Université de Montréal

Régulation de la mémoire par la plasticité des interneurones inhibiteurs de l'hippocampe

Par

Ève Honoré

Département de Neurosciences, Faculté de Médecine

Thèse présentée en vue de l'obtention du grade de Docteure en Philosophie (Ph. D)
en Neurosciences

© Ève Honoré, aout 2022

Université de Montréal
Département de Neurosciences, Faculté de Médecine

Cette thèse intitulée

Régulation de la mémoire par la plasticité des interneurones inhibiteurs de l'hippocampe

Présentée par

Ève Honoré

A été évaluée par un jury composé des personnes suivantes

Bénédicte Amilhon

Présidente du comité

Jean-Claude Lacaille

Directeur de recherche

Jonathan Brouillette

Membre du jury

Sylvain Williams

Examinateur externe

Elvire Vaucher

Représentante du doyen

Résumé

La mémoire explicite émerge de l'acheminement approprié de l'information à travers les circuits hippocampiques, et la formation d'un engramme qui encode cette mémoire. Les interneurones inhibiteurs régulent le flot d'information à travers ce réseau par leur contrôle dynamique des différents compartiments des cellules principales, ce qui contribue probablement à la formation de l'engramme. À cet égard, les interneurones somatostatinergiques (SOM-INs) et parvalbuminergiques (PV-INs), représentant les deux groupes majeurs de neurones inhibiteurs de l'hippocampe, sont particulièrement intéressants, car ils démontrent plusieurs formes de plasticité à long terme.

Cette thèse a pour objectif d'étudier le rôle spécifique des SOM-INs et PV-INs de l'aire CA1 ainsi que leurs plasticités à long terme dans le contrôle dynamique des réseaux de l'hippocampe et la formation de la mémoire.

Les SOM-INs expriment une potentialisation à long terme (PLT) à leurs synapses excitatrices venant des cellules pyramidales locales. Cette PLT a pour conséquence l'augmentation de l'inhibition des cibles des SOM-INs, les cellules pyramidales et interneurones locaux, ce qui contribue à la métaplasticité des circuits synaptiques de CA1. La PLT des SOM-INs contribue à la consolidation de la mémoire de peur contextuelle et la mémoire spatiale aversive. Cependant, nous ne savons pas si : 1) cette PLT est suffisante pour la formation de ces types de mémoire, ni si elle est impliquée dans la formation de la mémoire non aversive 2) si cette PLT est induite lors de l'acquisition ou de la consolidation de ces mémoires.

Pour l'étude de la PLT des SOM-INs, nous avons utilisé l'optogénétique afin d'avoir un contrôle sur la localisation et le moment des modifications de l'activité des SOM-INs. Nous avons montré que l'activité de ces interneurones était nécessaire durant l'apprentissage de la mémoire de peur contextuelle et de la mémoire spatiale épisodique non aversive. Nous avons établi un protocole de stimulation optogénétique capable d'induire *in vitro* une PLT aux synapses des cellules pyramidales de CA1 sur les SOM-INs. Nous avons démontré que cette PLT était nécessaire et suffisante pour moduler les réseaux synaptiques du CA1 *in vitro*, ainsi que les deux types de

mémoires étudiées. De plus, nous avons démontré de façon directe que l'induction de cette PLT induisait la synthèse protéique via l'activation de mTORC1 dans les SOM-INs *in vitro*.

Les PV-INs expriment également une PLT à leurs synapses excitatrices venant majoritairement des cellules pyramidales de l'aire CA3 à la suite d'un conditionnement à la peur, qui est nécessaire à la consolidation de cette mémoire. *In vitro*, la stimulation haute fréquence des afférences de CA3 entraine une PLT de l'excitabilité intrinsèque des PV-INs. Cependant, nous ne savons pas si cette forme de plasticité est également nécessaire pour la mémoire de peur contextuelle.

Pour l'étude de la PLT de l'excitabilité intrinsèque des PV-INs, nous avons d'abord établi qu'une perte de fonction hétérozygote et homozygote de mTORC1 dans les PV-INs ne change pas les propriétés de décharge de base de ces neurones, mais diminue la fréquence d'une décharge répétée et bloque l'induction de la PLT de l'excitabilité intrinsèque. De plus, nous avons montré que cette forme de PLT des PV-INs n'est pas nécessaire à la consolidation ni la discrimination de la mémoire de peur contextuelle.

En conclusion, ces travaux suggèrent que la plasticité synaptique des interneurones étudiés est nécessaire à la formation de la mémoire explicite. Celle des SOM-INs est nécessaire durant l'apprentissage, celle des PV-INs durant la consolidation.

L'ensemble de nos résultats mettent en évidence les rôles spécifiques des divers types de plasticité des interneurones inhibiteurs dans les fonctions mnésiques et soulignent leur rôle critique dans la régulation de la mémoire.

Mots clés :

Hippocampe, Interneurones inhibiteurs, Somatostatine, Parvalbumine, Potentialisation à long terme, Plasticité synaptique, Plasticité de l'excitabilité intrinsèque, Apprentissage et mémoire.

Abstract

Explicit memory emerges from the proper routing of information through hippocampal circuits, and the formation of an engram encoding this memory. Inhibitory interneurons regulate the flow of information in these networks by their dynamic control of the different compartments of pyramidal cells, which is likely to contribute to engram formation. In this regard, somatostatinergic (SOM-INs) and parvalbuminergic (PV-INs) interneurons, representing major groups of hippocampal inhibitory neurons, are particularly interesting because of the multiple forms of long-term plasticity they demonstrate.

The objective of this thesis is to study the specific roles of SOM-INs and PV-INs from hippocampal CA1 area, as well as their long-term plasticity in the dynamic control of the network and memory formation.

SOM-INs demonstrate long-term potentiation (LTP) at their excitatory synapses coming from local pyramidal cells. This LTP results in increased inhibition of SOM-INs targets, the local pyramidal cells and interneurons, which contributes to the metaplasticity of CA1 synaptic circuits. SOM-IN LTP is also involved in contextual fear memory and aversive spatial memory consolidation. However, it remains to be determined: 1) if this LTP is sufficient for the formation of these memory types, and if it is implicated in non-aversive memory formation; 2) if this LTP is induced during the acquisition or consolidation of these memories.

For studying SOM-IN LTP, we used optogenetics to control the place and time of SOM-IN activity. We showed that the activity of these interneurons is necessary during learning of contextual fear memory and non-aversive spatial episodic memory. We established an optogenetic stimulation protocol enabling us to induce LTP at synapses from CA1 pyramidal cells to SOM-INs *in vitro*. We demonstrated that this LTP is necessary and sufficient to modulate CA1 synaptic networks *in vitro*, as well as the two memory types studied. Moreover, we demonstrated a direct link between this LTP and mTORC1-dependent protein synthesis in SOM-INs *in vitro*.

PV-INs also express LTP at their excitatory synapses mainly coming from CA3 pyramidal cells after contextual fear conditioning, necessary for the consolidation of this memory. High frequency stimulation of CA3 afferents leads to PV-IN LTP of intrinsic excitability *in vitro*. Yet, we don't

know if this form of plasticity is also necessary for contextual fear memory. To study PV-INs LTP of intrinsic excitability, we established that heterozygous or homozygous mTORC1 loss of function in PV-INs did not change basic firing properties of these neurons but decreased repeated firing frequency and blocked LTP of intrinsic excitability. Besides, we showed that this form of PV-IN LTP is not necessary for the consolidation or discrimination of contextual fear memory.

In conclusion, these works suggest that synaptic plasticity of the studied interneurons is necessary for explicit memory formation. SOM-IN synaptic LTP is necessary during learning, while PV-INs LTP is necessary during consolidation.

Overall, our results highlight the specific roles of the various inhibitory interneuron plasticity in memory functions and emphasize their critical role in the regulation of memory.

Key words:

Hippocampus, Inhibitory interneurons, Somatostatin, Parvalbumin, Long-term potentiation, Synaptic plasticity, intrinsic excitability plasticity, Learning and memory.

Résumé vulgarisé

Pour beaucoup, l'hippocampe est un petit animal marin, mais c'est aussi une structure de votre cerveau nommée d'après lui car elle lui ressemble beaucoup. Cette structure est responsable de la création de la mémoire déclarative, c'est-à-dire celle dont on peut parler. C'est la mémoire des faits et des évènements. Mais comment notre hippocampe crée-t-il la mémoire ? Il reçoit de l'information d'autres structures du cerveau, par exemple : je vois qu'il y a des cerises sur l'arbre au loin. Il faut que je retienne cette information importante ! Dans le cerveau, l'information circule sous forme électrique dans des réseaux de neurones excitateurs. Ces réseaux sont finement régulés par des interneurones inhibiteurs. La première fois que je vois où se trouvent les cerises, un certain réseau de neurones va être activé, et la communication entre ces neurones va être facilitée. Une des fonctions des interneurones inhibiteurs est de faire la sélection des neurones activés et de faciliter de la communication entre eux tout en bloquant la communication avec d'autres neurones qui envoient des informations non pertinentes. Chaque fois que je vais retourner cueillir des cerises, le chemin que j'aurai pris sera plus fort, plus net, et facilité dans l'herbe, comme dans mes réseaux de neurones. Dans l'hippocampe, on connait bien ce phénomène de facilitation de la communication dans les réseaux de neurones excitateurs. Ce phénomène induit par l'apprentissage a aussi lieu entre les cellules excitatrices et certains interneurones, mais on en sait peu sur le rôle de cette facilitation dans la mémoire. Sert-elle à sélectionner le chemin du réseau de neurones qui encode le chemin pour me rendre au cerisier la première fois que je m'y rends (apprentissage) ? Sert-elle à rendre le chemin de neurones plus clair et plus fort (consolidation)? Ou encore à rendre possibles les modifications du chemin (reconsolidation) ? Mon projet de doctorat est d'étudier ce phénomène chez la souris.

Dans un premier temps, grâce à une technologie de pointe, j'ai induit artificiellement une facilitation entre des neurones excitateurs et un type d'interneurone inhibiteur qui les régulent juste avant des tâches d'apprentissages. Ainsi, j'ai étudié son effet sur deux types de mémoires créées par l'hippocampe : la mémoire spatiale et la mémoire de peur contextuelle, ainsi que sur les réseaux neuronaux qui les sous-tendent. Mes résultats montrent que l'activité de ces interneurones est cruciale pour la formation des deux types de mémoires, mais les mécanismes de facilitation de la communication entre les neurones semblent différents. Dans un second temps, j'ai effectué des

modifications génétiques dans un type d'interneurone particulier pour bloquer une autre forme de facilitation qui augmente l'activité du neurone globalement sans changer la force de ces connexions. Cette augmentation globale de l'activité n'a pas d'effet sur la mémoire de peur contextuelle alors que d'autres travaux avaient démontré que la facilitation des synapses de ces interneurones est nécessaire à la formation de ce type de mémoire.

Mis ensemble, mes travaux suggèrent qu'il faut une facilitation des synapses entre les cellules excitatrices et les interneurones inhibiteurs de l'hippocampe, pendant l'apprentissage pour le premier type d'interneurone, et pendant la consolidation pour le second, pour former la mémoire de façon adéquate. De plus, il a été montré dans des modèles de souris de la maladie d'Alzheimer, de l'autisme, de la schizophrénie et de l'épilepsie qu'il y avait un déficit de cette facilitation de la communication entre les cellules excitatrices et inhibitrices que j'étudie. Mon projet, en plus d'approfondir nos connaissances sur les bases neurobiologiques de la mémoire, pourrait nous aider à mieux comprendre ces maladies et nous diriger vers de meilleurs traitements.

Table des matières

Chapitre II

Chapitre III

Chapitre IV

Chapitre V

Table des figures

Chapitre I

Article de revue : Hippocampal Somatostatin Interneurons, Long-Term Synaptic Plasticity and Memory.

Chapitre II

Liste des tableaux

Liste des abréviations

	En Français	En Anglais
4E-BP		eIF4E-binding protein
aBFS		Associative burst frequency stimulation
aCSF		Artificial cerebrospinal fluid
AD		Alzheimer's disease
AEC	Avant l'ère commune	
AHP		After hyperpolarization
AKT	Protéine kinase B	Protein kinase B
AMPAR	Récepteur a l'acide a-amino-3-hydroxy-5-méthyl-1-4-isoxazole propionique	α-amino-3-hydroxy-5-methyl-4-isoxazolepropionic acid receptor
Arch	Archaerhodopsine	Archaerhodopsin
AP		Action potential
ARNm	Acide ribonucléique messagers	
BiCs		Bistratified cells
BP		Back-projecting
BTSP		Behavioral timescale synaptic plasticity
CA	Corne d'Ammon	
CaMKII		Ca2+/calmodulin-dependent protein kinase II
CB1R		Cannabinoid type 1 receptor
CFC	Conditionnement à la peur contextuelle	Contextual fear conditioning
CI-AMPARs		Calcium Impermeable AMPARs

CP	Cellules pyramidales	
CP-AMPAR	AMPAR permeables au calcium	Calcium permeable AMPAR
CPns	Cellules en panier	
CP-SOM	Synapses entre les cellules pyramidales et les interneurones exprimant la SOM	
CREB		cAMP responsive element binding protein
DG		Dentate gyrus
DHPG		(S)-3,5-dihydroxyphenylglycine (mGluR1/5 agonist)
DP		Double projecting interneurons
DPCPX		8-Cyclopentyl-1,3-dipropylxanthine (adenosine A1 receptor antagonist)
DREADD		Designer receptor exclusively activated by designer drug
eCB		Endocannabinoid
eIF2α		Eukaryotic initiation factor 2α
eIF4F		Eukaryotic initiation factor 4F
Elfn1		Extracellular leucine-rich repeat fibronectin containing 1
EPSC		Excitatory post-synaptic current
EPSP		Excitatory post-synaptic potential
ERK		Extracellular signal-regulated kinase
EYFP		Enhanced yellow fluorescent protein
fEPSP		Field EPSP
FS-PV INs		Fast-spiking parvalbumin-expressing interneurons
GABA	Acide γ-aminobutyrique	γ-aminobutyrique acid
GC		Granule cell

hChR2		Channelrhodopsin hChR2(E123T/T159C)
HFS		High frequency stimulation
HICAP		Hilar commissural associational path
HIL cells		Hilar cells
HIPP cells		Hilar perforant path cells
I-DLT	Dépression à long terme des synapses inhibitrices	
I-PLT	Potentialisation à long terme des synapses inhibitrices	
K2P		two-pore domain potassium channel
LFS		Low frequency stimulation
LFS_{opto}		Low frequency optogenetic stimulation
$L\text{-}LTP_{mGluR1}$		mGluR1-dependent late LTP
LTD		Long-term depression
LTD_{IE}		Long-term depression of intrinsic excitability
LTP		Long-term potentiation
LTP_{IE}		Long-term potentiation of intrinsic excitability
MAPK		Mitogen-activated protein kinase
MEF2		Myocyte enhancer Factor 2
MEK		Mitogen-activated protein kinase kinase
mEPSC		Miniature EPSC
mGluR1 to 7	Récepteurs métabotropiques au glutamate 1 à 7	Metabotropic glutamate receptor 1 to 7
mIPSC		Miniature inhibitory postsynaptic current
MPEP		2-methyl-6-(phenylethynyl)-pyridine (mGluR5 antagonist)

mTORC1	Protéine kinase cible de la rapamycine	Mechanistic target of rapamycin complex 1
NAPE-PLD		N-acylphosphatidylethanolamine phospholipase D
NCX		Sodium/calcium exchangers
Nkx-2.1		NK2 homeobox 1
NMDAR	Récepteur au n-méthyl-D-aspartate	N-methyl-D-aspartate receptor
OLM ou/or O-LM cells		Oriens Lacunosum-moleculare cells
OLMα2	Cellules OLM exprimant la sous-unité α2 du récepteur nicotinique	OLM cells expressing the nicotinic receptor α2 subunit
OLMt	Tâche de mémorisation de localisation d'objets	Object location memory task
ORP		Oriens-retrohippocampal projecting
PC		Principal cell or pyramidal cell
PC-SOM		synapses between PC and SOM-INs
PI3K		Phosphoinositide 3-kinase
PKA	Protéine kinase A	Protein kinase A
PKC	Protéine kinase C	Protein kinase C
PLT	Potentialisation à long terme	
PLT_{EI}	Potentialisation à long terme de l'excitabilité intrinsèque	
PLT_{opto}	PLT optogénétique	
PV	Parvalbumine	Parvalbumin
PV-INs	Interneurones exprimant la parvalbumine	Parvalbumin expressing interneurons
Raptor		Regulatory-Associated Protein of mTOR
REM sleep		Rapid eye movement sleep
Rin		Input resistance

RLM		Radiatum-lacunosum moleculare
Rptor	Gène de la protéine Raptor	Gene of the Raptor protein
RSK		Ribosomal S6 Kinase
S6K		ribosomal protein S6 kinase
SC		Schaffer collateral pathway
SC-PC		CA3 to CA1 PCs synapses
sEPSC		Spontaneous excitatory postsynaptic currents
sIPSCs		Spontaneous inhibitory postsynaptic currents
SL		Stratum lucidum
SOM	Somatostatine	Somatostatin
SOM-EYFP -Raptor KO		Sstires-Cre;Rosa26lsl-EYFP;Rptorfl/fl knock-out mice
SOM-EYFP -WT		Sstires-Cre;Rosa26lsl-EYFP mice
SOM-INs	Interneurones exprimant la somatostatine	Somatostatin expressing interneurons
SR		Stratum radiatum
SRIF		Somatotropin release inhibitory factor
SSTR1 to 5		Somatostatin receptor 1 to 5
SUnSET		SUrface SEnsing of Translation
SWR	Ondulation de vagues pointues	Sharp wave ripples
TAP ou TA		Temporo-ammonic pathway
TBS		Theta burst stimulation
TBS_{opto}		Optogenetic theta burst stimulation
TRP		Transient receptor potential

TSC1/2	Tuberous Sclerosis Complex 1/2
VGCCs	Voltage gated calcium channels
VIP	Vasoactive intestinal peptide
wTBS	Weak electrical TBS
γCaMKII	Gamma-Ca2+/calmodulin-dependent protein kinase II

Remerciements

La thèse est un travail solitaire sur bien des aspects, mais comme beaucoup de choses, elle ne se fait jamais vraiment seule. Je tiens donc à exprimer ma gratitude à toutes ces personnes qui ont d'une façon ou d'une autre contribué à la réussite de ce projet.

Tout d'abord, je voudrais remercier Jean-Claude Lacaille d'avoir accepté une dernière doctorante au sein de son laboratoire. Merci pour la confiance et la liberté de travail que tu m'as accordé, mais aussi pour ta disponibilité quand j'avais besoin d'être guidée.

Je souhaite également remercier mon comité de parrainage, Bénédicte Amilhon et Richard Robitaille pour les encouragements, et les conseils que vous m'avez donnés, si bien d'un point de vue scientifique que personnel.

Merci aux membres de mon jury, Bénédicte Amilhon, Jonathan Brouillette, Sylvain Williams et Elvire Vaucher pour avoir accepté d'examiner cette thèse.

To the Neurowire club organizers, thank you all, these seminars were a weekly source of marvel and inspiration. I loved the atmosphere you created, enabling tricky questions to be addressed in a very relaxed and respectful way. May this project prosper and last long!

Merci aux postdocs du laboratoire de Sylvain Williams de m'avoir initié à l'optogénétique, particulièrement à Guillaume Etter pour m'avoir montré comment on branche une souris et pour avoir relu la discussion de ma thèse.

Merci aux membres du lab, avec qui j'ai partagé des projets. Plus particulièrement Julien Artinian qui m'a intégré au lab, initié à l'art complexe du ducttaping, pour les longues pauses du midi qui me permettaient de voir la lumière du jour, et les longues longues longues discussions scientifiques et moins scientifiques. À Isabel, pour avoir toujours anticipé mes besoins en souris, s'être occupé de toutes les choses 'plates' du labo, pour les cours de québécois avec Julie, et pour m'avoir fait connaitre radio neige folle. Merci à Abdessattar pour tes mots d'encouragement, et pour avoir commencé à me montrer le patch. Merci aussi à François-Xavier pour avoir fini ma formation au patch, pour avoir couru à mon secours lorsque le fantôme de clampex faisait des siennes ou que j'étais simplement trop crevée pour voir que clampex était passé en mode démo, pour les pastis et autres apéros de soutiens. Merci à Darren, pour avoir relu ma revue à peine arrivé

au lab et le résumé de cette thèse, pour les excellentes suggestions de films et séries, et les bons moments passés en dehors du lab.

Merci à mes superviseurs précédents, Emmanuel Valjent, Kevin Mouzat, et Michel Vignes pour leur confiance, l'enseignement qu'ils m'ont apporté, ainsi que les conseils qu'ils continuent de me donner.

Merci à Gregory, même si tu as failli me couter cette thèse (malgré toi), c'est quand même grâce, ou à cause de toi que j'en suis là. Milles merci pour être le parfait 'partner in crime' et player 2, ainsi que pour ta propension à accepter n'importe lequel de mes plans sans poser de questions. Merci pour ton soutien indéfectible, et pour ta douce folie. Je suis admirative de ta capacité à avancer coute que coute et te souhaites une belle réussite maintenant que la neuroimmuno est devenue cool (c'est fou!). PS : J'espère que tu as pris des cours de forge.

À Neus, merci pour ta bonne humeur et ton énergie qui m'ont donné des courbatures et fait dépasser mes limites. Ces belles qualités qui poussent les sneaky racoons à explorer le Canada toujours plus loin. Merci pour ton oreille attentive quand j'ai juste besoin de me plaindre, et les mots d'apaisements '*we are not this next thought*'. Merci pour toutes les aventures partagées, je suis tellement heureuse qu'on ait commencé et fini ensemble ce doc! Je croise les doigts, touche du bois, lagarto lagarto pour que tes rêves se réalisent, et que peut-être on ouvre un lab au bord de la méditerranée un jour.

À François, merci de m'avoir fait entrer dans la secte Python, pour les révisions de code et avoir sacrifié ton ordi de gaming à un moment où il n'y avait pas vraiment autre chose à faire pour que je puisse faire mon analyse. Sans toi j'aurais perdu la vue à faire mon analyse à la main. Merci pour ton soutien moral, pour être passé par toutes les embuches du doc avant moi pour que je puisse les voir venir, pour m'avoir supporté tout au long de ce doc, surtout vers la fin, et ce après un nombre incalculable de confinements. Merci de me pousser à m'améliorer, mais aussi pour ta douceur quand j'en ai besoin, et bien sûr pour les multiples poulets au beurre de célébration.

Merci à mes amis, à François et à mes beaux-parents de m'avoir offert le meilleur, le plus beau, le plus doux chat de support moral. J'ai un nombre de commentaires suffisant de personnes n'ayant pas de conflits d'intérêts qui corroborent ces faits pour dire que ce n'est pas juste à cause de toxoplasma gondi que je trouve Ekeko aussi exceptionnel.

Merci à ma mère pour avoir cultivé ma curiosité, ma débrouillardise et m'avoir laissé expérimenter avec tout ce qui me tombait sous la main, mais aussi pour avoir lu ma revue pour trouver les abréviations.

Merci à ma belle-famille pour leur soutien.

Merci à l'ADENUM pour les belles années passées à tenter d'améliorer la vie des étudiants de neurosciences, j'ai rencontré de belles personnes dans cette asso. Merci aussi pour la bourse d'implication. Je vous souhaite à tous bon courage pour les années à venir.

À tous, il y a des chances non nulles que j'ai un, ou un sous-ensemble de neurones, qui encode chacun de vous spécifiquement dans mon hippocampe. C'est l'une des raisons pourquoi cette structure est sans équivoque la meilleure (Quiroga et al., 2005).

Quiroga, R., Reddy, L., Kreiman, G. et al. Invariant visual representation by single neurons in the human brain. Nature 435, 1102–1107 (2005). https://doi.org/10.1038/nature03687

Chapitre I

Introduction

1.1. Qu’est-ce que la mémoire ? Une question que l’on se pose depuis 3000 ans.

1.1.1 Définition de la mémoire

La mémoire est définie comme la capacité d'encoder, de conserver, et de restituer des informations. De façon plus générale, on peut dire que la mémoire est toute modification d’un système par un stimulus, qui persiste après la fin de ce stimulus et qui change la réponse de ce système aux présentations futures de stimulations similaires (Squire L. R., 2009; Kukushkin N. V. & Carew T. J., 2017; Zlotnik G. & Vansintjan A., 2019). Cette rétention d’information est indispensable à notre vie, car elle nous permet de nous adapter à de nouvelles situations grâce à l’expérience. Étant donné que l’expérience est unique à chaque individu, la mémoire l’est aussi. La mémoire nous définit donc en tant qu’individu par l’encodage, la conservation, et la restitution de nos expériences. Nos idées, nos peurs, nos désirs sont constitués par les impacts cumulés de ce dont nous nous souvenons. C’est pour ces raisons que la mémoire est si précieuse et que les affections qui la touchent nous semblent si graves. Ainsi, depuis des millénaires, l’humain se demande d’où vient la mémoire ? Comment se forme-t-elle ? Qu’est-ce qui la régule ?

1.1.2 Évolution du concept de mémoire.

Premières hypothèses sur la mémoire

Dans la Grèce antique, la mémoire était sacrée, donnée par Mnémosyne déesse de la mémoire et mère des muses (Hésiode, 8e-7e siecle AEC). Seuls les dieux étaient sages et détenaient la connaissance universelle. Les hommes avaient la philosophie pour étudier la mémoire via l’introspection et l’observation attentive, et faire l’inventaire de leurs connaissances pour se rendre compte qu’ils ne savent rien (Je ne sais qu’une chose, c’est que je ne sais rien. Attribué à Socrate par Platon) (Burnham W. H., 1888; Platon, -427 a -348). Même si l’interprétation de leurs

observations était teintée par leurs croyances, il en reste que les observations en elles même étaient très justes. Nous verrons au cours de cette thèse comment des concepts posés depuis l'antiquité reviennent encore et encore au fur et à mesure que nos connaissances sur la mémoire s'étoffent.

Il était communément admis dans l'antiquité que la mémoire était séparée en deux formes, la mémoire du corps : celle que l'on acquière par l'expérience des sensations et qui est trompeuse, et la mémoire de l'âme : celle des idées, de l'imagination et des savoirs qu'on n'apprend pas par les sens, mais par la cognition, telles que les sciences. Ce dernier type de mémoire était considéré (et l'est toujours) comme supérieur, si bien que Socrate se serait opposé à l'écriture de cette thèse, parce qu'il soutenait que l'écriture nuisait à la mémoire. L'apprenant se reposant sur l'écriture pour se rappeler ne développe pas sa mémoire, l'écriture est alors un remède pour la réminiscence, mais pas la mémorisation (Platon, -427 a -348). Il est intéressant de voir qu'à cette époque déjà, on séparait le rappel et la mémorisation comme fonctions distinctes de la mémoire. Par bonheur Platon a défié son maitre, nous communiquant non sans paradoxe un plaidoyer contre l'écriture, ainsi que les premiers traités sur la mémoire mettant en scène des discussions avec Socrate (Platon, -427 a -348). L'une des idées qui ressortent de ces écrits est que la perception (réunion de sensations en images mentales) et la réminiscence sont des occasions pour l'esprit de se détourner des sens pour se concentrer sur le monde intérieur des idées innées et universelles. La sensation seule ne nous donne pas ces idées, car elle nous donne des informations sur des aspects individuels et immédiats des choses. Pour concevoir des idées, il faut d'abord connaitre les faits et les associer pour avoir une compréhension d'ensemble des choses (Burnham W. H., 1888).

Aristote qui était contemporain à Platon avait une vision plus biophysique de la mémoire. La stimulation des organes sensoriels crée un mouvement appelé *pneuma* (qui se traduit littéralement par le souffle, mais aussi l'âme) transporté par le sang jusqu'au cœur. La fonction du cœur est alors de comparer, synthétiser et de rendre consciente la sensation. Les souvenirs sont déclenchés par l'initiation du même mouvement du *pneuma* par la même stimulation sensorielle ou une stimulation proche. Les souvenirs qui ne sont pas déclenchés par des stimulations sensorielles proviennent de l'âme qui agit via le cœur. Bien sûr cette hypothèse n'est plus admise de nos jours, néanmoins plusieurs concepts présentés par Aristote sont toujours valides et à l'étude de nos jours. Il faisait la différence entre la mémoire immédiate qui reproduit directement une représentation et la mémoire à long terme qui nécessite l'association d'idées. De plus, il démontre que l'habituation provoque le rappel d'une séquence de souvenirs, mais aussi que nous cherchons

dans notre mémoire par une succession de liens entre les souvenirs (Burnham W. H., 1888; Souques A. A., 1936).

Hippocrate qui est considéré comme le père de la médecine et le fondateur de la méthode d'observation clinique fut le premier dont nous ayons une trace écrite à proposer que la pensée et la mémoire aient lieu dans le cerveau suite à l'étude de nombreux cas de blessures à la tête (Souques A. A., 1936; Hippocrates, -460 a -377). Suivant cette méthode et grâce aux premières dissections humaines à but scientifiques documentées, Hérophile et Érasistrate décrivirent le système nerveux, et fournirent les premiers liens directs entre les circonvolutions cérébrales et fonctions intellectuelles (Souques A. A., 1936).

Ces trois théories de la mémoire ont peu évolué de l'antiquité jusqu'au 19^{èm} siècle. Les courants de pensée empruntaient un peu à l'une et à l'autre, mais se séparaient majoritairement entre l'explication platonicienne et aristotélicienne en gardant toujours ce dualisme entre la mémoire du corps et la mémoire de l'esprit (Burnham W. H., 1888; Souques A. A., 1936).

Débuts de la physiologie de la mémoire

À la façon d'Hippocrate, des avancées majeures sur la localisation de la mémoire furent faites via l'analyse de patients présentant des pertes de mémoire. Théodule-Armand Ribot dans les maladies de la mémoire (Ribot T.-A., 1881), propose que la perte de mémoire soit le symptôme d'une maladie progressive du cerveau. Il fut le premier à postuler que la mémoire venait d'un changement d'activité des cellules nerveuses. La spécificité de fonction des régions du cerveau avait été démontrée quelques années auparavant pour le langage (Broca P.-P., 1861b; a) et les fonctions sensorimotrices (Flourens M. J. P., 1842; Fritsch G. & Hitzig E., 1870; Ferrier D., 1876). Cependant, aucune région n'était directement associée à la mémoire. Étant donné la limitation de l'étude de lésions chez l'humain, puisqu'il fallait documenter les pertes de fonctions supposées sans connaitre les performances avant la lésion, puis espérer pouvoir avoir accès au cerveau du patient après sa mort et enfin avoir la chance de trouver une lésion et si possible qui ne s'étend qu'à une structure. L'expérimentation animale prit donc de plus en plus de place dans les neurosciences. La taille des lésions était alors contrôlée, on pouvait étudier les différences de performances de l'animal avant et après la lésion, puis vérifier son étendue et sa localisation. Une première publication rapporte un lien entre des lésions du lobe temporal et une perte de mémoire apparente chez les singes (Brown S. & Sharpey-Schafer E. A., 1888). Néanmoins, le but de ces travaux n'était

pas d'étudier la mémoire, et pour cause, il fallait d'abord concevoir des expériences permettant de tester la mémoire chez les animaux. En psychologie expérimentale, des tests chez l'humain avaient été créés afin de démontrer que la mémoire à court terme n'est pas définitive et qu'elle est sensible aux perturbations (Müller G. E. & Pilzecker A., 1900). Toutefois, ces expériences consistaient en une étape d'apprentissage d'association de syllabes, afin de tester la mémoire on donnait la première syllabe de la paire et le sujet devait répondre par la syllabe correspondante, ce qui est impossible à mettre en place chez l'animal.

Le comportementalisme

En 1890 Ivan Pavlov en voulant étudier la physiologie gastrique découvrit le réflexe conditionnel qu'on appela plus tard conditionnement pavlovien. Il avait remarqué qu'après quelques jours les chiens qu'il utilisait pour ses expériences commençaient à saliver en entrant dans le laboratoire, avant d'être en contact avec la nourriture. Ceci suggérait que les chiens étaient capables d'anticiper qu'ils allaient être nourris, en se souvenant de l'association de l'environnement avec la nourriture. Pour mieux étudier ce phénomène, il associa un son qui est un stimulus neutre qui ne produit pas de réaction particulière chez ses chiens avec la présentation de nourriture qui elle est une stimulation qui produit une réaction réflexe : la salivation. Il découvrit qu'après quelques entrainements, les chiens salivaient dès qu'ils entendaient le son, ce qui démontre qu'il y a eu association entre le son et la nourriture (figure 1 A) (Pavlov I. P., 1928).

A Conditionnement pavlovien (I. Pavlov)

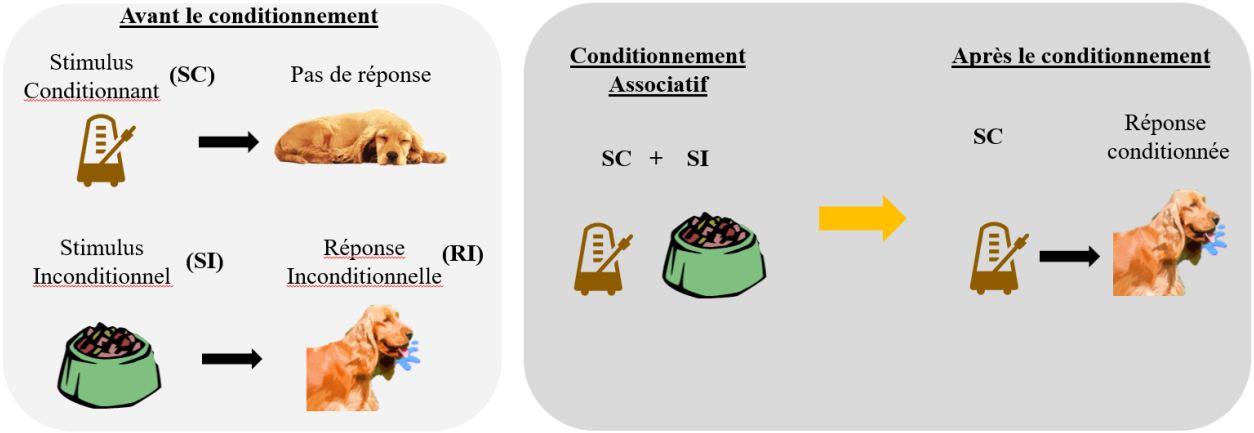

B Conditionnement opérant (B.F. Skinner)

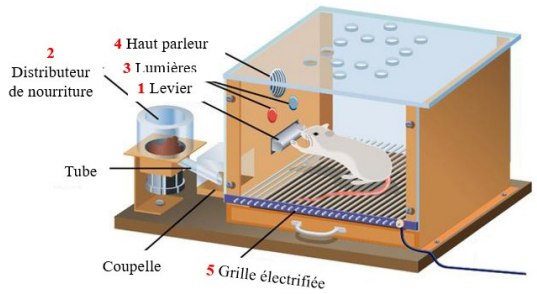

Paradigmes	Réponse comportementale
1 -> **2**	Augmentation du nombre de presse jusqu'à satiété.
Si **3** est activé, **1**->**2**	Presse seulement pendant le signal lumineux
Si **4** est activé, **1**-> **5**	Presse seulement quand il n'y a pas de signal sonore

Figure 1 : Méthodes d'étude du comportement animal. A, paradigme du conditionnement pavlovien. Le stimulus conditionnant n'induit pas de réponse de la part de l'animal, le stimulus inconditionnel, ici de la nourriture, induit une réponse inconditionnelle réflexe, la salivation. Si on couple le stimulus inconditionnel au stimulus conditionnant, l'animal va les associer. Plus tard, la présentation seule du stimulus conditionnant sera suffisante pour induire une réponse conditionnée, la salivation. **B**, paradigmes de conditionnement opérant. Un animal est mis dans la boite de Skinner, en l'explorant il va par hasard appuyer sur le levier (1) ce qui va déclencher la libération de nourriture (2). Dans ce cas, le rongeur va associer la presse de levier avec la nourriture, et continuera d'appuyer jusqu'à satiété. On peut également effectuer des séquences d'associations en ne libérant la nourriture que lorsqu'un indice est présenté, ou encore inhiber un comportement en ne donnant pas la récompense sous certaines conditions, ou en donnant une punition. B adapté de https://www.simplypsychology.org/operant-conditioning.html

Inspiré par cette expérience, John Watson voulait démontrer que ce genre de conditionnement réflexe pouvait avoir lieu chez l'humain aussi. Il développa le ``*behaviorism*`` ou comportementalisme, une théorie selon laquelle le comportement observable est le produit de conditionnements réflexes. Cette approche vise à démontrer des relations statistiquement significatives entre un comportement et des variables environnementales, par observation objective de sujets (Watson J. B., 1930). Dans la même lignée, Burrhus Frederic Skinner emmena plus loin le comportementalisme. Il pensait que les comportements complexes de l'humain ne pouvaient pas être expliqués par le conditionnement réflexe, mais voulait prouver que nos actions étaient conditionnées et les pures conséquences du renforcement ou de l'inhibition de nos actions passées (Skinner B. F., 1974). Pour prouver sa théorie, il développa une chambre de conditionnement permettant d'étudier le comportement d'animaux sans l'intervention directe de l'expérimentateur, l'expression de la mémoire se fait par l'adaptation du comportement, on quantifie donc la rapidité de l'adaptation et la fréquence à laquelle le comportement acquis se présente. Grâce à cet appareil,

appelé plus tard la boite de Skinner, il mit en place une nouvelle forme de conditionnement dit opérant. Dans le conditionnement pavlovien, il y a association d'un comportement naturel passif (par exemple la salivation) avec un stimulus neutre (par exemple un son de métronome ou une lumière qui s'allume). Dans le conditionnement opérant, une action spontanée est soit renforcée par une récompense, soit inhibée par association avec un stimulus aversif. Par exemple, une boite de Skinner adaptée pour les rats contient un levier et un distributeur de nourriture. Le rat en explorant la boite va appuyer sur le levier ce qui va déclencher la distribution de nourriture. Le rat va donc associer la pression du levier avec la récompense en nourriture et va continuer à activer le levier jusqu'à ce qu'il n'ait plus faim. On peut ensuite inhiber ce comportement en l'associant à un stimulus aversif en donnant des chocs électriques lorsque le rat presse le levier, ou encore conditionner la distribution de nourriture à un stimulus neutre se faisant le rat apprendra à ne presser le levier que lorsque le stimulus neutre est présenté. Plusieurs successions d'actions peuvent être additionnées pour produire des comportements complexes (figure 1 B) (Ferster C. & Skinner B., 1957; Skinner B. F., 1974). Ces travaux nous ont donné beaucoup d'informations sur comment la mémoire associative influence le comportement et surtout une nouvelle méthode d'exploration de la mémoire, mais pas sur la neurobiologie de la mémoire.

L'un des étudiants de Watson, Karl Lashley s'inspira aussi du *behaviorism* pour étudier la localisation du centre de la mémoire dans le cerveau. Il développa des labyrinthes de plus en plus complexes dans lesquels il entrainait des rats à trouver de la nourriture avant de faire des lésions corticales. Il observait alors le comportement d'exploration des rats lors de leur retour dans le labyrinthe pour déterminer si leur mémoire avait été affectée de manière significative ou pas par les différentes lésions. Ses résultats montrent que la taille de la lésion est directement proportionnelle à la diminution des fonctions mnésiques, mais que la localisation influençait peu. Il en conclut que la mémoire n'est pas située à un endroit précis, mais qu'elle est distribuée de façon égale dans le cortex et que toute partie intacte du cerveau a la capacité d'exécuter la fonction d'une partie lésée de la même zone fonctionnelle (Lashley K. S., 1929). Cette interprétation fut contestée par l'idée alternative selon laquelle la mémoire est bel et bien distribuée dans le cortex, mais chaque structure a une fonction bien déterminée encodant chacune différents aspects de la mémoire (Hunter W. S., 1930; Hebb D. O., 1949). La mémoire était donc vue comme intégrée avec

les fonctions perceptuelles (la mémoire motrice dans le cortex moteur, la mémoire visuelle dans le cortex visuel) et aucune région du cerveau n'avait pour rôle spécifique de produire la mémoire.

La formation de la mémoire dépend du lobe temporal médian. Travaux de Brenda Milner avec le patient HM :

À la fin des années 1950, les travaux de Brenda Milner et de ses collègues sur le patient H.M. vont marquer un tournant dans la recherche sur la question : "où se trouve la mémoire". En effet, H.M. souffrait d'épilepsie réfractaire causant des crises majeures très handicapantes et aucun foyer épileptogène précis n'a pu être identifié. Afin de réduire ses crises, H.M. a subi une résection bilatérale des lobes temporaux médians puisque l'hippocampe, l'une des structures qui composent ce cortex, était connu pour sa nature épileptogène (Scoville W. B. & Milner B., 1957). La partie du cerveau retirée correspond à la partie antérieure de l'hippocampe et au gyrus parahippocampique qui constituent la formation hippocampique, ainsi qu'à l'amygdale et l'uncus (Annese J. *et al.*, 2014). La chirurgie a effectivement réduit le nombre de crises épileptiques, toutefois elle a eu pour conséquence inattendue des troubles de la mémoire profonds, mais n'entraina aucun changement dans la personnalité ni aucune atteinte aux capacités intellectuelles

A Résection du lobe temporal médian

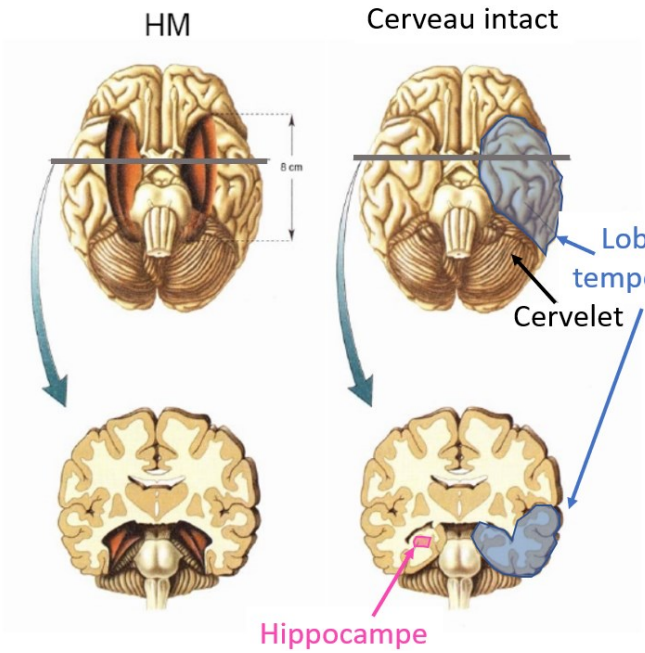

B Effets de la résection sur la mémoire autobiographique

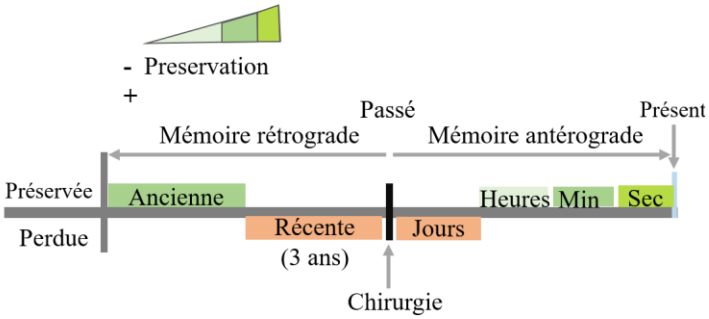

Figure 2 : Résection du lobe temporal médian et ses effets sur la mémoire autobiographique. A, schéma montrant la partie du lobe temporal excisé chez H.M. **B**, schéma représentant les formes de mémoires autobiographiques préservées ou perdues chez H.M. sur une échelle de temps. A adapté de Wolters Kluwer Health 2007, Ch.24.

générales d'H.M. (figure 2 A) (Scoville W. B. & Milner B., 1957; Milner B. *et al.*, 1968; Squire L. R., 2009). D'autres patients ayant subi une chirurgie similaire, mais avec une résection plus petite ont montré une perte des fonctions mnésiques moins importante. Quand la résection se limitait à l'uncus et a l'amygdale, il n'y avait pas de perte de mémoire (Scoville W. B. & Milner B., 1957; Squire L. R., 2009). Cela suggérait donc un rôle primordial de la formation hippocampique dans la mémoire.

Plus précisément, la mémoire rétrograde des faits antérieurs aux 3 années précédant la chirurgie d'H.M. était intacte. Sa mémoire à très court terme (quelques secondes) était meilleure que celle de personnes normales, à court terme (quelques minutes) elle était généralement bonne. Il pouvait se souvenir d'un nombre de choses restreint pour quelques minutes si on ne l'interrompait pas. Il était aussi capable d'améliorer ses performances de jour en jour dans des tâches de coordination sensorimotrice fine telle que dessiner une étoile en ne voyant son dessin qu'à partir d'un miroir, alors qu'il ne se souvenait pas avoir effectué ces tâches auparavant. Finalement, il démontrait des signes de conditionnement. Après plusieurs tests de sensibilité tactile où l'expérimentateur lui demandait de tendre les mains puis de fermer les yeux, H.M. fermait les yeux directement après avoir tendu les mains sans qu'on le lui demande et sans se souvenir qu'on lui eut déjà demandé de faire cela. Cependant, il avait globalement perdu la mémoire des faits et évènements récents et était incapable de former de nouveaux souvenirs à long terme (figure 2B) (Scoville W. B. & Milner B., 1957; Penfield W. & Milner B., 1958; Milner B. *et al.*, 1968).

En plus de démontrer que la mémoire n'est pas distribuée de façon égale dans tout le cerveau, et que la formation hippocampique joue un rôle fondamental dans la mémoire, les résultats des tests effectués sur le patient H.M. ont permis de mettre en évidence que le phénomène qu'on appelle mémoire n'est pas monolithique, mais représente une multitude de fonctions avec différentes temporalités, supportées par différentes régions du cerveau. En effet, la mémoire motrice et la mémoire de travail intactes, ainsi que le conditionnement involontaire d'H.M. démontrent que ces formes de mémoires sont encodées par des structures en dehors du lobe temporal médian. En outre, H.M. n'avait aucun problème à se souvenir de faits et d'évènements de son enfance. Cela met donc en lumière que la formation hippocampique n'est pas un lieu de stockage des souvenirs à long terme. Mais d'après ces résultats, sa fonction est de faire passer un souvenir à court terme vers une mémoire à long terme. Ceci souligne également le fait que la mémoire à court terme utilise des mécanismes différents de la mémoire à long terme, les souvenirs

durables ne le sont pas dès leurs premières secondes, et leur passage de mémoire à court terme vers une mémoire à long terme peut prendre des années comme l'indique l'amnésie rétrograde d'H.M. De façon alternative, cela peut aussi suggérer que l'hippocampe est nécessaire pour le rappel des informations récentes (les 3 années précédant la lobectomie pour H.M.), mais pas les plus anciennes. Plus tard dans sa vie H.M avait une moins bonne mémoire autobiographique, ses souvenirs étaient moins détaillés (Corkin 2002). L'imagerie par résonance magnétique (IRM) du cerveau d'H.M. à montré qu'il avait perdu du volume cortical et sous-cortical (Salat D. H. *et al.*, 2006) Cela pourrait indiquer que la formation hippocampique protège l'intégrité des souvenirs en les réactivant, en faisant des liens avec de nouvelles choses apprises.

Ces travaux ont permis d'identifier des fonctions de la formation hippocampique, mais plusieurs structures étaient atteintes. D'autres travaux furent donc nécessaires afin de mettre en évidence la contribution de chacune des structures.

Fonctions de l'hippocampe chez l'Humain

Ainsi commença une course acharnée qui a toujours lieu de nos jours, pour l'allocation de fonctions spécifiques à chacune des structures retirées dans la lobectomie temporo-médiane.

Des patients avec une lésion circonscrite à l'hippocampe avaient des déficits de mémoire moins sévères que ceux d'H.M., néanmoins ils montraient une moindre capacité à retenir la relation entre plusieurs choses. Par exemple, dans une tâche de mémorisation de places d'objets, les patients avec une lésion de l'hippocampe n'étaient pas capables de retenir la position de plus de 3 objets les uns par rapport aux autres alors que les personnes ayant un cerveau intact pouvaient retenir la disposition de 7 objets sans problème (Jeneson A. *et al.*, 2010). Ces mêmes patients avaient également un déficit de reconnaissance d'objet lorsqu'ils devaient déterminer si l'un des objets indicés lors du test était de la même couleur lors de l'entrainement parmi un set de plus de 3 objets (Jeneson A. *et al.*, 2012). Cependant ce déficit n'était pas présent si le délai entre l'entrainement et le test était d'une seconde. Ceci suggère que l'un des rôles de l'hippocampe est de soutenir la mémoire de travail par la rétention d'information à plus long terme, et par l'encodage de la mise relation des choses.

L'étude de lésion n'est pas la seule façon d'obtenir des informations sur les fonctions de l'hippocampe. L'une des questions soulevées par l'amnésie antérograde des patients lésés alors

que la mémoire rétrograde était relativement préservée était : l'hippocampe sert-il à encoder ces informations, mais n'est peut-être pas nécessaire pour le rappel ? De nombreuses études par IRM fonctionnelle et enregistrement par électrodes en profondeur ont démontré que l'activité de l'hippocampe était proportionnelle au succès de l'encodage et du rappel de mots, nom, visages et objets (Stark C., 2009; Asem J. S. A. & Fortin N. J., 2017). Le développement d'électrodes permit l'enregistrement de l'activité unitaire de neurones de l'hippocampe chez le rat pendant l'exploration d'un environnement. Grâce à cela, John O'Keefe et Jonathan Dostrovky (O'Keefe J. & Dostrovsky J., 1971) découvrirent que lors de l'exploration un sous-ensemble de cellules de l'hippocampe dorsal a une activité augmentée à un endroit donné de l'environnement (champ de lieu), ces cellules étaient majoritairement silencieuses en dehors de cette zone. Elles furent plus tard nommées cellules de lieu. Une partie des cellules de lieu ont une activité plus intense lorsque l'animal trouve un nouvel élément inattendu ou ne trouve pas un élément familier dans leur champ de lieu(Fyhn M. *et al.*, 2002{Anderson, 2003 #482; Valenti O. *et al.*, 2018)}. La découverte de ces cellules et de leurs propriétés a mené à la théorie de la carte cognitive selon laquelle l'hippocampe en mettant en relation les éléments qui composent un environnement, crée une représentation cognitive de l'espace (O'keefe J. & Nadel L., 1978). Chez l'humain, l'IRM structurelle de l'hippocampe postérieur (équivalent à l'hippocampe dorsal chez le rongeur) de conducteurs de taxis londoniens est significativement plus grand que celui de personnes normales. Cet élargissement est proportionnel au temps passé en tant que conducteur (Maguire E. A. *et al.*, 2000). Des cellules de lieu ont aussi été enregistrées chez l'humain (Ekstrom A. D. *et al.*, 2003), et les patients avec une lésion limitée à l'hippocampe sont incapables de former de nouvelles représentations spatiales, cependant ils sont capables de se diriger de façon flexible dans un environnement qui était connu longtemps avant la lésion (Asem J. S. A. & Fortin N. J., 2017). L'activité de l'hippocampe est donc nécessaire à la création de la carte mentale de l'environnement, cependant une fois encore l'hippocampe n'est pas un lieu de stockage à long terme.

Les travaux cités dans cette section et la précédente ont permis de montrer qu'il y avait plusieurs sortes de mémoires, celles qui est dépendent du fonctionnement de l'hippocampe pour rester persistantes et d'autres indépendantes de l'hippocampe.

1.1.3 Système de mémoires multiples

Nous l'avons vu précédemment, le terme mémoire est un mot parapluie qui englobe de nombreuses fonctions. Premièrement, il y a la mémoire à court terme qui ne dépend pas de l'hippocampe, qui dure quelques secondes à plusieurs minutes et qui inclut la mémoire de travail (Buchsbaum B. R. & D'Esposito M., 2017). Deuxièmement, il y la mémoire à long terme qui comprend plusieurs sous-systèmes. La dichotomie soulignée par les philosophes grecs entre la mémoire du corps et la mémoire de l'esprit reflète une réalité biologique. Il y a bien une différence d'encodage entre la mémoire sensorimotrice et la mémoire des savoirs, comme le suggèrent les travaux sur les patients ayant une résection du lobe temporal médian. Les types de mémoires encodés par la formation hippocampique peuvent être racontés, tandis que les types de mémoires qui n'en dépendent pas sont divers, leur apprentissage semble implicite, il est difficile de décrire comment nous les avons acquis. D'où la séparation des types de mémoires en deux groupes distincts : la mémoire déclarative et la mémoire implicite (figure 3) (Milner B. *et al.*, 1998; Squire L. R., 2009; Asem J. S. A. & Fortin N. J., 2017; Knowlton B. J. *et al.*, 2017; Bauer P. J. & Dugan J. A., 2020).

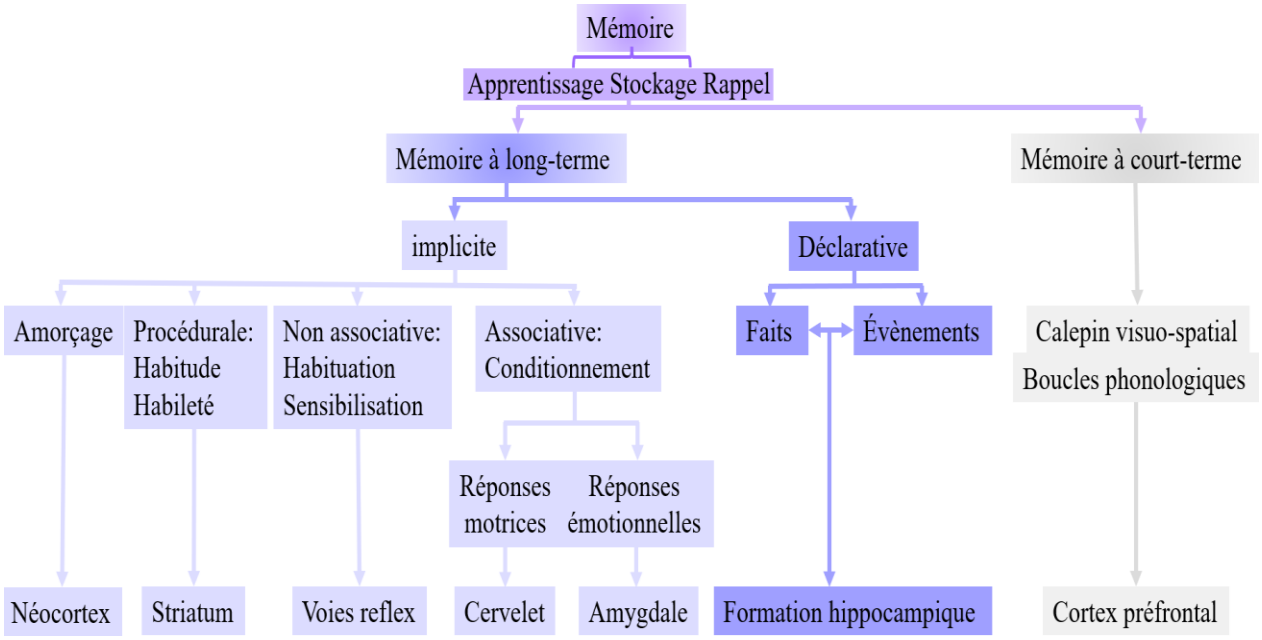

Figure 3 : Vue d'ensemble des différents types de mémoire. Adapté de Milner, Squire, and Kandel 1998.

La mémoire déclarative

La mémoire déclarative est la mémoire des faits, et des évènements (épisodique) et leurs mises en relations spatiale, chronologique et émotionnelle. C'est ainsi qu'elle constitue notre mémoire autobiographique, car la mémoire épisodique est toujours liée au contexte dans lequel elle fut acquise (quoi, où, quand ?). Ce type de mémoire comprend également la mémoire des connaissances (sémantique) qui n'est liée à aucun contexte. Le rappel de la mémoire déclarative peut se faire de façon consciente, et par association. Elle est vue comme une forme de mémoire très flexible, car elle encode une très large variété d'informations auxquelles on peut accéder par une grande variété d'associations logiques, ce qui permet son expression à travers des comportements très divers (Asem J. S. A. & Fortin N. J., 2017). Cette thèse porte sur l'étude de ce type de mémoire dans différents modèles rongeurs.

La mémoire implicite

Il est difficile d'expliquer comment on a acquis la mémoire implicite, car son rappel n'est pas conscient, il vient de façon automatique. L'expression de ce type de mémoire se fait par un changement de performance ou de comportement. Elle prend du temps pour se former, il faut généralement qu'il y ait plusieurs répétitions de l'évènement pour que ce type de mémoire se mette en place. Contrairement à la mémoire explicite, la mémoire implicite est rigide, elle est difficile à corriger et la mémoire acquise pour une chose en particulier est difficilement transférable à une autre mémoire (je connais par cœur mon clavier d'ordinateur, je suis capable de taper des mots rapidement, mais cela n'a pas influencé mes compétences au piano). Ce type de mémoire comprend de multiples formes : la mémoire procédurale qui comprend la mémoire motrice, et celle des habitudes ; la mémoire associative avec les formes simples de conditionnements (conditionnement réflexe) ; la mémoire non associative avec l'apprentissage sensoriel, l'habituation et la sensibilisation ; et enfin l'amorçage (Knowlton B. J. *et al.*, 2017; Bauer P. J. & Dugan J. A., 2020).

1.2 Modèles rongeurs de la mémoire déclarative

L'étude neuropsychologique des patients ayant perdu les fonctions hippocampiques a fourni de nombreuses informations sur la localisation des fonctions mnésiques, leurs natures, et leurs interactions. Afin d'étudier plus en détail la neurobiologie de ces phénomènes des modèles animaux d'amnésie furent développés grâce auxquels chaque sous-type de mémoire est plus précisément alloué aux structures, mais aussi aux circuits, et aux cellules qui les encodent, de même que les changements biophysiques que la mémoire engendre sur ces substrats.

Les rongeurs sont les animaux les plus utilisés en neurobiologie. Ils partagent de nombreuses similitudes anatomiques, physiologiques, et génétiques avec l'humain tout en ayant un cycle de vie très court, et une maintenance facile et abordable. Depuis le développement du système Cre-Lox, permettant notamment l'édition génétique dirigée a un tissu spécifique, les souris sont devenues le modèle de choix dans l'étude de la neurobiologie de la mémoire (Tsien J. Z., 2016).

1.2.1 L'apprentissage associatif

La mémoire de peur est l'un des types de mémoires le plus étudié chez le rongeur. Il est facile à mettre en place, très robuste, et le moment exact de l'apprentissage est connu et discret. Puisqu'il a été très utilisé, un autre avantage est que beaucoup de variations subtiles de ce test existent et permettent de tester un large éventail d'aspects de la mémoire. Habituellement, ce type de mémoire est étudié via un conditionnement pavlovien avec une association entre un environnement est un stimulus aversif qu'on appelle conditionnement à la peur contextuelle. Ce test se fait généralement en deux étapes, pendant l'entrainement l'animal est mis dans un contexte et après quelques minutes d'exploration libre, il va recevoir un ou plusieurs chocs électriques douloureux aux pattes via le sol grillagé. Étant donné qu'il ne peut pas fuir ni combattre ce qui cause cette douleur, l'animal va exprimer sa peur par des périodes d'immobilité. Le pourcentage de temps passé immobile est proportionnel au nombre de chocs reçus. Après un délai de quelques heures, pour tester la mémoire à court terme, à 24 h ou plus pour la mémoire à long terme, l'animal

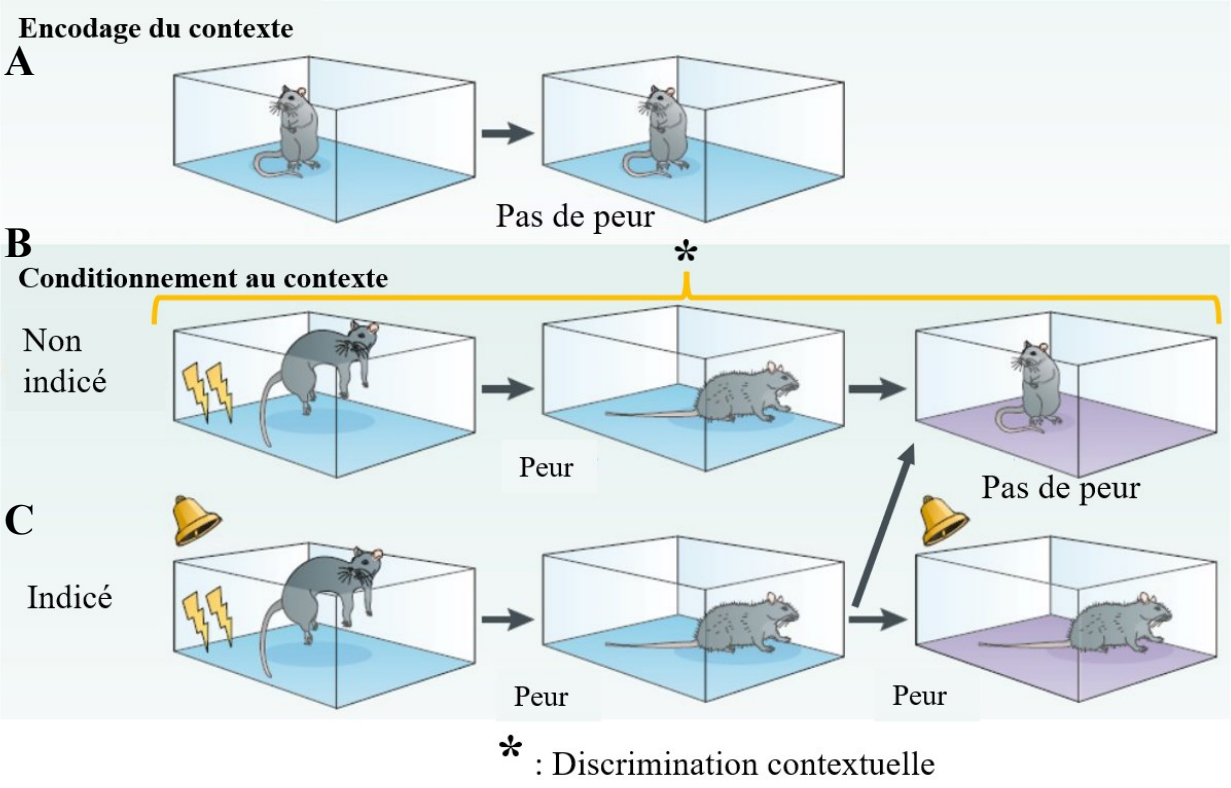

Figure 4 : Différents paradigmes du conditionnement a la peur. A, l'exploration du contexte neutre par le rongeur n'induit pas de peur. **B**, si le rongeur reçoit des chocs électriques dans un contexte neutre, il va associer ce contexte aux chocs. Si on remet le rongeur dans ce même contexte, il se souviendra des chocs et exprimera donc de la peur. Si on met ce rongeur dans un nouveau contexte différent, il n'exprimera pas de peur, c'est la discrimination contextuelle. **C**, Si on paire les chocs avec un indice, ici un son, le rongeur va associer les chocs au contexte dans lequel ils ont reçu ces chocs mais aussi à l'indice. Ainsi, si plus tard on remet l'animal dans le contexte dans lequel il a reçu des chocs, il exprimera sa peur. Si on le met dans un nouveau contexte diffèrent il n'exprimera pas de peur, sauf si on lui présente l'indice. Adapté de Maren, Phan, and Liberzon. Nature reviews Neuroscience 2013.

est replacé dans le même contexte, si sa mémoire est intacte il montrera un comportement d'immobilité proportionnel au nombre de chocs reçus lors de l'entrainement (figure 4 A). Cette forme de conditionnement, bien que pavlovienne, repose largement sur les fonctions de l'hippocampe étant donné que le stimulus inconditionnel n'est pas directement associé à un stimulus conditionnant, mais au contexte en entier soit l'association de l'environnement spatial, des odeurs, des sons, de la suite d'évènements qui a mené à ce moment-là. (Izquierdo I. *et al.*, 2016).

On peut d'ailleurs vérifier qu'une modification, par exemple génétique, d'un modèle animal n'atteint que les fonctions de l'hippocampe en associant un stimulus conditionnant avec les chocs.

Dans ce cas, la mémoire de peur est indépendante de l'hippocampe. Par exemple dans le cas de l'association de chocs avec un son, il y a une association anatomique directe des stimuli sensoriels électrique et auditif dans le noyau latéral de l'amygdale (Blair H. T. *et al.*, 2001). Une autre utilisation du conditionnement indicé est d'introduire un délai entre l'indice et le stimulus inconditionnel. Ici, pour qu'il y ait association entre l'indice et le stimulus aversif il y a nécessité de l'engagement de l'hippocampe puisqu'à cause du délai il ne peut pas y avoir concordance anatomique des entrées sensorielles (Carretero-Guillén A. *et al.*, 2015). C'est une forme de mémoire épisodique.

Le conditionnement à la peur contextuelle est utilisé comme modèle de syndrome post-traumatique. Une troisième version de ce test est conçue pour étudier les mécanismes de généralisation de la peur. La généralisation peut aussi être due à une perte de la spécificité de la mémoire. Grâce à ce paradigme, on peut également tester la qualité de l'encodage en évaluant la capacité de l'animal à discriminer deux contextes. Dans ce paradigme, on conditionne à la peur des souris dans le contexte A puis lors du test l'animal est mis dans un contexte B différent. On peut aussi faire un premier test dans le contexte A, puis un second dans le contexte B pour connaitre la capacité à discriminer les deux contextes de chaque animal. Enfin, on peut indicer le stimulus lors du conditionnement, et après une période d'exploration libre dans B induire la mémoire de peur en présentant l'indice. A et B peuvent être plus ou moins similaires selon le degré de généralisation ou discrimination que l'on veut montrer (figure 4 B)(Izquierdo I. *et al.*, 2016).

Finalement, l'extinction de la mémoire de peur, qui est un processus actif nécessaire à l'adaptation et différent de l'oubli, peut aussi être étudiée grâce à ce conditionnement. Il suffit de replacer l'animal dans l'environnement A sans stimulation aversive, après plusieurs minutes le comportement d'immobilité aura beaucoup diminué. On peut aussi utiliser la version indicée du conditionnement à la peur. Pour produire l'extinction, on met l'animal dans le contexte B et on présente le stimulus conditionnant plusieurs fois. L'immobilité est réduite de façon proportionnelle au nombre de présentations du stimulus conditionnant. Néanmoins, il faudra plusieurs jours, voire plusieurs semaines pour que le niveau de peur de l'animal revienne à la normale, selon la force du conditionnement. (Zelikowsky M. *et al.*, 2012; Izquierdo I. *et al.*, 2016)

Des formes de conditionnement opérant existent aussi pour la mémoire de peur. Dans ces expériences on peut premièrement inhiber un comportement naturel de la souris, tel que l'attirance

pour un lieu sombre et clos en l'associant avec un choc. La souris qui a retenu l'association choc-salle sombre mettra plus de temps à retenter d'entrer dans la pièce sombre (Jarvik M. E. & Kopp R., 1967). Deuxièmement on peut renforcer le comportement de fuite, pour cela dans une arène possédant deux chambres entre lesquelles l'animal peut circuler librement, on indice la stimulation aversive en commençant l'indice quelques secondes avant les chocs. Après l'association, l'animal qui a appris va échapper aux chocs en courant vers l'autre chambre dès le début de la présentation de l'indice (Diehl M. M. *et al.*, 2019).

Ces tests sont très flexibles et couvrent un large éventail de fonctions mnésiques. Cependant, le contexte de peur est un cas particulier de la mémoire et pour la comprendre dans sa globalité il faut l'étudier sur différents aspects.

1.2.2 La mémoire spatiale

La piscine de Morris

Inspiré par « the hippocampus as a cognitive map » (O'keefe J. & Nadel L., 1978) Richard Morris réalisat un nouveau test (la piscine de Morris) afin d'évaluer l'implication de l'hippocampe dans la mémoire spatiale chez les rongeurs. Cette tache de navigation spatiale est motivée par l'aversion des rongeurs pour l'eau. Pour échapper à la nage, l'animal doit utiliser des indices spatiaux distants afin d'atteindre une plateforme, cachée sous l'eau rendue opaque, dont la localisation est apprise progressivement aux cours de multiples sessions d'entrainement (Morris R., 1984).

La mémoire spatiale peut être achevée par le striatum, de façon indépendante de l'hippocampe, en utilisant des informations idiothétiques, c'est-à-dire des informations sensorielles intéroceptives, proprioceptives, et vestibulaires (McDonald R. J. & White N. M., 1994; Rinaldi A. *et al.*, 2020). Différentes stratégies de navigation sont donc utilisées selon la disponibilité ou non de l'hippocampe ou encore sa nécessité (Geva-Sagiv M. *et al.*, 2015; Nyberg N. *et al.*, 2022). L'une des forces de la piscine de Morris c'est qu'elle permet de mettre en lumière ces différentes stratégies utilisées pour naviguer pendant l'apprentissage. La plateforme n'est jamais située en

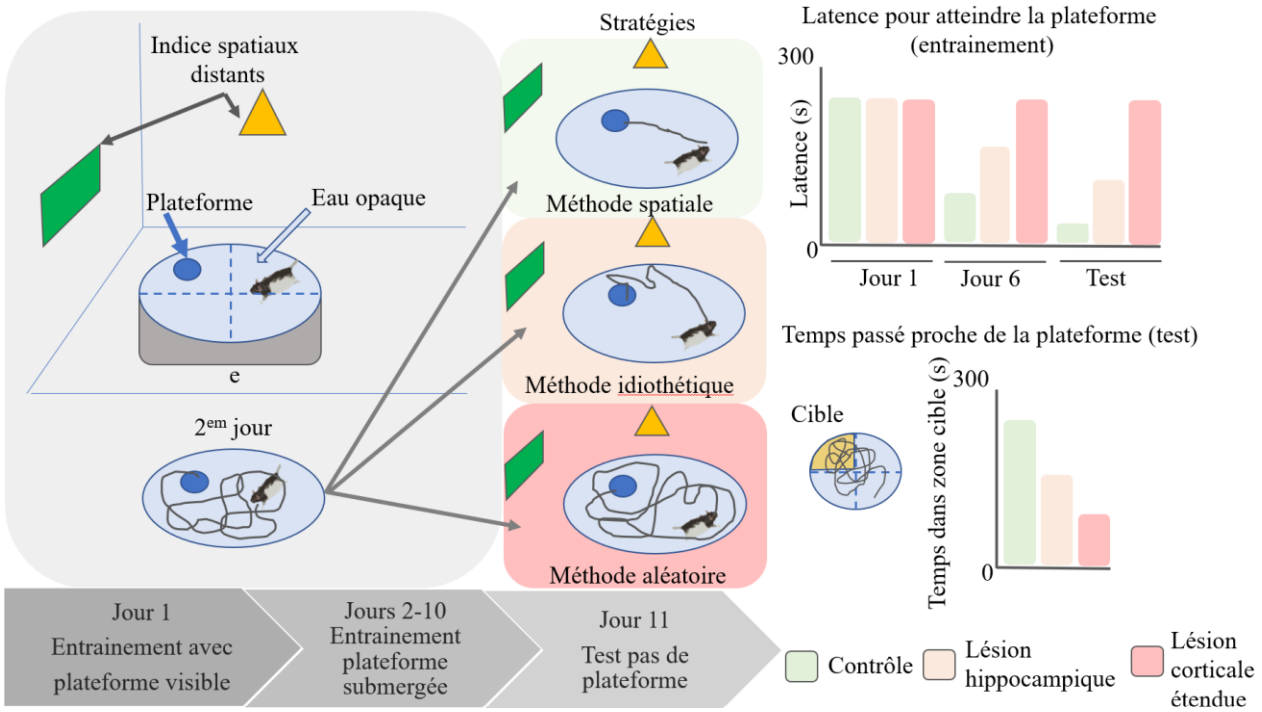

Figure 5 : La piscine de Morris. Description de l'expérience dans le texte. Exemple de résultats que l'on obtiendrait avec un rongeur contrôle intact (vert), un rongeur dont l'hippocampe a été lésé de façon bilatérale (orange), et un présentant des lésions corticales étendues (rouge).

alignement direct avec un indice visuel mais entre des indices, et l'animal n'est jamais déposé au même endroit de la piscine au départ. De plus, comme le test a lieu dans une piscine, les animaux ne peuvent pas utiliser d'indices proximaux tels que des traces odorantes laissées sur le sol ou des indices tactiles. Ainsi, l'animal intact choisira la stratégie spatiale allocentrique, la plus rapide dans ce cas, et après quelques secondes d'identification de l'environnement il effectuera une triangulation de sa position à partir des indices distaux et se rendra directement à la plateforme. L'animal dont l'hippocampe est lésé utilisera une combinaison de stratégies égocentriques telles que le balisage, qui nécessite de se déplacer vers un indice visuel (nager vers le triangle jaune), puis l'intégration de route qui utilise les informations intéroceptives (tourner à droite un peu avant le bord de la piscine puis nager encore un peu)(Geva-Sagiv M. *et al.*, 2015). Malgré tout, cette combinaison de stratégie est moins précise, et moins efficace, les rats lésés prennent donc significativement plus de temps pour localiser la plateforme. Le jour du test, la plateforme est retirée et on laisse l'animal explorer l'environnement plusieurs minutes. On détermine la précision de la mémoire par la stratégie utilisée pour se rendre à la place supposée de la plateforme, de même

que le nombre de fois où l'animal se rend à cet endroit et le temps passé proche (figure 5) (Morris R. G. M. *et al.*, 1982; Andersen P. *et al.*, 2007).

L'une des caractéristiques de la mémoire déclarative est sa flexibilité. Une façon d'étudier cette flexibilité est de regarder la vitesse d'adaptation à de nouvelles règles dans un même test. Avec la piscine de Morris, on peut évaluer la capacité d'édition de la mémoire en faisant un apprentissage inversé. À la suite du test, on en recommence l'expérience en inversant la place de la plateforme. On regarde alors la rapidité et la fidélité de la formation de la mémoire pour une nouvelle localisation (Morris R. G. *et al.*, 1986b).

Le labyrinthe de Barnes

Une limitation de la piscine de Morris est que cette tâche nécessite une bonne condition physique des animaux, puisqu'ils doivent nager parfois plusieurs minutes, ce qui est problématique lors d'études chez l'animal âgé par exemple. De plus, il induit beaucoup de stress, donc selon le modèle animal utilisé, de mauvaises performances à ce test peuvent être interprétées de façon erronée comme une détérioration de la mémoire spatiale alors qu'en réalité le seuil d'anxiété a pu être abaissé dans ces animaux et interférer avec les performances. Pour pallier ces limites, Carole Barnes à inventé un labyrinthe dont les principes fondamentaux et l'analyse sont très similaires à la piscine de Morris. Le labyrinthe de Barnes consiste en une table ronde avec des trous distribués de façon égale sur la périphérie. Tous les trous sont bouchés sauf celui qui mène à une boite sombre sous la table. Ce test est motivé par l'aversion des rongeurs pour les grands espaces ouverts et les lumières fortes. Il peut être renforcé par un son fort. Pendant les multiples sessions d'apprentissage, l'animal est placé dans un cylindre au centre de la table pour le désorienter, puis le cylindre est levé est l'animal doit utiliser des indices distants pour se diriger le plus vite possible vers la boite d'évasion. Si le comportement est renforcé par un son, on l'arrête dès que l'animal entre dans la boite. Le jour du test, le trou de la boite d'évasion est bouché, et on analyse les mêmes paramètres que dans le test de la piscine de Morris (Gawel K. *et al.*, 2019).

En conséquence, la piscine de Morris et le labyrinthe de Barnes ont une composante anxiogène et testent des mémoires aversives.

La mémoire de localisation d'objets

D'autres labyrinthes peuvent aussi être utilisés pour étudier la mémoire spatiale motivée par une récompense, tels que les labyrinthes en Y, en T, en croix, ou radial (Bird C. M. & Burgess N., 2009; Kraeuter A. K. *et al.*, 2019). Pour renforcer l'aspect récompense, les animaux sont préalablement restreints en nourriture ou en eau, ce qui peut engendrer un stress en dehors des séances d'entrainement. En outre, ce sont également des apprentissages qui se font sur plusieurs jours. Aussi, de plus en plus d'expériences utilisent des environnements virtuels avec associations de localisations virtuelles positives et négatives (Thurley K. & Ayaz A., 2017). Toutes les méthodes citées jusqu'à maintenant impliquent la mémorisation d'une cible, soit pour recevoir une récompense, soit pour échapper un environnement aversif. De façon alternative, on peut utiliser la curiosité naturelle des rongeurs pour l'exploration de nouveaux environnements ou objets. Comme nous l'avons vu précédemment, chez l'humain l'hippocampe est nécessaire pour l'association à long terme de l'organisation spatiale d'objets dans un environnement. La version adaptée aux rongeurs de ce test appelé tache de mémorisation de localisation d'objets se déroule comme suit (illustration figure 6) : pendant quatre jours, l'animal est familiarisé à un environnement qu'il peut librement explorer afin de réduire le stress dû à la nouveauté de l'environnement et favoriser sa mémorisation. L'arène est habituellement cubique, avec l'un des murs différenciés. Le cinquième jour deux objets sont introduits, tous les deux placés vers le mur différencié. Comme ces deux objets sont nouveaux et identiques, l'animal va les explorer de façon équivalente. Lors du test, de quelques heures à un jour après, l'un des deux objets est déplacé vers le mur opposé. Si l'animal se souvient de l'organisation spatiale des objets les uns par rapport aux autres et par rapport à l'environnement, l'objet déplacé constitue une nouveauté, il va donc préférentiellement l'explorer par rapport à l'objet qui n'a pas été déplacé. Dans cette expérience, on analyse donc le temps d'exploration des deux objets, et la préférence de l'animal pour l'un ou l'autre de ces objets. Ce qui est intéressant avec cette tâche,

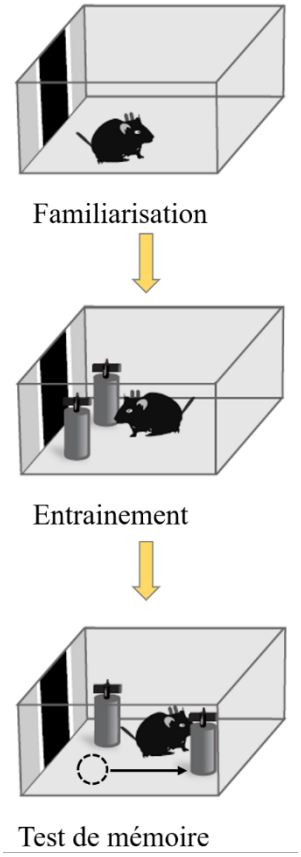

Figure 6 : Tache de mémorisation de localisation d'objets. Description dans le texte.

c'est qu'elle fait appel à la mémoire spatiale et épisodique. De plus, l'apprentissage se fait en une seule séance, comme dans le conditionnement à la peur, contre plusieurs dans les taches de localisation d'une cible. Enfin, elle induit peu de stress et ne nécessite pas que l'animal soit préalablement restreint en nourriture ou en eau. Néanmoins, étant donné que cette tâche est peu saillante, la mémoire engendrée est très sensible aux perturbations (Bird C. M. & Burgess N., 2009; Vogel-Ciernia A. & Wood M. A., 2014).

1.2.3 La mémoire, un processus

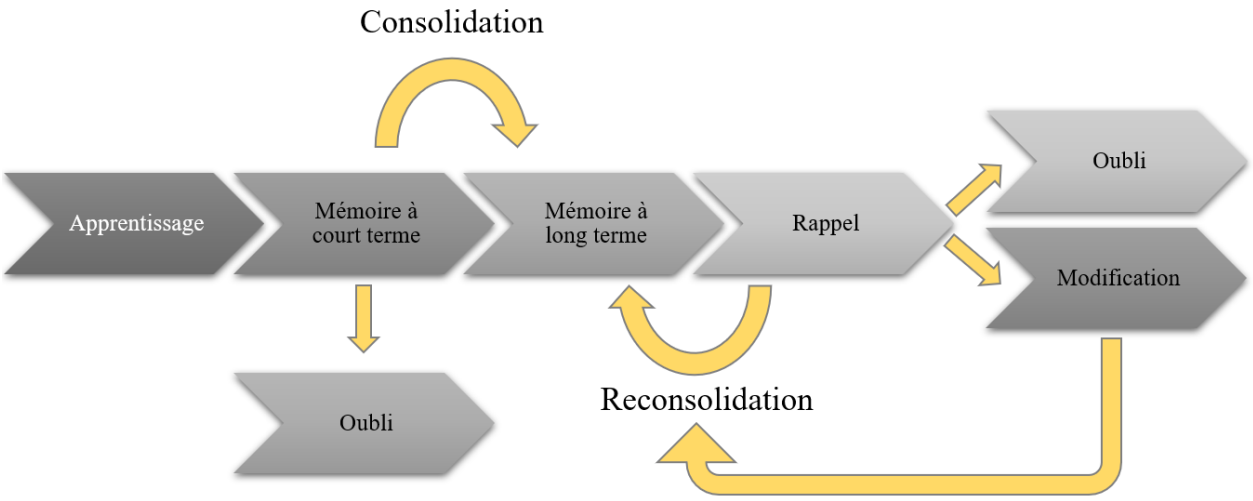

Figure 7 : Le processus de la mémoire. Description dans le texte.

La mémoire est un processus complexe et dynamique (figure 7). La survenue d'un évènement va immédiatement créer un souvenir à court terme qui repose sur des changements du niveau d'excitabilité des cellules qui encodent cet évènement. Cette mémoire est très labile, et la plupart du temps oubliée (Buchsbaum B. R. & D'Esposito M., 2017). Cependant, à certaines occasions, la mémoire à court terme va rester encodée à long terme via sa consolidation. Cette stabilisation de la mémoire n'est pas immédiate, elle repose sur des changements structurels qui nécessitent la synthèse de nouvelles protéines dans les cellules qui encodent ce souvenir (Kukushkin N. V. & Carew T. J., 2017). Mes travaux portent sur l'étude de ces mécanismes, nous les verrons plus en détail dans les sections suivantes. Le rappel est aussi un processus actif, afin de permettre la réédition de nos connaissances, à chaque fois que nous nous souvenons de quelque chose, nous soumettons ce souvenir à l'effacement. Ce processus appelé reconsolidation nécessite aussi la

synthèse de nouvelles protéines, même si l'information remémorée n'est pas changée (Nader K. & Hardt O., 2009). Ceci est valable pour la mémoire de peur acquise après un seul entrainement (Nader K. *et al.*, 2000) comme pour la mémoire spatiale apprise sur plusieurs jours (Artinian J. *et al.*, 2007). L'oubli réfère à la perte de disponibilité d'informations qui avaient été encodées avec succès, et repose également sur des mécanismes actifs qui nécessitent des changements structurels entre les cellules qui encodent un souvenir. Le souvenir pourrait être réactivé, car les cellules qui l'encodent n'ont pas disparu, mais ce sont les connexions entre ces cellules qui sont affaiblies (Ryan T. J. & Frankland P. W., 2022).

1.3 Caractérisation anatomique et fonctionnelle de l'hippocampe

Afin d'avoir une compréhension globale des mécanismes de la mémoire, il est nécessaire de savoir d'où l'information provient, et comment elle circule entre les différentes structures du cerveau qui encodent ses différents aspects. Étant donné la place cruciale que l'hippocampe a dans la formation de la mémoire, mes travaux se concentrent sur la modulation de ses fonctions. Je me concentrerai donc dans cette section sur les caractéristiques anatomiques et fonctionnelles de cette structure.

1.3.1 Circuits, composition, et fonctions de la formation hippocampique

La formation hippocampique est un ensemble bilatéral de structures corticales présent chez tous les mammifères comprenant l'hippocampe, le complexe subiculaire et le cortex entorhinal (figure 8). Lors de l'apprentissage, l'information circule majoritairement de façon unidirectionnelle entre ces trois structures à travers un réseau de neurones excitateurs comme suit. L'information en provenance des cortex associatifs et sensoriels sont intégrées au niveau des couches I à IV du cortex entorhinal où une première étape de la représentation d'environnement est faite. Le cortex entorhinal médian fournit des informations spatiales globales tandis que sa partie latérale apporte des informations individuelles et locales sur les objets ou les indices proximaux à l'hippocampe (Knierim J. J. *et al.*, 2014). Ces informations complexes transitent d'abord par le gyrus denté puis

par la corne d'Ammon et enfin dans le complexe subiculaire avant de retourner au cortex entorhinal, dans ses couches V et VI cette fois.

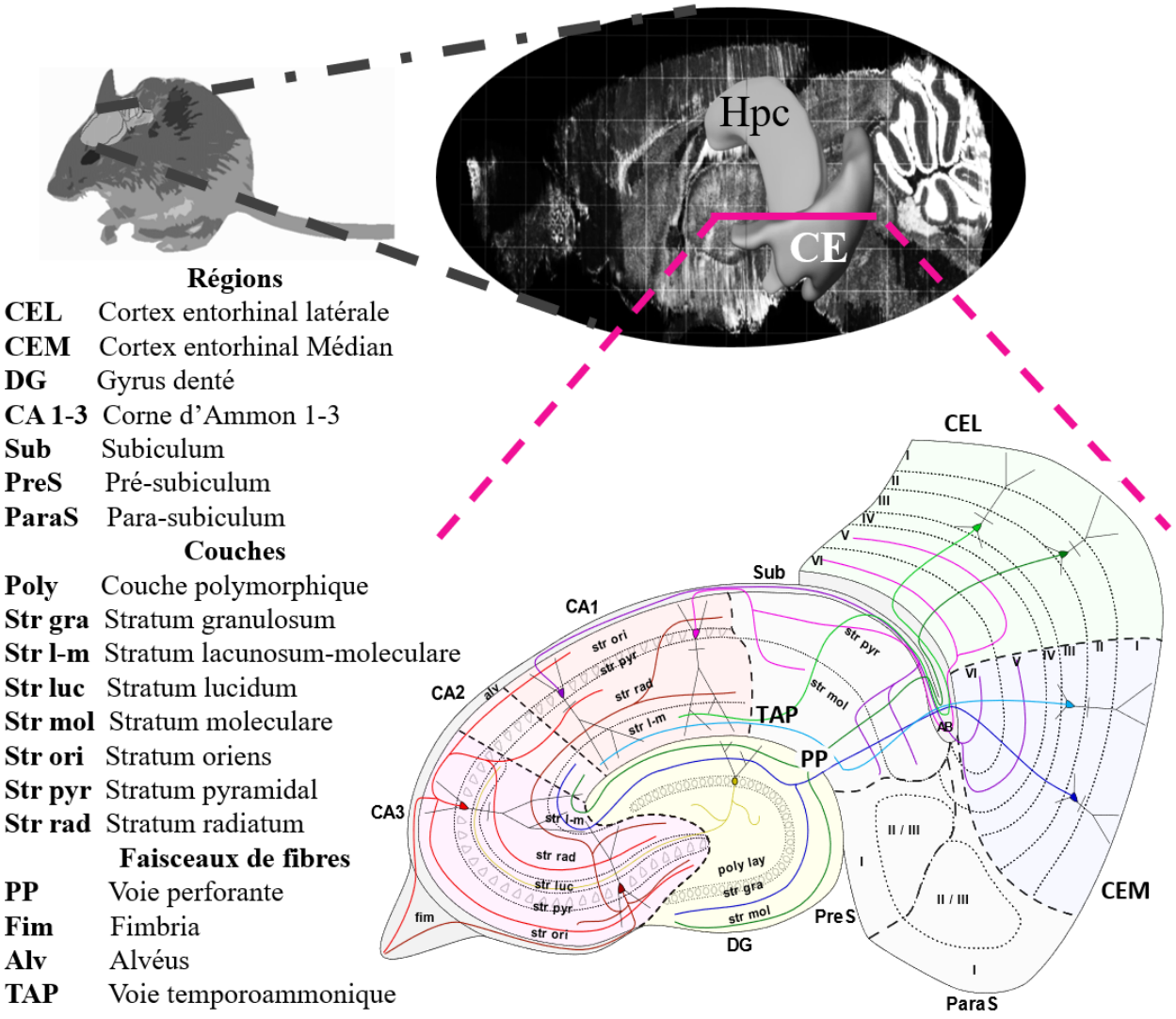

Figure 8 : Structures et connectivité de la formation hippocampique chez le rongeur. La formation hippocampique composée de l'hippocampe (Hpc), du subiculum, et du cortex entorhinal (CE) se situe dans la partie postérieure du cerveau rongeur. La barre rose pleine représente le plan de coupe que représente le schéma détaillé des circuits reliant ces structures les unes aux autres. Image de la coupe sagittale du cerveau entier avec Hpc et CE en 3D généré avec le Allen Mouse Brain Atlas. Schéma du circuit adapté de https:/ /github.com/MartinPyka/NeuroSVG.

Le gyrus denté

De façon plus détaillée, les cellules principales de la couche II du cortex entorhinal vont former un faisceau de fibres appelé voie perforante qui vont contacter les dendrites des cellules granulaires dans la couche moléculaire du gyrus denté. C'est aussi à cet endroit que le gyrus denté va recevoir des afférences sous-corticales directes, mais aussi de l'hippocampe controlatéral. Les corps des cellules granulaires sont alignés en une forme de V et forment la deuxième couche (couche granulaire) de cette structure stratifiée. Ce V entoure la troisième couche qui constitue le gyrus denté, le hile ou couche polymorphique. Dans le hile se trouvent les axones des cellules granulaires appelés fibres moussues, ainsi que de nombreux types cellulaires détaillés dans la section 1.7 (Cappaert N. L. M. *et al.*, 2015). Étant donné sa position dans le circuit, l'une des fonctions du gyrus denté est de filtrer les nombreuses afférences qu'il reçoit et de les intégrer pour former une représentation précise d'un évènement dans une population cellulaire discrète. Une des fonctions particulières de cette structure est d'ailleurs de détecter des différences subtiles entre deux représentations afin de les discriminer, on appelle cela séparation de motifs. Cela permet d'encoder de façon distincte et fidèle les différents souvenirs (Yassa M. A. & Stark C. E., 2011; Jonas P. & Lisman J., 2014).

La corne d'Ammon

L'information ainsi triée est envoyée via les fibres moussues à la corne d'Ammon (CA), qui entoure le gyrus denté. Cette structure est séparée en trois sous-régions, CA1, CA2, et CA3 organisées en cinq à six couches. Accolée au gyrus denté, il y a la *stratum lacunosum-moleculare*. Au-dessus, le *stratum radiatum*, puis les corps cellulaires des cellules principales de cette structure, appelées cellules pyramidales, définissent la couche pyramidale. Enfin, en périphérie de la CA se trouve le *stratum oriens*, coiffée par une couche fibreuse l'alvéus. Dans CA3 une couche supplémentaire, le *stratum lucidum* se trouve entre les couches *radiatum* et pyramidale.

<u>CA3</u>

Les fibres moussues des cellules granulaires vont contacter les dendrites proximales des cellules pyramidales de CA3 dans le *stratum lucidum*. Les cellules pyramidales de CA3 reçoivent

également des afférences sensorielles directes du cortex entorhinal via la voie perforante sur ses dendrites distales dans le *stratum lacunosum-moleculare*, ainsi que d'autres structures sous-corticales notamment via la fimbria et l'alvéus. L'une des caractéristiques anatomiques de CA3 est que ses cellules pyramidales innervent massivement d'autres cellules pyramidales locales via des connexions récurrentes à la fois sur les dendrites proximales dans la couche *oriens* et les dendrites distales dans la *radiatum* (Cappaert N. L. M. *et al.*, 2015). Ces connexions récurrentes sont associées avec la fonction de CA3 qui est d'amplifier le signal reçu du gyrus denté ainsi que d'associer des signaux similaires. Cette fonction appelée complémentation de motif associe des informations partielles avec celles déjà encodées pour créer une représentation globale, des prédictions, ou des catégories basées sur des similitudes (Yassa M. A. & Stark C. E., 2011).

CA2

Juxtaposé à CA3, CA2 reçoit des informations du cortex entorhinal, et du gyrus denté comme CA3. Les cellules pyramidales de CA3 dont la cible d'innervation principale sont les cellules pyramidales de CA1 font des synapses en passant sur les cellules pyramidales de CA2 via leurs axons appelés collatérales de Schaffer. Cette petite région relativement au reste de l'hippocampe est fortement innervée par des entrées extrahippocampiques, notamment par les noyaux supramammilaires et paraventriculaires. Cette balance d'entrées locales et extrahippocampiques pourrait expliquer les fonctions de CA2. Premièrement, les cellules pyramidales de CA2 sont plus sensibles aux changements subtils de l'environnement que celles des autres aires de l'hippocampe et pourraient fonctionner comme un détecteur de nouveauté. Elles ne semblent pas encoder l'espace de façon précise, mais plutôt de nouveaux indices proximaux ou des changements de ces indices (Wintzer M. E. *et al.*, 2014). Deuxièmement, l'encodage de l'espace par ces cellules est très dynamique et sensible au temps. Ceci suggère que les cellules pyramidales de CA2 pourraient être impliquées dans l'encodage du temps (Mankin Emily A. *et al.*, 2015). Finalement, cette région est particulièrement riche en récepteurs à la vasopressine et ocytocine, deux neurohormones déversées via les afférences du noyau paraventriculaire et impliquées dans le stress, les comportements agressifs d'une part, et de l'attachement d'autre part. Ceci confère à CA2 un rôle dans la reconnaissance sociale et l'association de la mémoire avec l'état émotionnel (Dudek S. M. *et al.*, 2016).

CA1

Les cellules pyramidales de CA1 intègrent donc de l'information spatiale spécifique de CA3, à la fois dans la couche *oriens*, mais majoritairement dans la couche *radiatum*. Elles reçoivent aussi des informations directes du cortex entorhinal (spatiales globales pour la partie médiale, et individuelles locales pour la partie latérale) sur leurs dendrites distales dans le stratum *lacunosum-moleculare,* mais à travers un autre faisceau de fibres venant de la couche III nommée voie temporoammonique. Tout comme les autres structures, CA1 reçoit également des informations sous-corticales directes via le faisceau de fibres que forme l'alveus dans la couche oriens. Enfin, CA2 innerve les cellules pyramidales de CA1 dans la couche oriens envoyant des informations sur la nouveauté, le temps, et les relations émotionnelles et sociales (Knierim J. J. *et al.*, 2014; Cappaert N. L. M. *et al.*, 2015; Dudek S. M. *et al.*, 2016). En associant ces sommes d'informations, CA1 va créer des représentations complexes de nos expériences de façon chronologique (Bittner K. C. *et al.*, 2015; Barrientos S. A. & Tiznado V., 2016). En outre, résultant de l'organisation de son circuit, l'une des fonctions supposées de CA1 est de détecter si une représentation est nouvelle ou familière. En effet, une des hypothèses concernant le fonctionnement de l'hippocampe suggère que les afférences venant du gyrus denté passant par CA3 comportent des informations associatives sur des choses apprises, et des estimations sur notre environnement. Ces afférences arrivent sur les mêmes cellules que l'information venant directement du cortex entorhinal sur les évènements qui se passe en effet à ce moment-là. La cooccurrence de ces deux entrées dans les cellules de lieu produit la formation rapide de champs de lieu, et augmente l'activité dans les champs de lieux déjà présents (Bittner K. C. *et al.*, 2015). Cela suggère donc que si l'information entre ces deux voies concorde de façon précise dans le temps, cela augmente l'activité dans les cellules ou cette concordance a lieu. Si l'information n'était pas connue, on l'imprime dans le circuit en créant des champs de lieu, si elle est déjà connue, les cellules qui l'encodaient sont réactivées ce qui déclenche le souvenir (Tayler Kaycie K. *et al.*, 2013).

Les cellules de lieu

Toutes les cellules excitatrices de ce circuit n'encodent donc pas l'environnement de la même façon. Comme évoqué précédemment, pour chaque environnement, seulement une partie

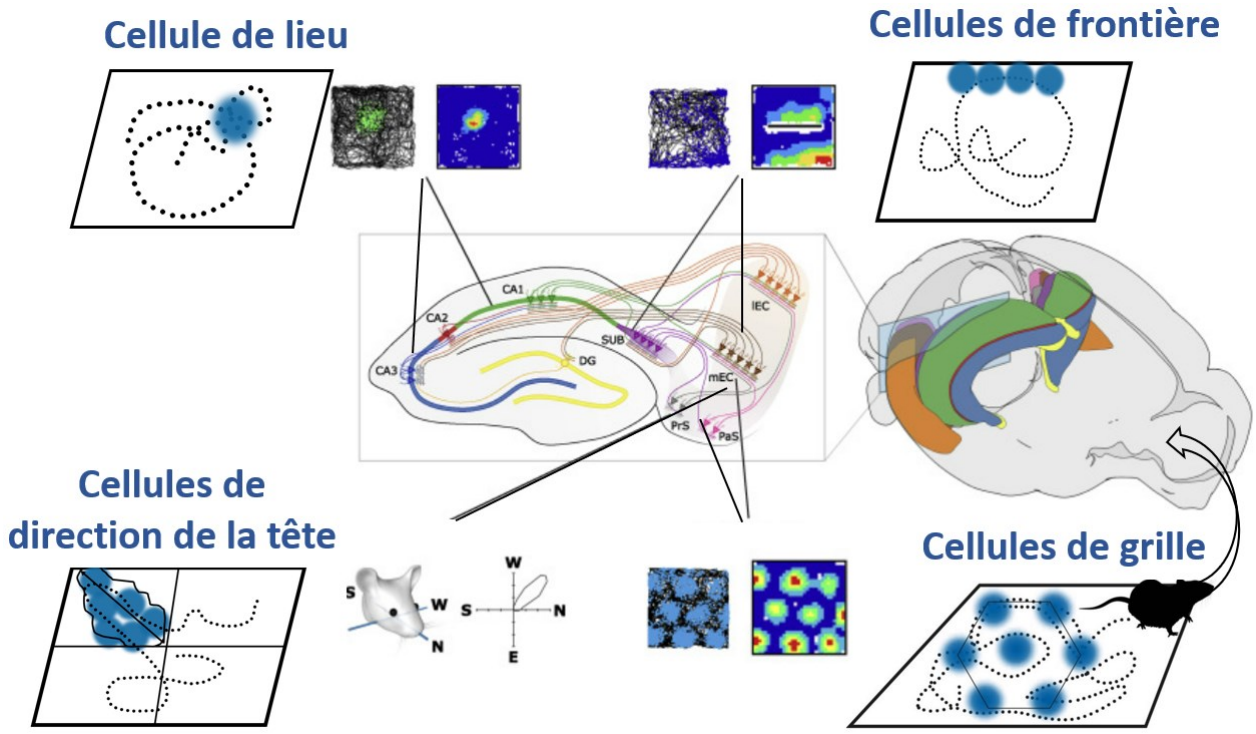

Figure 9 : Les différentes cellules qui encodent la mémoire spatiale et leurs localisations. Les différentes cellules qui encodent l'espace sont des cellules excitatrices de la formation hippocampiques qui échangent de l'information spatiale à travers les circuits de cette structure. Les cellules de lieu sont restreintes à la corne d'Ammon et encodent une partie précise de l'environnement, les autres cellules sont distribuées dans le cortex entorhinal et le subiculum, et encodent pour une bordure pour les cellules de frontière, une direction pour les cellules de direction de la tête, et un environnement au complet pour les cellules de grille. Ensembles ces cellules donnent naissance à une représentation complexe des environnements. Adapté de (Bjerknes T. & Moser M. B., 2013) et (Nyberg N. *et al.*, 2022).

des cellules pyramidales de l'hippocampe vont être des cellules de lieu, et chacune va encoder pour un seul lieu dans cet environnement ou quelques lieux si l'environnement est grand. Chaque cellule de lieu peut être active dans différents environnements (Jeffery K. J., 2017). Ces cellules montrent une activité intense dans leur champ de lieu, mais pas en dehors, et leur activité n'est généralement pas dépendante de la direction par laquelle l'animal entre dans le champ de lieu (figure 9) (McNaughton B. L. *et al.*, 1983), mais pas toujours (O'Keefe J. & Recce M. L., 1993; Battaglia F. P. *et al.*, 2004). Elle n'est pas non plus dépendante seulement des informations visuelles puisque les champs de lieu sont conservés dans l'obscurité (Quirk G. *et al.*, 1990), ce qui concorde avec le fait que les cellules de lieu intègrent des informations variées afin de représenter un lieu. Cependant, si un environnement est élargi, les champs de lieux le sont aussi, couvrant ainsi la

même proportion de la surface (Muller R. U. & Kubie J. L., 1987; O'Keefe J. & Burgess N., 1996; Huxter J. *et al.*, 2003). De plus, les champs de lieu suivent la conformation des indices spatiaux distants (O'Keefe J. & Speakman A., 1987). Les champs de lieu sont maintenus à long terme, mais ils sont plastiques si l'environnement change (O'Keefe J. & Burgess N., 1996; Kinsky N. R. *et al.*, 2018; Jayakumar R. P. *et al.*, 2019). Il est intéressant de noter que l'activité des cellules de lieu est seulement légèrement influencée par le fait que le lieu qu'elles encodent soit une cible associée à une récompense (Jeffery K. J., 2017). En revanche, certaines de ces cellules encodent spécifiquement pour un objet dans un environnement, deviennent silencieuses si l'objet est absent, ou le suivent s'il est déplacé (Rivard B. *et al.*, 2004; Vandrey B. *et al.*, 2021). D'autres cellules de lieu appelées cellules de déplacement sont activées par l'absence d'un objet à la localisation attendue (O'Keefe J., 1976; Vandrey B. *et al.*, 2021).

D'autres cellules qui encodent l'espace existent en dehors de l'hippocampe, et communiquent avec les cellules de lieu (figure 9). Sans entrer dans les détails, ces cellules se trouvent dans le pré-Subiculum et le cortex entorhinal médian, mais pas dans l'hippocampe. Il y a les cellules de frontière qui encodent pour les limites de l'environnement. Il y a les cellules de grille qui forment des motifs hexagonaux qui encodent pour un environnement complet. Les cellules de direction de la tête sont quant à elles activées quand la tête de l'animal est dans une direction spécifique (Asem J. S. A. & Fortin N. J., 2017; Nyberg N. *et al.*, 2022).

1.3.2 Ségrégation fonctionnelle de CA1

L'axe dorso-ventral

La plupart des études citées ont été faites dans l'hippocampe dorsal notamment dans l'aire CA1, qui est aussi la partie de l'hippocampe que j'étudie dans cette thèse. Cependant, les fonctions hippocampiques ne sont pas les mêmes selon son axe dorso-ventral aussi appelé septo-temporal (figure 10). Pour CA1,

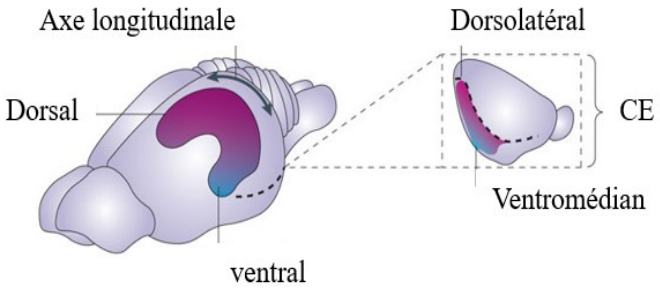

Figure 10 : Représentation de l'axe dorso-ventral de l'hippocampe rongeur et des projections respectives de ces sous parties sur le cortex entorhinal (CE). Adapté de Strange *et al*., 2014.

des changements graduels de l'expression génique, des propriétés électrophysiologiques, ainsi que des entrées extrahippocampiques le séparent en trois domaines fonctionnels, à savoir une partie dorsale, intermédiaire et ventrale. De nombreux travaux suggèrent que la partie dorsale est plus impliquée dans l'encodage des informations spatiales précises, et la détection de nouveauté. La partie ventrale aussi forme des représentations spatiales, mais elles sont beaucoup moins précises et concernent des espaces à grande échelle (toute une pièce plutôt que juste l'endroit où se trouve le bureau). L'environnement est donc encodé du plus précis au plus global en suivant l'axe dorso-ventral. Le rappel d'informations spatiales, quant à lui, implique les ¾ de l'hippocampe à partir de la partie dorsale. De son côté, le CA1 ventral est particulièrement impliqué dans la reconnaissance d'objets, le contrôle de comportements, la mémoire sociale et émotionnelle (Strange B. A. *et al.*, 2014; Cembrowski Mark S. *et al.*, 2016).

L'axe proximo-distal

Un niveau de complexité supplémentaire existe dans la ségrégation fonctionnelle des régions hippocampiques. Il existe également pour chaque sous-partie une séparation graduelle suivant l'axe proximo-distal (figure 11). Par exemple dans le CA1 dorsal, la partie proximale, qui fait suite à CA2, est innervée par le cortex entorhinal médian et encode des informations spatiales sur l'environnement en général. La partie distale, proche du subiculum, est quand a-t-elle innervée par le cortex entorhinal latéral, et encode des informations liées aux objets se trouvant dans l'environnement (Vandrey B. *et al.*, 2021). Cette séparation fonctionnelle est donc en accord avec les rôles respectifs des entrées du cortex entorhinal médian et latéral (Knierim J. J. *et al.*, 2014).

L'axe superficiel-profond

Finalement, en plus des différenciations dorso-ventrales et proximo-distales un dernier niveau de séparation existe entre les cellules pyramidales de CA1. Au sein de la couche pyramidale, les cellules qui se trouvent en superficie, c'est à dire proche de la couche *radiatum*, et celles qui sont en profondeur, donc proche de l'*oriens,* (figure11) montrent des différences dans leur expression génique, leurs propriétés électrophysiologiques, et leurs afférences (Lee S.-H. *et al.*, 2014; Cembrowski Mark S. *et al.*, 2016; Sharif F. *et al.*, 2021). Les cellules pyramidales superficielles ont une arborisation dendritique enrichie dans le stratum *radiatum*, sont fortement innervées par les collatérales de Schaffer, et le cortex entorhinal latéral (Li Y. *et al.*, 2017; Sharif F. *et al.*, 2021). Ces cellules sont recrutées préférentiellement lors de la navigation dans des environnements pauvres en indices (Sharif F. *et al.*, 2021). Elles encodent de façon stable des représentations plus globales du contexte et sont capables de discriminer différents contextes de manière fiable (Danielson N. B. *et al.*, 2016). Les cellules profondes quant à elles, ont une arborisation dendritique enrichie dans les couches *oriens* et *lacunosum-moleculare*, sont fortement innervées par les afférences de CA2 et le cortex entorhinal médian (Li Y. *et al.*, 2017; Sharif F. *et al.*, 2021). Ces cellules sont recrutées lors de la navigation dans des environnements riches en indices (Sharif F. *et al.*, 2021). Elles encodent particulièrement les repères, forment des champs de lieu de façon très dynamique qui sont stabilisés par la saillance d'un lieu (but ou récompense) (Danielson N. B. *et al.*, 2016; Geiller T. *et al.*, 2017). En plus de permettre l'encodage simultané des différents aspects d'une expérience (Knierim J. J. *et al.*, 2014), cette spécialisation dans la fonction des cellules pyramidales pourrait

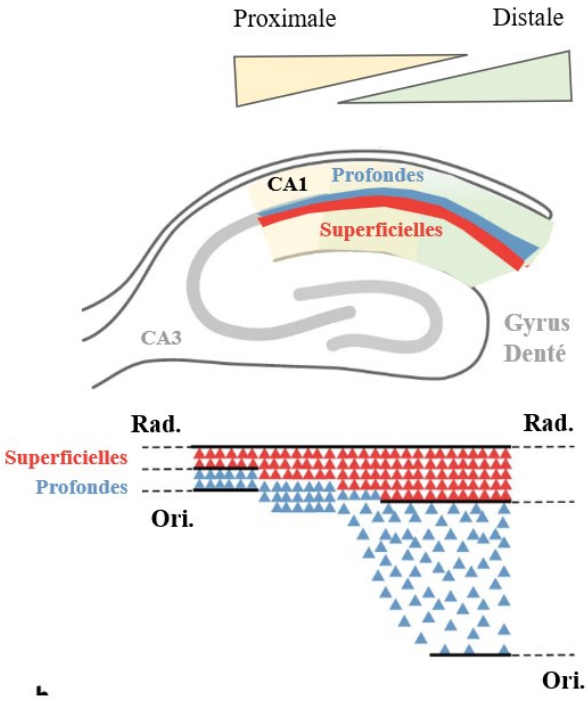

Figure 11 : Représentations des différentes cellules pyramidales de CA1 en fonction des axes proximodistal et dorsoventral. Rad, radiatum; Ori, oriens**.** Adapté de (Soltesz I. & Losonczy A., 2018).

permettre d'avoir en même temps une stabilité et une plasticité des souvenirs (Soltesz I. & Losonczy A., 2018).

Étant donné que les cellules pyramidales de CA1 se contactent très peu les unes aux autres, la question de comment le flux d'information est régulé à travers ces compartiments fonctionnels de cellules pyramidales se pose. L'autre type neuronal présent dans l'hippocampe sont les interneurones inhibiteurs exprimant le GABA. Les cellules pyramidales superficielles stimulent plus fortement l'un des types d'interneurones qui exprime la parvalbumine. En réponse à cette excitation, les interneurones parvalbuminergiques inhibent fortement les cellules pyramidales profondes et dans une moindre mesure les superficielles (Lee S.-H. *et al.*, 2014). Ce microcircuit local pourrait expliquer comment le routage entre les différents modules se fait de façon dynamique en fonction de l'environnement, ou de la tâche effectuée (Soltesz I. & Losonczy A., 2018).

1.4 Les interneurones inhibiteurs de l'hippocampe

Les interneurones inhibiteurs ne représentent que 10 à 20% des neurones composant l'hippocampe, cependant ils sont très diversifiés. On dénombre jusqu'à 30 sous-types, classées selon leur morphologie, la position de leur corps cellulaire, dendrites et axone dans les couches de l'hippocampe, leur expression protéique, ainsi que leurs propriétés électrophysiologiques. Ce qui a pour conséquence que chaque sous-type d'interneurone va inhiber un compartiment différent des cellules pyramidales (figure 12) avec chacun sa propre dynamique (Pelkey K. A. *et al.*, 2017; Booker S. A. & Vida I., 2018; Topolnik L. & Tamboli S., 2022). Malgré cette hétérogénéité, l'une des façons de catégoriser les interneurones est de les regrouper en fonction de la localisation de leurs synapses sur les neurones qu'ils ciblent. Il en découle quatre catégories majoritaires, les interneurones qui inhibent les dendrites, ceux qui inhibent le corps cellulaire et ceux qui inhibent le segment initial de l'axone des cellules pyramidales, finalement il y a les interneurones qui inhibent d'autres interneurones seulement (figure 12) (Booker S. A. & Vida I., 2018).

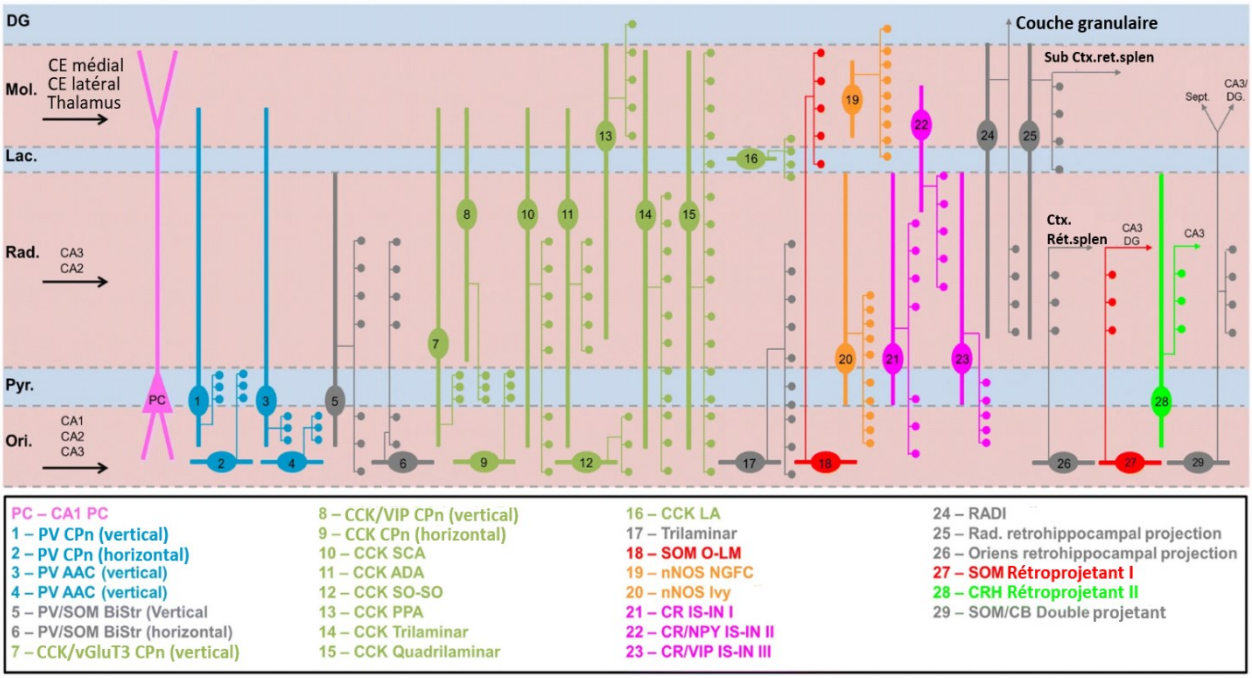

Figure 12 : Localisation et morphologie des interneurones de l'aire CA1. Afférences excitatrices principales (flèches noires), arborisations dendritiques (lignes en gras), axone et lieux de contact des interneurones sur les CP (lignes minces et petits cercles), CP : Cellules pyramidales, PV CPn : Cellules en panier exprimant la parvalbumine (PV), PV AAC : Cellules axo-axoniques exprimant la PV, PV/SOM BiStr : Cellules bistratifiées exprimant la PV et la somatostatine (SOM), CCK/vGluT3 CPn : Cellules en panier exprimant la cholécystokinine (CCK), CCK/VIP CPn Cellules en panier exprimant la CCK et le peptide vasoactif intestinal (VIP), CCK CPn : Cellules en panier exprimant la CCK: CCK SCA : Cellules associées aux collatérales de Schaffer exprimant la CCK, CCK ADA : Cellules associées aux dendrites apicales exprimant la CCK, CCK SO-SO : Cellules stratum oriens-stratum oriens exprimant la CCK, CCK PPA : Cellules associées à la voie perforante exprimant la CCK, CCK LA : Cellules associées à la stratum lacunosum exprimant la CCK, SOM O-LM : Cellules oriens-lacunosome moleculare exprimant la somatostatine (SOM), nNos NGFC : Cellules neurogliaformes exprimant l'oxyde nitrique synthase neuronale (nNOS), nNos Ivy : Cellules ivy exprimant le nNos, CR IS-IN I : Interneurones spécifique interneurones de type I exprimant la calretinine (CR), CR/NPY IS-IN II : Interneurones spécifique interneurones de type II exprimant la CR et le neuropeptide Y (NPY), CR/VIP IS-IN III : Interneurones spécifique interneurones de type I exprimant CR et VIP, RADI : Interneurone de la radiatum, CB : calbindine. Couches : Mol: Moleculare, Lac : Lacunosum, Rad : Radiatum, Pyr : Pyramidale, Ori : Oriens. Structures: CE : Cortex entorhinal, DG: Gyrus denté, Sub : Subiculum, Ctx.ret.splen : Cortex rétro splénial, Sept : septum.

Les interneurones dendritiques ont pour fonction commune de contrôler l'entrée de l'information des cellules pyramidales. Les interneurones somatiques et ceux qui inhibent le segment initial de l'axone ont pour fonction commune de contrôler la sortie de l'information des cellules pyramidales. Les interneurones qui ciblent d'autres interneurones ont pour fonction de désinhiber l'activité des différents compartiments des cellules pyramidales en inhibant les interneurones qui les contrôlent (Topolnik L. & Tamboli S., 2022). Les interneurones qui ciblent les dendrites sont majoritairement somatostatinergiques (SOM-INs), et ceux qui ciblent le corps cellulaire parvalbuminergiques (PV-INs) (Pelkey K. A. *et al.*, 2017). Nous verrons plus en détail les caractéristiques et fonctions de ces neurones dans les sections 1.6 et 1.7.

L'apprentissage, la consolidation de la mémoire, et le rappel nécessitent une synchronisation de l'activité des cellules qui encodent cette mémoire. Lors de ces taches mnésiques, les circuits de l'hippocampe sont synchronisés à travers plusieurs rythmes oscillatoires dépendant de l'interaction des entrées extrahippocampiques ainsi que de son rythme propre. L'émergence et la modulation de ces rythmes sont fortement liées à l'activité des différents interneurones. Durant les fonctions mnésiques, le circuit de CA1 se synchronise entre autres au rythme thêta (4 à 12 Hz). L'activité de chaque type cellulaire est ancrée dans une phase spécifique de chaque cycle. Au cours d'un cycle thêta, les cellules pyramidales ont leur activité minimale concordante avec la phase d'activité maximale des interneurones somatiques. L'entrée excitatrice majeure des interneurones somatiques provient des collatérales de Schaffer, suivant l'augmentation des entrées de CA3, ces interneurones vont inhiber de façon anticipative (feedforward) les cellules pyramidales. La phase ascendante du cycle des cellules pyramidales est corrélée avec l'activation des entrées du cortex entorhinal. L'augmentation de l'activité des cellules pyramidales va activer à leurs tours les interneurones dendritiques qui vont en retour inhiber les entrées des cellules pyramidales (inhibition rétroactive ou feedback). Ceci a pour effet d'une part de maximiser l'activité des cellules pyramidales en synchronisant les entrées, et d'autre part d'inhiber les afférences hors contexte (Somogyi P. *et al.*, 2014; Topolnik L. & Tamboli S., 2022).

1.5 Bases neurobiologiques de la mémoire

La circulation des informations à travers les réseaux hippocampiques seule ne constitue pas la mémoire. Comme postulé par Donald Hebb en 1949, pour qu'il y ait persistance des traces mnésiques, il faut qu'il y ait des changements durables entre les cellules du réseau qui encodent un souvenir. La synchronisation de l'activité entre les cellules qui constituent une trace mnésique provoque de tels changements de connectivité (Hebb D. O., 1949; Hölscher C. *et al.*, 1997; Siegle J. H. & Wilson M. A., 2014).

1.5.1 La plasticité

Plus précisément, la théorie Hebbienne de l'apprentissage stipule que non seulement les neurones activés ensemble se connectent '*Cells that fire together, wire together'*, mais également que l'activation d'un neurone A doit causer l'activation du neurone B. De plus, il faut que ces neurones soient activés ensemble de façon répétée, afin que l'activation de A facilite l'activation de B au cours des répétitions (Hebb D. O., 1949). Ce phénomène fut observé pour la première fois dans l'hippocampe, où la stimulation répétée des fibres de la voie perforante potentialise la réponse des cellules granulaires de façon durable. Il fut alors nommé potentialisation à long terme (PLT). Cette PLT est le résultat d'une augmentation de l'efficacité synaptique avec à la fois une augmentation de la transmission synaptique des fibres de la voie perforante et une excitabilité augmentée des cellules granulaires (Bliss T. V. & Lomo T., 1973). L'étude plus en profondeur de ce mécanisme mit au jour la bidirectionnalité de la plasticité synaptique. Les synapses peuvent être renforcées via la PLT, mais aussi affaiblies à travers les mécanismes de dépression à long terme (DLT) et dépotentialisation (Malenka R. C. & Bear M. F., 2004). Tous ces changements de l'efficacité synaptiques sont induits par l'apprentissage (Moser E. I. *et al.*, 1998; Whitlock J. R. *et al.*, 2006; Di Prisco G. V. *et al.*, 2014; Kandel *et al.*, 2014).

La potentialisation à long terme

La PLT est donc un renforcement des connexions synaptiques entre deux neurones.

Mécanismes d'induction

Tout comme la mémoire, et les neurones qui l'encodent, la PLT n'est pas monolithique, mais regroupe une multitude de phénomènes, qui varient dans leurs mécanismes d'induction et d'expression. La PLT peut être induite par des bouffées de stimulations données à des fréquences autour de celles du rythme thêta, une stimulation à haute fréquence (100 Hz) ou encore chimiquement via l'activation de divers récepteurs au glutamate, chaque mécanisme d'induction pouvant produire des formes de potentialisation différentes. La PLT est toutefois caractérisée par des mécanismes généraux. Premièrement, elle est spécifique à l'entrée, elle n'a pas lieu à travers l'intégralité des synapses d'un neurone, mais est spécifique aux synapses activées. Deuxièmement, elle peut être induite par coopération ou par association. La coopérativité fait référence au fait qu'il faille l'activation simultanée d'un nombre seuil d'entrées afin de produire une PLT. L'associativité quant à elle est la propriété par laquelle un stimulus fort associé dans le temps ou l'espace à un stimulus faible (sous le seuil) va permettre la potentialisation des deux voies indépendantes. D'un point de vue comportemental, la coopérativité pourrait servir de filtre ne potentialisant que les afférences suffisamment saillantes, alors que l'associativité pourrait être le substrat synaptique de l'apprentissage associatif (tel que l'association audiotactile dans les neurones de l'amygdale lors du conditionnement à la peur indicé voir 1.2.1) (Blair H. T. *et al.*, 2001; Bliss T. V. P. *et al.*, 2018). Finalement, plusieurs stimulations subséquentes peuvent augmenter progressivement la potentialisation jusqu'à un maximum appelé saturation (Abraham W. C., 2008).

La forme classique de la PLT requiert l'activation des récepteurs NMDA (NMDAR), qui sont des récepteurs glutamatergiques et canaux cationiques fortement perméables au calcium. Ces récepteurs dont les propriétés rappellent celles de la PLT sont des détecteurs de coïncidence. Leur blocage n'a pas d'influence sur la transmission synaptique basale. Cependant, leur activation nécessite soit un relargage massif de glutamate par une stimulation très forte des fibres afférentes, soit la synchronisation de plusieurs entrées afin de dépolariser la membrane suffisamment pour libérer l'ion magnésium qui bloque les NMDARs via l'activation des récepteurs AMPA (AMPARs) plus sensibles au glutamate. Ils nécessitent aussi la libération astrocytaire de D-sérine ou glycine (Blanke M. L. & VanDongen A., 2009; Papouin T. *et al.*, 2017).

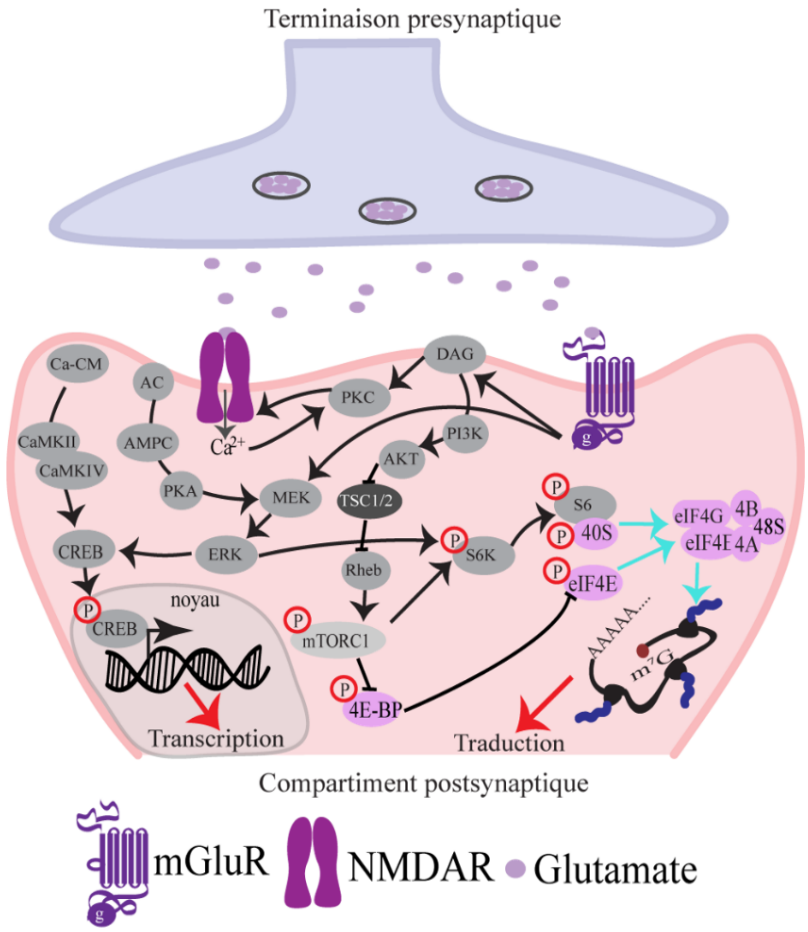

Figure 13 : Mécanismes post-synaptiques d'induction des PLTs tardives. La terminaison présynaptique excitatrice va relâcher du glutamate dans la fente synaptique. Ce glutamate va activer ses nombreux récepteurs canaux et métabotropiques postsynaptiques ce qui va entrainer une cascade de phosphorylations et activations (flèches noires). L'activation de la voie PI3K-AKT va inhiber le complexe protéique TSC1/2, ce qui va lever l'inhibition de Rheb, un activateur du complexe mTORC1. A son tour mTORC1 va activer d'un côté 4E-BP puis eIF4E et de l'autre côté S6K puis S6. Ceci a pour conséquences l'assemblages (flèches bleues) des complexes ribosomiques et l'initiation de la traduction d'ARNm en nouvelles protéines nécessaires pour l'expression de la première phase de la PLT tardive. La voie de signalisation MEK/ERK va elle aussi contribuer à l'activation de la traduction via la phosphorylation de la S6K. D'autre part, l'élévation massive de calcium cytosolique va activer les CAMK II et IV, la PKA et les signaux de la voie MEK/ERK qui vont être envoyés au noyau ou ils vont activer CREB en le phosphorylant ce qui va avoir pour conséquence la transcription de gènes spécifiques, nécessaires aux Figure 13 : Mécanismes post-synaptiques d'induction de la PLT tardive. La terminaison présynaptique excitatrice va relâcher du glutamate dans la fente synaptique. Ce glutamate va activer ses nombreux récepteurs canaux et métabotropiques postsynaptiques ce qui va entrainer une cascade de phosphorylations et activations (flèches noires). L'activation de la voie PI3K-AKT va inhiber le complexe protéique TSC1/2, ce qui va lever l'inhibition de Rheb, un activateur du complexe

mTORC1. A son tour mTORC1 va activer d'un côté 4E-BP puis eIF4E et de l'autre côté S6K puis S6. Ceci a pour conséquences l'assemblages (flèches bleues) des complexes ribosomiques et l'initiation de la traduction d'ARNm en nouvelles protéines nécessaires pour l'expression première phase de la PLT. La voie MEK/ERK va elle aussi contribuer à l'activation de la traduction via la phosphorylation de la S6K. D'autre part, l'élévation massive de calcium cytosolique va activer les CAMK II et IV, la PKA et les effecteurs de la voie MEK/ERK qui vont être envoyer au noyau ou ils vont activer CREB en le phosphorylant ce qui va avoir pour conséquence la transcription de gènes spécifiques, nécessaires aux transformations synaptiques qui sous-tendent la PLT

Mécanismes d'expression

Généralement, l'expression de la PLT, comme suggéré par les expériences de Tim Bliss et Terje Lømo, se fait des deux côtés de la synapse. Dans la partie présynaptique (neurone A) il y a une augmentation de la probabilité et de la quantité de la libération de neurotransmetteurs. Dans la partie postsynaptique (neurone B), il y a une augmentation du nombre et de la conductance des AMPARs. Cependant ce n'est pas toujours le cas, et différentes combinaisons d'expressions peuvent exister (Bliss T. V. & Lomo T., 1973; Bliss T. V. P. *et al.*, 2018). Quel que soit le récepteur stimulé, le point clef de l'induction de la PLT est l'augmentation massive et prolongée de calcium dans la synapse. Si cette élévation du calcium est faite par un seul épisode de stimulation, on induit une PLT précoce durant une à quelques heures, dont l'expression dépend de la phosphorylation de protéines déjà présentes à la synapse, ainsi que l'insertion de nouveau AMPAR à la membrane (Malenka R. C. & Bear M. F., 2004; Bliim N. *et al.*, 2016). Si la stimulation est répétée, on induit une PLT tardive, qui dure de nombreuses heures voire plusieurs jours. Son expression repose sur la synthèse de nouvelles protéines. Cette PLT tardive est également composée de plusieurs phases. Dans un premier temps, les protéines nouvellement synthétisées proviennent de la traduction d'ARNs messagers déjà prêts dans les dendrites via l'activation des complexes mTORC1 (*Mechanistic target of rapamycin complex 1*) et eIF4F (*eukaryotic initiation factor 4F*). En effet, l'élévation massive de calcium engendrée par l'ouverture des récepteurs NMDA ou la libération des protéines G par l'activation des récepteurs métabotropiques au glutamate va activer une cascade de phosphorylations à travers les voies PI3K-AKT (Phosphoinositide 3-kinase – Protéine kinase B) et MEK/ERK (*Mitogen-activated protein kinase-kinase/ Extracellular signal-regulated kinase*) menant à l'assemblage des ribosomes et à la synthèse protéique locale (figure 13) (Costa-Mattioli M. *et al.*, 2009; Bliss T. V. P. *et al.*, 2018). Dans un second temps, les CaMK

(*calcium/calmodulin-dependent protein kinase*), Protéines kinase A et RSK (*Ribosomal S6 Kinase*) vont être transloquées vers le noyau du neurone où elles déclencheront la transcription de gènes spécifiques en nouveaux ARNs messagers par l'activation de CREB (*cAMP responsive element binding protein*) (Bliim N. *et al.*, 2016). Ces ARNs messagers sont alors sélectivement adressés au niveau des synapses activées où ils sont à leur tour traduits en protéines. Il faut noter que ce n'est probablement pas le cas pour toutes les protéines nécessaires à l'expression de la PLT. Certaines seraient plutôt synthétisées dans le corps cellulaire, notamment celles de grosse taille, puis adressées à la synapse (figure 13) (Farris S. *et al.*, 2017). Ces nouvelles protéines vont alors servir d'une part à modifier la composition, et la forme des synapses activées (élargissement de la tête, raccourcissement du cou des épines)(Matsuzaki M. *et al.*, 2004; Tazerart S. *et al.*, 2020). D'autre part, elles vont participer à la création de nouvelles épines dendritiques proche de la synapse activée, afin de former un groupe synaptique fonctionnel (Hedrick N. G. *et al.*, 2022).

Induction de la potentialisation à long terme par la stimulation en bouffées thêta.

Dans trois des quatre articles de recherche présentés dans cette thèse nous utilisons la stimulation en bouffée thêta (TBS pour *theta burst stimulation*) afin d'induire une potentialisation à long terme. Ce patron de stimulation mime deux propriétés de l'activité des cellules pyramidales de l'hippocampe. Les décharges complexes des neurones pyramidaux sont imitées par les bouffées de stimulations, qui sont données au rythme thêta, rythme dans lequel l'excitabilité de ces cellules est verrouillée lors de l'exploration par exemple (Larson J. & Munkácsy E., 2015). Pour ces raisons, ce modèle d'induction est supposé plus physiologique qu'une stimulation à haute fréquence continue. De plus, la synapse étudiée dans ces articles, à savoir la synapse excitatrice entre une cellule pyramidale et un interneurone somatostatinergique, exprime un ensemble spécifique de protéines qui facilite la transmission excitatrice et la maximise dans la gamme de fréquence thêta (Shigemoto R. *et al.*, 1996; Sylwestrak E. L. & Ghosh A., 2012)(voir Chapitre1.7 section 3.1). Finalement, le TBS est également plus efficace que la stimulation tétanique (stimulation à haute fréquence continue) pour induire une PLT (Larson J. & Munkácsy E., 2015).

La dépression à long terme

Par opposition, la dépression à long terme est un affaiblissement persistant des connexions entre deux neurones. Elle nécessite l'activation des mêmes récepteurs que ceux impliqués dans la

PLT, et l'élévation du calcium dans la synapse. Cependant, l'élévation du calcium a une cinétique différente, la DLT est induite par une stimulation prolongée à basse fréquence (0.5 à 5 Hz) ou le couplage clairsemé d'entrées faibles. Comme la PLT, la DLT est aussi entrée spécifique, implique les parties pré et post-synaptiques et nécessite la synthèse de nouvelles protéines. Cependant, cette fois-ci la phase précoce implique la diminution du nombre et de la conductance des AMPARs. Les protéines synthétisées lors de la phase tardive provoquent dans ce cas une diminution de la taille des épines dendritiques, voire leur effacement (Malenka R. C. & Bear M. F., 2004). D'un point de vue fonctionnel, la DLT est aussi importante que la PLT dans la formation de la mémoire puisqu'elle raffine le réseau de neurones en retirant des synapses, ce qui contribue probablement à aiguiser la précision de la mémoire. Elle sert également à découpler d'anciennes connexions afin de pouvoir mettre à jour nos souvenirs et adapter des comportements acquis (Malenka R. C. & Bear M. F., 2004; Stacho M. & Manahan-Vaughan D., 2022).

La dépotentialisation

La dépotentialisation réfère au renversement de la PLT. Si une potentialisation est initiée, mais suivie par une période de stimulation à basse fréquence, alors elle sera annulée et la synapse retournera à son état basal. La dépotentialisation repose comme la PLT et la DLT sur l'activation des NMDARs ou des mGluRs, cependant son induction dépend de mécanismes légèrement différents. Alors que la DLT implique la sous-unité GluN2B, la dépotentialisation requière l'activation de la sous-unité GluN2A. Son expression est également similaire à la DLT, avec une déphosphorylation et une endocytose des AMPAR. Mais là encore des différences subtiles existent entre ces deux formes de plasticité. Les sites de déphosphorylation et les sous-unité d'AMPAR régulées ne sont pas les mêmes (Sanderson T. M., 2012).

Les mécanismes de PLT, DLT et dépotentialisation prennent du temps. Les modifications de l'activité par des mécanismes de phosphorylation sont presque immédiats, la synthèse de protéines à partir d'ARN déjà présents aux abords de la synapse prend quelques minutes alors que la transcription génique dépendante de l'activité prend quelques heures. Cela fait partie des raisons pourquoi la mémoire n'est pas immédiatement encodée de façon permanente (Kukushkin N. V. & Carew T. J., 2017).

La métaplasticité

Un autre niveau de complexité dans la régulation des phénomènes plastiques s'ajoute à ceux décrits au-dessus. En effet, la plasticité synaptique est aussi modulée par l'activité antérieure de la synapse, de la cellule ou encore du réseau dans lequel elles se trouvent (Abraham W. C., 2008; Hulme S. R. *et al.*, 2014a). Ce phénomène est appelé métaplasticité, car c'est la plasticité de la plasticité synaptique (Abraham W. C. & Bear M. F., 1996). Un premier évènement peut réguler de façon positive ou négative la capacité d'induire de la plasticité subséquente à une synapse sans forcément modifier sa transmission de base, mais aussi la direction (PLT ou DLT), l'amplitude, et la persistance de cette plasticité (Bear M. F., 1995; Abraham W. C. & Bear M. F., 1996) (Voir exemple Chapitre 1.7 section 5 et figure 5). Les processus de métaplasticité homosynaptiques peuvent impliquer l'activation des récepteurs glutamatergiques. L'activation préalable des récepteurs NMDA pouvant générer une réduction durable de la PLT et l'augmentation de la DLT, alors que l'activation des mGluRs du groupe 1 facilite la PLT subséquente (Abraham W. C., 2008; Hulme S. R. *et al.*, 2014b). Les processus hétérosynaptiques sont extrêmement variés. La potentialisation d'une synapse peut faciliter la PLT de synapses proches plus faiblement activées (Abraham W. C., 2008; Hulme S. R. *et al.*, 2014b). Des changements dans la transmission GABAergique proche peuvent modifier dans les deux sens la capacité de la synapse à être potentialisée (Chapitre 1.7 section 5)(Hulme S. R. *et al.*, 2014b). Des régulations locales (à la synapse) et étendues peuvent aussi être opérées par les astrocytes (Hulme S. R. *et al.*, 2014b), le stress (Schmidt M. V. *et al.*, 2013), ou encore les rythmes biologiques (Hartsock M. J. *et al.*, 2022).

1.5.2 Formation de l'engramme

Décrit pour la première fois en 1904 par Richard Semon, l'engramme est défini comme le substrat neuronal où sont stockés les souvenirs (Semon R., 1904; Schacter D. L. *et al.*, 1978). Comme décrit plus haut, l'activité neuronale lors de l'apprentissage provoque des changements morphologiques, biophysiques et chimiques durables au sein d'un ensemble restreint de cellules qui forment l'engramme. Notamment, ces changements comprennent une augmentation en nombre et en efficacité (PLT) des connexions spécifiquement entre les cellules qui composent l'engramme (Choi J. H. *et al.*, 2018). La réactivation de cet ensemble provoque le rappel. Les cellules qui composent un engramme sont distribuées à travers plusieurs régions du cerveau, chaque région

apportant une contribution spécifique à l'encodage de l'expérience dans sa globalité (Josselyn S. A. & Tonegawa S., 2020).

Dans le CA1, la plupart des cellules formant un engramme sont des cellules de lieu, mais seulement une partie des cellules de lieu qui encodent un environnement donné font partie de l'engramme (Tanaka K. Z. *et al.*, 2018). De façon générale, le nombre de cellules qui composent un engramme est invariable. Quelle que soit la force de la mémoire qu'il encode, le nombre de cellules qui composent chaque engramme est relativement semblable. C'est plutôt le nombre de synapses entre les cellules de l'engramme qui représentent la force d'une mémoire (Josselyn S. A. & Tonegawa S., 2020). Il y a donc une sélection des cellules actives lors d'une expérience pour les inclure ou non dans l'engramme. D'une part cette sélection est faite par l'excitabilité intrinsèque des cellules pyramidales. Les cellules les plus excitables au moment de l'évènement ayant le plus de chances d'être recrutées (Josselyn & Frankland, 2018). Un autre mécanisme de sélection peut être effectué par les interneurones en synchronisant ou inhibant l'activité des cellules excitatrices via l'inhibition anticipative, rétroactive et l'inhibition latérale (ex : inhibition des cellules pyramidales profondes par les superficielles via PV-INs) (Raven F. & Aton S. J., 2021).

1.6 Interneurones parvalbuminergiques de l'hippocampe.

Les interneurones inhibiteurs de l'hippocampe démontrent eux aussi de la plasticité. Notamment, les deux classes prédominantes d'interneurones exprimant la parvalbumine ou la somatostatine (Kullmann D. M. & Lamsa K. P., 2011). Les interneurones parvalbuminergiques représentent l'un des types d'interneurones majoritaire dans l'hippocampe. Ils ont leurs corps cellulaires dans la couche de cellules principales ou proche de cette dernière dans les couches oriens et radiatum pour le CA ou le hilus pour le gyrus denté. Leurs cibles sont le corps cellulaire et le segment initial des cellules principales (figure 12). Les PV-INs ont des propriétés intrinsèques et synaptiques qui favorisent une réponse rapide courte et fiable avec une grande précision temporelle (Pelkey K. A. *et al.*, 2017; Booker S. A. & Vida I., 2018). À travers leur positionnement dans le circuit et leur patron de décharge, les PV-INs ont un rôle primordial dans la régulation de la sortie d'information des cellules pyramidales et la synchronisation des ensembles neuronaux (Somogyi P. *et al.*, 2014).

1.6.1 Différents interneurones parvalbuminergiques dans CA1

Dans CA1, les PV-INs comprennent trois sous-types d'interneurones : Les cellules en panier, les cellules axo-axoniques, et les cellules bistratifiées. Les cellules bistratifiées qui coexpriment la somatostatine ont déjà été présentées dans la partie 1.6.

Les cellules en panier (CPns) ont leurs dendrites principalement dans le *stratum radiatum* ou elles reçoivent leurs entrées excitatrices majoritaires venant des cellules pyramidales de CA3, ce qui leur confère un rôle important dans l'inhibition anticipative (Pelkey K. A. *et al.*, 2017; Booker S. A. & Vida I., 2018). Elles présentent aussi des dendrites dans le *stratum lacunosum-moleculare* ou elles reçoivent des afférences du cortex entorhinal, et le *stratum oriens* ou elles reçoivent des afférences des cellules pyramidales locales, particulièrement celles présentes dans la couche superficielle (Lee S.-H. *et al.*, 2014). Les CPns reçoivent dans une moindre mesure des entrées inhibitrices, venant principalement d'autres CPns, mais aussi des interneurones spécifiques aux interneurones et des SOM-INs (voir Chapitre 1.7, section 3) (Booker S. A. & Vida I., 2018). Ces neurones peuvent donc contrôler les réseaux de CA1 de trois façons. Lorsqu'ils sont activés par les collatérales de Schaffer, ils exercent une inhibition proactive sur les cellules pyramidales de CA1 (figure 14 A). Leur connectivité différente entre les cellules pyramidales profondes et superficielles leur confère un rôle d'inhibition latérale (figure 14 B). Enfin, suite à leur activation

pas les cellules pyramidales de CA1, les PV-INs exercent une rétroaction inhibitrice sur ces même neurones (figure 14 C) (Lee S.-H. *et al.*, 2014; Booker S. A. & Vida I., 2018).

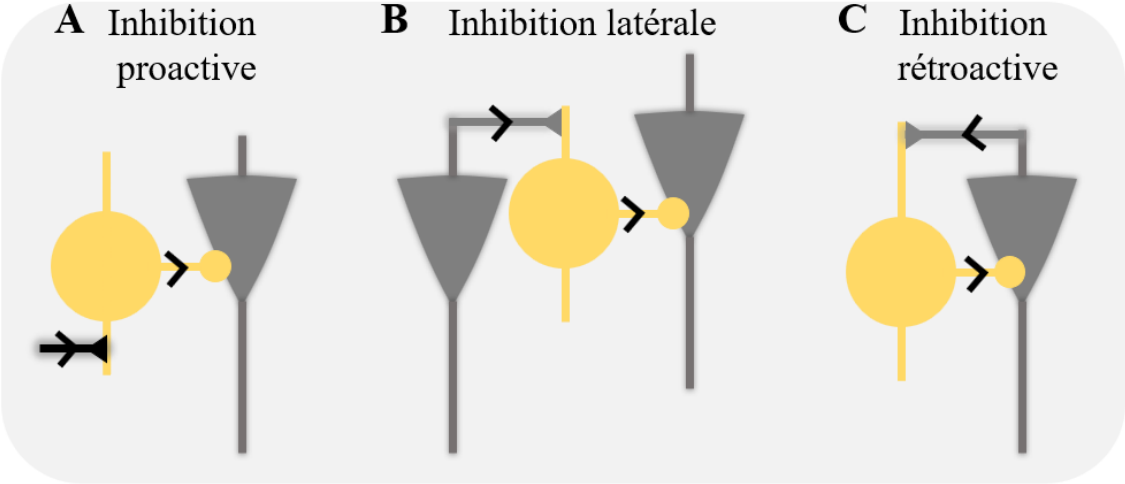

Figure 14 : Trois types d'inhibition des PV-INs. A, Les PV-INs peuvent exercer une inhibition proactive des cellules pyramidales de CA1 via leur activation par les collatérales de Schaffer. **B**, Ils peuvent également agir comme relais inhibiteurs dans l'inhibition latérale d'une cellule pyramidale locale sur une autre. **C**, Enfin ils exercent un rétrocontrôle inhibiteur en inhibant les cellules pyramidales qui les activent.

Les cellules axo-axoniques ont les dendrites organisées de la même façon que les CPns et reçoivent les mêmes entrées excitatrices hormis que pour elles il n'a pas été prouvé qu'il y ait une différence entre les cellules pyramidales superficielles ou profondes. Leur arborisation axonale forme de nombreuses collatérales qui innervent densément le segment initial de l'axone des cellules pyramidales de CA1, et réduisent donc les décharges des cellules pyramidales (Booker S. A. & Vida I., 2018; Dudok B. *et al.*, 2021).

1.6.2 régulations des rythmes de CA1 par les interneurones parvalbuminergiques

Les PV-INs déchargent dans la phase descendante du cycle thêta des cellules pyramidales, avec leur pic d'activité au creux de celui des cellules pyramidales, ce qui traduit bien le contrôle que les PV-INs exercent sur l'activité de ces neurones (Somogyi P. *et al.*, 2014). En effet, dans l'hippocampe isolé des entrées extrahippocampiques, le rythme thêta est conservé (Goutagny R. *et al.*, 2009). Dans ces conditions, la synchronisation des cellules pyramidales menant à l'émergence

de ce rythme thêta intrinsèque est fortement liée à l'activité des PV-INs (Amilhon B. *et al.*, 2015). *In vivo* , l'ablation des NMDARs spécifiquement dans les interneurones PV altère également l'amplitude et la rythmicité du thêta (Korotkova T. *et al.*, 2010). L'activité des PV-INs augmente la puissance des rythme theta et delta de CA1 spécifiquement durant la consolidation (Ognjanovski N. *et al.*, 2017).

La nature rapide et précise dans le temps des patrons de décharge des PV-IN leur permet de réguler des rythmes rapides. Les PV-INs contribuent à la génération des rythmes gamma de (Antonoudiou P. *et al.*, 2020), et notamment à ceux de la couche pyramidale de CA1 (Lasztóczi B. & Klausberger T., 2014). Cette fonction de générateur de rythme émerge de leur position dans le réseau, les PV-IN reçoivent une stimulation des cellules pyramidales de CA3 au rythme gamma et contraignent l'activité des cellules pyramidales de CA1 via l'inhibition proactive de leurs corps cellulaires et axones (Zemankovics R. *et al.*, 2013). Cette faculté provient aussi des propriétés biophysiques des dendrites des PV-IN (Kriener B. *et al.*, 2022).

Lors de l'apprentissage, les rythmes gamma lents provenant de l'intégration synaptique des afférences de CA3 sont couplés au rythme thêta de CA1(Wulff P. *et al.*, 2009; Fernández-Ruiz A. *et al.*, 2017). La force de ce couplage est directement corrélée avec l'augmentation des performances, et la précision du rappel (Wulff P. *et al.*, 2009; Fernández-Ruiz A. *et al.*, 2017). Le couplage des rythmes gamma de CA3 et thêta de CA1 dépend à la fois de l'inhibition des PV-INs (Wulff P. *et al.*, 2009), et de la plasticité de leurs afférences excitatrices (Korotkova T. *et al.*, 2010; He X. *et al.*, 2021).

Un autre rythme lie l'activité rythmique de CA3 et CA1 durant la consolidation et le rappel et est fortement régulé par les PV-INs. Ces interneurones ont un rôle clef dans la mise en forme et la synchronisation des ondulations de vagues pointues (SWR, *sharp wave ripples*). Leur plasticité synaptique induite par le conditionnement à la peur contextuelle et modulée par la dopamine augmente la fréquence et l'amplitude des SWR(Karunakaran S. *et al.*, 2016; Ognjanovski N. *et al.*, 2017).

Cette combinaison de régulation des rythmes par les PV-INs durant la consolidation de la mémoire et le rappel augmente la stabilisation et la réactivation consistante des ensembles neuronaux de CA1 (Ognjanovski N. *et al.*, 2017).

1.6.3 Plasticité des interneurones parvalbuminergiques

La régulation de ces rythmes est modulée par la plasticité des PV-INs. Ces interneurones démontrent un large éventail de changements plastiques. Ces formes de plasticité sont spécifiques aux différents récepteurs au glutamate exprimés par les PV-INs. Ces interneurones ont des synapses riches en AMPARs perméables au calcium (CP-AMPAR), expriment une PLT anti Hebbienne induite à des rythmes proches du gamma lent (20-55 Hz). Ils expriment aussi des NMDAR qui stimulés à haute fréquence (100 Hz ou TBS) induisent une PLT Hebbienne. Ces deux formes de plasticité sont exprimées exclusivement dans la partie postsynaptique, et dépendent de la CaMKII gamma (Le Roux N. *et al.*, 2013; He X. *et al.*, 2021). La perte de ces mécanismes de potentialisation par la délétion de ces récepteurs dans les PV-INs induit des altérations de la mémoire (voir 1.7.4). La stimulation haute fréquence des afférences de CA3 peut aussi induire une PLT de l'excitabilité intrinsèque des PV-INs via l'activation des mGluR5 qui induit une diminution des canaux potassiques Kv1 *in vitro* (Campanac E. *et al.*, 2013). La stimulation à basse fréquence (5 Hz) des afférences des PV-INs n'induit pas de DLT (Le Roux N. *et al.*, 2013). Par contre, le couplage des afférences excitatrices et des PV-INs à un rythme thêta produit une DLT Hebbienne par l'activation des CP-AMPAR présynaptique (Camiré O. & Topolnik L., 2014; Lau P. Y.-P. *et al.*, 2017).

1.6.4 Rôle des interneurones parvalbuminergiques dans la mémoire dépendante de l'hippocampe

L'activité et la plasticité des PV-INs sont important pour la consolidation de la mémoire. Durant la navigation spatiale, les PV-INs ont leur activité maximale juste avant l'entrée dans un champ de lieu, puis leur activité décroît pendant la traversée, libérant ainsi l'activité des cellules pyramidales, leur permettant de former un champ de lieu (Royer S. *et al.*, 2012; Fernández-Ruiz A. *et al.*, 2017; Dudok B. *et al.*, 2021). Inhiber les cellules axo-axoniques durant l'exploration mène à la création de champs de lieu surnuméraires à l'endroit où ces interneurones ont été inhibés (Dudok B. *et al.*, 2021). Par conséquent, l'un des rôles des PV-INs dans la mémoire spatiale est l'affûtage de la carte cognitive par l'inhibition de l'activité hors champ.

La perte de PLT synaptique des PV-INs par la délétion des NMDARs ou de sous-unités d'AMPARs dans ces cellules n'a pas d'effet sur la mémoire spatiale de référence, mais induit une

diminution de la mémoire de travail, ainsi qu'un déficit de la mémoire de reconnaissance d'objet et de localisation d'objets (Fuchs E. C. *et al.*, 2007; Korotkova T. *et al.*, 2010). Ces différences d'implication pourraient émerger du fait que les CPns inhibent particulièrement les cellules pyramidales profondes, qui encodent plus particulièrement les repères locaux ainsi que les informations saillantes (Soltesz I. & Losonczy A., 2018). Ainsi les types de mémoires reposant particulièrement sur ce type d'information sont plus affectés par la perte de fonction des PV-INs.

Alors que l'inhibition de l'activité PV-IN durant le conditionnement à la peur n'a pas d'effet sur la mémoire contextuelle de peur (Lovett-Barron M. *et al.*, 2014), leur inhibition pendant la consolidation, et particulièrement durant le sommeil REM altère cette mémoire. Dans les heures qui suivent le conditionnement à la peur, l'activité des PV-INs montre plus de cohérence avec les oscillations de CA1, et leur activation augmente la mémoire de peur (Ognjanovski N. *et al.*, 2017).

De plus, l'ablation de la CaMKII gamma, provoquant l'abolition de la PLT entre les cellules pyramidales de CA3 et les PV-INs, mais ne modifiant pas leur transmission basale, altère également la mémoire contextuelle de peur. Ce rôle de l'activité et de la PLT des PV-INs dans la consolidation est lié à leur régulation des SWR qui ont lieu durant la réactivation séquentielle des engrammes (replay) renforçant les connexions entre les cellules qui le composent (Buzsáki G., 2015; Ognjanovski N. *et al.*, 2017; Joo H. R. & Frank L. M., 2018). Durant le rappel, les réactivations séquentielles et les SWRs qui leur sont associées ont également lieu, ce qui suggère que leur régulation par les PV-INs est importante lors de cette fonction mnésique aussi (Buzsáki G., 2015; Joo H. R. & Frank L. M., 2018).

Ainsi, le rôle des PV-INs dans la formation de la mémoire dépendante de l'hippocampe semble être de synchroniser les ensembles neuronaux afin d'avoir une représentation précise des expériences, ainsi que la consolidation des engrammes ainsi formés. Enfin ils régulent également la réactivation de ces engrammes durant le rappel.

1.7 Les interneurones somatostatinergiques

Dans l'article qui suit, nous avons fait une revue de littérature sur les interneurones somatostatinergiques de l'hippocampe ainsi que leur rôle dans la régulation des circuits hippocampiques et la formation de la mémoire par leur activité durant l'apprentissage, mais aussi par leur plasticité à long terme. Nous couvrons aussi brièvement comment les astrocytes participent aux fonctions des SOM-INs et finalement comment un dysfonctionnement de la plasticité des SOM-INs pourrait contribuer aux troubles cognitifs.

Article de revue publié le 2 juin 2021 dans le journal « *Frontiers in Neural Circuits* »
doi:10.3389/fncir.2021.687558

Hippocampal Somatostatin Interneurons, Long-Term Synaptic Plasticity and Memory.

Honoré Eve, Khlaifia Abdessattar, Bosson Anthony, Lacaille Jean-Claude.

Department of Neurosciences, Centre for Interdisciplinary Research on Brain and Learning, Research Group on the Central Nervous System, Université de Montréal, Montreal, QC, Canada
Edited by: Maria Gutierrez-Mecinas, University of Glasgow, United Kingdom
Reviewed by: Rebecca Ann Piskorowski, INSERM U1266 Institut de Psychiatrie et Neurosciences de Paris, France; Marco Fuenzalida, Universidad de Valparaiso, Chile

Conflict of interest statement

The authors declare that the research was conducted in the absence of any commercial or financial relationships that could be construed as a potential conflict of interest

Funding statement

-Canadian Institutes of Health Research, PJT-153311 (JCL).

-Canada Research Chair in Cellular and Molecular Neurophysiology, CRC 950-231066 (JCL)
-Fonds de la Recherche du Québec – Santé (FRQS), Research Centre grant, Centre Interdisciplinaire de Recherche sur le Cerveau et l'Apprentissage (CIRCA), JCL member
-Université de Montréal, Research Group grant, Groupe de recherche sur le système nerveux central (GRSNC), JCL member

Abstract

A distinctive feature of the hippocampal structure is the diversity of inhibitory interneurons. These complex inhibitory interconnections largely contribute to the tight modulation of hippocampal circuitry, as well as to the formation and coordination of neuronal assemblies underlying learning and memory. Inhibitory interneurons provide more than a simple transitory inhibition of hippocampal principal cells. The synaptic plasticity of inhibitory neurons provides long-lasting changes in the hippocampal network and is a key component of memory formation. The dendrite targeting interneurons expressing the peptide somatostatin (SOM) are particularly interesting in this regard because they display unique long-lasting synaptic changes leading to metaplastic regulation of hippocampal networks. In this article we examine the actions of the neuropeptide SOM on hippocampal cells, synaptic plasticity, learning and memory. We address the different subtypes of hippocampal SOM interneurons. We describe the long-term synaptic plasticity that takes place at the excitatory synapses of SOM interneurons, its singular induction and expression mechanisms, as well as the consequences of these changes on hippocampal network, learning and memory. We also review evidence that astrocytes provide cell-specific dynamic regulation of inhibition of PC dendrites by SOM interneurons. Finally, we cover how, in mouse models of Alzheimer's disease (AD), dysfunction of plasticity of SOM interneuron excitatory synapses may also contribute to cognitive impairments in brain disorders.

Contribution to the field

A distinctive feature of the hippocampal structure is the diversity of inhibitory interneurons. These complex inhibitory interconnections largely contribute to the tight modulation of hippocampal circuitry, as well as to the formation and coordination of neuronal assemblies underlying learning and memory. Inhibitory interneurons provide more than a simple transitory inhibition of hippocampal principal cells. The synaptic plasticity of inhibitory neurons provides long-lasting changes in the hippocampal network and is a key component of memory formation. The dendrite targeting interneurons expressing the peptide somatostatin (SOM) are particularly interesting in this regard because they display unique long-lasting synaptic changes leading to metaplastic regulation of hippocampal networks. In this review, we shed light on this specific subpopulation of interneurons focussing on the role of SOM interneurons activity and synaptic plasticity in the regulation of hippocampal networks and memory functions. This review improves our understanding of SOM interneuron synaptic plasticity and help uncover how these specific inhibitory cells contribute to hippocampal memory processes.

1. INTRODUCTION

Hippocampal learning and memory emerge from the proper routing of information throughout its networks and the formation of enduring neuronal assemblies encoding a memory (Kandel *et al.*, 2014). These neuronal assemblies, also called engrams, are formed by a discrete population of excitatory glutamatergic principal cells (PCs) between which synaptic transmission is potentiated (Josselyn S. A. & Frankland P., 2018; Tonegawa S. *et al.*, 2018).

A distinctive feature of the hippocampal structure is the diversity of inhibitory interneurons. PCs represent the majority of neurons in every hippocampal region. While interneurons only represent 10 to 20% of the total neuron population, they can be divided into many subgroups based on their laminar position, dendritic and axonal morphology, protein expression, electrophysiological features and functions (Freund T. F. & Buzsáki G., 1996; Somogyi P. &

Klausberger T., 2005; Tricoire L. *et al.*, 2011; Kepecs A. & Fishell G., 2014; Pelkey K. A. *et al.*, 2017; Booker S. A. & Vida I., 2018). Interestingly, the different interneuron types have preferred synaptic connections on specific and distinct subcellular domains of the principal cells including the apical and proximal dendrites, cell body, and the axon initial segment. Due to their specific characteristics, inhibitory interneurons play various roles in fine tuning signal integration and firing of PCs. Additional levels of control of the hippocampal network is achieved by interneurons targeting other interneurons (Katona I. *et al.*, 1999; Pelkey K. A. *et al.*, 2017; Artinian J. & Lacaille J.-C., 2018) along with interneuron-astrocyte interactions (Mederos S. & Perea G., 2019).

These complex inhibitory interconnections largely contribute to the tight modulation of hippocampal circuitry, providing means for the formation and coordination of neuronal assemblies. Hence, hippocampal interneurons also participate in the mechanisms underlying hippocampus-dependent memory. In this review, we aim to shed light on a major subpopulation of GABAergic interneurons specifically inhibiting PC dendrites and characterized by the expression of the peptide somatostatin (SOM). As the morphological and neurochemical profiles of these interneurons were reviewed (Pelkey K. A. *et al.*, 2017; Booker S. A. & Vida I., 2018), we will focus on the role of SOM interneurons activity and synaptic plasticity in the regulation of hippocampal networks and memory functions.

2. SOMATOSTATIN IN THE HIPPOCAMPUS

The peptide SOM, also referred initially as somatotropin release inhibitory factor (SRIF), was originally discovered in the hypothalamus where it acts as growth hormone inhibitor (Krulich L. *et al.*, 1968; Brazeau P. *et al.*, 1973). In the cerebral cortex, SOM is stored in dense-core vesicles in a specific subset GABAergic interneuron and released by intense neuronal activity (Vezzani A. *et al.*, 1993; Hou Z.-H. & Yu X., 2013; Liguz-Lecznar M. *et al.*, 2016). SOM can bind to five metabotropic receptors (SSTR1 to 5) which are coupled to G protein from the Gi/o and Gq/G11 families. Thus, SSTR activation downregulates adenylyl cyclase activity, and activates the phosphoinositide 3-kinase and phospholipase Cβ signaling pathways (Liguz-Lecznar M. *et al.*, 2016; Thomas Günther G. T., Pascal Dournaud, Corinne Bousquet, Zsolt Csaba, Hans-Jürgen Kreienkamp, Amelie Lupp, Márta Korbonits, Justo P. Castaño, Hans-Jürgen Wester, Michael Culler, Shlomo Melmed and Stefan Schulz, 2018). SSTR1-4, but not SSTR5, are present in the

hippocampus in PCs and as auto-receptors in SOM interneurons. Although the distribution of SSTRs overlaps within and across hippocampal regions, SSTR subtypes preferentially occupy specific cell compartments. SSTR1 are preferentially located pre-synaptically, SSTR2 and 4 post-synaptically, and SSTR3 extra-synaptically. Yet, which cell type expresses the receptors and whether they are pre or postsynaptic remain unclear (Csaba Z. & Dournaud P., 2001; Liguz-Lecznar M. *et al.*, 2016; Cammalleri M. *et al.*, 2019).

The systematic distribution of SSTRs suggests a precise regulation of hippocampal networks by SOM. However, the mechanisms by which SOM regulates hippocampal networks remain ambiguous. Reports of membrane and synaptic effects are diverse and sometimes contradictory. On the one hand, SOM has an inhibitory effect on pyramidal neurons exhibiting hyperpolarizing effect, decreasing evoked and spontaneous activity, persistently reducing NMDA and AMPA currents and reducing spine density (Pittman Q. J. & Siggins G. R., 1981; Tallent M. K. & Siggins G. R., 1997; Hou Z.-H. & Yu X., 2013). On the other hand, SOM also produces excitatory effects on pyramidal cells inducing membrane depolarization, as well as increasing spontaneous and evoked excitatory post-synaptic potentials (EPSPs) (Olpe H.-R. *et al.*, 1980; Delfs J. & Dichter M., 1983; Scharfman H. & Schwartzkroin P. A., 1988; Scharfman H. E. & Schwartzkroin P. A., 1989).

Many factors may explain these discrepancies. First, in many studies the effect of SOM is concentration dependent, and the number of PCs responding to SOM application with a depolarization follows an inverted U-shaped curve between 100 pM and 1 µM, until it reaches potent toxic concentrations over 10 µM (Olpe H.-R. *et al.*, 1980; Pittman Q. J. & Siggins G. R., 1981; Delfs J. & Dichter M., 1983; Scharfman H. & Schwartzkroin P. A., 1988; Tallent M. K. & Siggins G. R., 1997). Second, the location of SOM application is also important. In rabbit hippocampal slices, SOM application on the soma of CA1 PCs induces membrane depolarization often accompanied by action potentials. When applied on the dendrites of PCs SOM produces depolarization or hyperpolarization. Larger SOM applications further away from PCs induce membrane hyperpolarization (Scharfman H. & Schwartzkroin P. A., 1988). Third, inhibitory interneurons also express SSTRs. SOM application at the soma of interneurons at the border between *stratum pyramidale* and *oriens* produces a depolarization accompanied by action potential in these cells. When applied at their dendrites, SOM produces either depolarization followed by

increased action potentials, or hyperpolarization also followed by increased action potentials, or a combination of depolarization and action potential discharge followed by a hyperpolarization (Scharfman H. & Schwartzkroin P. A., 1988).

The effect of SOM on interneuron output also appears complex. Blocking SSTR1 resulted in an increase in SOM concentration but had no effect on GABA concentration *in vivo* (De Bundel D. *et al.*, 2010). This finding may indicate that SOM release from an interneuron can promote auto-inhibition *via* SSTR1 presynaptic activation without interfering with GABA transmission. Bath application of somatostatin did not affect isolated GABAergic inhibitory postsynaptic currents induced by stimulation close to the pyramidal cell layer, nor the density of inhibitory synapses (Tallent M. K. & Siggins G. R., 1997; Hou Z.-H. & Yu X., 2013). However, earlier research demonstrated persistent reduction or blockade of spontaneous or evoked inhibitory postsynaptic potentials (Pittman Q. J. & Siggins G. R., 1981; Scharfman H. & Schwartzkroin P. A., 1988; Scharfman H. E. & Schwartzkroin P. A., 1989).

Finally, another level of complexity with SOM effects arises from its long-lasting action. SOM produces long-lasting increases in spontaneous activity and evoked responses of pyramidal cells *via* postsynaptic effects (Delfs J. & Dichter M., 1983; Scharfman H. & Schwartzkroin P. A., 1988). In addition, transgenic mice with ablation of the SOM gene or mice with pharmacological depletion of SOM by cysteamine treatment, have normal basal transmission but a deficit in long-term potentiation (LTP) in CA1 (Kluge C S. C., Szinyei C, Stork O, Pape HC, 2008). Taken altogether this *corpus* of data suggests that SOM has a complex function which is dependent on the location and concentration released, the activated receptor subtype, and experimental conditions (for details see Table 1).

TABLE 1 | Effects of somatostatin (SOM) on hippocampal pyramidal cell activity.

Reference	Model	Experiment	Results
Hou and Yu (2013)	Rat hippocampal neuronal-glial culture	1 day SOM application 1 μM.	↘ Spine density (excitatory) and density of pre-post synaptic markers. No effect on inhibitory synapses.
Kluge et al. (2008)	Mouse acute slices	SOM-KO mice or cysteamine application.	SOM KO show normal basal synaptic transmission and ↘ LTP in CA1; same results with cysteamine.
Tallent and Siggins (1997)	Rat, acute slices	1 μM SOM superfusion.	SOM persistently ↘ NMDA and AMPA currents in a time and dose-dependent manner. It has no effect on isolated GABAergic currents elicited by pyramidal layer stimulation.
Scharfman and Schwartzkroin (1989)	Rabbit, acute slices	Pressure application of SOM on distinct CA1 pyramidal cell compartment.	Soma application of SOM depolarizes CA1-PCs and persistently ↘ or blocks IPSPs evoked by *oriens* electrical stimulation.
Scharfman and Schwartzkroin (1988)	Rabbit, acute slices	Pressure application of SOM on distinct CA1 pyramidal cell compartment.	SOM application on pyramidal cell soma elicits depolarization often accompanied by action potentials. On dendrites, it produces depolarization or hyperpolarization. Applied in larger quantities further from the cell it hyperpolarizes CA1-PCs. Potentiation with ↗ spontaneous activity and evoked responses due to postsynaptic effects.
Delfs and Dichter (1983)	Rat cortical neurons in culture	100 pM to 100 μM SOM application just over the studied neuron.	Concentration/response curve inverted U- shaped from 100 pM to 1 μM. 30–50% of the neurons respond ↗ with EPSPs and IPSPs amplitude, and ↗ spontaneous action potentials frequency.
Pittman and Siggins (1981)	Rat, acute slices	Application of 0.12 μM to 1.2 μM SOM superfusion on the slice.	Hyperpolarization of PCs and ↘ evoked and spontaneous activity. Slight ↘IPSPs amplitude. Slight↗ EPSPs amplitude evoked by *radiatum* stimulation.
Olpe et al. (1980)	Rat, *in vivo*, anesthetized	Hippocampal 60 s micro-injection of SOM.	↗ Number of neurons responding with excitation, following ↗ SOM concentration. No alteration of GABA release.

↗ = increase; ↘ = decrease.

Interestingly, at the behavioral level, SOM appears important as a neuromodulator of hippocampal function. Genetic ablation of the SOM gene or SOM depletion by cysteamine impairs contextual fear memory and has no effect on cued fear memory, indicating a specific action on hippocampus-dependent memory (Kluge C S. C., Szinyei C, Stork O, Pape HC, 2008). Moreover, intracerebroventricular injection of SOM, or a non-hydrolyzable SOM analog, before or after learning, increases active and passive avoidance behaviors 24 hours after the acquisition, and prevents their extinction (Vécsei L. & Widerlöv E., 1988; Vécsei L. *et al.*, 1989). However, both treatments have no effect on spatial discrimination learning and reversal learning in the T-maze test (Vécsei L. *et al.*, 1984). Again, SOM concentration is critical, low concentrations increase passive avoidance memory, while 10-fold higher concentrations have the opposite effect (Vécsei L. *et al.*, 1984; Vécsei L. & Widerlöv E., 1988; Vécsei L. *et al.*, 1989; Schettini G., 1991) . Pre-training intra-hippocampal injection of SOM or a SSTR4 agonist impairs spatial memory in a dose-dependent manner. In addition, the SSTR4 agonist decreases cued memory and enhances the

retention of bar pressing task. Intriguingly, the administration of SSTR1-3 agonists do not evoke any behavioral change (Gastambide F. *et al.*, 2008). The timing of SOM treatment is also critical. When injected before the memory acquisition trials in the 8-arm radial maze task, SOM increases acquisition rates. However, when administered before the memory probe test, it impairs performance. Thus, SOM has different effects on acquisition and memory probe tests (Guillou J.-L. *et al.*, 1993; Lamirault L. *et al.*, 2001). Finally, it is important to note that hippocampal injections of SOM or agonists of SSTR4 and SSTR2 have anxiolytic and antidepressant-like effects *via* the inhibition of the hypothalamic-pituitary-adrenal axis. Through this mechanism, SOM also regulates emotions and stress responses which strongly modulate learning and memory (Prévôt T. D. *et al.*, 2017) (for details see Table 2).

Thus, at the behavioral level, SOM is required for proper memory formation. The location, timing, and concentration of SOM release by interneurons appears crucial for SOM functional outcomes, perhaps because of the distribution and types of receptors involved. However, a better understanding of how, where and when SOM is released to fulfill its functions requires new precise tools.

TABLE 2 | Effects of somatostatin (SOM) on hippocampus-dependent behavior.

Reference	Model	Experiment	Results
Gastambide et al. (2008)	Mouse	Intra-hippocampal injection of SOM or SSTR agonist at different concentrations before spatial and cued versions of Morris water maze and bar pressing conditioning.	SOM and SST_4R agonist injection ↘ spatial memory dose-dependently. $SST_{1-3}R$ agonist does not affect these behavioral tasks. SST_4R agonist ↘ cued memory but ↗ bar pressing retention.
Kluge et al. (2008)	Mouse	SOM KO mice or cysteamine injection in wild type mice. Contextual fear conditioning and cued fear conditioning.	SOM KO ↘ contextual fear but not cued fear memory. Pre-conditioning cysteamine injection in wild type mice has the same effect, but post-conditioning injection induces unspecific increase of fear response.
Lamirault et al. (2001)	Mouse	Intra-hippocampal injection of SOM or cysteamine prior spatial discrimination eight-arm radial maze task acquisition or test.	SOM injection prior acquisition (0.2 μg/0.2 μl/hippocampus) ↗ acquisition speed but ↘ performances during the test. Injection before the test does not affect memory.
Guillou et al. (1993)	Mouse	Intra hippocampal injection of SOM or cysteamine prior to spatial discrimination eight-arm radial maze task.	SOM injection (0.2 μg/0.2 μl/hippocampus) ↗ acquisition speed, but impairs the ability to change strategies. Cysteamine injection impairs memory.
Vécsei et al. (1989)	Rat	Intra-cerebroventricular SOM or SOM fragments injection in male rats directly after passive avoidance acquisition.	0.6 nM SOM ↗ avoidance latency and 6 nM ↘ it in a passive avoidance task during the test 24 h after. In open field task 6 nM SOM ↘ rearing and 0.6 nM has no effect. Injections above 12 nM are lethal.
Vécsei and Widerlöv (1988)	Rat	Intra-cerebroventricular SOM injection in male rats 30 min before passive avoidance, or active avoidance acquisition.	In passive avoidance: 1 μg of SOM ↗ avoidance latency at 24 h but not 48 h after acquisition. 10 μg ↘ avoidance latency 24 h after acquisition. In active avoidance: 1 μg SOM ↗ learning curve.
Vécsei et al. (1984)	Rat	Intra-cerebroventricular SOM or subcutaneous cysteamine injection in male rats directly after active avoidance and T-maze acquisition.	SOM ↘ extinction of active avoidance but has no effect on T-maze. Cysteamine ↗ extinction in both behavioral tasks. SOM ↗ locomotion in open field 10 min after injection. Cysteamine ↘ locomotion, rearing, and grooming.

↗ = increase; ↘ = decrease.

3. HIPPOCAMPAL SOMATOSTATIN INTERNEURONS

Although hippocampal SOM interneurons release the peptide SOM, in hippocampal research SOM has largely been regarded only as a neurochemical marker for a subset of GABAergic interneurons. Through their GABAergic actions, SOM interneurons provide local inhibition to regulate hippocampal networks, and distal inhibition to synchronize hippocampal activity with other brain areas. Hippocampal SOM interneurons have been the subject of recent comprehensive reviews (Muller C. & Remy S., 2014; Pelkey K. A. *et al.*, 2017; Booker S. A. & Vida I., 2018). In this section we will highlight the features of SOM interneurons in various hippocampal regions that are critical for later sections.

A cardinal feature of SOM interneurons is that they synaptically target the dendrites of local PCs, and other interneurons, to provide inhibition of synaptic and peri-synaptic compartments. Thus, they gate the synaptic inputs of their targets (Katona I. *et al.*, 1999; Muller C. & Remy S., 2014). SOM interneurons preferentially receive excitatory inputs from local PCs to which they send inhibitory feedback (Lacaille J. C. *et al.*, 1987; Blasco-Ibáñez J. M. & Freund T. F., 1995). Yet, there is more to SOM interneuron function than negative feedback. SOM interneurons dynamically regulate the input-output transformation and firing of PCs both in slices and during exploration *in vivo* (Lovett-Barron M. *et al.*, 2012; Royer S. *et al.*, 2012). In addition, SOM interneurons are diverse, and each type has a different contribution to the regulation of information flow through PCs (Figure 1).

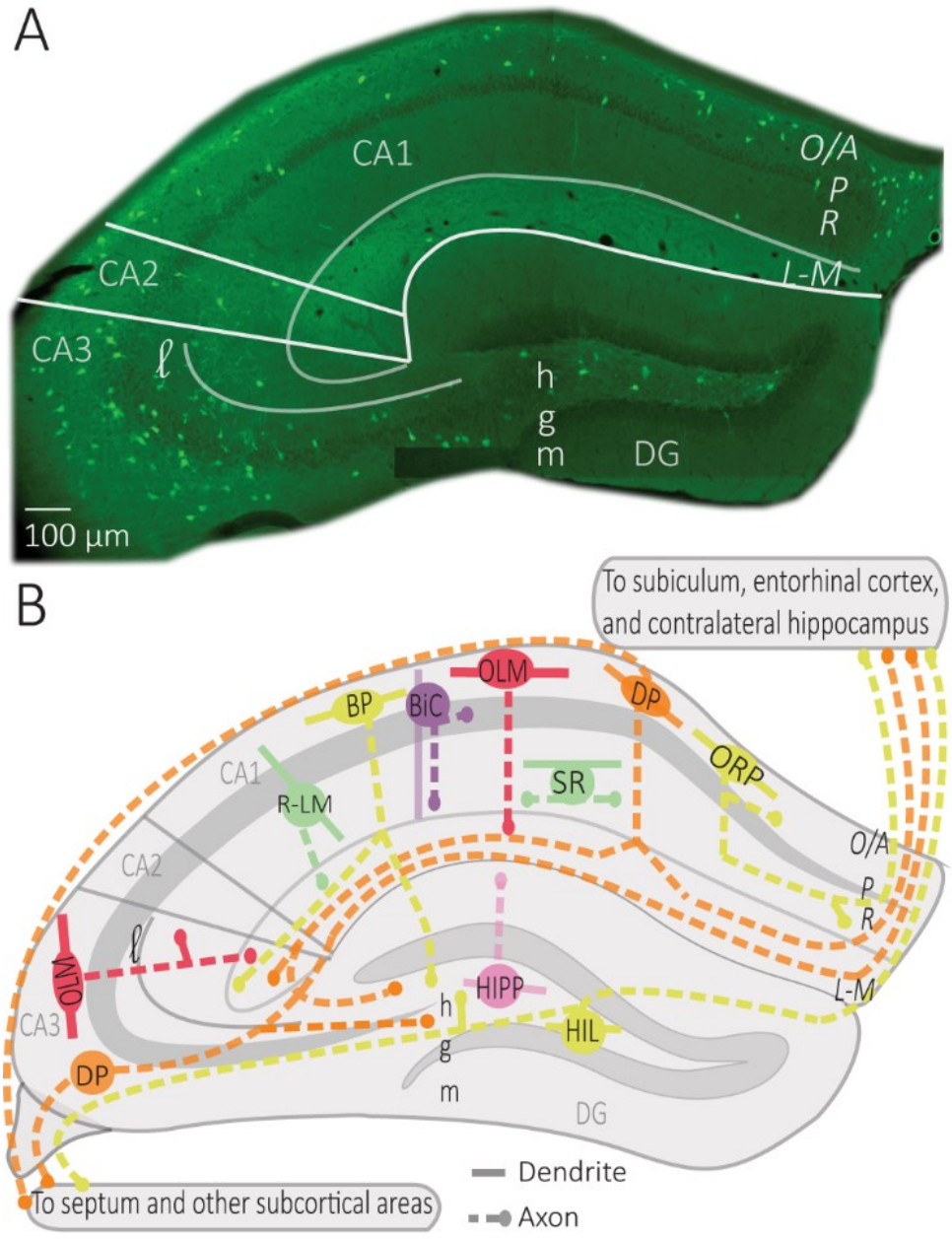

Figure 1

Figure 1. Distribution of SOM interneurons in hippocampus. (A) Representative montage of fluorescence images showing the soma location of SOM interneurons expressing enhanced yellow fluorescent protein in dorsal hippocampus of *Sst*$^{ires\text{-}Cre}$;*Rosa26*$^{lsl\text{-}EYFP}$ mice (Vasuta C. *et al.*, 2015; Artinian J. *et al.*, 2019), with indicated anatomical landmarks. (B) Simplified diagram illustrating the characteristic position of soma, dendrites and axons of the different types of SOM interneurons in hippocampus. Abbreviations for hippocampus: CA1-3, *cornu ammonis* 1-3; DG, dentate gyrus; O/A, *oriens*/*alveus*; P, *pyramidale*; R, *radiatum*; L-M, *lacunosum-moleculare*; l, *lucidum*; h, hilus; g, granule cell layer; m, *moleculare*. Abbreviations for SOM interneuron types: OLM, *oriens/lacunosum-moleculare* cell; ORP, *oriens*-retrohippocampal projecting cell; DP, double

projecting cell; BP, back-projecting cell; BiC, bistratified cell; R-LM, *radiatum/lacunosum-moleculare* cell; SR, *stratum radiatum* cell; HIPP, hilar perforant path cell; HIL, hilar cell.

3.1 .Oriens Lacunosum-Moleculare (OLM) cells

OLM cells are the most extensively studied SOM interneurons in the hippocampus. They are located in CA3 and CA1 along the complete dorso-ventral axis of the hippocampus (Mikulovic S. *et al.*, 2015). Their designation comes from the location of their soma and dendrites in *stratum oriens* and their rich axonal arborization in *stratum lacunosum-moleculare* (Lacaille J. C. *et al.*, 1987; Chittajallu R. *et al.*, 2013) (Figure 1). Their main excitatory input comes from local PCs to which they send inhibitory feedback (Lacaille J. C. *et al.*, 1987), as well as from cholinergic afferents from the septum and diagonal band of Broca (Lovett-Barron M. *et al.*, 2012; Sun Y. *et al.*, 2014). They receive inhibition from local inhibitory neurons, mostly vasoactive intestinal peptide (VIP) expressing interneurons, and inhibitory afferents from septal regions (Tyan L. *et al.*, 2014) and the nucleus incertus (Szonyi A. *et al.*, 2019).

The main targets of OLM cell axons are the distal dendrites and spines of PCs (Maccaferri G. *et al.*, 2000) They also target dendrites of other interneurons, such as bistratified cells, basket cells, and interneurons located in *stratum radiatum* (Shaffer collateral associated cells, perforant path associated cells, and neurogliaform cells) (Katona I. *et al.*, 1999; Elfant D. *et al.*, 2008) (Figure 2). Consequently, CA1 OLM cells provide differential control of PC excitatory afferents: 1) OLM cell activation directly inhibits the distal excitatory inputs of the temporoammonic pathway (TAP); 2) they also inhibit other interneurons, which themselves inhibit the proximal dendrites of CA1 PCs in *stratum radiatum*, providing indirect disinhibition of the excitatory inputs from the Schaffer collateral pathway (SC). Hence, OLM cells differentially modulate the excitatory synaptic inputs coming from the entorhinal cortex and CA3 onto PCs (Leao R. N. *et al.*, 2012; Katona L. *et al.*, 2014).

Interestingly, OLM cells express a specific set of proteins regulating their excitatory synaptic inputs. They express high level of the metabotropic glutamate receptor type 1α (mGlur1α) (Ferraguti F. *et al.*, 2004) which localize perisynaptically at their dendritic synapses (Luján R. *et al.*, 1996). They also express the postsynaptic adhesion molecule, extracellular leucine-rich repeat

fibronectin containing 1 (Elfn1) protein, that interacts with the presynaptic receptor mGluR7, expressed specifically at afferent excitatory synapses of OLM cell (Shigemoto R. *et al.*, 1996; Sylwestrak E. L. & Ghosh A., 2012). The Elfn1-mGluR7 interaction facilitates excitatory transmission at these synapses and maximizes excitation in the theta frequency range (4-10 Hz) (Sylwestrak E. L. & Ghosh A., 2012).

The hippocampus displays characteristic oscillatory activities, theta and gamma oscillations as well as sharp wave ripples, during exploration and rapid eye movement (REM) sleep (Vanderwolf C. H., 1969; O'keefe J. & Nadel L., 1978; Buzsaki G. *et al.*, 1992; Buzsáki G., 2002). Thus, the relation of interneuron firing to hippocampal oscillations provides useful functional information (Somogyi P. *et al.*, 2014). OLM interneurons fire during theta activity at the trough of theta oscillations (Klausberger T. *et al.*, 2003; Varga C. *et al.*, 2012; Katona L. *et al.*, 2014; Somogyi P. *et al.*, 2014). However, their firing is not coupled to gamma oscillations (Tukker J. J. *et al.*, 2007). Also, OLM cell firing is decreased during slow wave sleep and mostly inhibited during sharp wave ripples (Klausberger T. *et al.*, 2003; Varga C. *et al.*, 2012; Katona L. *et al.*, 2014). The precise timing of synchronized spikes is crucial for the integration of information because excitatory synapses from CA1 PCs onto SOM interneurons display facilitation on repetitive activation (Ali A. B. & Thomson A. M., 1998).

The membrane potential of OLM cells shows intrinsic theta frequency resonance with frequency preferences in theta and low theta ranges (1-5 Hz) (Pike F. G. *et al.*, 2000). OLM cells display a substantial spike frequency adaptation during sustained discharges (Lacaille J. C. & Williams S., 1990; Tricoire L. *et al.*, 2011). These properties constrain OLM cells to delayed low frequency sustained activity (Pouille F. & Scanziani M., 2004). Thus, the facilitation of synaptic activation of SOM interneurons results in gradual recruitment of sustained inhibition of CA1 PCs (Pouille F. & Scanziani M., 2004).

3.2 . Bistratified cells (BiC)

BiCs express the peptide SOM as well as the other interneuron-specific marker, parvalbumin (PV) (Pelkey K. A. *et al.*, 2017). Their somas are located in or around the CA1 pyramidal cell layer (BiCs; Figure 1). Their vertical aspinous dendrites arborize in *stratum oriens* and *radiatum* (Figure 2) (Maccaferri G. *et al.*, 2000). They receive both feedforward excitation

from SC of CA3 PCs and feedback excitation from CA1 PCs (Klausberger T. *et al.*, 2004). These two major inputs show different short-term dynamics. Repeated stimulation of SC inputs to BiCs show marked and sustained facilitation, whereas similar stimulation of CA1 PCs inputs to BiCs display only an initial transient facilitation (Wierenga C. J. & Wadman W. J., 2003; Pouille F. & Scanziani M., 2004). BiCs receive inhibitory synaptic inputs from OLM cells (Leao R. N. *et al.*, 2012) and from septal GABAergic neurons (Unal G. *et al.*, 2018). The designation of BiC comes from the two-layered distribution of their axonal arborizations in the *stratum oriens* and *stratum radiatum* (Figure 2). Accordingly, BiCs strongly inhibit the basal and proximal apical dendrites of CA1 PCs, as well as other interneurons (Halasy K. *et al.*, 1996; Maccaferri G. *et al.*, 2000).

The action potentials and subsequent after-hyperpolarization of BiCs are fast, enabling these cells to withstand high frequency stimulation with high temporal reliability (Buhl E. H. *et al.*, 1996; Pouille F. & Scanziani M., 2004). In relation to hippocampal oscillatory activity, BiCs fire during theta activity in the trough of theta oscillation (Klausberger T. *et al.*, 2004). In contrast to OLM cells, BiCs show strong modulation of activity during gamma oscillations and fire during the ascending phase of oscillations (Tukker J. J. *et al.*, 2007) In addition, BiCs demonstrate high activity during sharp wave ripples (Katona L. *et al.*, 2014). BiCs fast spiking features and the dynamics of their excitatory and inhibitory inputs influence the way they provide recurrent inhibition of PCs. At the beginning of sustained activation of CA1 PC inputs, BiCs respond with reliable time-locked excitation that shows transient facilitation, resulting in onset-transient inhibition of CA1 PCs proximal dendrites (Wierenga C. J. & Wadman W. J., 2003; Pouille F. & Scanziani M., 2004). In contrast, OLM cell firing shows a gradual recruitment during sustained activation of CA1 PC inputs, thereby providing a late-persistent type of inhibition (Pouille F. & Scanziani M., 2004).Thus, BiCs and OLM cells provide recurrent inhibition with distinct dynamics, targeting proximal versus distal CA1 PC dendrites respectively (Wierenga C. J. & Wadman W. J., 2003; Pouille F. & Scanziani M., 2004; Muller C. & Remy S., 2014).

3.3. Hilar perforant path (HIPP) cells

HIPP cells of the dentate gyrus (DG) have their soma and dendritic arborizations in the hilus (Sik A. *et al.*, 1997; Yuan M. *et al.*, 2017). Their axonal projections heavily ramify in the outer two thirds of the molecular layer (Figure 1) (Han Z. S. *et al.*, 1993; Yuan M. *et al.*, 2017).

Although the majority of HIPP axon processes terminate in the DG, some branches traverse the hippocampal fissure and project to the CA1 *stratum lacunosum-moleculare* (Han Z. S. *et al.*, 1993; Houser C. R., 2007). HIPP cells are mainly excited by granule cell (GC) axons and provide feedback inhibition to distal dendrites of GCs, thereby showing functional similarities with OLM cells. (Hosp J. A. *et al.*, 2014). HIPPs form functional synapses with GCs, but also with PV interneurons and other HIPP cells. They also rarely connect to CCK hilar commissural associational path (HICAP) interneurons (Savanthrapadian S. *et al.*, 2014). HIPP provide weak and slow dendritic inhibition (Yuan M. *et al.*, 2017). However, their inhibition of PV cells is sufficient to regulate their action potential generation and spike timing precision, and hence, control information flow within the DG circuitry (Savanthrapadian S. *et al.*, 2014).

3.4. Radiatum (R) cells

Other subtypes of SOM cells, that are sparse in number, are found in *stratum radiatum* (Figure 1) (Oliva A. A., Jr. *et al.*, 2000; Tricoire L. *et al.*, 2011). One type of SOM interneuron was identified in a transgenic mice line (GFP-expressing Inhibitory Neurons, GIN mice) (Oliva A. A., Jr. *et al.*, 2000). These CA1 SOM interneurons have a cell body in *stratum radiatum* and dendrites that span *stratum oriens* and *stratum radiatum*. Their axonal projections ramify in *stratum lacunosum-moleculare* and these cells were designated *radiatum-lacunosum moleculare* (RLM cells; Figure 1) (Oliva A. A., Jr. *et al.*, 2000). RLM cells show similar firing properties to OLM cells (Oliva A. A., Jr. *et al.*, 2000). Hence, RLM cells may provide feedforward inhibition of entorhinal cortex input of PCs (Oliva A. A., Jr. *et al.*, 2000). Another type of SOM cell was identified with the soma, dendrites and axonal projections restricted to *stratum radiatum* (SR cells; Figure 1) (Oliva A. A., Jr. *et al.*, 2000; Tricoire L. *et al.*, 2011). These SOM cells have similar firing properties to OLM cells and may provide feedforward inhibition of Schaffer collateral input to CA1 pyramidal cells (Oliva A. A., Jr. *et al.*, 2000; Tricoire L. *et al.*, 2011).

3.5. Projection cells

Distinct SOM interneurons, in addition to providing local inhibition, have projections to other hippocampal and subcortical areas, where they target many cell types including PCs and GABA interneurons (Gulyas A. I. *et al.*, 2003; Katona L. *et al.*, 2017; Eyre M. D. & Bartos M., 2019). In CA1, these SOM projecting cells have their soma and dendrites in *stratum oriens*, as well as local

axonal arborizations in *stratum oriens* and *stratum radiatum*. Distinct CA1 SOM projection cells are distinguished by their axonal projection targets (Figure 1). Back-projecting (BP) cells have axonal projections to CA3 and DG (Goldin M. *et al.*, 2007; Katona L. *et al.*, 2017). Oriens-retrohippocampal projecting (ORP) cells project to the subiculum (Jinno S. *et al.*, 2007; Melzer S. *et al.*, 2012). Double-projecting (DP) cells have axons projecting to the septum, as well as to CA3 and DG (Gulyas A. I. *et al.*, 2003; Katona L. *et al.*, 2017; Eyre M. D. & Bartos M., 2019), Subiculum (Goldin M. *et al.*, 2007; Jinno S. *et al.*, 2007; Melzer S. *et al.*, 2012) or the medial entorhinal cortex and contralateral hippocampus (Goldin M. *et al.*, 2007; Jinno S. *et al.*, 2007; Melzer S. *et al.*, 2012; Eyre M. D. & Bartos M., 2019). Much less is known about the physiological properties of these cell types, although *in vivo* recordings indicate that most projection cells discharge during theta activity in the descending slope or at the trough of theta cycles during movement (Jinno S. *et al.*, 2007; Katona L. *et al.*, 2017). Some projection cells fire preferentially on the ascending phase of gamma oscillations (Jinno S. *et al.*, 2007). Most of them also increase their firing during sharp wave ripples (Jinno S. *et al.*, 2007; Katona L. *et al.*, 2017). Thus, SOM projection cells tend to fire similarly to BiC cells during hippocampal oscillations.

In CA3, DP cells were described with soma in *stratum oriens*, *pyramidale*, and *lucidum* (Gulyas A. I. *et al.*, 2003; Jinno S. *et al.*, 2007) (Figure 1). CA3 DP cells have dendrites in *stratum oriens* and *radiatum*, as well as local axons in *stratum oriens*, *pyramidale* and *radiatum* (Jinno S. *et al.*, 2007). CA3 DP cells have axonal long-range projections that target the septum, as well as CA1 and subiculum (Jinno S. *et al.*, 2007) and ventral hippocampal areas (Gulyas A. I. *et al.*, 2003). CA3 DP cell axonal long-range projections make synaptic contacts with PCs and GABA interneurons (Gulyas A. I. *et al.*, 2003; Jinno S. *et al.*, 2007).

In DG, another type of SOM cell is the hilar cell (HIL, Figure 1). HIL cells have a cell body, dendrites and local axonal projections in the hilus (Yuan M. *et al.*, 2017). Their activity is driven by excitatory inputs from GCs and DG mossy cells (Larimer P. & Strowbridge B. W., 2008; Yuan M. *et al.*, 2017). HIL cells provide perisomatic inhibition of hilar GABAergic cells and mossy cells, and send long-range axonal projections to the medial septum (Gulyas A. I. *et al.*, 2003; Larimer P. & Strowbridge B. W., 2008; Yuan M. *et al.*, 2017) and contralateral DG (Gulyas A. I. *et al.*, 2003; Goldin M. *et al.*, 2007; Jinno S. *et al.*, 2007; Eyre M. D. & Bartos M., 2019). By exerting a powerful inhibition onto local GABAergic and mossy cells, as well as septal neurons, HIL cells can

coordinate activities in these areas as a function of GC and mossy cell activation (Larimer P. & Strowbridge B. W., 2008; Yuan M. *et al.*, 2017).

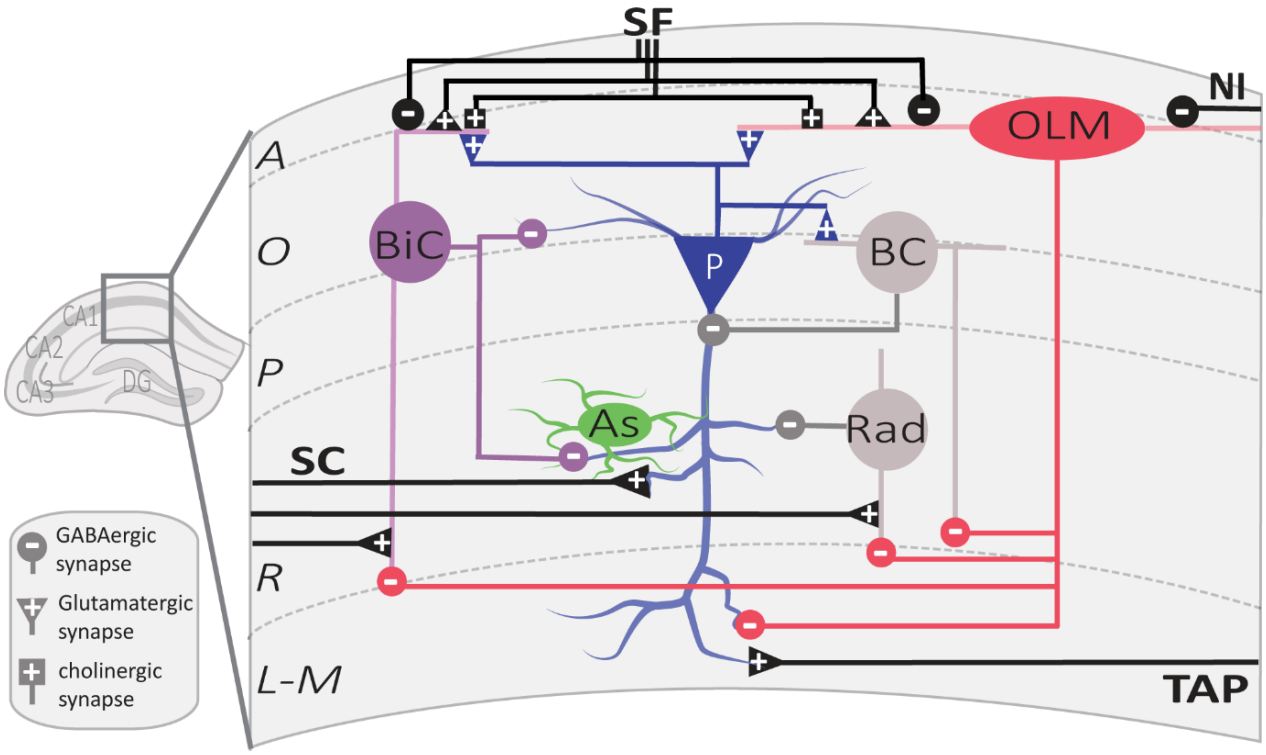

Figure 2

FIGURE 2. Local circuit of CA1 SOM interneurons. Simplified diagram illustrating the local synaptic circuits of OLM cells and BiCs with other cell types in dorsal CA1 hippocampus. Abbreviations for CA1 layers: A, alveus; O, oriens; P, pyramidale; R, radiatum; L-M, lacunosum-moleculare. Abbreviations for CA1 afferent inputs: SF, septal fibers; NI, nucleus incertus fibers; SC, Schaffer collateral pathway from CA3 pyramidal cells; TAP, temporo-ammonic pathway from entorhinal cortex. Abbreviations for SOM cell types: (red) OLM, oriens/lacunosum-moleculare cell; (violet) BiC, bistratified cell. Abbreviations for other cell types: (blue) P, pyramidal cell; (gray) BC, basket cell; (green) As, astrocyte; (gray) Rad, unidentified stratum radiatum interneurons targeted by OLM cells.

4. SOM-INTERNEURONS LONG-TERM SYNAPTIC PLASTICITY

In the central nervous system, two widely studied forms of long-term synaptic plasticity are long-term potentiation (LTP), a long-lasting strengthening of synaptic efficacy, and long-term depression (LTD), a long-lasting weakening of synaptic efficacy (Malenka R. C. & Bear M. F., 2004). These forms of synaptic plasticity at hippocampal excitatory synapses are linked to memory storage (Morris R. G., 2003). *In vitro*, several protocols of electrical stimulations, or repetitive pairing of pre- and post-synaptic firing, induce long-term changes of synaptic transmission (Malenka R. C. & Bear M. F., 2004; Caporale N. & Dan Y., 2008). With electrical stimulation, LTP is generally associated with high-frequency afferent stimulation, and LTD with low frequency stimulation. With pre- and post-synaptic pairing, a presynaptic spike preceding the postsynaptic spike within a narrow time window induces LTP, whereas the reverse produces LTD (Feldman D. E., 2012). Although it has been known for some time that blocking GABAergic transmission facilitates the induction of LTP at excitatory synapses (Wigstrom H. & Gustafsson B., 1983) and that afferents of inhibitory interneurons display long-term potentiation (Buzsaki G. & Eidelberg E., 1982), synaptic plasticity at excitatory synapses onto interneurons has recently attracted more attention (Kullmann D. M. & Lamsa K. P., 2007; Pelletier J. G. & Lacaille J. C., 2008). It is becoming increasingly apparent that hippocampal inhibitory neurons, including SOM interneurons, have highly dynamic activity and express long-lasting changes at their excitatory input synapses and inhibitory output synapses (Maccaferri G. & McBain C. J., 1996; Perez Y. *et al.*, 2001; Lamsa K. *et al.*, 2005; Chevaleyre V. *et al.*, 2006; Kullmann D. M. & Lamsa K. P., 2007; Pelletier J. G. & Lacaille J. C., 2008; Kullmann D. M. & Lamsa K. P., 2011; Vasuta C. *et al.*, 2015; Udakis M. *et al.*, 2020). In this section, we will focus on long-term plasticity at excitatory synapses onto hippocampal SOM interneurons Perez Y. *et al.* (2001) and later examine its role in hippocampus-dependent memory.

4.1. Excitatory synapses onto CA1 SOM interneurons

Plasticity of excitatory synapses onto SOM interneurons has been characterized the most in CA1 OLM cells (Lacaille J. C. *et al.*, 1987; Maccaferri G. & McBain C. J., 1996; Perez Y. *et al.*, 2001; Lamsa K. P. *et al.*, 2007). Excitatory synapses made by CA1 PC axons that feedback on CA1 SOM interneurons (notably OLM cells) are composed of Ca^{2+} permeable AMPA receptors (CP-AMPARs). These synapses show inward rectification of their current-voltage (I-V) relationship, display short-term facilitation with repeated stimulation, and are inhibited by mGluR2/3 (Croce A. *et al.*, 2010). In contrast, excitatory synapses made by axons of CA3 PCs that feed-forward onto CA1 SOM interneurons (OLM cells) are composed of Ca^{2+} impermeable AMPARs (CI-AMPARs), and these synapses show linear I-V relationships, display short-term depression with repeated stimulation, and are mGluR2/3-insensitive (Croce A. *et al.*, 2010). These input-specific properties of excitatory synapses differentially control the SOM interneuron output firing, resulting in gradual sustained recruitment of evoked firing with repetitive feedback input activation, and transient evoked firing with repetitive feedforward input activation of SOM cells (Croce A. *et al.*, 2010). It is interesting to note that input-specific rules of excitatory synapses also occur for other types of interneurons in CA3 *stratum lucidum* (SL) but with opposite organization (Toth K. & McBain C. J., 1998). Thus, excitatory synapses onto single SOM cells originate from multiple sources and display afferent-specific mechanisms. In addition, these afferent-specific mechanisms differ from those in other types of interneurons.

4.2. Long-term potentiation at excitatory synapses onto SOM interneurons

The synapse between CA1 PC axons and SOM interneurons, notably BiC and OLM cells, express a Hebbian form of LTP that requires the coincident activity of both pre- and postsynaptic neurons for induction (Perez Y. *et al.*, 2001; Lapointe V. *et al.*, 2004; Vasuta C. *et al.*, 2015).

Multiple lines of evidence indicate that this SOM interneuron LTP is not due to passive propagation of di-synaptic LTP at Schaffer collateral synapses on CA1 pyramidal cells (SC-CA1 synapses) (McBain C. J. *et al.*, 1999). First, SOM interneuron LTP is insensitive to the NMDA receptor blocker AP-5 (Perez Y. *et al.*, 2001), unlike LTP at SC-CA1 PC synapses (Morris R. G. *et al.*, 1986a). Second, LTP is induced directly at putative single fiber synapses onto SOM interneurons by using minimal stimulation (Perez Y. *et al.*, 2001; Lapointe V. *et al.*, 2004; Vasuta C. *et al.*, 2015). Finally, interfering with Ca^{2+} influx in the postsynaptic SOM interneuron prevents LTP induction (Lapointe V. *et al.*, 2004).

This LTP is considered Hebbian since it is induced by presynaptic theta-burst stimulation (TBS) paired with postsynaptic depolarization (Figure 3), but not by presynaptic stimulation alone nor postsynaptic depolarization alone (Perez Y. *et al.*, 2001). Hebbian LTP is expressed as a decrease in failure rates of EPSCs and an increase in the potency of EPSCs (amplitude of EPSCs excluding failures) (Perez Y. *et al.*, 2001; Lapointe V. *et al.*, 2004). It is also accompanied by a change in paired-pulse facilitation and the coefficient of variation of EPSCs, parameters associated presynaptic changes (Lapointe V. *et al.*, 2004). Thus, Hebbian LTP may be expressed by both pre- and post-synaptic mechanisms.

Hebbian LTP in SOM interneurons shows afferent input specificity. Pairing presynaptic TBS with postsynaptic depolarization elicits LTP at synapses between CA1 PCs and SOM interneurons, but not at the synapses between CA3 PCs and SOM interneurons (Croce A. *et al.*, 2010). Also, it displays cell-type specificity. Pairing presynaptic TBS with postsynaptic depolarization evoked LTP in SOM interneurons (BiC and OLM cells) (Perez Y. *et al.*, 2001; Lapointe V. *et al.*, 2004; Vasuta C. *et al.*, 2015) but not in PV interneurons (Vasuta C. *et al.*, 2015) nor in unidentified interneurons in *stratum radiatum* (Perez Y. *et al.*, 2001).

Induction of Hebbian LTP in SOM interneurons involves a very different signaling cascade than LTP in PCs (Figure 3). Most notably, Hebbian LTP in SOM interneurons does not involve NMDA receptors (Perez Y. *et al.*, 2001), but requires the activation of mGluR1α receptors, a glutamate metabotropic receptor highly expressed in SOM interneurons (Perez Y. *et al.*, 2001; Kougioumoutzakis A. *et al.*, 2020). Pharmacologically blocking mGluR1α, or genetically deleting mGluR1 ($mGluR1^{-/-}$ mice), prevents Hebbian LTP induction, indicating a crucial role of mGluR1α (Perez Y. *et al.*, 2001; Lapointe V. *et al.*, 2004; Topolnik L. *et al.*, 2005; Vasuta C. *et al.*, 2015).

During induction of Hebbian LTP, the activation of postsynaptic mGluR1α stimulates Src and extracellular signal-regulated kinase (ERK) pathways, causing opening of transient receptor potential (TRP) channels and Ca^{2+} influx, as well as Ca^{2+} release from intracellular stores (Topolnik L. *et al.*, 2006) (Figure 3). TRPC1 interaction with mGluR1α in SOM interneuron dendrites mediates a mGluR1α-dependent slow EPSC in SOM interneurons, supporting the importance of TRP channels in SOM interneurons LTP (Kougioumoutzakis A. *et al.*, 2020).

Endocannabinoid (eCB) signalling mainly mediates short- and long-term depression of excitatory and inhibitory transmission (Chevaleyre V. *et al.*, 2006). In addition, synaptic activation of group I mGluRs (mGluR1/5) is a major pathway for the production of eCBs (Chevaleyre V. *et al.*, 2006). Interestingly in SOM interneurons, eCBs may be involved as a retrograde messenger in LTP (Friend L. N. *et al.*, 2019). SOM interneurons express the endocannabinoid-synthesizing enzyme diacylglycerol lipase α (DGLα) and n-acylphosphatidylethanolamine phospholipase D (NAPE-PLD) (Friend L. N. *et al.*, 2019). Moreover, inhibition of cannabinoid type 1 receptor (CB1R) prevents LTP in SOM interneurons (Friend L. N. *et al.*, 2019). Thus, synaptic activation of mGluR1/5 may lead to production of eCBs (anandamide, AEA; 2-arachadonyl glycerol, 2-AG) that act retrogradely on presynaptic CB1Rs to potentiate synaptic transmission (Figure 3) (Friend L. N. *et al.*, 2019).

Activation of mGluR5 in SOM interneurons (OLM cells) also elicits postsynaptic Ca^{2+} rises from intracellular stores release, independent of Src-ERK activation (Topolnik L. *et al.*, 2006). Moreover, this type of Ca^{2+} signaling is not involved directly in Hebbian LTP induction (Topolnik L. *et al.*, 2006). Pharmacological activation of mGluR5 is sufficient to induce LTP at excitatory synapses onto SOM interneurons (OLM cells), indicating multiple types of LTP linked to mGluRs in SOM interneurons (Le Vasseur M. *et al.*, 2008). In addition, local mGluR5 activation by agonist application or high frequency synaptic stimulation leads to sustained enhancement of action potential evoked Ca^{2+} transients in dendrites of SOM interneurons (OLM cells) (Topolnik L. *et al.*, 2009). This augmentation of postsynaptic Ca^{2+} transients is expressed as a selective potentiation of L-type voltage gated calcium channels (VGCCs) function and controlled by mGluR5-mediated intracellular Ca^{2+} release as well as protein kinase C (PKC) activation (Figure 3) (Topolnik L. *et*

al., 2009). This activity-dependent regulation of VGCCs by mGluR5 may serve as mechanism for positively regulating Hebbian synaptic plasticity of SOM interneurons (Topolnik L. *et al.*, 2009).

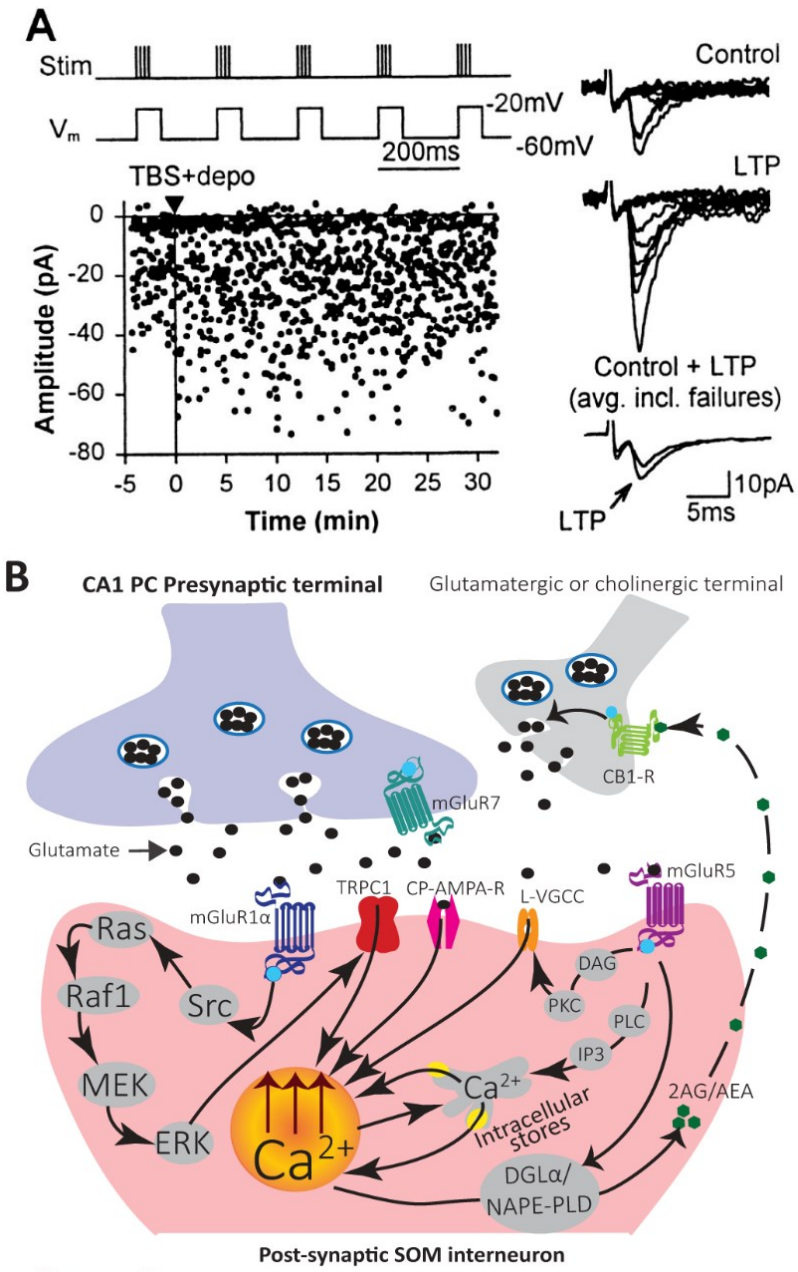

Figure 3

FIGURE 3. Mechanisms of induction and modulation of Hebbian LTP in SOM interneurons. (A) Graph of EPSC amplitude from a representative cell showing LTP after TBS paired with depolarization (TBS + depo; protocol shown above and delivered at time indicated by black triangle and vertical line). Examples of control and potentiated EPSCs (10 consecutive responses) at 30 min after induction (Right). Superimposed average EPSCs (bottom traces; n = 64 responses each, failures included) from control and 30 min after induction also show LTP. Adapted from Perez et al. (2001). (B) Diagram of LTP induction mechanisms leading to postsynaptic Ca2+ elevation in SOM interneurons. Stimulation of the presynaptic terminal releases glutamate that activates postsynaptic CP-AMPAR and mGluR1α. Activation of mGluR1α stimulates the Src signaling cascade leading to ERK activation. ERK leads to postsynaptic Ca2+ rise via activation of non-selective cationic channels TRPC1 and Ca2+ entry, as well as mobilization of Ca2+ from intracellular stores. A retrograde signaling mechanism may involve eCBs. Synaptic activation of mGluR1/5 stimulates synthesizing enzymes DGLα and/or NAPE-PLD to produce the eCBs 2-AG and/or AEA. 2-AG/AEA act retrogradely to activate CB1Rs on glutamatergic or cholinergic terminals and potentiate transmission. A potential mechanism of LTP modulation may involve activation of mGluR5 that

produces postsynaptic Ca2+ rises via two pathways. First, mGluR5 activates the PLC/IP3 pathway which leads to Ca2+ release from internal stores. Second, mGluR5 activates DAG-PKC pathway to potentiate L-type VGCC function and may regulate LTP induction.

In pyramidal cells, $GABA_BRs$ mediate a slow K^+-mediated inhibitory postsynaptic current (sIPSC) (Dutar P. & Nicoll R. A., 1988; Degro C. E. *et al.*, 2015) and promote excitatory synapses LTP *via* a presynaptic disinhibition mechanism (Davies C. H. *et al.*, 1991; Mott D. D. & Lewis D. V., 1991). In SOM interneurons, $GABA_BRs$ are also highly expressed in dendrites. But instead of activating postsynaptic K^+ currents, $GABA_BRs$ inhibit postsynaptic L-type VGCCs in SOM interneurons (Booker S. A. *et al.*, 2018). By negatively regulating VGCCs, $GABA_BRs$ inhibit Hebbian LTP in SOM interneurons (Booker S. A. *et al.*, 2018). Thus, $GABA_BR$-mediated inhibition of L-type VGCCs provide a mechanism for negative regulation of Hebbian synaptic plasticity of SOM interneurons. Interestingly, excitatory and inhibitory synaptic inputs onto SOM interneurons are inhibited presynaptically by $GABA_BRs$, as well as SOM interneuron inhibitory synapses onto PCs (Booker S. A. *et al.*, 2020). Thus, $GABA_BR$ activation may also functionally uncouple SOM interneurons from the CA1 network (Booker S. A. *et al.*, 2020).

4.3. Persistent long-term potentiation at excitatory synapses onto SOM interneurons

LTP in principal cells is divided into two phases: an early phase (early LTP, E-LTP) that is induced by brief high frequency stimulation, lasts several minutes to hours and depends on post-translational mechanisms; and a late phase (late LTP, L-LTP) that requires repetitive high frequency stimulation, lasts several hours to days and depends on new gene expression and protein synthesis (Kandel E. R., 2001; Abraham W. C. *et al.*, 2019). Although the study of late LTP has mainly focused on excitatory synapses onto principal cells (Malenka R. C. & Bear M. F., 2004), recent studies revealed that excitatory synapses onto CA1 SOM interneurons can also undergo L-LTP (Ran I. *et al.*, 2009; Ran I. *et al.*, 2012; Artinian J. *et al.*, 2019).

In hippocampal slice culture, repetitive stimulation of mGluR1, by the repeated application of the mGluR1/5 agonist (RS)-3,5-dihydroxyphenylglycine (DHPG), in the presence of the mGluR5 antagonist 2-methyl-6-(phenylethynyl)pyridine (MPEP), induces a persistent potentiation

of excitatory synapses onto SOM interneurons that can last at least 24 hours, termed mGluR1-dependent late LTP (L-LTP$_{mGluR1}$) (Figure 4) (Ran I. *et al.*, 2009; Ran I. *et al.*, 2012; Artinian J. *et al.*, 2019). L-LTP$_{mGluR1}$ is prevented by inhibitors of transcription and translation, indicating that it is dependent on new gene expression and protein synthesis (Figure 4) (Ran I. *et al.*, 2009). L-LTP$_{mGluR1}$ is also induced in acute hippocampal slices by repeated mGluR1 stimulation with DHPG, or by repetitive theta-burst stimulation of afferents (Artinian J. *et al.*, 2019). Interestingly, using *ex vivo* whole-cell recordings in acute slices 24 hours after contextual fear conditioning, training was found to induce mGluR1-mediated, translation-dependent L-LTP at SOM interneuron excitatory synapses, indicating that L-LTP$_{mGluR1}$ may be linked to hippocampus-dependent memory (Artinian J. *et al.*, 2019).

Mechanistically, L-LTP$_{mGluR1}$ shares many features of Hebbian LTP. Repetitive stimulation of mGluR1 by DHPG during action potentials blockade with tetrodotoxin prevent L-LTP$_{mGluR1}$, suggesting a Hebbian induction (Ran I. *et al.*, 2012). L-LTP$_{mGluR1}$ is also NMDAR independent, and prior induction of L-LTP$_{mGluR1}$ occludes induction of Hebbian LTP, indicating that they share similar mechanisms (Ran I. *et al.*, 2012).

The mechanisms of induction of L-LTP$_{mGluR1}$ (Figure 4) requires activation of mGluR1a, as it is prevented by the selective antagonist LY367385 (Ran I. *et al.*, 2009; Artinian J. *et al.*, 2019). Activation of mGluR1a stimulates both phosphoinositide 3-kinase (PI3K) and mitogen-activated protein kinase kinase (MEK)/extracellular signal-regulated kinase (ERK) pathways resulting in mTORC1 phosphorylation. In turn mTORC1 activates ribosomal protein S6 kinase (S6K) and S6 phosphorylation, as well as phosphorylation of eIF4E-binding protein (4E-BP), to stimulate eIF4E-dependent translation necessary for L-LTP$_{mGluR1}$ (Ran I. *et al.*, 2009; Artinian J. *et al.*, 2019). In addition activation of mGluR1a stimulates phosphorylation of cAMP response element-binding protein (CREB) *via* ERK signalling, to activate CREB-dependent transcription also necessary for L-LTP$_{mGluR1}$ (Ran I. *et al.*, 2012). A cell-specific conditional knock-out in SOM interneurons of the Regulatory-Associated Protein of mTOR (Raptor) gene, a necessary component of mTORC1, reduces mTORC1 activity and prevents L-LTP$_{mGluR1}$ (Artinian J. *et al.*, 2019). Conversely, cell-specific conditional heterozygous knock-out in SOM interneurons of the Tuberous Sclerosis Complex 1 (TSC1) gene, a repressor of mTORC1, increases mTORC1 activity in SOM interneurons and facilitates L-LTP$_{mGluR1}$ by lowering the threshold for induction (Artinian J. *et al.*,

2019). Knock-out of the 4E-BP gene, which removes the repression of eIF4E-dependent translation, similarly causes a facilitation of L-LTP$_{mGluR1}$ by lowering the threshold for induction (Ran I. *et al.*, 2009), further highlighting the critical role of mTORC1-dependent translation in L-LTP$_{mGluR1}$ (Figure 4).

The mechanisms of expression of synaptic plasticity in central neurons are varied and complex (Citri A. & Malenka R. C., 2008). In SOM interneurons, L-LTP$_{mGluR1}$ expression may involve both pre- and postsynaptic mechanisms, not occurring necessarily jointly (Figure 4) (Ran I. *et al.*, 2009; Ran I. *et al.*, 2012; Artinian J. *et al.*, 2019). In slice cultures, L-LTP$_{mGluR1}$ is expressed by an increase in potency of EPSCs evoked by minimal stimulation (Ran I. *et al.*, 2009; Artinian J. *et al.*, 2019), and in amplitude of miniature EPSC (mEPSCs) (Ran I. *et al.*, 2009), suggesting postsynaptic mechanisms of expression. L-LTP$_{mGluR1}$ in slice cultures is accompanied by a reduction in the paired-pulse ratio of EPSCs evoked by minimal stimulation (Ran I. *et al.*, 2009; Artinian J. *et al.*, 2019) and by an increase in mEPSC frequency (Ran I. *et al.*, 2009), suggesting presynaptic mechanisms of expression. Moreover, quantal analysis of EPSCs evoked by minimal stimulation in slice culture indicated an increase in quantal content and quantal size during L-LTP$_{mGluR1}$, consistent with coordinated pre- and post-synaptic changes (Ran I. *et al.*, 2012). The increase in quantal content may result from increased release probability or new release sites (Ran I. *et al.*, 2012). Conforming with the increase in quantal size, peak-scaled nonstationary fluctuation analysis of mEPSCs indicated that an increase in both single-channel conductance and number of functional receptors contribute to the increase in the postsynaptic response during L-LTP$_{mGluR1}$ (Ran I. *et al.*, 2012). In acute slices, L-LTP$_{mGluR1}$ induced by DHPG is expressed by an increase in EPSC potency, but no change in paired-pulse ratio, whereas L-LTP$_{mGluR1}$ induced by TBS stimulation is expressed by an increase in EPSC potency and a decrease in paired-pulse ratio (Artinian J. *et al.*, 2019). Similarly, L-LTP$_{mGluR1}$ induced by contextual fear conditioning is expressed by an increase in spontaneous EPSC amplitude and frequency, as well as increase in potency of EPSCs evoked by minimal stimulation but no change in paired-pulse ratio (Artinian J. *et al.*, 2019), indicating that pre- and post-synaptic expression mechanisms do not always occur jointly during L-LTP$_{mGluR1}$.

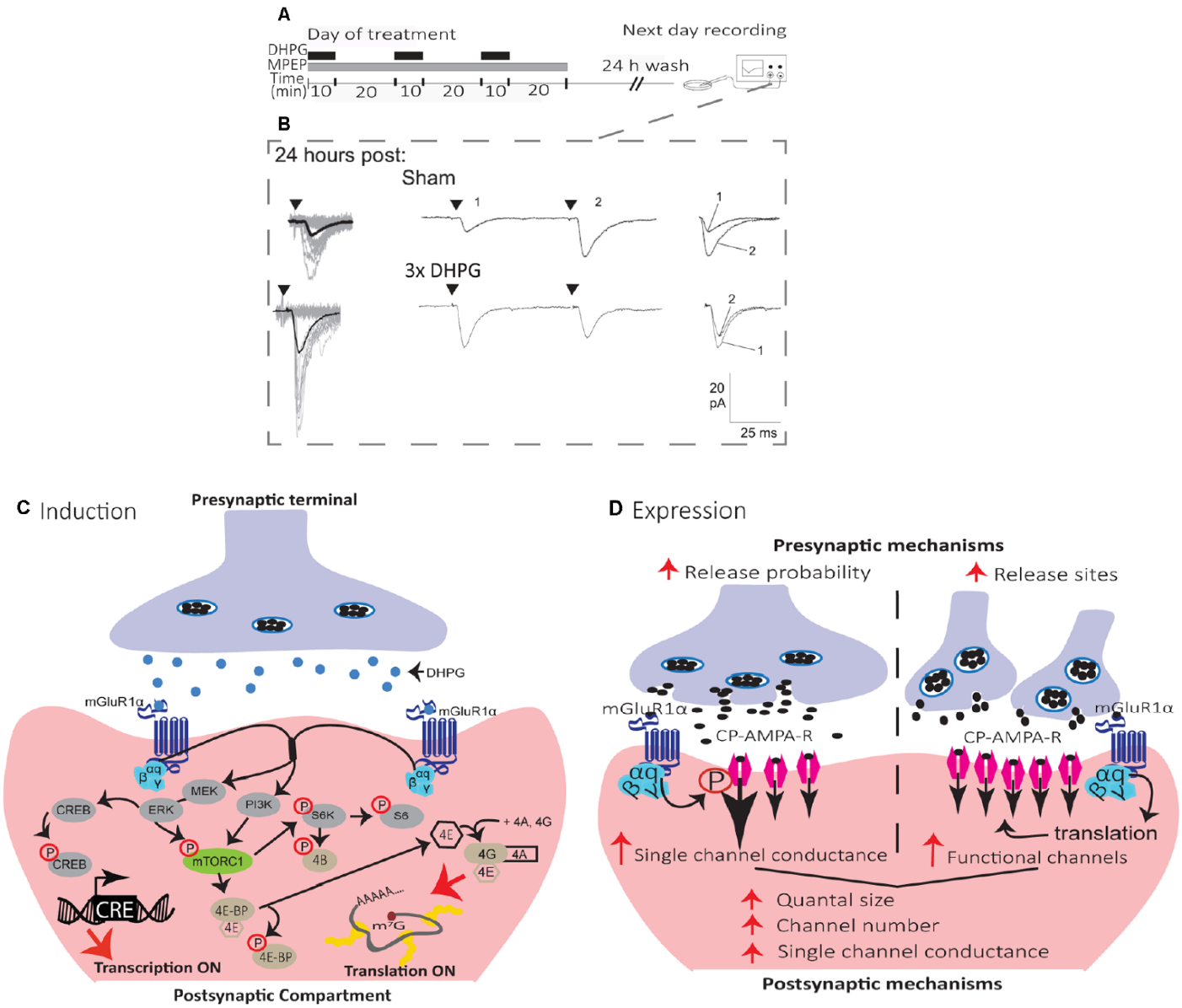

Figure 4. Mechanisms of induction and expression of L-LTP$_{mGluR1}$ in SOM interneurons. (A) Schematics of induction and recording protocol. Cultured hippocampal slices were treated with repetitive (3×) applications of the mGluR1/5 agonist (DHPG, 5 μM, black bars) in the presence of the mGluR5 antagonist (MPEP, 25 μM, gray bar). On the next day, after a 24 h wash-out, whole cell recordings were obtained from visually identified CA1 SOM interneurons in agonist- or sham-treated slices. (B) Representative EPSCs evoked by minimal stimulation at 24 h after sham-treatment (top), repetitive (3×; bottom) mGluR1 agonist-stimulation, showing larger responses after repetitive treatment. Left, superimposed 20 successive events (EPSCs + failures; gray) with average EPSC (including failures; solid black line) of 100 events. Middle, average of EPSC pairs (100 events) evoked by paired-pulse stimulation (50 ms interstimulus interval), showing loss of paired-pulse facilitation after repetitive treatment. Right, superimposed first and second EPSCs of

average pair. Black triangles indicate time of stimulation. Adapted from (Ran I. *et al.*, 2009). (C) Diagram of L-LTP$_{mGluR1}$ induction mechanisms. Repeated stimulation of mGluR1 by DHPG engages PI3K and MEK/ERK signalling pathways to phosphorylate mTORC1. Activation of mTORC1 leads to initiation of eIF4E-mediated mRNA translation *via* to pathways: (1) ribosomal S6 protein kinase (S6K) stimulation of S6 phosphorylation; and (2) phosphorylation of 4E-BPs repressors proteins which release eIF4E. Subsequently, eIF4E associates with eIF4A and eIF4G to form the cap-binding complex, eIF4F, which initiates translation. Activation of MEK–ERK signaling by repeated mGluR1 stimulation also leads to phosphorylation of CREB to control CRE-dependent gene expression. (D) Diagram of L-LTP$_{mGluR1}$ expression mechanisms. The maintenance of L-LTP$_{mGluR1}$ involves both pre- and post-synaptic modifications. At the presynaptic level, transmitter release is increased (increase in release probability and/or addition of functional release site). At the postsynaptic level, postsynaptic responsiveness is increased (recruitment of functional receptors and increase in single channel conductance).

4.4. Other types of synaptic plasticity in SOM interneurons

Interestingly, another form of plasticity called anti-Hebbian LTP is induced at excitatory synapses onto CA1 OLM interneurons by pairing presynaptic stimulation with postsynaptic membrane hyperpolarization (Kullmann D. M. & Lamsa K. P., 2007). The anti-Hebbian LTP is NMDAR-independent and dependent on CP-AMPARs. This form of LTP is not specific to SOM interneurons and can be induced in fast spiking PV interneurons (axo-axonic cells and basket cells) (Kullmann D. M. & Lamsa K. P., 2007). The diversity in types of long-term plasticity at SOM interneuron synapses in hippocampal CA1 region suggest multiple roles in long-lasting regulation of the CA1 network.

In CA3, excitatory synapses onto interneurons display different types of synaptic plasticity including NMDA-dependent LTP and NMDAR-independent LTD (Laezza F. *et al.*, 1999; Laezza F. & Dingledine R., 2004). However, whether synaptic plasticity occurs at synapses onto CA3 SOM interneurons remains to be determined.

In DG however, excitatory synapses onto both types of SOM interneurons, HIPP and HIL cells, show long-term synaptic plasticity (Yuan M. *et al.*, 2017). In these cases, plasticity is induced by the application of an associative burst frequency stimulation at 30 Hz (aBFS) of afferents paired with postsynaptic action potentials, a stimulation protocol aimed at mimicking fast rhythmic neuronal network activity patterns at gamma (30–100 Hz) frequencies in DG. Remarkably, aBFS

induces long-lasting depression (LTD) of excitatory synapses from GC onto HIPP cells, but LTP of excitatory synapses from GC and mossy cells onto HIL cells (Yuan M. *et al.*, 2017). The increase and the decrease in failure rate of synaptic transmission accompanying LTD in HIPP cells and LTP in HIL cells, respectively, suggest that both phenomena involve presynaptic expression mechanisms (Yuan M. *et al.*, 2017). These results indicate that long-term synaptic plasticity in DG HIPP cells differ from that in CA1 OLM cells. Thus, although both cell types provide local dendritic feedback inhibition, their synapses from excitatory inputs display different types of long-term changes, indicating region-specific plasticity properties.

5. REGULATION OF CA1 NETWORK METAPLASTICITY BY PLASTICITY OF EXCITATORY SYNAPSES OF SOM INTERNEURONS

As mentioned previously, early work established that afferents of inhibitory interneurons express long-term potentiation (Buzsaki G. & Eidelberg E., 1982). Coupled with the finding that pharmacological inhibition of GABAergic transmission facilitated the induction of LTP at PC excitatory synapses (Wigstrom H. & Gustafsson B., 1983), this led to the concept that plasticity at excitatory synapses in interneurons increase inhibition of PCs and dampen LTP at PC excitatory synapses. However, more recent work indicates that multiple types of synaptic plasticity at excitatory synapses onto inhibitory interneurons have more complex actions in hippocampal networks (Kullmann D. M. & Lamsa K. P., 2007; Pelletier J. G. & Lacaille J. C., 2008).

5.1. Long-term plasticity of excitatory synapses controls SOM interneuron firing and synaptic output

Dendrite-projecting SOM interneurons provide efficient suppression of CA1 PC dendritic excitatory synaptic inputs and synaptically-evoked burst firing (Lovett-Barron M. *et al.*, 2012). *In vivo* during spatial navigation, dendritic inhibition by SOM interneurons supresses firing of PCs in their place fields, as well as PC burst firing (Royer S. *et al.*, 2012). But dendritic inhibition is not static, and the recruitment of recurrent dendritic inhibition in PCs is dynamic during short trains of stimulation (Pouille F. & Scanziani M., 2004). At the onset of a series of stimuli, soma- and proximal dendrite-targeting recurrent inhibition are elicited. Later in the series of stimuli, recurrent inhibition is evoked in the distant dendritic regions. Thus, during repetitive activation of PCs, recurrent inhibition switches from transient somatic inhibition to late persistent dendritic inhibition (Pouille F. & Scanziani M., 2004). These dynamic changes in dendritic inhibition are due in part to a late and persistent recruitment on SOM interneuron (OLM cell) firing during short trains of CA1 PC stimulation.

Induction of Hebbian LTP during voltage clamp recordings requires the pairing of presynaptic stimulation with postsynaptic depolarization (Perez Y. *et al.*, 2001). However, during current clamp recordings, presynaptic TBS stimulation alone is sufficient to activate mGluR1a and evoke EPSPs that trigger postsynaptic firing of action potentials in SOM interneurons, and thus, induce Hebbian LTP (Vasuta C. *et al.*, 2015). Using the TBS induction protocol in slices permits the assessment of the functional impact of Hebbian LTP in SOM interneurons. As synaptic efficacy is improved during Hebbian LTP at excitatory synapses in SOM interneurons, synaptically-evoked firing of SOM interneurons should show long-lasting increases after Hebbian LTP. Indeed, short trains of afferents stimulation in slices elicit two patterns of evoked firing in SOM interneurons (BiC and OLM cells): an onset-transient firing consistent with activation of CA3 afferents; or a late-persistent firing consistent with activation of CA1 afferents (Croce A. *et al.*, 2010). After application of the TBS induction protocol for Hebbian LTP, onset-transient responses are unchanged but late-persistent firing responses of SOM interneurons show long-term increases (Croce A. *et al.*, 2010). These long-term changes in synaptically-evoked firing are prevented by application of the selective mGluR1a antagonist LY367385 during the TBS induction (Croce A. *et al.*, 2010). These results suggest that Hebbian LTP at excitatory synapses translates into an increase in output firing of SOM interneurons (Croce A. *et al.*, 2010).

Using a similar approach during whole-cell recording of inhibitory postsynaptic currents (IPSCs) in CA1 pyramidal cells, the TBS induction protocol for Hebbian LTP produces long-term increases in postsynaptic inhibitory responses in pyramidal cells (Lapointe V. *et al.*, 2004). The long-term increase in inhibition is not accompanied by any change in excitatory postsynaptic response, and is prevented in mGluR1 knockout mice that lack Hebbian LTP in SOM interneurons (Lapointe V. *et al.*, 2004). These findings suggest that Hebbian LTP at excitatory synapses of SOM interneurons translates in long-term increases in SOM cell firing and pyramidal cell inhibition (Figure 5).

5.2. Long-term plasticity of SOM interneuron excitatory synapses controls CA1 network metaplasticity

Synaptic plasticity is bidirectionally modulated by prior cellular and/or synaptic activity, a phenomena called metaplasticity (plasticity of synaptic plasticity) (Bear M. F., 1995). In the hippocampus, long-term plasticity at SC-CA1 PC synapses is regulated by multiple metaplastic mechanisms, including both homo- and hetero-synaptic processes (Abraham W. C., 2008). In CA1, the dendrite-projecting SOM interneurons have emerged as central players in the regulation of the local network metaplasticity. Optogenetic activation of CA1 SOM interneurons (OLM cells) dampens information flow from entorhinal cortex through the TA pathway *via* direct inhibition of CA1 PCs distal dendrites, and facilitates information flow from CA3 through the SC pathway *via* inhibition of other inhibitory interneurons (Leao R. N. *et al.*, 2012). In addition, CA1 OLM cells regulate the metaplasticity of TA and SC pathways (Figure 5). Optogenetic activation of OLM cells during LTP induction decreases LTP at TA-PC synapses, whereas it facilitates LTP at SC-PC synapses (Leao R. N. *et al.*, 2012).

For Hebbian LTP at excitatory synapses onto SOM interneurons results in long-term changes in their output firing and inhibition of pyramidal cells, it should also result in long-term regulation of plasticity at SC and TA synapses onto PCs (Figure 5). Indeed, application of the TBS induction protocol for Hebbian LTP in SOM interneurons does not affect basal transmission at SC-PC synapses, but increases the magnitude of LTP at SC-PC synapses elicited 30 min later (Vasuta C. *et al.*, 2015). This facilitation of LTP at SC-PC synapses is prevented by optogenetic silencing of SOM interneurons during the TBS induction protocol, or by the mGluR1a antagonist LY367385,

suggesting that Hebbian LTP in SOM interneurons result in long-term upregulation of plasticity of SC-PC synapses (Vasuta C. *et al.*, 2015). Likewise, application of the induction protocol for mGluR1-dependent late LTP (L-LTP$_{mGluR1}$) in SOM interneurons facilitates LTP of SC-PC synapses elicited 2 hours later (Artinian J. *et al.*, 2019). This persistent facilitation of LTP at SC-PC synapses is absent in mice with conditional knock-out of *Rptor* in SOM interneurons that lack L-LTP$_{mGluR1}$, suggesting that long-term upregulation of plasticity of SC-PC synapses lasting hours results from late-LTP at excitatory synapses onto SOM interneurons (Artinian J. *et al.*, 2019). De-phosphorylation of the eukaryotic initiation factor 2 α subunit (eIF2a) by synaptic activity is a key regulator of mRNA translation and late-LTP in PCs (Costa-Mattioli M. *et al.*, 2007). Knock-in mice with a mutated non-phosphorylatable eIF2a (eIF2a^{S51A}) show facilitation of late-LTP in CA1 PCs (Costa-Mattioli M. *et al.*, 2007). Interestingly, conditional knock-in of eIF2a^{S51A} specifically in SOM interneurons, upregulates mRNA translation in SOM interneurons, reduces inhibitory synaptic transmission in CA1 PCs and facilitates induction of L-LTP at SC-PC synapses (Sharma V. *et al.*, 2020). Altogether these findings suggest that synaptic plasticity at excitatory synapses of SOM interneurons act as a long-term metaplasticity switch at SC-PCs synapses *via* disinhibition (Figure 5).

Similarly, long-term plasticity at excitatory synapses of SOM interneurons may also regulate metaplasticity of TA synapses of PCs. Application of the TBS induction protocol for Hebbian LTP in SOM interneurons does not affect basal transmission at TA-PC synapses but decreases the magnitude of LTP that is elicited 30 min later at these synapses (Sharma V. *et al.*, 2020). Importantly, this down-regulation of LTP at TA-PC synapses is increased in mice with conditional knock-in of the non-phosphorylatable eIF2a^{S51A} in SOM interneurons that result in upregulated mRNA translation in these cells and impaired inhibition of PCs (Sharma V. *et al.*, 2020). Thus, long-term plasticity at excitatory synapses of SOM interneurons may act as bidirectional long-term metaplasticity switch in the CA1 network to differentially regulate long-term plasticity of SC and TA synapses of PCs (Figure 5).

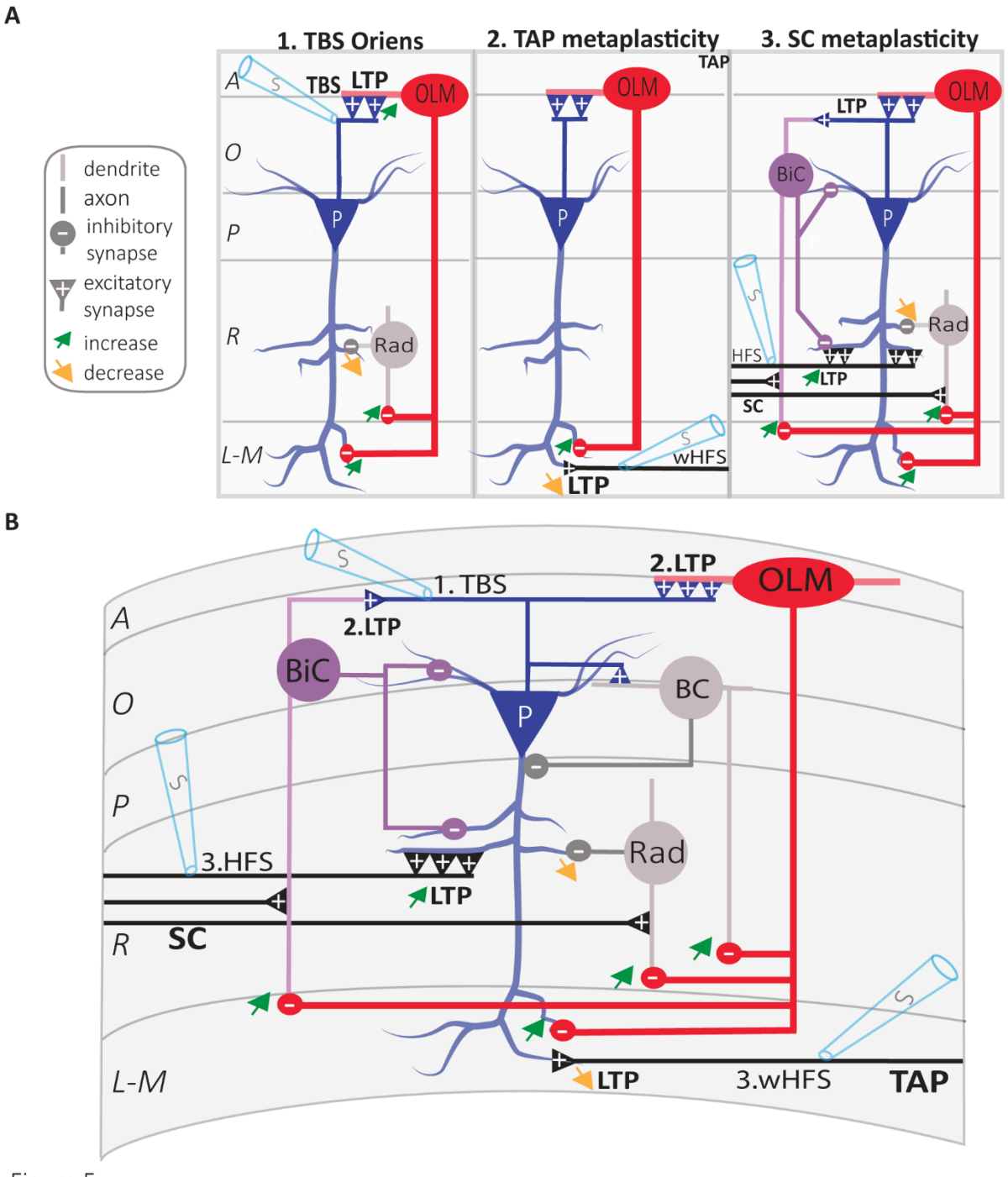

Figure 5

Figure 5. Regulation of CA1 network metaplasticity by plasticity at excitatory synapses of SOM interneurons. (A) Diagrams of synaptic plasticity of SOM interneurons and regulation of CA1 network. (A1) Theta burst stimulation (TBS) at the O/A border induces LTP of CA1 PC

synapses onto SOM interneurons (OLM cell). LTP at input synapses results in increased firing of OLM cell, which leads to increased postsynaptic inhibition of (i) PC distal dendrites and (ii) *radiatum* interneurons (rad). This leads to the increased inhibition of distal dendrites in *stratum lacunosum-moleculare* (L-M), and disinhibition of more proximal dendrites in *stratum radiatum* (R). (A2) LTP of excitatory inputs of OLM cell results in TA pathway metaplasticity. Because of distal dendritic inhibition increase, tetanization of the temporoammonic (TA) pathway produces less LTP at TA-PC synapses. (A3) LTP of excitatory inputs of OLM cell results in SC pathway metaplasticity. Because of proximal dendritic disinhibition, tetanization of Schaffer collaterals (SC) produces larger LTP at SC-PC synapses. As electrically induced TBS also produces LTP at PC-BiC synapses, the overall results on BiC inhibition of PCs remains undetermined. (B) Integration of synaptic mechanisms described above: 1. TBS of PC axons; 2. LTP at PC-OLM synapses results in more inhibition of distal PC dendrites and disinhibition of proximal PC dendrites; the end-result of LTP at PC-BiC synapses on BiC inhibition of PC remains undetermined. 3. Metaplastic changes of CA1 circuit: increased LTP at SC-PC synapses and decreased LTP at TA-PC synapses. Abbreviations for CA1 layers: A, *alveus*; O, *oriens*; P, *pyramidale*; R, *radiatum*; L-M, *lacunosum-moleculare.* Abbreviations for CA1 afferent inputs: SC, Schaffer collateral pathway; TAP, temporo-ammonic pathway. Abbreviations for SOM cell types: (red) OLM, o*riens/lacunosum-moleculare* cell; (violet) BiC, bistratified cell. Abbreviations for other cell types: (blue) P, pyramidal cell; (grey) BC, basket cell; (grey) Rad, unidentified *stratum radiatum* interneurons. Other Abbreviation: S, stimulation electrode.

6. SOM INTERNEURONS IN HIPPOCAMPUS-DEPENDENT LEARNING AND MEMORY.

At the behavioral level, the dendritic inhibition mediated by SOM interneurons plays a key role in hippocampus-dependent learning and memory (Lovett-Barron M. *et al.*, 2014). The contribution of SOM interneurons has been studied particularly in the dorsal part of CA1, in relation to the encoding of spatial and contextual memory by PCs.

A combination of *in vivo* calcium imaging with pharmacogenetic and optogenetic manipulations of SOM interneurons in CA1 hippocampus of mice revealed that dendritic inhibition by SOM interneurons is necessary for contextual fear memory formation (Lovett-Barron M. *et al.*, 2014). During contextual conditioning, aversive stimuli activate, *via* septal cholinergic inputs,

SOM interneurons that target PC dendrites. The activation of SOM interneurons leads to inhibition of PC distal dendrites that receive aversive sensory excitation from the entorhinal cortex (Lovett-Barron M. *et al.*, 2014). Inactivating dendrite-targeting SOM interneurons during aversive stimuli increases PC responses and prevents fear learning (Lovett-Barron M. *et al.*, 2014). Thus, activation of dendritic inhibition by SOM interneurons may be a mechanism for exclusion of aversive stimuli from hippocampal contextual representations that is necessary during fear learning (Lovett-Barron M. *et al.*, 2014).

Interestingly, GABAergic cells from the brainstem nucleus incertus (NI) selectively inhibit hippocampal SOM interneurons directly, and indirectly by inhibiting septal excitatory inputs to SOM interneurons (Szonyi A. *et al.*, 2019). NI GABAergic inputs to the hippocampus are activated by relevant salient environmental stimuli *in vivo* (Szonyi A. *et al.*, 2019). In addition, optogenetic manipulations of NI GABAergic neurons during contextual fear conditioning modify the strength of contextual fear memory: activation of NI GABA neurons impairs, whereas inhibition improves contextual fear memory (Szonyi A. *et al.*, 2019). Thus, SOM interneuron gating of PC TA sensory inputs during contextual learning may be regulated by the brainstem NI inhibitory system.

6.1. Long-term plasticity of SOM interneuron excitatory synapses in learning and memory

Cell-specific transgenic mouse approaches were used to test whether there is a functional role of long-term plasticity at SOM interneuron excitatory synapses in hippocampal learning and memory (Artinian J. *et al.*, 2019). Downregulation of mTORC1 activity was achieved by cell-specific conditional knock-down of the gene for the essential mTORC1 component *Rptor* in SOM interneurons, whereas upregulation of mTORC1 activity was attained by cell-specific conditional knock-down of the mTORC1 repressor *Tsc1* gene. At the behavioral level, loss of mTORC1 function specifically in SOM interneurons impaired contextual fear and spatial long-term memories, but spared sensory-motor gating, hippocampus-dependent short-term contextual memory and hippocampus-independent long-term auditory-cued fear memory (Artinian J. *et al.*, 2019). In contrast, upregulation of mTORC1 activity specifically in SOM interneurons augmented spatial and contextual fear memories, and impaired discrimination (Artinian J. *et al.*, 2019).

As mentioned before, at the cellular level, bidirectional regulation of mTORC1 activity in SOM interneurons differentially regulates mGluR1-mediated late-LTP at SOM interneurons excitatory synapses, whereas at the network level, the SOM interneuron late-LTP induction protocol upregulates metaplasticity of the SC pathway in PCs, in a mTORC1-dependent manner. Moreover, using *ex vivo* whole-cell recordings after training, contextual fear learning was found to persistently increase the efficacy of excitatory synapses of SOM interneurons *via* mGluR1 and mTORC1. These findings link mTORC1 to learning-induced long term plasticity of SOM interneuron excitatory synapses, regulation of CA1 network metaplasticity, and hippocampal long-term memory consolidation (Artinian J. *et al.*, 2019). Thus, long-term plasticity at SOM interneuron excitatory synapses may play a role in spatial/contextual information encoding by CA1 PCs, by promoting on a long timescale the internal representations by the hippocampal CA3 pathway while dampening external representations *via* the extrahippocampal entorhinal inputs (Artinian J. *et al.*, 2019).

Recent work manipulating another pathway to enhance memory, de-phosphorylation of the translation initiation factor eIF2a (Costa-Mattioli M. *et al.*, 2007), further support the idea that SOM interneurons synaptic plasticity is important for memory formation (Sharma V. *et al.*, 2020). Contextual fear learning reduces the phosphorylation of eIF2α in hippocampal PCs and SOM interneurons, but not in PV interneurons (Sharma V. *et al.*, 2020). Moreover, cell-specific conditional knock-in of the non-phosphorylatable $eIF2a^{S51A}$ in PCs or in SOM interneurons upregulates general mRNA translation in these cells and is sufficient to increase long-term contextual fear memory (Sharma V. *et al.*, 2020). Silencing CA1 SOM interneurons, using the inhibitory designer receptor exclusively activated by designer drug (DREADD), during the consolidation of fear memory, reverses the increase in contextual fear memory in the SOM interneurons conditional knock-in mice (Sharma V. *et al.*, 2020), indicating that hippocampal CA1 SOM interneurons are pivotal for memory consolidation. As mentioned above, these behavioral changes suggest that a reduction in eIF2a phosphorylation in SOM interneurons promotes memory formation *via* two mechanisms; first, it increases the responsiveness of PCs to SC inputs by disinhibition and thereby facilitates LTP at these synapses; and second, it suppresses LTP in the TA pathway, thereby modulating sensory inputs from entorhinal cortex (Sharma V. *et al.*, 2020). These findings suggest the existence of two autonomous and complementary memory consolidation processes mediated by eIF2a-dependent translational control in PCs and SOM

interneurons: (i) translational changes in excitatory PCs help to facilitate memory consolidation by mediating synaptic plasticity in a sparse population of CA1 PCs, and (ii) translational changes in SOM interneurons facilitate memory consolidation by gating synaptic plasticity in the CA1 PCs circuit.

6.2. Dorso-ventral differences in SOM interneuron function

The research reviewed so far on CA1 SOM interneurons and hippocampal function has been mostly concerned with interneurons of dorsal hippocampus. However, recent work suggests differences in function of CA1 SOM interneurons along the dorsoventral hippocampal axis (Siwani S. *et al.*, 2018). Targeted expression of optogenetic tools in CA1 OLM cells expressing the nicotinic receptor α2 subunit (OLMα2) was used to activate or silence these cells in freely moving mice during contextual passive avoidance tasks and novel object recognition (Siwani S. *et al.*, 2018). Activation of intermediate CA1 OLMα2 interneurons during passive avoidance learning impairs aversive memory, whereas silencing of these OLMα2 cells has no effect. In contrast, silencing of dorsal CA1 OLMα2 interneurons impairs aversive memory (Siwani S. *et al.*, 2018). For object recognition, silencing of intermediate CA1 OLMα2 interneurons during training enhances object memory, while their activation impairs it. In contrast, silencing dorsal CA1 OLMα2 cells has no effect on object memory (Siwani S. *et al.*, 2018). To summarize, in contrast to dorsal CA1, intermediate CA1 OLMα2 cell activity is not required for contextual fear memory. However, their activation reduces both contextual fear and object memory (Siwani et al., 2018). Thus, intermediate OLMα2 cells can modulate object or fear-related representations. These findings suggest that intermediate OLMα2 cells may be silenced during fear memory formation, meaning that in the intermediate CA1, the inputs from the TAP to CA1 PCs may not be dampened in the learning process. This is consistent with the memory impairment induced by the optogenetic activation of these cells during the aversive stimuli presentation or during object exploration (Siwani et al., 2018). Alternatively, the memory impairment induced by intermediate OLMα2 cell activation may mean that proper memory formation requires the activation of a sparse number of cells and that optogenetic stimulation activates many of them. Interestingly, intermediate OLMα2 cells display increased sensitivity for acetylcholine compared to dorsal CA1 OLMα2 cells which

could mean that these cells are more entrained by septal inputs and play a role in timing the inputs onto CA1 PCs. Thus, activating intermediate OLMα2 cells with optogenetics could have disrupted the proper convergence of inputs. Lastly, the increase of object recognition following intermediate OLMα2 cell inhibition during object exploration could indicate that their role is to gate the size of the engram encoding object memory, as seen in other hippocampal areas (see below Stefanelli et al., 2016), and inhibiting these cells would lead to a stronger but less precise memory. The role of SOM interneurons in contextual fear memory also appears different in the dentate gyrus (DG) than in dorsal CA1 hippocampus (Stefanelli T. *et al.*, 2016). Silencing DG SOM interneurons with inhibitory DREADD, during contextual fear conditioning, increases contextual fear memory and the size of the c-Fos expressing granule cell engram (Stefanelli T. *et al.*, 2016). Activation of DG SOM interneurons using excitatory DREADD during contextual fear training, impairs contextual fear memory and reduces the number of c-Fos expressing granule cells (Stefanelli T. *et al.*, 2016). Thus, DG SOM interneurons, most likely HIPP cells, may gate the size of the DG neuronal ensemble encoding contextual memory *via* dendritic lateral inhibition of granule cells (Stefanelli T. *et al.*, 2016).

6.3 SOM interneurons and place cells

During spatial exploration, a subset of dorsal CA1 pyramidal cells progressively display increased firing when the animal approach a specific location. Each place cell demonstrates a preference for a different location (place field) (O'Keefe J. & Dostrovsky J., 1971). Place cells are characterized by a slow ramp-like depolarization of membrane potential (*Vm*) driving increased AP discharge when the animal passes through the place field (Harvey C. D. *et al.*, 2009; Lee D. *et al.*, 2012; Bittner K. C. *et al.*, 2015). The fluctuations in PCs *Vm* drive their output firing, and the formation of place cells are mediated by synaptic potentiation of a specific subset of excitatory inputs (Bittner K. C. *et al.*, 2015; Sheffield M. E. J. *et al.*, 2017). In CA1 PCs, dendritic plateau potentials are generated by the coincident activation of CA3 and entorhinal cortex inputs, leading to increased output firing and LTP of perforant path synapses (Takahashi H. & Magee J. C., 2009), and the induction of place field in PCs (Bittner et al. 2015).

Inhibitory interneurons play a cardinal role in achieving input selectivity necessary to drive place cells output firing (Grienberger C. *et al.*, 2017). Optogenetic silencing of CA1 SOM or PV

interneurons, or both populations, in awake head-fixed mice, performing a spatial navigation task increases PCs output firing in their place fields, without affecting their firing rate out-of-field (Royer S. *et al.*, 2012; Grienberger C. *et al.*, 2017). This is consistent with the dendrite-targeting interneurons role in regulating complex spiking and perisomatic-targeting interneurons regulating AP timing (Royer S. *et al.*, 2012). Thus, inhibitory interneurons may be critical during place cell firing by controlling their excitatory inputs, by limiting dendritic amplification and suppressing out-of-field excitatory inputs (Grienberger C. *et al.*, 2017). By that mean, SOM interneurons participate in the control of the plasticity of specific relevant inputs (Takahashi H. & Magee J. C., 2009).

Recent works *in vivo* revealed that CA1 PCs exhibit place field plasticity following the initiation of dendritic plateau potentials occurring naturally in behaving mice or induced artificially by the injection of a depolarizing current through the recording pipette (Bittner K. C. *et al.*, 2015; Bittner K. C. *et al.*, 2017). This synaptic plasticity is termed behavioral timescale synaptic plasticity (BTSP), in which active excitatory inputs within seconds before or after the generation of dendritic plateau potentials are selectively potentiated, contrary to the classical Hebbian plasticity in which a coincident activation of the presynaptic and the postsynaptic neuron within a narrow time window is required (Bittner K. C. *et al.*, 2017; Magee J. C. & Grienberger C., 2020). BTSP can be induced *ex vivo* in hippocampal acute slices by pairing stimulations of the presynaptic input with dendritic plateau potential in the postsynaptic PC, is pathway specific and requires the activation of NMDAR and L-type Ca^{2+} channels (Bittner K. C. *et al.*, 2017; Magee J. C. & Grienberger C., 2020). Interestingly, during spatial navigation, when an animal transits from familiar to new environment, SOM interneurons-mediated dendritic inhibition transiently decreases which causes short-lasting increase in PCs dendritic excitability, whereas during the same period, PV interneurons-mediated perisomatic inhibition increases (Sheffield M. E. J. *et al.*, 2017; Sheffield M. E. & Dombeck D. A., 2019). Notably, the transient decrease in dendritic inhibition may serve as a time window in which increased dendritic plateau potentials in PCs promotes synaptic potentiation to occur in selective inputs to drive place output firing once the inhibitory system recovers in the familiar environment.

Hence, SOM interneurons have a determining role in place field formation by regulating dendritic plateau potentials and synaptic plasticity induction in selective excitatory inputs necessary for network adaptation to environmental changes.

7. SOM INTERNEURONS AND ASTROCYTES

In addition to pre- and post-synaptic neurons, glial cells and particularly astrocytes can actively modulate synaptic transmission in hippocampal circuits through bidirectional communication with neurons. The term "tripartite synapse" (Araque A. *et al.*, 1999) encompasses the structural enwrapping of the synaptic cleft that allows astrocytes to sense neuronal activity through membrane receptors, leading to spatiotemporally coordinated fluctuations of intracellular Ca^{2+} levels and their ability to trigger gliotransmitters release (Araque A. *et al.*, 2014; Bazargani N. & Attwell D., 2016; Durkee C. A. & Araque A., 2019). Despite multiple interactions between inhibitory networks and excitatory circuits (Klausberger T. & Somogyi P., 2008), current understanding of the bidirectional communications between neurons and astrocytes emerged mainly from studies focusing on excitatory transmission leaving their involvement at inhibitory synapses ill-defined (Losi G. *et al.*, 2014). However recent studies indicate that astrocytes also interact dynamically with inhibitory interneurons.

Through expression of GABA receptors ($GABA_A$Rs (Egawa K. *et al.*, 2013; Ishibashi M. *et al.*, 2019) and $GABA_B$Rs (Kang J. *et al.*, 1998; Serrano A. *et al.*, 2006; Ding S. *et al.*, 2009; Haustein M. D. *et al.*, 2014; Ishibashi M. *et al.*, 2019)) and transporters (GAT-1 and GAT-3 (Borden L. A. & Caplan M. J., 1996; Ribak C. E. *et al.*, 1996; Ishibashi M. *et al.*, 2019)), astrocytes can detect and respond to GABAergic activity with Ca^{2+} oscillations (Nilsson M. *et al.*, 1993; Lia A. *et al.*, 2019). Astrocytic GABAergic Ca^{2+} activities are mediated by several mechanisms involving voltage-sensitive Ca^{2+} channels, release from internal stores, G proteins, GATs and sodium/calcium exchangers (NCXs) (Perea G. *et al.*, 2016; Ishibashi M. *et al.*, 2019; Lia A. *et al.*, 2019; Mederos S. & Perea G., 2019). GABAergic activation of astrocytes can lead to the release of various gliotransmitters such as glutamate (Kang J. *et al.*, 1998; Andersson M. *et al.*, 2007;

Mariotti L. *et al.*, 2016; Perea G. *et al.*, 2016; Mederos S. & Perea G., 2019), GABA (Lee S. *et al.*, 2010; Yoon B.-E. *et al.*, 2011), ATP (Serrano A. *et al.*, 2006; Boddum K. *et al.*, 2016; Covelo A. & Araque A., 2018; Matos M. *et al.*, 2018) or efflux of chloride (Egawa K. *et al.*, 2013) to modulate both excitatory and inhibitory transmission (Figure 6) (Perea G. *et al.*, 2016). While the heterogeneity of interneurons subtypes can give rise to diverse GABAergic signaling, we focus here on the interplay between hippocampal SOM interneurons, PCs and astrocytes.

Intense depolarization of astrocytes induces Ca^{2+} increases that potentiate miniature inhibitory postsynaptic currents (mIPSCs) in pyramidal cells (Kang J. *et al.*, 1998), that could originate at least in part from SOM interneurons with axons in *stratum radiatum* (eg. BiC). In addition, calcium uncaging in hippocampal astrocytes leads to an increase in spontaneous inhibitory postsynaptic currents (sIPSCs) frequency in *stratum radiatum* interneurons, which is induced by astrocytic glutamate release targeting kainate receptors on PCs (Liu Q. S. *et al.*, 2004). These studies show that astrocytes are well suited to establish another level of connection and regulation between inhibitory and excitatory networks in the hippocampus. Indeed GABAergic activation of hippocampal astrocytes was found to induce the release of ATP, which is converted extracellularly into adenosine in order to activate presynaptic adenosine A_1 receptors (A_1R) on PCs in the context of heterosynaptic depression at excitatory synapses of CA1 PCs (Serrano A. *et al.*, 2006). This demonstrated a functional interplay between glial and GABAergic neuronal networks during heterosynaptic plasticity.

More recently, the use of optogenetic tools (Goshen I., 2014) allowed the specific stimulation of different subtypes of interneurons to decipher the complex modulatory mechanisms of inhibitory synapses. In acute hippocampal slices, astrocytes specifically upregulate synaptic inhibition of PCs by SOM interneurons but not PV interneurons (Matos M. *et al.*, 2018). Using cell-specific expression of channelrhodopsin-2 in SOM or PV interneurons, optogenetic activation of SOM interneurons (evoking one or two action potentials) was found to induce Ca^{2+} activities in astrocyte processes mediated by $GABA_BR$ and GAT-3 (Figure 6) (Matos M. *et al.*, 2018). This in turn leads to astrocytic release of ATP, converted extracellularly into adenosine that acts on postsynaptic A_1R to upregulate SOM interneuron inhibition onto PCs (Figure 6). This suggests an endogenous astrocyte-mediated positive feedback autoregulation of SOM interneuron dendritic inhibition of PCs (Matos M. *et al.*, 2018). Importantly, this mechanism may be specific to SOM

interneuron synapses as blockers of A_1R (DPCPX) or GAT-3 (SNAP-5114) failed to affect IPSCs evoked in PCs by optogenetic activation of PV interneuron (Matos M. *et al.*, 2018). In addition, spontaneous synaptic inhibition (sIPSC) in PCs (which reflects more global inhibition of PCs coming from many interneurons subtypes), was depressed by inhibition of A_1R, GAT-3 or astrocytic Ca^{2+} oscillations (Matos M. *et al.*, 2018). These findings point toward the possible existence of multiple astrocyte-mediated modulations of synaptic inhibition originating from different interneuron subtypes.

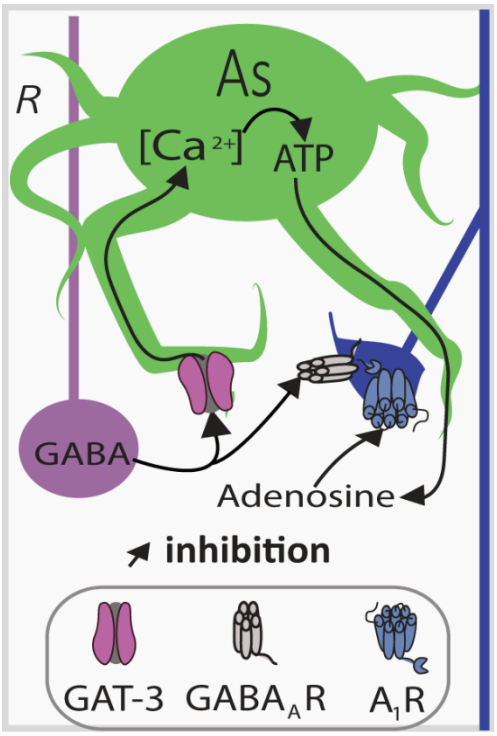

FIGURE 6. Astrocytes upregulate synaptic inhibition and excitation of PC apical dendrites via SOM interneuron GABA release. Diagram of endogenous astrocyte-mediated positive feedback autoregulation of SOM interneuron (violet) dendritic inhibition of CA1 PCs (blue) and putative regulation of excitatory inputs. Astrocytes (green) sense GABA release through the GABA transporter GAT-3 and GABABRs which induce an increase in astrocyte calcium concentration ([Ca2+]) leading to the liberation of ATP in the extracellular compartment. After its release, ATP is converted into adenosine, which then activates pyramidal cell adenosine 1 receptors (A1Rs). Activation of these receptors enhances SOM interneuron synaptic inhibition by a mechanism leading to gain of function of postsynaptic GABAARs. Parallel to this mechanism, as a consequence of Ca2+ rise, astrocytes can probably release other gliotransmitters like glutamate to coordinate different synapses (black, excitatory synapse). Abbreviations: Glut, Glutamate; R, radiatum.

Figure 6

Consistent with this concept, other groups have shown different astrocyte modulation based on interactions with specific interneuron subtype. Optogenetic activation of CA1 hippocampal astrocytes in slices increases the firing rate of CCK interneurons, but not PV interneurons, dependent on the release of ATP acting on P2Y-1R which led to inhibition of a two-pore domain potassium channel (K2P) (Tan Z. *et al.*, 2017). In contrast, optogenetic activation of astrocytic ATP release induces hyperpolarization of PCs mediated by its conversion into adenosine acting on A_1R (Tan Z. *et al.*, 2017). Interestingly in neocortex, astrocyte Ca^{2+} elevations are differentially modulated by GABAergic signaling originating from PV or SOM interneurons. Optogenetic

activation of PV interneurons induces weak Ca^{2+} elevations whereas SOM interneuron activation results in robust $GABA_B$ receptor-mediated Ca^{2+} elevations (Mariotti L. *et al.*, 2018). Moreover, these astrocyte Ca^{2+} responses present a form of plasticity, with depression of Ca^{2+} elevations upon repetitive PV interneuron stimulations and enhancement after repetitive SOM interneuron stimulations. The latter relies on somatostatin released by SOM interneurons acting on somatostatin receptors along astrocytic processes (Mariotti L. *et al.*, 2018).

Taken together these results show that astrocytes dynamically influence both the input and output of inhibitory interneurons, notably SOM interneurons, and thus, as for excitatory synapses of PCs, astrocyte do not have only a passive role in inhibitory circuits. Astrocytes are at the interface between excitatory and inhibitory synapses, and more detailed and comprehensive studies *in situ* and *in vivo* are required to refine our understanding of the inhibitory-glial-excitatory networks interplay involving SOM interneurons and its role in hippocampal synaptic plasticity and function.

8. SOM INTERNEURONS IN DISEASE

Given that hippocampal synaptic function and plasticity are impaired in brain disease with cognitive disorder, notably Alzheimer's disease (AD), SOM interneuron dysfunction may also contribute to these cognitive impairments.

In his initial observations after the death of the patient A. Deter suffering from dementia, Alois Alzheimer identified two characteristic cerebral lesions, neurofibrillary tangles made of Tau and senile plaques consisting of Aβ peptide aggregation (Graeber M. *et al.*, 1997). Accumulation of $A\beta_{1\text{-}42}$ oligomers is one of the earliest events leading to direct or indirect synaptic alterations in AD (Huang Y. & Mucke L., 2012; Mucke L. & Selkoe D. J., 2012). Electron microscopy and immunohistochemistry quantifications reported a significant decrease of synaptic density in the hippocampus of AD patients (Davies C. *et al.*, 1987; Masliah E. *et al.*, 2001). There is also a strong correlation between Aβ load in patient brain and the extent of synapse loss (Wang J. *et al.*, 1999). However, in many animal models of AD, despite cognitive alterations, these dendritic spine losses

are not always present or as pronounced as in the human form of the disease (Auld D. S. *et al.*, 2002; Elder G. A. *et al.*, 2010). Accordingly, previous works have shown that different neuronal populations such as excitatory neurons *versus* inhibitory interneurons, are differentially affected (Davies P. *et al.*, 1980; Ramos B. *et al.*, 2006). Moreover, inhibitory interneuron damage may occur before principal neuron alterations and the manifestation of symptoms. Focusing on SOM interneurons, a selective and early neurodegeneration of O-LM and HIPP cells was reported (Ramos B. *et al.*, 2006). In APP/PS1 transgenic mouse model of AD, several features of these SOM interneurons are altered. Using quantitative RT-PCR, SOM mRNA level is decreased as early as 4 months of age. Quantification of SOM interneurons showed a 60% reduction in cell numbers and the presence of dystrophic SOM interneurons in transgenic compared to wildtype animals (Ramos B. *et al.*, 2006). Importantly, these alterations precede PC loss. Moreover, SOM interneuron modifications showed a linear relationship with Aβ presence/concentration indicating that SOM interneuron loss is an early hippocampal neuropathology in this mouse model of AD.

Functional alterations of hippocampal SOM interneurons also accompany the early neuropathological changes in AD mouse model. In an elegant *in vivo* study taking advantage of Gad1-eGFP mice crossbred with APP/PS1AD mouse model, structural changes consisting of SOM interneuron axon losses were observed at 4 months of age (Schmid L. C. *et al.*, 2016). Moreover, chronic imaging of individual eGFP positive O-LM cells revealed that the normal age-dependent increase in number of SOM interneuron dendritic spines is impaired in APP/PS1 mice. As for excitatory neurons (Koffie R. M. *et al.*, 2009; Wei W. *et al.*, 2010), the reduction in SOM interneuron spine density was correlated with Aβ proximity (< 50 µm). Nevertheless, spine stability was impaired in APP/PS1 mice with a greater spine turnover associated with Aβ distance. These structural modifications may represent primary mechanisms to cope with pathological alterations of synapses during AD (Schmid L. C. *et al.*, 2016). However, contextual fear learning-associated plasticity of dendritic spines of SOM interneurons are also affected in APP/PS1 mice. *In vivo* imaging showed that, after contextual fear conditioning, the gain of SOM interneuron dendritic spines is impaired in APP/PS1 mice, and this is associated with impaired contextual fear memory, compared to control mice (Schmid L. C. *et al.*, 2016). Based on the cholinergic input that O-LM cells receive from the medial septum during aversive stimuli (Lovett-Barron M. *et al.*, 2014) and the well-documented cholinergic degeneration in AD (Auld D. S. *et al.*, 2002; Perez S. E. *et al.*, 2007), the reduction in spine formation could be an indirect result of presynaptic cholinergic

deficits. Using imaging with GCaMP6m calcium indicator, delivery of aversive air puffs in awake head-fixed mice evoked reduced Ca^{2+} responses in putative O-LM cells of APP/PS1 mice (Schmid L. C. *et al.*, 2016). These observations are consistent with the observed reduction of medial septum trans-synaptically labelled monosynaptic afferents to SOM interneurons in APP/PS1 mice. In addition, pharmacological blockade of m1AChR or chemogenetic silencing of SOM interneurons during fear conditioning were sufficient to mimic the spine gain reduction and impair fear memory in control mice. Conversely, application of the m1AChR agonist Cevimeline during fear conditioning restored fear memory in APP/PS1 mice (Schmid L. C. *et al.*, 2016). These findings demonstrate that early alterations in SOM interneuron spine plasticity may be linked to behavioral impairment and memory loss in AD. Thus, targeting presynaptic inputs or postsynaptic SOM interneurons may offer complementary therapeutic strategies. Indeed, strategies targeting somatostatin receptor subtype-4 (SSTR4) with agonists have recently been proposed to promote and restore the expression of altered subcortical mRNA genes in AD (Sandoval K. *et al.*, 2019).

Another key function of SOM interneurons is their involvement in the generation of theta rhythms, which among other hippocampal network oscillations are impaired in AD models (Villette V. *et al.*, 2010; Palop J. J. & Mucke L., 2016; Mondragon-Rodriguez S. *et al.*, 2018). An alternative to transgenic AD models is to inject directly soluble oligomers of Aβ peptide (Abo). Recently, co-injection of Aβo and AAV5-Ef1a-DIO-hChR2(ET/TC)-mCherry to SST-Cre mice hippocampi was shown to replicate theta oscillations impairments (Villette V. *et al.*, 2010; Palop J. J. & Mucke L., 2016), and optogenetic activation of SOM interneurons restored the power of theta oscillations in Aβo injected animals (Chung H. *et al.*, 2020). In addition, Aβo injection desynchronized SOM interneuron firing relative to theta oscillations, which was restored by optogenetic activation of SOM interneurons (Chung H. *et al.*, 2020). Finally, in slices from Aβo-injected animals, optogenetic stimulation of SOM interneurons enhances sIPSCs received by CA1 PCs at theta frequencies (Chung H. *et al.*, 2020). Together with the reported loss of SOM interneurons in perirhinal cortex of AD patients correlated with Aβ load (Sanchez-Mejias E. *et al.*, 2020), these findings suggest that targeting SOM interneurons may help restore network oscillations, which are heavily impacted during AD (Palop J. J. & Mucke L., 2016). Interestingly, transplantation of interneuron progenitors can restore learning and memory in APOE4-KI mice in the presence of Aβ (Tong L. M. *et al.*, 2014). Thus, maintaining proper SOM interneurons synaptic

function and plasticity could be crucial to reduce the impact of AD on cognitive functions, as soon as Aβ production starts, or even later.

CONCLUSIONS AND FUTURE DIRECTIONS

The rapid pace of development of new experimental tools for cell-specific identification and manipulation of distinct neuron types will likely provide means to address many interesting questions that remain unresolved about long-term plasticity at excitatory synapses of SOM interneurons and its role in hippocampal memory processes.

As mentioned above, hippocampal SOM interneurons are part of a group composed of many different cell types, even in a specific hippocampal region like CA1 (Pelkey K. A. *et al.*, 2017). Presently, studies on synaptic plasticity of SOM interneurons have focused largely on CA1 BiC and OLM cells (Perez Y. *et al.*, 2001; Lamsa K. P. *et al.*, 2007). However, other types of SOM interneurons include cells with both local and long-range projections (DP, BP and ORP cells) (Gulyas A. I. *et al.*, 2003; Goldin M. *et al.*, 2007; Jinno S. *et al.*, 2007). The DP cells that project to the septum, as well as other hippocampal areas, may be particularly interesting to investigate given the crucial role of septal afferents to hippocampus during spatial and contextual learning (Lovett-Barron M. *et al.*, 2014; Schmid L. C. *et al.*, 2016). Coupling of trans-synaptic monosynaptic labeling with DP cell-specific identification could be used to characterize and manipulate their excitatory synapses and potential long-term plasticity. It would be of interest to determine how plasticity of DP interneuron excitatory synapses may play a role in coordinating changes across septal and hippocampal areas during hippocampal learning.

Another interesting issue is the regional difference in function of SOM interneurons in hippocampal learning, and particularly that of OLM cells along the CA1 dorsoventral axis (Lovett-Barron M. *et al.*, 2014; Siwani S. *et al.*, 2018). The different roles of OLM cells in hippocampal learning were suggested to be due to a difference in septal cholinergic inputs along the dorsoventral

axis (Siwani S. *et al.*, 2018). As long-term plasticity of SOM interneuron synapses in hippocampal learning has been examined mostly in dorsal hippocampus (Artinian J. *et al.*, 2019), it would be of interest to examine if there is a difference in SOM interneuron long-term synaptic plasticity along the dorsal-ventral axis, and if so, does it parallels the difference in functional role of SOM interneurons in hippocampal learning.

Much progress has been achieved on characterizing Hebbian and mGluR1-mediated LTP at excitatory synapses of SOM interneurons, and its role in regulation of hippocampal network and memory (Artinian J. *et al.*, 2019). However other types of long-term synaptic plasticity occur at excitatory synapses of SOM interneurons, notably anti-Hebbian LTP at BiC and OLM cells synapses (Lamsa K. P. *et al.*, 2007), LTP at HIL cell synapses, and LTD at HIPP cell synapses (Yuan M. *et al.*, 2017). These multiple types of synaptic plasticity may each supports a different function in the formation and consolidation of hippocampus-dependent memory. Therefore, it would be important to demonstrate these roles in hippocampal function using cell-specific manipulations and hippocampal learning tasks.

Another largely unresolved question is the role of the release of the endogenous peptide SOM in SOM interneuron function. Ablation of the SOM gene or depletion of SOM by cysteamine treatment, impairs LTP in CA1 PCs and impedes contextual fear memory (Kluge C S. C., Szinyei C, Stork O, Pape HC, 2008). Similarly, blocking LTP at excitatory synapses of SOM interneurons decreases contextual fear memory and prevents facilitation of SC-PC LTP by SOM interneuron synaptic plasticity (Artinian J. *et al.*, 2019). These effects on contextual fear memory and on CA1 PC synaptic plasticity suggest a possible link between the peptide SOM and long-term plasticity at SOM interneuron excitatory synapses. This would be interesting to explore given that endogenous SOM release is considered to be activity-dependent.

Work on astrocyte regulation of SOM interneuron synapses focused largely on astrocyte interactions at inhibitory synapses made by SOM interneurons on PC dendrites (Matos M. *et al.*, 2018). However, astrocyte interactions are largely documented at excitatory synapses onto PCs and linked to regulation of long-term plasticity at these synapses (Araque A. *et al.*, 2014). Interestingly, the activity of astrocytic glutamate transporters GLT-1 and GLAST regulate mGluR1-mediated slow EPSCs in CA1 OLM cells, indicating a functional interaction of astrocytes at excitatory synapses onto SOM interneurons (Huang Y. H. *et al.*, 2004). Thus, it would be interesting to

characterize further astrocyte interactions at these excitatory synapses and determine how astrocytes may influence long-term synaptic plasticity of SOM interneurons, and consequently, hippocampal learning and memory.

Astrocytes also display functional heterogeneity, at least in term of GABAergic-induced Ca^{2+} oscillation and gliotransmitter release. Single astrocytes can be modulated by distinct mechanisms (endocannabinoids and GABA) and can release at least two different gliotransmitters (ATP/adenosine and glutamate) (Covelo A. & Araque A., 2018). Given the different astrocytic modulation uncovered with SOM and other interneuron subtypes (Mariotti L. *et al.*, 2018; Matos M. *et al.*, 2018), it raises the question whether different subtypes of astrocytes may co-exist within a brain region. Astrocyte heterogeneity has already reported between brain regions (Chai H. *et al.*, 2017; Khakh B. S. & Deneen B., 2019; Kohler S. *et al.*, 2021). However, given the different firing properties of specific interneurons, do specific firing patterns govern the astrocytic responses or is it another level of modulation? These questions still need to be addressed.

Future progress on these and other questions will likely move forward our understanding of SOM interneuron synaptic plasticity and help uncover how these specific inhibitory cells contribute to hippocampal memory processes.

Références

Abraham, W.C. (2008) Metaplasticity: tuning synapses and networks for plasticity. *Nature Reviews Neuroscience*, **9**, 387-387.

Abraham, W.C. & Bear, M.F. (1996) Metaplasticity: the plasticity of synaptic plasticity. *Trends Neurosci*, **19**, 126-130.

Abraham, W.C., Jones, O.D. & Glanzman, D.L. (2019) Is plasticity of synapses the mechanism of long-term memory storage? *NPJ Sci Learn*, **4**, 9.

Ali, A.B. & Thomson, A.M. (1998) Facilitating pyramid to horizontal oriens-alveus interneurone inputs: dual intracellular recordings in slices of rat hippocampus. *J Physiol*, **507**, 185-199.

Amilhon, B., Huh, Carey Y.L., Manseau, F., Ducharme, G., Nichol, H., Adamantidis, A. & Williams, S. (2015) Parvalbumin Interneurons of Hippocampus Tune Population Activity at Theta Frequency. *Neuron*, **86**, 1277-1289.

Andersen, P., Morris, R., Amaral, D., O'Keefe, J. & Bliss, T. (2007) *The Hippocampus Book*. Oxford University Press, USA.

Andersson, M., Blomstrand, F. & Hanse, E. (2007) Astrocytes play a critical role in transient heterosynaptic depression in the rat hippocampal CA1 region. *J Physiol*, **585**, 843-852.

Annese, J., Schenker-Ahmed, N.M., Bartsch, H., Maechler, P., Sheh, C., Thomas, N., Kayano, J., Ghatan, A., Bresler, N., Frosch, M.P., Klaming, R. & Corkin, S. (2014) Postmortem examination of patient H.M.'s brain based on histological sectioning and digital 3D reconstruction. *Nature Communications*, **5**, 3122.

Antonoudiou, P., Tan, Y.L., Kontou, G., Upton, A.L. & Mann, E.O. (2020) Parvalbumin and Somatostatin Interneurons Contribute to the Generation of Hippocampal Gamma Oscillations. *The Journal of Neuroscience*, **40**, 7668-7687.

Araque, A., Carmignoto, G., Haydon, P.G., Oliet, S.H., Robitaille, R. & Volterra, A. (2014) Gliotransmitters travel in time and space. *Neuron*, **81**, 728-739.

Araque, A., Parpura, V., Sanzgiri, R.P. & Haydon, P.G. (1999) Tripartite synapses: glia, the unacknowledged partner. *Trends Neurosci*, **22**, 208-215.

Artinian, J., Jaeger, X.D., Fellini, L., Saint Blanquat, P.d. & Roullet, P. (2007) Reactivation with a simple exposure to the experimental environment is sufficient to induce reconsolidation requiring protein synthesis in the hippocampal CA3 region in mice. *Hippocampus*, **17**, 181-191.

Artinian, J., Jordan, A., Khlaifia, A., Honore, E., La Fontaine, A., Racine, A.S., Laplante, I. & Lacaille, J.C. (2019) Regulation of Hippocampal Memory by mTORC1 in Somatostatin Interneurons. *J Neurosci*, **39**, 8439-8456.

Artinian, J. & Lacaille, J.-C. (2018) Disinhibition in learning and memory circuits: New vistas for somatostatin interneurons and long-term synaptic plasticity. *Brain Research Bulletin*, **141**, 20-26.

Asem, J.S.A. & Fortin, N.J. (2017) 1.15 - Memory for Space, Time, and Episodes☆. In Byrne, J.H. (ed) *Learning and Memory: A Comprehensive Reference (Second Edition)*. Academic Press, Oxford, pp. 255-283.

Auld, D.S., Kornecook, T.J., Bastianetto, S. & Quirion, R. (2002) Alzheimer's disease and the basal forebrain cholinergic system: relations to β-amyloid peptides, cognition, and treatment strategies. *Prog Neurobiol*, **68**, 209-245.

Barrientos, S.A. & Tiznado, V. (2016) Hippocampal CA1 Subregion as a Context Decoder. *The Journal of Neuroscience*, **36**, 6602-6604.

Battaglia, F.P., Sutherland, G.R. & McNaughton, B.L. (2004) Local Sensory Cues and Place Cell Directionality: Additional Evidence of Prospective Coding in the Hippocampus. *The Journal of Neuroscience*, **24**, 4541-4550.

Bauer, P.J. & Dugan, J.A. (2020) Chapter 18 - Memory development. In Rubenstein, J., Rakic, P., Chen, B., Kwan, K.Y. (eds) *Neural Circuit and Cognitive Development (Second Edition)*. Academic Press, pp. 395-412.

Bazargani, N. & Attwell, D. (2016) Astrocyte calcium signaling: the third wave. *Nat Neurosci*, **19**, 182-189.

Bear, M.F. (1995) Mechanism for a sliding synaptic modification threshold. *Neuron*, **15**, 1-4.

Bird, C.M. & Burgess, N. (2009) Spatial Memory: Assessment in Animals. In Squire, L.R. (ed) *Encyclopedia of Neuroscience*. Academic Press, Oxford, pp. 187-194.

Bittner, K.C., Grienberger, C., Vaidya, S.P., Milstein, A.D., Macklin, J.J., Suh, J., Tonegawa, S. & Magee, J.C. (2015) Conjunctive input processing drives feature selectivity in hippocampal CA1 neurons. *Nat Neurosci*, **18**, 1133-1142.

Bittner, K.C., Milstein, A.D., Grienberger, C., Romani, S. & Magee, J.C. (2017) Behavioral time scale synaptic plasticity underlies CA1 place fields. *Science*, **357**, 1033-1036.

Bjerknes, T. & Moser, M.B. (2013) A sense of place. *The Biologist* **66**, 10-13.

Blair, H.T., Schafe, G.E., Bauer, E.P., Rodrigues, S.M. & LeDoux, J.E. (2001) Synaptic plasticity in the lateral amygdala: a cellular hypothesis of fear conditioning. *Learn Mem*, **8**, 229-242.

Blanke, M.L. & VanDongen, A. (2009) Chapter 13: Activation mechanisms of the NMDA receptor. *Biology of the NMDA Receptor; Van Dongen, AM, Ed.; CRC Press/Taylor & Francis: Boca Raton, FL, USA*.

Blasco-Ibáñez, J.M. & Freund, T.F. (1995) Synaptic Input of Horizontal Interneurons in Stratum Oriens of the Hippocampal CA1 Subfield: Structural Basis of Feed-back Activation. *Eur J Neurosci*, **7**, 2170-2180.

Bliim, N., Leshchyns'ka, I., Sytnyk, V. & Janitz, M. (2016) Transcriptional regulation of long-term potentiation. *neurogenetics*, **17**, 201-210.

Bliss, T.V. & Lomo, T. (1973) Long-lasting potentiation of synaptic transmission in the dentate area of the anaesthetized rabbit following stimulation of the perforant path. *J Physiol*, **232**, 331-356.

Bliss, T.V.P., Collingridge, G.L., Morris, R.G.M. & Reymann, K.G. (2018) Long-term potentiation in the hippocampus: discovery, mechanisms and function. *Neuroforum*, **24**, A103-A120.

Boddum, K., Jensen, T.P., Magloire, V., Kristiansen, U., Rusakov, D.A., Pavlov, I. & Walker, M.C. (2016) Astrocytic GABA transporter activity modulates excitatory neurotransmission. *Nat Commun*, **7**, 13572.

Booker, S.A., Harada, H., Elgueta, C., Bank, J., Bartos, M., Kulik, A. & Vida, I. (2020) Presynaptic GABAB receptors functionally uncouple somatostatin interneurons from the active hippocampal network. *Elife*, **9**, e51156.

Booker, S.A., Loreth, D., Gee, A.L., Watanabe, M., Kind, P.C., Wyllie, D.J.A., Kulik, A. & Vida, I. (2018) Postsynaptic GABABRs Inhibit L-Type Calcium Channels and Abolish Long-Term Potentiation in Hippocampal Somatostatin Interneurons. *Cell Reports*, **22**, 36-43.

Booker, S.A. & Vida, I. (2018) Morphological diversity and connectivity of hippocampal interneurons. *Cell and Tissue Research*, **373**, 619-641.

Borden, L.A. & Caplan, M.J. (1996) GABA transporter heterogeneity: Pharmacology and cellular localization. *Neurochem Int*, **29**, 335-356.

Brazeau, P., Vale, W., Burgus, R., Ling, N., Butcher, M., Rivier, J. & Guillemin, R. (1973) Hypothalamic Polypeptide That Inhibits the Secretion of Immunoreactive Pituitary Growth Hormone. *Science*, **179**, 77-79.

Broca, P.-P. (1861a) Perte de la parole, ramollissement chronique et destruction partielle du lobe antérieur gauche. [Sur le siège de la faculté du langage.]. *Bulletin de la Société d"Anthropologie*, **II**, 235-238.

Broca, P.-P. (1861b) Sur le principe des localisations cérébrales. *Bulletin de la Société d'Antropologie*, **II**, 190-204.

Brown, S. & Sharpey-Schafer, E.A. (1888) XI. An investigation into the functions of the occipital and temporal lobes of the monkey's brain. *Philosophical Transactions of the Royal Society of London. (B.)*, **179**, 303-327.

Buchsbaum, B.R. & D'Esposito, M. (2017) 3.15 - Short-Term and Working Memory☆. In Byrne, J.H. (ed) *Learning and Memory: A Comprehensive Reference (Second Edition)*. Academic Press, Oxford, pp. 263-274.

Buhl, E.H., Szilágyi, T., Halasy, K. & Somogyi, P. (1996) Physiological properties of anatomically identified basket and bistratified cells in the CA1 area of the rat hippocampus in vitro. *Hippocampus*, **6**, 294-305.

Burnham, W.H. (1888) Memory, Historically and Experimentally Considered. I. An Historical Sketch of the Older Conceptions of Memory. *The American Journal of Psychology*, **2**, 39-90.

Buzsáki, G. (2002) Theta oscillations in the hippocampus. *Neuron*, **33**, 325-340.

Buzsáki, G. (2015) Hippocampal sharp wave-ripple: A cognitive biomarker for episodic memory and planning. *Hippocampus*, **25**, 1073-1188.

Buzsaki, G. & Eidelberg, E. (1982) Direct afferent excitation and long-term potentiation of hippocampal interneurons. *J Neurophysiol*, **48**, 597-607.

Buzsaki, G., Horvath, Z., Urioste, R., Hetke, J. & Wise, K. (1992) High-frequency network oscillation in the hippocampus. *Science*, **256**, 1025-1027.

Camiré, O. & Topolnik, L. (2014) Dendritic Calcium Nonlinearities Switch the Direction of Synaptic Plasticity in Fast-Spiking Interneurons. *The Journal of Neuroscience*, **34**, 3864-3877.

Cammalleri, M., Bagnoli, P. & Bigiani, A. (2019) Molecular and Cellular Mechanisms Uderlying Somatostatin-Based Signaling in Two Model Neural Networks, the Retina and the Hippocampus. *International Journal of Molecular Sciences*, **20**.

Campanac, E., Gasselin, C., Baude, A., Rama, S., Ankri, N. & Debanne, D. (2013) Enhanced Intrinsic Excitability in Basket Cells Maintains Excitatory-Inhibitory Balance in Hippocampal Circuits. *Neuron*, **77**, 712-722.

Caporale, N. & Dan, Y. (2008) Spike timing-dependent plasticity: a Hebbian learning rule. *Annu Rev Neurosci*, **31**, 25-46.

Cappaert, N.L.M., Van Strien, N.M. & Witter, M.P. (2015) Chapter 20 - Hippocampal Formation. In Paxinos, G. (ed) *The Rat Nervous System (Fourth Edition)*. Academic Press, San Diego, pp. 511-573.

Carretero-Guillén, A., Pacheco-Calderón, R., Delgado-García, J.M. & Gruart, A. (2015) Involvement of hippocampal inputs and intrinsic circuit in the acquisition of context and cues during classical conditioning in behaving rabbits. *Cereb Cortex*, **25**, 1278-1289.

Cembrowski, Mark S., Bachman, Julia L., Wang, L., Sugino, K., Shields, Brenda C. & Spruston, N. (2016) Spatial Gene-Expression Gradients Underlie Prominent Heterogeneity of CA1 Pyramidal Neurons. *Neuron*, **89**, 351-368.

Chai, H., Diaz-Castro, B., Shigetomi, E., Monte, E., Octeau, J.C., Yu, X., Cohn, W., Rajendran, P.S., Vondriska, T.M., Whitelegge, J.P., Coppola, G. & Khakh, B.S. (2017) Neural Circuit-Specialized Astrocytes: Transcriptomic, Proteomic, Morphological, and Functional Evidence. *Neuron*, **95**, 531-549 e539.

Chevaleyre, V., Takahashi, K.A. & Castillo, P.E. (2006) Endocannabinoid-mediated synaptic plasticity in the CNS. *Annu Rev Neurosci*, **29**, 37-76.

Chittajallu, R., Craig, M.T., McFarland, A., Yuan, X., Gerfen, S., Tricoire, L., Erkkila, B., Barron, S.C., Lopez, C.M., Liang, B.J., Jeffries, B.W., Pelkey, K.A. & McBain, C.J. (2013) Dual origins of functionally distinct O-LM interneurons revealed by differential 5-HT3AR expression. *Nat Neurosci*, **16**, 1598-1607.

Choi, J.H., Sim, S.E., Kim, J.I., Choi, D.I., Oh, J., Ye, S., Lee, J., Kim, T., Ko, H.G., Lim, C.S. & Kaang, B.K. (2018) Interregional synaptic maps among engram cells underlie memory formation. *Science*, **360**, 430-435.

Chung, H., Park, K., Jang, H.J., Kohl, M.M. & Kwag, J. (2020) Dissociation of somatostatin and parvalbumin interneurons circuit dysfunctions underlying hippocampal theta and gamma oscillations impaired by amyloid beta oligomers in vivo. *Brain structure & function*, **225**, 935-954.

Citri, A. & Malenka, R.C. (2008) Synaptic plasticity: multiple forms, functions, and mechanisms. *Neuropsychopharmacology*, **33**, 18-41.

Costa-Mattioli, M., Gobert, D., Stern, E., Gamache, K., Colina, R., Cuello, C., Sossin, W., Kaufman, R., Pelletier, J., Rosenblum, K., Krnjević, K., Lacaille, J.C., Nader, K. & Sonenberg, N. (2007) eIF2alpha phosphorylation bidirectionally regulates the switch from short- to long-term synaptic plasticity and memory. *Cell*, **129**, 195-206.

Costa-Mattioli, M., Sossin, W.S., Klann, E. & Sonenberg, N. (2009) Translational control of long-lasting synaptic plasticity and memory. *Neuron*, **61**, 10-26.

Covelo, A. & Araque, A. (2018) Neuronal activity determines distinct gliotransmitter release from a single astrocyte. *eLife*, **7**.

Croce, A., Pelletier, J.G., Tartas, M. & Lacaille, J.C. (2010) Afferent-specific properties of interneuron synapses underlie selective long-term regulation of feedback inhibitory circuits in CA1 hippocampus. *J Physiol*, **588**, 2091-2107.

Csaba, Z. & Dournaud, P. (2001) Cellular biology of somatostatin receptors. *Neuropeptides*, **35**, 1-23.

Danielson, N.B., Zaremba, J.D., Kaifosh, P., Bowler, J., Ladow, M. & Losonczy, A. (2016) Sublayer-Specific Coding Dynamics during Spatial Navigation and Learning in Hippocampal Area CA1. *Neuron*, **91**, 652-665.

Davies, C., Mann, D., Sumpter, P. & Yates, P. (1987) A quantitative morphometric analysis of the neuronal and synaptic content of the frontal and temporal cortex in patients with Alzheimer's disease. *J Neurol Sci*, **78**, 151-164.

Davies, C.H., Starkey, S.J., Pozza, M.F. & Collingridge, G.L. (1991) GABA autoreceptors regulate the induction of LTP. *Nature*, **349**, 609-611.

Davies, P., Katzman, R. & Terry, R.D. (1980) Reduced somatostatin-like immunoreactivity in cerebral cortex from cases of Alzheimer disease and Alzheimer senile dementa. *Nature*, **288**, 279-280.

De Bundel, D., Aourz, N., Kiagiadaki, F., Clinckers, R., Hoyer, D., Kastellakis, A., Michotte, Y., Thermos, K. & Smolders, I. (2010) Hippocampal sst1 receptors are autoreceptors and do not affect seizures in rats. *Neuroreport*, **21**, 254-258.

Degro, C.E., Kulik, A., Booker, S.A. & Vida, I. (2015) Compartmental distribution of GABAB receptor-mediated currents along the somatodendritic axis of hippocampal principal cells. *Front Synaptic Neurosci*, **7**, 6.

Delfs, J. & Dichter, M. (1983) Effects of somatostatin on mammalian cortical neurons in culture: physiological actions and unusual dose response characteristics. *J Neurosci*, **3**, 1176-1188.

Di Prisco, G.V., Huang, W., Buffington, S.A., Hsu, C.-C., Bonnen, P.E., Placzek, A.N., Sidrauski, C., Krnjević, K., Kaufman, R.J., Walter, P. & Costa-Mattioli, M. (2014) Translational control of mGluR-dependent long-term depression and object-place learning by eIF2α. *Nature Neuroscience*, **17**, 1073-1082.

Diehl, M.M., Bravo-Rivera, C. & Quirk, G.J. (2019) The study of active avoidance: A platform for discussion. *Neurosci Biobehav Rev*, **107**, 229-237.

Ding, S., Wang, T., Cui, W. & Haydon, P.G. (2009) Photothrombosis ischemia stimulates a sustained astrocytic Calcium signaling in vivo. *Glia*, **57**, 767-776.

Dudek, S.M., Alexander, G.M. & Farris, S. (2016) Rediscovering area CA2: unique properties and functions. *Nat Rev Neurosci*, **17**, 89-102.

Dudok, B., Szoboszlay, M., Paul, A., Klein, P.M., Liao, Z., Hwaun, E., Szabo, G.G., Geiller, T., Vancura, B., Wang, B.-S., McKenzie, S., Homidan, J., Klaver, L.M.F., English, D.F., Huang, Z.J., Buzsáki, G., Losonczy, A. & Soltesz, I. (2021) Recruitment and inhibitory action of hippocampal axo-axonic cells during behavior. *Neuron*, **109**, 3838-3850.e3838.

Durkee, C.A. & Araque, A. (2019) Diversity and specificity of astrocyte–neuron communication. *Neuroscience*, **396**, 73-78.

Dutar, P. & Nicoll, R.A. (1988) A physiological role for GABAB receptors in the central nervous system. *Nature*, **332**, 156-158.

Egawa, K., Yamada, J., Furukawa, T., Yanagawa, Y. & Fukuda, A. (2013) Choride homeodynamics in gap junction-coupled astrocytic networks on activation of GABAergic synapses. *J Physiol*, **591**, 3901-3917.

Ekstrom, A.D., Kahana, M.J., Caplan, J.B., Fields, T.A., Isham, E.A., Newman, E.L. & Fried, I. (2003) Cellular networks underlying human spatial navigation. *Nature*, **425**, 184-188.

Elder, G.A., Gama Sosa, M.A. & De Gasperi, R. (2010) Transgenic mouse models of Alzheimer's disease. *Mt Sinai J Med*, **77**, 69-81.

Elfant, D., Pál, B.Z., Emptage, N. & Capogna, M. (2008) Specific inhibitory synapses shift the balance from feedforward to feedback inhibition of hippocampal CA1 pyramidal cells. *Eur J Neurosci*, **27**, 104-113.

Eyre, M.D. & Bartos, M. (2019) Somatostatin-expressing interneurons form axonal projections to the contralateral hippocampus. *Front Neural Circuits*, **13**, 56.

Farris, S., Dynes, J.L. & Steward, O. (2017) 4.06 - mRNA Trafficking to Synapses and Memory Formation☆. In Byrne, J.H. (ed) *Learning and Memory: A Comprehensive Reference (Second Edition)*. Academic Press, Oxford, pp. 153-178.

Feldman, D.E. (2012) The spike-timing dependence of plasticity. *Neuron*, **75**, 556-571.

Fernández-Ruiz, A., Oliva, A., Nagy, G.A., Maurer, A.P., Berényi, A. & Buzsáki, G. (2017) Entorhinal-CA3 Dual-Input Control of Spike Timing in the Hippocampus by Theta-Gamma Coupling. *Neuron*, **93**, 1213-1226.e1215.

Ferraguti, F., Cobden, P., Pollard, M., Cope, D., Shigemoto, R., Watanabe, M. & Somogyi, P. (2004) Immunolocalization of metabotropic glutamate receptor 1α (mGluR1α) in distinct

classes of interneuron in the CA1 region of the rat hippocampus. *Hippocampus*, **14**, 193-215.

Ferrier, D. (1876) *The functions of the brain*. London Smith, Elder.

Ferster, C. & Skinner, B. (1957) Schedules of Reinforcement. New York: Appleton Century.

Flourens, M.J.P. (1842) *Recherches expérimentales sur les propriétés et les fonctions du système nerveux, dans les animaux vertébrés*. J.-B. Balliere.

Freund, T.F. & Buzsáki, G. (1996) Interneurons of the hippocampus. *Hippocampus*, **6**, 347-470.

Friend, L.N., Williamson, R.C., Merrill, C.B., Newton, S.T., Christensen, M.T., Petersen, J., Wu, B., Ostlund, I. & Edwards, J.G. (2019) Hippocampal Stratum Oriens Somatostatin-Positive Cells Undergo CB1-Dependent Long-Term Potentiation and Express Endocannabinoid Biosynthetic Enzymes. *Molecules*, **24**.

Fritsch, G. & Hitzig, E. (1870) Über die elektrische Erregbarkeit des Grosshirns. *Arch Anat Physiol Wissen*, **37**, 300-332.

Fuchs, E.C., Zivkovic, A.R., Cunningham, M.O., Middleton, S., LeBeau, F.E.N., Bannerman, David M., Rozov, A., Whittington, M.A., Traub, R.D., Rawlins, J.N.P. & Monyer, H. (2007) Recruitment of Parvalbumin-Positive Interneurons Determines Hippocampal Function and Associated Behavior. *Neuron*, **53**, 591-604.

Fyhn, M., Molden, S., Hollup, S., Moser, M.-B. & Moser, E.I. (2002) Hippocampal Neurons Responding to First-Time Dislocation of a Target Object. *Neuron*, **35**, 555-566.

Gastambide, F., Viollet, C., Lepousez, G., Epelbaum, J. & Guillou, J.-L. (2008) Hippocampal SSTR4 somatostatin receptors control the selection of memory strategies. *Psychopharmacology*, **202**, 153.

Gawel, K., Gibula, E., Marszalek-Grabska, M., Filarowska, J. & Kotlinska, J.H. (2019) Assessment of spatial learning and memory in the Barnes maze task in rodents-methodological consideration. *Naunyn Schmiedebergs Arch Pharmacol*, **392**, 1-18.

Geiller, T., Fattahi, M., Choi, J.-S. & Royer, S. (2017) Place cells are more strongly tied to landmarks in deep than in superficial CA1. *Nature Communications*, **8**, 14531.

Geva-Sagiv, M., Las, L., Yovel, Y. & Ulanovsky, N. (2015) Spatial cognition in bats and rats: from sensory acquisition to multiscale maps and navigation. *Nat Rev Neurosci*, **16**, 94-108.

Goldin, M., Epsztein, J., Jorquera, I., Represa, A., Ben-Ari, Y., Crépel, V. & Cossart, R. (2007) Synaptic Kainate Receptors Tune Oriens-Lacunosum Moleculare Interneurons to Operate at Theta Frequency. *J Neurosci*, **27**, 9560-9572.

Goshen, I. (2014) The optogenetic revolution in memory research *Trends Neurosci*, pp. 511-522.

Goutagny, R., Jackson, J. & Williams, S. (2009) Self-generated theta oscillations in the hippocampus. *Nature Neuroscience*, **12**, 1491-1493.

Graeber, M., Kösel, S., Egensperger, R., Banati, R., Müller, U., Bise, K., Hoff, P., Möller, H., Fujisawa, K. & Mehraein, P. (1997) Rediscovery of the case described by Alois Alzheimer in 1911: historical, histological and molecular genetic analysis. *Neurogenetics*, **1**, 73-80.

Grienberger, C., Milstein, A.D., Bittner, K.C., Romani, S. & Magee, J.C. (2017) Inhibitory suppression of heterogeneously tuned excitation enhances spatial coding in CA1 place cells. *Nat Neurosci*, **20**, 417-426.

Guillou, J.-L., Micheau, J. & Jaffard, R. (1993) Effects of intrahippocampal injections of somatostatin and cysteamine on spatial discrimination learning in mice. *Psychobiology*, **21**, 265-271.

Gulyas, A.I., Hajos, N., Katona, I. & Freund, T.F. (2003) Interneurons are the local targets of hippocampal inhibitory cells which project to the medial septum. *Eur J Neurosci*, **17**, 1861-1872.

Halasy, K., Buhl, E.H., Lörinczi, Z., Tamás, G. & Somogyi, P. (1996) Synaptic target selectivity and input of GABAergic basket and bistratified interneurons in the CA1 area of the rat hippocampus. *Hippocampus*, **6**, 306-329.

Han, Z.S., Buhl, E.H., Lorinczi, Z. & Somogyi, P. (1993) A high degree of spatial selectivity in the axonal and dendritic domains of physiologically identified local-circuit neurons in the dentate gyrus of the rat hippocampus. *Eur J Neurosci*, **5**, 395-410.

Hartsock, M.J., Strnad, H.K. & Spencer, R.L. (2022) Iterative Metaplasticity Across Timescales: How Circadian, Ultradian, and Infradian Rhythms Modulate Memory Mechanisms. *J Biol Rhythms*, **37**, 29-42.

Harvey, C.D., Collman, F., Dombeck, D.A. & Tank, D.W. (2009) Intracellular dynamics of hippocampal place cells during virtual navigation. *Nature*, **461**, 941-946.

Haustein, M.D., Kracun, S., Lu, X.H., Shih, T., Jackson-Weaver, O., Tong, X., Xu, J., Yang, X.W., O'Dell, T.J., Marvin, J.S., Ellisman, M.H., Bushong, E.A., Looger, L.L. & Khakh, B.S. (2014) Conditions and constraints for astrocyte calcium signaling in the hippocampal mossy fiber pathway. *Neuron*, **82**, 413-429.

He, X., Li, J., Zhou, G., Yang, J., McKenzie, S., Li, Y., Li, W., Yu, J., Wang, Y., Qu, J., Wu, Z., Hu, H., Duan, S. & Ma, H. (2021) Gating of hippocampal rhythms and memory by synaptic plasticity in inhibitory interneurons. *Neuron*, **109**, 1013-1028.e1019.

Hebb, D.O. (1949) The organization of behavior: A neuropsychological theory. . *Science Education*, **34**, 337.

Hedrick, N.G., Lu, Z., Bushong, E., Singhi, S., Nguyen, P., Magaña, Y., Jilani, S., Lim, B.K., Ellisman, M. & Komiyama, T. (2022) Learning binds new inputs into functional synaptic clusters via spinogenesis. *Nature Neuroscience*, **25**, 726-737.

Hésiode (8e-7e siecle AEC) *La théogonie d'Hésiode traduction nouvelle*. Typographie Georges Chamerot

Hippocrates (-460 a -377) *De la maladie sacrée*. Bailliere, Paris.

Hölscher, C., Anwyl, R. & Rowan, M.J. (1997) Stimulation on the Positive Phase of Hippocampal Theta Rhythm Induces Long-Term Potentiation That Can Be Depotentiated by Stimulation on the Negative Phase in Area CA1 In Vivo. *The Journal of Neuroscience*, **17**, 6470-6477.

Hosp, J.A., Struber, M., Yanagawa, Y., Obata, K., Vida, I., Jonas, P. & Bartos, M. (2014) Morpho-physiological criteria divide dentate gyrus interneurons into classes. *Hippocampus*, **24**, 189-203.

Hou, Z.-H. & Yu, X. (2013) Activity-regulated Somatostatin Expression Reduces Dendritic Spine Density and Lowers Excitatory Synaptic Transmission Via Postsynaptic Somatostatin Reptor 4. *Journal od Biological Chemistry*, **288**, 2501-2509.

Houser, C.R. (2007) Interneurons of the dentate gyrus: an overview of cell types, terminal fields and neurochemical identity. *Prog Brain Res*, **163**, 217-232.

Huang, Y. & Mucke, L. (2012) Alzheimer mechanisms and therapeutic strategies. *Cell*, **148**, 1204-1222.

Huang, Y.H., Sinha, S.R., Tanaka, K., Rothstein, J.D. & Bergles, D.E. (2004) Astrocyte glutamate transporters regulate metabotropic glutamate receptor-mediated excitation of hippocampal interneurons. *J Neurosci*, **24**, 4551-4559.

Hulme, S.R., Jones, O.D., Raymond, C.R., Sah, P. & Abraham, W.C. (2014a) Mechanisms of heterosynaptic metaplasticity. *Philos Trans R Soc Lond B Biol Sci*, **369**, 20130148.

Hulme, S.R., Jones, O.D., Raymond, C.R., Sah, P. & Abraham, W.C. (2014b) Mechanisms of heterosynaptic metaplasticity. *Philosophical Transactions of the Royal Society B: Biological Sciences*, **369**, 20130148.

Hunter, W.S. (1930) A Consideration of Lashley's Theory of the Equipotentiality of Cerebral Action. *The Journal of General Psychology*, **3**, 455-468.

Huxter, J., Burgess, N. & O'Keefe, J. (2003) Independent rate and temporal coding in hippocampal pyramidal cells. *Nature*, **425**, 828-832.

Ishibashi, M., Egawa, K. & Fukuda, A. (2019) Diverse Actions of Astrocytes in GABAergic Signaling. *Int J Mol Sci*, **20**, 2964.

Izquierdo, I., Furini, C.R.G. & Myskiw, J.C. (2016) Fear Memory. *Physiological Reviews*, **96**, 695-750.

Jarvik, M.E. & Kopp, R. (1967) An Improved One-Trial Passive Avoidance Learning Situation. *Psychological Reports*, **21**, 221-224.

Jayakumar, R.P., Madhav, M.S., Savelli, F., Blair, H.T., Cowan, N.J. & Knierim, J.J. (2019) Recalibration of path integration in hippocampal place cells. *Nature*, **566**, 533-537.

Jeffery, K.J. (2017) 3.13 - Spatial Memory. In Byrne, J.H. (ed) *Learning and Memory: A Comprehensive Reference (Second Edition)*. Academic Press, Oxford, pp. 209-231.

Jeneson, A., Mauldin, K.N. & Squire, L.R. (2010) Intact Working Memory for Relational Information after Medial Temporal Lobe Damage. *The Journal of Neuroscience*, **30**, 13624-13629.

Jeneson, A., Wixted, J.T., Hopkins, R.O. & Squire, L.R. (2012) Visual Working Memory Capacity and the Medial Temporal Lobe. *The Journal of Neuroscience*, **32**, 3584-3589.

Jinno, S., Klausberger, T., Marton, L.F., Dalezios, Y., Roberts, J.D., Fuentealba, P., Bushong, E.A., Henze, D., Buzsaki, G. & Somogyi, P. (2007) Neuronal diversity in GABAergic long-range projections from the hippocampus. *J Neurosci*, **27**, 8790-8804.

Jonas, P. & Lisman, J. (2014) Structure, function, and plasticity of hippocampal dentate gyrus microcircuits. *Frontiers in Neural Circuits*, **8**.

Joo, H.R. & Frank, L.M. (2018) The hippocampal sharp wave–ripple in memory retrieval for immediate use and consolidation. *Nature Reviews Neuroscience*, **19**, 744-757.

Josselyn & Frankland (2018) Memory allocation: Mechanisms and function. *Annual Review of Neuroscience*, **41**, 389-413.

Josselyn, S.A. & Frankland, P. (2018) Memory allocation: Mechanisms and function. *Annu Rev Neurosci*, **41**, 389-413.

Josselyn, S.A. & Tonegawa, S. (2020) Memory engrams: Recalling the past and imagining the future. *Science*, **367**.

Kandel, Dudai & Mayford (2014) The Molecular and Systems Biology of Memory. *Cell*, **157**, 163-186.

Kandel, E.R. (2001) The molecular biology of memory storage: a dialogue between genes and synapses. *Science*, **294**, 1030-1038.

Kang, J., Jiang, L., Goldman, S.A. & Nedergaard, M. (1998) Astrocyte-mediated potentiation of inhibitory synaptic transmission. *Nat Neurosci*, **1**, 683-692.

Karunakaran, S., Chowdhury, A., Donato, F., Quairiaux, C., Michel, C.M. & Caroni, P. (2016) PV plasticity sustained through D1/5 dopamine signaling required for long-term memory consolidation. *Nature Neuroscience*, **19**, 454-464.

Katona, I., Acsády, L. & Freund, T.F. (1999) Postsynaptic targets of somatostatin-immunoreactive interneurons in the rat hippocampus. *Neuroscience*, **88**, 37-55.

Katona, L., Lapray, D., Viney, Tim J., Oulhaj, A., Borhegyi, Z., Micklem, Benjamin R., Klausberger, T. & Somogyi, P. (2014) Sleep and Movement Differentiates Actions of Two Types of Somatostatin-Expressing GABAergic Interneuron in Rat Hippocampus. *Neuron*, **82**, 872-886.

Katona, L., Micklem, B., Borhegyi, Z., Swiejkowski, D.A., Valenti, O., Viney, T.J., Kotzadimitriou, D., Klausberger, T. & Somogyi, P. (2017) Behavior-dependent activity patterns of GABAergic long-range projecting neurons in the rat hippocampus. *Hippocampus*, **27**, 359-377.

Kepecs, A. & Fishell, G. (2014) Interneuron cell types are fit to function. *Nature*, **505**, 318-326.

Khakh, B.S. & Deneen, B. (2019) The Emerging Nature of Astrocyte Diversity. *Annu Rev Neurosci*, **42**, 187-207.

Kinsky, N.R., Sullivan, D.W., Mau, W., Hasselmo, M.E. & Eichenbaum, H.B. (2018) Hippocampal Place Fields Maintain a Coherent and Flexible Map across Long Timescales. *Current Biology*, **28**, 3578-3588.e3576.

Klausberger, T., Magill, P.J., Márton, L.F., Roberts, J.D.B., Cobden, P.M., Buzsáki, G. & Somogyi, P. (2003) Brain-state- and cell-type-specific firing of hippocampal interneurons in vivo. *Nature*, **421**, 844-848.

Klausberger, T., Marton, L.F., Baude, A., Roberts, J.D., Magill, P.J. & Somogyi, P. (2004) Spike timing of dendrite-targeting bistratified cells during hippocampal network oscillations in vivo. *Nat Neurosci*, **7**, 41-47.

Klausberger, T. & Somogyi, P. (2008) Neuronal diversity and temporal dynamics: The unity of hippocampal circuit operations. *Science*, **321**, 53-57.

Kluge C, S.C., Szinyei C, Stork O, Pape HC (2008) Role of the somatostatin system in contextual fear memory and hippocampal plasticity. *Learn Mem*, **3**, 252-260.

Knierim, J.J., Neunuebel, J.P. & Deshmukh, S.S. (2014) Functional correlates of the lateral and medial entorhinal cortex: objects, path integration and local-global reference frames. *Philosophical Transactions of the Royal Society B: Biological Sciences*, **369**, 20130369.

Knowlton, B.J., Siegel, A.L.M. & Moody, T.D. (2017) 3.17 - Procedural Learning in Humans☆. In Byrne, J.H. (ed) *Learning and Memory: A Comprehensive Reference (Second Edition)*. Academic Press, Oxford, pp. 295-312.

Koffie, R.M., Meyer-Luehmann, M., Hashimoto, T., Adams, K.W., Mielke, M.L., Garcia-Alloza, M., Micheva, K.D., Smith, S.J., Kim, M.L. & Lee, V.M. (2009) Oligomeric amyloid β associates with postsynaptic densities and correlates with excitatory synapse loss near senile plaques. *PNAS*, **106**, 4012-4017.

Kohler, S., Winkler, U. & Hirrlinger, J. (2021) Heterogeneity of Astrocytes in Grey and White Matter. *Neurochem Res*, **46**, 3-14.

Korotkova, T., Fuchs, E.C., Ponomarenko, A., von Engelhardt, J. & Monyer, H. (2010) NMDA Receptor Ablation on Parvalbumin-Positive Interneurons Impairs Hippocampal Synchrony, Spatial Representations, and Working Memory. *Neuron*, **68**, 557-569.

Kougioumoutzakis, A., Pelletier, J.G., Laplante, I., Khlaifia, A. & Lacaille, J.C. (2020) TRPC1 mediates slow excitatory synaptic transmission in hippocampal oriens/alveus interneurons. *Mol Brain*, **13**, 12.

Kraeuter, A.K., Guest, P.C. & Sarnyai, Z. (2019) The Y-Maze for Assessment of Spatial Working and Reference Memory in Mice. *Methods Mol Biol*, **1916**, 105-111.

Kriener, B., Hu, H. & Vervaeke, K. (2022) Parvalbumin interneuron dendrites enhance gamma oscillations. *Cell Reports*, **39**, 110948.

Krulich, L., Dhariwal, A.P.S. & McCann, S.M. (1968) Stimulatory and Inhibitory Effects of Purified Hypothalamic Extracts on Growth Hormone Release from Rat Pituitary in Vitro1. *Endocrinology*, **83**, 783-790.

Kukushkin, N.V. & Carew, T.J. (2017) Memory Takes Time. *Neuron*, **95**, 259-279.

Kullmann, D.M. & Lamsa, K.P. (2007) Long-term synaptic plasticity in hippocampal interneurons. *Nat Rev Neurosci*, **8**, 687-699.

Kullmann, D.M. & Lamsa, K.P. (2011) Interneurons go plastic. *Neuropharmacology*, **60**, 711.

Lacaille, J.C., Mueller, A.L., Kunkel, D.D. & Schwartzkroin, P.A. (1987) Local circuit interactions between oriens/alveus interneurons and CA1 pyramidal cells in hippocampal slices: electrophysiology and morphology. *J Neurosci*, **7**, 1979-1993.

Lacaille, J.C. & Williams, S. (1990) Membrane properties of interneurons in stratum oriens-alveus of the CA1 region of rat hippocampus in vitro. *Neuroscience*, **36**, 349-359.

Laezza, F. & Dingledine, R. (2004) Voltage-controlled plasticity at GluR2-deficient synapses onto hippocampal interneurons. *J Neurophysiol*, **92**, 3575-3581.

Laezza, F., Doherty, J.J. & Dingledine, R. (1999) Long-term depression in hippocampal interneurons: joint requirement for pre- and postsynaptic events. *Science*, **285**, 1411-1414.

Lamirault, L., Guillou, J.L., Micheau, J. & Jaffard, R. (2001) Intrahippocampal injections of somatostatin dissociate acquisition from the flexible use of place responses. *Eur J Neurosci*, **14**, 567-570.

Lamsa, K., Heeroma, J.H. & Kullmann, D.M. (2005) Hebbian LTP in feed-forward inhibitory interneurons and the temporal fidelity of input discrimination. *Nat Neurosci*, **8**, 916-924.

Lamsa, K.P., Heeroma, J.H., Somogyi, P., Rusakov, D.A. & Kullmann, D.M. (2007) Anti-Hebbian long-term potentiation in the hippocampal feedback inhibitory circuit. *Science*, **315**, 1262-1266.

Lapointe, V., Morin, F., Ratte, S., Croce, A., Conquet, F. & Lacaille, J.C. (2004) Synapse-specific mGluR1-dependent long-term potentiation in interneurones regulates mouse hippocampal inhibition. *J Physiol*, **555**, 125-135.

Larimer, P. & Strowbridge, B.W. (2008) Nonrandom local circuits in the dentate gyrus. *J Neurosci*, **28**, 12212-12223.

Larson, J. & Munkácsy, E. (2015) Theta-burst LTP. *Brain Research*, **1621**, 38-50.

Lashley, K.S. (1929) *Brain mechanisms and intelligence: A quantitative study of injuries to the brain*. University of Chicago Press, Chicago, IL, US.

Lasztóczi, B. & Klausberger, T. (2014) Layer-Specific GABAergic Control of Distinct Gamma Oscillations in the CA1 Hippocampus. *Neuron*, **81**, 1126-1139.

Lau, P.Y.-P., Katona, L., Saghy, P., Newton, K., Somogyi, P. & Lamsa, K.P. (2017) Long-term plasticity in identified hippocampal GABAergic interneurons in the CA1 area in vivo. *Brain Structure and Function*, **222**, 1809-1827.

Le Roux, N., Cabezas, C., Böhm, U.L. & Poncer, J.C. (2013) Input-specific learning rules at excitatory synapses onto hippocampal parvalbumin-expressing interneurons. *J Physiol*, **591**, 1809-1822.

Le Vasseur, M., Ran, I. & Lacaille, J.C. (2008) Selective induction of metabotropic glutamate receptor 1- and metabotropic glutamate receptor 5-dependent chemical long-term potentiation at oriens/alveus interneuron synapses of mouse hippocampus. *Neuroscience*, **151**, 28-42.

Leao, R.N., Mikulovic, S., Leao, K.E., Munguba, H., Gezelius, H., Enjin, A., Patra, K., Eriksson, A., Loew, L.M., Tort, A.B. & Kullander, K. (2012) OLM interneurons differentially modulate CA3 and entorhinal inputs to hippocampal CA1 neurons. *Nat Neurosci*, **15**, 1524-1530.

Lee, D., Lin, B.J. & Lee, A.K. (2012) Hippocampal place fields emerge upon single-cell manipulation of excitability during behavior. *Science*, **337**, 849-853.

Lee, S.-H., Marchionni, I., Bezaire, M., Varga, C., Danielson, N., Lovett-Barron, M., Losonczy, A. & Soltesz, I. (2014) Parvalbumin-Positive Basket Cells Differentiate among Hippocampal Pyramidal Cells. *Neuron*, **82**, 1129-1144.

Lee, S., Yoon, B.-E., Berglund, K., Oh, S.-J., Park, H., Shin, H.-S., Augustine, G.J. & Lee, C.J. (2010) Channel-mediated tonic GABA release from glia. *Science*, **330**, 790-796.

Li, Y., Xu, J., Liu, Y., Zhu, J., Liu, N., Zeng, W., Huang, N., Rasch, M.J., Jiang, H., Gu, X., Li, X., Luo, M., Li, C., Teng, J., Chen, J., Zeng, S., Lin, L. & Zhang, X. (2017) A distinct entorhinal cortex to hippocampal CA1 direct circuit for olfactory associative learning. *Nature Neuroscience*, **20**, 559-570.

Lia, A., Zonta, M., Requie, L.M. & Carmignoto, G. (2019) Dynamic interactions between GABAergic and astrocytic networks. *Neuroscience Letters*, **689**, 14-20.

Liguz-Lecznar, M., Urban-Ciecko, J. & Kossut, M. (2016) Somatostatin and Somatostatin-Containing Neurons in Shaping Neuronal Activity and Plasticity. *Front Neural Circuits*, **10**.

Liu, Q.S., Xu, Q., Arcuino, G., Kang, J. & Nedergaard, M. (2004) Astrocyte-mediated activation of neuronal kainate receptors. *PNAS USA*, **101**, 3172-3177.

Losi, G., Mariotti, L. & Carmignoto, G. (2014) GABAergic interneuron to astrocyte signalling: A neglected form of cell communication in the brain. *Philos Trans R Soc Lond B Biol Sci*, **369**, 20130609.

Lovett-Barron, M., Kaifosh, P., Kheirbek, M.A., Danielson, N., Zaremba, J.D., Reardon, T.R., Turi, G.F., Hen, R., Zemelman, B.V. & Losonczy, A. (2014) Dendritic inhibition in the hippocampus supports fear learning. *Science*, **343**, 857-863.

Lovett-Barron, M., Turi, G.F., Kaifosh, P., Lee, P.H., Bolze, F., Sun, X.H., Nicoud, J.F., Zemelman, B.V., Sternson, S.M. & Losonczy, A. (2012) Regulation of neuronal input transformations by tunable dendritic inhibition. *Nat Neurosci*, **15**, 423-430, S421-423.

Luján, R., Nusser, Z., Roberts, J.D.B., Shigemoto, R. & Somogyi, P. (1996) Perisynaptic Location of Metabotropic Glutamate Receptors mGluR1 and mGluR5 on Dendrites and Dendritic Spines in the Rat Hippocampus. *Eur J Neurosci*, **8**, 1488-1500.

Maccaferri, G., David, J., Roberts, B., Szucs, P., Cottingham, C.A. & Somogyi, P. (2000) Cell surface domain specific postsynaptic currents evoked by identified GABAergic neurones in rat hippocampus in vitro. *J Physiol*, **524**, 91-116.

Maccaferri, G. & McBain, C.J. (1996) Long-term potentiation in distinct subtypes of hippocampal nonpyramidal neurons. *J Neurosci*, **16**, 5334-5343.

Magee, J.C. & Grienberger, C. (2020) Synaptic Plasticity Forms and Functions. *Annu Rev Neurosci*, **43**, 95-117.

Maguire, E.A., Gadian, D.G., Johnsrude, I.S., Good, C.D., Ashburner, J., Frackowiak, R.S.J. & Frith, C.D. (2000) Navigation-related structural change in the hippocampi of taxi drivers. *Proceedings of the National Academy of Sciences*, **97**, 4398-4403.

Malenka, R.C. & Bear, M.F. (2004) LTP and LTD: an embarrassment of riches. *Neuron*, **44**, 5-21.

Mankin, Emily A., Diehl, Geoffrey W., Sparks, Fraser T., Leutgeb, S. & Leutgeb, Jill K. (2015) Hippocampal CA2 Activity Patterns Change over Time to a Larger Extent than between Spatial Contexts. *Neuron*, **85**, 190-201.

Mariotti, L., Losi, G., Lia, A., Melone, M., Chiavegato, A., Gómez-Gonzalo, M., Sessolo, M., Bovetti, S., Forli, A., Zonta, M., Requie, L.M., Marcon, I., Pugliese, A., Viollet, C., Bettler, B., Fellin, T., Conti, F. & Carmignoto, G. (2018) Interneuron-specific signaling evokes distinctive somatostatin-mediated responses in adult cortical astrocytes. *Nat Commun*, **9**, 82.

Mariotti, L., Losi, G., Sessolo, M., Marcon, I. & Carmignoto, G. (2016) The inhibitory neurotransmitter GABA evokes long-lasting Ca(2+) oscillations in cortical astrocytes. *Glia*, **64**, 363-373.

Masliah, E., Mallory, M., Alford, M., DeTeresa, R., Hansen, L., McKeel, D. & Morris, J. (2001) Altered expression of synaptic proteins occurs early during progression of Alzheimer's disease. *Neurology*, **56**, 127-129.

Matos, M., Bosson, A., Riebe, I., Reynell, C., Vallée, J., Laplante, I., Panatier, A., Robitaille, R. & Lacaille, J.-C. (2018) Astrocytes detect and upregulate transmission at inhibitory synapses of somatostatin interneurons onto pyramidal cells. *Nat commun*, **9**, 1-15.

Matsuzaki, M., Honkura, N., Ellis-Davies, G.C. & Kasai, H. (2004) Structural basis of long-term potentiation in single dendritic spines. *Nature*, **429**, 761-766.

McBain, C.J., Freund, T.F. & Mody, I. (1999) Glutamatergic synapses onto hippocampal interneurons: precision timing without lasting plasticity. *Trends Neurosci*, **22**, 228-235.

McDonald, R.J. & White, N.M. (1994) Parallel information processing in the water maze: Evidence for independent memory systems involving dorsal striatum and hippocampus. *Behavioral and Neural Biology*, **61**, 260-270.

McNaughton, B.L., Barnes, C.A. & O'Keefe, J. (1983) The contributions of position, direction, and velocity to single unit activity in the hippocampus of freely-moving rats. *Experimental Brain Research*, **52**, 41-49.

Mederos, S. & Perea, G. (2019) GABAergic-astrocyte signaling: A refinement of inhibitory brain networks. *Glia*, **67**, 1842-1851.

Melzer, S., Michael, M., Caputi, A., Eliava, M., Fuchs, E.C., Whittington, M.A. & Monyer, H. (2012) Long-range-projecting GABAergic neurons modulate inhibition in hippocampus and entorhinal cortex. *Science*, **335**, 1506-1510.

Mikulovic, S., Restrepo, C.E., Hilscher, M.M., Kullander, K. & Leao, R. (2015) Novel markers for OLM interneurons in the hippocampus. *Front Cell Neurosci*, **9**, 201.

Milner, B., Corkin, S. & Teuber, H.-L. (1968) Further analysis of the hippocampal amnesic syndrome: 14-year follow-up study of HM. *Neuropsychologia*, **6**, 215-234.

Milner, B., Squire, L.R. & Kandel, E.R. (1998) Cognitive Neuroscience and the Study of Memory. *Neuron*, **20**, 445-468.

Mondragon-Rodriguez, S., Salas-Gallardo, A., Gonzalez-Pereyra, P., Macias, M., Ordaz, B., Pena-Ortega, F., Aguilar-Vazquez, A., Orta-Salazar, E., Diaz-Cintra, S., Perry, G. & Williams, S. (2018) Phosphorylation of Tau protein correlates with changes in hippocampal theta oscillations and reduces hippocampal excitability in Alzheimer's model. *J Biol Chem*, **293**, 8462-8472.

Morris, R. (1984) Developments of a water-maze procedure for studying spatial learning in the rat. *Journal of Neuroscience Methods*, **11**, 47-60.

Morris, R.G. (2003) Long-term potentiation and memory. *Philos Trans R Soc Lond B Biol Sci*, **358**, 643-647.

Morris, R.G., Anderson, E., Lynch, G.S. & Baudry, M. (1986a) Selective impairment of learning and blockade of long-term potentiation by an N-methyl-D-aspartate receptor antagonist, AP5. *Nature*, **319**, 774-776.

Morris, R.G., Hagan, J.J. & Rawlins, J.N. (1986b) Allocentric spatial learning by hippocampectomised rats: a further test of the "spatial mapping" and "working memory" theories of hippocampal function. *Q J Exp Psychol B*, **38**, 365-395.

Morris, R.G.M., Garrud, P., Rawlins, J.N.P. & O'Keefe, J. (1982) Place navigation impaired in rats with hippocampal lesions. *Nature*, **297**, 681-683.

Moser, E.I., Krobert, K.A., Moser, M.B. & Morris, R.G. (1998) Impaired spatial learning after saturation of long-term potentiation. *Science*, **281**, 2038-2042.

Mott, D.D. & Lewis, D.V. (1991) Facilitation of the induction of long-term potentiation by GABAB receptors. *Science*, **252**, 1718-1720.

Mucke, L. & Selkoe, D.J. (2012) Neurotoxicity of amyloid beta-protein: synaptic and network dysfunction. *Cold Spring Harb Perspect Med*, **2**, a006338.

Muller, C. & Remy, S. (2014) Dendritic inhibition mediated by O-LM and bistratified interneurons in the hippocampus. *Front Synaptic Neurosci*, **6**, 23.

Müller, G.E. & Pilzecker, A. (1900) *Experimentelle beiträge zur lehre vom gedächtniss*. JA Barth.

Muller, R.U. & Kubie, J.L. (1987) The effects of changes in the environment on the spatial firing of hippocampal complex-spike cells. *J Neurosci*, **7**, 1951-1968.

Nader, K. & Hardt, O. (2009) A single standard for memory: the case for reconsolidation. *Nature Reviews Neuroscience*, **10**, 224-234.

Nader, K., Schafe, G.E. & Le Doux, J.E. (2000) Fear memories require protein synthesis in the amygdala for reconsolidation after retrieval. *Nature*, **406**, 722-726.

Nilsson, M., Eriksson, P.S., Rönnbäck, L. & Hansson, E. (1993) GABA induces Ca2+ transients in astrocytes. *Neuroscience*, **54**, 605-614.

Nyberg, N., Duvelle, É., Barry, C. & Spiers, H.J. (2022) Spatial goal coding in the hippocampal formation. *Neuron*, **110**, 394-422.

O'Keefe, J. (1976) Place units in the hippocampus of the freely moving rat. *Experimental Neurology*, **51**, 78-109.

O'Keefe, J. & Burgess, N. (1996) Geometric determinants of the place fields of hippocampal neurons. *Nature*, **381**, 425-428.

O'Keefe, J. & Dostrovsky, J. (1971) The hippocampus as a spatial map. Preliminary evidence from unit activity in the freely-moving rat. *Brain Research*, **34**, 171-175.

O'keefe, J. & Nadel, L. (1978) *The hippocampus as a cognitive map*. Oxford: Clarendon Press.

O'Keefe, J. & Recce, M.L. (1993) Phase relationship between hippocampal place units and the EEG theta rhythm. *Hippocampus*, **3**, 317-330.

O'Keefe, J. & Speakman, A. (1987) Single unit activity in the rat hippocampus during a spatial memory task. *Exp Brain Res*, **68**, 1-27.

Ognjanovski, N., Schaeffer, S., Wu, J., Mofakham, S., Maruyama, D., Zochowski, M. & Aton, S.J. (2017) Parvalbumin-expressing interneurons coordinate hippocampal network dynamics required for memory consolidation. *Nature Communications*, **8**, 15039.

Oliva, A.A., Jr., Jiang, M., Lam, T., Smith, K.L. & Swann, J.W. (2000) Novel hippocampal interneuronal subtypes identified using transgenic mice that express green fluorescent protein in GABAergic interneurons. *J Neurosci*, **20**, 3354-3368.

Olpe, H.-R., Balcar, V.J., Bittiger, H., Rink, H. & Sieber, P. (1980) Central actions of somatostatin. *Eur J Pharmacol*, **63**, 127-133.

Palop, J.J. & Mucke, L. (2016) Network abnormalities and interneuron dysfunction in Alzheimer disease. *Nat Rev Neurosci*, **17**, 777-792.

Papouin, T., Henneberger, C., Rusakov, D.A. & Oliet, S.H.R. (2017) Astroglial versus Neuronal D-Serine: Fact Checking. *Trends in Neurosciences*, **40**, 517-520.

Pavlov, I.P. (1928) *Lectures on conditioned reflexes: Twenty-five years of objective study of the higher nervous activity (behaviour) of animals*. Liverwright Publishing Corporation, New York, NY, US.

Pelkey, K.A., Chittajallu, R., Craig, M.T., Tricoire, L., Wester, J.C. & McBain, C.J. (2017) Hippocampal GABAergic Inhibitory Interneurons. *Physiol Rev*, **97**, 1619-1747.

Pelletier, J.G. & Lacaille, J.C. (2008) Long-term synaptic plasticity in hippocampal feedback inhibitory networks. *Prog Brain Res*, **169**, 241-250.

Penfield, W. & Milner, B. (1958) Memory Deficit Produced by Bilateral Lesions in the Hippocampal Zone. *A.M.A. Archives of Neurology & Psychiatry*, **79**, 475-497.

Perea, G., Gómez, R., Mederos, S., Covelo, A., Ballesteros, J.J., Schlosser, L., Hernández-Vivanco, A., Martín-Fernández, M., Quintana, R. & Rayan, A. (2016) Activity-dependent switch of GABAergic inhibition into glutamatergic excitation in astrocyte-neuron networks. *Elife*, **5**, e20362.

Perez, S.E., Dar, S., Ikonomovic, M.D., DeKosky, S.T. & Mufson, E.J. (2007) Cholinergic forebrain degeneration in the APPswe/PS1ΔE9 transgenic mouse. *Neurobiol Disease*, **28**, 3-15.

Perez, Y., Morin, F. & Lacaille, J.C. (2001) A hebbian form of long-term potentiation dependent on mGluR1a in hippocampal inhibitory interneurons. *Proc Natl Acad Sci U S A*, **98**, 9401-9406.

Pike, F.G., Goddard, R.S., Suckling, J.M., Ganter, P., Kasthuri, N. & Paulsen, O. (2000) Distinct frequency preferences of different types of rat hippocampal neurones in response to oscillatory input currents. *J Physiol*, **529**, 205-213.

Pittman, Q.J. & Siggins, G.R. (1981) Somatostatin hyperpolarizes hippocampal pyramidal cells in vitro. *Brain Res*, **221**, 402-408.

Platon (-427 a -348) *Oeuvres de Platon : Ion, Lysis, Protagoras, Phèdre , le banquet / traduction nouvelle, avec des notices et des notes*. Librairie Garnier Freres.

Pouille, F. & Scanziani, M. (2004) Routing of spike series by dynamic circuits in the hippocampus. *Nature*, **429**, 717-723.

Prévôt, T.D., Gastambide, F., Viollet, C., Henkous, N., Martel, G., Epelbaum, J., Béracochéa, D. & Guillou, J.-L. (2017) Roles of Hippocampal Somatostatin Receptor Subtypes in Stress Response and Emotionality. *Neuropsychopharmacology*, **42**, 1647-1656.

Quirk, G., Muller, R. & Kubie, J. (1990) The firing of hippocampal place cells in the dark depends on the rat's recent experience. *The Journal of Neuroscience*, **10**, 2008-2017.

Ramos, B., Baglietto-Vargas, D., del Rio, J.C., Moreno-Gonzalez, I., Santa-Maria, C., Jimenez, S., Caballero, C., Lopez-Tellez, J.F., Khan, Z.U., Ruano, D., Gutierrez, A. & Vitorica, J. (2006) Early neuropathology of somatostatin/NPY GABAergic cells in the hippocampus of a PS1xAPP transgenic model of Alzheimer's disease. *Neurobiol Aging*, **27**, 1658-1672.

Ran, I., Laplante, I., Bourgeois, C., Pepin, J., Lacaille, P., Costa-Mattioli, M., Pelletier, J., Sonenberg, N. & Lacaille, J.C. (2009) Persistent transcription- and translation-dependent long-term potentiation induced by mGluR1 in hippocampal interneurons. *J Neurosci*, **29**, 5605-5615.

Ran, I., Laplante, I. & Lacaille, J.C. (2012) CREB-dependent transcriptional control and quantal changes in persistent long-term potentiation in hippocampal interneurons. *J Neurosci*, **32**, 6335-6350.

Raven, F. & Aton, S.J. (2021) The Engram's Dark Horse: How Interneurons Regulate State-Dependent Memory Processing and Plasticity. *Frontiers in Neural Circuits*, **15**.

Ribak, C.E., Tong, W.M. & Brecha, N.C. (1996) GABA plasma membrane transporters, GAT-1 and GAT-3, display different distributions in the rat hippocampus. *J Comp Neurol*, **367**, 595-606.

Ribot, T.-A. (1881) *Les maladies de la memoire*. Paris Balliere.

Rinaldi, A., De Leonibus, E., Cifra, A., Torromino, G., Minicocci, E., De Sanctis, E., López-Pedrajas, R.M., Oliverio, A. & Mele, A. (2020) Flexible use of allocentric and egocentric spatial memories activates differential neural networks in mice. *Scientific Reports*, **10**, 11338.

Rivard, B., Li, Y., Lenck-Santini, P.P., Poucet, B. & Muller, R.U. (2004) Representation of objects in space by two classes of hippocampal pyramidal cells. *J Gen Physiol*, **124**, 9-25.

Royer, S., Zemelman, B.V., Losonczy, A., Kim, J., Chance, F., Magee, J.C. & Buzsaki, G. (2012) Control of timing, rate and bursts of hippocampal place cells by dendritic and somatic inhibition. *Nat Neurosci*, **15**, 769-775.

Ryan, T.J. & Frankland, P.W. (2022) Forgetting as a form of adaptive engram cell plasticity. *Nature Reviews Neuroscience*, **23**, 173-186.

Salat, D.H., van der Kouwe, A.J.W., Tuch, D.S., Quinn, B.T., Fischl, B., Dale, A.M. & Corkin, S. (2006) Neuroimaging H.M.: A 10-year follow-up examination. *Hippocampus*, **16**, 936-945.

Sanchez-Mejias, E., Nunez-Diaz, C., Sanchez-Varo, R., Gomez-Arboledas, A., Garcia-Leon, J.A., Fernandez-Valenzuela, J.J., Mejias-Ortega, M., Trujillo-Estrada, L., Baglietto-Vargas, D., Moreno-Gonzalez, I., Davila, J.C., Vitorica, J. & Gutierrez, A. (2020) Distinct disease-sensitive GABAergic neurons in the perirhinal cortex of Alzheimer's mice and patients. *Brain Pathol*, **30**, 345-363.

Sanderson, T.M. (2012) Molecular mechanisms involved in depotentiation and their relevance to schizophrenia. *Chonnam Med J*, **48**, 1-6.

Sandoval, K., Umbaugh, D., House, A., Crider, A. & Witt, K. (2019) Somatostatin Receptor Subtype-4 Regulates mRNA Expression of Amyloid-Beta Degrading Enzymes and Microglia Mediators of Phagocytosis in Brains of 3xTg-AD Mice. *Neurochem Res*, **44**, 2670-2680.

Savanthrapadian, S., Meyer, T., Elgueta, C., Booker, S.A., Vida, I. & Bartos, M. (2014) Synaptic properties of SOM- and CCK-expressing cells in dentate gyrus interneuron networks. *J Neurosci*, **34**, 8197-8209.

Schacter, D.L., Eich, J.E. & Tulving, E. (1978) Richard Semon's theory of memory. *Journal of Verbal Learning and Verbal Behavior*, **17**, 721-743.

Scharfman, H. & Schwartzkroin, P.A. (1988) Further studies of the effects of somatostatin and related peptides in area CA1 of rabbit hippocampus. *Cell Mol Biol*, **8**, 411-429.

Scharfman, H.E. & Schwartzkroin, P.A. (1989) Selective depression of GABA-mediated IPSPs by somatostatin in area CA1 of rabbit hippocampal slices. *Brain Res*, **493**, 205-211.

Schettini, G. (1991) Brain somatostatin: Receptor-coupled transducing mechanisms and role in cognitive functions. *Pharmacol Res*, **23**, 203-215.

Schmid, L.C., Mittag, M., Poll, S., Steffen, J., Wagner, J., Geis, H.R., Schwarz, I., Schmidt, B., Schwarz, M.K., Remy, S. & Fuhrmann, M. (2016) Dysfunction of Somatostatin-Positive Interneurons Associated with Memory Deficits in an Alzheimer's Disease Model. *Neuron*, **92**, 114-125.

Schmidt, M.V., Abraham, W.C., Maroun, M., Stork, O. & Richter-Levin, G. (2013) Stress-induced metaplasticity: from synapses to behavior. *Neuroscience*, **250**, 112-120.

Scoville, W.B. & Milner, B. (1957) Loss of recent memory after bilateral hippocampal lesions. *J Neurol Neurosurg Psychiatry*, **20**, 11-21.

Semon, R. (1904) Dze Mneme als erhaltendes Prznzip zm Wechsel des organischen Geschehens. Leipzig.

Serrano, A., Haddjeri, N., Lacaille, J.-C. & Robitaille, R. (2006) GABAergic Network Activation of Glial Cells Underlies Hippocampal Heterosynaptic Depression. *J Neurosci*, **16**, 5073-5081.

Sharif, F., Tayebi, B., Buzsáki, G., Royer, S. & Fernandez-Ruiz, A. (2021) Subcircuits of Deep and Superficial CA1 Place Cells Support Efficient Spatial Coding across Heterogeneous Environments. *Neuron*, **109**, 363-376.e366.

Sharma, V., Sood, R., Khlaifia, A., Eslamizade, M.J., Hung, T.-Y., Lou, D., Asgarihafshejani, A., Lalzar, M., Kiniry, S.J., Stokes, M.P., Cohen, N., Nelson, A.J., Abell, K., Possemato, A.P., Gal-Ben-Ari, S., Truong, V.T., Wang, P., Yiannakas, A., Saffarzadeh, F., Cuello, A.C., Nader, K., Kaufman, R.J., Costa-Mattioli, M., Baranov, P.V., Quintana, A., Sanz, E., Khoutorsky, A., Lacaille, J.-C., Rosenblum, K. & Sonenberg, N. (2020) eIF2α controls memory consolidation via excitatory and somatostatin neurons. *Nature*, **586**, 412-416.

Sheffield, M.E. & Dombeck, D.A. (2019) Dendritic mechanisms of hippocampal place field formation. *Curr Opin Neurobiol*, **54**, 1-11.

Sheffield, M.E.J., Adoff, M.D. & Dombeck, D.A. (2017) Increased Prevalence of Calcium Transients across the Dendritic Arbor during Place Field Formation. *Neuron*, **96**, 490-504 e495.

Shigemoto, R., Kulik, A., Roberts, J.D.B., Ohishi, H., Nusser, Z., Kaneko, T. & Somogyi, P. (1996) Target-cell-specific concentration of a metabotropic glutamate receptor in the presynaptic active zone. *Nature*, **381**, 523-525.

Siegle, J.H. & Wilson, M.A. (2014) Enhancement of encoding and retrieval functions through theta phase-specific manipulation of hippocampus. *eLife*, **3**, e03061.

Sik, A., Penttonen, M. & Buzsaki, G. (1997) Interneurons in the hippocampal dentate gyrus: an in vivo intracellular study. *Eur J Neurosci*, **9**, 573-588.

Siwani, S., França, A.S.C., Mikulovic, S., Reis, A., Hilscher, M.M., Edwards, S.J., Leão, R.N., Tort, A.B.L. & Kullander, K. (2018) OLMα2 Cells Bidirectionally Modulate Learning. *Neuron*, **99**, 404-412.e403.

Skinner, B.F. (1974) *About behaviorism*. Vintage Books.

Soltesz, I. & Losonczy, A. (2018) CA1 pyramidal cell diversity enabling parallel information processing in the hippocampus. *Nature neuroscience*, **21**, 484-493.

Somogyi, P., Katona, L., Klausberger, T., Lasztóczi, B. & Viney, T.J. (2014) Temporal redistribution of inhibition over neuronal subcellular domains underlies state-dependent rhythmic change of excitability in the hippocampus. *Philosophical Transactions of the Royal Society B: Biological Sciences*, **369**, 20120518.

Somogyi, P. & Klausberger, T. (2005) Defined types of cortical interneurone structure space and spike timing in the hippocampus. *J Physiol*, **562**, 9-26.

Souques, A.A. (1936) *Etapes de la neurologie dans l'antiquité grecque: d'Homère à Galien*. Masson.

Squire, L.R. (2009) Memory and brain systems: 1969–2009. *Journal of Neuroscience*, **29**, 12711-12716.

Stacho, M. & Manahan-Vaughan, D. (2022) The Intriguing Contribution of Hippocampal Long-Term Depression to Spatial Learning and Long-Term Memory. *Frontiers in Behavioral Neuroscience*, **16**.

Stark, C. (2009) Functional Role of the Human Hippocampus. In Per Andersen, Richard Morris, David Amaral, Tim Bliss, O'Keefe, a.J. (eds) *The hippocampus book*. Oxford University Press, pp. 549-580.

Stefanelli, T., Bertollini, C., Lüscher, C., Muller, D. & Mendez, P. (2016) Hippocampal Somatostatin Interneurons Control the Size of Neuronal Memory Ensembles. *Neuron*, **89**, 1074-1085.

Strange, B.A., Witter, M.P., Lein, E.S. & Moser, E.I. (2014) Functional organization of the hippocampal longitudinal axis. *Nature Reviews Neuroscience*, **15**, 655-669.

Sun, Y., Nguyen, A.Q., Nguyen, J.P., Le, L., Saur, D., Choi, J., Callaway, Edward M. & Xu, X. (2014) Cell-Type-Specific Circuit Connectivity of Hippocampal CA1 Revealed through Cre-Dependent Rabies Tracing. *Cell Reports*, **7**, 269-280.

Sylwestrak, E.L. & Ghosh, A. (2012) Elfn1 regulates target-specific release probability at CA1-interneuron synapses. *Science*, **338**, 536-540.

Szonyi, A., Sos, K.E., Nyilas, R., Schlingloff, D., Domonkos, A., Takacs, V.T., Posfai, B., Hegedus, P., Priestley, J.B., Gundlach, A.L., Gulyas, A.I., Varga, V., Losonczy, A., Freund, T.F. & Nyiri, G. (2019) Brainstem nucleus incertus controls contextual memory formation. *Science*, **364**.

Takahashi, H. & Magee, J.C. (2009) Pathway interactions and synaptic plasticity in the dendritic tuft regions of CA1 pyramidal neurons. *Neuron*, **62**, 102-111.

Tallent, M.K. & Siggins, G.R. (1997) Somatostatin Depresses Excitatory but not Inhibitory Neurotransmission in Rat CA1 Hippocampus. *J Neurophysiol*, **78**, 3008-3018.

Tan, Z., Liu, Y., Xi, W., Lou, H.F., Zhu, L., Guo, Z., Mei, L. & Duan, S. (2017) Glia-derived ATP inversely regulates excitability of pyramidal and CCK-positive neurons. *Nat Commun*, **8**, 13772.

Tanaka, K.Z., He, H., Tomar, A., Niisato, K., Huang, A.J.Y. & McHugh, T.J. (2018) The hippocampal engram maps experience but not place. *Science*, **361**, 392-397.

Tayler, Kaycie K., Tanaka, Kazumasa Z., Reijmers, Leon G. & Wiltgen, Brian J. (2013) Reactivation of Neural Ensembles during the Retrieval of Recent and Remote Memory. *Current Biology*, **23**, 99-106.

Tazerart, S., Mitchell, D.E., Miranda-Rottmann, S. & Araya, R. (2020) A spike-timing-dependent plasticity rule for dendritic spines. *Nature Communications*, **11**, 4276.

Thomas Günther, G.T., Pascal Dournaud, Corinne Bousquet, Zsolt Csaba, Hans-Jürgen Kreienkamp, Amelie Lupp, Márta Korbonits, Justo P. Castaño, Hans-Jürgen Wester, Michael Culler, Shlomo Melmed and Stefan Schulz (2018) International Union of Basic and Clinical Pharmacology. CV. Somatostatin Receptors: Structure, Function, Ligands, and New Nomenclature. *Pharmacol Rev*, **70**, 763-835.

Thurley, K. & Ayaz, A. (2017) Virtual reality systems for rodents. *Curr Zool*, **63**, 109-119.

Tonegawa, S., Morrissey, Mark D. & and Kitamura, T. (2018) The role of engram cells in the systems consolidation of memory. *Nat Neurosci*, **19**, 485-498.

Tong, L.M., Djukic, B., Arnold, C., Gillespie, A.K., Yoon, S.Y., Wang, M.M., Zhang, O., Knoferle, J., Rubenstein, J.L., Alvarez-Buylla, A. & Huang, Y. (2014) Inhibitory interneuron progenitor transplantation restores normal learning and memory in ApoE4 knock-in mice without or with Abeta accumulation. *J Neurosci*, **34**, 9506-9515.

Topolnik, L., Azzi, M., Morin, F., Kougioumoutzakis, A. & Lacaille, J.C. (2006) mGluR1/5 subtype-specific calcium signalling and induction of long-term potentiation in rat hippocampal oriens/alveus interneurones. *J Physiol*, **575**, 115-131.

Topolnik, L., Chamberland, S., Pelletier, J.G., Ran, I. & Lacaille, J.C. (2009) Activity-dependent compartmentalized regulation of dendritic Ca2+ signaling in hippocampal interneurons. *J Neurosci*, **29**, 4658-4663.

Topolnik, L., Congar, P. & Lacaille, J.C. (2005) Differential regulation of metabotropic glutamate receptor- and AMPA receptor-mediated dendritic Ca2+ signals by presynaptic and postsynaptic activity in hippocampal interneurons. *J Neurosci*, **25**, 990-1001.

Topolnik, L. & Tamboli, S. (2022) The role of inhibitory circuits in hippocampal memory processing. *Nature Reviews Neuroscience*.

Toth, K. & McBain, C.J. (1998) Afferent-specific innervation of two distinct AMPA receptor subtypes on single hippocampal interneurons. *Nat Neurosci*, **1**, 572-578.

Tricoire, L., Pelkey, K.A., Erkkila, B.E., Jeffries, B.W., Yuan, X. & McBain, C.J. (2011) A Blueprint for the Spatiotemporal Origins of Mouse Hippocampal Interneuron Diversity. *The Journal of Neuroscience*, **31**, 10948-10970.

Tsien, J.Z. (2016) Cre-Lox Neurogenetics: 20 Years of Versatile Applications in Brain Research and Counting…. *Frontiers in Genetics*, **7**.

Tukker, J.J., Fuentealba, P., Hartwich, K., Somogyi, P. & Klausberger, T. (2007) Cell type-specific tuning of hippocampal interneuron firing during gamma oscillations in vivo. *J Neurosci*, **27**, 8184-8189.

Tyan, L., Chamberland, S., Magnin, E., Camiré, O., Francavilla, R., David, L.S., Deisseroth, K. & Topolnik, L. (2014) Dendritic Inhibition Provided by Interneuron-Specific Cells Controls the Firing Rate and Timing of the Hippocampal Feedback Inhibitory Circuitry. *J Neurosci*, **34**, 4534-4547.

Udakis, M., Pedrosa, V., Chamberlain, S.E.L., Clopath, C. & Mellor, J.R. (2020) Interneuron-specific plasticity at parvalbumin and somatostatin inhibitory synapses onto CA1 pyramidal neurons shapes hippocampal output. *Nat Commun*, **11**, 4395.

Unal, G., Crump, M.G., Viney, T.J., Éltes, T., Katona, L., Klausberger, T. & Somogyi, P. (2018) Spatio-temporal specialization of GABAergic septo-hippocampal neurons for rhythmic network activity. *Brain structure & function*, **223**, 2409-2432.

Valenti, O., Mikus, N. & Klausberger, T. (2018) The cognitive nuances of surprising events: exposure to unexpected stimuli elicits firing variations in neurons of the dorsal CA1 hippocampus. *Brain Structure and Function*, **223**, 3183-3211.

Vanderwolf, C.H. (1969) Hippocampal electrical activity and voluntary movement in the rat. *Electroencephalography and clinical neurophysiology*, **26**, 407-418.

Vandrey, B., Duncan, S. & Ainge, J.A. (2021) Object and object-memory representations across the proximodistal axis of CA1. *Hippocampus*, **31**, 881-896.

Varga, C., Golshani, P. & Soltesz, I. (2012) Frequency-invariant temporal ordering of interneuronal discharges during hippocampal oscillations in awake mice. *PNAS*, **109**, E2726-E2734.

Vasuta, C., Artinian, J., Laplante, I., Hebert-Seropian, S., Elayoubi, K. & Lacaille, J.C. (2015) Metaplastic Regulation of CA1 Schaffer Collateral Pathway Plasticity by Hebbian MGluR1a-Mediated Plasticity at Excitatory Synapses onto Somatostatin-Expressing Interneurons. *eNeuro*, **2**.

Vécsei, L., Király, C., Bollók, I., Nagy, A., Varga, J., Penke, B. & Telegdy, G. (1984) Comparative studies with somatostatin and cysteamine in different behavioral tests on rats. *Pharmacol Biochem Behav*, **21**, 833-837.

Vécsei, L., Pavo, I., Zsigo, J., Penke, B. & Widerlöv, E. (1989) Comparative studies of somatostatin-14 and some of its fragments on passive avoidance behavior, open field activity and on barrel rotation phenomenon in rats. *Peptides*, **10**, 1153-1157.

Vécsei, L. & Widerlöv, E. (1988) Effects of intracerebroventricularly administered somatostatin on passive avoidance, shuttle-box behaviour and open-field activity in rats. *Neuropeptides*, **12**, 237-242.

Vezzani, A., Ruiz, R., Monno, A., Rizzi, M., Lindefors, N., Samanin, R. & Brodin, E. (1993) Extracellular Somatostatin Measured by Microdialysis in the Hippocampus of Freely Moving Rats: Evidence for Neuronal Release. *J Neurochem*, **60**, 671-677.

Villette, V., Poindessous-Jazat, F., Simon, A., Lena, C., Roullot, E., Bellessort, B., Epelbaum, J., Dutar, P. & Stephan, A. (2010) Decreased rhythmic GABAergic septal activity and memory-associated theta oscillations after hippocampal amyloid-beta pathology in the rat. *J Neurosci*, **30**, 10991-11003.

Vogel-Ciernia, A. & Wood, M.A. (2014) Examining Object Location and Object Recognition Memory in Mice. *Current Protocols in Neuroscience*, **69**, 8.31.31-38.31.17.

Wang, J., Dickson, D.W., Trojanowski, J.Q. & Lee, V.M.-Y. (1999) The levels of soluble versus insoluble brain Aβ distinguish Alzheimer's disease from normal and pathologic aging. *Exp Neurol*, **158**, 328-337.

Watson, J.B. (1930) *Behaviorism, Rev. ed*. W W Norton & Co, New York, NY, US.

Wei, W., Nguyen, L.N., Kessels, H.W., Hagiwara, H., Sisodia, S. & Malinow, R. (2010) Amyloid beta from axons and dendrites reduces local spine number and plasticity. *Nat Neurosci*, **13**, 190-196.

Whitlock, J.R., Heynen, A.J., Shuler, M.G. & Bear, M.F. (2006) Learning induces long-term potentiation in the hippocampus. *Science*, **313**, 1093-1097.

Wierenga, C.J. & Wadman, W.J. (2003) Excitatory inputs to CA1 interneurons show selective synaptic dynamics. *J Neurophysiol*, **90**, 811-821.

Wigstrom, H. & Gustafsson, B. (1983) Facilitated induction of hippocampal long-lasting potentiation during blockade of inhibition. *Nature*, **301**, 603-604.

Wintzer, M.E., Boehringer, R., Polygalov, D. & McHugh, T.J. (2014) The Hippocampal CA2 Ensemble Is Sensitive to Contextual Change. *The Journal of Neuroscience*, **34**, 3056-3066.

Wulff, P., Ponomarenko, A.A., Bartos, M., Korotkova, T.M., Fuchs, E.C., Bähner, F., Both, M., Tort, A.B.L., Kopell, N.J., Wisden, W. & Monyer, H. (2009) Hippocampal theta rhythm and its coupling with gamma oscillations require fast inhibition onto parvalbumin-positive interneurons. *Proceedings of the National Academy of Sciences*, **106**, 3561-3566.

Yassa, M.A. & Stark, C.E. (2011) Pattern separation in the hippocampus. *Trends Neurosci*, **34**, 515-525.

Yoon, B.-E., Jo, S., Woo, J., Lee, J.-H., Kim, T., Kim, D. & Lee, C.J. (2011) The amount of astrocytic GABA positively correlates with the degree of tonic inhibition in hippocampal CA1 and cerebellum. *Mol Brain*, **4**, 1-7.

Yuan, M., Meyer, T., Benkowitz, C., Savanthrapadian, S., Ansel-Bollepalli, L., Foggetti, A., Wulff, P., Alcami, P., Elgueta, C. & Bartos, M. (2017) Somatostatin-positive interneurons in the dentate gyrus of mice provide local- and long-range septal synaptic inhibition. *Elife*, **6**.

Zelikowsky, M., Pham, D.L. & Fanselow, M.S. (2012) Temporal factors control hippocampal contributions to fear renewal after extinction. *Hippocampus*, **22**, 1096-1106.

Zemankovics, R., Veres, J.M., Oren, I. & Hájos, N. (2013) Feedforward Inhibition Underlies the Propagation of Cholinergically Induced Gamma Oscillations from Hippocampal CA3 to CA1. *The Journal of Neuroscience*, **33**, 12337-12351.

Zlotnik, G. & Vansintjan, A. (2019) Memory: An Extended Definition. *Frontiers in Psychology*, **10**.

1.8 Objectifs de la thèse

Vue d'ensemble du sujet de thèse

Comme nous l'avons vu, la mémoire explicite émerge de l'acheminement approprié de l'information à travers le réseau hippocampique, et la formation d'un assemblage persistant en un réseau de neurones qui encode un souvenir (Kandel *et al.*, 2014). Ces assemblages de neurones, également nommés engrammes, sont formés par une population discrète de neurones excitateurs, entre lesquels une potentialisation de la transmission synaptique s'opère lors de l'apprentissage (Josselyn & Frankland, 2018; Tonegawa *et al.*, 2018). Cependant, nous ne savons toujours pas clairement comment ces engrammes ne se forment ni pourquoi un neurone est sélectionné parmi ceux qui l'entourent. Depuis plusieurs années, de plus en plus d'études se tournent vers les interneurones, qui modulent l'activité des cellules excitatrices. D'une part, ils contrôlent leurs intégrations en inhibant leurs afférences ou dendrites, en les facilitant par des mécanismes de désinhibition (inhibition d'autres interneurones inhibiteurs), ou encore en les synchronisant. Les interneurones contrôlent aussi les sorties des cellules pyramidales via l'inhibition de leurs corps cellulaires ou de leurs axones pour synchroniser les ensembles neuronaux (Pelkey K. A. *et al.*, 2017; Artinian J. & Lacaille J.-C., 2018; Honoré E. *et al.*, 2021; Raven F. & Aton S. J., 2021; Topolnik L. & Tamboli S., 2022).

Dans leur ensemble, mes travaux visent à mieux comprendre le rôle spécifique des interneurones de l'aire CA1 de l'hippocampe dans le contrôle dynamique des fonctions mnésiques de l'hippocampe. Notre hypothèse est que les différents interneurones, notamment les interneurones somatostatinergiques et parvalbuminergiques, et les types spécifiques de plasticité qu'ils expriment, contrôlent des aspects différents des fonctions de l'hippocampe. Nous verrons dans les prochains chapitres comment nos résultats apportent des éléments de réponse à cette question.

Problématique :

I. Rôle des interneurones somatostatinergiques

Parmi les différents types d'interneurones qui peuplent l'aire CA1 de l'hippocampe, un sous-ensemble exprimant la somatostatine (SOM-INs) est particulièrement intéressant dans ce contexte, car l'activité de ces interneurones est nécessaire à la formation de la mémoire contextuelle de peur (Lovett-Barron M. *et al.*, 2014). Leurs afférences excitatrices montrent une potentialisation à long terme (PLT) particulière, dépendante des récepteurs métabotropiques au glutamate mGluR1a, et de la traduction via mTORC1 (Ran I. *et al.*, 2009). Cette PLT spécifique aux synapses entre les cellules excitatrices locales, les cellules pyramidales (CP), et les SOM-INs (synapses CP-SOM) est induite par le conditionnement à la peur contextuelle et régule la formation de la mémoire contextuelle de peur et la mémoire spatiale (Artinian et al. 2019). Cependant, nous ne savons pas si cette PLT est 1) nécessaire à la bonne formation des mémoires contextuelle de peur et spatiale, 2) ni si elle est induite lors de l'acquisition ou de la consolidation de ces mémoires.

Notre hypothèse est que lors de l'apprentissage des mémoires contextuelles de peur (chapitre II) et spatiales (Chapitre IV), une PLT hebbienne des synapses CP-SOM de CA1 est induite, et que cette PLT provoque des modifications du réseau de l'hippocampe.

Ainsi, le premier objectif de cette thèse est de déterminer le rôle de la plasticité synaptique des interneurones SOM dans l'apprentissage et la mémoire dépendants de l'hippocampe, et d'approfondir nos connaissances sur les mécanismes de cette PLT.

II. Rôle des interneurone parvalbuminergiques.

Un autre type principal d'interneurones de l'aire CA1 de l'hippocampe, les interneurones parvalbuminergiques, ciblent les corps cellulaires et dendrites proximales des CP (Pelkey K. A. *et al.*, 2017; Booker S. A. & Vida I., 2018). Leur activité est nécessaire à la consolidation de la mémoire contextuelle de peur (Ognjanovski N. *et al.*, 2017). Les PV-INs démontrent de la plasticité synaptique à leurs afférences excitatrices principales, les collatérales de Schaffer (Campanac E. *et al.*, 2013). De plus la stimulation à haute fréquence de ces afférences induit dans les PV-INs une potentialisation à long terme de l'excitabilité intrinsèque (PLT_{EI}) (Campanac E. *et al.*, 2013). La PLT_{EI} est dépendante de l'activation des récepteurs mGluR5 et est sensible à la rapamycine, un inhibiteur de mTORC1 (Campanac E. *et al.*, 2013). Étant donné l'importance des PV-INs dans la consolidation de la mémoire de peur, et le rôle de la voie de signalisation de mTORC1 dans la PLT_{EI} des PV-INs, l'objectif de cette section est d'évaluer le rôle de mTORC1 dans la plasticité à long terme de l'excitabilité intrinsèque des PV-INs et dans la mémoire contextuelle de peur.

Chapitre II

Long-term potentiation at pyramidal cell to somatostatin interneuron synapses controls hippocampal network plasticity and memory

Azam Asgarihafshejani[1] #, Ève Honoré[1] #, François-Xavier Michon[1], Isabel Laplante[1], and Jean-Claude Lacaille[1]. #Contributions égales. 2022, iScience doi.org/10.1016/j.isci.2022.104259

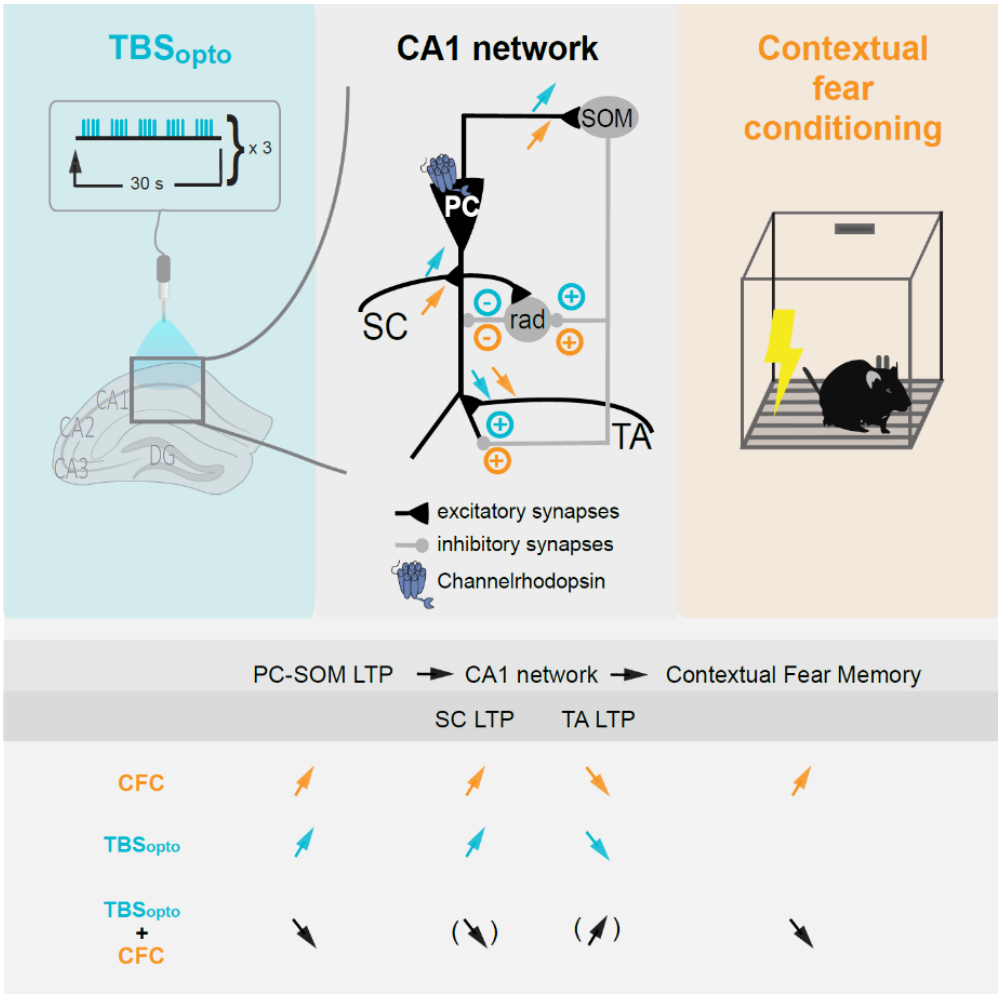

[1]Department of Neurosciences, Center for Interdisciplinary Research on Brain and Learning (CIRCA) and Research Group on Neural Signaling and Circuitry (GRSNC), Université de Montréal, Montreal, Quebec H3C 3J7, Canada

Ce chapitre présente l'article de recherche: « Long-term Potentiation at Pyramidal Cell to Somatostatin Interneuron Synapses Controls Hippocampal Network Plasticity and Memory ». Azam Asgarihafshejani #, Ève Honoré #, François-Xavier Michon, Isabel Laplante, and Jean-Claude Lacaille. Publié en 2022 dans le journal iScience doi.org/10.1016/j.isci.2022.104259 # Contributions égales.

Objectifs spécifiques de l'article :

De précédents travaux de notre laboratoire ont démontré que la PLT des synapses CP-SOM de CA1 est dépendante de l'activité de mTORC1, et contribue à la métaplasticité du réseau de CA1 ainsi qu'à la consolidation de la mémoire (Artinian J. *et al.*, 2019). L'objectif du présent chapitre est de vérifier si cette PLT est suffisante pour réguler ces phénomènes. Le premier but de ces expériences est d'établir un protocole d'induction optogénétique de la PLT aux synapses CP-SOM de CA1. Ensuite d'étudier si cette PLT partage les mêmes mécanismes que celle induite par une stimulation électrique ou le conditionnement à la peur. Enfin, le dernier objectif de ces expériences est d'examiner l'effet de cette PLT sur les réseaux de l'hippocampe ainsi que lors de l'acquisition de la mémoire contextuelle de peur. Pour ces séries d'expériences, des stimulations optogénétiques des efférences excitatrices des CP de CA1 ont été effectuées après l'injection dans l'aire CA1 dorsale d'un virus exprimant la rhodopsine modifiée hChR2 (E123T/T159C) sous le contrôle du promoteur de la CaMKIIa, lors d'enregistrements électrophysiologiques sur des tranches *in vitro*, ou chez la souris *in vivo* lors du conditionnement à la peur contextuelle.

SUMMARY

Hippocampal somatostatin (SOM) cells are dendrite-projecting inhibitory interneurons. CA1 SOM cells receive major excitatory inputs from pyramidal cells (PC-SOM synapses) which show mGluR1a- and mTORC1-mediated long-term potentiation (LTP). PC-SOM synapse LTP contributes to CA1 network metaplasticity and memory consolidation, but whether it is sufficient to regulate these processes remains unknown. Here we used optogenetic stimulation of CA1 pyramidal cells and whole cell recordings in slices to show that optogenetic theta burst stimulation (TBS_{opto}) produces LTP at PC-SOM synapses. At the network level, we found that TBS_{opto} differentially regulates metaplasticity of pyramidal cell inputs: enhancing LTP at Schaffer collateral synapses and depressing LTP at temporo-ammonic synapses. At the behavioral level, we uncovered that *in vivo* TBS_{opto} regulates learning-induced LTP at PC-SOM synapses, as well as contextual fear memory. Thus, LTP of PC-SOM synapses is a long-term feedback mechanism controlling pyramidal cell synaptic plasticity, sufficient to regulate memory consolidation

KEY WORDS

Optogenetics; inhibitory interneuron; somatostatin interneurons; mGluR1a; mTORC1; Schaffer collateral synapse; temporoammonic synapse; pyramidal cell metaplasticity; contextual fear memory

INTRODUCTION

Hippocampal interneurons are heterogeneous populations of GABAergic inhibitory cells with varied morphological, molecular and electrophysiological properties, as well as specialized network functions (Freund T. F. & Buzsáki G., 1996; Klausberger T. & Somogyi P., 2008; Bezaire M. J. & Soltesz I., 2013; Booker S. A. & Vida I., 2018). CA1 somatostatin-expressing (SOM) cells are a major interneuron subgroup comprised notably of Oriens-Lacunosum/Moleculare (O-LM) cells, bistratified cells and long-range projecting cells (Katona L. *et al.*, 2014; Pelkey K. A. *et al.*, 2017; Honore E. *et al.*, 2021). SOM cells have axons that target dendrites of pyramidal cells (Klausberger T. *et al.*, 2003; Lovett-Barron M. *et al.*, 2014; Muller C. & Remy S., 2014; Pelkey K. A. *et al.*, 2017) as well as other interneurons (Leao R. N. *et al.*, 2012; Fuhrmann F. *et al.*, 2015). SOM cells suppress spike rate and burst firing of pyramidal cells *in vitro* (Lovett-Barron M. *et al.*, 2012) and of place cells during exploration *in vivo* (Royer S. *et al.*, 2012). SOM cells fire with specific phase-coupling during hippocampal theta and gamma network oscillations that are hallmarks of hippocampal function and occur during spatial navigation, memory tasks, and rapid-eye-movement sleep (Klausberger T. & Somogyi P., 2008; Katona L. *et al.*, 2014). Indeed, SOM cell regulation of pyramidal neuron activity is critical for hippocampus-dependent learning and memory, as silencing SOM cells during contextual fear conditioning impairs long-term contextual memory (Lovett-Barron M. *et al.*, 2014).

SOM cells, like other hippocampal interneurons, show long-term synaptic plasticity of their input synapses (Pelletier J. G. & Lacaille J. C., 2008; Kullmann D. M. *et al.*, 2012; Honore E. *et al.*, 2021). CA1 pyramidal cell excitatory synapses onto SOM cells (PC-SOM synapses) display a Hebbian form of long-term potentiation (LTP) (Perez Y. *et al.*, 2001; Lapointe V. *et al.*, 2004; Croce A. *et al.*, 2010; Vasuta C. *et al.*, 2015; Honore E. *et al.*, 2021) dependent on metabotropic glutamate receptor subtype 1a (mGluR1a) activation and postsynaptic Ca^{2+} rise (Perez Y. *et al.*, 2001; Lapointe V. *et al.*, 2004). This form of long-term plasticity is cell-specific and absent in parvalbumin-expressing cells (Vasuta C. *et al.*, 2015) and radiatum interneurons (Perez Y. *et al.*, 2001). LTP at input synapses enables long-term regulation of interneuron firing (Croce A. *et al.*, 2010) and pyramidal cell inhibition (Lapointe V. *et al.*, 2004).

A critical SOM cell function is the differential regulation of afferents onto pyramidal cell dendrites: via distal dendritic inhibition, SOM cells downregulate activity and LTP in the temporo-ammonic pathway (TA-PC); whereas via proximal dendritic disinhibition (inhibition of other inhibitory interneurons), they upregulate activity and LTP in the CA3-CA1 Schaffer collateral pathway (SC-PC) (Leao R. N. *et al.*, 2012). Remarkably, Hebbian LTP at PC-SOM synapses increases subsequent LTP at SC-PC synapses (Vasuta C. *et al.*, 2015) and decreases subsequent LTP at TA-PC synapses (Sharma V. *et al.*, 2020), showing that plasticity at PC-SOM input synapses controls durably CA1 network metaplasticity (Honore E. *et al.*, 2021).

LTP at PC-SOM synapses can be persistent, as repeated activation of mGluR1a induces LTP of excitatory synapses lasting hours and involving gene transcription and mRNA translation (Ran I. *et al.*, 2009; Artinian J. *et al.*, 2019). mTORC1 signaling controls translation during LTP at PC-SOM synapses (Ran I. *et al.*, 2009; Artinian J. *et al.*, 2019). Interestingly, mTORC1 activity in SOM cells is required for learning-induced LTP of PC-SOM synapses, regulation of CA1 network plasticity, and long-term consolidation of spatial and contextual fear memory (Artinian J. *et al.*, 2019). However, whether LTP at PC-SOM synapses is sufficient for the regulation of CA1 network metaplasticity and hippocampus-dependent memory remains to be determined.

In the present study, we address this question by using optogenetics to induce long-term plasticity at PC-SOM excitatory synapses. We found that optogenetic stimulation of pyramidal cells induces LTP at PC-SOM synapses in slices. Furthermore, optogenetic induction of LTP at PC-SOM synapses bi-directionally controls CA1 network plasticity by facilitating SC-PC LTP and suppressing TA-PC LTP. Moreover, we uncover that optogenetic induction of LTP at PC-SOM synapses *in vivo* regulates learning-induced LTP at these synapses and controls contextual fear memory. Our findings suggest that LTP at PC-SOM synapses is sufficient to control the state of plasticity in the CA1 network and the consolidation of contextual fear memory, uncovering a long-term feedback control mechanism via PC-SOM synapses sufficient for regulation of CA1 pyramidal cell metaplasticity and hippocampus-dependent memory.

RESULTS

Optogenetically-induced LTP at PC-SOM synapses

CA1 pyramidal cells are the major excitatory synaptic inputs to SOM interneurons in CA1 stratum oriens (Croce A. *et al.*, 2010; Honore E. *et al.*, 2021). We used a combination of optogenetic stimulation after injection of AAV2/9-CaMKIIa-hChR2(E123T/T159C)-mCherry in SOM-Cre-EYFP mice to activate CA1 pyramidal cells, and of whole cell current clamp recordings in slices with synaptic inhibition intact to monitor excitatory postsynaptic potentials (EPSPs) in CA1 SOM interneurons resulting from activation of PC-SOM synapses (Figure 1A). Local optogenetic stimulation (470 nm) through the objective was adjusted (pulse duration 0.5-2.0 ms) to elicit light-evoked EPSPs in SOM interneurons (Figures 1B-G and S1A-G), similar to EPSPs evoked by electrical stimulation (Figure S2B-F) (Vasuta C. *et al.*, 2015). Theta burst stimulation (TBS) is an effective induction protocol for eliciting Hebbian LTP at PC-SOM excitatory synapses (Perez Y. *et al.*, 2001; Croce A. *et al.*, 2010; Vasuta C. *et al.*, 2015). Therefore, we developed an optogenetic TBS protocol (TBS_{opto}; bursts of 4 light pulses at 80 Hz, given 5 times with 300 ms inter-burst intervals, repeated 3 times at 30 s intervals) effective in eliciting EPSP summation and burst firing of SOM cells (Figure 1B). The TBS_{opto} protocol induced LTP of light-evoked EPSPs at PC-SOM synapses. Light-evoked EPSP amplitude showed a slow onset, gradual increase, lasting at least 30 min after TBS_{opto} (132.0% of baseline at 20-30 min post-induction; Figure 1B and 1J).

Next, we examined the mechanisms involved in the optogenetically-induced LTP at PC-SOM synapses. First, low frequency optogenetic stimulation (LFS_{opto}; 20 Hz) that elicited EPSP summation but a lower rate of firing in SOM cells (Figure 1C) did not induce lasting changes in light-evoked EPSP amplitude (103.0% of baseline at 20-30 min post-induction; Figure 1C and 1J, Figure S1B). Second, in recordings with no optogenetic tetanization, light-evoked EPSP amplitude was unchanged over the same time period (95.7% of baseline at 20-30 min post-induction; Figure 1D and 1J, Figure S1C). Third, to determine whether the optogenetically-induced LTP at PC-SOM synapses was mGluR1a-dependent, TBS_{opto} was given in the presence of the mGluR1a antagonist LY367385 (40 μM) (Figure 1E). In these conditions, TBS_{opto} failed to induce lasting changes in EPSP amplitude (111.0% of baseline at 20-30 min post-induction; Figure 1E and 1J, Figure S1D).

Fourth, to determine whether optogenetically-induced LTP at PC-SOM synapses is dependent on mTORC1-mediated translation, we used SOM-Raptor-KO mice that are deficient in mTORC1 signaling and late-LTP in SOM cells (Artinian J. *et al.*, 2019). In these mice, TBS_{opto} failed to induce lasting changes in light-evoked EPSP amplitude (104.0% of baseline at 20-30 min post-induction; Figure 1F and 1J, Figure S1E). Fifth, we examined if optogenetically-induced LTP requires transcription by pre-incubating hippocampal slices with 2 µM of the irreversible transcription inhibitor actinomycin D for 15 min prior to recording (Yuan S. & Burrell B. D., 2013; Younts T. J. *et al.*, 2016). In these conditions, TBS_{opto} induced a slow onset LTP of light-evoked EPSP amplitude (119.5% of baseline at 20-30 min post-induction; Figure 1G and 1J, Figure S1F) that was comparable to the LTP induced in control (Figure 1B and 1J) or in vehicle (DMSO; Figure S1G-H). Sixth, we determined if optogenetic stimulation elicited LTP at PC synapses onto parvalbumin-expressing interneurons (PC-Pvalb synapses) using injection of AAV2/9-CaMKIIa-hChR2(E123T/T159C)-mCherry and AAV2/9-EF1a-DIO-EYFP in Pvalb-Cre mice (Figure 1H). In these mice, TBS_{opto} failed to induce lasting increases in light-evoked EPSPs at PC-Pvalb synapses (90.0% of baseline at 20-30 min post-induction; Figure 1I-J, Figure S1I). In all these experiments, cell input resistance was unchanged after TBS_{opto} (Figure 1K). Together, these results suggest that optogenetic stimulation of CA1 pyramidal cells produces a frequency-dependent LTP at PC-SOM synapses that is dependent on mGluR1a activation and mTORC1-mediated translation, but independent of transcription. Moreover, optogenetic stimulation of CA1 pyramidal cells does not induce LTP at PC-Pvalb synapses.

These properties of optogenetically-induced LTP at PC-SOM synapses are similar to those previously reported for Hebbian LTP at excitatory synapses onto SOM cells characterized using electrical stimulation (Perez Y. *et al.*, 2001; Croce A. *et al.*, 2010; Honore E. *et al.*, 2021). So, next we determined if TBS_{opto} can induce LTP of EPSPs evoked in SOM cells by electrical stimulation (Figure S2A). We found that TBS_{opto} induced a similar LTP of electrically-evoked EPSPs that was dependent on mGluR1a and mTORC1, required tetanization and was absent in mice that received only the control CaMKIIa-mCherry injection without hChR2 (Figure S2B-G), indicating similar mechanisms as at PC-SOM synapses activated optogenetically.

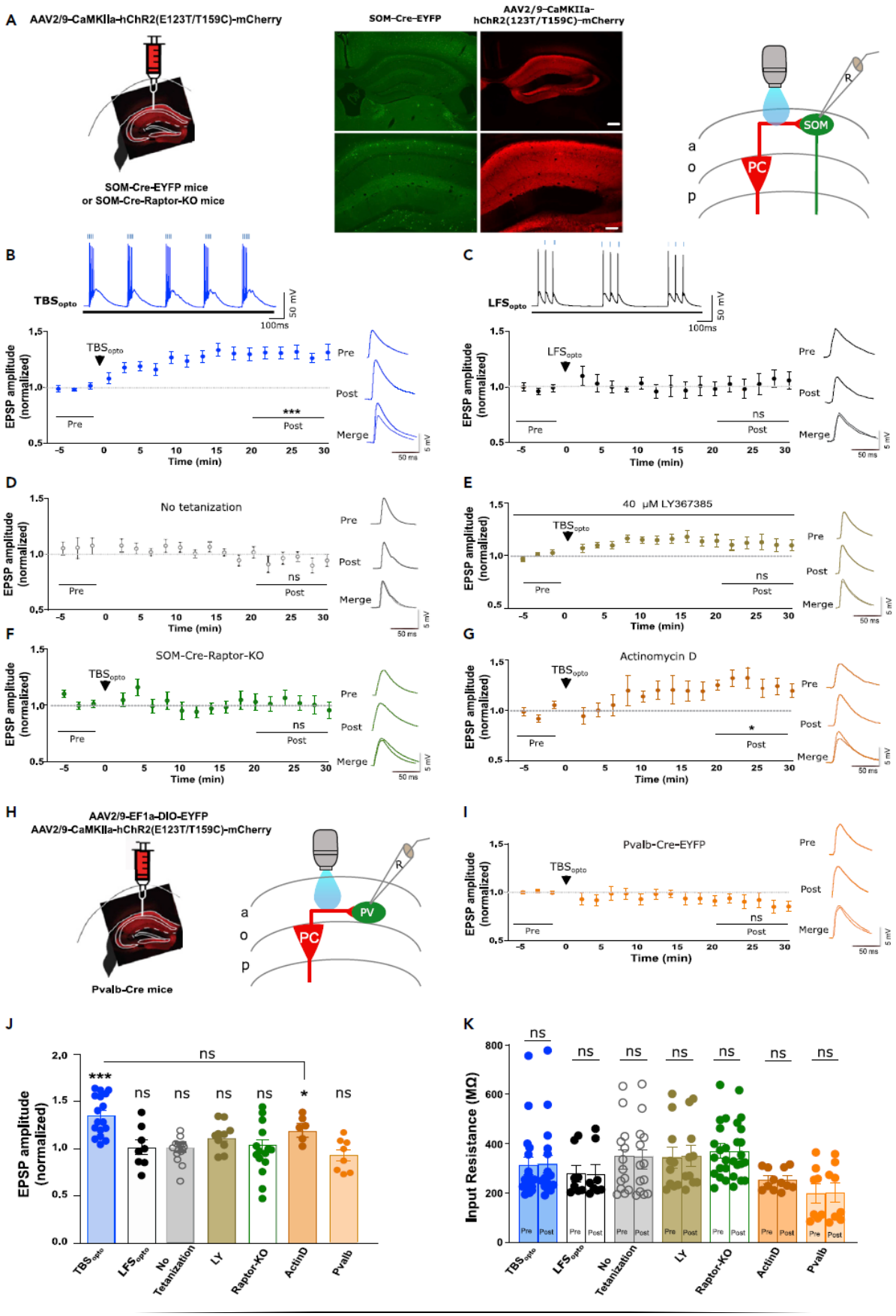
A
AAV2/9-CaMKIIa-hChR2(E123T/T159C)-mCherry
SOM-Cre-EYFP mice
or SOM-Cre-Raptor-KO mice
SOM-Cre-EYFP
AAV2/9-CaMKIIa-
hChR2(123T/T159C)-mCherry
SOM
PC
R
a
o
p
B
TBSopto
100ms
50 mV
EPSP amplitude (normalized)
Time (min)
Pre
Post
Merge
***
ns
C
LFSopto
D
No tetanization
E
40 μM LY367385
F
SOM-Cre-Raptor-KO
G
Actinomycin D
*
H
AAV2/9-EF1a-DIO-EYFP
AAV2/9-CaMKIIa-hChR2(E123T/T159C)-mCherry
Pvalb-Cre mice
PV
I
Pvalb-Cre-EYFP
J
EPSP amplitude (normalized)
TBSopto
LFSopto
No Tetanization
LY
Raptor-KO
ActinD
Pvalb
K
Input Resistance (MΩ)

Figure 1. Optogenetically induced LTP at PC-SOM synapses. (A) Left: schematic of experimental paradigm showing viral injections in the dorsal hippocampus of SOM-Cre-EYFP or SOM-Cre-Raptor-KO mice. Middle: representative images of EYFP expression in SOM cells and mCherry expression in CA1 pyramidal cells (calibration bar: 100 μm bottom; 250 μm top). Right: diagram of local optogenetic stimulation of CA1 pyramidal cells and whole-cell recording from SOM interneurons in stratum oriens. (B and C) Bottom left: time plots of light-evoked EPSP amplitude for all SOM cells, showing LTP at PC-SOM synapses following TBSopto (B; n = 17 cells) but not after LFSopto (C; n = 8 cells). Right: example of representative cells of average EPSPs before (pre) and 20–30 min after (post) TBSopto or LFSopto. Top: EPSP summation and cell firing during TBSopto (80 Hz) or LFSopto (20 Hz). Paired t-tests; ∗∗∗$p < 0.0001$; ns, $p > 0.05$. See Figures S1A and S1B for the respective time plots of EPSP amplitude of representative cells in (B) and (C), respectively. (D–G) Left: time plots of light-evoked EPSP amplitude for all SOM cells, showing absence of LTP at PC-SOM synapses following no tetanization (D; n = 13 cells), TBSopto in the presence of the mGluR1a antagonist LY367385 (40 μM) (E; n = 10 cells), or TBSopto in SOM-Cre-Raptor-KO mice (F; n = 15 cells); but LTP after TBSopto in slices pre-incubated with the transcription inhibitor actinomycin D (2μM) (G; n = 6 cells). Right: representative example of average EPSPs before (pre) and after (post) each treatment condition. Paired t-tests; ∗$p < 0.05$; ns, $p > 0.05$. See Figures S1C, S1D, and S1F for the respective time plots of EPSP amplitude of representative cells in (D), (E), (F), and (G), respectively; and Figure S1G for representative cells and S1H for time plot for all cells, showing LTP after TBSopto in DMSO (vehicle for actinomycin D). (H) Schematic of experimental paradigm with (left) viral injections in the dorsal hippocampus of Pvalb-Cre mice and (right) local optogenetic stimulation of pyramidal cells and recording from CA1 PV interneurons. (I) Time plot of light-evoked EPSP amplitude for all PV cells (left) and example of average EPSPs from a representative cell (right), showing absence of LTP at PC-PV synapses following TBSopto (n = 8 cells). Paired t-test; ns, $p > 0.05$. See Figure S1I for the time plot of EPSP amplitude of the representative PV cell in (I). (J) Summary graph of EPSP amplitude for all cells at 20–30 min post-induction, showing LTP after TBSopto in ACSF and after incubation with actinomycin D, but no LTP after LFSopto, in absence of tetanization, or after TBSopto in LY367385, in Som-Cre-Raptor-KO mice, or in PV cells. Paired t-tests (post vs pre in B-I) and unpaired t-test (post in B vs post in G); ∗∗∗$p < 0.0001$; ∗$p < 0.05$; ns, $p > 0.05$. (K) Summary graph for all cells, showing no change in cell input resistance at 20–30 min post-induction in any experimental group. Wilcoxon matched-pairs signed-rank test (TBSopto and LFSopto), or paired t-test (other groups); ns, $p > 0.05$. Data are represented as mean ± SEM here and below. ∗$p < 0.05$, ∗∗$p < 0.01$, ∗∗∗$p < 0.001$; $p > 0.5$ is considered not significant (ns). Statistical tests and actual p values for each comparison here and below are given in Table S1.

TBS_{opto} differentially regulates LTP at Schaffer collateral and temporo-ammonic synapses

CA1 SOM cells (notably OLM cells) differentially control transmission at Schaffer collateral and temporo-ammonic synapses of CA1 pyramidal cells (Leao R. N. *et al.*, 2012). In consequence, Hebbian LTP at excitatory synapses onto SOM cells is associated with increased LTP at Schaffer collateral inputs and reduced LTP at temporo-ammonic synapses of CA1 pyramidal cells (Vasuta C. *et al.*, 2015; Artinian J. *et al.*, 2019; Sharma V. *et al.*, 2020). So, next we studied if TBS_{opto}-induced LTP at PC-SOM synapses was sufficient to regulate metaplasticity of the CA1 network using whole-field optogenetic stimulation and field potential recordings in slices with synaptic inhibition intact. First, we established that whole-field optogenetic stimulation also elicited LTP at PC-SOM synapses (Figure 2A). Whole-field TBS_{opto} elicited EPSP summation and burst firing of SOM cells, and induced LTP of light-evoked EPSP amplitude (125.0% of baseline at 20-30 min post-induction; Figure 2B and S3E). LTP was absent in cells that received no optogenetic tetanization (light-evoked EPSP amplitude 97.8% of baseline at 30 min post-induction; Figure S3B and S3E), or with TBS_{opto} given in the presence of the mGluR1a antagonist LY367385 (40 μM) (light-evoked EPSP amplitude 97.0% of baseline at 20-30 min post-induction; Figure S3C and S3E), or in SOM cells of SOM-Raptor-KO mice (light-evoked EPSP amplitude 96.3% of baseline at 20-30 min post-induction; Figure S3D and S3E). Thus, whole-field TBS_{opto} induced a similar mGluR1a- and mTORC1-mediated LTP at PC-SOM synapses as local optogenetic stimulation.

Next, we examined the long-lasting effects of whole-field TBS_{opto} on plasticity at Schaffer collateral synapses (SC-PC synapses) and temporo-ammonic synapses (TA-PC synapses) onto CA1 PCs in slices with synaptic inhibition intact. In these experiments, we used whole-field optogenetic stimulation and fEPSP recordings so that we could obtain long-term stable recordings of synaptic responses, for a 15 min baseline period before TBS_{opto} and a 25 min period after TBS_{opto}, to assess effects of TBS_{opto} on basal transmission, and for another 35 min period after tetanization of SC-PC or TA-PC synapses, to assess effects on LTP at these synapses (Figure 2). First, we investigated regulation of plasticity at SC-PC synapses (Figure 2C and Figure S3F). A weak electrical TBS (wTBS) of the SC pathway failed to induce LTP of fEPSP slope (107.0% of baseline at 25-35 min post-induction; Figure 2D and Figure S3G). In contrast, when the wTBS was preceded

25 min earlier by TBS_{opto}, LTP was induced at SC-PC synapses (125.7% of baseline at 25-35 min post-induction; Figure 2D and 2F, and Figure S3H). Thus, TBS_{opto} facilitated LTP at SC-PC synapses. TBS_{opto} did not affect basal transmission at SC-PC synapses (Figure 2G). In mice with control CaMKIIa-mCherry injection without hChR2, TBS_{opto} failed to facilitate LTP at SC-PC synapses (104.0% of baseline at 25-35 min post-induction; Figure 2D and 2F), indicating that the LTP facilitation was not due to unspecific effects of light stimulation. To determine if the facilitation of LTP at SC-PC synapses was due to plasticity at SOM-PC synapses induced by TBS_{opto}, we examined if the facilitation was dependent on mGluR1a and on mTORC1 in SOM cells. When wTBS was preceded 25 min earlier by TBS_{opto} in the presence of the mGluR1a antagonist LY367385 (40 μM), the facilitation of LTP at SC-PC synapses was absent (107.0% of baseline at 25-35 min post-induction; Figure 2D and 2F). Similarly, when wTBS was preceded 25 min earlier by TBS_{opto} in slices from SOM-Raptor-KO mice, the facilitation of LTP at SC-PC synapses was also absent (112.0% of baseline at 25-35 min post-induction without TBS_{opto} and 1007.0% of baseline at 25-35 min post-induction with TBS_{opto}; Figure 2E and 2H). These results suggests that the facilitation of LTP at SC-PC synapses was due to mGluR1a- and mTORC1-dependent plasticity at SOM-PC synapses induced by TBS_{opto}.

Second, we investigated regulation of plasticity at TA-PC synapses (Figure 2I and Figure S3I). A weak electrical TBS (wTBS) of the TA pathway induced LTP of fEPSP slope (126.7% of baseline at 25-35 min post-induction; Figure 2J and 2L and Figure S3J). In contrast, when the wTBS was preceded 25 min earlier by TBS_{opto}, LTP was prevented at TA-PC synapses (95.5% of baseline at 25-35 min post-induction; Figure 2J and 2L, and Figure S3K). Thus, TBS_{opto} depressed LTP at TA-PC synapses. TBS_{opto} did not affect basal transmission at TA-PC synapses (Figure 2M). In mice with control CaMKIIa-mCherry injection without hChR2, TBS_{opto} failed to depress LTP at TA-PC synapses (127.0% of baseline at 25-35 min post-induction; Figure 2J and 2L), indicating that the LTP depression was not due to unspecific effects of light stimulation. The depression of LTP at TA-PC synapses was likely due to plasticity at SOM-PC synapses induced by TBS_{opto} since it was dependent on mGluR1a and on mTORC1 in SOM cells. The depression of LTP at TA-PC synapses was absent when wTBS was preceded by TBS_{opto} in the presence of the mGluR1a antagonist LY367385 (126.0% of baseline at 25-35 min post-induction; Figure 2J and 2L). Similarly, the depression of LTP at TA-PC was absent when wTBS was preceded by TBS_{opto} in slices from SOM-Raptor-KO mice (123.0% of baseline at 25-35 min post-induction without

TBS_{opto} and 118.9% of baseline at 25-35 min post-induction with TBS_{opto}; Figure 2K and 2N). These results suggest that the TBS_{opto}-induced depression of LTP at TA-PC synapses is the result of mGluR1a- and mTORC1-dependent plasticity at SOM-PC synapses. Thus, TBS_{opto}-induced LTP at PC-SOM synapses appears sufficient to regulate metaplasticity of the CA1 network, upregulating LTP at SC-PC synapses and downregulating LTP at TA-PC synapses.

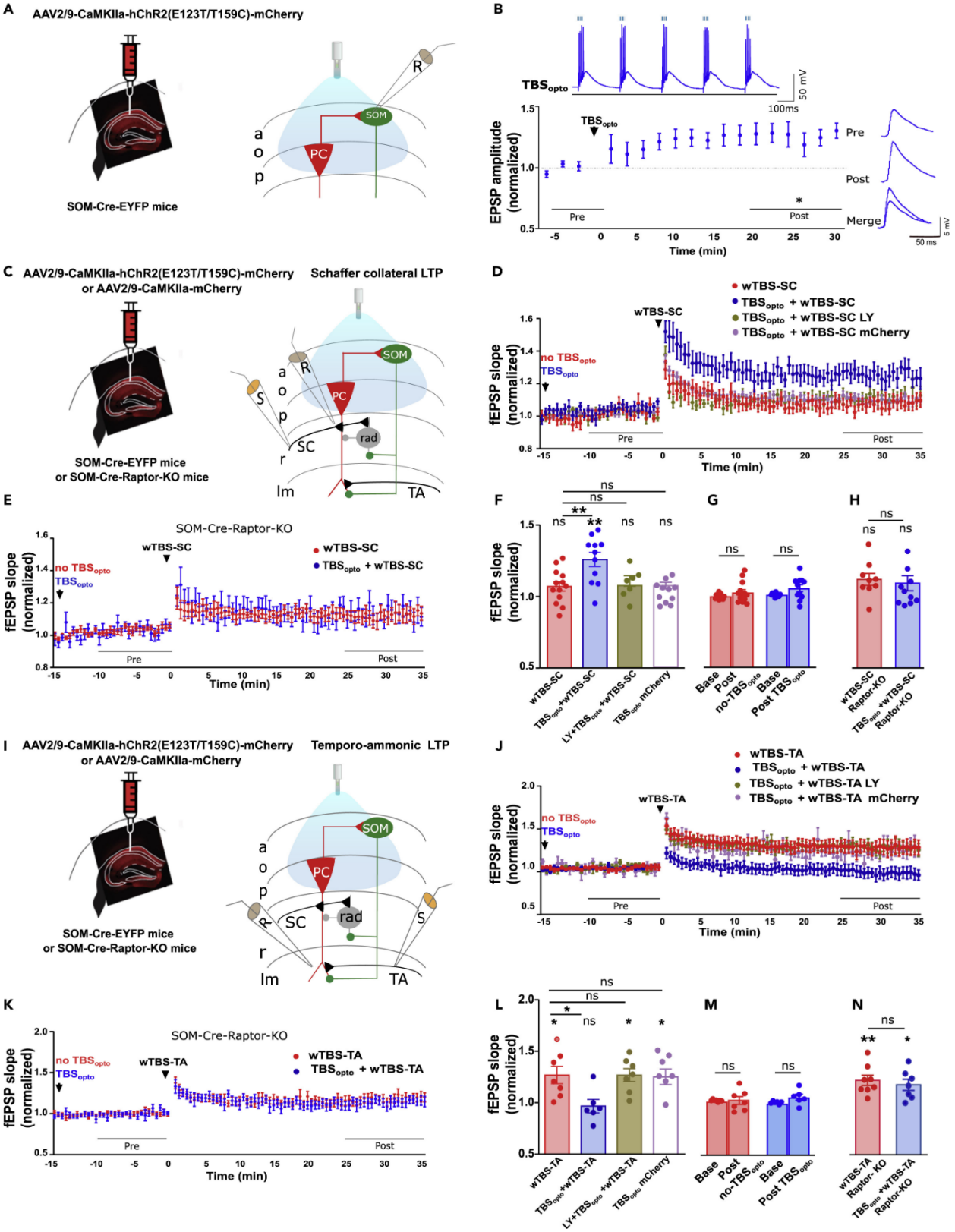
A
AAV2/9-CaMKIIa-hChR2(E123T/T159C)-mCherry
SOM-Cre-EYFP mice
SOM
PC
R
a
o
p
B
TBSopto
50 mV
100ms
EPSP amplitude (normalized)
Pre
Post
Merge
5 mV
50 ms
Time (min)
C
AAV2/9-CaMKIIa-hChR2(E123T/T159C)-mCherry
or AAV2/9-CaMKIIa-mCherry
Schaffer collateral LTP
SOM-Cre-EYFP mice
or SOM-Cre-Raptor-KO mice
S
SC
r
rad
lm
TA
D
wTBS-SC
TBSopto + wTBS-SC
TBSopto + wTBS-SC LY
TBSopto + wTBS-SC mCherry
no TBSopto
fEPSP slope (normalized)
E
SOM-Cre-Raptor-KO
F
G
H
ns
I
AAV2/9-CaMKIIa-hChR2(E123T/T159C)-mCherry
or AAV2/9-CaMKIIa-mCherry
Temporo-ammonic LTP
J
wTBS-TA
TBSopto + wTBS-TA
TBSopto + wTBS-TA LY
TBSopto + wTBS-TA mCherry
K
L
M
N

Figure 2. Whole-field TBS_{opto} induces LTP at PC-SOM synapses and differentially regulates LTP at SC-PC and TA-PC synapses. (A) Left: schematic of experimental paradigm with hippocampal viral injections in SOM-Cre-EYFP mice. Right: diagram of whole-field optogenetic stimulation of CA1 pyramidal cells and whole-cell recording from SOM interneurons. (B) Left bottom: time plot of light-evoked EPSP amplitude for all SOM cells, showing LTP at PC-SOM synapses following TBSopto (n = 7 cells). Left top: EPSP summation and cell firing during TBSopto in a representative cell. Right: example from a representative cell of average light-evoked EPSPs before (pre) and 20–30 min after (post) TBSopto. Paired t-test; $*p < 0.05$. See Figures S3A–S3E for the dependence of whole-field TBSopto-induced LTP on tetanization (S3B and S3E), mGluR1a (S3C and S3E), and mTORC1 (S3D and S3E). (C) Left: schematic of experimental paradigm with hippocampal viral injections in SOM-Cre-EYFP or SOM-Cre-Raptor-KO mice. Right: diagram of whole-field optogenetic stimulation of CA1 pyramidal cells, with electrical stimulation and recording of SC-PC fEPSPs in stratum radiatum. (D) Time plot of fEPSP slope for all slices, showing that LTP at SC-PC synapses (n = 13 slices, red) is facilitated by prior application of TBSopto (n = 11 slices, blue), but not in the presence of the mGluR1a antagonist LY367385 (n = 7 slices, brown) nor in slices from mice with control CaMKIIa-mCherry injection without hChR2 (n = 11 slices, magenta). See Figures S3G and S3H for time plots of fEPSP slope in representative slices without and with TBSopto, respectively. (E) Time plot of fEPSP slope for all slices from SOM-Cre-Raptor-KO mice, showing that prior application of TBSopto (n = 10 slices, blue) does not facilitate LTP at SC-PC synapses (n = 9 slices; red) in these mutant mice. (F) Summary graph of fEPSP slope for all slices at 25–35 min post-induction of LTP at SC-PC synapses, showing that LTP at SC-PC synapses (red) is facilitated by prior application of TBSopto (blue), but not in LY367385 (brown) or in slices from mice injected with mCherry (magenta). Paired t-tests (pre vs post); ANOVA, Tukey's multiple comparisons tests (post wTBS-SC vs post other conditions); $*p < 0.05$, ns $p > 0.05$. (G) Summary bar graph of fEPSP slope before (−10 to 0 min) and after (15–25 min) TBSopto, showing that basal transmission at SC-PC synapses is unchanged after TBSopto or no TBSopto. Paired t-test, ns $p > 0.05$. (H) Summary graph of fEPSP slope for all slices at 25–35 min post-induction of LTP at SC-PC synapses, showing that LTP at SC-PC synapses (red) is not facilitated by prior application of TBSopto (blue) in SOM-Cre-Raptor-KO mice. Unpaired t-test, ns $p > 0.05$. (I) Left: schematic of experimental paradigm with hippocampal viral injections in SOM-Cre-EYFP or SOM-Cre-Raptor-KO mice. Right: diagram of whole-field optogenetic stimulation of CA1 pyramidal cells, with electrical stimulation and recording of TA-PC fEPSPs in stratum lacunosum-moleculare. (J) Time plot of fEPSP slope for all slices, showing that LTP at TA-PC synapses (n = 7 slices, red) is depressed by prior application of TBSopto (n = 6 slices, blue), but not by TBSopto in the presence of the mGluR1a antagonist LY367385 (n = 7 slices, brown), nor by TBSopto in slices from mice with CaMKIIa-mCherry injection (n = 7 slices, magenta). See Figures S3J and S3K for time plots of fEPSP slope in representative slices without and with TBSopto, respectively. (K) Time plot of fEPSP slope for all slices from SOM-Cre-Raptor-KO mice, showing that LTP at TA-PC synapses (n = 8 slices; red) is not depressed by prior application of TBSopto (n = 7 slices, blue) in these mutant mice. (L) Summary graph of fEPSP slope for all

slices at 25–35 min post-induction of LTP at TA-PC synapses, showing LTP at TA-PC synapses (red) is depressed by prior application of TBSopto (blue), but not by TBSopto in LY367385 (brown) or in slices from mice injected with mCherry (magenta). Paired t-tests (pre vs post); ANOVA, Tukey's multiple comparisons tests (post wTBS-TA vs post other conditions); $*p < 0.05$, ns $p > 0.05$. (M) Summary bar graph of fEPSP slope before (−10 to 0 min) and after (15–25 min) TBSopto, showing that basal transmission at TA-PC synapses is unchanged after TBSopto or no TBSopto. Paired t-test, ns $p > 0.05$. (N) Summary graph of fEPSP slope for all slices at 25–35 min post-induction of LTP at TA-PC synapses, showing that LTP at TA-PC synapses (red) is not depressed by prior application of TBSopto (blue) in SOM-Cre-Raptor-KO mice. Paired t-tests (pre vs post); unpaired t-test (wTBS-TA vs TBSopto + wTBS-TA); $**p < 0.01$, $*p < 0.05$, ns $p > 0.05$.

TBS_{opto} interferes with contextual fear memory consolidation

At the behavioral level, mTORC1 activity in SOM cells, that is required for learning-induced LTP of PC-SOM synapses, contributes to long-term consolidation of spatial and contextual fear memory (Artinian J. *et al.*, 2019). So, next we examined if LTP at PC-SOM synapses is sufficient to regulate hippocampus-dependent memory. First, we verified that, as previously reported (Lovett-Barron M. *et al.*, 2014), activity of CA1 SOM cells is necessary for long-term contextual fear memory using optogenetic silencing of CA1 SOM cells with archaerhodopsin (Arch) (Vasuta C. *et al.*, 2015) during contextual fear conditioning (Figure 3A and 3B). Optogenetic activation of Arch in phase with the presentation of shocks during conditioning, resulted in reduced freezing during the long-term contextual fear memory test, relative to light stimulation in absence of Arch (51.4% reduction; Figure 3C) or to activation of Arch out of phase (shifted) with presentation of shocks (64.9% reduction; Figure 3C). In the open field test (Figure S4A), silencing of CA1 SOM cells with light stimulation of Arch did not affect anxiety level (time spent in periphery or center, and ratio of time in center/periphery; Figure S4B) or locomotion (total distance traveled and zone transitions; Figure S4C) relative to mice receiving light stimulation without Arch. These results indicate that silencing SOM cells during contextual fear conditioning impairs long-term contextual fear memory, confirming that SOM cell activity is necessary during long-term contextual fear learning (Lovett-Barron M. *et al.*, 2014).

Next, we determined if LTP at PC-SOM synapses is sufficient to regulate hippocampus-dependent memory. We used CA1 injection of AAV2/9-CaMKIIa-hChR2(E123T/T159C)-mCherry in SOM-Cre-EYFP mice and the same TBS_{opto} induction protocol that elicit LTP at PC-SOM synapses in slices. We delivered the optogenetic stimulation *in vivo* and investigated its

effect on contextual fear memory (Figure 3D and 3E). TBS_{opto} given in CA1 30 min prior to conditioning resulted in reduced freezing during the long-term contextual fear memory test, relative to mice receiving no TBS_{opto} prior to conditioning (73.7% reduction; Figure 3F) or TBS_{opto} in the absence of hChR2 (71.5% reduction; Figure 3F). Mice in the three groups showed similar normal anxiety level (time spent in periphery or center, and ratio of time in center/periphery; Figure S4E) and locomotion (total distance traveled and zone transitions; Figure S4F) in the open field test. These results indicate that the TBS_{opto} induction protocol that elicit LTP at PC-SOM synapses is sufficient to regulate long-term contextual fear memory *in vivo* .

Since LTP induced by TBS_{opto} at PC-SOM synapses, and its regulation of CA1 PC metaplasticity, are blocked by conditional knock-out of *Rptor* in SOM cells (Figures 1 and 2), we tested next if the reduction of fear memory by TBS_{opto} was due to mTORC1 signaling in SOM cells. TBS_{opto} in CA1 given 30 min prior to conditioning in SOM-Cre-Raptor-KO mice did not affect freezing during the long-term contextual fear memory test, relative to mice not receiving TBS_{opto} prior to conditioning (Figure 3F). Both mice groups showed increased freezing in the memory tests demonstrating significant contextual fear learning (Figure 3F) and behaved similarly in the open field test (Figure S4D-S4F) indicating normal anxiety level and locomotion. These results indicate that the TBS_{opto}-induced impairment of fear memory was dependent on mTORC1 signaling in SOM interneurons and not due to other non-specific effects of optogenetic activation of CA1 PCs, suggesting that TBS_{opto}-induced LTP at PC-SOM synapses is sufficient for the regulation of hippocampus-dependent memory.

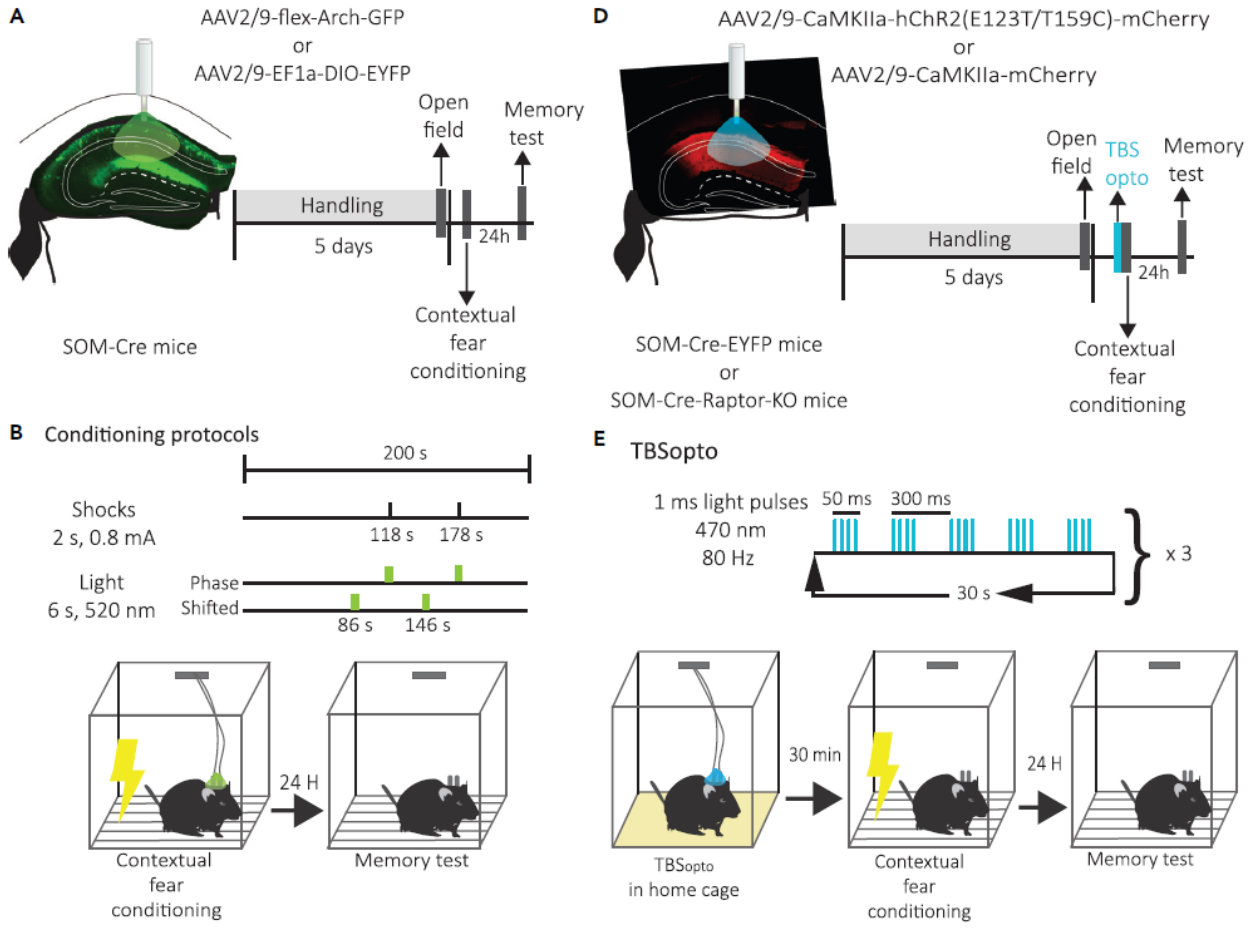
A
AAV2/9-flex-Arch-GFP
or
AAV2/9-EF1a-DIO-EYFP
Open field
Memory test
Handling
5 days
24h
Contextual fear conditioning
SOM-Cre mice
D
AAV2/9-CaMKIIa-hChR2(E123T/T159C)-mCherry
or
AAV2/9-CaMKIIa-mCherry
Open field
TBS opto
Memory test
Handling
5 days
24h
Contextual fear conditioning
SOM-Cre-EYFP mice
or
SOM-Cre-Raptor-KO mice
B
Conditioning protocols
200 s
Shocks
2 s, 0.8 mA
118 s
178 s
Light
6 s, 520 nm
Phase
Shifted
86 s
146 s
24 H
Contextual fear conditioning
Memory test
E
TBSopto
1 ms light pulses
470 nm
80 Hz
50 ms
300 ms
x 3
30 s
30 min
24 H
TBSopto in home cage
Contextual fear conditioning
Memory test
C
Conditioning
Memory test
Freezing (% of time)
AAV
Light
EYFP
Phase
Arch
Shifted
Arch
Phase
F
Conditioning
Memory test
Freezing (% of time)
Mice
AAV
TBSopto
EYFP
mCherry
+
EYFP
hChR2
-
EYFP
hChR2
+
Raptor-KO
hChR2
-
Raptor-KO
hChR2
+

Figure 3. Silencing of SOM cells and TBSopto impair contextual fear memory. (A) Left: schematic of cannulation and injection site of AAV2/9-flex-Arch-GFP or AAV2/9-EF1a-DIO-EYFP in dorsal CA1 hippocampus of SOM-Cre mice with the representative image of Arch expression. Right: diagram of behavioral testing sequence (open field and contextual fear conditioning). (B) Experimental protocol of optogenetic stimulation (in phase or shifted with respect to shocks) during contextual fear conditioning. (C) Summary graph for all mice, showing reduced freezing in the long-term memory test in mice that received Arch activation in phase with shocks (n = 9 mice, dark green), relative to those that received light stimulation without Arch (n = 8 mice, gray) or Arch activation out of phase with shocks (shifted; n = 7 mice, light green). Mann-Whitney Rank-Sum test or paired t-test (pre vs post-conditioning), ∗∗∗p < 0.001 (gray). One way ANOVA(Memory tests), Holm-Sidak pairwise comparisons, ∗p < 0.05, ∗∗∗p < 0.001, ns p > 0.05. (D) Schematic of cannulation and injection site of AAV2/9-CaMKIIa-hChR2(E123T/T159C)-mCherry or AAV2/9-CaMKIIa-mCherry in dorsal CA1 hippocampus of SOM-Cre-EYFP or SOM-Cre-Raptor-KO mice with a representative image of hChR2-mCherry expression, and diagram of behavioral testing sequence (open field and contextual fear conditioning). (E) Experimental protocol of TBSopto given 30 min before contextual fear conditioning. (F) Left: Summary graph for all SOM-Cre-EYFP mice, showing reduced freezing in the long-term memory test in mice that received TBSopto (n = 8 mice, blue), relative to mice that received no TBSopto (n = 7 mice, violet) or TBSopto without hChR2 (n = 8 mice, gray). Mann-Whitney Rank-Sum test (pre vs post-conditioning), ∗∗∗p < 0.001 (gray). Kruskal-Wallis One-way ANOVA on Ranks (Memory tests), Dunn's pairwise comparisons test, ∗∗∗p = 0.001, ns p > 0.05. Right: Similar data presentation for SOM-Cre-Raptor-KO mice, showing significant freezing in the memory test relative to pre-conditioning, and no difference in freezing in the long-term memory test in mice that received TBSopto (n = 6 mice, blue) or no TBSopto (n = 7 mice, violet). Mann-Whitney Rank-Sum test (pre vs post-conditioning), ∗∗p < 0.005 (gray). Unpaired t-test (Memory tests), ns p > 0.05.

Prior induction of LTP by TBS_{opto} results in subsequent TBS- and learning-induced depotentiation

Since the behavior experiments indicate that TBS_{opto} impairs contextual fear memory consolidation when given prior to contextual fear conditioning, we examined the interaction

between optogenetically- and electrically-induced LTP of electrically-evoked EPSPs in SOM cells in slices (Figure 4A).

After a baseline period, a first episode of electrical TBS elicited LTP of EPSP amplitude (134.0% of baseline at 10-15 min post-induction TBS#1), and a second TBS episode induced a further increase in LTP (164.0% of baseline at 30-35 min post-induction TBS#1; Figure 4B). In contrast, a first episode of TBS_{opto} elicited LTP of EPSP amplitude (140.0% of baseline at 10-15 min post-induction of TBS_{opto} #1), and a second TBS_{opto} episode did not induce a further increase in LTP (142.0% of baseline at 30-35 min post-induction TBS_{opto} #1; Figure 4C). Interestingly, after a first episode of TBS_{opto} that elicited LTP of EPSP amplitude (121.0% of baseline at 10-15 min post-induction of TBS_{opto} #1), a subsequent TBS episode induced depotentiation of EPSP amplitude (94.0% of baseline at 30-35 min post-induction TBS_{opto} #1; Figure 4D). Such a depotentiation was absent when a first episode of TBS (130.0% of baseline at 10-15 min post-induction of TBS #1) was followed by a subsequent TBS_{opto} episode (141.0% of baseline at 30-35 min post-induction TBS #1; Figure 4E). Finally, a single TBS episode given at the later time point induced LTP (129.0% of baseline; Figure 4F), suggesting that the depotentiation induced by TBS was not due to a response run-down due to recording time, or dialysis of cell content. Thus, prior induction of LTP by TBS_{opto} engages some mechanisms resulting in depotentiation when TBS is given subsequently.

Contextual fear conditioning induces a persistent LTP of PC-SOM synapses, that can be recorded ex vivo 24h after conditioning (Artinian J. *et al.*, 2019). Therefore, we used ex vivo whole cell recordings in slices 24 hours after conditioning, to examine if *in vivo* TBS_{opto} given 30 min prior to contextual fear conditioning interferes with learning-induced LTP at excitatory synapses of SOM cells (Figure 4G). SOM cells from mice that received TBS_{opto} prior to contextual fear conditioning exhibited decreases in spontaneous EPSC frequency and amplitude, relative to cells from mice with contextual fear conditioning only (56.1% decrease in frequency, 31.9% decrease in amplitude; Figure 4H). Similarly, the input-output function of electrically-evoked EPSCs was decreased in SOM cells from mice that received TBS_{opto} prior to contextual fear conditioning, relative to cells from mice with contextual fear conditioning only (64.1% decrease in slope of EPSC input-output function; Figure 4I). These results suggest that *in vivo* TBS_{opto} given 30 min prior to contextual fear conditioning interferes with learning-induced LTP at PC-SOM synapses, consistent

with our findings that induction of Hebbian LTP results in depotentiation at PC-SOM synapses after prior induction of LTP by TBS_{opto} in slices. Overall, our findings indicate that LTP at PC-SOM synapses is sufficient to regulate CA1 pyramidal cell metaplasticity and hippocampus-dependent memory.

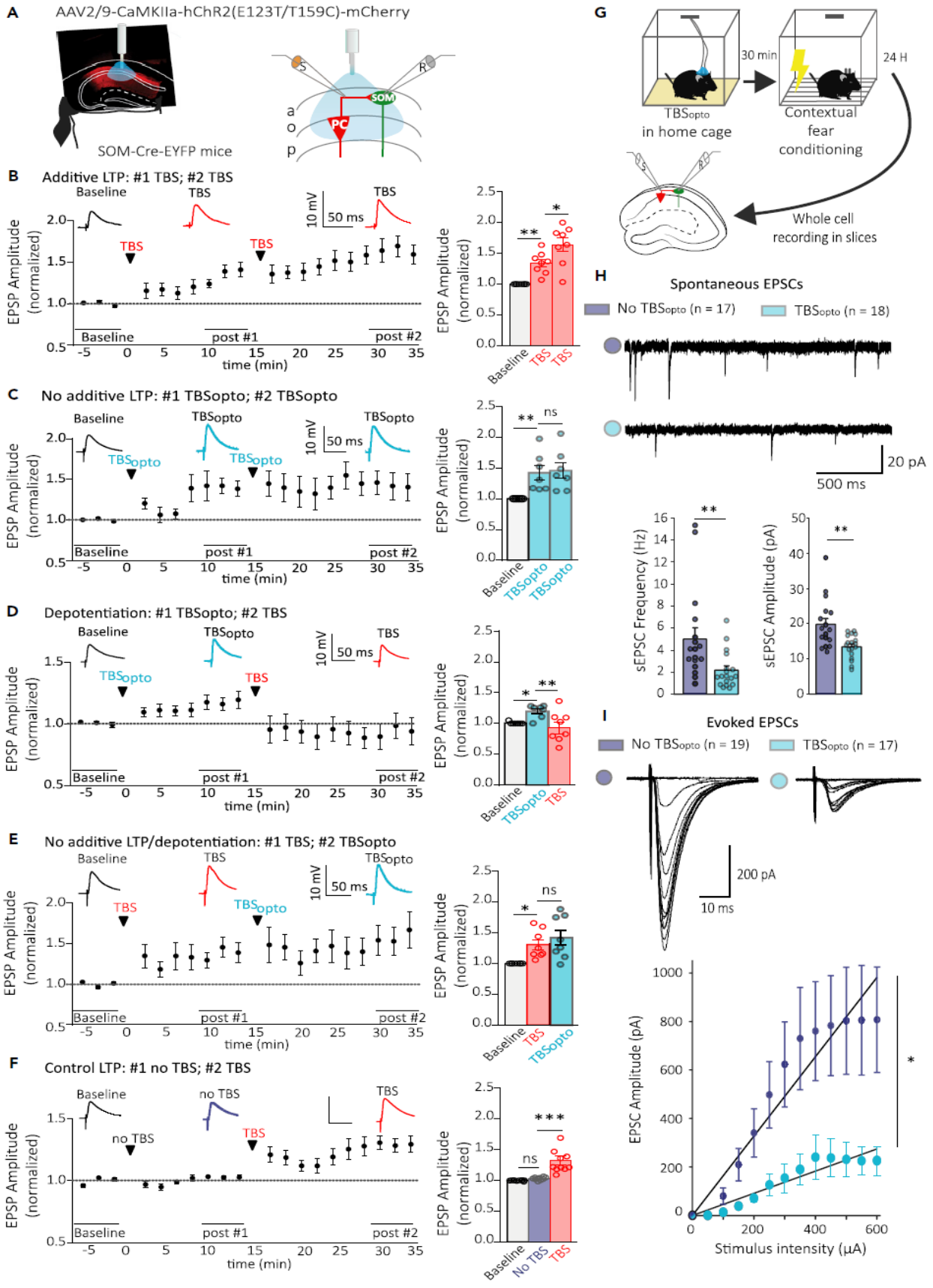
A
AAV2/9-CaMKIIa-hChR2(E123T/T159C)-mCherry
SOM-Cre-EYFP mice
S
R
a
o
p
SOM
PC
B
Additive LTP: #1 TBS; #2 TBS
Baseline
TBS
10 mV
50 ms
EPSP Amplitude (normalized)
Baseline
post #1
post #2
time (min)
C
No additive LTP: #1 TBSopto; #2 TBSopto
TBSopto
ns
D
Depotentiation: #1 TBSopto; #2 TBS
E
No additive LTP/depotentiation: #1 TBS; #2 TBSopto
F
Control LTP: #1 no TBS; #2 TBS
no TBS
G
30 min
24 H
TBSopto
in home cage
Contextual
fear
conditioning
Whole cell
recording in slices
H
Spontaneous EPSCs
No TBSopto (n = 17)
TBSopto (n = 18)
20 pA
500 ms
sEPSC Frequency (Hz)
sEPSC Amplitude (pA)
I
Evoked EPSCs
No TBSopto (n = 19)
TBSopto (n = 17)
200 pA
10 ms
EPSC Amplitude (pA)
Stimulus intensity (μA)

Figure 4. LTP induction by TBSopto interferes with subsequent induction of Hebbian or learning-related LTP. (A) Left: schematic of experimental paradigm with viral injections in the dorsal hippocampus of SOM-Cre-EYFP mice. Right: diagram of whole-field optogenetic stimulation of CA1 pyramidal cells (TBSopto), electrical stimulation of afferents in stratum oriens/alveus (S), and whole-cell recording (R) of electrically evoked EPSPs in SOM interneurons. (B–F) (Left) Time plots of electrically evoked EPSP amplitude for all cells (with above, representative average EPSPs during baseline, post-induction #1 and #2), and (right) summary bar graphs of EPSP amplitude for all cells during baseline, 10–15 min after induction #1 and 15–20 min after induction #2, showing: (B) LTP following a first episode of TBS of afferents (TBS#1) that is further increased after a second TBS episode (n = 8 cells); (C) LTP following the first episode of TBSopto without further increase following a second TBSopto episode (n = 7 cells); (D) LTP following the first episode of TBSopto followed by depotentiation after a subsequent episode of TBS (n = 8 cells); (E) LTP following a first episode of TBS and absence of depotentiation after a subsequent TBSopto episode (n = 8 cells); and (F) LTP following TBS given at the induction #2 time point only (n = 10 cells). rmANOVA, Tukey's multiple comparisons test; $*p < 0.05$, $**p < 0.01$, $***p < 0.0001$, ns $p > 0.05$. (G) Diagram of experimental paradigm with in vivo optogenetic stimulation of CA1 pyramidal cells (TBSopto) before contextual fear conditioning, and ex vivo whole-cell recording of spontaneous and electrically evoked EPSCs (electrical stimulation in stratum oriens/alveus) in SOM interneurons in slices at 24 h post-conditioning. (H) Top: Spontaneous EPSCs from representative cells from mice receiving contextual fear conditioning only (violet) or TBSopto before contextual fear conditioning (blue). Bottom: Summary bar graphs of sEPSC frequency and amplitude for all cells, showing a decrease in frequency and amplitude of sEPSCs in cells from mice with TBSopto before contextual fear conditioning (blue; n = 18 cells, three mice), relative to cells from mice with contextual fear conditioning only (violet; n = 17 cells, four mice). Mann-Whitney Rank-Sum Test, $**p < 0.01$.(I) Top: Family of EPSCs evoked by increasing intensity of stimulation in representative cells from mice receiving contextual fear conditioning only (violet) or TBSopto before contextual fear conditioning (blue). Bottom: Summary plots of input–output function of EPSC amplitude as a function of stimulation intensity and linear fit (synaptic gain), showing that the input–output function of evoked EPSCs was decreased in cells from mice with TBSopto before contextual fear

conditioning (blue; n = 17 cells, three mice), relative to cells from mice that received contextual fear conditioning only (violet; n = 19 cells, four mice). Mann-Whitney Rank-Sum Test, $*p < 0.05$.

DISCUSSION

Long-term synaptic plasticity at excitatory input synapses onto specific inhibitory interneurons is an intriguing feature of hippocampal synaptic networks but its role in hippocampal memory function has remained largely undetermined (McBain C. J. & Kauer J. A., 2009; Bartos M. *et al.*, 2011; Kullmann D. M. *et al.*, 2012; Honore E. *et al.*, 2021). Brain-wide manipulation of mTORC1 activity specifically in SOM cells indicated that LTP at afferent synapses of hippocampal SOM cells contributes to regulation of CA1 network plasticity and long-term consolidation of spatial and contextual fear memory (Artinian J. *et al.*, 2019). Here we used hippocampal CA1-specific optogenetic approaches to establish that LTP at PC-SOM synapses is sufficient to differentially control metaplasticity of SC-PC and TA-PC synapses, and regulate contextual fear memory, uncovering a long-term feedback mechanism controlling pyramidal cell synaptic plasticity and memory consolidation.

TBS_{opto}-induced LTP

TBS_{opto} was sufficient to induce LTP of synaptic responses elicited by optogenetic activation or local electrical stimulation of PC-SOM synapses. Optogenetically-induced LTP at PC-SOM synapses shared key features with Hebbian LTP induced by electrical tetanization: slow onset potentiation, frequency-dependence, mGluR1a-mediated, and SOM *versus* Pvalb cell-specificity (Perez Y. *et al.*, 2001; Lapointe V. *et al.*, 2004; Croce A. *et al.*, 2010; Vasuta C. *et al.*, 2015). Since TBS_{opto} restricts activation to CA1 PCs, without affecting other CA1 afferent fibers potentially activated with tetanization by electrical stimulation (Cardin J. A. *et al.*, 2010; Nabavi S. *et al.*, 2014; Nicholson E. & Kullmann D. M., 2021), selective activation of CA1 PC axons may, thus, be sufficient to induce Hebbian LTP at PC-SOM synapses. CA1 SOM cells receive other afferents, notably cholinergic projections from septum (Leao R. N. *et al.*, 2012; Lovett-Barron M. *et al.*, 2012), GABAergic fibers from septum (Sun Y. *et al.*, 2014), brainstem nucleus incertus (Szonyi

A. *et al.*, 2019) and local interneurons (Tyan L. *et al.*, 2014), as well as noradrenergic, serotonergic and dopaminergic inputs (Oleskevich S. *et al.*, 1989; Pelkey K. A. *et al.*, 2017). Our findings establish that activation of these other projection systems is not required for LTP at PC-SOM synapses. This is in contrast to another form of plasticity at excitatory synapses onto putative-SOM cells in CA1 stratum oriens, anti-Hebbian LTP (Lamsa K. P. *et al.*, 2007; Nicholson E. & Kullmann D. M., 2021), which can be induced by optogenetic activation of cholinergic afferents but not of CA1 PCs, and, thus, is due to cholinergic heterosynaptic LTP at PC-oriens interneurons excitatory synapses (Nicholson E. & Kullmann D. M., 2021). Our finding that TBS_{opto} of PC-SOM synapses is sufficient for induction of LTP is consistent with previous work that Hebbian LTP is afferent pathway-specific, occurring at CA1 PC-SOM synapses but not at CA3 PC-SOM synapses (Croce A. *et al.*, 2010).

Interestingly, we uncovered that TBS_{opto}-induced LTP at PC-SOM synapses was mTORC1-dependent and transcription-independent. A more persistent (lasting many hours) form of mGluR1a-mediated LTP at PC-SOM synapses is both transcription- and translation-dependent (Ran I. *et al.*, 2009; Artinian J. *et al.*, 2019). Since mTORC1 is a key signaling control mechanism of translation (Costa-Mattioli M. *et al.*, 2009), our results suggest that mGluR1a-mediated LTP at PC-SOM synapse is translation-dependent. Thus, LTP at PC-SOM synapses may be mediated by mechanisms analogous to mGluR-mediated, mTORC1- and translation-dependent, transcription-independent LTD at SC-PC synapses (Huber K. M. *et al.*, 2000; Banko J. L. *et al.*, 2006). Such a mTORC1- and protein synthesis-dependent mechanism is consistent with the slow onset gradual development over minutes of LTP at PC-SOM synapses (Huber K. M. *et al.*, 2000). SOM interneurons express both mGluR1 and mGluR5 (van Hooft J. A. *et al.*, 2000; Topolnik L. *et al.*, 2006). Previous work indicated that mGluR1a and mGluR5 signal via distinct pathways in SOM intermeurons, notably OLM cells (Topolnik L. *et al.*, 2006). Activation of mGluR1a leading to Src/ERK-dependent Ca^{2+} entry via TRP channels and intracellular Ca^{2+} release are necessary for LTP induction at SOM interneuron excitatory synapses, whereas mGluR5 activation and intracellular Ca^{2+} release are not involved in LTP induction (Topolnik L. *et al.*, 2006). Here we examined the role of mGluR1a in TBS_{opto}-induced LTP at PC-SOM synapses, however additional work will be necessary to clarify if mGluR5 is implicated in this plasticity.

Network regulation

Our finding that TBS_{opto} up-regulated LTP at SC-PC synapses and down-regulated LTP at TA-PC synapses in a mGluR1a- and SOM cell-mTORC1-dependent manner, is consistent with a differential gating of plasticity at PC input pathways by SOM cells (Leao R. N. *et al.*, 2012) that is controlled over long-term periods by plasticity of SOM cell input synapses (Leao R. N. *et al.*, 2012; Vasuta C. *et al.*, 2015; Artinian J. *et al.*, 2019; Sharma V. *et al.*, 2020). It is noteworthy that TBS_{opto} did not affect basal transmission at SC- and TA-PC synapses, but regulated theta burst induced plasticity at these synapses. This modulation of plasticity reflects the property of PC-SOM synapses that show facilitation and postsynaptic firing with repeated stimulation, resulting in effective recruitment with repetitive activation of PCs (Pouille F. & Scanziani M., 2004; Croce A. *et al.*, 2010; Honore E. *et al.*, 2021).

What are the network mechanisms responsible for the differential modulation of LTP of CA3 and entorhinal inputs of pyramidal cells? Previous work indicated that somatostatin-expressing oriens lacunosum-moleculare (OLM) interneurons differentially modulate CA3 and entorhinal inputs to CA1 pyramidal cells (Leao R. N. *et al.*, 2012). OLM inhibitory interneurons suppress entorhinal inputs via postsynaptic inhibition of PC distal dendrites in stratum lacunosum-moleculare (Leao R. N. *et al.*, 2012). In addition, OLM inhibitory interneurons facilitate CA3 inputs by disinhibition of the more proximal dendrites of pyramidal cells, i.e. OLM interneurons inhibit other inhibitory interneurons in stratum radiatum which themselves inhibit local pyramidal cell dendrites (Leao R. N. *et al.*, 2012). Moreover, OLM interneurons similarly modulated LTP in these pathways, depressing LTP of entorhinal inputs and facilitating LTP of CA3 inputs (Leao R. N. *et al.*, 2012). Our present findings are consistent with these mechanisms of regulation of CA1 network plasticity. In addition, previous work showed that a consequence of LTP at PC-SOM input synapses is to enhance synaptically-evoked firing of SOM interneurons (Croce A. *et al.*, 2010). Thus, our present results and previous reports (Croce A. *et al.*, 2010; Leao R. N. *et al.*, 2012) are consistent with network mechanisms whereby LTP at input synapses of SOM INs increases their firing output, which enhances LTP of the CA3 input pathway via an increased disinhibitory action in proximal dendrites of pyramidal cells (Vasuta C. *et al.*, 2015; Artinian J. *et al.*, 2019), and suppresses LTP of the entorhinal input pathway via an increased inhibitory action in distal dendrites of pyramidal cells (Sharma V. *et al.*, 2020).

Our findings highlight the different roles of long-term synaptic plasticity at excitatory synapses onto PC *versus* SOM interneurons. It has been proposed that LTP at PC excitatory synapses serves to generate enduring changes at synapses of engram cells that encode memories (Nabavi S. *et al.*, 2014; Choi J. H. *et al.*, 2018). In contrast, our results suggest that LTP at SOM cell excitatory synapses may serve to regulate the state of plasticity (or metaplasticity) of PC input synapses (Honore E. *et al.*, 2021). These distinct roles suggest that hippocampal-dependent encoding of memories, via LTP in PCs, can still occur, albeit in a reduced manner, in the absence of LTP at SOM cell synapses, as for example in mice with conditional knockout of *Rptor* in SOM cells (Artinian J. *et al.*, 2019). However, LTP at PC-SOM synapses controls the efficiency of hippocampal-dependent encoding memories by PCs, providing additional versatility to CA1 network plasticity. Our findings provide a link between LTP at PC-SOM synapses, regulation of metaplasticity at SC-PC and TA-PC synapses, and modulation of contextual fear memory. Contextual fear learning was previously shown to induce LTP at PC-SOM synapses (Artinian J. *et al.*, 2019). Thus, during contextual fear learning, LTP is induced at PC-SOM synapses, and this may cause an upregulation of the CA1 network plasticity changes, such as LTP at SC-PC synapses, that encode memory. Thus, impairment in learning-induced plasticity at PC-SOM synapses caused by TBS_{opto} *in vivo* (Figure 4) may result in a loss of upregulation of metaplasticity in the CA1 network during learning (Figure 2), and in a deficit in memory consolidation (Figure 3). Such a link would be strengthened by a demonstration that contextual fear learning induces long-term changes at SC-PC and TA-PC synapses, and that these changes are modulated by *in vivo* manipulation of LTP at PC-SOM synapses. However, given the spatially restricted synaptic plasticity changes in pyramidal cells (Whitlock J. R. *et al.*, 2006) and the sparse coding of synaptic changes in hippocampal engram cells (Choi J. H. *et al.*, 2018), such experiments require different approaches that those used in the present study.

The gating of PC input pathways has been well established for OLM cells, a subtype of SOM cells (Leao R. N. *et al.*, 2012). However, SOM cells also include other types of interneurons: bistratified cells, and other cells with both local projections and distal projections to septum, subiculum or retrohippocampal areas (CA3, dentate gyrus, entorhinal cortex) (Pelkey K. A. *et al.*, 2017; Booker S. A. & Vida I., 2018; Honore E. *et al.*, 2021). Although excitatory synapses onto bistratified cells and OLM cells show Hebbian LTP (Perez Y. *et al.*, 2001; Croce A. *et al.*, 2010), it remains to be determined if SOM projection cells also do. Thus, it will be interesting to build on our findings and

determine how plasticity at input synapses of other CA1 SOM cell types may participate in network regulation, possibly even controlling more distant hippocampal-related pathways.

Learning-induced changes at the input synapses of SOM cells may only be part of a more integrated response of SOM cells during learning. An increase in the intrinsic excitability of CA1 SOM cells, due to a reduced Ca^{2+}-dependent K^+ conductance, was found after learning a hippocampus-dependent trace eyeblink conditioning task (McKay B. M. *et al.*, 2013). Although it remains to be determined if SOM cell inhibitory synapses demonstrate learning-induced changes (Chiu C. Q. *et al.*, 2018; Udakis M. *et al.*, 2020), mTORC1-dependent axonal sprouting by CA1 SOM cells takes place in the CACNA1A mouse model of epilepsy which is characterized by impaired synaptic inhibition by Pvalb interneurons (Jiang X. *et al.*, 2018). These previous works and our findings indicate that multiple plasticity mechanisms occur in SOM cells at the level of their input function, intrinsic excitability and perhaps even output synapses, suggesting that an integrated gain-of-function response may occur in SOM cells during learning.

TBS_{opto} interaction with Hebbian and learning-induced LTP

Our results that TBS_{opto} given *in vivo* prior to contextual fear conditioning affects long-term contextual fear memory suggests that LTP at PC-SOM synapses regulates hippocampal memory. In these experiments, TBS_{opto} was given *in vivo* . Thus, it is conceivable that optogenetic activation of PCs in the CA1 region also activated the other major synaptic target of pyramidal cells, subicular pyramidal neurons (Taube J. S., 1993; Cenquizca L. A. & Swanson L. W., 2007), inducing long-term plasticity at these synapses (O'Mara S. M. *et al.*, 2000; Huang Y. Y. & Kandel E. R., 2005) and influencing hippocampal memory function. To examine this possibility, we examined the effects of TBS_{opto} in mice with a cell-specific conditional knockout of *Rptor* in somatostatin interneurons, in which LTP at PC-SOM synapses is blocked. We found that the regulation of long-term contextual fear memory by TBS_{opto} was absent in these mice (Figure 3), suggesting that the regulation of hippocampal memory by TBS_{opto} was due to changes at PC-SOM synapses and not at other efferent targets of CA1 PCs, like subicular neurons. However, it would be interesting in future experiments to design an induction protocol applicable *in vivo* that selectively activates CA1 PC-SOM synaptic plasticity and, thus, rule out actions via other synaptic targets of CA1 PCs. Nonetheless, our results are consistent with our other observations that PC-SOM synapse efficacy

was reduced, like fear memory, by TBS_{opto} given prior to learning (Figure 4), as well as with our previous findings that learning-induced LTP at PC-SOM synapses is necessary for long-term contextual fear memory (Artinian J. *et al.*, 2019). It is noteworthy that TBS_{opto} in slices produces LTP at PC-SOM synapses and not at PC-PV synapses, indicating some CA1 PC target cell-specificity in TBS_{opto} induced long-term plasticity.

Our results indicate that LTP at PC-SOM synapses induced by TBS_{opto} share similar mechanisms as Hebbian LTP induced by electrical TBS and LTP induced by contextual fear learning at excitatory synapses onto SOM cells. As reported for LTP at hippocampal synapses (Bliss T. V. & Lomo T., 1973), LTP induced by a first episode of TBS_{opto} occluded further LTP by a second TBS_{opto}. However, LTP induced by a first episode of electrical TBS did not, and more LTP was induced by a second episode of TBS. In contrast, when electrical TBS was given after LTP induced by a first TBS_{opto} episode, depotentiation occurred at PC-SOM synapses. Similarly, *in vivo* , when contextual fear conditioning was given 30 min after TBS_{opto}, the efficacy of PC-SOM synapses was reduced during *ex vivo* recordings 24 hours later. These results indicate that although they share similar mechanisms, LTP induced by TBS_{opto}, electrical TBS and fear learning are not identical. This is not surprising given that electrical stimulation may activate additional intra-hippocampal fibers, and learning may implicate other systems in addition to CA1 PC-SOM synapses. These additional mechanisms are likely implicated in the depotentiation of PC-SOM synapses. Multiple mechanisms regulate PC-SOM synapse function and plasticity, notably pre- and post-synaptic $GABA_B$-receptor mediated inhibition (Booker S. A. *et al.*, 2018; Booker S. A. *et al.*, 2020), astrocyte-mediated regulation of glutamate uptake (Huang Y. H. *et al.*, 2004), and $GABA_A$ synaptic inhibition by vasoactive intestinal polypeptide inhibitory interneurons (Tyan L. *et al.*, 2014). It will be important to determine if any of these control mechanisms are implicated in the modulation/depotentiation of PC-SOM synapses. Importantly, our findings that learning-induced potentiation is impaired by prior application of TBS_{opto} *in vivo* may explain why contextual fear memory may be impaired by TBS_{opto}, providing further support that LTP induced at PC-SOM synapses is sufficient to regulate CA1 network metaplasticity and the contextual fear memory.

Limitations of the study

Some limitations should be considered when interpreting our results. First, although our interpretation of the results is concordant with optical stimulation resulting in LTP at PC-SOM synapses *in vivo*, this remains to be demonstrated directly. This would require recording synaptic activity of SOM INs *in vivo* and assessing the effect of optogenetic induction *in vivo* on this synaptic activity. Such experiments however require different experimental approaches than those used here. Instead, we addressed this issue using the approach shown in Figure 4, with optical stimulation *in vivo*, contextual fear conditioning and *ex vivo* recordings. Our *ex vivo* results are consistent with optical stimulation *in vivo* eliciting LTP and with subsequent contextual fear conditioning resulting in depotentiation, instead of the late form of LTP that is normally elicited (Artinian J. *et al.*, 2019). These results are analogous to the effect found in the slice experiments whereby optical stimulation *in vitro* elicits LTP and subsequent TBS with electrical stimulation results in depotentiation, instead of the LTP normally elicited. Thus, our results are consistent with the notion that optical stimulation elicits LTP at PC-SOM synapses both *in vivo* and *in vitro*. Previous work showed that a different induction protocol with repeated episodes of stimulation elicits a late, persistent form of LTP that lasts many hours to a day at SOM interneuron excitatory synapses (Ran I. *et al.*, 2009; Artinian J. *et al.*, 2019). Thus, it would be important to test if such a repeated optical stimulation protocol *in vivo* can produce persistent changes at PC-SOM synapses that can be detected with *ex vivo* recordings.

Second, a caveat of our study concerns our results that the regulation of long-term contextual fear memory by TBS_{opto} was absent in mice with conditional knockout of *Rptor* in somatostatin cells, suggesting that the regulation of hippocampal memory by TBS_{opto} was due to changes at PC-SOM synapses. The lack of effect of TBS_{opto} on contextual fear memory in the Raptor-KO model could be due to the low level of freezing response in these mice, indicating that these animals cannot learn any worse. In our experiments we used a weak contextual fear conditioning protocol based on previous work showing that inactivating SOM interneurons impairs contextual fear memory (Lovett-Barron M. *et al.*, 2014). It is important to note that with this contextual fear conditioning protocol, SOM-Cre-Raptor-KO mice show impaired fear memory relative to control mice, however the SOM-Cre-Raptor-KO mice do display significant freezing responses in the memory probe test relative to pre-conditioning, indicating some level of contextual

memory (Figure 3F). Using a stronger contextual fear conditioning protocol, previous work showed also that although the SOM-Cre-Raptor-KO mice display a memory impairment, they still show significant contextual fear learning (Artinian J. *et al.*, 2019). Thus, these findings suggest that a component of contextual fear learning requires mTORC1 and SOM interneurons, but another component does not. A similar conclusion was found for spatial learning in the Barnes maze (Artinian J. *et al.*, 2019). Thus, repeating the present experiments with a stronger contextual fear conditioning protocol (Artinian J. *et al.*, 2019) could help resolve the possibility of a floor effect in our experiments. However, the residual significant freezing responses in SOM-Cre-Raptor-KO mice in the contextual fear memory probe test suggest the absence of a floor effect, and, thus, are consistent with the effects of TBS_{opto} on contextual fear memory being due to LTP at PC-SOM synapses.

ACKNOWLEDGMENTS

This work was supported by grants to J.C.L. from the Canadian Institutes of Health Research (CIHR MOP-125985 and PJT-153311) and a Research Centre grant (Centre Interdisciplinaire de Recherche sur le Cerveau et l'Apprentissage; CIRCA) from the Fonds de la Recherche du Québec – Santé (FRQS). J.C.L. is the recipient of the Canada Research Chair in Cellular and Molecular Neurophysiology (CRC 950-231066) and a member of the Research Group on Neural Signaling and Circuitry (GRSNC) at Université de Montréal.

AUTHOR CONTRIBUTIONS

Conceptualization, J.C.L., A.A. and E.H.; Methodology, A.A., E.H and I.L.; Software, E.H.; Formal Analysis, A.A. and E.H.; Investigation, A.A., E.H., I.L. and F.X.M.; Writing – Original Draft, J.C.L., A.A., E.H. and I.L.; Writing – Review & Editing, J.C.L., A.A. and E.H.; Visualization, A.A., E.H. and I.L.; Supervision, Project Administration, and Funding Acquisition, J.C.L.

DECLARATION OF INTERESTS

The authors declare no competing interests.

STAR METHODS

RESOURCE AVAILABILITY

Lead Contact

Further information and requests for resources should be directed to and will be fulfilled by the Lead Contact, Dr. Jean-Claude Lacaille (jean-claude.lacaille@umontreal.ca).

Materials Availability

This study did not generate new unique reagents.

Data and Code Availability

The published article includes all datasets generated or analyzed during this study. The raw electrophysiology data supporting the current study have not been deposited in a public repository because there is currently no standardized format or repository for such data, but they are available from the corresponding author on request.

EXPERIMENTAL MODEL AND SUBJECT DETAILS

Animals

Experimental protocols were approved by the Animal Care Committee at the Université de Montréal (Comité de Déontologie de l'Expérimentation sur les Animaux; CDEA Protocols # 17-

001, 17-002, 18-002, 18-003, 19-003, 19-004, 20-001, 20-002, 21-001, 21-002) and experiments were performed in accordance with the Canadian Council of Animal Care guidelines.

Sst$^{ires\text{-}Cre}$ mice (Taniguchi H. *et al.*, 2011) were crossed with *Rosa26*$^{lsl\text{-}EYFP}$ reporter mice (Madisen L. *et al.*, 2010) to generate Cre-dependent Enhanced Yellow Fluorescent Protein (EYFP) expression in SOM interneurons (SOM-Cre-EYFP mice) (Artinian J. *et al.*, 2019). *Sst*$^{ires\text{-}Cre}$;*Rosa26*$^{lsl\text{-}EYFP}$ mice were crossed with floxed *Rptor* mice (Sengupta S. *et al.*, 2010) for cell-specific homozygous knock-out of *Rptor* in SOM cells (SOM-Cre-Raptor-KO mice) (Artinian J. *et al.*, 2019). *Pvalb*$^{ires\text{-}Cre}$ mice (Hippenmeyer S. *et al.*, 2005) were used for Cre-dependent targeting of PV interneurons (Pvalb-Cre mice). Mice were housed 2-4 animals per cage, except for *in vivo* optogenetic studies in which mice were housed singly after cannula implantation. Food and water were *given ad libitum*. The mice were maintained on a 12 h light/dark cycle with all experiments performed during the light phase.

The *in vitro* electrophysiological slice experiments were performed on 6-7 weeks old male or female mice at the diestrus phase to reduce possible variability in responses. Behavioral studies and *ex vivo* electrophysiological slice experiments were carried out on 8-10 weeks old male mice.

METHOD DETAILS

Virus injection

Four weeks old mice were given an intraperitoneal (IP) injection of ketamine (50 mg/kg i.p.) and xylazine (5 mg/kg i.p.) and placed in a stereotaxic frame (Stoelting). For *in vitro* slice experiments, AAV2/9-CaMKIIa-hChR2(E123T/T159C)-mCherry (1.5-1.77×10^{12} particles/ml) or AAV2/9-CaMKIIa-mCherry (2.20×10^{13} particles/ml) were injected bilaterally in CA1 hippocampus (coordinates relative to bregma: −1.95 mm AP, ±1.3 mm ML, and -1.3 mm DV) of mice of either sex. Viral solution (0.5-0.8µl) was delivered at a flow rate of 50-100 nl/min using a 10µl Hamilton syringe and a microfluidic pump (Harvard Apparatus). The needle was left in place for at least 5 minutes after injection. For some slice experiments, Pvalb-Cre mice were injected, in addition, with AAV2/9-EF1a-DIO-EYFP (3.95×10^{13} particles/ml). For *in vivo* optogenetic experiments, 7-8 weeks old male mice were used and treated as above. In some *in vivo* experiments, mice were

injected bilaterally 0.5µl of AAV2/9-flex-Arch-GFP (1.74-1.83×10^{13} particles/ml) or AAV2/9-EF1a-DIO-EYFP (3.95×10^{13} particles/ml) as above.

Hippocampal slice preparation

Six to seven weeks old animals (10-18 days after viral injection) were anesthetized by isoflurane inhalation and the brain was rapidly removed and placed in cold (4°C) sucrose-based cutting solution saturated with 95% O_2 and 5% CO_2 containing the following (in mM): 87 NaCl, 2.5 KCl, 1.25 NaH_2PO_4, 7 $MgSO_4$, 0.5 $CaCl_2$, 25 $NaHCO_3$, 25 glucose, 9.5 ascorbic acid, 3.0 pyruvic acid and 75 sucrose, pH 7.4, and 295-300 mOsmol/L. A block of tissue containing the hippocampus was prepared and transverse hippocampal slices (300 and 400 µm thickness for whole-cell and field recordings, respectively) were cut with a vibratome (Leica VT1000S). Slices were transferred to artificial CSF (ACSF; saturated with 95% O_2 and 5% CO_2) containing the following (in mM): 124 NaCl, 2.5 KCl, 1.25 NaH_2PO_4, 4 $MgSO_4$, 4 $CaCl_2$, 26 $NaHCO_3$, and 10 glucose (pH 7.3–7.4, and 295–300 mOsmol/L) at 32°C for 30 minutes, and afterward maintained at room temperature (20–22°C) for at least 90 minutes and until recording experiments. Individual slices were transferred to a submersion chamber perfused (3-4 ml/min) with ACSF at 31 ± 0.5°C, and with CA1 and CA3 regions separated by a surgical cut. Synaptic inhibition was intact in most experiments, except for voltage clamp recordings of EPSCs (see below). For *ex vivo* recordings after learning, slices were obtained as above from animals 24 hours after optogenetic stimulation and contextual fear conditioning.

Whole-cell patch clamp recording

EYFP-expressing CA1 interneurons were identified using an upright microscope (Nikon Eclipse, E600FN), equipped with a water-immersion long-working distance objective (40x; differential interference contrast, DIC), epifluorescence and an infrared CCD camera (CXE-B013-U; Mightex). Whole-cell current-clamp recordings were obtained using borosilicate glass pipettes (3-5 MΩ) filled with intracellular solution containing (in mM): 120 $KMeSO_4$, 10 KCl, 0.5 EGTA, 10 HEPES, 2.5 MgATP, 0.3 NaGTP and 10 Na_2-phosphocreatine (pH 7.3, 290-298 mOsmol/L). For whole-cell voltage-clamp recordings, the intracellular solution contained (in mM): 120 $CsMeSO_3$,

5 CsCl, 2 $MgCl_2$, 10 HEPES, 0.5 EGTA, 10 Na_2-phosphocreatine, 2 ATP-Tris, 0.4 GTP-Tris, 0.1 spermine, 2 QX314 (pH 7.2–7.3, 300 mOsmol/L). Data was acquired using a Multiclamp 700B amplifier (Molecular Devices) and digitized at 10-20 kHz using Digidata 1440A and pClamp 10.5/10.7 software (Molecular Devices). Recordings were low-pass filtered at 2 kHz and membrane potential was corrected for liquid junction potential (11 mV). Access resistance was monitored throughout experiments and data were included only if the holding current and series resistance were stable (changes <20% of initial value).

Whole cell recording of synaptic responses

EPSPs and EPSCs evoked by electrical stimulation were elicited using constant current pulses (50 µs duration) via an ACSF-filled bipolar theta-glass electrode positioned approximately 100-150 µm lateral from the recorded cell soma in the alveus near the border with CA1 stratum oriens. EPSCs were recorded in the presence of DL-2-Amino-5-phosphonopentanoic acid (DL-AP5; 50 µM) and SR-95531 (Gabazine, 5 µM) to block NMDA and $GABA_A$ receptors, respectively. Input-output function of EPSCs was studied by delivering current pulses of incremental intensity (0–600µA, 50µA steps); 10 trials per pulse intensity were delivered and responses averaged to determine EPSC amplitude (initial EPSC peak). The slope (synaptic gain) and *x*-intercept (minimal stimulation intensity) of the linear regression of the input-output relationship were measured on averaged responses of individual cells. Spontaneous EPSCs were recorded over a period of 5 min and generally 300 consecutive events were analyzed (except for some cells with low frequency of events: TBS_{opto} group 4 cells with 168, 188, 200 and 261 events; no TBS_{opto} group 2 cells with 279 and 294 event) for frequency and amplitude (Clampfit 10.7).

EPSPs evoked by focal optogenetic stimulation through the objective were elicited using a Polygon400 Multiwavelength Dynamic Patterned Illuminator (Mightex). An area (20x20 to 20x30 µm) lateral to the recorded cell soma was illuminated with brief pulses of blue light (470 nm; duration 0.5-2 ms). EPSPs evoked by whole field optogenetic stimulation were elicited using a 4-Channel LED Driver (DC4104; Thorlabs) coupled to an optical fiber (MF79L01; 400 µm core diameter, 0.39 NA; Thorlabs) and fiber optic cannula (CFM14L20; 400 µm core diameter, 0.39 NA; Thorlabs) positioned above the CA1 stratum oriens region of the slice with brief light pulses (470 nm; duration 0.5-2 ms). In some experiments, the mGluR1a antagonist LY367385 (40 µM)

was added in the ACSF during recordings. In other experiments, slices were pre-incubated in ACSF with 2 μM of the irreversible transcription inhibitor actinomycin D for 15 min prior to recording (Yuan S. & Burrell B. D., 2013; Younts T. J. *et al.*, 2016).

LTP induction protocol during whole cell current clamp recording

Test EPSPs were evoked at 0.1Hz. LTP induced by electrical stimulation was elicited by theta burst stimulation (TBS) consisting of 3 episodes (given at 30 s intervals) of 5 bursts (at 250 ms interburst intervals) of 4 electrical pulses at 100 Hz (Vasuta C. *et al.*, 2015). LTP induced by optogenetic stimulation of CA1 pyramidal cells (TBS_{opto}) was elicited by TBS consisting of 3 episodes (given at 30 s intervals) of 5 bursts (at 300 ms inter-burst interval) of 4 light pulses at 80 Hz. In some experiments, low frequency optogenetic stimulation (LFS_{opto}) was given as 3 episodes (given at 30 s intervals) of 3 bursts (at 500 ms inter-burst interval) of 3 light pulses at 20 Hz. Test EPSP amplitude was averaged in 2 minutes bins before and after LTP induction. EPSPs were characterized in one cell per slice, and responses were analyzed off-line using Clampfit (pClamp 10.5/10.6; Molecular Devices) and GraphPad Prism 6.

Field potential recording

For experiments with field potential recordings, transverse hippocampal slices were prepared as described above, except oxygenated ACSF contained 1.3 mM $MgSO_4$ and 2.5 mM $CaCl_2$. The slices were let to recover for at least 2 h at 32°C in ACSF, and for an additional 30 minutes at 27°–28°C while submerged in a recording chamber continuously perfused (2–2.5 ml/min) with ACSF. Extracellular field EPSPs were recorded with borosilicate glass pipettes (3–4MΩ) filled with ACSF using a differential extracellular amplifier (Microelectrode AC Amplifier Model 1800, A-M Systems), filtered at 2 kHz, digitized at 10 kHz (Digidata 1440A), and analyzed with pClamp10.5. For Schaffer collateral-evoked fEPSPs, the concentric bipolar tungsten stimulating electrode (FHC) and recording pipette were placed in stratum radiatum. For temporo-ammonic pathway evoked fEPSPs, the stimulation and recording electrodes were positioned in stratum lacunosum-moleculare. Stimulus (0.1 ms duration; 15 sec^{-1}) strength was adjusted to elicit 50% of maximal fEPSP and fEPSP slope was measured at 10–90% of fEPSP amplitude. CA1 pyramidal cell long-

term potentiation was induced by weak theta burst stimulation (wTBS; 2 bursts of 4 pulses at 100 Hz, with 200 ms inter-burst interval) (Leao R. N. *et al.*, 2012). Optogenetic induction of LTP in SOM interneurons was elicited as described above through a fiber optic positioned above the CA1 stratum oriens/alveus region of the slice.

Optogenetic stimulation *in vivo*

One week after viral injections, mice were anesthetised using ketamine and xylazine as described above, and fiber cannulas were stereotaxically implanted bilaterally (coordinates relative to bregma: -1.95 AP; ±1.60 ML; and -1.15 DV) and sealed with dental cement (Metabond, Parkell Inc). Animals were housed singly after the optic fiber implantation and allowed to rest for a week before behavioral experimentation. For *in vivo* optogenetic stimulation, a Quadruple Laser Diode Fiber Light Source (LDFLS_405/100_450/070_520/060_638/080; Doric Lenses Inc) was coupled to Mono Fiberoptic Patchcords (MFP_200/240/900-0.22_2m_FC-ZF1.25(F), 200 µm Core diameter, 0.22 NA; Doric Lenses Inc) and hand-made fiber optic cannulas (optic fiber: FT200EMT, 200 µm Core diameter, 0.22 NA; ceramic ferrule: CFLC230-10; Thorlabs).

Behavioral experiments

For all behavioral experiments, the experimenter was blind to the experimental groups (opsin *versus* reporter) from the day habituation began until data analysis was completed.

Habituation. Mice were gently handled daily for 5 days (5min/day) to progressively habituate them to the experimenter and reduce the stress related to the experimental handling and optic fiber connection (without light stimulation).

Open field test. Mice were allowed to freely explore a square arena (45 x 45 cm; Pan-Lab) for 15 min for the Arch experiments and 5 min for the hChR2 experiments. The anxiety level was assessed by measuring the time spent and the distance travelled in the center (1/3 central zone) of the arena compared to the periphery (1/3 peripheral zone). Locomotion was evaluated by measuring the total distance traveled and the number of zone transitions (16 equal squared zones). Mice were first video-tracked at 25 frames/s and their movements subsequently analyzed using a position tracking system (Smart 3.0; PanLab). For the Arch experiments, mice received continuous light stimulation (520 nm) for the 5-10 min period.

Contextual fear conditioning. Mice were trained in conditioning chambers that were housed in sound- and light-isolated cubicles (Coulbourn Instruments). The chambers contained a stainless-steel grid floor, overhead LED lighting, camera and were supplied with background noise (60 dB) by an air extractor fan. The experimental protocol was based on Lovett-Baron and coworkers (Lovett-Barron M. *et al.*, 2014) with slight modifications. The training context was rectangular with 2 transparent and 2 stainless steel walls, was cleaned with 70% ethanol solution before and after each trial, and ethanol solution was added under the grid floor as a contextual smell. After 2 min free exploration, the animals received a weak fear conditioning consisting of 2 presentations of unconditioned stimulus (2 sec foot shock, 0.8mA; separated by 60 sec). To test for long-term contextual fear memory, the mice were returned to the training context during a test period of 3 min, at 24 h after conditioning. The freezing behavior was assessed using FreezeFrame (Coulbourn Instruments).

For the Arch optogenetic experiments, mice received light stimulation (520 nm; 6 sec pulses) in phase (starting 2 sec before) or shifted (30 sec before) relative to foot shocks during conditioning. For the TBS optogenetic experiments, mice were brought in the testing room on the training day and, in their home cage, given the optogenetic TBS protocol (473 nm; 5 bursts of 4 light pulses of 1ms duration at 80 Hz, given at 300 ms interburst interval, and repeated 3 times with 30 s interval) or no light stimulation, 30 min prior to contextual fear conditioning.

Histology

Following *in vivo* optogenetic experiments, mice were deeply anesthetized intraperitoneally with sodium pentobarbital (MTC Pharmaceuticals), perfused transcardially first with 0.1M phosphate buffer saline (PBS) and next with 4% paraformaldehyde in 0.1M PBS (PFA). Brains were isolated, postfixed in 4% PFA for 24 hours and cryoprotected in 30% sucrose. Coronal brain sections (50 µm thick) were obtained using freezing microtome (SM200R; Leica) and mounted in ProLong Gold (Invitrogen). Sections were examined using an epifluorescence microscope (Eclipse E600; Nikon) and images were acquired with the Simple PCI software. Immunofluorescence was used to enhance GFP fluorescence associated with Arch. For these mice, brain sections were obtained as described above, permeabilized with 0.5% Triton X-100 in PBS for 15 minutes, and unspecific binding was blocked with 10% normal goat serum in 0.1% Triton X-100/PBS for 1 hour. Rabbit

polyclonal GFP (1/200) antibodies were incubated for 48 hours at 4°C. Sections were subsequently incubated at room temperature with Alexa Fluor 594-conjugated goat anti-rabbit IgG (1/500; 90 min), mounted in ProLong Gold, and imaged as described above. For behavioral experiments, data were excluded if mice did not show virus expression restricted to CA1, and if optic fibers placement was outside the CA1 hippocampus.

QUANTIFICATION AND STATISTICAL ANALYSIS

No statistical methods were used to predetermine the sample size, but our sample sizes are similar to those used in the field. Statistical analysis was performed using SigmaPlot or GraphPad Prism 6 and 9. Data were tested for normality using the Shapiro–Wilk, D'Agostino and Pearson, Kolmogorov-Smirnov, and Brown–Forsythe tests. We used Student's *t* tests, one- or two-way ANOVA, and one- or two-way mixed repeated-measures ANOVA, with Tukey's pairwise comparison tests (with Bonferroni adjustments for multiple comparisons) or with Holm-Sidak pairwise comparison tests, when data passed normality and homoscedasticity assumptions. Wilcoxon matched pairs signed rank tests, Mann–Whitney Rank Sum tests and Kruskal-Wallis one-way ANOVA on Ranks with Dunn's pairwise comparisons, were used when data did not pass normality and homoscedasticity assumptions. All the tests were two-sided. All data in the Figures are presented as mean ± SEM. Asterisks in Figures denote statistical significance levels for specified tests (* $p < 0.05$; ** $p < 0.01$; *** $p < 0.001$; ns, not significant). Detailed results of all statistical tests referenced per Figure panel are given in Supplemental Table 1. Baseline EPSP amplitudes are reported for all groups in Supplemental Table 2, with Dunn's multiple comparisons tests indicating no differences between SOM interneuron groups.

Supplemental Information

Table S1. Details of statistical comparisons, related to Figures 1-4, S1-4

Figure	Panel	Group size	Test	Statistic	P values	Statistic 2	P values 2
1	B	TBS_{opto} n=17	Paired t-test	t(16)=6.312	P < 0.0001		
1	C	LFS_{opto} n=8	Paired t-test	t(7)=0.449	P = 0.667		
1	D	No tetanization n=13	Paired t-test	t(12)=1.138	P= 0.277		
1	E	LY n=10	Paired t-test	t(9)=2.141	P = 0.06		
1	F	SOM-Cre-Raptor-KO n=15	Paired t-test	t(14)=0.5457	P = 0.5939		
1	G	Actin D n=6	Paired t-test	t(5)=3.482	P = 0.0176		
1	I	Pvalb-Cre-EYFP n=8	Paired t-test	t(7)=1.578	P = 0.158		
1	J	TBS_{opto} n=17	Paired t-tests (as above, B-I)	as above, B-I	as above, B-I	Unpaired t-test,20-30 min post induction,TBS_{opto} vs Actin D, t(21)=1.396	P= 0.1772
		LFS_{opto} n=8					
		No tetanization n=13					
		LY n=10					
		SOM-Cre-Raptor-KO n=15					
		Actin D n=6					
		Pvalb-Cre-EYFP n=8					
1	K	TBS_{opto} n=17	Wilcoxon matched pairs signed rank test		P=0.0655		
		LFS_{opto} n=8	Wilcoxon matched pairs signed rank test		P=0.9688		

		No tetanization n=13	Paired t-test	t(12)=0.3049	P=0.7656		
		LY n=10	Paired t-test	t(9)=1.245	P=0.2446		
		SOM-Cre-Raptor-KO n=15	Paired t-test	t(14)=0.4623	P=0.6510		
		Actin D n=6	Paired t-test	t(5)=0.05801	P=0.9560		
		Pvalb-Cre-EYFP n=8	Paired t-test	t(7)=0.8685	P=0.4139		
SUP1	A	TBS_{opto}	Paired t-test	t(35) =8.243	P<0.0001		
		Pre n=36					
		Post n=36					
SUP1	B	LFS_{opto}	Paired t-test	t(35)=0.6396	P=0.5266		
		Pre n=36					
		Post n=36					
SUP1	C	No tetanization	Paired t-test	t(35)=0.3376	P=0.7377		
		Pre n=36					
		Post n=36					
SUP1	D	LY	Paired t-test	t(35)=0.7724	P=0.4450		
		Pre n=36					
		Post n=36					
SUP1	E	SOM-Cre-Raptor-KO	Paired t-test	t(35)=0.3611	P=0.7202		
		Pre n=36					
		Post n=36					
SUP1	F	Actin D	Paired t-test	t(35)=2.624	P=0.0128		
		Pre n=36					
		Post n=36					
SUP1	G	DMSO	Paired t-test	t(35)=3.354	P=0.0019		
		Pre n=36					
		Post n=36					
SUP1	H (left)	DMSO n=6	Paired t-test	t(5)=4.175	P = 0.0087		
SUP1	H (right)	Actin D n=6	Paired t-test, as above (Fig 1G and SUP 1H left)	Actin D t(5)=3.482	Actin D P = 0.0176	Unpaired t-test, 20-30 min post induction, Actin D vs	P= 0.3272
		DMSO n=6		DMSO t(5)=4.175	DMSO P = 0.0087		

						DMSO, t(10)=1.03	
SUP1	I	Pvalb-Cre-EYFP	Paired t-test	t(35)=0.2349	P=0.8157		
		Pre n=36					
		Post n=36					
SUP2	B left	TBS_{opto} n=9	Paired t-test	t(8)=3.248	P=0.0117		
SUP2	B right	TBS_{opto}	Paired t-test	t(35)=3.129	P=0.0035		
		Pre n=36					
		Post n=36					
SUP2	C left	No tetanization n=8	Paired t-test	t(7)=1.198	P = 0.270		
SUP2	C right	No tetanization	Paired t-test	t(35)=1.346	P= 0.1871		
		Pre n=36					
		Post n=36					
SUP2	D left	AAV9-CaMKIIa-mCherry n=8	Paired t-test	t(7)=0.04446	P = 0.965		
SUP2	D right	AAV9-CaMKIIa-mCherry	Paired t-test	t(35)=0.6835	P=0.4988		
		Pre n=36					
		Post n=36					
SUP2	E left	LY n=8	Paired t-test	t(7)=1.058	P = 0.325		
SUP2	E right	LY	Paired t-test	t(35)=1.299	P=0.2026		
		Pre n=36					
		Post n=36					
SUP2	F left	SOM-Cre-Raptor-KO n=8	Paired t-test	t(7)=0.3832	P = 0.712		
SUP2	F right	SOM-Cre-Raptor-KO	Paired t-test	t(35)=1.352	P=0.1850		
		Pre n=36					
		Post n=36					
SUP2	G	TBS_{opto} n=9					

		No tetanization n=8 9-CaMKIIa-mCherry n=8 LY n=8 SOM-Cre-Raptor-KO n=8	Paired t-tests (as above, B-F left)	as above, B-F left	as above, B-F left		
SUP3	B	No tetanization n=6	Paired t-test	t(5)=0.6528	P = 0.542		
SUP3	C	LY n=6	Paired t-test	t(5)=0.3449	P = 0.744		
SUP3	D	SOM-Cre-Raptor-KO n=8	Paired t-test	t(7)=0.4145	P = 0.690		
SUP3	E	TBS_{opto} n=7 No tetanization n=6 LY n=6 SOM-Cre-Raptor-KO n=8	Paired t-tests (as above, B-D; and Fig 2B below)	as above, B-D; and Fig 2B below	as above, B-D; and Fig 2B below		
SUP3	G	wTBS-SC Pre n=24 Post n=24	Paired t-test	t(24)= 0.3405	P = 0.7365		
SUP3	H	TBS_{opto}+wTBS-SC Pre n=24 Post n=24	Paired t-test	t(24)=22.14	P <0.0001		
SUP3	J	wTBS-TA Pre n=24 Post n=24	Paired t-test	t(24)=60.20	P <0.0001		
SUP3	K	TBS_{opto}+wTBS-TA Pre n=24 Post n=24	Paired t-test	t(24)=0.7208	P = 0.4780		
2	B	TBS_{opto} n=7	Paired t-test	t(6)= 3.455	P = 0.0135		
2	D	wTBS-SC n=13	Paired t-test	t(12)=1.183	P=0.2596		

		TBS_{opto}+wTBS-SC n=11	Paired t-test	t(10) =4.410	P = 0.0013		
		LY+TBS_{opto} +wTBS-SC n=7	Paired t-test	t(6)= 1.618	P = 0.1568		
		TBS_{opto} mCherry n=11	Paired t-test	t(10)=0.4497	P = 0.6625		
2	E	wTBS-SC Raptor-KO n=9	Paired t-test	t(8)= 2.215	P= 0.0576		
		TBS_{opto} +wTBS-SC Raptor-KO n=10	Paired t-test	t(9) =1.350	P= 0.2243		
2	F	wTBS-SC n=13 TBS_{opto}+wTBS n=11 LY+TBS_{opto} +wTBS-SC n=7 TBS_{opto}+wTBS-SC mCherry n=11	One-way ANOVA Multiple comparison	F (3, 38) = 6.053	P = 0.0018	Tukey's multiple comparisons test	25-35 min post induction TBS_{opto} + wTBS-SC vs. wTBS-SC P= 0.0067 TBS_{opto} + wTBS-SC vs. LY+TBS_{opto} + wTBS-SC P= 0.0359 TBS_{opto} + wTBS-SC vs. TBS_{opto}+wTBS-SC mCherry P= 0.0028 wTBS-SC vs. LY+TBS_{opto} + wTBS-SC

							P= 0.9993 wTBS-SC vs. TBS_{opto}+wTBS-SC mCherry P= 0.9645
2	G	SC no TBS_{opto} n=13 SC + TBS_{opto} n=11	Paired t test (Post no-TBS_{opto} vs. Base) Paired t test (Post TBS_{opto} vs. Base)	(12)=1.325 t(10)=1.925	P= 0.2099 P= 0.0832		
2	H	wTBS-SC Raptor-KO n=9 TBS_{opto} +wTBS-SC Raptor-KO n=10				Unpaired t-test, 25-35 min post induction	wTBS-SC Raptor-KO vs. TBS_{opto} +wTBS-SC Raptor-KO P= 0.4222 t(17)=0.8225
2	J	wTBS-TA n=7	Paired t-test	t(6)=2.985	P = 0.0245		
		TBS_{opto}+wTBS-TA n=6	Paired t-test	t(5)=0.955	P = 0.3833		
		LY+TBS_{opto} +wTBS-TA n=7	Paired t-test	t(6)=4.022	P = 0.0069		
		TBS_{opto}+wTBS-TA mCherry n=7	Paired t-test	t(6)=2.695	P = 0.0358		
2	K	wTBS-TA Raptor-KO n=8	Paired t-test	t(7)=4.385	P = 0.0032		
		TBS_{opto} +wTBS-TA Raptor-KO n=7	Paired t-test	t(6)=3.660	P = 0.0106		

2	L	wTBS-TA n=7 TBS_{opto}+wTBS n=6 LY+TBS_{opto} +wTBS-TA n=7 TBS_{opto}+wTBS-TA mCherry n=7	One-way ANOVA Multiple comparison	F (3, 23) = 3.667	P = 0.0270	Tukey's multiple comparisons test	25-35 min post induction TBS_{opto} + wTBS-TA vs. wTBS-TA P= 0.0420 TBS_{opto} + wTBS-TA vs. LY+TBS_{opto} + wTBS-TA P= 0.0289 TBS_{opto} + wTBS-TA vs. TBS_{opto}+wTBS-TA mCherry P= 0.0405 wTBS-TA vs. LY+TBS_{opto} + wTBS-TA P=0.999 wTBS-TA vs. TBS_{opto}+wTBS-TA mCherry P >0.9999
2	M	TA no TBS_{opto} n=7	Paired t test (Post no-TBS_{opto} vs. Base)	t(6)=0.5498	P= 0.6023		
		TA + TBS_{opto} n=6	Paired t test (Post TBS_{opto} vs. Base)	t(5)=2.177	P= 0.0815		

2	N	wTBS-TA Raptor-KO n=8 TBS_{opto} +wTBS-TA Raptor-KO n=7				Unpaired t-test,25-35 min post induction	wTBS-TA Raptor-KO vs. TBS_{opto} +wTBS-TA Raptor-KO P= 0.5516 t(13)=0.6113
3	C	EYFP-Phase n=8 Conditioning vs test	Mann-Whitney Rank Sum Test	T=106	P=0.001		
3	C	Arch-Phase n=9 Conditioning vs test	Mann-Whitney Rank Sum Test	T=84	P<0.001		
3	C	Arch-Shifted n=7 Conditioning vs test	Paired t-test	T=5.136	P<0.001		
3	C	EYFP-Phase n=8 Arch-Phase n=9 Arch-Shifted n=7	One-way ANOVA	F=10.188	P < 0.001	Holm-Sidak multiple comparisons test	Arch-Phase vs EYFP-Phase t = 2.627, P = 0.016 Arch-Phase vs Arch-Shifted t = 4.463, P <0.001 EYFP-Phase vs Arch-Shifted t = 1.879, P = 0.074
3				T=36	P<0.001		

	F Left	SOM-Cre-EYFP mice TBS_{opto} hChR2 n=8 Conditioning vs test	Mann-Whitney Rank Sum Test				
3	F Left	SOM-Cre-EYFP mice no TBS_{opto} hChR2 n=7 Conditioning vs test	Mann-Whitney Rank Sum Test	T=28	P<0.001		
3	F Left	SOM-Cre-EYFP mice TBS_{opto} EYFP n=8	Mann-Whitney Rank Sum Test	T=36	P<0.001		
3	F Left	SOM-Cre-EYFP mice TBS_{opto} hChR2 n=8 no TBS_{opto} hChR2 n=7 TBS_{opto} EYFP n=8	Kruskal-Wallis One-way ANOVA on Ranks	H = 17.626	P = 0.001	Dunn's multiple comparisons test	TBS_{opto} vs. no TBS_{opto} P=0.001 TBS_{opto} vs. TBS_{opto} no hChR2 P=0.001 No TBS_{opto} vs. TBS_{opto} no hChR2 P >0.05
3	F Right	SOM-Cre-Raptor-KO mice no TBS_{opto} n=7 Conditioning vs test	Mann-Whitney Rank Sum Test	T=31	P= 0.004		
3	F Right	SOM-Cre-Raptor-KO mice TBS_{opto} n=6 Conditioning vs test	Mann-Whitney Rank Sum Test	T=21	P= 0.002		
3				T =-0.653	P = 0.527		

	F Right	SOM-Cre-Raptor-KO mice TBS_{opto} n=6 no TBS_{opto} n=7	Unpaired t-test				
SUP4	B (Left) Time spent in periphery	EYFP n=6 Arch n=9	Two-way repeated measure ANOVA	EYFP vs Arch F = 0.12 no light vs light F = 0.0207 EYFP/Arch vs no light/light F = 0.892	EYFP vs Arch P = 0.734 no light vs light P = 0.888 EYFP/Arch vs no light/light P = 0.362		
SUP4	B (middle) Time spent in center	EYFP n=6 Arch n=9	Two-way repeated measure ANOVA	EYFP vs Arch F = 0.0688 no light vs light F = 0.000023 EYFP/Arch vs no light/light F = 0.00168	EYFP vs Arch P = 0.797 no light vs light P = 0.996 EYFP/Arch vs no light/light P = 0.968		
SUP4	B (Right) Ratio of time in center /periphery	EYFP n=6 Arch n=9	Mann-Whitney Rank Sum Test	T = 54	P = 0.517		
SUP4	C Total distance travelled	EYFP n=6 Arch n=9	Unpaired t-test	T = -0.0335	P = 0.974		
SUP4	C Zone	EYFP n=6 Arch n=9	Mann-Whitney	T = 54	P = 0.517		

	transitions		Rank Sum Test				
SUP4	E (Left) Time spent in periphery	SOM-Cre-EYFP mice mCherry n=6 SOM-Cre-EYFP mice hChR2 n=16 SOM-Cre-Raptor-KO mice hChR2 n=13	Kruskal-Wallis One Way Analysis of Variance on Ranks	H = 0.44	P = 0.802		
SUP4	E (middle) Time spent in center	SOM-Cre-EYFP mice mCherry n=6 SOM-Cre-EYFP mice hChR2 n=16 SOM-Cre-Raptor-KO mice hChR2 n=13	Kruskal-Wallis One Way Analysis of Variance on Ranks	H = 0.284	P = 0.868		
SUP4	E (Right) Ratio of time in center /periphery	SOM-Cre-EYFP mice mCherry n=6 SOM-Cre-EYFP mice hChR2 n=16 SOM-Cre-Raptor-KO mice hChR2 n=13	Kruskal-Wallis One Way Analysis of Variance on Ranks	H = 0.0549	P = 0.973		
SUP4	F (Left) Total distance	SOM-Cre-EYFP mice mCherry n=6 SOM-Cre-EYFP mice	Kruskal-Wallis One Way Analysis of Variance on Ranks	H = 1.274	P = 0.529		

		hChR2 n=16 SOM-Cre-Raptor-KO mice hChR2 n=13					
SUP4	F (Right) Zone transitions	SOM-Cre-EYFP mice mCherry n=6 SOM-Cre-EYFP mice hChR2 n=16 SOM-Cre-Raptor-KO mice hChR2 n=13	One-way ANOVA	F =0.781	P = 0.466		
4	B	Baseline TBS #1 TBS #2, n=8	rmANOVA	F (2, 14) = 22.41	P<0.0001	Tukey's multiple comparisons tests	Baseline vs. TBS #1 P= 0.0079 TBS #1 vs. TBS #2 P=0.0199
4	C	Baseline TBS_{opto} #1 TBS_{opto} #2, n=7	rmANOVA	F (2, 12) = 14.71	P=0.0006	Tukey's multiple comparisons test	Baseline vs. TBS_{opto} #1 P=0.0029 TBS_{opto} #1 vs. TBS_{opto} #2 P=0.7365
4	D	Baseline TBS_{opto} #1 TBS #2, n=8	rmANOVA	F (2, 14) = 9.137	P=0.0029	Tukey's multiple comparisons test	Baseline vs. TBS_{opto} #1 P=0.0180 TBS_{opto} #1 vs. TBS #2 P= 0.0031
4	E	Baseline TBS #1 TBS_{opto} #2, n=8	rmANOVA	F (2, 14) = 8.467	P=0.0039	Tukey's multiple	Baseline vs. TBS #1

						comparisons test	P=0.0290 TBS #1 vs. TBS_{opto} #2 P=0.5483
4	F	Baseline no TBS #1 TBS #2, n=10	rmANOVA	F (2, 18) = 24.33	P<0.0001	Tukey's multiple comparisons test	Baseline vs. no TBS #1 P=0.8039 No TBS #1 vs. TBS #2 P<0.0001
4	H sEPSC frequency	TBS_{opto} and CFC n=18 cells, 3 mice No TBS_{opto} and CFC n=17 cells, 4 mice	Mann-Whitney Rank Sum Test	t = 389	P = 0.006		
4	H sEPSC amplitude	TBS_{opto} and CFC n=18 cells, 3 mice No TBS_{opto} and CFC n=17 cells, 4 mice	Mann-Whitney Rank Sum Test	t =397	P = 0.003		
4	I Slope of EPSC I-O	TBS_{opto} and CFC n=17 cells, 3 mice No TBS_{opto} and CFC n=19 cells, 4 mice	Mann-Whitney Rank Sum Test	t = 221	P = 0.028		

Table S2. Light-evoked EPSP and electrical-evoked EPSP amplitude pre-TBS in all related experiments, related to Figures 1, 4, S2, and S3.

Experiments Figure 1	**N**	**EPSP Amplitude (mV) Mean±SEM**	**Statistic**
TBS_{opto}	17	7.786±0.6659	Dunn's multiple comparisons test
LFS_{opto}	8	7.106±0.6369	P= 0.9999
No tetanization	13	7.811±0.9687	P= 0.9999
LY	10	8.533±0.6725	P= 0.9999
Raptor-KO	15	6.448±0.4820	P= 0.7334
ActinD	6	5.840±0.8812	P= 0.6247
DMSO	6	6.106±0.6708	P= 0.9999
Pvalb	8	4.872±0.4452	P= 0.0167*
Experiments Figure S2	**N**	**EPSP Amplitude (mV) Mean±SEM**	**Statistic**
TBS_{opto}	9	4.339±0.4648	Dunn's multiple comparisons test
No tetanization	8	5.967±0.5759	P= 0.2202
mCherry	8	6.026±0.7012	P= 0.2202
LY	8	6.270±0.5736	P= 0.0563
Raptor-KO	8	5.631±0.6788	P= 0.7228
Experiments Figure S3	**N**	**EPSP Amplitude (mV) Mean±SEM**	**Statistic**
TBS_{opto}	7	8.852±0.5967	Dunn's multiple comparisons test
No tetanization	6	7.375±1.299	P= 0.9999
LY	6	10.52±0.4438	P= 0.4059
Raptor-KO	8	6.532±0.7446	P= 0.2394
Experiments Figure 4	**N**	**EPSP Amplitude (mV) Mean±SEM**	**Statistic**
B	8	4.540±0.4835	0.2089
C	7	4.248±0.3853	0.0937
D	8	6.427± 0.4251	0.5308
E	8	5.367±0.3607	0.9694
F	10	5.660±0.4683	F (4, 36) = 3.802

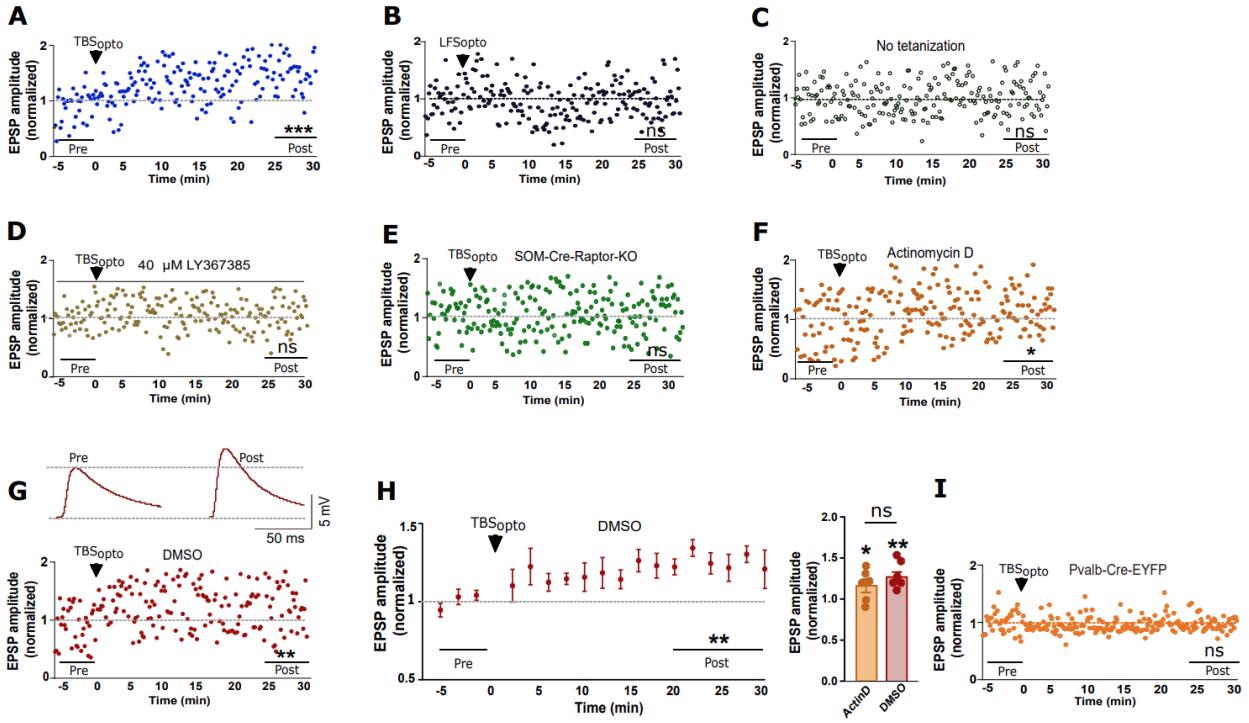

Figure S1. Optogenetically-induced LTP at PC-SOM synapses in representative cells, related to Figure 1. (A to E) Time plots of light-evoked EPSP amplitude from representative SOM cells (EPSPs shown in Figure 1B to 1G) showing LTP at PC-SOM synapses after TBSopto (A), but not after LFSopto (B), no tetanization (C), TBSopto in LY367385 (D), or TBSopto in SOM-Cre-Raptor-KO mice (E). Paired t-tests at 25-30 min after induction (Post) relative to baseline (Pre), *** $p < 0.0001$, ns $p > 0.05$. (F and G) Time plots of light-evoked EPSP amplitude from representative SOM cells (EPSPs shown in Figure 1G for cell in F), showing LTP at PC-SOM synapses after TBSopto after incubation with the transcription inhibitor actinomycin D (F) or its vehicle DMSO (G; EPSPs above). Paired t-tests, * $p < 0.05$,** $p < 0.01$. (H) Left: time plot of light-evoked EPSP amplitude for all SOM cells tested showing LTP at PC-SOM synapses following TBSopto after incubation with DMSO (n = 6 cells). Right: Summary graph of EPSP amplitude for all cells at 20-30 min post induction, showing similar LTP after TBSopto after incubation in actinomycin D or its vehicle DMSO. Paired t-tests (Pre vs Post) and unpaired t-test (Post Actin D vs Post DMSO), * $p < 0.05$, ** $p < 0.01$, ns $p > 0.05$. (I) Time plots of light-evoked EPSP amplitude from representative Pvalb cell (EPSPs shown in Figure 1I) showing absence of LTP at PC-Pvalb synapses after TBSopto. Paired t-test, ns $p > 0.05$.

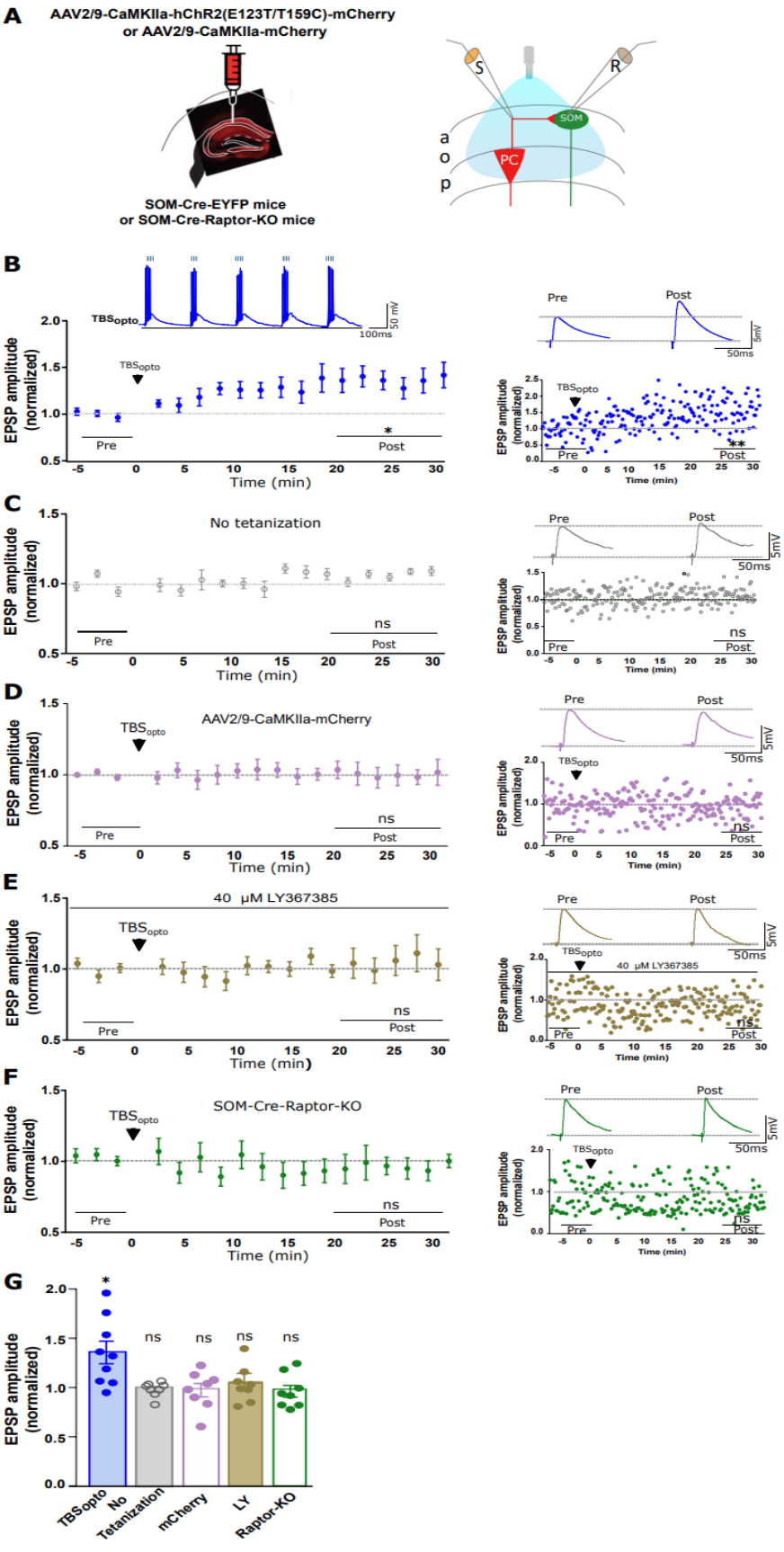
A
AAV2/9-CaMKIIa-hChR2(E123T/T159C)-mCherry
or AAV2/9-CaMKIIa-mCherry
SOM-Cre-EYFP mice
or SOM-Cre-Raptor-KO mice
S
R
SOM
PC
a
o
p
B
TBSopto
50 mV
100ms
EPSP amplitude (normalized)
Pre
Post
Time (min)
5mV
50ms
C
No tetanization
ns
D
AAV2/9-CaMKIIa-mCherry
E
40 μM LY367385
F
SOM-Cre-Raptor-KO
G
TBSopto
No Tetanization
mCherry
LY
Raptor-KO

Figure S2. Optogenetically-induced LTP of electrically-evoked EPSPs in SOM cells, related to Figure 1. (A) Left: schematic of experimental paradigm with viral injections in dorsal hippocampus of SOM-Cre-EYFP or SOM-Cre-Raptor-KO mice. Right: diagram of local optogenetic stimulation of CA1 pyramidal cells, electrical stimulation of afferents and whole cell recording from SOM cells. (B) Left: time plot of electrically evoked EPSP amplitude for all SOM cells, showing LTP at 20-30 min following TBSopto (n = 9 cells). Inset above: EPSP summation and cell firing during TBSopto. Right: example of EPSPs (top) and time plot (bottom) from a representative cell, before (Pre) and 25-30 min after (Post) induction. Paired t-tests; ** $p < 0.01$, * $p < 0.05$. (C - F) Time plots of electrically-evoked EPSP amplitude for all SOM cells (left) and example of EPSPs (top) and time plot (bottom) from a representative cell (right), showing absence of LTP of electrically-evoked EPSP amplitude following no tetanization (C; n = 8 cells), or following TBSopto in slices from mice with control CaMKIIa-mCherry injection without hChR2 (D; n = 8 cells), TBSopto in the presence of the mGluR1a antagonist LY367385 (40 μM) (E; n = 8 cells), or TBSopto in SOM-Cre-Raptor-KO mice (F; n = 8 cells). Paired t-tests; ns, $p > 0.05$. (G) Summary graph of EPSP amplitude for all cells at 20-30 min post induction, showing LTP after TBSopto, but no LTP in absence of tetanization, or after TBSopto in mice injected with mCherry, in LY367385, or in SOM-Cre-Raptor-KO mice. Paired t-tests (Pre vs Post); * $p < 0.05$, ns $p > 0.05$.

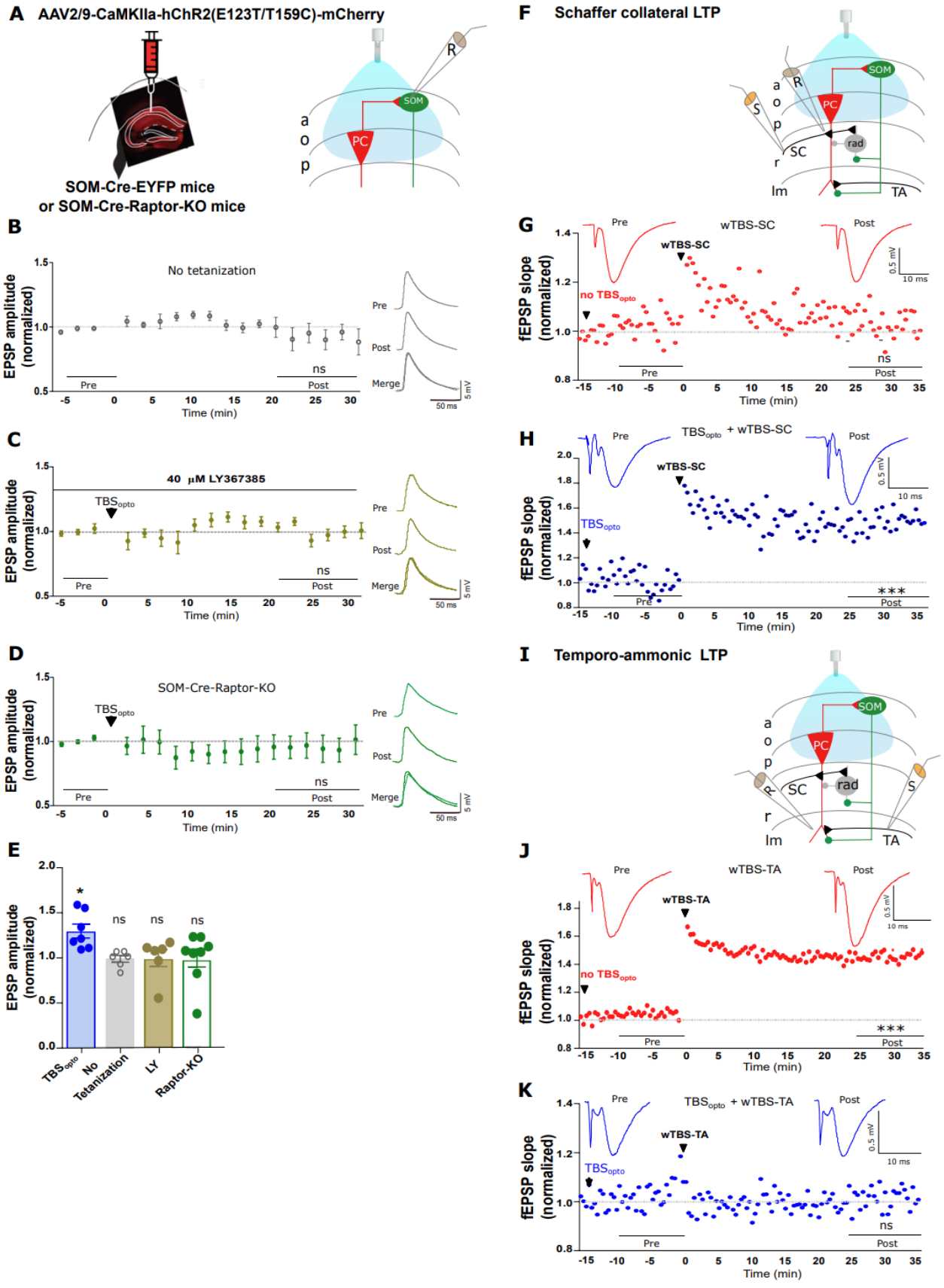
A
AAV2/9-CaMKIIa-hChR2(E123T/T159C)-mCherry
SOM-Cre-EYFP mice
or SOM-Cre-Raptor-KO mice
R
SOM
PC
a
o
p
B
No tetanization
EPSP amplitude (normalized)
Time (min)
Pre
Post
Merge
ns
5 mV
50 ms
C
40 µM LY367385
TBSopto
D
SOM-Cre-Raptor-KO
E
EPSP amplitude (normalized)
*
ns
TBSopto
No Tetanization
LY
Raptor-KO
F
Schaffer collateral LTP
S
SC
rad
lm
TA
G
wTBS-SC
fEPSP slope (normalized)
no TBSopto
***
H
TBSopto + wTBS-SC
I
Temporo-ammonic LTP
J
wTBS-TA
K
TBSopto + wTBS-TA

Figure S3. Whole-field TBSopto-induced LTP at PC-SOM synapses and differential regulation of LTP at SC-PC and TA-PC synapses, related to Figure 2. (A) Left: schematic of experimental paradigm with viral injections in dorsal hippocampus of SOM-Cre-EYFP or SOM-Cre-Raptor-KO mice. Right: diagram of whole-field optogenetic stimulation of CA1 pyramidal cells and whole cell recording from SOM interneurons. (B-D) Left: time plots of light-evoked EPSP amplitude for all SOM cells, showing absence of LTP at PCSOM synapses following no tetanization (B; n = 6 cells), TBSopto in the presence of the mGluR1a antagonist LY367385 (C; n = 6 cells), or TBSopto in SOM-Cre-Raptor-KO mice (D; n =8 cells). Right: representative example of average EPSPs before (Pre) and 20-30 min after (Post) induction in each treatment condition. Paired t-tests, ns $p > 0.05$. (E) Summary graph of light-evoked EPSP amplitude for all cells at 20-30 min post induction, showing LTP after TBSopto, but not in absence of tetanization, nor after TBSopto in LY367385 or SOM-Cre-Raptor-KO mice. Paired t-tests; * $p < 0.05$, ns $p > 0.05$. (F) Diagram of whole-field optogenetic stimulation of CA1 pyramidal cells, with electrical stimulation and recording of SC-PC fEPSPs in stratum radiatum. (G-H) Time plots of fEPSP slope (with average fEPSPs above) from representative slices, showing that LTP at SC-PC synapses (G; red) is facilitated by prior application of TBSopto (H; blue). Paired t-tests, *** $p < 0.001$, ns, $p > 0.05$. (I) Diagram of whole-field optogenetic stimulation of CA1 pyramidal cells, with electrical stimulation and recording of TA-PC fEPSPs in stratum lacunosum-moleculare. (J-K) Time plots of fEPSP slope (with average fEPSPs above) from representative slices, showing that LTP at TA-PC synapses (J; red) is depressed by prior application of TBSopto (H; blue). Paired t-tests, *** $p < 0.001$, ns, $p > 0.05$.

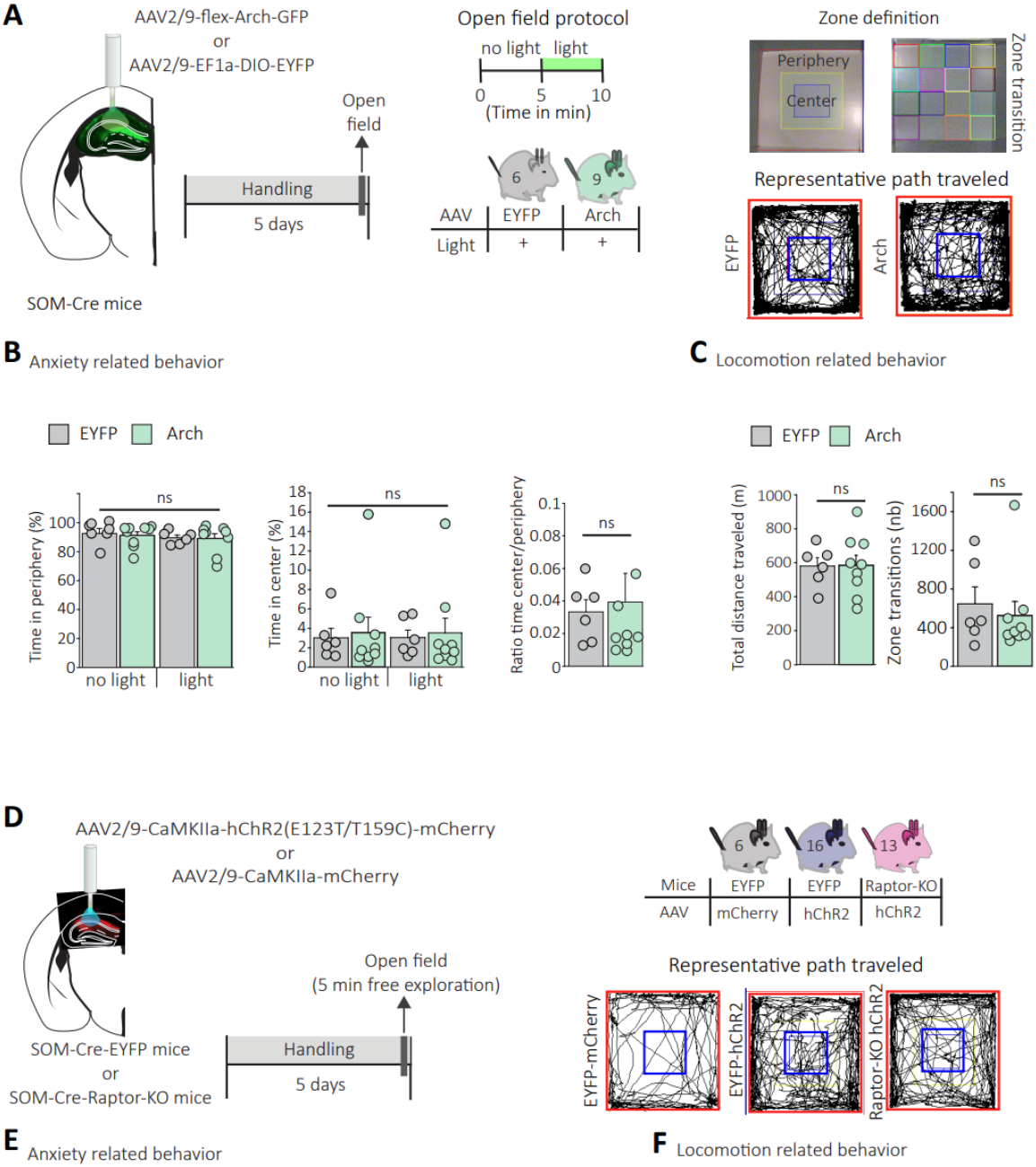
A
AAV2/9-flex-Arch-GFP
or
AAV2/9-EF1a-DIO-EYFP
Open field
Handling
5 days
SOM-Cre mice
Open field protocol
no light light
0 5 10
(Time in min)
6
9
AAV EYFP Arch
Light + +
Zone definition
Periphery
Center
Zone transition
Representative path traveled
EYFP
Arch
B Anxiety related behavior
EYFP Arch
Time in periphery (%)
ns
no light light
Time in center (%)
Ratio time center/periphery
C Locomotion related behavior
Total distance traveled (m)
Zone transitions (nb)
D
AAV2/9-CaMKIIa-hChR2(E123T/T159C)-mCherry
or
AAV2/9-CaMKIIa-mCherry
SOM-Cre-EYFP mice
or
SOM-Cre-Raptor-KO mice
Open field
(5 min free exploration)
Handling
5 days
6
16
13
Mice EYFP EYFP Raptor-KO
AAV mCherry hChR2 hChR2
Representative path traveled
EYFP-mCherry
EYFP-hChR2
Raptor-KO hChR2
E Anxiety related behavior
F Locomotion related behavior
EYFP-mCherry
EYFP-hChR2
Raptor-KO-hChR2
Time in periphery (%)
Time in center (%)
Ratio time center/periphery
Total distance traveled (m)
Zone transitions (nb)

Figure S4. Normal anxiety and locomotion in open field tests, related to Figure 3. (A) Left: schematic of experimental paradigm with injections of AAV2/9-flex-Arch-GFP or AAV2/9-EF1aDIO-EYFP in dorsal CA1 hippocampus of SOM-Cre mice. Middle: diagram of protocol during two open field test episodes, first without light and second with light for optogenetic silencing of SOM interneurons. Right: (top) zone separations used for analysis and (bottom) representative examples of path traveled by mice with EYFP (left) or Arch (right) expression in open field test. (B) Summary graphs for all mice showing unchanged time spent in periphery (left) and center (middle), and ratio of time in center/periphery (right), of mice that received light activation of Arch (Arch; n=9 mice, green) relative to mice with light stimulation without Arch (EYFP; n=6 mice, grey) during open field tests without and with light, indicating normal anxiety level in both groups. Two-way repeated measures ANOVA (time spent in periphery and center); MannWhitney Rank Sum Test (ratio of time center/periphery); ns $p>0.05$. (C) Summary graphs for all mice showing unchanged total distance traveled and zone transitions in mice that received light activation of Arch (green) relative to mice with light stimulation without Arch (gray) during open field tests, indicating normal locomotion in both groups. Unpaired t-test (distance traveled) and MannWhitney Rank Sum Test (zone transitions), ns $p>0.05$. (D) Left: Schematic of experimental paradigm with injections of AAV2/9-CaMKIIa-hChR2(E123T/T159C)- mCherry or AAV2/9-CaMKIIa-mCherry in dorsal CA1 hippocampus of SOM-Cre-EYFP and SOM-CreRaptor-KO mice, and diagram of behavioral testing sequence (open field test). Right: representative examples of path traveled in open field test by SOM-Cre-EYFP mice with mCherry or hChR2 expression, and SOM-Cre-Raptor-KO mice with hChR2 expression. (E) Summary graphs for all mice showing unchanged time spent in periphery (left) and center (middle), and ratio of time in center/periphery (right), of SOM-Cre-EYFP mice with mCherry expression (n=6 mice, grey) or hChR2 expression (n=16 mice, violet), and SOM-Cre-Raptor-KO mice with hChR2 expression (n=13 mice, pink), indicating normal anxiety level. Kruskal-Wallis one-way ANOVA on Ranks, ns $p>0.05$. (F) Summary graphs for all mice showing unchanged total distance traveled and zone transition number of SOM-Cre-EYFP mice with mCherry expression (n=6 mice, pink) or hChR2 expression (n=15 mice, blue), and SOM-Cre-Raptor-KO mice with hChR2 expression (n=13 mice, green), indicating normal locomotion. Kruskal-Wallis one-way ANOVA on Ranks (distance traveled), one-way ANOVA (zone transitions), ns $p>0.05$.

REFERENCES

ARTINIAN, J., JORDAN, A., KHLAIFIA, A., HONORE, E., LA FONTAINE, A., RACINE, A. S., LAPLANTE, I. & LACAILLE, J. C. 2019. Regulation of Hippocampal Memory by mTORC1 in Somatostatin Interneurons. J Neurosci, 39, 8439-8456.

BANKO, J. L., HOU, L., POULIN, F., SONENBERG, N. & KLANN, E. 2006. Regulation of eukaryotic initiation factor 4E by converging signaling pathways during metabotropic glutamate receptor-dependent long-term depression. J Neurosci, 26, 2167-73.

BARTOS, M., ALLE, H. & VIDA, I. 2011. Role of microcircuit structure and input integration in hippocampal interneuron recruitment and plasticity. Neuropharmacology, 60, 730-9.

BEZAIRE, M. J. & SOLTESZ, I. 2013. Quantitative assessment of CA1 local circuits: knowledge base for interneuron-pyramidal cell connectivity. Hippocampus, 23, 751-85.

BLISS, T. V. & LOMO, T. 1973. Long-lasting potentiation of synaptic transmission in the dentate area of the anaesthetized rabbit following stimulation of the perforant path. J Physiol, 232, 331-56.

BOOKER, S. A., HARADA, H., ELGUETA, C., BANK, J., BARTOS, M., KULIK, A. & VIDA, I. 2020. Presynaptic GABAB receptors functionally uncouple somatostatin interneurons from the active hippocampal network. Elife, 9.

BOOKER, S. A., LORETH, D., GEE, A. L., WATANABE, M., KIND, P. C., WYLLIE, D. J. A., KULIK, A. & VIDA, I. 2018. Postsynaptic GABABRs Inhibit L-Type Calcium Channels and Abolish Long-Term Potentiation in Hippocampal Somatostatin Interneurons. Cell Rep, 22, 36-43.

BOOKER, S. A. & VIDA, I. 2018. Morphological diversity and connectivity of hippocampal interneurons. Cell Tissue Res, 373, 619-641.

CARDIN, J. A., CARLEN, M., MELETIS, K., KNOBLICH, U., ZHANG, F., DEISSEROTH, K., TSAI, L. H. & MOORE, C. I. 2010. Targeted optogenetic stimulation and recording of neurons *in vivo* using cell-type-specific expression of Channelrhodopsin-2. Nat Protoc, 5, 247-54.

CENQUIZCA, L. A. & SWANSON, L. W. 2007. Spatial organization of direct hippocampal field CA1 axonal projections to the rest of the cerebral cortex. Brain Res Rev, 56, 1-26.

CHIU, C. Q., MARTENSON, J. S., YAMAZAKI, M., NATSUME, R., SAKIMURA, K., TOMITA, S., TAVALIN, S. J. & HIGLEY, M. J. 2018. Input-Specific NMDAR-Dependent Potentiation of Dendritic GABAergic Inhibition. Neuron, 97, 368-377 e3.

CHOI, J. H., SIM, S. E., KIM, J. I., CHOI, D. I., OH, J., YE, S., LEE, J., KIM, T., KO, H. G., LIM, C. S. & KAANG, B. K. 2018. Interregional synaptic maps among engram cells underlie memory formation. Science, 360, 430-435.

COSTA-MATTIOLI, M., SOSSIN, W. S., KLANN, E. & SONENBERG, N. 2009. Translational control of long-lasting synaptic plasticity and memory. Neuron, 61, 10-26.

CROCE, A., PELLETIER, J. G., TARTAS, M. & LACAILLE, J. C. 2010. Afferent-specific properties of interneuron synapses underlie selective long-term regulation of feedback inhibitory circuits in CA1 hippocampus. J Physiol, 588, 2091-107.

FREUND, T. F. & BUZSAKI, G. 1996. Interneurons of the hippocampus. Hippocampus, 6, 347-470.

FUHRMANN, F., JUSTUS, D., SOSULINA, L., KANEKO, H., BEUTEL, T., FRIEDRICHS, D., SCHOCH, S., SCHWARZ, M. K., FUHRMANN, M. & REMY, S. 2015. Locomotion, Theta Oscillations, and the Speed-Correlated Firing of Hippocampal Neurons Are Controlled by a Medial Septal Glutamatergic Circuit. Neuron, 86, 1253-64.

HIPPENMEYER, S., VRIESELING, E., SIGRIST, M., PORTMANN, T., LAENGLE, C., LADLE, D. R. & ARBER, S. 2005. A developmental switch in the response of DRG neurons to ETS transcription factor signaling. PLoS Biol, 3, e159.

HONORE, E., KHLAIFIA, A., BOSSON, A. & LACAILLE, J. C. 2021. Hippocampal Somatostatin Interneurons, Long-Term Synaptic Plasticity and Memory. Front Neural Circuits, 15, 687558.

HUANG, Y. H., SINHA, S. R., TANAKA, K., ROTHSTEIN, J. D. & BERGLES, D. E. 2004. Astrocyte glutamate transporters regulate metabotropic glutamate receptor-mediated excitation of hippocampal interneurons. J Neurosci, 24, 4551-9.

HUANG, Y. Y. & KANDEL, E. R. 2005. Theta frequency stimulation up-regulates the synaptic strength of the pathway from CA1 to subiculum region of hippocampus. Proc Natl Acad Sci U S A, 102, 232-7.

HUBER, K. M., KAYSER, M. S. & BEAR, M. F. 2000. Role for rapid dendritic protein synthesis in hippocampal mGluR-dependent long-term depression. Science, 288, 1254-7.

JIANG, X., LUPIEN-MEILLEUR, A., TAZERART, S., LACHANCE, M., SAMAROVA, E., ARAYA, R., LACAILLE, J. C. & ROSSIGNOL, E. 2018. Remodeled cortical inhibition prevents motor seizures in generalized epilepsy. Ann Neurol, 84, 436-451.

KATONA, L., LAPRAY, D., VINEY, T. J., OULHAJ, A., BORHEGYI, Z., MICKLEM, B. R., KLAUSBERGER, T. & SOMOGYI, P. 2014. Sleep and movement differentiates actions of two types of somatostatin-expressing GABAergic interneuron in rat hippocampus. Neuron, 82, 872-86.

KLAUSBERGER, T., MAGILL, P. J., MARTON, L. F., ROBERTS, J. D., COBDEN, P. M., BUZSAKI, G. & SOMOGYI, P. 2003. Brain-state- and cell-type-specific firing of hippocampal interneurons in vivo. Nature, 421, 844-8.

KLAUSBERGER, T. & SOMOGYI, P. 2008. Neuronal diversity and temporal dynamics: the unity of hippocampal circuit operations. Science, 321, 53-7.

KULLMANN, D. M., MOREAU, A. W., BAKIRI, Y. & NICHOLSON, E. 2012. Plasticity of inhibition. Neuron, 75, 951-62.

LAMSA, K. P., HEEROMA, J. H., SOMOGYI, P., RUSAKOV, D. A. & KULLMANN, D. M. 2007. Anti-Hebbian long-term potentiation in the hippocampal feedback inhibitory circuit. Science, 315, 1262-6.

LAPOINTE, V., MORIN, F., RATTE, S., CROCE, A., CONQUET, F. & LACAILLE, J. C. 2004. Synapse-specific mGluR1-dependent long-term potentiation in interneurones regulates mouse hippocampal inhibition. J Physiol, 555, 125-35.

LEAO, R. N., MIKULOVIC, S., LEAO, K. E., MUNGUBA, H., GEZELIUS, H., ENJIN, A., PATRA, K., ERIKSSON, A., LOEW, L. M., TORT, A. B. & KULLANDER, K. 2012. OLM interneurons differentially modulate CA3 and entorhinal inputs to hippocampal CA1 neurons. Nat Neurosci, 15, 1524-30.

LOVETT-BARRON, M., KAIFOSH, P., KHEIRBEK, M. A., DANIELSON, N., ZAREMBA, J. D., REARDON, T. R., TURI, G. F., HEN, R., ZEMELMAN, B. V. & LOSONCZY, A. 2014. Dendritic inhibition in the hippocampus supports fear learning. Science, 343, 857-63.

LOVETT-BARRON, M., TURI, G. F., KAIFOSH, P., LEE, P. H., BOLZE, F., SUN, X. H., NICOUD, J. F., ZEMELMAN, B. V., STERNSON, S. M. & LOSONCZY, A. 2012. Regulation of neuronal input transformations by tunable dendritic inhibition. Nat Neurosci, 15, 423-30, S1-3.

MADISEN, L., ZWINGMAN, T. A., SUNKIN, S. M., OH, S. W., ZARIWALA, H. A., GU, H., NG, L. L., PALMITER, R. D., HAWRYLYCZ, M. J., JONES, A. R., LEIN, E. S. & ZENG, H. 2010. A robust and high-throughput Cre reporting and characterization system for the whole mouse brain. Nat Neurosci, 13, 133-40.

MCBAIN, C. J. & KAUER, J. A. 2009. Presynaptic plasticity: targeted control of inhibitory networks. Curr Opin Neurobiol, 19, 254-62.

MCKAY, B. M., OH, M. M. & DISTERHOFT, J. F. 2013. Learning increases intrinsic excitability of hippocampal interneurons. J Neurosci, 33, 5499-506.

MULLER, C. & REMY, S. 2014. Dendritic inhibition mediated by O-LM and bistratified interneurons in the hippocampus. Front Synaptic Neurosci, 6, 23.

NABAVI, S., FOX, R., PROULX, C. D., LIN, J. Y., TSIEN, R. Y. & MALINOW, R. 2014. Engineering a memory with LTD and LTP. Nature, 511, 348-52.

NICHOLSON, E. & KULLMANN, D. M. 2021. Nicotinic receptor activation induces NMDA receptor independent long-term potentiation of glutamatergic signalling in hippocampal oriens interneurons. J Physiol, 599, 667-676.

O'MARA, S. M., COMMINS, S. & ANDERSON, M. 2000. Synaptic plasticity in the hippocampal area CA1-subiculum projection: implications for theories of memory. Hippocampus, 10, 447-56.

OLESKEVICH, S., DESCARRIES, L. & LACAILLE, J. C. 1989. Quantified distribution of the noradrenaline innervation in the hippocampus of adult rat. J Neurosci, 9, 3803-15.

PELKEY, K. A., CHITTAJALLU, R., CRAIG, M. T., TRICOIRE, L., WESTER, J. C. & MCBAIN, C. J. 2017. Hippocampal GABAergic Inhibitory Interneurons. Physiol Rev, 97, 1619-1747.

PELLETIER, J. G. & LACAILLE, J. C. 2008. Long-term synaptic plasticity in hippocampal feedback inhibitory networks. Prog Brain Res, 169, 241-50.

PEREZ, Y., MORIN, F. & LACAILLE, J. C. 2001. A hebbian form of long-term potentiation dependent on mGluR1a in hippocampal inhibitory interneurons. Proc Natl Acad Sci U S A, 98, 9401-6.

POUILLE, F. & SCANZIANI, M. 2004. Routing of spike series by dynamic circuits in the hippocampus. Nature, 429, 717-23.

RAN, I., LAPLANTE, I., BOURGEOIS, C., PEPIN, J., LACAILLE, P., COSTA-MATTIOLI, M., PELLETIER, J., SONENBERG, N. & LACAILLE, J. C. 2009. Persistent transcription- and translation-dependent long-term potentiation induced by mGluR1 in hippocampal interneurons. J Neurosci, 29, 5605-15.

ROYER, S., ZEMELMAN, B. V., LOSONCZY, A., KIM, J., CHANCE, F., MAGEE, J. C. & BUZSAKI, G. 2012. Control of timing, rate and bursts of hippocampal place cells by dendritic and somatic inhibition. Nat Neurosci, 15, 769-75.

SENGUPTA, S., PETERSON, T. R., LAPLANTE, M., OH, S. & SABATINI, D. M. 2010. mTORC1 controls fasting-induced ketogenesis and its modulation by ageing. Nature, 468, 1100-4.

SHARMA, V., SOOD, R., KHLAIFIA, A., ESLAMIZADE, M. J., HUNG, T. Y., LOU, D., ASGARIHAFSHEJANI, A., LALZAR, M., KINIRY, S. J., STOKES, M. P., COHEN, N., NELSON, A. J., ABELL, K., POSSEMATO, A. P., GAL-BEN-ARI, S., TRUONG, V. T., WANG, P., YIANNAKAS, A., SAFFARZADEH, F., CUELLO, A. C., NADER, K., KAUFMAN, R. J., COSTA-MATTIOLI, M., BARANOV, P. V., QUINTANA, A., SANZ, E., KHOUTORSKY, A.,

LACAILLE, J. C., ROSENBLUM, K. & SONENBERG, N. 2020. eIF2alpha controls memory consolidation via excitatory and somatostatin neurons. Nature, 586, 412-416.

SUN, Y., NGUYEN, A. Q., NGUYEN, J. P., LE, L., SAUR, D., CHOI, J., CALLAWAY, E. M. & XU, X. 2014. Cell-type-specific circuit connectivity of hippocampal CA1 revealed through Cre-dependent rabies tracing. Cell Rep, 7, 269-80.

SZONYI, A., SOS, K. E., NYILAS, R., SCHLINGLOFF, D., DOMONKOS, A., TAKACS, V. T., POSFAI, B., HEGEDUS, P., PRIESTLEY, J. B., GUNDLACH, A. L., GULYAS, A. I., VARGA, V., LOSONCZY, A., FREUND, T. F. & NYIRI, G. 2019. Brainstem nucleus incertus controls contextual memory formation. Science, 364.

TANIGUCHI, H., HE, M., WU, P., KIM, S., PAIK, R., SUGINO, K., KVITSIANI, D., FU, Y., LU, J., LIN, Y., MIYOSHI, G., SHIMA, Y., FISHELL, G., NELSON, S. B. & HUANG, Z. J. 2011. A resource of Cre driver lines for genetic targeting of GABAergic neurons in cerebral cortex. Neuron, 71, 995-1013.

TAUBE, J. S. 1993. Electrophysiological properties of neurons in the rat subiculum in vitro. Exp Brain Res, 96, 304-18.

TOPOLNIK, L., AZZI, M., MORIN, F., KOUGIOUMOUTZAKIS, A. & LACAILLE, J. C. 2006. mGluR1/5 subtype-specific calcium signalling and induction of long-term potentiation in rat hippocampal oriens/alveus interneurones. J Physiol, 575, 115-31.

TYAN, L., CHAMBERLAND, S., MAGNIN, E., CAMIRE, O., FRANCAVILLA, R., DAVID, L. S., DEISSEROTH, K. & TOPOLNIK, L. 2014. Dendritic inhibition provided by interneuron-specific cells controls the firing rate and timing of the hippocampal feedback inhibitory circuitry. J Neurosci, 34, 4534-47.

UDAKIS, M., PEDROSA, V., CHAMBERLAIN, S. E. L., CLOPATH, C. & MELLOR, J. R. 2020. Interneuron-specific plasticity at parvalbumin and somatostatin inhibitory synapses onto CA1 pyramidal neurons shapes hippocampal output. Nat Commun, 11, 4395.

VAN HOOFT, J. A., GIUFFRIDA, R., BLATOW, M. & MONYER, H. 2000. Differential expression of group I metabotropic glutamate receptors in functionally distinct hippocampal interneurons. J Neurosci, 20, 3544-51.

VASUTA, C., ARTINIAN, J., LAPLANTE, I., HEBERT-SEROPIAN, S., ELAYOUBI, K. & LACAILLE, J. C. 2015. Metaplastic Regulation of CA1 Schaffer Collateral Pathway Plasticity by Hebbian MGluR1a-Mediated Plasticity at Excitatory Synapses onto Somatostatin-Expressing Interneurons. eNeuro, 2.

WHITLOCK, J. R., HEYNEN, A. J., SHULER, M. G. & BEAR, M. F. 2006. Learning induces long-term potentiation in the hippocampus. Science, 313, 1093-7.

YOUNTS, T. J., MONDAY, H. R., DUDOK, B., KLEIN, M. E., JORDAN, B. A., KATONA, I. & CASTILLO, P. E. 2016. Presynaptic Protein Synthesis Is Required for Long-Term Plasticity of GABA Release. Neuron, 92, 479-492.

YUAN, S. & BURRELL, B. D. 2013. Endocannabinoid-dependent long-term depression in a nociceptive synapse requires coordinated presynaptic and postsynaptic transcription and translation. J Neurosci, 33, 4349-58.

Chapitre III

Stimulation of protein synthesis by optogenetic and chemical induction of excitatory synaptic plasticity in hippocampal somatostatin interneurons

Ève Honoré[1#], Inês Belo do Nascimento[1#], Isabel Laplante[1] and Jean-Claude Lacaille[1*].

[#]Contributions égales. 2022, Molecular Brain. doi.org/10.1186/s13041-022-00967-y

[1]Centre for Interdisciplinary Research on Brain and Learning, Research Group on Neural Signaling and Circuits, Department of Neurosciences, Université de Montréal, P.O. Box 6128, Station Downtown, Montreal, Qc H3C 3J7, Canada

Ce chapitre présente l'article de recherche: « Stimulation of protein synthesis by optogenetic and chemical induction of excitatory synaptic plasticity in hippocampal somatostatin interneurons. » Ève Honoré #, Ines Belo do Nascimento #, Isabel Laplante and Jean-Claude Lacaille. # Contributions égales. Publié en 2022 dans le journal Molecular Brain.

Objectifs spécifiques de l'article :

Les études suggérant l'implication de la synthèse protéique lors de la plasticité synaptique des SOM INs ont utilisé des approches pharmacologiques avec des inhibiteurs de traduction. Le but premier de ce chapitre est de déterminer de façon directe si les formes courtes et longues de la plasticité synaptique des SOM-INs, induites par optogénétique ou via l'activation pharmacologique des récepteurs mGluR1, provoquent la synthèse protéique par l'activation de mTORC1. Puisque l'induction de la PLT par optogénétique bloque l'induction subséquente d'une PLT par stimulation électrique ou par l'apprentissage de la peur (chapitre II), le second objectif de ce chapitre est de déterminer si l'induction optogénétique de la PLT des SOM-INs affecte la synthèse protéique induite lors d'une PLT subséquente. Pour ces expériences, la technique de « SUrface SEnsing of Translation (SUnSET) » a été utilisée pour quantifier la synthèse protéique dans les SOM-INs, suite à l'induction de PLT par stimulation pharmacologique ou optogénétique sur des tranches aigües de souris.

Abstract

Somatostatin-expressing interneurons (SOM-INs) are a major subpopulation of GABAergic cells in CA1 hippocampus that receive excitation from pyramidal cells (PCs) and provide feedback

control of synaptic inputs onto PC dendrites. Excitatory synapses from PCs onto SOM-INs (PC-SOM synapses) exhibit long-term potentiation (LTP) mediated by type 1a metabotropic glutamate receptors (mGluR1a). LTP at PC-SOM synapses translates in lasting regulation of metaplasticity of entorhinal and CA3 synaptic inputs on PCs and contributes to hippocampus-dependent learning. A persistent form of PC-SOM synapse LTP lasting hours is prevented by blockers of transcription and translation, and a more transient form of PC-SOM synapse LTP lasting tens of minutes requires mTORC1-signaling, suggesting an involvement of protein synthesis. However, the role of protein synthesis in these forms of plasticity has not been directly demonstrated. Here we use the SUrface SEnsing of Translation (SUnSET) assay of protein synthesis to directly show that the induction protocols for both forms of LTP at PC-SOM synapses stimulate protein synthesis in SOM-INs. Moreover, protein synthesis stimulated by persistent LTP induction was prevented in mice with a SOM-IN conditional knock-out of Raptor, an essential component of mTORC1, indicating a critical role of mTORC1 in the control of translation in PC-SOM synapse plasticity. Moreover, protein synthesis induced by both forms of LTP may share common mechanisms as transient LTP induction occluded further stimulation of protein synthesis by persistent LTP induction. Our findings highlight a crucial role of protein synthesis and its control by mTORC1 in SOM-INs that is important for hippocampus-dependent memory function.

Keywords: GABA interneurons, Hebbian LTP, Late LTP, SUnSET assay, Puromycin translation assay, Raptor, Translation.

Introduction

Somatostatin-expressing interneurons in CA1 hippocampus (SOM-INs) are a major subpopulation of local inhibitory interneurons [1]. SOM-INs receive their major excitatory inputs from local pyramidal cells (PCs), and, in turn, provide feedback inhibition onto dendrites of PCs [1, 2]. SOM-INs regulate PC synaptic integration [3], action potential rate and burst firing [4] as well as synaptic plasticity [2, 5, 6], and are critical for contextual fear and spatial learning [6, 7, 8, 9]. A notable feature of SOM-INs is long-term plasticity of their excitatory synapses from PCs (PC-SOM synapses). These synapses show a transient form of Hebbian long-term potentiation (LTP) mediated by type 1a metabotropic glutamate receptors (mGluR1a) that lasts tens of minutes [2, 9, 10, 11]. Importantly, optogenetic induction of transient LTP at PC-SOM synapses involves mechanistic target of rapamycin complex 1 (mTORC1) signaling and regulates hippocampal memory function [9]. In addition, contextual fear learning induces a persistent mGluR1a-dependent LTP at PC-SOM synapses, that lasts 24 h and requires mTORC1 signaling [6]. Repeated mGluR1 chemical stimulation or electrical theta burst stimulation (TBS) in slices also elicit persistent LTP at PC-SOM synapses which lasts hours and is transcription- and translation-dependent [6, 12]. Moreover, down-regulation of mTORC1 selectively in SOM-INs impairs mGluR1a-dependent persistent LTP and contextual fear and spatial memory consolidation, suggesting a necessary role of PC-SOM synapse LTP in hippocampal memory [6]. Conditional knock-in of the non-phosphorylatable translation initiation factor eIF2α (eIF2αS51A) in SOM-INs upregulates their general mRNA translation, gates CA1 network plasticity and increases long-term contextual fear memory [8]. Thus, protein synthesis and both transient and persistent long-term synaptic plasticity in SOM-INs are critically implicated in hippocampal learning and memory [6, 8, 9]. However, a direct link remains to be demonstrated between transient and persistent LTP at PC-SOM synapses and protein synthesis in SOM-INs via mGluR1a and mTORC1.

Here, we investigate the involvement of protein synthesis in plasticity at PC-SOM synapses using the SUrface SEnsing of Translation (SUnSET) assay [13] in SOM-INs in combination with chemical and optogenetic induction of persistent and transient forms of LTP, respectively, in slices from transgenic mice expressing EYFP in SOM-INs. We test also the role of mTORC1 in protein

synthesis, using mice with a conditional knockout of the essential component of mTORC1, regulatory-associated protein of mTOR (Raptor), in SOM-INs.

Results

First, we established the specificity of puromycin labeling in the SUnSET assay [8, 13] of EYFP-expressing CA1 SOM-INs of acute hippocampal slices obtained from Sstires−Cre;Rosa26lsl−EYFP mice (SOM-EYFP-WT mice) [6] (Additional file 1—Materials and methods). Puromycin immunolabeling was present in approximately 25% of EYFP-expressing SOM-INs, but was absent in slices not treated with puromycin, or slices processed for SUnSET assay but without puromycin primary antibody (Additional file 2: Fig. S1). These results confirm the specificity of puromycin immunolabeling and indicate a detectable basal level of protein synthesis in SOM-INs of hippocampal slices.

Synaptic mechanisms that induce chemical late LTP in CA1 pyramidal cells (NMDAR, cAMP) [14] are different from the induction mechanisms implicated in chemical persistent LTP in CA1 SOM interneurons (mGluR1a) [6, 12]. So next, we examined if repeated mGluR1 chemical stimulation, an effective protocol for induction of mTORC1-mediated persistent LTP at PC-SOM synapses [6, 12], increases protein synthesis in SOM-INs of control SOM-EYFP-WT mice. After repeated application of the mGluR1/5 agonist (S)-3,5-dihydroxyphenylglycine (DHPG) in presence of the mGluR5 antagonist 2-methyl-6-(phenylethynyl)-pyridine (MPEP), puromycin immunolabeling was increased in SOM-INs relative to sham-treated slices (Fig. 1a), indicating that chemical induction of persistent LTP stimulates protein synthesis in SOM-INs. We tested the role of mTORC1 in persistent LTP-induced protein synthesis using mice with a conditional knockout of Raptor, an essential component of mTORC1, in SOM-INs (Sstires−Cre;Rosa26lsl−EYFP;Rptorfl/fl knock-out mice; SOM-EYFP-Raptor-KO mice) [6]. Repeated mGluR1 stimulation of slices from SOM-EYFP-Raptor-KO mice failed to increase puromycin immunolabeling in SOM-INs (Fig. 1a), indicating that protein synthesis elicited by induction of persistent LTP in SOM-INs is mediated by mTORC1 signaling. Basal level of puromycin immunofluorescence in SOM-INs of sham-treated slices was similar in SOM-EYFP-WT and SOM-EYFP-Raptor-KO mice (Additional file 2: Fig. S2a), suggesting undetectable

mTORC1 control of basal protein synthesis in SOM-INs. We also examined puromycin immunofluorescence in CA1 stratum pyramidale after repeated mGluR1 stimulation. DHPG treatment did not increase stratum pyramidale puromycin immunofluorescence in slices of SOM-EYFP-WT or SOM-EYFP-Raptor-KO mice (Additional file 2: Fig. S2b-c), suggesting that induction protocol for persistent LTP at PC-SOM synapses stimulates protein synthesis in SOM-INs, but may not in PCs.

Next, we determined if optogenetic theta-burst stimulation (TBSopto), an effective protocol to induce transient LTP at PC-SOM synapses [6, 9], increases protein synthesis in SOM-INs. hChR2 was expressed in PCs by CA1 injections of AAV2/9-CaMKIIa-hChR2(E123T/T159C)-mCherry in SOM-EYFP-WT mice, as previously [9] (Additional file 1—Materials and methods). Optogenetic theta burst stimulation (TBSopto) was then given as previously [9] in slices prepared for SUnSET assay (Fig. 1b). Puromycin immunolabeling was increased in SOM-INs after TBSopto relative to unstimulated slices from hChR2-expressing mice (Fig. 1b), indicating that optogenetic induction of transient LTP stimulates protein synthesis in SOM-INs.

Next, we examined if protein synthesis elicited in SOM-INs by TBSopto and repeated mGluR1 stimulation interact with each other. TBSopto was given to slices in absence of puromycin and repeated mGluR1 stimulation was applied 30 min later in presence of puromycin (Fig. 1c). In control slices (without prior TBSopto), puromycin immunofluorescence was increased in SOM-INs after DHPG treatment (Fig. 1c). But in slices with prior TBSopto, the increase in puromycin immunofluorescence after DHPG treatment was impaired (Fig. 1c). Thus, induction of transient LTP prevents further stimulation of protein synthesis by persistent LTP induction, suggesting both forms of LTP share signaling mechanisms.

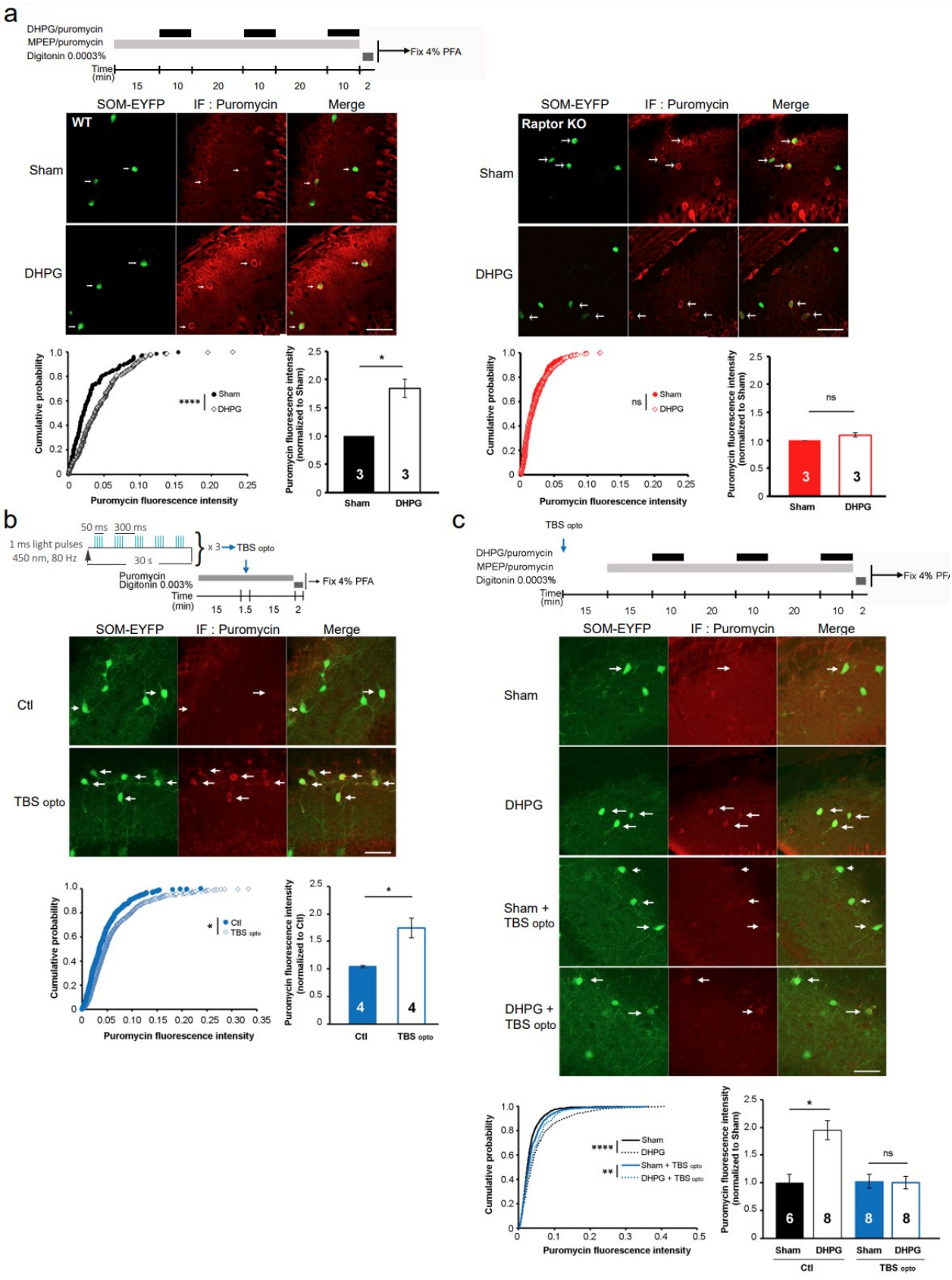
a
DHPG/puromycin
MPEP/puromycin
Digitonin 0.0003%
Fix 4% PFA
Time (min)
15 10 20 10 20 10 2
SOM-EYFP
IF : Puromycin
Merge
WT
Sham
DHPG
Raptor KO
Cumulative probability
Puromycin fluorescence intensity
****
Sham
DHPG
ns
Puromycin fluorescence intensity (normalized to Sham)
*
3
b
50 ms 300 ms
1 ms light pulses
450 nm, 80 Hz
30 s
x 3
TBS opto
Puromycin
Digitonin 0.003%
Ctl
TBS opto
Puromycin fluorescence intensity (normalized to Ctl)
4
c
DHPG + TBS opto
Sham + TBS opto
**
Puromycin fluorescence intensity (normalized to Sham)
6
8

Figure 1. Stimulation of protein synthesis in SOM-INs by chemical and optogenetic LTP induction. (a) Protocol of chemical persistent LTP induction (top left), representative images (middle), cumulative distribution plots and summary bar graphs (bottom; each group 3 independent slice experiments from 3 animals, 3-6 sections analyzed per experiment) of puromycin immunofluorescence in SOM-INs of control SOM-EYFP-WT mice (left) and conditional SOM-EYFP-Raptor-KO mice (right), showing increase in fluorescence after DHPG treatment relative to Sham-treatment in control mice, but not in conditional knockout mice. Summary bar graph (mean ± SEM; SOM-EYFP-WT mice, Sham = 395 cells and DHPG = 396 cells; SOM-EYFP-Raptor KO mice, Sham = 457 cells and DHPG = 487 cells). (b) Protocol of optogenetic (TBSopto) transient LTP induction (top), representative images (middle), cumulative distribution plot and summary bar graph (bottom; each group 4 independent slice experiments from 2 animals, 4-6 sections analyzed per experiment) of puromycin immunofluorescence in SOM-INs of SOM-EYFP-WT mice, showing an increase in fluorescence after TBSopto relative to control (unstimulated) slices. Summary bar graph (mean ± SEM; Control 570 cells and TBSopto 761 cells). (c) Protocol of consecutive induction of TBSopto (in absence of puromycin) and repeated mGluR1 (in presence of puromycin) LTP (top), representative images (middle), cumulative distribution plot and summary bar graph (bottom; each group 6-8 independent slice experiments from 3-4 animals, 3-6 sections analyzed per experiment) of puromycin immunofluorescence in SOM-INs of SOM-EYFP-WT mice, showing that the increase in fluorescence after DHPG treatment is impaired by prior application of TBSopto. Summary bar graph (mean ± SEM; Ctl, Sham 781 cells and DHPG 805 cells; TBSopto, Sham 925 cells and DHPG: 869 cells). In all panels: arrows indicate cells with colocalization of EYFP with puromycin immunofluorescence; scale bars, 50 μm; Kolmogorov-Smirnov tests (cumulative distribution tests) or Student's t-tests (group mean tests), * $p < 0.05$, ** $p < 0.01$, **** $p < 0.0001$ and ns not significant.

Discussion

Here, we demonstrate that protein synthesis is stimulated in SOM-INs by induction protocols for transient and persistent LTP at PC-SOM synapses. Moreover, stimulation of protein synthesis by persistent LTP induction requires mTORC1 signaling. Transient LTP induced by TBSopto is known to be mTORC1-dependent [9], thus protein synthesis induced by TBSopto is also likely mTORC1-mediated. Our results suggest a causal role of protein synthesis in PC-SOM LTP because both transient LTP [9] and persistent LTP [6] were previously shown to be blocked in mice with conditional knockout of Rptor in SOM-INs. Since transient and persistent LTP at PC-SOM synapses contribute to long-term contextual fear and spatial learning [6, 9], our findings highlight

a crucial role of translational control by mTORC1 in SOM-INs that is important for hippocampus-dependent memory processes.

Protein synthesis induced by optogenetic and repeated mGluR1 stimulation share mechanisms since TBSopto induction occludes activation of protein synthesis by subsequent repeated mGluR1 stimulation. These results are consistent with previous evidence that TBSopto induction *in vivo* prior to contextual fear conditioning impairs learning-induced potentiation of PC-SOM synapses, and reduces contextual fear memory consolidation [9]. Prior induction of persistent LTP by repeated mGluR1 stimulation in SOM-INs was also found to occlude subsequent transient LTP elicited by electrical TBS [12]. Our findings indicate that the interaction may occur upstream of protein synthesis. Thus, it will be of interest to determine where the occlusion occurs in the signaling cascade between mGluR activation and protein synthesis.

Our finding of long-term potentiation of PC-SOM synapses mediated by mGluR1a and associated with protein synthesis in SOM-INs, contrasts with the long-term depression (LTD) of Schaffer collateral synapses in PCs mediated by mGluR5 and protein synthesis [15]. Our observation that stimulation of protein synthesis by mGluR1-mediated persistent LTP induction protocol was observed in SOM-INs and absent in stratum pyramidale, is consistent with the requirement of activation of mGluR5 for LTD and protein synthesis in PCs [15]. Given the functional specificity of mGluR stimulated protein synthesis in SOM-INs (potentiation of synapses) and PCs (depression of synapses), it will be important to identify the cell-specific mRNAs controlled by synaptic activity and mTORC1 which determine the type of synaptic plasticity in SOM-INs and PCs.

References

1. Pelkey KA, Chittajallu R, Craig MT, Tricoire L, Wester JC, McBain CJ. Hippocampal GABAergic inhibitory interneurons. Physiol Rev. 2017;97(4):1619–747.

2. Honore E, Khlaifa A, Bosson A, Lacaille JC. Hippocampal somatostatin interneurons, long-term synaptic plasticity and memory. Front Neural Circuits. 2021;15: 687558.

3. Lovett-Barron M, Turi GF, Kaifosh P, Lee PH, Bolze F, Sun XH, et al. Regulation of neuronal input transformations by tunable dendritic inhibition. Nat Neurosci. 2012;15(3):423–30, S1-3.

4. Royer S, Zemelman BV, Losonczy A, Kim J, Chance F, Magee JC, et al. Control of timing, rate and bursts of hippocampal place cells by dendritic and somatic inhibition. Nat Neurosci. 2012;15(5):769–75.

5. Leao RN, Mikulovic S, Leao KE, Munguba H, Gezelius H, Enjin A, et al. OLM interneurons diferentially modulate CA3 and entorhinal inputs to hippocampal CA1 neurons. Nat Neurosci. 2012;15(11):1524–30.

6. Artinian J, Jordan A, Khlaifa A, Honore E, La Fontaine A, Racine AS, et al. Regulation of hippocampal memory by mTORC1 in somatostatin interneurons. J Neurosci. 2019;39(43):8439–56.

7. Lovett-Barron M, Kaifosh P, Kheirbek MA, Danielson N, Zaremba JD, Reardon TR, et al. Dendritic inhibition in the hippocampus supports fear learning. Science. 2014;343(6173):857–63.

8. Sharma V, Sood R, Khlaifa A, Eslamizade MJ, Hung TY, Lou D, et al. eIF2alpha controls memory consolidation via excitatory and somatostatin neurons. Nature. 2020;586(7829):412–6.

9. Asgarihafshejani A, Honore E, Michon FX, Laplante I, Lacaille JC. Long-term potentiation at pyramidal cell to somatostatin interneuron synapses controls hippocampal network plasticity and memory. iScience.

2022;25(5): 104259.

10. Perez Y, Morin F, Lacaille JC. A hebbian form of long-term potentiation dependent on mGluR1a in hippocampal inhibitory interneurons. Proc Natl Acad Sci USA. 2001;98(16):9401–6.

11. Booker SA, Loreth D, Gee AL, Watanabe M, Kind PC, Wyllie DJA, et al. Postsynaptic GABABRs inhibit L-type calcium channels and abolish longterm potentiation in hippocampal somatostatin interneurons. Cell Rep.2018;22(1):36–43.

12. Ran I, Laplante I, Bourgeois C, Pepin J, Lacaille P, Costa-Mattioli M, et al. Persistent transcription- and translation-dependent long-term potentiation induced by mGluR1 in hippocampal interneurons. J Neurosci. 2009;29(17):5605–15.

13. Schmidt EK, Clavarino G, Ceppi M, Pierre P. SUnSET, a nonradioactive method to monitor protein synthesis. Nat Methods. 2009;6(4):275–7.

14. Otmakhov N, Khibnik L, Otmakhova N, Carpenter S, Riahi S, Asrican B, et al. Forskolin-induced LTP in the CA1 hippocampal region is NMDA receptor dependent. J Neurophysiol. 2004;91(5):1955–62.

15. Huber KM, Roder JC, Bear MF. Chemical induction of mGluR5- and protein synthesis-dependent long-term depression in hippocampal area CA1. J Neurophysiol. 2001;86(1):321–5.

Supplementary Information

Materials and methods.

Animals

All animal procedures and experimental protocols were performed in accordance with the guidelines of the Animal Care Committee of University of Montreal and of the Canadian Council on Animal Care.

Transgenic mice lines

Knock-in mice expressing Cre under a ribosomal entry site (IRES) downstream of Sst locus (Sstires-Cre mice; The Jackson Laboratory, Bar Harbor, ME; JAX #013044) (1) were crossed with Rosa26lsl-EYFP reporter mice (Ai3; JAX#007903) (2) to generate mice with Cre-dependent Enhanced Yellow Fluorescent Protein (EYFP) expression in SOM-INs (SOM-EYFP-WT mice) (3). Sstires-Cre;Rosa26lsl-EYFP mice were crossed with floxed Rptor mice (JAX#013188) (4) for cell-specific knock-out of Rptor in SOM cells (SOM-EYFP-Raptor-KO mice) (3). Heterozygous offsprings were backcrossed together and homozygous animals were isolated. Mice were housed 2–5 animals per cage and given ad libitum access to food and water, in temperature (~22°C) and humidity (~55%) controlled rooms with a normal 12h light/dark cycle. Experiments were carried out on 4-9 weeks old mice from both sexes.

Viral constructs injection

Four to six weeks old mice were anesthetized with an intraperitoneal injection of ketamine (50 mg/kg) and xylazine (5 mg/kg) and placed in a stereotaxic apparatus (Stoelting). AAV2/9-CaMKIIa-hChR2(E123T/T159C)-mCherry (1.5x1012 particles/ml) was injected bilaterally in dorsal CA1 hippocampus (coordinates from bregma: -2.46 mm AP; ± 1.75 mm ML; -1.5 mm DV). Viral solution (0.8 µl) was delivered at a flow rate of 100 nl/min using a 10 µl Hamilton syringe

coupled to a G26 beveled needle. The needle was left in place for at least 5 minutes after injection. Mice were allowed to recover for 2 weeks prior to slice experiments.

Hippocampal slice preparation

Mice were anesthetized with isoflurane inhalation and the brain was rapidly removed and placed in ice-cold sucrose-based cutting solution containing (in mM): 75 sucrose, 87 NaCl, 2.5 KCl, 1.25 NaH2PO4, 7 MgCl2, 0.5 CaCl2, 25 NaHCO3, 25 D-glucose (pH 7.4 and 330 mOsmol/L). Three hundred microns thick transverse dorsal hippocampal slices were cut with a Leica VT1000S vibratome (Leica, Germany). Slices were transferred for a recovery period of one hour in artificial cerebrospinal fluid (ACSF) at room temperature (20 –22°C) containing (in mM): 124 NaCl, 2.5 KCl, 1.25 NaH2PO4, 2 MgCl2, 2 CaCl2, 26 NaHCO3, 10 D-glucose, 1.3 ascorbic acid (pH 7.4 and 295-305 mOsmol/L). Both cutting solution and ACSF were saturated with 95% O2/5% CO2.

Protein synthesis assay

To measure protein synthesis in SOM-INs we used the immunohistochemical version of the assay called SUrface SEnsing of Translation (SUnSET) (also called puromycin translation assay) (5-8). Individual slices were pre-incubated for 15 minutes in ACSF containing puromycin (100 µM; Sigma-Aldrich, P8833) and saturated with 95% O2/5% CO2 at 30-33ºC. Slices received the LTP induction protocol (see below) in the presence of puromycin, followed by a post-incubation period of 2 minutes in digitonin (0.0003%; Sigma-Aldrich; D141). Slices were then fixed in 4% paraformaldehyde in 0.1 M phosphate buffer (PB) overnight at 4ºC before processing for immunofluorescence. Slices were rinsed in 0.01 M PB saline (PBS), cryoprotected with 30% sucrose in 0.1 M PB, and re-sectioned (50 µm thickness) using a Leica freezing microtome (SM 2000R). Sections were permeabilized in 0.3% Triton X-100 in 0.01 M PBS for 15 min. To block unspecific binding sections were incubated in 10% normal goat serum, 0.1% Triton X-100 in PBS for 1 hour, followed by overnight incubation at 4ºC with a mouse monoclonal IgG2a puromycin antibody (1/1000; Millipore #MABE343). Sections were then incubated at room temperature

(1h30) with a goat anti-mouse IgG2a-conjugated to Rhodamine-Red™X (1/200) or Alexa Fluor™ 647 (1/200; for AAV2/9-CaMKIIa-hChR2(E123T/T159C)-mCherry experiments) and mounted in Prolong Diamond. Images were acquired with a confocal microscope (LSM510 or LSM880, Zeiss) at excitation wavelength 488 nm and 543 nm (Rhodamine-Red labeling) or 633 nm (Alexa Fluor 647 labeling). Images were acquired using the exact same parameters set on control sections. In each section, the intensity of puromycin immunofluorescence was quantified in EYFP-expressing SOM-INs in similar sized fields of view (150 x 150 µm) in oriens-alveus region of the CA1 hippocampus using ImageJ software (National Institute of Health; https://imagej.nih.gov/ij/download.html) by comparing integrated intensity in cells corrected for background fluorescence. In each immunofluorescence independent experiment, control and treated slices were processed together and analyzed using the same equipment settings. Immunofluorescence intensity of cells from treated slices was normalized to values of cells in associated control slices. In summary bar graphs, immunofluorescence intensity was expressed as mean of independent experiments (numbers for different experiments indicated in Figure 1 legend). For measurement of puromycin immunofluorescence in the CA1 pyramidal layer, the integrated fluorescence intensity was measured in similar sized fields of view (30 x 20 µm) in the pyramidal cell layer and corrected for background fluorescence.

LTP induction protocols

The protocol for chemical induction of persistent mGluR1-mediated LTP was as previously (9). Briefly, induction consisted of three applications (10 min duration each at 30 min intervals) of the mGluR1/5 agonist (S)-3,5-dihydroxyphenylglycine (DHPG, 5 µM, Abcam) in the presence of the mGluR5 antagonist 2-methyl-6-(phenylethynyl)-pyridine (MPEP, 40 µM, Abcam) and puromycin. Puromycin incubation was terminated after the last DHPG application.

The protocol for optogenetic theta burst stimulation (TBSopto) induction of transient LTP was as previously (10) in slices preincubated in ACSF and puromycin for 15 min, as described above. Briefly, whole field optogenetic stimulation of slices were elicited using a Quadruple Laser Diode Fiber Light Source (LDFLS_405/100_450/070_520/060_638/080; Doric Lenses Inc) coupled to Mono Fiberoptic Patchcords (MFP_200/240/900–0.22_2m_FC-ZF1.25(F), 200 mm Core diameter, 0.22 NA; Doric Lenses Inc) and hand-made fiber optic cannulas (optic fiber: FT200EMT,

200 mm Core diameter, 0.22 NA; ceramic ferrule: CFLC230-10; Thorlabs) positioned above the CA1 stratum oriens region of the slice with brief light pulses (450 nm; duration 1 ms). Optogenetic stimulation of CA1 pyramidal cells (TBSopto) consisted of 3 episodes (given at 30 s intervals) of 5 bursts (at 300 ms inter-burst interval) of 4 light pulses at 80 Hz. Slices were incubated in ACSF with puromycin for a further 15 min after the TBSopto induction protocol. In experiments with TBSopto preceding chemical LTP induction, slices received TBSopto (or no light) without puromycin and, after 15 min, were exposed to the chemical LTP induction protocol in the presence of puromycin as detailed above.

Statistical Analysis

No statistical methods were used to predetermine sample size but our sample sizes are comparable to those used generally in the field. Statistical analysis was performed using Sigma Stat, Excel and ClampFit. Student's t tests were used to determine difference between control and treatment groups, and Fisher tests to validate homoscedasticity. Kolmogorov-Smirnov tests were used to compare cumulative probability distributions. All data in the Figures are presented as mean ± SEM. Asterisks in Figures denote statistical significance levels for specified tests (* $p < 0.05$; ** $p < 0.01$; *** $p < 0.001$; ns, not significant).

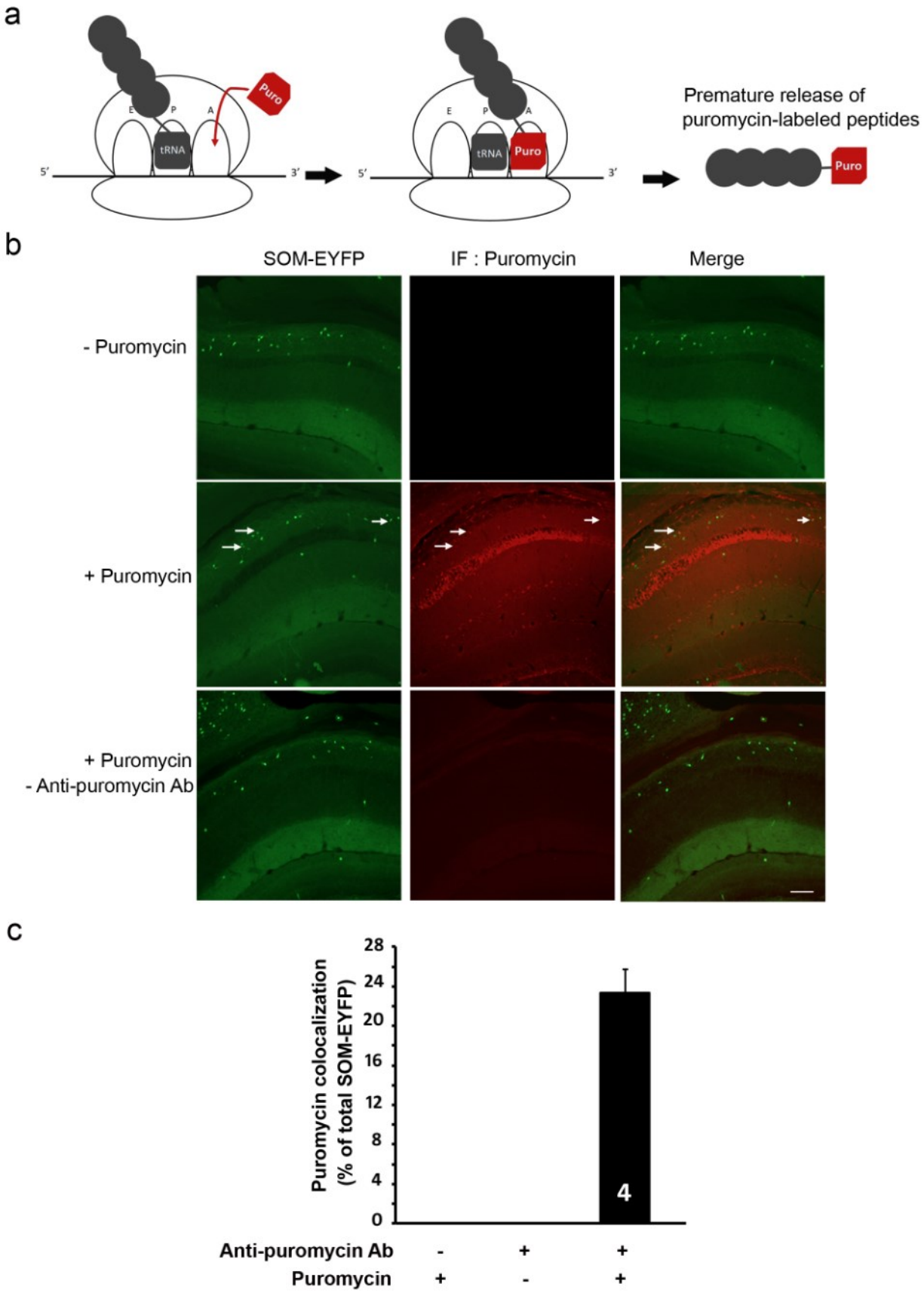
a
E
P
A
tRNA
Puro
5'
3'
Premature release of
puromycin-labeled peptides
b
SOM-EYFP
IF : Puromycin
Merge
- Puromycin
+ Puromycin
+ Puromycin
- Anti-puromycin Ab
c
Puromycin colocalization
(% of total SOM-EYFP)
28
24
20
16
12
8
4
0
4
Anti-puromycin Ab - + +
Puromycin + - +

Figure S1. Specificity of puromycin labeling in SUnSET assay. (a) Diagram of puromycin entering the ribosomal A-site, arrest of protein synthesis and release of premature peptides, later detected using a puromycin specific antibody. (b) Representative images of EYFP and puromycin immunofluorescence showing specificity of puromycin antibody in absence (upper panels) or presence (middle panels) of puromycin, and no puromycin labeling without puromycin antibody (bottom panels). Hippocampal slices were exposed with or without puromycin to Sham-treatment of late LTP protocol. Arrows indicate cells with colocalization of EYFP and puromycin fluorescence signal. Scale bar, 100 μm. (c) Summary bar graph of puromycin colocalization in EYFP cells expressed as percentage of total EYFP cells (4 independent experiments with 1-2 sections analyzed per experiment, in each group; n = 275 EYFP cells with puromycin co-localization).

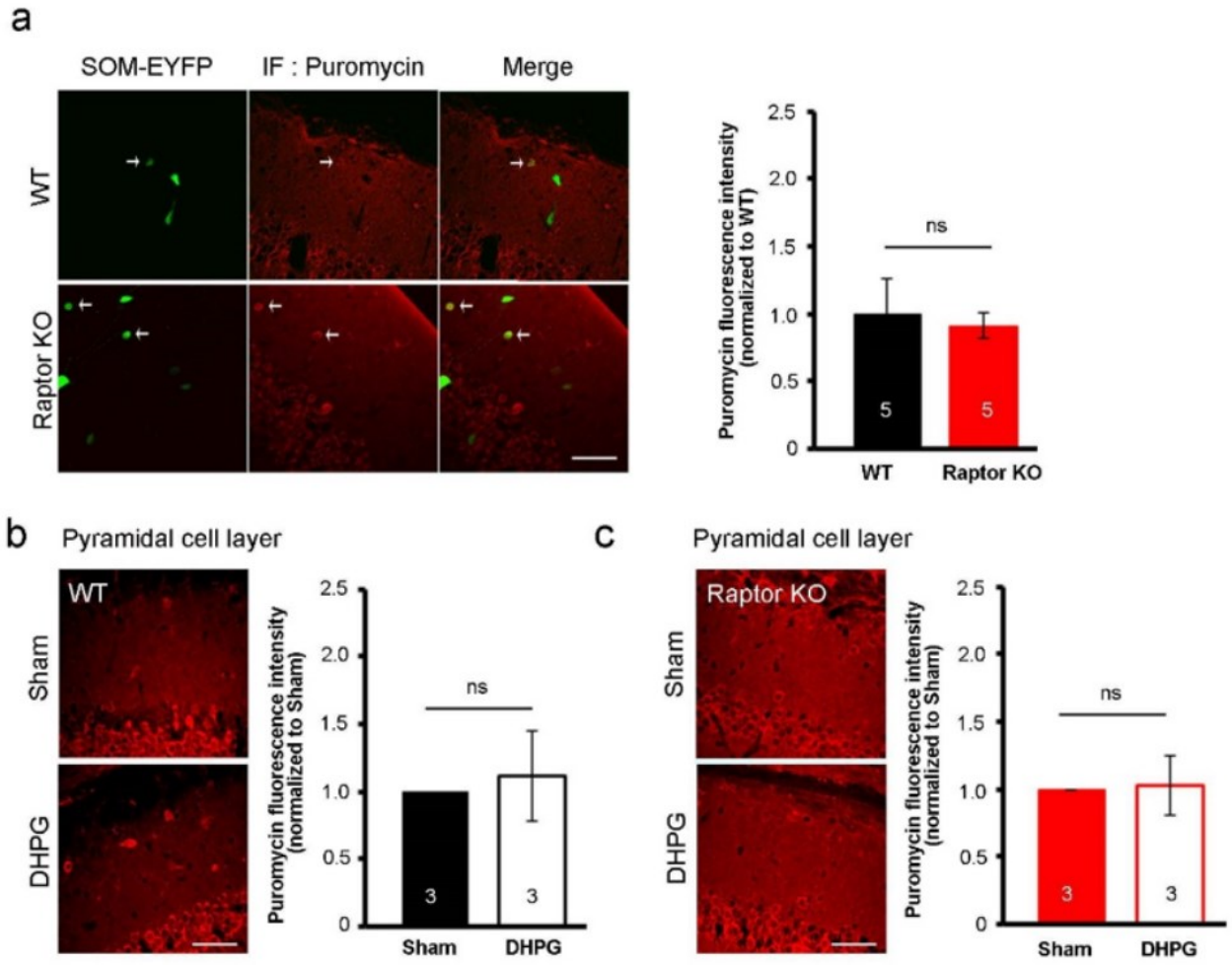

Figure S2. Intact SOM-IN basal protein synthesis in mice with conditional Rptor knock-out, and unchanged pyramidal cell layer puromycin immunofluorescence after chemical LTP induction. (a) Representative images and summary bar graph (each group 5 independent slice experiments from 5 animals, 1-5 sections analyzed per experiment) of puromycin immunofluorescence in SOM-INs of SOM-EYFP WT and SOM-EYFP-Raptor KO mice, showing no difference of puromycin fluorescence in SOM-INs (sham-treatment) of control and knockout mice. Arrows indicate cells with colocalization of EYFP with puromycin immunofluorescence. Summary bar graph (mean ± SEM; WT 570 cells and Raptor KO 722 cells). (b-c) Representative images and summary bar graphs (each group 3 independent slice experiments from 3 animals, 1-3 sections analyzed per experiment) of puromycin immunofluorescence in the CA1 pyramidal layer of SOM-EYFP WT (b) and SOM-EYFP-Raptor KO (c), showing no difference in puromycin fluorescence following chemical late LTP induction. Summary bar graph (mean ± SEM; number

of fields of view for WT, Sham 53 and DHPG 88; for Raptor-KO, Sham 75 and DHPG 101). Scale bars, 50 μm. Student's t-tests, ns not significant.

Acknowledgements

The authors wish to thank Julie Pépin for technical support.

Authors' contributions

JCL designed and supervised the project. EH, IL and JCL designed experiments. EH, IBN and IL performed experiments and analysed data. EH, IBN, IL and JCL wrote the paper. All authors read and approved the final manuscript.

Funding

This work was supported by an operating grant from the Canadian Institutes of Health Research (CIHR PJT-153311), a Research Centre grant (Centre Interdisciplinaire de Recherche sur le Cerveau et l'Apprentissage; CIRCA) from the Fonds de la Recherche du Québec – Santé (FRQS), and a Group grant from Université de Montréal (Groupe de recherche sur la signalisation et circuiterie neurale; GRSNC) to JCL. JCL is the recipient of the Canada Research Chair in Cellular and Molecular Neurophysiology (CRC 950-231066).

Availability of data and material

All data and materials are available upon request.

Declarations

Ethics approval and consent to participate

All animal procedures and experiments were performed in accordance with guidelines for maintenance and care of animals of the Canadian Council of Animal Care and in accordance with the Université de Montréal animal care committee regulations (Protocol #: 18-002 and 18-003; 19-003 and 19-004; 20-001 and 20-002; 21-001 and 21-002; 22-008 and 22-009).

Consent for publication

All authors gave their consent for publication

Competing interests

The authors declare that they have no competing interests.

Supplementary References

1. Taniguchi H, He M, Wu P, Kim S, Paik R, Sugino K, et al. A resource of Cre driver lines for genetic targeting of GABAergic neurons in cerebral cortex. Neuron. 2011;71(6):995-1013.

2. Madisen L, Zwingman TA, Sunkin SM, Oh SW, Zariwala HA, Gu H, et al. A robust and high-throughput Cre reporting and characterization system for the whole mouse brain. Nature neuroscience. 2010;13(1):133-40.

3. Artinian J, Jordan A, Khlaifia A, Honore E, La Fontaine A, Racine AS, et al. Regulation of Hippocampal Memory by mTORC1 in Somatostatin Interneurons. J Neurosci. 2019;39(43):8439-56.

4. Sengupta S, Peterson TR, Laplante M, Oh S, Sabatini DM. mTORC1 controls fasting-induced ketogenesis and its modulation by ageing. Nature. 2010;468(7327):1100-4.

5. Schmidt EK, Clavarino G, Ceppi M, Pierre P. SUnSET, a nonradioactive method to monitor protein synthesis. Nat Methods. 2009;6(4):275-7.

6. Goodman CA, Mabrey DM, Frey JW, Miu MH, Schmidt EK, Pierre P, et al. Novel insights into the regulation of skeletal muscle protein synthesis as revealed by a new nonradioactive in vivo technique. FASEB J. 2011;25(3):1028-39.

7. Ma T, Trinh MA, Wexler AJ, Bourbon C, Gatti E, Pierre P, et al. Suppression of eIF2alpha kinases alleviates Alzheimer's disease-related plasticity and memory deficits. Nature neuroscience. 2013;16(9):1299-305.

8. Sharma V, Sood R, Khlaifia A, Eslamizade MJ, Hung TY, Lou D, et al. eIF2alpha controls memory consolidation via excitatory and somatostatin neurons. Nature. 2020;586(7829):412-6.

9. Ran I, Laplante I, Bourgeois C, Pepin J, Lacaille P, Costa-Mattioli M, et al. Persistent transcription- and translation-dependent long-term potentiation induced by mGluR1 in hippocampal interneurons. J Neurosci. 2009;29(17):5605-15.

10. Asgarihafshejani A, Honore E, Michon FX, Laplante I, Lacaille JC. Long-term potentiation at pyramidal cell to somatostatin interneuron synapses controls hippocampal network plasticity and memory. iScience. 2022;25(5):104259.

Chapitre IV

Object location learning in mice requires hippocampal somatostatin interneuron activity and is facilitated by mTORC1-mediated long-term potentiation of their excitatory synapses

Eve Honoré[1] and Jean-Claude Lacaille[1*]. 2022, Molecular brain

doi.org/10.1186/s13041-022-00988-7

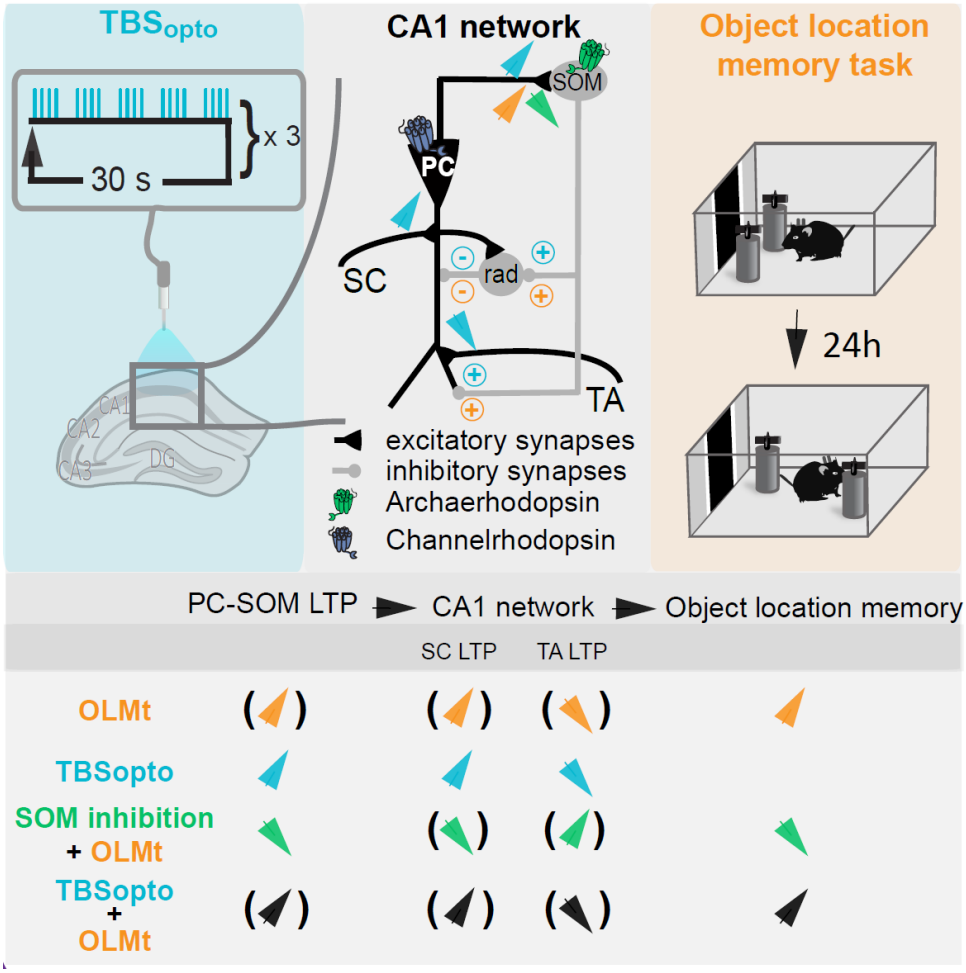

[1]Department of Neurosciences, Center for Interdisciplinary Research on Brain and Learning (CIRCA) and Research Group on Neural Signaling and Circuitry (GRSNC), Université de Montréal, Montreal, Quebec, H3C 3J7, Canada.

Ce chapitre présente l'article de recherche: « Object location learning in mice requires hippocampal somatostatin interneuron activity and is facilitated by mTORC1-mediated long-term potentiation of their excitatory synapses». Par Ève Honoré et Jean-Claude Lacaille. Publié en 2022 dans le journal Molecular Brain.

Objectifs spécifiques de l'article :

L'activité et la PLT des SOM-INs durant l'acquisition de la mémoire contextuelle de peur sont nécessaires à la bonne formation de cette mémoire (Chapitre II). De plus la PLT des SOM-INs est nécessaire pour la consolidation de la mémoire spatiale aversive (Artinian J. *et al.*, 2019). Cependant nous ne savons pas si l'activité ou la PLT des SOM-INs est nécessaire pour la formation de la mémoire spatiale dans un contexte non aversif et peu saillant. De plus, lors de quelles phases de l'apprentissage ou de la consolidation de la mémoire spatiale l'activité ou la PLT des SOM-INs est nécessaire, demeurent inconnues. Le premier but des travaux de ce chapitre est de déterminer si l'activité des SOM-INs est nécessaire pendant l'acquisition de la mémoire spatiale non aversive. Pour ces expériences, l'injection dans l'aire CA1 dorsale d'une construction virale pour l'expression d'archaerhodopsine spécifiquement dans les SOM INs est utilisée pour déterminer l'effet de l'inhibition des SOM-INs de CA1 durant l'acquisition d'une tâche de localisation d'objets (*object location memory task*). Le deuxième but des travaux est de tester si la PLT des synapses CP-SOM est suffisante pour réguler l'acquisition de cette mémoire.

Abstract

Hippocampus-dependent learning and memory originate from long-term synaptic changes in hippocampal networks. The activity of CA1 somatostatin interneurons (SOM-INs) during aversive stimulation is necessary for contextual fear memory formation. In addition, mTORC1-dependent long-term potentiation (LTP) of SOM-IN excitatory input synapses from local pyramidal cells (PC-SOM synapses) contributes to the consolidation of fear motivated spatial and contextual memories. Although, it remains unknown if SOM-IN activity and LTP are necessary and sufficient for novelty motivated spatial episodic memory such as the object location memory, and if so when it is required. Here we use optogenetics to examine whether dorsal CA1 SOM-IN activity and LTP are sufficient to regulate object location memory. First, we found that silencing SOM-INs during object location learning impaired memory. Second, optogenetic induction of PC-SOM synapse LTP (TBSopto) given 30 minutes before object location training, resulted in facilitation of memory. However, in mice with mTORC1 pathway genetically inactivated in SOM-INs, which blocks PC-SOM synapse LTP, TBSopto failed to facilitate object location memory. Our results indicate that SOM-IN activity is necessary during object location learning and that optogenetic induction of PC-SOM synapse LTP is sufficient to facilitate consolidation of object location memory. Thus, hippocampal somatostatin interneuron activity is required for object location learning, a hippocampus-dependent form of novelty motivated spatial learning that is facilitated by plasticity at PC-SOM synapses.

Keywords: Dorsal CA1 hippocampus, Somatostatin interneurons, Long-term potentiation, Object location memory, mTORC1, Optogenetic silencing, Optogenetic synaptic plasticity.

1 Introduction

Hippocampal somatostatin expressing interneurons (SOM-INs) are dendrite-projecting inhibitory cells (1). The activity of CA1 SOM-INs is necessary for the proper formation of contextual fear memory (2, 3). SOM-INs may also be critical during place cell firing by controlling pyramidal cell excitatory inputs, limiting dendritic amplification and suppressing out-of-field excitatory inputs (4, 5). The contribution of SOM-INs has been studied particularly in the dorsal part of CA1, in relation to the encoding of spatial and contextual memory by PCs. However, the contribution to aversive episodic memory of a subset of SOM-INs, the oriens lacunosum-moleculare interneurons that express the nicotinic a2 subunit (OLMα2), varies depending on their location along the dorsoventral axis of the hippocampus, with activation of cells in intermediate hippocampus inhibiting fear-related memories (6).

A large body of evidence suggests that long-term synaptic plasticity between hippocampal principal cells is a fundamental substrate supporting memory (7-11). Inhibitory interneuron synapses also display a wide range of plasticity (1, 12, 13). Notably, SOM-INs display an input-specific long-term potentiation (LTP) at their main excitatory inputs coming from local pyramidal cells (PC; PC-SOM synapses) (14-16). This LTP is Hebbian and depends on the activation of the metabotropic glutamate receptor subtype 1a (mGluR1a) and mechanistic target of rapamycin complex 1 (mTORC1) pathways (14, 15, 17-19). PC-SOM synapse LTP is triggered by theta burst stimulation (TBS) of PCs or contextual fear conditioning and is absent in parvalbumin expressing interneurons or in interneurons of stratum radiatum (3, 17-19). PC-SOM synapse LTP in turn regulates CA1 network metaplasticity at CA3 and entorhinal inputs to PCs (3, 15, 18, 20). Besides, PC-SOM synapse LTP is required during learning for the consolidation of contextual fear memory (3, 19). Moreover, SOM-IN activity after contextual fear conditioning supports memory consolidation (20). SOM-IN mTORC1 dependent plasticity also contributes to fear motivated spatial memory, as in the Barnes maze, in which mice need to learn over repeated trials the location of a target hole to escape a bright, loud, open environment (19). Thus, SOM-IN activity and PC-SOM synapse LTP during learning and consolidation, control the formation of fear-related contextual and spatial memories.

Hippocampal synaptic plasticity also plays an important role in novelty driven learning, particularly in the processing of novel object spatial configuration (21-23). Novel spatial learning such as spatial object recognition triggers long-term depression (LTD) that curtails LTP at hippocampal PC synapses (21, 24). Hippocampal PC LTD creates a neuronal representation of spatial content by eliminating weakly potentiated synapses and by dictating temporal constraints and the dendritic distribution of LTP (25). Therefore, the hippocampus recognizes and encodes the novel spatial component of an object through LTD and metaplastic changes at PC synapses (21, 23, 25).

The activity of SOM-IN from dorsal CA1 is not required for the encoding of object shape while inhibiting intermediate CA1 SOM-INs during learning facilitates later novel object recognition (6). The object location memory task, which largely depends on dorsal CA1 function, is a one trial, novelty driven, spatial episodic memory test (26-29). Given the role of PC-SOM synapse LTP in spatial memory (19) and the dependency of object location memory task on dorsal CA1 (26-29), we asked if dorsal CA1 SOM-IN activity and PC-SOM synapse LTP contribute to the encoding of such non-aversive forms of spatial episodic memory.

To address this question, we used optogenetics to silence SOM-IN activity during training of an object location memory task. We found that silencing dorsal hippocampal SOM-INs during training impaired object location memory tested 24 hours later. Furthermore, optogenetic induction of PC-SOM synapse LTP given 30 minutes before training resulted in facilitation of object location memory tested 24 hours later. This facilitation was absent in mice with conditional knock-out of Rptor in SOM-INs which lack PC-SOM synapse LTP. Hence, our results indicate that SOM-IN activity is necessary during object location learning and that optogenetic induction of PC-SOM synapse LTP is sufficient to facilitate consolidation of object location memory. These findings shed new light on the essential role of activity of SOM-INs in novelty-driven spatial episodic memory that is facilitated by plasticity at PC-SOM synapses.

2 Methods

2.1 Animals

Animal procedures and experiments were performed in accordance with the Université de Montréal Animal Care Committee (Comité de Déontologie de l'Expérimentation sur les Animaux; CDEA Protocols # 17-001, 17-002, 18-002, 18-003, 19-003, 19-004, 20-001, 20-002, 21-001, 21-002, 22-008, 22-009) and the Canadian Council of Animal Care guidelines.

Mice with Cre-dependent Enhanced Yellow Fluorescent Protein (EYFP) expression in SOM-INs (SOM-Cre-EYFP mice) were produced by crossing Sstires-Cre mice (Jackson Labs #013044) with Rosa26lsl-EYFP reporter mice (Ai3, Jackson Labs # 007903) as previously (3, 19). Mice with a conditional homozygous knock-out of Rptor in SOM-INs (SOM-Cre-Raptor-KO mice) were obtained by crossing Sstires-Cre; Rosa26lsl-EYFP with Rptorfl/fl mice as previously (3, 19). Mice were housed 2-4 animals per cage, until optogenetic cannula implantation after which they were singly housed in larger cages (rat cage) with some object enrichment (small plastic weight boat and PVC tube). Food and water were given ad libitum. Mice were maintained on a 12 h light/dark cycle. Experiments were performed during the light phase on male mice.

2.2 Virus injection, optic fiber implantation and optogenetic stimulation

Six to eight weeks old mice were anesthetized with intraperitoneal injection of ketamine (50mg/kg) and xylazine (5mg/kg). For experiments with SOM-IN silencing, 0.5 µL of AAV2/9-flex-Arch-GFP (1.74-1.83×1013 particles/ml) or AAV2/9-EF1a-DIO-EYFP (3.95 × 1013 particles/ml) were injected bilaterally (0.05 µL/min) in dorsal CA1 hippocampus (coordinates relative to bregma: -1.95 mm AP; ±1.30 mm ML; and -1.30 mm DV) as previously (3). For experiments with TBS optogenetic induction, 0.5 µL of AAV2/9-CaMKIIa-hChR2(E123T/T159C)-mCherry (1.5-1.77×1012 particles/ml) was injected as described above. After a recovery period of one week, mice were re-anesthetized as described above, and optic fiber cannulas (multimode optic fiber FT200EMT: 0.39 NA, Low OH, 200 µm core diameter; Thorlabs) were implanted bilaterally to target dorsal CA1 hippocampus just above stratum oriens (coordinates relative to bregma: -1.95 mm AP; ±1.60 mm ML; and -1.15 mm DV) and sealed with dental cement mixed with carbon

powder (Metabond, Parkell Inc). Mice were allowed to rest for a week before behavioral experiments.

For *in vivo* optogenetic stimulation, a Quadruple Laser Diode Fiber Light Source (LDFLS_405_450_520_638; Doric Lenses Inc) was coupled to Mono Fiberoptic Patchcords (MFP_200/240/900-0.22_2m_FC-ZF1.25(F), 200 µm Core diameter, 0.22 NA; Doric Lenses Inc) and hand-made fiber optic cannulas (optic fiber: FT200EMT, 200 µm Core diameter, 0.39 NA; ceramic ferrule: CFLC230-10; Thorlabs).

2.3 Behavioral experiments

For the SOM-IN silencing experiments, mice had 1 week recovery between viral injection and cannula implantation. Handling started after 2 weeks recovery (9-11 weeks old mice). For the optogenetic LTP experiments, mice underwent viral injection and cannula implantation the same day. Handling started after 1 week recovery (7-9 weeks old mice). Before each experimental session, the arena and objects were thoroughly cleaned with a 10% Versaclean solution.

Handling. Animals were handled for 5 days (5 min/day) and progressively habituated to contention and optic fibers connection (without light stimulation).

Open field test. On the last day of habituation, mice were allowed to freely explore a square arena (45 × 45 cm; Panlab) for 10 minutes. The anxiety level was assessed by measuring the time spent and the distance traveled in the center (1/3 central zone) and the periphery (1/3 peripheral zone) of the arena. Locomotion was assessed by measuring the total distance traveled and the number of zone transitions (16 equal square zones). Mice were video-tracked and their movements analyzed using a position tracking system (Smart 3.0; PanLab). Animals showing abnormal levels of anxiety in the open field test were excluded from the study.

Object Location Memory Task. The task consisted of four days of habituation, one day of object location training and one day of object location memory test. For this task, the square arena (45 × 45 cm; Panlab) had three uniform light gray walls and one differentiated wall with a glossy black square in the center (1/3 of the wall). For habituation, mice were connected to the patch cord either immediately before entering the arena for experiments with SOM-IN silencing, or 30 minutes

before in the home cage for the experiments with TBS optogenetic induction. Mice were allowed to explore the empty arena for 5 minutes a day.

For object location training, two identical objects (aluminum post with black plastic star grip screw on top; Siskiyou Design-Instruments) were placed 10 cm from the differentiated wall, each in line with one end of the glossy black square. For SOM-IN silencing experiments, the animals were attached to the patch cord, placed in the arena and allowed to explore the arena and objects for 10 minutes. SOM-INs were silenced during the complete training session with continuous 520 nm light stimulation. For experiments with optogenetic TBS (TBSopto) induction in the home cage before training, mice were given the TBSopto protocol (450 nm; 5 bursts of 4 light pulses of 1 ms duration at 80 Hz, given at 300 ms interburst interval, and repeated 3 times with 30 s interval), or no light stimulation. Thirty minutes later, mice were allowed to explore the arena and objects for 10 minutes. For object location memory test 24 h later, one object was moved to a new location across the arena, 10 cm from the opposite wall. Mice were placed in the arena and allowed to explore the arena and objects for 10 minutes.

Object location experiments were carried out using 2 contiguous arenas. The allocation to arena 1 or 2, and the object to be moved during the test (right or left), were counterbalanced between mice and groups. All sessions were video tracked at 30 frame/sec (1080 pixels). Behavior was analyzed using DeepLabCut (30), as follows. The deep neural network was trained to detect the head, body, and tail base of the mice, as well as the object that stayed at the original place (immobile object) and the object that moved for the test session (mobile object), on a randomly generated sample of frames taken from memory acquisition and test videos from each batch of experiments (≥ 20 frames per videos, > 200 frames per batches). The object exploration time was measured as the time the mouse's head was in a 3 cm zone around each object (see analysis code in Supplemental file 2). ResNet50 deep neural network was trained until tests and trained errors where approximately 3 pixels. All analyzed videos were watched by the experimenter to ensure there was no failure to detect object exploration. The exploration time for each object was expressed as a percentage of total object exploration time: (time exploring mobile object)/(time exploring mobile object + immobile object) x100. The object preference ratio was calculated as: (time exploring mobile object)/(time exploring immobile object). Mice were excluded if the discrimination index (time exploring mobile object - time exploring immobile object)/(time

exploring mobile object + time exploring immobile object) during training was not between -30 and 30, if the time of exploration of one object was <3 sec, or if total exploration time was <10 sec during the test (31).

2.4 Histology

After behavioral experiments, animals were deeply anesthetized with intraperitoneal injection of sodium pentobarbital (MTC Pharmaceuticals), trans-cardially perfused first with 0.1 M phosphate buffer saline (PBS) and next with 4% paraformaldehyde diluted in 0.1 M PBS (PFA). The brains were isolated, postfixed in 4% PFA for 24 h and cryoprotected in 30% sucrose. Coronal brain sections (50 μm thick) were obtained using freezing microtome (SM200R; Leica) and mounted in ProLong Gold (Invitrogen). Immunofluorescence was used to enhance GFP fluorescence associated with Arch. Brain sections of mice injected with AAV9.flex.CBA.Arch-GFP.WPRE.SW40 were prepared as described above, permeabilized with 0.5% Triton X-100 in PBS for 30 minutes and unspecific binding was blocked with 10% normal goat serum in 0.1% Triton X-100/PBS for 1 h. Rabbit polyclonal anti GFP (1/200) antibodies were incubated 24 h at 4° C. Sections were subsequently incubated at room temperature with Alexa Fluor 594-conjugated goat anti-rabbit IgGs (1/500; 60 min). Sections were mounted in ProLong Gold (Invitrogen), examined using an epifluorescence microscope (Eclipse E600; Nikon) and images were acquired with the Simple PCI software. Mice were excluded if virus expression was not restricted to dorsal CA1 hippocampus, or optic fiber placement was not correct (just above stratum oriens of dorsal CA1 hippocampus).

2.5 Statistical Analysis

Statistical analysis was performed using SigmaPlot (Systat Software) or SPSS (IBM Statistics). Data were tested for normality and equal variability. Mann–Whitney Rank Sum tests and Kruskal-Wallis one-way ANOVA on Ranks with Dunn's pairwise comparisons were used when data did not pass normality and/or homoscedasticity assumptions. Otherwise, Student's t-tests, paired t-test, one-way ANOVA, or 2- repeated measures ANOVA followed by Bonferroni pairwise

comparisons, were used. All tests were two-sided. All data in the Figures are presented as mean ± SEM. Box plots in Figures represent mean, 25th and 75th percentiles, and ± SEM. Asterisks in Figures denote statistical significance levels for specified tests (* $p < 0.05$; ** $p < 0.01$; *** $p < 0.005$; ns, not significant). Sample size required to reach significance were determined with a power analysis with power=0.8 and alpha=0.05. Details of every statistical test are listed in Supplemental file 1 and identified per Figure panel.

3 Results

3.1 Somatostatin interneuron activity is necessary during object location learning

Activity of dorsal CA1 SOM-INs is necessary during the presentation of aversive stimuli for the formation of contextual fear memory (2, 3). To determine if the activity of SOM-INs is also necessary during learning for object location memory, we used optogenetic inhibition of CA1 SOM-INs. The light-gated proton pump archaerhodopsin (Arch) was expressed in SOM-INs using bilateral injections of AAV2/9-flex-Arch-GFP to the dorsal CA1 region of SOM-Cre mice and control mice received injections of AAV2/9-EF1a-DIO-EYFP (Figure 1A) (3, 18). In all experiments, post-hoc histology showed selective expression of Arch-GFP in CA1 SOM interneurons (ex. Figure 1A), as previously (3).

The object location memory task consisted of a training during which the animal was exposed to two identical new objects in an environment, and a memory test 24 hours later when the animal was exposed to the same environment but with one object moved to a new location (Figure 1B-C). The time spent exploring each object was measured and object location memory assessed as the preference for exploration of the object with a novel location in the memory test (31). During training, silencing SOM-INs by optogenetic activation of Arch (Arch Light) did not affect total exploration time relative to control mice with light stimulation of EYFP expressing SOM-INs (EYFP Light) or without light activation of Arch expressing SOM-INs (Arch No light) (Figure 1D left). Also, control mice did not show preference for exploration of any object and silencing SOM-INs did not affect the percent exploration time of the mobile object (Figure 1D middle). Thus, silencing SOM-INs did not affect object exploration during training.

However silencing SOM-INs during training affected object location memory tested 24 h later. Control mice with light stimulation of EYFP expressing SOM-INs during training, or without light stimulation of Arch expressing SOM-INs, spent more time exploring the mobile object during the memory test, but mice with SOM-IN silencing during training did not (Figure 1D middle). The preference ratio of mobile/immobile object was elevated in both control mice but not in mice with silencing of SOM-INs (Figure 1D right). Thus, silencing SOM-INs during training results in impairment of object location memory, indicating that activity of SOM-INs supports object location learning.

The effects of silencing SOM-INs were not due to changes in anxiety levels or locomotion since in open field tests (Figure 1E-G), mice from the 3 groups showed equivalent anxiety levels (% time spent in periphery or center, and ratio of time in center/periphery; Figure 1F) or locomotion (total distance traveled and zone transitions; Figure 1G). Thus, dorsal CA1 SOM-IN activity is necessary during learning for formation of object location memory.

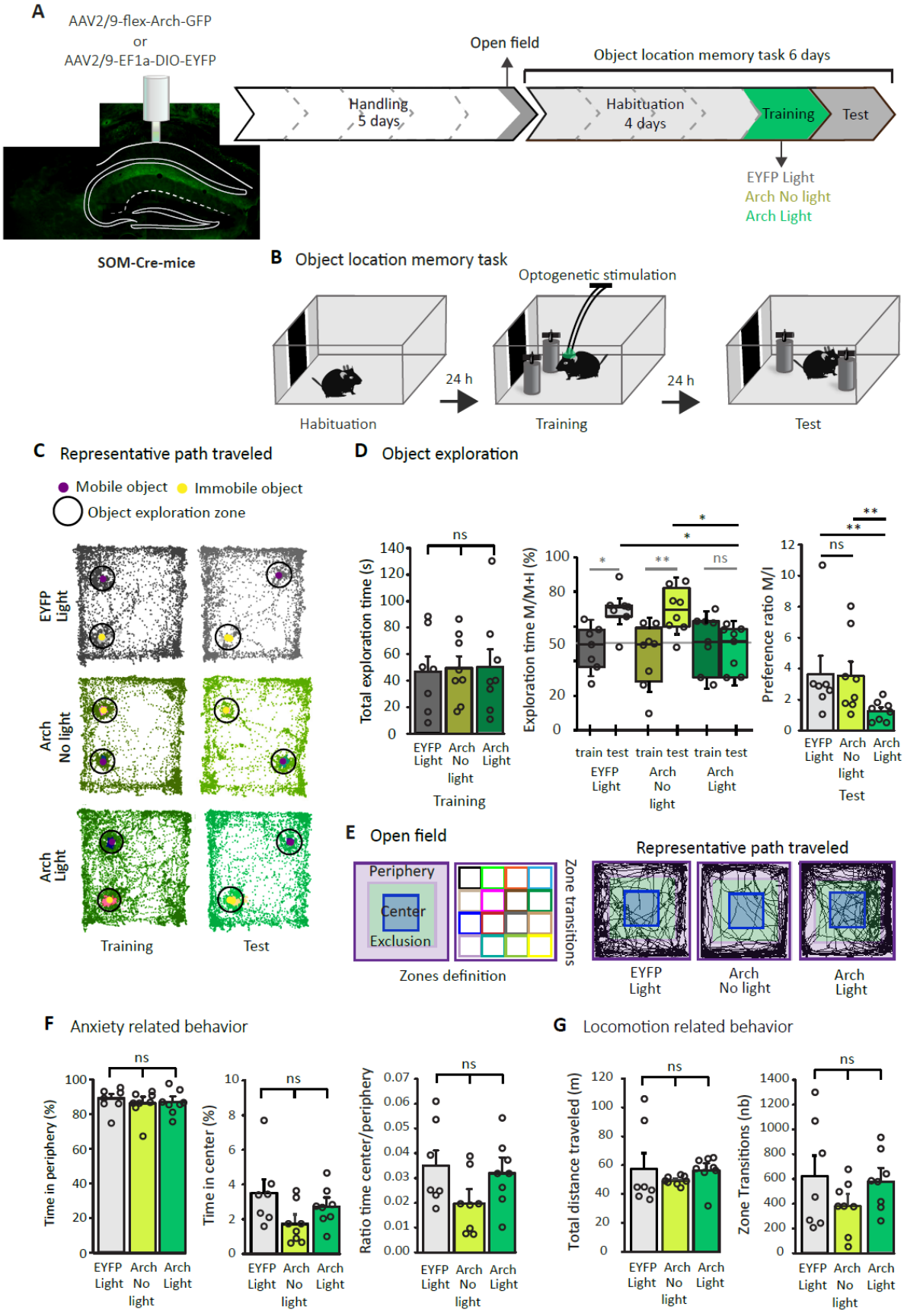
A
AAV2/9-flex-Arch-GFP
or
AAV2/9-EF1a-DIO-EYFP
SOM-Cre-mice
Open field
Object location memory task 6 days
Handling
5 days
Habituation
4 days
Training
Test
EYFP Light
Arch No light
Arch Light
B Object location memory task
Optogenetic stimulation
24 h
24 h
Habituation
Training
Test
C Representative path traveled
Mobile object
Immobile object
Object exploration zone
EYFP Light
Arch No light
Arch Light
Training
Test
D Object exploration
Total exploration time (s)
Exploration time M/M+I (%)
Preference ratio M/I
ns
train test
EYFP Light
Arch No light
Arch Light
Training
Test
E Open field
Periphery
Center
Exclusion
Zones definition
Zone transitions
Representative path traveled
EYFP Light
Arch No light
Arch Light
F Anxiety related behavior
Time in periphery (%)
Time in center (%)
Ratio time center/periphery
G Locomotion related behavior
Total distance traveled (m)
Zone Transitions (nb)

Figure 1. Somatostatin interneuron activity is necessary during object location memory acquisition. (A) Left: representative image of CAG-driven cre-dependent Arch-GFP expression in a SOM-Cre mice. Right: diagram of behavioral testing sequence. **(B)** Experimental protocol of the object location memory task with optogenetic light stimulation (520 nm) for the duration of the training session. **(C-G)** Color coding of groups is as follows. Grey: EYFP injected mice with light, n=7 mice. Chartreuse green: Arch injected mice without light (Arch No light), n=8 mice. Emerald green: Arch injected mice with light (Arch Light) n=8 mice. Dark colors, training; light colors, test. **(C)** Representative path traveled during training and test sessions. **(D)** Left: graph of the total exploration time of objects during the training session, showing no difference between groups (One way ANOVA). Middle: graph of the percentage of time spent exploring the mobile object during training and test sessions, showing no difference during training sessions, but reduced exploration time during test session for mice with SOM-INs silencing (Arch Light) relative to controls. Two-way repeated measures ANOVA, Bonferroni pairwise multiple comparisons. Right: graph of preference ratio indicating a deficit in mice with SOM-INs silencing (Arch Light) relative to control mice (EYFP and Arch No light) (Kruskal-Wallis one-way ANOVA on ranks). ns $p > 0.05$, * $p < 0.05$, ** $p < 0.01$. **(E)** Open field. Left: zone separations used for analysis. Right: representative path traveled during the open field test for EYFP, Arch No light and Arch Light mice. **(F)** Graphs showing similar times spent in periphery (left) or center (middle), and ratio of time in center/periphery (right), indicating normal anxiety. One-way ANOVA, ns $p > 0.05$. **(G)** Graphs showing similar total distance traveled (left) and zone transitions (right) in all groups. Total distance: Kruskal-Wallis one-way ANOVA on Ranks. Zone transitions: one-way ANOVA, ns $p > 0.05$. Details of all statistical tests in this and following figures are listed in Supplemental File 1.

3.2 Object location memory is facilitated by optogenetic induction of long-term potentiation of SOM interneuron excitatory afferents

mTORC1-dependent LTP is induced at PC-SOM synapses by contextual fear learning and contributes to fear motivated contextual and spatial memories (19). Optogenetic theta burst stimulation (TBSopto) of CA1 PCs induces mGluR1a- and mTORC1-mediated LTP at PC-SOM synapses, and TBSopto given *in vivo* 30 minutes before contextual fear conditioning negatively regulates contextual fear memory (3). Thus, we next determined if optogenetic induction of PC-SOM synapse LTP also regulates spatial episodic memory in object location memory task. Modified hChR2 was expressed in CA1 PCs using bilateral injections of AAV2/9-CaMKIIa-hChR2 (E123T/T159C)-mCherry in dorsal CA1 region of SOM-Cre-EYFP mice, and TBSopto protocol (450 nm; 5 bursts of 4 light pulses of 1 ms duration at 80 Hz, given at 300 ms interburst

interval, and repeated 3 times with 30 s interval) was delivered in CA1 region, as previously (3) (Figure 2 A-B). In all experiments, post-hoc histology showed selective expression of hChR2-mCherry in CA1 pyramidal cells (ex. Figure 2A), as previously (3).

TBSopto given 30 min prior to training did not affect total exploration time of objects during training, relative to control mice that did not receive TBSopto (Figure 2 C-D). During training, control mice did not show preference for exploration of any object and TBSopto did not affect the percent exploration time of the mobile object (Figure 2D middle). Thus, TBSopto given 30 min prior to learning did not affect object exploration during training.

However, TBSopto given prior to training affected object location memory tested 24 h later. In these experiments, modifications of the surgical timeline and behavioral paradigm (see methods) resulted in subthreshold learning of the object location memory task in control mice in our conditions. Although the discrepancy with the control mice showing significant learning in the SOM-IN inhibition experiments (Figure 1D) prevented us to make comparisons between these experimental cohorts, it allowed us to test whether TBSopto could facilitate object location learning under conditions that were subthreshold for learning. During memory tests, control mice did not spend more time exploring the mobile object, but mice given TBSopto showed increased exploration of the mobile object (Figure 2D middle). Preference ratio of mobile/immobile object was elevated in mice that received TBSopto relative to control mice (Figure 2D right). Thus, TBSopto given 30 min prior to training results in facilitation of object location memory, suggesting that induction of synaptic plasticity at PC-SOM synapses facilitates object location learning.

Effects of TBSopto were not due to changes in anxiety levels or locomotion since in open field tests (Figure 2E-G), mice from both groups showed equivalent anxiety levels (Figure 2F) or locomotion (Figure 2G). Thus, optogenetic induction of synaptic plasticity at PC-SOM synapses prior to learning may facilitate the formation of object location memory.

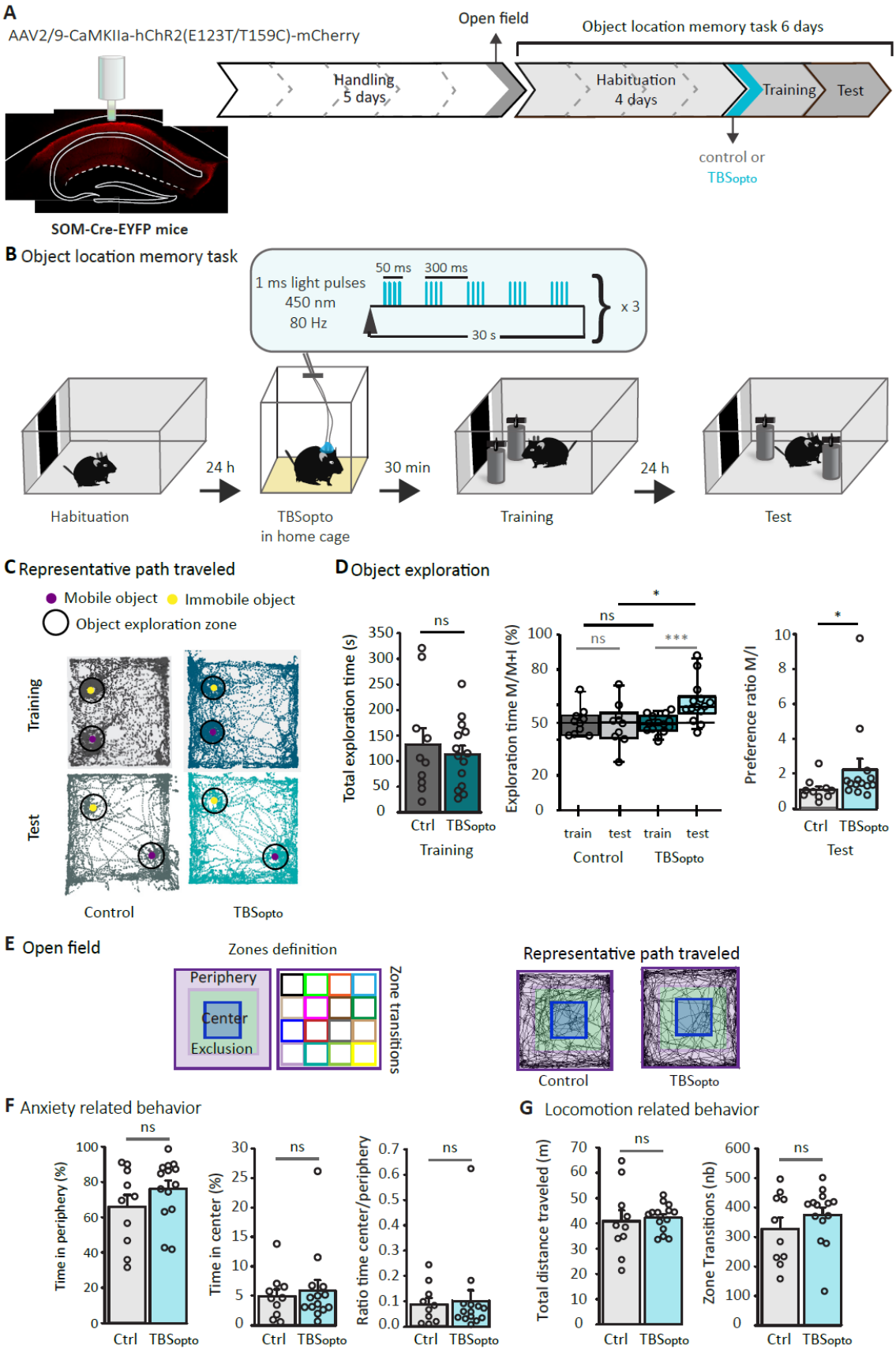
A
AAV2/9-CaMKIIa-hChR2(E123T/T159C)-mCherry
SOM-Cre-EYFP mice
Open field
Object location memory task 6 days
Handling
5 days
Habituation
4 days
Training
Test
control or
TBSopto
B Object location memory task
1 ms light pulses
450 nm
80 Hz
50 ms
300 ms
30 s
x 3
24 h
30 min
24 h
Habituation
TBSopto
in home cage
Training
Test
C Representative path traveled
Mobile object
Immobile object
Object exploration zone
Training
Test
Control
TBSopto
D Object exploration
Total exploration time (s)
ns
Ctrl
TBSopto
Training
Exploration time M/M+I (%)
ns
ns
***
*
train
test
train
test
Control
TBSopto
Preference ratio M/I
*
Ctrl
TBSopto
Test
E Open field
Zones definition
Periphery
Center
Exclusion
Zone transitions
Representative path traveled
Control
TBSopto
F Anxiety related behavior
Time in periphery (%)
Time in center (%)
Ratio time center/periphery
G Locomotion related behavior
Total distance traveled (m)
Zone Transitions (nb)

Figure 2. Object location memory is facilitated by optogenetic induction of long-term potentiation of SOM-IN excitatory afferents. (A) Left: schematic of cannulation with representative image of hChR2-mCherry expression of the AAV2/9-CaMKIIa-hChR2(E123T/T159C)-mCherry in dorsal CA1 hippocampus of SOM-Cre-EYFP mice. Right: diagram of behavioral testing sequence (open field and object location memory task). **(B)** Experimental protocol of the object location memory task with optogenetic induction of PC-SOM synapse LTP (TBSopto) 30 min before the training session. **(C- G)** Color coding of groups is as follows. Grey: control mice without TBSopto, n=10 mice. Blue: mice with TBSopto, n=14 mice. Dark colors = training, light colors = test. **(C)** Representative path traveled during training and test sessions. **(D)** Left: graph of total exploration time of objects during the training session, showing no difference between groups (t-test). Middle: graph of the percentage of time spent exploring the mobile object during training and test sessions, showing no difference during training sessions, but increased exploration time during test session for mice that received TBSopto before training, relative to controls. Two-way repeated measures ANOVA, Bonferroni pairwise multiple comparisons. Right: graph of preference ratio showing facilitation of object location memory for mice that received TBSopto relative to control mice without TBSopto (Mann-Witney Rank Sum Test). ns $p > 0.05$, * $p < 0.05$, ***$p < 0.005$. **(E)** Open field. Left: zone separations used for analysis. Right: representative path traveled during the open field test for control and mice receiving TBSopto. **(F)** Graphs showing similar time spent in periphery (left) or center (middle), and ratio of time in center/periphery (right), indicating normal anxiety in both groups. Mann-Witney Rank Sum Tests, ns $p > 0.05$. **(G)** Graphs showing similar total distance traveled (left) and zone transitions (right) in both groups, indicating normal locomotion. Total distance: Mann-Witney Rank Sum Test. Zone transitions: t-test. ns $p > 0.05$.

3.3 Conditional knock-out of *Rptor* in SOM interneurons prevents facilitation of object location memory by TBS_{opto}

LTP induced by TBSopto at PC-SOM synapses and its regulation of CA1 network metaplasticity and contextual fear memory are blocked by conditional knock-out of Rptor in SOM-INs (3). Although conditional knockout may have occurred in a minority of CA3 pyramidal cells in the SOM-Cre-Raptor-KO mice (32), we have previously shown that the Cre expression in these mice is highly selective to SOM interneurons (18) and that conditional knockout is specific to SOM interneurons and does not affect significantly hippocampal principal cells (19). Therefore, we tested next if the facilitation of object location memory by TBSopto was due to mTORC1 signaling in SOM-INs, by using the same TBSopto protocol and expressing hChR2 in CA1 pyramidal cells of mice with a conditional knock-out of Rptor in SOM-INs (SOM-Cre-Raptor-KO mice) in which TBSopto-induced plasticity in SOM-INs is blocked (3).

TBSopto given 30 min prior to training in SOM-Cre-Raptor-KO mice did not affect total exploration time of objects during training, relative to control mice without TBSopto (Figure 3 C-D). During training, control mice did not show preference for exploration of any object and TBSopto did not affect the percent exploration time of the mobile object (Figure 3D middle). Thus, TBSopto given 30 min prior to learning did not affect object exploration during training in SOM-Cre-Raptor-KO mice.

TBSopto given prior to training in SOM-Cre-Raptor-KO mice failed to facilitate object location memory tested 24 h later. During memory tests, both control mice and mice that received TBSopto did not spend more time exploring the mobile object (Figure 3D middle). Preference ratio of mobile/immobile object was not different in mice that received TBSopto relative to control mice (Figure 3D right). Thus, TBSopto given 30 min prior to training did not result in facilitation object location memory in SOM-Cre-Raptor-KO mice, suggesting that facilitation of object location learning by TBSopto in SOM-Cre-EYFP mice was due to induction of mTORC1-mediated synaptic plasticity at PC-SOM synapses.

Failure to observe facilitating effects of TBSopto was not due to changes in anxiety levels or locomotion since in open field tests (Figure 3E-G) mice from both groups showed equivalent anxiety levels (Figure 3F) or locomotion (Figure 3G).

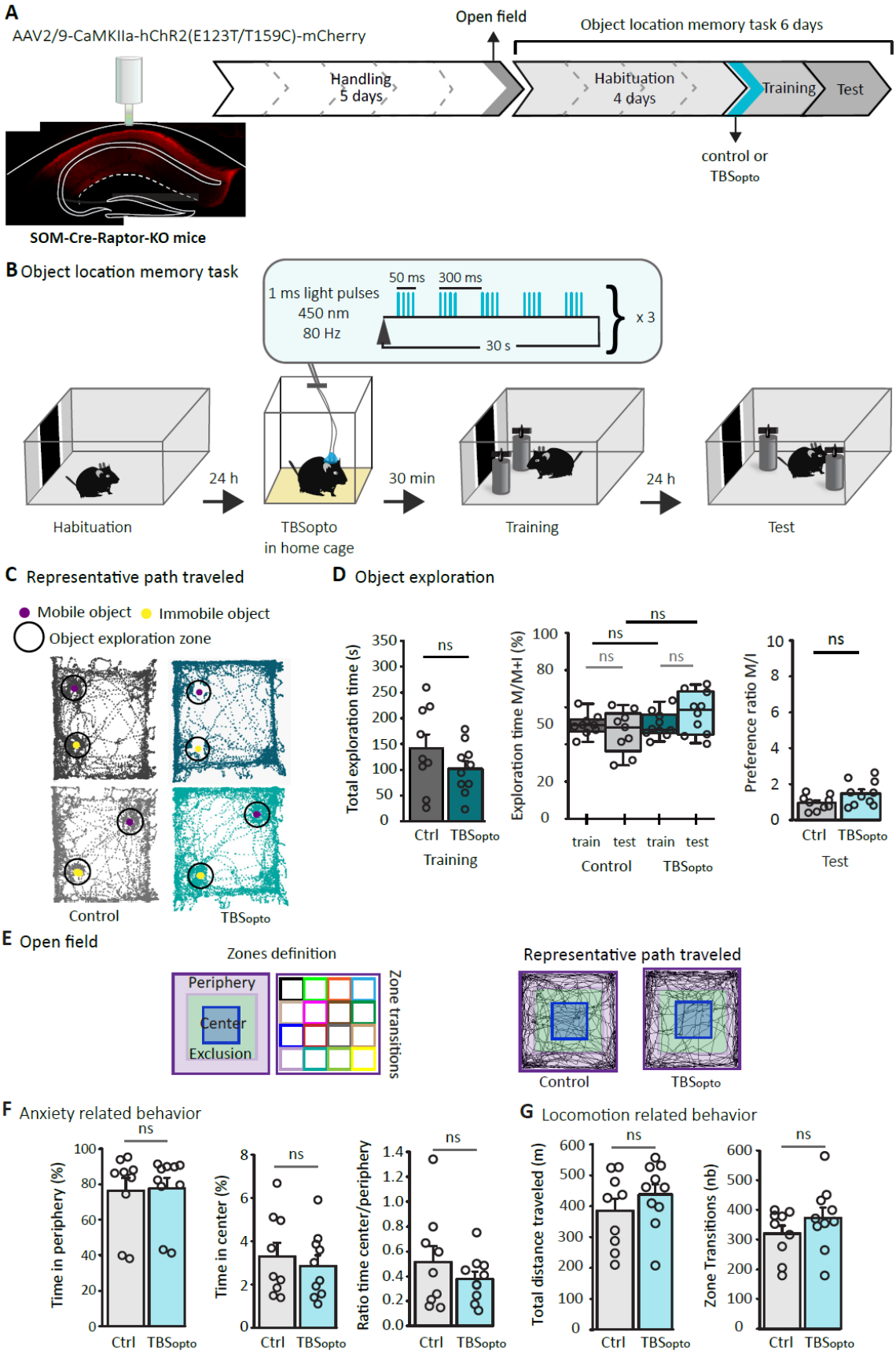
A
AAV2/9-CaMKIIa-hChR2(E123T/T159C)-mCherry
Open field
Object location memory task 6 days
Handling
5 days
Habituation
4 days
Training
Test
control or
TBSopto
SOM-Cre-Raptor-KO mice
B Object location memory task
1 ms light pulses
450 nm
80 Hz
50 ms
300 ms
x 3
30 s
24 h
30 min
24 h
Habituation
TBSopto
in home cage
Training
Test
C Representative path traveled
Mobile object
Immobile object
Object exploration zone
Control
TBSopto
D Object exploration
Total exploration time (s)
ns
Ctrl
TBSopto
Training
Exploration time M/M+I (%)
ns
ns
ns
ns
train
test
train
test
Control
TBSopto
Preference ratio M/I
ns
Ctrl
TBSopto
Test
E Open field
Zones definition
Periphery
Center
Exclusion
Zone transitions
Representative path traveled
Control
TBSopto
F Anxiety related behavior
Time in periphery (%)
ns
Ctrl
TBSopto
Time in center (%)
ns
Ctrl
TBSopto
Ratio time center/periphery
ns
Ctrl
TBSopto
G Locomotion related behavior
Total distance traveled (m)
ns
Ctrl
TBSopto
Zone Transitions (nb)
ns
Ctrl
TBSopto

Figure 3. Conditional knock-out of Rptor in SOM-INs prevents facilitation of object location memory by TBSopto. (A) Left: schematic of cannulation with representative image of hChR2-mCherry expression of the AAV2/9-CaMKIIa-hChR2(E123T/T159C)-mCherry in dorsal CA1 hippocampus of SOM-Cre-Raptor-KO mice. Right: diagram of behavioral testing sequence (open field and object location memory task). **(B)** Experimental protocol of the object location memory task with TBSopto 30 min before the training session. **(C–G)** Color coding of groups is as follows. Grey: control mice without TBSopto, n = 9 mice. Blue: mice with TBSopto, n = 10 mice. Dark colors = training, light colors = test. **(C)** Representative path traveled during training and test sessions. **(D)** Left: graph of total exploration time of objects during the training session, showing no difference between groups (t-test). Middle: graph of the percentage of time spent exploring the mobile object during training and test sessions, showing no difference during training and test sessions in both groups, indicating no facilitation of object location memory by TBSopto in SOM-Cre-Raptor-KO mice. Two-way repeated measures ANOVA, Bonferroni pairwise multiple comparisons. Right: graph of preference ratio showing absence of facilitation of object location memory for SOM-Cre-Raptor-KO mice that received TBSopto (t-test). ns $p > 0.05$. **(E)** Open field. Left: zone separations used for analysis. Right: representative path traveled during the open field test for control and mice receiving TBSopto. **(F)** Graphs showing similar time spent in periphery (left) or center (middle), and ratio of time in center/periphery (right), indicating normal anxiety in both groups. Time in periphery and ratio, Mann-Witney Rank Sum Tests. Time in center, t-test. Ns $p > 0.05$. **(G)** Graphs showing similar total distance traveled (left) and zone transitions (right) in both groups, indicating normal locomotion (t-tests). ns $p > 0.05$

4 Discussion

The main observations of the study were that I) silencing SOM-INs during training results in impairment of object location memory, indicating that activity of SOM-INs supports object location learning; II) TBSopto given 30 min prior to training results in facilitation of object location memory, suggesting that induction of synaptic plasticity at PC-SOM synapses facilitates object location learning; and III) TBSopto given 30 min prior to training did not result in facilitating object location memory in SOM-Cre-Raptor-KO mice, suggesting that facilitation of object location learning by TBSopto in SOM-Cre-EYFP mice was due to induction of mTORC1-mediated synaptic plasticity at PC-SOM synapses. Thus, hippocampal somatostatin interneuron activity is required for object location learning, a hippocampus-dependent form of novelty motivated spatial learning that is facilitated by plasticity at PC-SOM synapses.

4.1 SOM cells activity is necessary for encoding multiple types of memory

Our results indicate that SOM-IN activity is necessary during object location learning. SOM-IN activity is also required for linking context to fear. In contextual fear conditioning, inhibition of

SOM-INs during the application of the conditioning stimulus (shocks) reduces contextual fear memory, but inhibition during the context exploration does not (2, 3). In a passive avoidance task, in which mice avoid an attractive context that is associated with an aversive stimulus, inhibition of the OLMα2 sub-population of SOM-INs during training also reduces fear memory (6). Our results show that SOM-IN activity is not only necessary for associating fear to context, but also for encoding object relations in space in a novelty-driven task that does not involve aversive stimuli. Although we did not provide electrophysiological confirmation of optogenetic inhibition of SOM-INs by Arch activation in the present work, we showed in a previous report with whole-cell recording in slices that optogenetic activation of Arch hyperpolarizes SOM-INs (18). A paradoxical release of neurotransmitters from Arch-expressing terminals has been reported with prolonged stimulation with yellow light (33), which could potentially have interfered with our behavioral experiments. Additional experiments using the light-gated chloride pump halorhodopsin (eNpHR3.0) which lacks such paradoxical effects would be useful to confirm our results. However, we have previously shown that sustained Arch activation does not affect basal transmission at Schaffer collateral synapses in hippocampal slices (18). In addition, we found previously that in open-field control experiments, 5 min continuous yellow light activation or Arch inhibition of SOM-INs did not affect mice exploration, anxiety and locomotion (3), suggesting that the Arch-induced impairment of object location learning was due to SOM-IN silencing. Thus, our findings of an essential role of SOM-IN activity in object location learning, specifically in a mismatch novelty paradigm, extend the necessary role of SOM-IN activity in encoding a wide range of aspects of the context and its relation to salient events in mice.

Interestingly, SOM-IN activity after contextual fear conditioning supports memory consolidation (20). If the same timing to plasticity is involved in non-aversive behavior - such as the object location task - it would be useful to determine if, using the protocols developed in the present study, activation or inhibition of SOM-IN function, either before or after the object location learning phase, affects consolidation of this memory circuit. Also, the role of SOM-INs vary along the dorso-ventral axis of the hippocampus. Inhibiting OLMα2 cells of intermediate CA1 during passive avoidance training had no effect on fear memory. Furthermore, an opposite role was found in the object recognition task, another novelty motivated memory task where the animal learns the features of objects to differentiate familiar and novel objects. Inhibition of dorsal OLMα2 cells during training has no effect on novel object recognition, while inhibition of intermediate OLMα2

cells facilitates novel object recognition (6). In this context, it will be interesting to examine the role of SOM-INs in object location memory according to their position along the dorso-ventral axis.

4.2 LTP at PC-SOM synapses facilitates object location memory

Our results indicate that object location memory is facilitated by optogenetic induction of long-term potentiation of SOM interneuron excitatory afferents. It is noteworthy that control mice in our three experimental groups (Figures 1D, 2D and 3D) did not show similar levels of object location learning. The reason for this discrepancy is unclear but may be due to differences in experimental protocols. For example, the timeline of surgical procedures differed in the Arch and hChR2 groups. Viral injection and cannulation were performed in two separate sessions separated by a one-week recovery period for Arch experiments, while viral injection and cannulation were carried out in one session for hChR2 experiments. However, the three groups of control mice showed normal anxiety and locomotion in the open-field test (Figure 1E-G, Figure 2E-G, and Figure 3E-G). Alternatively, the TBSopto control experiments included an additional session with connection to the optic probe without optogenetic stimulation in home cage, and 30 min later the training session (Figure 1B versus Figure 2B), which may have negatively affected the object location learning during the training session. However, it is important to note that both control groups in SOM-Cre-EYFP and SOM-Cre-Raptor-KO mice showed similar behavior in the object location learning task, i.e. sub-threshold for learning, validating the comparison of the effects of TBSopto between these mice. The results that facilitation of object location learning was absent in SOM-Cre-Raptor-KO mice indicates that facilitation of object location learning by TBSopto requires mTORC1 function in SOM-INs, suggesting that LTP at PC-SOM synapse positively regulates object location learning.

Previous work indicates that TBSopto given before contextual fear conditioning has the opposite effect and negatively regulates contextual fear memory (3). In addition, optogenetic induction of PC-SOM synapse LTP prior to contextual fear conditioning, leads to a reduction of subsequent contextual fear conditioning-induced LTP at PC-SOM synapses (3). In slices, TBSopto given 15 min prior to chemically inducing PC-SOM synapses LTP blocks the protein synthesis normally produced by the chemical LTP induction (34), strengthening the idea that TBSopto

interacts with later LTP induction. Interestingly, passive avoidance learning induces long-term potentiation in a subset of pyramidal neurons and this learning-induced potentiation occludes subsequent high frequency stimulation-induced LTP (35). Thus, an analogous situation may occur in SOM-INs, with induction of LTP by TBSopto at PC-SOM synapses preventing and even reducing LTP induced subsequently during contextual fear conditioning, leading to a deficit in contextual fear memory (3).

Hence the question of why TBSopto-induced LTP has different effects on contextual fear and object location memory, when SOM-IN activity is required for both contextual fear and object location learning? An explanation could be that depotentiation of PC-SOM synapses may be required for object location learning. This may be analogous to plasticity at pyramidal cell synapses, where object location learning generally induces long-term depression at Schaffer collateral synapses onto pyramidal cells (36). LTD of SC-PC synapses may passively propagate to PC-SOM synapses (37) and negatively affect metaplasticity of Schaffer collateral synapses of the CA1 network during learning (3). Thus, it would be interesting to examine how long-term depression at PC-SOM synapses regulates plasticity of CA3 and entorhinal inputs to pyramidal cells, and how it is influenced by prior induction of TBSopto.

However, in pyramidal cells, the saturation of hippocampal LTP impairs spatial learning in the Morris water maze task (38). Also, in mice with cell-specific impairment of mTORC1 activity in SOM-INs, basal synaptic transmission is normal, but LTP is impaired at PC-SOM synapses, and spatial memory in the Barnes maze is deficient. Conversely, in mice with cell-specific facilitation of mTORC1 activity in SOM-INs, LTP at PC-SOM synapses and spatial memory in the Barnes maze are increased (19). Thus, LTP at PC-SOM synapses appears to be necessary for spatial learning. Consequently, a more plausible explanation for the opposite effect of TBSopto on contextual fear and object location memory, may be that in the present control conditions object location learning was subthreshold for the consolidation of memory, and therefore, long-term plasticity at PC-SOM synapses was likely not induced by learning in these control training conditions. In such “weak” training conditions, prior induction of PC-SOM synapse LTP by TBSopto may not lead later to occlusion of learning-induced long-term plasticity at PC-SOM synapses but to facilitation, resulting in memory formation. Hence, induction of PC-SOM synaptic plasticity by contextual fear and spatial learning may differ, resulting in different sensitivity to

occlusion. It will be important in future experiments to determine the plasticity mechanisms induced by spatial learning at PC-SOM synapses. Given that we observed TBSopto-induced facilitation of object location learning in "weak" training conditions, it would be important to test if TBSopto also induces a facilitation of object location learning in "stronger" training conditions (ie. that induce learning), to clarify the role of PC-SOM plasticity in spatial learning. Since learning of novel object location involves an interplay of LTD, LTP, and metaplasticity at CA1 PC synapses (23, 25), it would also be pertinent to examine how LTP at PC-SOM synapses modulates CA1 network metaplasticity induced by novel object location. Whether synaptic plasticity of PC-SOM synapses also regulates other novelty mismatch learning paradigms (23) is another interesting question to address.

Our results of facilitation of object location memory by TBSopto suggests that LTP at PC-SOM synapse regulates hippocampal spatial memory. Because TBSopto was given *in vivo*, it may have stimulated other synaptic targets of CA1 pyramidal cells, such as subicular neurons, potentially resulting in plasticity at these other output synapses and influencing hippocampal memory (39-41). To address this possibility, the effect of TBSopto was examined in mice with conditional knock-out of Rptor in SOM-INs in which mTORC1-mediated LTP at PC-SOM synapses is blocked (3). The finding that facilitation of object location memory is absent in these mice, suggests that facilitation of object location memory was due to TBSopto-induced plasticity in SOM-INs, and not to actions via other synaptic targets of CA1 pyramidal cells. The finding is also consistent with previous work indicating that, in parvalbumin expressing interneurons, which are another synaptic target of CA1 pyramidal cells, TBSopto does not induce LTP at PC-parvalbumin cell synapses (3). Interestingly, a subset of the subicular neurons targeted by CA1 pyramidal cells, project back to CA1 pyramidal neurons. Moreover, this feedback from the subiculum is important for formation of object location memory and regulation of pyramidal cell place fields, but not for object recognition (42). Furthermore, these subicular neurons that feedback to CA1 are inhibited by CA1 SOM-INs (42), likely SOM projection cells (1). It will be interesting to determine if the synaptic inputs of these SOM projection cells are potentiated by TBSopto and if so, how this regulates the subicular-CA1 network and hippocampal memory. Finally, another useful point in future experiments may be to relate the degree of pyramidal cell recruitment, perhaps visualized with immediate early gene expression, with the TBSopto-induced changes in

behavioral performance. Such experiments would provide important information about network changes associated with PC-SOM synaptic plasticity and learning.

4.3 Limitations

Our findings are consistent with previous demonstrations that the optogenetic LTP induction protocol (TBSopto) *in vitro* elicits specific long-term potentiation at PC-SOM synapses during whole-cell recordings from SOM-INs in slices, and *in vivo* regulates contextual fear learning-induced LTP at PC-SOM synapses (3). However, a caveat of our work is that we did not provide direct proof that the TBSopto induces LTP in vivo. Hence, it would be important to develop an *in vivo* assay for LTP at PC-SOM synapses to confirm directly the optogenetic induction of *LTP in vivo* (3). In addition, it is unlikely that the effects of TBSopto in the present study were due to light-generated heat effect since previous whole-cell experiments in slices have shown that the same TBSopto given to control slices from mice with pyramidal cell expression of mCherry (and no hChR2) did not affect transmission at PC-SOM synapses, and neither did TBSopto given to hChR2-expressing pyramidal cells in the presence of a mGluR1a antagonist, or in mice with a conditional knockout of Rptor, an essential component of mTORC1, in SOM-INs (3). Moreover, in previous behavioral experiments, TBSopto given to mice expressing mCherry (and no hChR2) in pyramidal cells showed normal contextual fear learning compared to unstimulated control mice (3). Finally, in the present study, TBSopto did not facilitate object location learning in mice with a conditional knockout of Rptor in SOM-INs (Figure 3), suggesting that TBSopto facilitation of object location memory in control mice was unlikely to be due to light-generated heat effects.

A second caveat of our study is the use of mice with global conditional knock-out of Rptor in SOM cells that will impair mTORC1 function in SOM cells in other non-hippocampal brain regions and may result in non-specific behavioral changes. However previous work has shown that object location memory is critically dependent on dorsal CA1 hippocampus, compared to other brain regions (26-28). In addition, these mice display normal exploratory behavior, anxiety level and locomotion in the open field test (Figure 3), intact sensorimotor gating measured during fear conditioning, and intact non-hippocampal memory such as auditory-cued fear memory (3, 19). Hence, the effect of the global conditional deletion of Rptor in SOM cells is most likely due to

interfering with hippocampal SOM-IN mTORC1 function rather than non-hippocampal effects. However, regional- and cell-specific conditional deletion of Rptor would be useful for confirmation.

5 List of abbreviations

EYFP Enhanced Yellow Fluorescent Protein

LTD Long-term depression

LTP Long-term potentiation

mGluR1a Metabotropic glutamate receptor 1a

mTORC1 Mechanistic target of rapamycin complex 1

OLMα2 Oriens lacunosum-moleculare interneurons that express the nicotinic a2 subunit

PC Pyramidal cells

PC-SOM synapse SOM-IN excitatory input synapses from local pyramidal cells

SOM-IN Somatostatin expressing interneuron

TBS Theta burst stimulation

TBSopto Optogenetic theta burst stimulation

6 Supplementary Information

Supplemental table 1: statistical tests details

Figure	*Variable*	*Group:size*	*Test*	*Mean± sem*	*Statistic*	*Pvalue*
1 D	OLM total exploration time (s) training	EYFP L:7 Arch U:8 Arch L:8	One way ANOVA	EYFP L 46.6 ± 11.76 Arch U 49.4 ± 8.9 Arch L 50.3 ± 13.5	F=0.0269	P=0.973
1 D	OLM exploration time (%)	EYFP L:7 Arch U:8 Arch L:8	Two way repeated measures ANOVA Bonferroni pairwise multiple comparison	Training: EYFP L 50.64 ± 5.47 Arch U 46.31 ± 5.12 Arch L 53.38 ±5.47 Test: EYFP L 72.54 ± 5.47 Arch U 72.07 ± 5.12 Arch L 49.9 ± 5.47	Training/TestF=7.876 P=0.011 Groups x training/test F=3.024 P=0.07	EYFP Train vs test p=0.029 Arch U Train vs test p=0.008 Arch L Train vs test P=0.712 Training: EYFP vs Arch U p=1 EYFP vs Arch L p=1 Arch U vs Arch L p=0.706 Test: EYFP vs Arch U p=1 EYFP vs Arch L p=0.013 Arch U vs Arch L p=0.012

1 D	OLM test preference ratio	EYFP L:7 Arch U:8 Arch L:8	Kruskal-Wallis One Way ANOVA on ranks Multiple comparison Dunn's method	EYFP L 3.63 ± 1.2 Arch U 3.55 ± 0.91 Arch L 1.27 ± 0.655	P=0.011	EYFP vs Arch L Q=2.634 P<0.05 EYFP vs Arch U Q=0.133 P>0.05 Arch U vs Arch L Q=2.588 P<0.05
1 F	OF % time in periphery	EYFP L:7 Arch U:8 Arch L:8	One way ANOVA	EYFP L 100.35 ± 8.6 Arch U 86.07 ± 3.9 Arch L 87.13 ± 3.32	F= 1.718 Power analysis sample size to reach significance overall n= 66	P=0.211
1 F	OF % time in center	EYFP L:7 Arch U:8 Arch L:8	One way ANOVA	EYFP L 3.52 ± 0.77 Arch U 1.72 ± 0.55 Arch L 2.71 ± 0.53	F=1.971 Power analysis sample size to reach	P=0.172

					significance overall n= 57	
1 F	OF ratio time in center/periphery	EYFP L:7 Arch U:8 Arch L:8	One way ANOVA	EYFP L 0.035± 0.006 Arch U 0.02 ± 0.006 Arch L 0.032± 0.006	F=1.658 Power analysis sample size to reach significance overall n= 69	P=0.222
1 G	Total distance	EYFP L:7 Arch U:8 Arch L:8	Kruskal-Wallis One way ANOVA on Ranks	EYFP L 57.65 ± 1.06 Arch U 49.45 ± 1.43 Arch L 56.31±0.5	H=2.025 Power analysis sample size to reach significance overall n= 201	P=0.363
1 G	Zone transitions	EYFP L:7 Arch U:8 Arch L:8	One way ANOVA	EYFP L 620.43±166	F=0.894	P=0.429

				Arch U 380.83±100.5 Arch L 578±111.07	Power analysis sample size to reach significance overall n= 93	
2 D	OLM total exploration time (s) training	Ctrl :10 TBS_{opto} :14	t-test	Ctrl 131.94 ± 32.4 TBS_{opto} 112.71 ± 17.22	.t=-0.566	P=0.577
2 D	OLM exploration time (%)	Ctrl :10 TBS_{opto} :14	Two way repeated measures ANOVA Bonferroni pairwise multiple comparison	Training: Ctrl 50.2 ± 3.114 TBS_{opto} 48.36 ± 2.631 Test: Ctrl 48.8 ± 3.114 TBSopto 61.48 ± 2.631	Ctrl/ TBS_{opto} x training/test F = 8.65 P = 0.008	Ctr Train vs test p=1 TBS_{opto} Train vs test p=0.003 Training: Ctrl vs TBS_{opto} p=1 Test: Ctrl vs TBS_{opto} p=0.02

2 D	OLM test preference ratio	Ctrl :10 TBS_{opto} :14	Mann-Witney Rank Sum Test	Ctrl 1.07 ± 0.194 TBS_{opto} 2.221 ± 0.63	T=84	P=0.018
2 F	OF % time in periphery	Ctrl :10 TBS_{opto} :14	Mann-Witney Rank Sum Test	Ctrl 65.76 ± 6.97 TBS_{opto} 76.12 ± 4.64	T=106.5	P=0.292
2 F	OF % time in center	Ctrl :10 TBS_{opto} :14	Mann-Witney Rank Sum Test	Ctrl 4.918 ± 1.22 TBS_{opto} 5.95 ± 1.71	T=123	P=0.930
2 F	OF ratio time in center/periphery	Ctrl :10 TBS_{opto} :14	Mann-Witney Rank Sum Test	Ctrl 0.089 ± 0.025 TBS_{opto} 0.101 ± 0.042	T=130.5	P=0.77
2 G	Total distance	Ctrl :10 TBS_{opto} :14	Mann-Witney Rank Sum Test	Ctrl 40.81 ± 0.4 TBS_{opto} 42.19 ± 0.15	T=125.5	P=0.482
2 G	Zone transitions	Ctrl :10 TBS_{opto} :14	t-test	Ctrl 327.5 ± 37.85 TBS_{opto} 385.71 ± 24.8	.t=-1.344	P=0.193
3 D	OLM total exploration time (s) training	Ctrl :9 TBS_{opto} :10	t-test	Ctrl 144.6 ± 27.7 TBS_{opto} 103.9 ± 15.6	.t=1.311	P=0.207

3 D	OLM exploration time (%)	Ctrl :9 TBS_{opto} :10	Two way repeated measures ANOVA Bonferroni pairwise multiple comparison	Training: Ctrl 50.57 ± 3.077 TBS_{opto} 50.49 ± 2.919 Test: Ctrl 46.79 ± 3.077 TBS_{opto} 56.94 ± 2.919	Ctrl/ TBS_{opto}x training/test F = 5.448 P = 0.032	Ctrl: train/test p=1 TBS_{opto} : train/test p=0.284 Training: ctrl/ TBS_{opto} p=1 Test: ctrl/ TBS_{opto} p=0.143
3 D	OLM test Preference ratio	Raptor U:9 Raptor L :10	t-test	Ctrl 0.957 ± 0.137 TBS_{opto} 1.482 ± 0.218	.t= -1.986	P=0.063
3 F	OF % time in periphery	Raptor U:9 Raptor L :10	Mann-Witney Rank Sum Test	Ctrl 76.22 ± 7.315 TBS_{opto} 77.7 ± 5.95	T=87	P=0.838
3 F	OF % time in center	Raptor U:9 Raptor L :10	t-test	Ctrl 3.31 ± 0.63 TBS_{opto} 2.87 ± 0.48	.t=0.555	P=0.586
3 F	OF ratio time in center/periphery	Raptor U:9 Raptor L :10	Mann-Witney Rank Sum Test	Ctrl 0.51 ± 0.013 TBS_{opto} 0.38 ± 0.005	T= 96	P=0.653

3 G	Total distance	Raptor U:9 Raptor L :10	t-test	Ctrl 38.44 ± 0.4 TBS_{opto} 43.83 ± 0.33	.t= -1.046	P=0.31
3 G	Zone transitions	Raptor U 9 Raptor L 10	t-test	Ctrl 317.78 ± 27.28 TBS_{opto} 370.8 ± 33.66	.t=1.206	P=0.244

Abbreviations:

OLM: Object location memory U: Unlit

OF: Open field L: Light

Object location task analysis script

```
# Put this script in the folder with deeplabcut's csv results files, it will open all csv files in this folder. Then you can choose to directly print the results in your prompt, the script will then print the file name taken from the deeplabcut results csv which is the same as the video it summarizes, and then the results. I called my videos by  the test session (acq for training and tst for test) and the animals number so in the end I had: acq or tst, animal number, time in IOZ xx time in MOZ xx; with I/M OZ being Immobile/Mobile object zone. The other option is to print the results in a csv, to build this csv, I took the test session (acq or tst) mice number from the deeplabcut result csv name. So for this script to work you will need to call your videos the same way or to change the script (I will show you where).

import pandas as pd

import os

import re

import csv


if not os.path.exists('results'):

    os.mkdir('results')


def isInside(IOZ_x, IOZ_y, rad, x, y):

    # Compare radius of circle with distance of its center from given point to tell if the animal's head is within the 3 cm radius circular zone around the objects.

    if ((x - IOZ_x) * (x - IOZ_x) +

        (y - IOZ_y) * (y - IOZ_y) <= rad * rad):

        return 1

    else:

        return 0

results = {}

list_csv = os.listdir()

for filename in list_csv:

    if not filename.endswith('.csv'):

        continue

    df = pd.read_csv(filename, header=[1,2])

    print(filename)


    df.astype("float")
```

```
  # This defines the objects positions
  IOZ_x = df['imobilobj']['x'].mean()
  IOZ_y = df['imobilobj']['y'].mean()
  MOZ_x = df['movedobj']['x'].mean()
  MOZ_y = df['movedobj']['y'].mean()
  rad = 75 # nb of pixels = to 3 cm in my arena.


  df["insIOZ"] = df.apply(lambda row: isInside(IOZ_x, IOZ_y, rad, row['head']['x'], row['head']['y']),
axis=1)
  df["insMOZ"] = df.apply(lambda row: isInside(MOZ_x, MOZ_y, rad, row['head']['x'], row['head']['y']),
axis=1)
  # This divide the number of frames where the animal's head is in the zone by the video speed to have
  the time spent in the zone
  insIOZtime = df['insIOZ'].sum()/30 #30 is the nb of frame/s in my videos, change it according to your
videos speed.
  insMOZtime = df['insMOZ'].sum()/30 # and here
# To print directly in powershell
  # print(f'time in IOZ {insIOZtime}')
  # print(f'time in MOZ {insMOZtime}')
 #  print()


  # print these results in results folder output csv: mouse; acq immobile object; acq mobile objects; test
  immobile object; test mobile object.
  test_name = re.search(r'tst[0-9]', filename) # If you did not put tst in the test video name, change it
here
  if test_name:
     mouse = test_name.group(0).replace('tst', 'm') # and here, and maybe m ( because I called my mice
m1,m2…)


     if mouse not in results:
        results[mouse] = {}
     results[mouse]['test'] = [insIOZtime, insMOZtime]
```

```
    acq_name = re.search(r'acq[0-9]', filename) # If you did not put acq in the training video name, change
it here
    if acq_name:
        mouse = acq_name.group(0).replace('acq', 'm') #and here
         if mouse not in results:
            results[mouse] = {}
         results[mouse]['acquisition'] = [insIOZtime, insMOZtime]


    if not test_name and not acq_name:
        print('Huh oh')


# print(results)
header = ['mouse','acq immobile', 'acq mobile', 'test immobile', 'test mobile']


with open('results/output.csv', 'w', newline='') as f:
# create the csv writer
    writer = csv.writer(f)
# write a row to the csv file
    writer.writerow(header)
    for mouse in results:
          writer.writerow([mouse, results[mouse]['acquisition'][0], results[mouse]['acquisition'][1],
results[mouse]['test'][0],  results[mouse]['test'][1]])
```

7 Ethics approval

All animal procedures and experiments were performed in accordance with the Université de Montréal animal care committee regulations.

8 Consent for publication

All authors have given their consent for publication.

9 Availability of data and materials

The datasets used and/or analyzed during the current study are available from the corresponding author on reasonable request.

10 Competing interests

The authors declare that they have no competing interests.

11 Funding

This work was supported by grants to J.C.L. from the Canadian Institutes of Health Research (CIHR MOP-125985 and PJT-153311) and a Research Centre grant (Centre Interdisciplinaire de Recherche sur le Cerveau et l'Apprentissage; CIRCA) from the Fonds de la Recherche du Québec – Santé (FRQS). J.C.L. is the recipient of the Canada Research Chair in Cellular and Molecular Neurophysiology (CRC 950-231066) and a member of the Research Group on Neural Signaling and Circuitry (GRSNC) at Université de Montréal.

12 Author Contributions

Conceptualization, E.H. and J.C.L; Methodology, Software, Analysis, Investigation, E.H. Writing – Original Draft, E.H. and J.C.L.; Writing – Review & Editing, E.H. and J.C.L; Visualization, E.H.; Supervision, Project Administration, and Funding Acquisition, J.C.L.

13 Acknowledgments

We would like to thank Dr. François Labrèche for material support and the review of analysis code.

References

1. Honoré E, Khlaifia A, Bosson A, Lacaille J-C. Hippocampal somatostatin interneurons, long-term synaptic plasticity and memory. Frontiers in Neural Circuits. 2021;15.

2. Lovett-Barron M, Kaifosh P, Kheirbek MA, Danielson N, Zaremba JD, Reardon TR, et al. Dendritic inhibition in the hippocampus supports fear learning. Science. 2014;343(6173):857-63.

3. Asgarihafshejani A, Honoré È, Michon F-X, Laplante I, Lacaille J-C. Long-term potentiation at pyramidal cell to somatostatin interneuron synapses controls hippocampal network plasticity and memory. iScience. 2022;25(5):104259.

4. Grienberger C, Milstein AD, Bittner KC, Romani S, Magee JC. Inhibitory suppression of heterogeneously tuned excitation enhances spatial coding in CA1 place cells. Nat Neurosci. 2017;20(3):417-26.

5. Royer S, Zemelman BV, Losonczy A, Kim J, Chance F, Magee JC, et al. Control of timing, rate and bursts of hippocampal place cells by dendritic and somatic inhibition. Nat Neurosci. 2012;15(5):769-75.

6. Siwani S, Franca ASC, Mikulovic S, Reis A, Hilscher MM, Edwards SJ, et al. OLMalpha2 Cells Bidirectionally Modulate Learning. Neuron. 2018.

7. Tonegawa, Morrissey, Kitamura. The role of engram cells in the systems consolidation of memory. Nature Neuroscience. 2018;19:485-98.

8. Josselyn, Frankland. Memory allocation: Mechanisms and function. Annual Review of Neuroscience. 2018;41:389-413.

9. Kandel, Dudai, Mayford. The Molecular and Systems Biology of Memory. Cell. 2014;157(1):163-86.

10. Lynch MA. Long-Term Potentiation and Memory. Physiological Reviews. 2004;84(1):87-136.

11. Abraham WC, Jones OD, Glanzman DL. Is plasticity of synapses the mechanism of long-term memory storage? NPJ Sci Learn. 2019;4:9.

12. Kullmann Dimitri M, Moreau Alexandre W, Bakiri Y, Nicholson E. Plasticity of Inhibition. Neuron. 2012;75(6):951-62.

13. Lamsa K, Lau P. Long-term plasticity of hippocampal interneurons during in vivo memory processes. Current Opinion in Neurobiology. 2019;54:20-7.

14. Lapointe V, Morin F, Ratte S, Croce A, Conquet F, Lacaille JC. Synapse-specific mGluR1-dependent long-term potentiation in interneurones regulates mouse hippocampal inhibition. J Physiol. 2004;555(Pt 1):125-35.

15. Croce A, Pelletier JG, Tartas M, Lacaille JC. Afferent-specific properties of interneuron synapses underlie selective long-term regulation of feedback inhibitory circuits in CA1 hippocampus. J Physiol. 2010;588(Pt 12):2091-107.

16. Booker SA, Loreth D, Gee AL, Watanabe M, Kind PC, Wyllie DJA, et al. Postsynaptic GABABRs Inhibit L-Type Calcium Channels and Abolish Long-Term Potentiation in Hippocampal Somatostatin Interneurons. Cell Rep. 2018;22(1):36-43.

17. Perez Y, Morin F, Lacaille JC. A hebbian form of long-term potentiation dependent on mGluR1a in hippocampal inhibitory interneurons. Proc Natl Acad Sci U S A. 2001;98(16):9401-6.

18. Vasuta C, Artinian J, Laplante I, Hebert-Seropian S, Elayoubi K, Lacaille JC. Metaplastic Regulation of CA1 Schaffer Collateral Pathway Plasticity by Hebbian MGluR1a-Mediated Plasticity at Excitatory Synapses onto Somatostatin-Expressing Interneurons. eNeuro. 2015;2(4).

19. Artinian J, Jordan A, Khlaifia A, Honore E, La Fontaine A, Racine AS, et al. Regulation of Hippocampal Memory by mTORC1 in Somatostatin Interneurons. J Neurosci. 2019;39(43):8439-56.

20. Sharma V, Sood R, Khlaifia A, Eslamizade MJ, Hung T-Y, Lou D, et al. eIF2α controls memory consolidation via excitatory and somatostatin neurons. Nature. 2020.

21. Goh JJ, Manahan-Vaughan D. Spatial object recognition enables endogenous LTD that curtails LTP in the mouse hippocampus. Cereb Cortex. 2013;23(5):1118-25.

22. Izquierdo LA, Viola H, Barros DM, Alonso M, Vianna MR, Furman M, et al. Novelty enhances retrieval: molecular mechanisms involved in rat hippocampus. Eur J Neurosci. 2001;13(7):1464-7.

23. Aidil-Carvalho MF, Carmo AJS, Ribeiro JA, Cunha-Reis D. Mismatch novelty exploration training enhances hippocampal synaptic plasticity: A tool for cognitive stimulation? Neurobiol Learn Mem. 2017;145:240-50.

24. Qi Y, Hu NW, Rowan MJ. Switching off LTP: mGlu and NMDA receptor-dependent novelty exploration-induced depotentiation in the rat hippocampus. Cereb Cortex. 2013;23(4):932-9.

25. Stacho M, Manahan-Vaughan D. The Intriguing Contribution of Hippocampal Long-Term Depression to Spatial Learning and Long-Term Memory. Front Behav Neurosci. 2022;16:806356.

26. Barrett RM, Malvaez M, Kramar E, Matheos DP, Arrizon A, Cabrera SM, et al. Hippocampal focal knockout of CBP affects specific histone modifications, long-term potentiation, and long-term memory. Neuropsychopharmacology. 2011;36(8):1545-56.

27. Assini FL, Duzzioni M, Takahashi RN. Object location memory in mice: pharmacological validation and further evidence of hippocampal CA1 participation. Behav Brain Res. 2009;204(1):206-11.

28. Aggleton JP, Nelson AJD. Distributed interactive brain circuits for object-in-place memory: A place for time? Brain and Neuroscience Advances. 2020;4:2398212820933471.

29. Vogel-Ciernia A, Matheos DP, Barrett RM, Kramár EA, Azzawi S, Chen Y, et al. The neuron-specific chromatin regulatory subunit BAF53b is necessary for synaptic plasticity and memory. Nature neuroscience. 2013;16(5):552-61.

30. Mathis A, Mamidanna P, Cury KM, Abe T, Murthy VN, Mathis MW, et al. DeepLabCut: markerless pose estimation of user-defined body parts with deep learning. Nature Neuroscience. 2018;21(9):1281-9.

31. Vogel-Ciernia A, Wood MA. Examining Object Location and Object Recognition Memory in Mice. Current Protocols in Neuroscience. 2014;69(1):8.31.1-8..17.

32. Muller-Komorowska D, Opitz T, Elzoheiry S, Schweizer M, Ambrad Giovannetti E, Beck H. Nonspecific Expression in Limited Excitatory Cell Populations in Interneuron-Targeting Cre-driver Lines Can Have Large Functional Effects. Front Neural Circuits. 2020;14:16.

33. Mahn M, Prigge M, Ron S, Levy R, Yizhar O. Biophysical constraints of optogenetic inhibition at presynaptic terminals. Nat Neurosci. 2016;19(4):554-6.

34. Honoré È, Belo do Nascimento I, Laplante I, Lacaille J-C. Stimulation of protein synthesis by optogenetic and chemical induction of excitatory synaptic plasticity in hippocampal somatostatin interneurons. Molecular Brain. 2022;15(1):81.

35. Whitlock JR, Heynen AJ, Shuler MG, Bear MF. Learning induces long-term potentiation in the hippocampus. Science. 2006;313(5790):1093-7.

36. Di Prisco GV, Huang W, Buffington SA, Hsu C-C, Bonnen PE, Placzek AN, et al. Translational control of mGluR-dependent long-term depression and object-place learning by eIF2α. Nature Neuroscience. 2014;17(8):1073-82.

37. Maccaferri G, McBain CJ. Passive propagation of LTD to stratum oriens-alveus inhibitory neurons modulates the temporoammonic input to the hippocampal CA1 region. Neuron. 1995;15(1):137-45.

38. Moser EI, Krobert KA, Moser MB, Morris RG. Impaired spatial learning after saturation of long-term potentiation. Science. 1998;281(5385):2038-42.

39. O'Mara SM, Commins S, Anderson M. Synaptic plasticity in the hippocampal area CA1-subiculum projection: implications for theories of memory. Hippocampus. 2000;10(4):447-56.

40. Taube JS. Electrophysiological properties of neurons in the rat subiculum in vitro. Exp Brain Res. 1993;96(2):304-18.

41. Cenquizca LA, Swanson LW. Spatial organization of direct hippocampal field CA1 axonal projections to the rest of the cerebral cortex. Brain Res Rev. 2007;56(1):1-26.

42. Sun Y, Jin S, Lin X, Chen L, Qiao X, Jiang L, et al. CA1-projecting subiculum neurons facilitate object–place learning. Nature Neuroscience. 2019;22(11):1857-70.

Chapitre V

mTORC1 function in hippocampal parvalbumin interneurons: regulation of firing and long-term potentiation of intrinsic excitability but not long-term contextual fear memory and context discrimination

Abdessattar Klaifia[1] #, Eve Honoré[1] #, Julien Artinian[1], Isabel Laplante[1], Jean-Claude Lacaille[1].
2022 doi.org/10.1186/s13041-022-00941-8 Molecular Brain # Contributions égales.

[1]Department of Neurosciences, Center for Interdisciplinary Research on Brain and Learning (CIRCA) and Research Group on Neural Signaling and Circuitry (GRSNC), Université de Montréal, Montreal, Quebec, H3C 3J7, Canada.

Ce chapitre présente l'article de recherche « mTORC1 function in hippocampal parvalbumin interneurons: regulation of firing and long-term potentiation of intrinsic excitability but not long-term contextual fear memory and context discrimination. » Abdessattar Klaifia #, Eve Honoré #, Julien Artinian, Isabel Laplante, Jean-Claude Lacaille # Contributions égales. Publié en 2022 dans le journal Molecular Brain.

Objectifs spécifiques de l'article :

Pour ces travaux, des souris transgéniques ont été utilisées avec un knock-out hétéro- et homozygote du gène *Rptor*, codant la composante nécessaire du complexe mTORC1 « Regulatory-Associated Protein of mTOR » (Raptor), conditionnellement dans les PV-INs. Ces travaux ont pour premier objectif d'utiliser des enregistrements de patch clamp en configuration cellule entière sur tranches d'hippocampe de ces souris afin étudier l'effet de l'inactivation de mTORC1 sur la PLT_{EI} des PV-INs. Le deuxième objectif est d'utiliser les souris hétéro- et homozygotes knock-out pour *Rptor* dans le but d'évaluer l'effet de l'inactivation de mTORC1 dans les PV-INs sur la mémoire contextuelle de peur et la discrimination de contexte dans la mémoire de peur.

Abstract

Hippocampal CA1 parvalbumin-expressing interneurons (PV INs) play a central role in controlling principal cell activity and orchestrating network oscillations. PV INs receive excitatory inputs from CA3 Schaffer collaterals and local CA1 pyramidal cells, and they provide perisomatic inhibition. Schaffer collateral excitatory synapses onto PV INs express Hebbian and anti-Hebbian types of long-term potentiation (LTP), as well as elicit LTP of intrinsic excitability (LTPIE). LTPIE requires the activation of type 5 metabotropic glutamate receptors (mGluR5) and is mediated by downregulation of potassium channels Kv1.1. It is sensitive to rapamycin and thus may involve activation of the mammalian target of rapamycin complex 1 (mTORC1). LTPIE facilitates PV INs recruitment in CA1 and maintains an excitatory-inhibitory balance. Impaired CA1 PV INs activity or LTP affects network oscillations and memory. However, whether LTPIE in PV INs plays a role in hippocampus-dependent memory remains unknown. Here, we used conditional deletion of the obligatory component of mTORC1, the Regulatory-Associated Protein of mTOR (Raptor), to directly manipulate mTORC1 in PV INs. We found that homozygous, but not heterozygous, conditional knock-out of Rptor resulted in a decrease in CA1 PV INs of mTORC1 signaling via its downstream effector S6 phosphorylation assessed by immunofluorescence. In whole-cell recordings from hippocampal slices, repetitive firing of CA1 PV INs was impaired in mice with either homozygous or heterozygous conditional knock-out of Rptor. High frequency stimulation of Schaffer collateral inputs that induce LTPIE in PV INs of control mice failed to do so in mice with either heterozygous or homozygous conditional knock-out of Rptor in PV INs. At the behavioral level, mice with homozygous or heterozygous conditional knock-out of Rptor showed similar long-term contextual fear memory or contextual fear memory discrimination relative to control mice. Thus, mTORC1 activity in CA1 PV INs regulates CA1 PV INs repetitive firing and LTPIE but is dispensable fornot consolidation of long-term contextual fear memory and context discrimination. Our results indicate that mTORC1 plays cell-specific roles in synaptic plasticity of hippocampal inhibitory interneurons that are differentially involved in hippocampus-dependent learning and memory.

Keywords: GABA interneurons, Raptor conditional knock-out mice, whole-cell recordings, CA1 hippocampus, contextual fear conditioning.

Introduction

Cortical neurons consist of glutamatergic excitatory neurons and GABAergic inhibitory interneurons that represent, respectively, approximately 80% and 20% of the total number (Aika et al., 1994; Freund & Buzsáki, 1996; Tremblay et al., 2016; Pelkey et al., 2017). Although highly outnumbered, inhibitory interneurons are crucial for normal cortical function by providing a tight control of excitatory neuron activity (Somogyi & Klausberger, 2005; Roux & Buzsaki, 2015; Tremblay et al., 2016; Pelkey et al., 2017). Given their importance in gating information flow and sculpting network activity, their dysfunction can result in abnormal brain function and the development of neurological and neuropsychiatric disorders (Chattopadhyaya & Cristo, 2012; Marin, 2012).

Inhibitory interneurons display a high diversity at anatomical, neurochemical, transcriptomic and electrophysiological levels (Petilla Interneuron Nomenclature et al., 2008; Tremblay et al., 2016; Pelkey et al., 2017; Tasic et al., 2018; Yu et al., 2021). In the hippocampus CA1 region, feedforward and feedback inhibition are mediated in part by perisomatic-targeting parvalbumin interneurons (PV INs) and dendritic-targeting somatostatin interneurons (SOM INs) (Pouille & Scanziani, 2001; 2004; Honore et al., 2021). These populations of interneurons are highly dynamic and express multiple types of plasticity at their excitatory input and inhibitory output synapses (Kullmann & Lamsa, 2007; Pelletier & Lacaille, 2008; Castillo et al., 2011; Udakis et al., 2020; Honore et al., 2021). In addition, PV INs and SOM INs express long-term potentiation of intrinsic excitability (LTPIE) and long-term depression of intrinsic excitability (LTDIE) respectively (Campanac et al., 2013; Incontro et al., 2021).

Interestingly, plasticity of intrinsic excitability, which is expressed by a change in action potential firing, is present in both excitatory and inhibitory neurons (Debanne et al., 2018; Incontro et al., 2021) and plays an important role in memory allocation, consolidation, and updating (Zhang & Linden, 2003; Debanne et al., 2018; Chen et al., 2020). Mechanistically, plasticity of intrinsic excitability is manifested as changes in action potential threshold, spike accommodation and burst-evoked afterhyperpolarization (AHP), due to alterations in ion channel expression, distribution and function, and which involve several intracellular signaling pathways, like PKA, PKC, CaMKII and mTORC1 (Zhang & Linden, 2003; Chandra & Barkai, 2018; Debanne et al., 2018). In PV-INs,

LTPIE is induced by mGluR5 activation that causes a downregulation of Kv1.1 potassium channels, resulting in a sustained increase in PV IN intrinsic excitability (Campanac et al., 2013).

The mechanistic target of rapamycin (mTOR) is a serine/threonine kinase that regulates many aspects of the cell physiology such as cell growth, proliferation and metabolism (Laplante & Sabatini, 2012). mTOR interacts with two structurally and functionally distinct protein complexes, mTOR complex 1 (mTORC1) and 2 (mTORC2). mTORC1 is defined by its specific components Raptor (regulatory-associated protein of mTOR) and PRAS40 (proline-rich Akt substrate 40 kDa), whereas mTORC2 is characterized by Rictor (rapamycin insensitive companion of TOR), the mammalian stress-activated MAP kinase-interacting protein 1 (mSin1), and Protor1 and 2 (protein observed with Rictor 1 and 2) (Laplante & Sabatini, 2012). The two protein complexes display different sensitivity to rapamycin as well as different upstream regulators and downstream targets (Laplante & Sabatini, 2012). mTORC1 activation promotes protein synthesis and cell growth through the regulation of the translational initiation machinery by phosphorylating eukaryotic initiation factor 4e (eIF4E) binding proteins (4EBPs) and p70 S6 kinases (S6K1 and S6K2), whereas mTORC2 activation promotes cell proliferation and survival via Akt (Laplante & Sabatini, 2012; Costa-Mattioli & Monteggia, 2013).

mTORC1, as a key regulator of protein synthesis, plays a cardinal role in long-term synaptic plasticity and memory in excitatory neurons (Costa-Mattioli et al., 2009b). However, it is also implicated in interneuron synaptic and intrinsic excitability plasticity (Costa-Mattioli et al., 2009b; Ran et al., 2009; Campanac et al., 2013; Younts et al., 2016; Artinian et al., 2019). In CA1 SOM INs, mTORC1 mediates learning-induced LTP at these interneuron input synapses, which in turn regulates CA1 network metaplasticity and hippocampal-dependent contextual fear and spatial memory consolidation (Costa-Mattioli et al., 2009b; Ran et al., 2009; Artinian et al., 2019; Sharma et al., 2020). In PV INs, mTORC1 may regulate LTPIE since treatment with rapamycin, an inhibitor of mTORC1, impairs LTPIE (Campanac et al., 2013). Although rapamycin is considered a more effective mTORC1 inhibitor (Kang et al., 2013), prolonged treatment (Sarbassov et al., 2006) or higher concentration (Foster & Toschi, 2009) of rapamycin also inhibits mTORC2. Thus, sensitivity to rapamycin treatment does not necessarily indicate mTORC1 implication.

Interestingly, activity of PV INs and LTP at their excitatory input synapses are critical for CA1 network oscillations and memory consolidation. Following contextual fear conditioning

(CFC), PV INs show higher firing coherence with CA1 network oscillations (Ognjanovski et al., 2017). Moreover, inactivation of PV INs prevents CFC-induced changes in network oscillations and impairs fear memory consolidation (Ognjanovski et al., 2017). In addition, genetic deletion of γCaMKII in PV INs prevents LTP at Schaffer collateral excitatory synapses onto PV INs and impairs fear memory consolidation (He et al., 2021). Furthermore, augmented mTORC1 signaling in PV INs impairs contextual fear discrimination (Haji et al., 2020).

Given the possible role of mTORC1 signaling in plasticity of intrinsic excitability of PV INS and the implication of PV INs in hippocampus-dependent memory, we investigated whether a cell-specific conditional deletion of Raptor, the obligatory component of mTORC1, in PV INs impairs LTPIE in these cells and affects hippocampus-dependent contextual fear memory and context discrimination. Using whole-cell recordings in hippocampal slices, we found that conditional heterozygous and homozygous deletion of Rptor in parvalbumin-expressing cells impaired firing and prevented LTPIE in CA1 PV INs. At the behavioral level, mice with conditional heterozygous and homozygous deletion of Rptor in parvalbumin-expressing cells showed intact long-term contextual fear memory and context discrimination. Our findings indicate a requirement of mTORC1 activity in PV INs for the normal expression of LTPIE in PV INs that is dispensable but not for hippocampus-dependent contextual fear memory and context discrimination.

Materials and Methods

Animals

All animal protocols were in accordance with the Université de Montréal Animal Care Committee (Comité de Déontologie de l'Expérimentation sur les Animaux; CDEA Protocols # 17-001, 17-002, 18-002, 18-003, 19-003, 19-004, 20-001, 20-002, 21-001, 21-002) and experiments were performed in accordance with the Canadian Council of Animal Care guidelines.

Mice with a cell-specific conditional knock-out of Rptor in parvalbumin-expressing cells were generated by crossing first, female homozygous PvalbIRES-Cre (The Jackson Laboratory, JAX #008069) with male homozygous Rptorfl/fl (JAX #013188). Heterozygous female offsprings PvalbIRES-Cre/wt;Rptorwt/fl were then crossed with homozygous male Rptorfl/fl to generate

PvalbIRES-Cre/wt;Rptorfl/wt (PV-Raptor-Het mice) and PvalbIRES-Cre/wt;Rptorfl/fl (PV-Raptor-Homo mice) littermates. Homozygous PvalbIRES-Cre mice served as control (PV-Raptor-WT mice). Mice were housed in group of 2-5 per cage with ad libitum access to food and water and maintained under 12 h light/dark cycle, with controlled temperature (~21°C) and humidity (~55%). All experiments were conducted during the light period. Immunohistochemistry and electrophysiology experiments were carried out on 5 to 11 weeks old male and female mice. For behavioral experiments, 6 to 8 weeks old male mice were used.

Virus injection

To label PV interneurons in hippocampus, AAV2/9-EF1a-DIO-EYFP (Addgene #27056; 3.95x1012 particles/ml) was injected bilaterally in dorsal CA1 hippocampus. Four to five weeks old mice were given an intraperitoneal (IP) injection of ketamine (50 mg/kg i.p.) and xylazine (5 mg/kg i.p.) and placed in a stereotaxic frame (Stoelting). Viral solution (0.8µL) of AAV2/9-EF1a-DIO-EYFP was injected using a 10µl Hamilton syringe (coordinates relative to bregma: AP -2.46 mm; L ±1.75 mm; DV -01.5 mm). The needle was left in place for 5 min after injection. Whole-cell patch-clamp recording experiments were performed between 7 to 15 days after AAV injection to allow animals recovery and EYFP expression.

Immunohistochemistry

Mice were anaesthetized with sodium pentobarbital (MTC Pharmaceuticals, Cambridge, Ontario, Canada) and transcardially perfused with ice-cold 0.1M phosphate buffer (PB) and then with 4% paraformaldehyde in 0.1 M PB. Brains were postfixed overnight and then cryopreserved in 30% sucrose. Coronal brain sections were obtained with a freezing microtome (Leica SM200R, Germany) at 50 µm thickness. Membrane permeabilization was performed by incubating sections in 0.3-0.5% Triton X-100 in 0.01M saline PB (PBS) for 15 min. Unspecific binding was blocked by incubating sections for 1h in 10% normal goat serum in 0.1% Triton X-100/PBS. Sections were incubated in primary antibody for 48 hours at 4°C (Mouse monoclonal Raptor; 1/500; Millipore catalog #05–1470, Burlington, MA, RRID:AB_11212192). Sections were then washed in PBS and incubated with secondary antibody (Rhodamine-conjugated goat anti-mouse IgG1; 1/200; Jackson

Immunoresearch Laboratories, West Grove, PA) for 90 min at room temperature. Sections were washed in PBS before mounting, coverslipped with ProLong™ Diamond (Life technologies) and examined using a Nikon microscope (Nikon Eclipse E600; Nikon, Japan) equipped with epifluorescence. Images were acquired with the Simple PCI software (CImaging Systems, Compix Inc., PA). The number of EYFP-positive interneurons in CA1 with colocalization of Raptor immunofluorescence were counted and expressed as percentage of the total EYFP-positive cells per sections. A total of 3 animals per group coming from 3 independent experiments were analyzed (2-4 sections/animal for a total of 97 cells in PV-Raptor-WT, 61 cells in PV-Raptor-Het, and 89 cells in PV-Raptor-Homo mice).

S6 phosphorylation immunofluorescence

Brain sections were prepared as described above for EYFP-positive parvalbumin interneuron visualization and immunostaining for phospho-S6S240/244 was performed. Individualized free-floating sections were permeabilized and treated for unspecific binding as described above. Slices were then incubated with rabbit monoclonal phospho-S6 antibody (1/1000; anti-phospho-S6S240/244; Cell Signaling catalog #5364, Beverly, MA, RRID:AB 10694233) for 48 h at 4°C, and subsequently with Alexa Fluor 594-conjugated goat anti-rabbit IgGs (1/500; Jackson Immunoresearch Laboratories) for 90 min at room temperature. Images were acquired with a Zeiss LSM 880 (Carl Zeiss, Oberkochen, Germany) confocal microscope at excitation 488 and 543 nm. Images in wild-type and conditional knock-out mice were acquired using the same parameters. Phospho-S6 cell fluorescence was quantified using ImageJ software (National Institute of Health; https://github.com/imagej/imagej1) by comparing density in cells corrected for background. Cell fluorescence was measured typically in 9-28 field of views from 3-4 sections per animal and was averaged per animal. A total of 5 animals per group coming from 5 independent experiments were analyzed (total of 441 cells in PV-Raptor-WT; 362 cells PV-Raptor-Het; 444 cells in PV-Raptor-Homo mice).

Slice preparation and electrophysiology

Hippocampal slices (300 µm thickness) were prepared from PV-Raptor-Het, PV-Raptor-Homo and PV-Raptor-WT mice. Mice were anesthetized with isoflurane and the brain was quickly

removed and placed in ice-cold oxygenated (95% O2, 5% CO2) sucrose-based cutting solution containing the following (in mM): 87 mM NaCl, 2.5 mM KCl, 1.25 mM NaH2PO4, 7 mM MgSO4, 25 mM NaHCO3, 25 mM D-glucose, 75 mM sucrose, 1 mM ascorbic acid, 3 mM pyruvic acid and 0.5 mM CaCl2. Hippocampal slices were obtained using a vibratome (Leica, VT1005) and transferred to oxygenated artificial cerebrospinal fluid (aCSF) containing the following (in mM): 124 mM NaCl, 5 mM KCl, 1.25mM NaH2PO4, 2mM MgSO4, 2mM CaCl2, 26 mM NaHCO3 and 10 mM dextrose (pH = 7.3–7.4; 295-300 mOsmol/L) for 30 min at 30°C. Slices were left in aCSF at room temperature for an additional 30 min. Individual hippocampal slices were then placed in a submerged recording chamber on the stage of an upright microscope (Nikon Eclipse, E600FN), equipped with a water immersion long-working distance objective (× 40, Nomarski optics) and an infrared video camera. Slices were perfused at 2.5 ml/min with aCSF at 30°C. Whole-cell current-clamp recordings were obtained from identified EYFP-expressing PV interneurons located in or at the border of CA1 stratum pyramidale. Patch glass electrodes (3-5 MΩ) were filled with internal solution containing the following (in mM): 120 K-gluconate, 10 KCl, 0.5 EGTA, 10 HEPES, 2.5 MgATP, 0.3 NaGTP, 10 Na2-phosphocreatine, 0.1 spermine, pH 7.3–7.4, and 280 ± 10 mOsmol. Recordings were performed using Multiclamp 700A/B amplifier (Molecular Devices) and digitized using Digidata 1440A and pClamp 10 software (Molecular Devices). Signals were filtered at 2 kHz, digitized at 10 kHz and stored on a PC. Recordings were included if the series resistance varied by < 20% and if the holding current was stable.

Membrane properties were recorded in current-clamp mode at a holding potential of -60 mV. Resting membrane potential (RMP) was directly measured after rupturing the cell membrane at a holding current I = 0 pA. Input resistance (Rin) was calculated using a linear regression of voltage deflections (±15 mV) in response to current steps (800 ms, 20 pA increment, holding membrane potential -60 mV). Action potential (AP) amplitude was measured as the difference in membrane potential between the threshold and the peak. The time difference between the current pulse onset and the AP peak was defined as AP latency. Action potential threshold was taken as the first voltage point at which the slope of the membrane potential exceeded 20 mV/ms. AP half-width was measured as action potential duration at half-amplitude. Fast-afterhyperpolarization (fAHP) amplitude was measured as the difference between AP threshold and the negative voltage peak after the AP. PV interneuron firing rate was evaluated using a series of depolarizing current pulses (800 ms duration) from 100 to 440 pA with increments of 20 pA.

Long-term potentiation of intrinsic excitability was induced in the presence of the GABAA channel blocker picrotoxin (100 µM) by high frequency stimulation (HFS) consisting of 10 bursts of 10 stimulations delivered at 100 Hz every 3 seconds through a theta-glass stimulating electrode filled with aCSF and placed in stratum radiatum.

Contextual fear conditioning

Mice were handled for 3 days prior to fear conditioning experiments to familiarize them with the experimenter, room and procedures. Mice were trained in conditioning chambers that were housed in sound- and light-isolated cubicles (Coulbourn Instruments, Withehall, PA). The chambers were made of a stainless-steel grid floor, overhead LED lighting, camera and supplied with background noise (60 dB) by an air extractor fan. The experimental protocol was based on Artinian and coworkers (Artinian et al., 2019). The training context was rectangular with 2 transparent walls and 2 stainless-steel walls and was cleaned with 70% ethanol before and after each trial. For context discrimination, the neutral context was triangular with transparent walls. For conditioning, mice were placed in the conditioning chamber, allowed to freely explore for 2.5 min, and then received 5 presentations of unconditioned stimuli (1 s foot shock, 0.8 mA). To test for long-term contextual fear memory, mice were returned to the training context 24 hours after conditioning during a test period of 2.5 min. To test for contextual discrimination, 5 hours after the test in the training context on the memory test day, a sub-group of mice were allowed to explore the new neutral context for 2.5 min. Freezing behavior was assessed using FreezeFrame (Coulbourn Instruments). Discrimination ratio was calculated as the amount of freezing in (training context)/(training context + neutral context) (Artinian et al., 2019). A ratio of 1 indicates that mice were able to discriminate the contexts perfectly, and a ratio of 0.5 means that they were unable to discriminate.

Statistical analysis

Data were expressed as mean ± S.E.M. and analyzed using GraphPad Prism 8 (GraphPad Software Inc.). Data were tested for normality using Shapiro-Wilk test and equal variance with Kolmogorov-Smirnov. For within-group comparisons, paired t-test and Wilcoxon signed-rank test

were used for normally and non-normally distributed distributed data, respectively. For multiple comparisons, one-way ANOVA and two-way ANOVA were used, followed by Tukey's post hoc test.

Results

Conditional knock-out of Rptor in PV interneurons causes a deficit in mTORC1 signaling

First, we verified that deleting Rptor specifically in PV cells affects Raptor expression in hippocampal CA1 PV interneurons. We quantified the number of EYFP-expressing hippocampal CA1 PV INs that are immunopositive for Raptor in PV-Raptor-WT, PV-Raptor-Het and PV-Raptor-Homo mice. We found that the number of PV INs expressing EYFP and immunopositive for Raptor are significantly reduced in PV-Raptor-Homo mice relative to PV-Raptor-WT mice (PV-Raptor-WT n=8 sections, PV-Raptor-Het n=6 sections, PV-Raptor-Homo n=7 sections, for 3 mice in each group; One Way ANOVA, $F(2, 18)=4$ $p<0.0001$, Tukey's multiple comparisons test, PV-Raptor-WT vs PV-Raptor-Het, $p=0.5$; PV-Raptor-WT vs PV-Raptor-Homo, $p<0.0001$; PV-Raptor-Het vs PV-Raptor-Homo, $p<0.0001$; Fig. 1A-B). PV-Raptor-Het mice failed to show such a decrease in number of PV INs expressing EYFP and immunopositive for Raptor. Thus, Raptor expression is impaired in hippocampal PV INs of PV-Raptor-Homo mice.

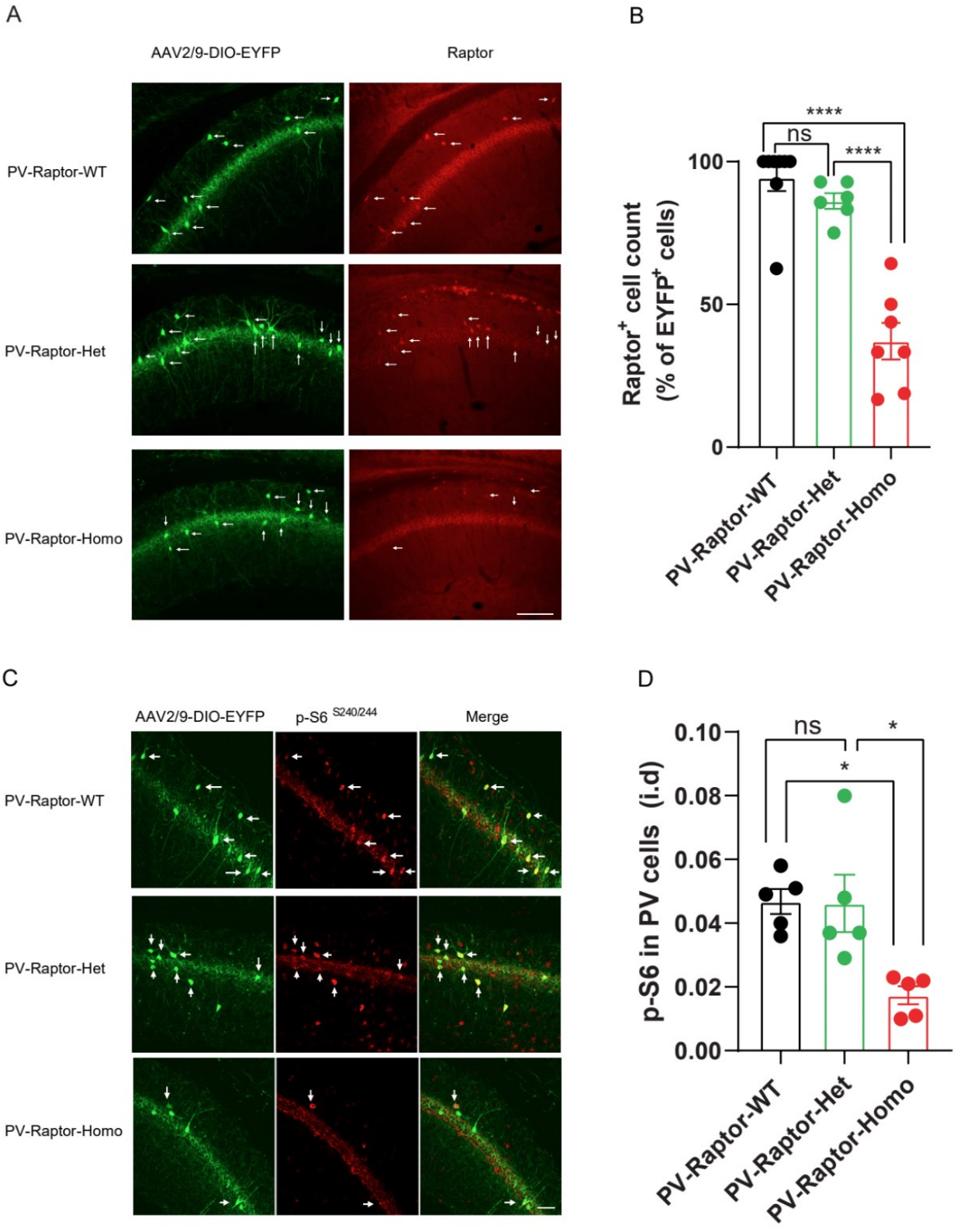
A
AAV2/9-DIO-EYFP
Raptor
PV-Raptor-WT
PV-Raptor-Het
PV-Raptor-Homo
B
Raptor+ cell count
(% of EYFP+ cells)
100
50
0
ns
****
****
PV-Raptor-WT
PV-Raptor-Het
PV-Raptor-Homo
C
AAV2/9-DIO-EYFP
p-S6 S240/244
Merge
PV-Raptor-WT
PV-Raptor-Het
PV-Raptor-Homo
D
p-S6 in PV cells (i.d)
0.10
0.08
0.06
0.04
0.02
0.00
ns
*
*
PV-Raptor-WT
PV-Raptor-Het
PV-Raptor-Homo

Figure 1. Homozygous conditional knock-out of Rptor in PV interneurons causes a deficit in mTORC1 activity. A Left, representative images of EYFP-positive PV interneurons (white arrows) in PV-Raptor-WT, PV-Raptor-Het and PV-Raptor-Homo mice injected with AAV2/9-DIO-EYFP in dorsal CA1 hippocampus. Right, representative images of Raptor-positive (red) EYFP-expressing PV interneurons (white arrows, co-labeling) in PV-Raptor-WT, PV-Raptor-Het and PV-Raptor-Homo mice. Scale bar 100 μm. **B**. Summary graph showing reduced percentage of EYFP-positive cells that are also Raptor-positive in PV-Raptor-Homo mice relative to PV-Raptor-Het and PV-Raptor-WT mice (n=7 sections from 3 PV-Raptor-WT mice, 6 sections from 3 PV-Raptor-Het mice, and 7 sections from 3 PV-Raptor-Homo mice, from 3 independent experiments). **C**. Representative images showing EYFP-positive cells (green), S6S240/244 phosphorylation (red) and co-labeling (merged) in CA1 hippocampus of PV-Raptor-WT, PV-Raptor-Het and PV-Raptor-Homo mice. **D**. Summary graph showing reduced p-S6 immunofluorescence in CA1 PV interneurons of PV-Raptor-Homo mice relative to PV-Raptor-Het and PV-Raptor-WT mice (n=5 mice/group from 5 independent experiments, scale bar 50 μm). **** $p<0.0001$, * $p<0.05$, ns not significant.

Next, we examined the effects of conditional knock-out of Rptor on mTORC1 activity by assessing phosphorylation of ribosomal protein S6S240/244 (p-S6), a downstream effector of mTORC1, in CA1 PV INs using immunofluorescence. The level of p-S6 was reduced in EYFP-expressing CA1 PV INs of PV-Raptor-Homo mice relative to PV-Raptor-WT or PV-Raptor-Het mice (n=5 mice in each group; one-way ANOVA, $F(2, 12)=8$, $p=0.006$; Tukey's multiple comparisons test, PV-Raptor-WT vs PV-Raptor-Het, $p=0.99$; PV-Raptor-WT vs PV-Raptor-Homo, $p=0.01$; PV-Raptor-Het vs PV-Raptor-Homo, $p=0.01$; Fig. 1C-D). The level of p-S6 was unaffected in CA1 PV INs of PV-Raptor-Het mice relative to PV-Raptor-WT mice. These results confirm that mTORC1 signaling, as assessed by p-S6, is impaired in hippocampal PV INs of PV-Raptor-Homo mice.

Conditional Rptor knock-out in PV interneurons impairs repetitive firing

Activation of mTORC1 is generally linked to stimulation of protein synthesis (Costa-Mattioli et al., 2009a; Costa-Mattioli et al., 2009b; Switon et al., 2017). However, mTORC1 activation also represses the synthesis of specific mRNAs, such as the Kv1.1 channel, a voltage-gated potassium channel that regulates neuronal excitability (Raab-Graham et al., 2006; Sosanya et al., 2013). Therefore, we determined if conditional Rptor knock-out in PV INs affected their membrane and firing properties. Whole-cell patch-clamp recordings were obtained from EYFP-

expressing PV INs located in or near the CA1 stratum pyramidale in acute slices from control and PV conditional Rptor knock-out mice (PV-Raptor-WT n=9 cells in 4 mice, PV-Raptor-Het n=10 cells in 3 mice and PV-Raptor-Homo n=11 cells in 3 mice). We found that PV INs from control and conditional knock-out mice had similar resting membrane potential (One Way ANOVA, F (2, 27) =0.65 p=0.52; Fig. 2A) and input resistance (One Way ANOVA, F(2, 27) =1.93 p=0.16; Fig. 2B), suggesting intact basic membrane properties.

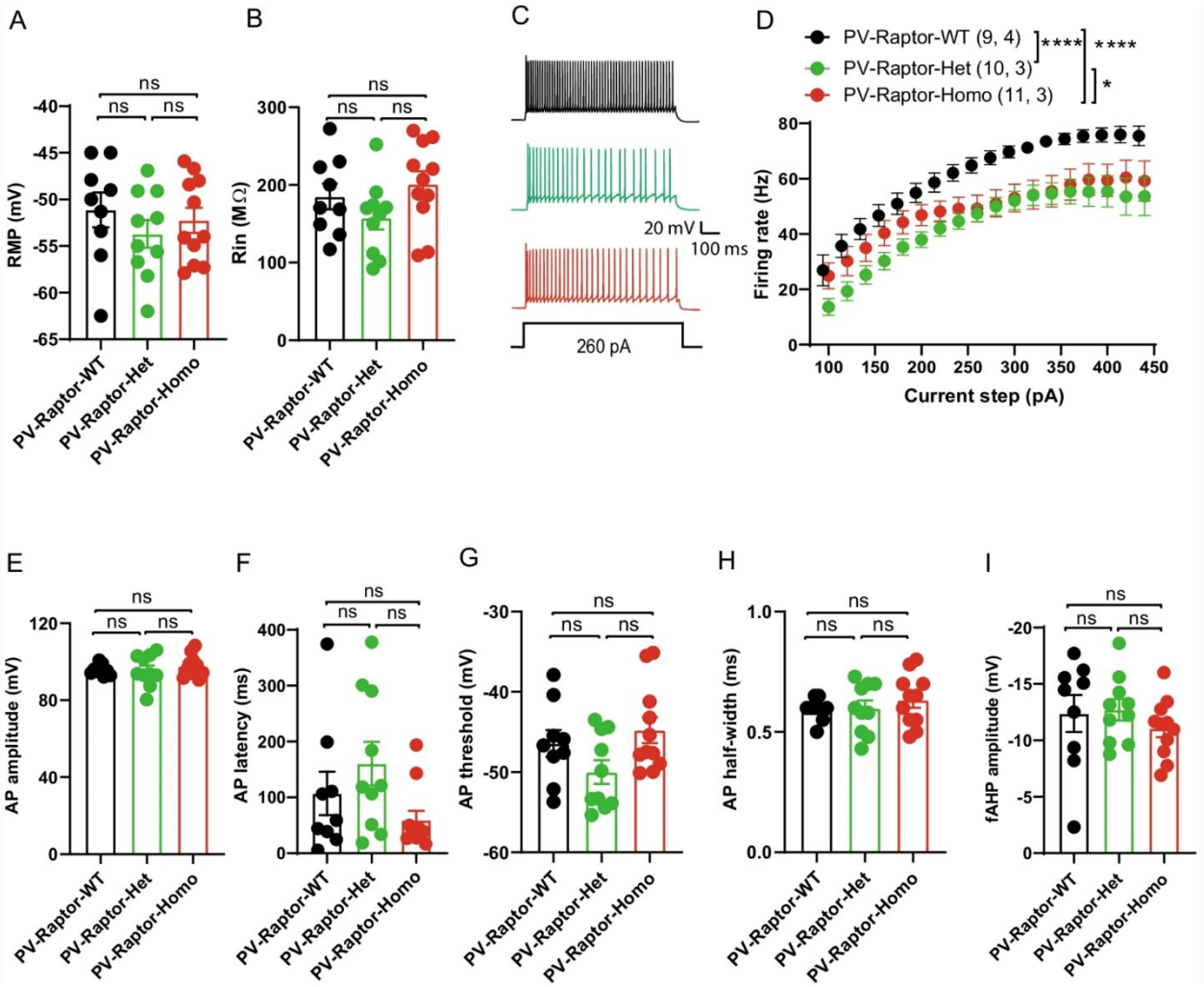

Figure 2. Conditional knock-out of Rptor in PV interneurons impairs firing properties. A and **B** Summary bar graphs showing intact: resting membrane potential (**A**) and input resistance (**B**) of CA1 PV interneurons from PV-Raptor-Het (green) and PV-Raptor-Homo (red) relative to PV-Raptor-WT mice (black). **C** Representative voltage responses of PV interneurons in response to a somatic depolarization (260 pA), illustrating the decrease in evoked firing of PV cells from PV-Raptor-Het and PV-Raptor-Homo mice relative to PV-Raptor-WT mice. **D** Summary plot of

frequency-current relationship for all cells showing reduced evoked firing of PV interneurons from PV-Raptor-Homo (n = 11 cells, 3 mice) and PV-Raptor-Het (n = 10 cells, 3 mice) mice relative to PV-Raptor-WT mice (n = 9 cells, 4 mice). E–I Summary bar graphs showing intact: action potential amplitude **(E)**, action potential latency (**F**), action potential threshold (**G**), action potential half-width (**H**) and fast after-hyperpolarization amplitude (**I**) of CA1 PV interneurons from PV-Raptor-Het (green) and PV-Raptor-Homo (red) relative to PV-Raptor-WT mice (black). * $p < 0.05$, **** $p < 0.0001$, ns not significant

Then, we assessed PV interneurons repetitive firing properties in response to somatic depolarizations. PV INs from control and mutant mice responded to incremental somatic depolarization with increasing number of action potentials (Fig. 2 C, D). However, PV INs from PV-Raptor-Het and PV-Raptor-Homo mutant mice fired less action potentials compared to those from PV-Raptor-WT mice (Two Way ANOVA, $F(2, 27) = 7.73$ $p=0.002$; Tukey's multiple comparisons tests, PV-Raptor-WT vs. PV-Raptor-Het $p<0.0001$, PV-Raptor-WT vs PV-Raptor-Homo $p<0.0001$, PV-Raptor-Het vs. PV-Raptor-Homo $p=0.012$; Fig. 2C-D). The impairment in firing was greater in PV INS from PV-Raptor-Het mice compared to those from PV-Raptor-Homo mice, suggesting possibly some compensatory mechanisms in the latter group. These results suggest that conditional hetero- and homozygous knock-out of Rptor in PV interneurons have impaired firing output.

Next, we examined whether the firing impairment of PV INs could be explained by changes in action potential properties. We found that PV INs from PV-Raptor-Het and PV-Raptor-Homo mice display similar action potential amplitude (One Way ANOVA, $F(2, 27) = 0.44$ $p=0.65$, Fig. 2E), latency to first action potential (One Way ANOVA, $F(2, 27) = 2.60$ $p=0.09$ Fig. 2F), action potential threshold (One Way ANOVA, $F(2, 27) = 02.89$ $p=0.07$, Fig. 2G), action potential half-width (One Way ANOVA, $F(2, 27) = 0.54$ $p=0.58$, Fig. 2H) and fast afterhyperpolarization amplitude (One Way ANOVA, $F(2, 27) = 0.64$ $p=0.53$, Fig. 2I). Together, these data indicate that conditional hetero- and homozygous knock-out of Rptor in PV interneurons impairs their repetitive firing properties without affecting their resting membrane potential, input resistance and action potential properties.

Conditional Rptor knock-out in PV interneurons impairs long-term potentiation of intrinsic excitability

Hippocampal GABAergic interneurons are highly dynamic and display several forms of long-term plasticity of synapses and intrinsic excitability (Kullmann & Lamsa, 2007; Campanac et al., 2013; Debanne et al., 2018; Chittajallu et al., 2020; Honore et al., 2021; Incontro et al., 2021). CA1 parvalbumin-expressing basket cells show long-term potentiation of intrinsic excitability (LTPIE) via mGluR5 activation and down-regulation of Kv1.1 channels, which is prevented by rapamycin, an inhibitor of mTORC1 (Campanac et al., 2013). Given that Raptor is obligatory for mTORC1 function, we tested if conditional knock-out of Rptor in PV INs could affect LTPIE. We obtained whole-cell patch-clamp recording from EYFP-positive PV interneurons located in or near CA1 stratum pyramidale. After establishing their fast-spiking phenotype in current-clamp mode via the injection of depolarizing currents, we adjusted i) the intracellular depolarizing current to evoke approximately 5 action potentials, and ii) the extracellular electrode simulation in stratum radiatum to elicit an EPSP of approximately 2 mV in amplitude (Campanac et al., 2013). After obtaining a stable baseline (5 min) of depolarization-evoked firing, we applied a high frequency stimulation (HFS) to the Schaffer collaterals pathway that consisted of 10 pulses at 100 Hz, repeated 10 times at the frequency of 3 Hz, and recorded PV interneuron spiking induced by the same somatic depolarization for up to 30 min (Campanac et al., 2013).

As previously reported in rat (Campanac et al., 2013), we found that in PV INs from PV-Raptor-WT mice (n=10 cells in 6 mice), HFS of Schaffer collaterals resulted in long-lasting potentiation of PV IN evoked firing (159.8% ± 15.8% of baseline at 10-15 min and 197.3% ± 3.3% of baseline at 25-30 min post-HFS, paired t-tests, p=0.013 and p=0.011 respectively, Fig. 3A-B). In the absence of HFS of Schaffer collateral pathway, we observed no change in evoked firing of PV INs (n=5 cells from 5 mice, 105.18% ± 14% of baseline at 10-15 min and 118.65% ± 15% of baseline at 25-30 min post-HFS, paired t-tests, p=0.88 and p=0.21 respectively, Fig. 3A-B). LTPIE was associated with a reduction in the latency of the first action potential (79.89 ± 5.49% of baseline at 10-15 min post-HFS and 68.17 ± 6.67% of baseline at 25-30 min post-HFS, Wilcoxon tests, p=0.004 and 0.004 respectively, Fig. 3C) and a hyperpolarization of the first action potential threshold (102.8 ± 0.54% of baseline at 10-15 min post-HFS and 106.54 ± 1.16% of baseline at 25-30 min post-HFS, paired t-tests, p=0.0007 and 0.0003 respectively, Fig. 3D). In the absence of HFS

of Schaffer collateral pathway, no change was observed in the first action potential latency (97.13 ± 14.73% of baseline at 10-15 min post-HFS and 91.8 ± 15.23% of baseline at 25-30 min post-HFS, paired t-tests, p=0.83 and 0.55 respectively, Fig. 3C), and only a depolarization of the first action potential threshold was seen at 10-15 min post-HFS (95.04 ± 0.7% of baseline at 10-15 min post-HFS and 98.2 ± 2.76% of baseline at 25-30 min post-HFS, paired t-tests, p=0.0018 and 0.55 respectively, Fig. 3D). The reduction in the first spike latency and threshold in the HFS group but not in the No HFS group is consistent with a modulation of Kv1.1 during LTPIE in PV interneurons, as previously reported (Campanac et al., 2013). Overall, these data confirm that HFS of Schaffer collateral pathway causes LTPIE in PV interneurons, which is dependent on tetanization, not due to unspecific effects of recording conditions and is associated with a modulation of Kv1.1 channels.

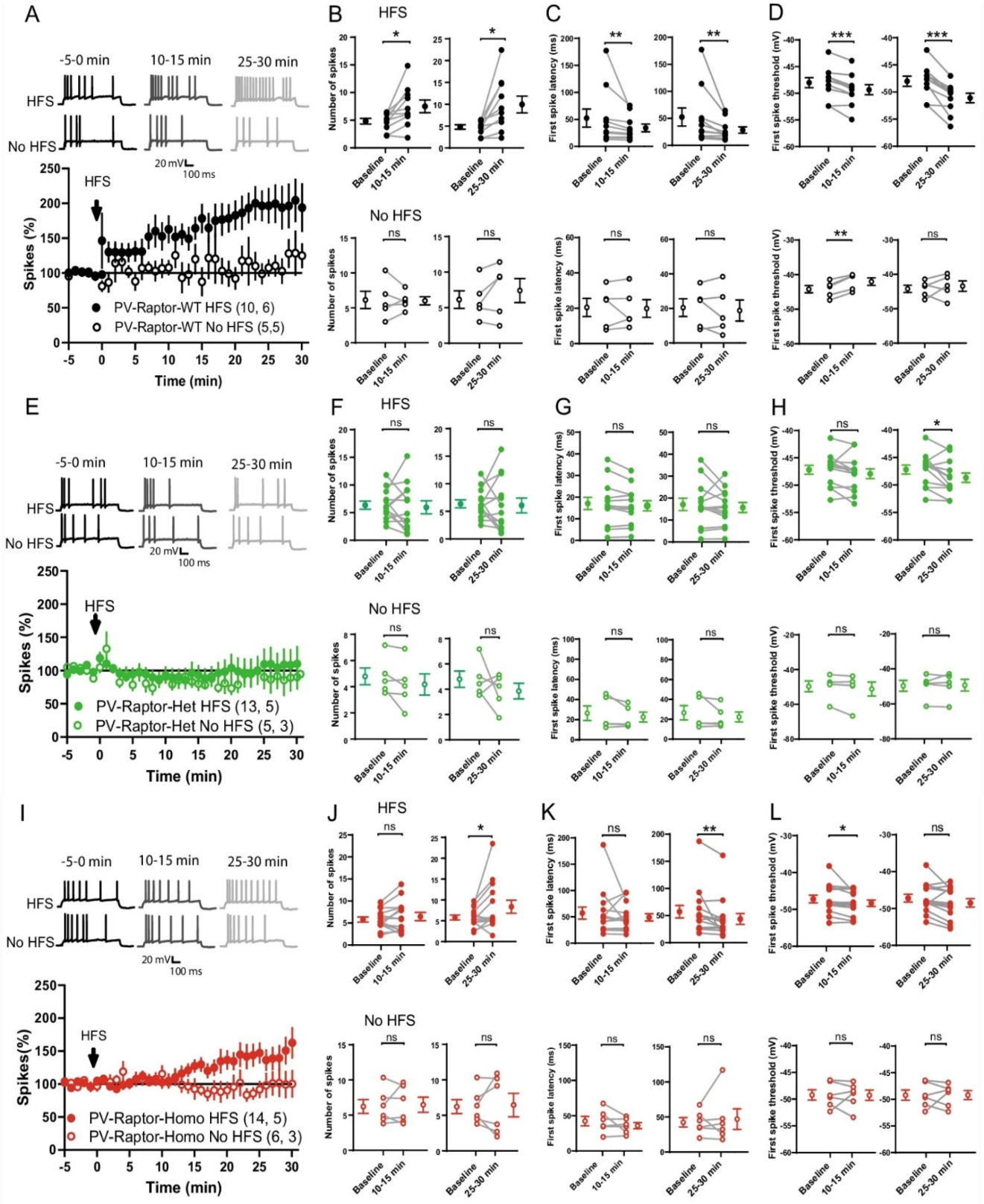
A
-5-0 min
10-15 min
25-30 min
HFS
No HFS
20 mV
100 ms
HFS
Spikes (%)
PV-Raptor-WT HFS (10, 6)
PV-Raptor-WT No HFS (5,5)
Time (min)
B
HFS
Number of spikes
Baseline
10-15 min
25-30 min
No HFS
C
First spike latency (ms)
D
First spike threshold (mV)
E
PV-Raptor-Het HFS (13, 5)
PV-Raptor-Het No HFS (5, 3)
F
G
H
I
PV-Raptor-Homo HFS (14, 5)
PV-Raptor-Homo No HFS (6, 3)
J
K
L
ns

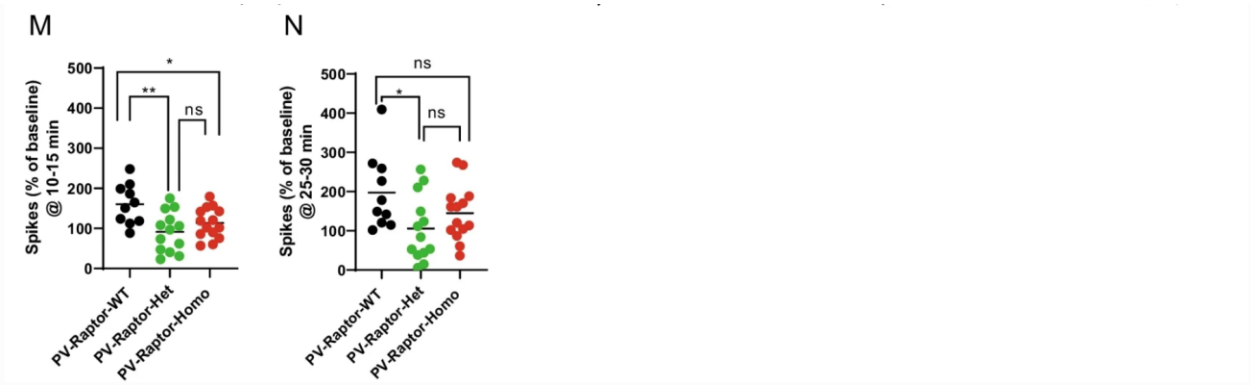

Figure 3. Conditional knock-out of Rptor in PV interneurons impairs LTPIE. A Representative trace (top) and time plot for all cells (bottom) of depolarization evoked firing showing long-lasting increase of firing in the group receiving HFS (filled circles, HFS) but not in the non-tetanized control group (open circles, No HFS) in CA1 PV interneuron from PV-Raptor-WT mice. **B-D** Summary plots of spikes number (**B**), latency to first spike (**C**) and first spike threshold (**D**) measured at -5 to 0 min baseline versus 10–15 min (left), or 25–30 min (right) post-HFS in cells of the tetanized group (HFS, top) and control group (No HFS, bottom). Individual data points before and after are joined by lines; means ± sem are indicated to the side for each group. **E–H** Similar data representation showing absence of long-lasting potentiation of intrinsic excitability at 10–15 min and 25–30 min after HFS in PV interneurons from PV-Raptor-Het mice. **I–L** Similar data representation showing a block of long-lasting potentiation of intrinsic excitability at 10–15 min, but not at 25–30 min, after HFS in PV interneurons from PV-Raptor-Homo mice. **M** and **N** Summary plots of spike increases relative to baseline for all cells measured at 10–15 min (**M**) and 25–30 min (**N**) after HFS in PV interneurons, showing block of LTPIE at 10–15 and 25–30 min after HFS in PV-Raptor-Het mice, and at 10–15 min post HFS in PV-Raptor-Homo mice, relative to PV-Raptor-WT mice. *** $p < 0.001$, ** $p < 0.01$, * $p < 0.05$, ns not significant

Next, we assessed whether the conditional knock-out of Rptor in PV interneurons affected LTPIE since it was reported to be sensitive to the mTORC1 inhibitor rapamycin (Campanac et al., 2013). In PV-Raptor-Het mice, we found that HFS of Schaffer collaterals failed to induce long-term potentiation of evoked firing in PV mice (n=13 cells from 5 mice, 91.1% ± 14% of baseline at 10-15 min and 105.5% ± 23.1% of baseline at 25-30 min post-HFS, paired t-tests, p=0.67 and p=0.8 respectively, Fig. 3H-I). HFS also failed to alter consistently the first action potential latency (99.66 ± 3.26% of baseline at 10-15 min post-HFS and 98.98 ± 7.33% of baseline at 25-30 min post-HFS, paired t-tests, p=0.09 and 0.43 respectively, Fig. 3J) and threshold (101.53 ± 1% of baseline at 10-15 min post-HFS and 103.22 ± 1.24% of baseline at 25-30 min post-HFS, paired t-tests, p=0.15 and 0.02 respectively, Fig. 3K). As in PV-Raptor-WT mice, the absence of HFS stimulation in PV-

Raptor-Het mice did not affect PV interneuron evoked firing (n=5 cells from 3 mice, 85.11% ± 9.6% of baseline at 10-15 min and 88.9% ± 20% of baseline at 25-30 min post-HFS, paired t-tests, p=0.16 and p=0.37 respectively, Fig. 3H-I), latency of first action potential (91.86 ± 6.73% of baseline at 10-15 min post-HFS and 91.1 ± 8.35% of baseline at 25-30 min post-HFS, paired t-tests, p=0.23 and 0.31 respectively, Fig. 3J) or threshold of first action potential (102.66 ± 1.57% of baseline at 10-15 min post-HFS and 99.27 ± 2.27% of baseline at 25-30 min post-HFS, paired t-tests, p=0.20 and 0.76 respectively, Fig. 3K). These data suggest that conditional heterozygous deletion of Rptor in PV interneurons is sufficient to prevent LTPIE.

In PV-Raptor-Homo mice, HFS failed to induce a potentiation of evoked firing at 10-15 min but did elicit an increase in firing at 25-30 min post-HFS (n=14 cells from 5 mice, 115.53% ± 10% of baseline at 10-15 min and 144.9% ± 18.7% of baseline at 25-30 min post-HFS, paired t-tests, p=0.23 and p=0.04 respectively, Fig. 3O-P). Similarly, HFS failed to alter latency of the first action potential at 10-15 min but not at 25-30 min post-HFS (97.67 ± 9.64% of baseline at 10-15 min post-HFS, paired t-test, p=0.4, and 80.95 ± 6.95% of baseline at 25-30 min post-HFS, Shapiro-Wilk test, p=0.008, Fig. 3Q). HFS reduced threshold of the first action potential at 10-15 min but not at 25-30 min post-HFS (102.62 ± 1.28% of baseline at 10-15 min post-HFS and 102.86 ± 1.5% of baseline at 25-30 min post-HFS, paired t-tests, p=0.04 and p=0.07 respectively, Fig. 3R). These results suggest that LTPIE is impaired by homozygous deletion of Rptor, but that an mTORC1-independent late component of LTPIE remains, as previously reported in experiments using the mTORC1 inhibitor rapamycin (Campanac et al., 2013). In the absence of HFS, PV interneuron from PV-Raptor-Homo mice did not show change over the same time period in evoked firing (n=6 cells from 3 mice, 100.3% ± 11% of baseline at 10-15 min and 99.9% ± 20% of baseline at 25-30 min post-HFS, paired t-tests, p=0.56 and p=0.72 respectively, Fig. 3O-P), latency to first action potential (90.06 ± 9.35% of baseline at 10-15 min post-HFS, paired t-test, p=0.64 and 104.66 ± 16.60% of baseline at 25-30 min post-HFS, Shapiro-Wilk test, p=0.68 respectively, Fig. 3Q) and threshold of first action potential (100.15 ± 1.58% of baseline at 10-15 min post-HFS and 100.05 ± 1.6% of baseline at 25-30 min post-HFS, paired t-tests, p=0.95 and p=0.98 respectively, Fig. 3R), confirming stable evoked firing over the recording period in these mice also.

Overall, these results show that i) HFS of Schaffer collaterals induces LTPIE in PV interneurons of PV-Raptor-WT mice, ii) LTPIE is blocked at both 10-15 min and 25-30 min post-

HFS in PV-Raptor-Het mice, and iii) LTPIE is deficient at 10-15 min but not 25-30 min post-HFS in PV-Raptor-Homo mice (Fig. 3S, 10-15 min post-HFS: One way ANOVA, F (2, 34) =6 p=0.003, Tukey's multiple comparisons test, PV-Raptor-WT vs PV-Raptor-Het, p=0.004, PV-Raptor-WT vs PV-Raptor-Homo, p=0.036, PV-Raptor-Het vs PV-Raptor-Homo, p=0.53; Fig. 3T, 25-30 min post-HFS: One way ANOVA, F (2, 34) =3 p=0.04, Tukey's multiple comparisons test, PV-Raptor-WT vs PV-Raptor-Het, p=0.03, PV-Raptor-WT vs PV-Raptor-Homo, p=0.27, PV-Raptor-Het vs. PV-Raptor-Homo, p=0.48). These findings indicate that the hetero- and homozygous conditional knock-out of Rptor in PV INs impairs LTPIE, consistent with previous report that this plasticity is sensitive to the mTORC1 inhibitor rapamycin (Campanac et al., 2013).

Mice with conditional Rptor knock-out in PV interneurons show normal contextual fear memory and fear discrimination

LTP of PV interneuron excitatory synapses and coherence of PV interneuron firing with CA1 network oscillations are required for contextual fear memory consolidation (Ognjanovski et al., 2017; He et al., 2021). Since we found a deficit in LTPIE in PV interneurons with conditional Rptor knock-out, next we examined fear memory consolidation and discrimination in these mice. During contextual fear conditioning, PV-Raptor-Het and PV-Raptor-Homo mice showed similar freezing responses to foot shocks relative to PV-Raptor-WT mice (n= 21 PV-Raptor-WT mice, 13 PV-Raptor-Het mice, and 15 PV-Raptor-Homo mice; Two way ANOVA F (2, 46) = 0.358, p=0.7, Fig. 4A-B), indicating normal anxiety and sensorimotor gating in the mutant mice.

During the long-term memory test in the training context (24 hours after conditioning), PV-Raptor-Het and PV-Raptor-Homo mice showed similar freezing responses relative to PV-Raptor-WT mice (One way ANOVA, F (2, 46) = 0.5923 p=0.5572, Fig. 4A-C), indicating intact long-term contextual memory in the mutant mice. During the context discrimination test in a new neutral context, the three mice groups showed less freezing responses relative to the trained context, indicating significant contextual discrimination (paired t-tests; n=12 PV-Raptor-WT mice, p<0.0001; n=7 PV-Raptor-Het mice, p=0.0026; n=6 PV-Raptor-Homo mice, p=0.026; Fig. 4D). In the neutral context, PV-Raptor-Het and PV-Raptor-Homo mice showed similar freezing responses relative to PV-Raptor-WT mice (n=12 PV-Raptor-WT mice, 7 PV-Raptor-Het mice, and 6 PV-

Raptor-Homo mice; One way ANOVA, F (2, 22) = 0.4621 p=0.6359, Fig. 4A-DE). Similarly, discrimination ratios to assess context discrimination normalized to the freezing level in the training context were similar in control and mutant mice (One way ANOVA, F (2, 22) = 2.83 p=0.08, Fig. 4A-DF). These results indicate suggest that long-term contextual fear memory and context discrimination are intact in mice with conditional Rptor knock-out in PV INs, and, thus, suggesting that mTORC1 regulation of firing and long-term potentiation of intrinsic excitability of PV INs is dispensable may not be necessary for long-term contextual fear memory and context discrimination.

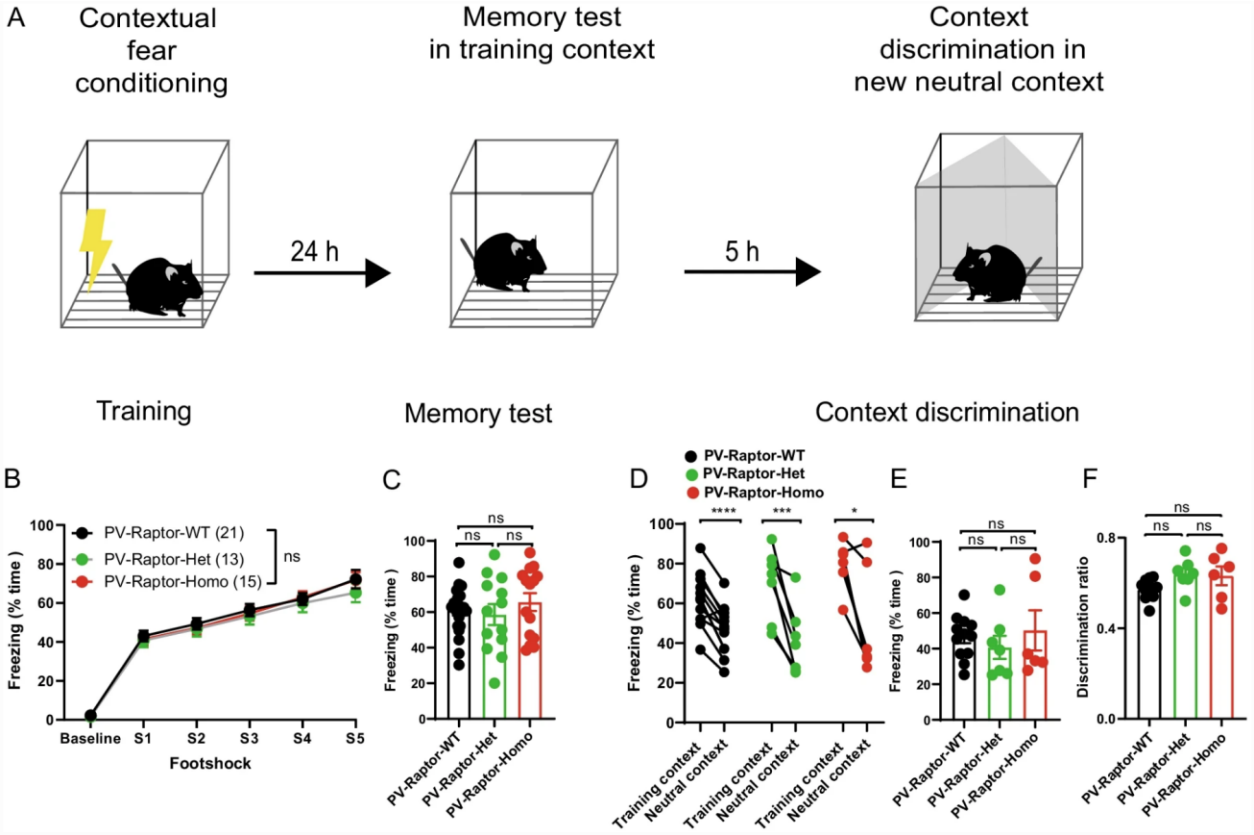

Figure 4. Conditional knock-out of Rptor in PV interneurons does not affect contextual fear memory or context discrimination. A Diagram of the contextual fear memory and context discrimination protocol. **B** Percentage of time freezing after each foot shock during the training session for PV-Raptor-WT (n = 21), PV-Raptor-Het (n = 13) and PV-Raptor-Homo (n = 15) mice (Baseline: before the first foot shock), indicating similar anxiety level and sensorimotor gating in the three groups. **C** Percentage of time freezing during the long-term memory tests at 24 h in the PV-Raptor-WT, PV-Raptor-Het and PV-Raptor-Homo mice (same mice as in B), indicating similar long-term contextual memory in the three groups. **D–F** Percentage of time freezing during the contextual discrimination test, relative to the training context (**D**), in the new neutral context (**E**)

and discrimination ratio (**F**; amount of freezing in [training context]/[training context + neutral context]) for PV-Raptor-WT (n = 12), PV-Raptor-Het (n = 7) and PV-Raptor-Homo (n = 6) mice, indicating similar context discrimination in the three mice groups. **** $p < 0.0001$, *** $p < 0.001$, * $p < 0.05$, ns not significant

Discussion

The major results of the present study are, first, that homozygous conditional knock-out of Rptor in parvalbumin-expressing cells decreases the level of expression of Raptor, as well as mTORC1 signaling as assessed by immunofluorescence of S6 phosphorylation, in CA1 PV INs (Fig. 1). Second, using whole-cell recordings from CA1 PV INs we found that repetitive firing induced by depolarizing pulses was impaired in mice with either homozygous or heterozygous conditional knock-out of Rptor, whereas basic membrane properties and single action potential firing characteristics were unaffected, indicating an impairment in repetitive firing output (Fig. 2). Third, we showed that brief high frequency stimulation of Schaffer collateral synaptic inputs induces LTPIE in PV INs of control mice but failed to do so in mice with either heterozygous or homozygous conditional knock-out of Rptor in PV INs, indicating that mTORC1 function is necessary for long-term potentiation of intrinsic excitability (Fig. 3). Fourth, at the behavioral level, we found that mice with homozygous or heterozygous conditional knock-out of Rptor showed similar long-term contextual fear memory or contextual fear memory discrimination relative to control mice (Fig. 4). Overall, our results establish a role of mTORC1 in the regulation of repetitive firing and of LTPIE in CA1 PV INs and suggest that mTORC1-regulation of firing and of LTPIE in these interneurons is dispensablemay not be necessary for hippocampus-dependent contextual fear memory and context discrimination.

Raptor expression and mTORC1 signaling

Raptor constitutes an essential component of the mTORC1 complex (Hara et al., 2002), whose activation regulates major cellular function such as growth, proliferation and cell metabolism (Laplante & Sabatini, 2012), as well as regulation of protein synthesis necessary for synaptic plasticity and memory (Jaworski & Sheng, 2006; Costa-Mattioli et al., 2009b). Using immunohistochemical assays for Raptor expression and phospho-specific S6

immunohistochemical assay for mTORC1 signaling, we found reduced level of Raptor expression and mTORC1 activity in PV INs from PV-Raptor-Homo mice but not from PV-Raptor-Het mice. However, we found significant impairment in cell firing and LTPIE in PV INs, consistent with some reduction in mTORC1 function in both PV-Raptor-Homo and PV-Raptor-Het mice. Thus, our results suggest that a reduction in mTORC1 function may occur in PV INs with conditional Rptor haploinsufficiency which is sufficient to affect mTORC1-dependent firing output and LTPIE, but which the Raptor and phospho-S6 immunocytochemical assays are not sensitive enough to detect. Although, pS6 phosphorylation is considered a readout of mTORC1 activity (Biever et al., 2015), other non-mTORC1 intracellular mechanisms also regulate S6 phosphorylation at serine240/244 sites, such as PKA-dependent inhibition of the Protein-Phosphatase-1 (PP-1) (Bonito-Oliva et al., 2013), thus possibly affecting the pS6 assay.

mTORC1 signals to its downstream targets, including S6 phosphorylation, to promote protein synthesis in long-term synaptic plasticity and memory. Indeed, heterozygous knock-out of mTOR in hippocampal pyramidal cells (Stoica et al., 2011) and of Rptor in somatostatin interneurons (Artinian et al., 2019) are not sufficient to impair mTORC1-mediated protein synthesis and long-term synaptic plasticity. Thus, homozygous deletions seem necessary to impair mTORC1-mediated protein synthesis, which may appear inconsistent with our results. However, mTORC1 activity represses the local, dendritic mRNA translation of the voltage-gated potassium channel subunit Kv1.1 (Raab-Graham et al., 2006) and reduction in mTORC1 signaling by rapamycin treatment causes the degradation of high affinity HuD target mRNAs, freeing HuD to bind Kv1.1 mRNA and promoting its translation (Sosanya et al., 2013). Thus, mTORC1 regulation of Kv1.1 channel is not via activation of protein synthesis. Our results suggest that heterozygous deletion of Rptor is sufficient to reduce mTORC1 signaling involved in regulation of repetitive firing and of Kv1.1 channels during LTPIE in PV IN, in contrast to mTORC1 signaling and p-S6 mediated activation of protein synthesis in synaptic plasticity (Stoica et al., 2011; Artinian et al., 2019).

mTORC1 downstream signaling involves multiple pathways. Another primary mTORC1 downstream signaling pathway is via phosphorylation of eIF4E-binding proteins (4E-BPs) to activate eIF4E-dependent translation (Costa-Mattioli et al., 2009b). In addition, via phosphorylation of S6 kinase it targets phosphorylation of S6, but also phosphorylation of eIF4B,

inhibition of FMRP signaling, and inhibition of eEF2-kinase (Costa-Mattioli et al., 2009b; Panja & Bramham, 2014). Moreover, mTORC1 controls translation via upregulation of 5' terminal oligopyrimidine (5' TOP) mRNAs that encode components of the translational machinery (Ruvinsky & Meyuhas, 2006; Gobert et al., 2008; Costa-Mattioli et al., 2009b). We used p-S6 as a readout of mTORC1 signaling and found a deficit in p-S6 signaling in PV-Raptor-Homo but not PV-Raptor-Het mice. However, we observed altered repetitive firing and LTPIE phenotypes in both PV-Raptor-Homo and -Het mice. These results suggest that mTORC1-mediated p-S6 signaling is not associated with the firing and LTPIE phenotypes. Thus, mTORC1 regulation of firing and LTPIE may involve a downstream signaling pathway other than p-S6. Further experiments will be necessary to distinguish possible roles via 4E-BPs, 5' TOP mRNAs, or other targets of S6K, in these mTORC1 mechanisms.

mTORC1 and PV IN excitability

Our results indicate that impairing mTORC1 function by conditional hetero- and homozygous Rptor knock-out selectively decreased firing output of PV INs, without altering their basic membrane properties and single action potential firing characteristics. Rptor knock-out in neurons has been associated with numerous morphological abnormalities, such as reduced soma size and dendritic length (Urbanska et al., 2012; Angliker et al., 2015; McCabe et al., 2020), as well as impaired passive and active membrane properties, including input resistance and action potential amplitude (McCabe et al., 2020). Thus, the reduced cell excitability of PV INs after conditional Rptor knock-out could be related to somatic or dendritic morphological changes. Although we did not examine the morphology of recorded cells, the impairment in PV cell firing is unlikely to be due to morphological changes, since we found that basic membrane properties such as resting membrane potential and input resistance, as well as single action potential properties, were intact in PV INs with conditional hetero- or homozygous Rptor knock-out. It is important to note that in PV IN conditional knock-out mice, Cre recombination occurs postnatally in hippocampal PV interneurons. Our results corroborate the lack of morphological and membrane properties changes with conditional homozygous Rptor knock-out in CA1 somatostatin INs, another mouse model with Cre recombination late in development of interneurons (Artinian et al., 2019). Interestingly, in contrast to PV INs, Rptor knock-out in somatostatin INs is associated with

an increase in evoked firing output (Artinian et al., 2019), suggesting that mTORC1 regulates interneuron excitability in a cell type-specific manner.

Fast-spiking interneurons excitability is strongly influenced by Kv1.1-containing potassium channels through regulation of action potential voltage threshold and near-threshold responsiveness (Goldberg et al., 2008). These channels are localized in the soma, dendrites, axon initial segment and synaptic terminals of neurons (Wang et al., 1994) and their activation dampens neuronal excitability (D'Adamo et al., 2020). However, repetitive firing of fast-spiking interneurons is controlled largely by Kv3 potassium channels (Martina et al., 1998; Jonas et al., 2004). Importantly, mTORC1 inhibition with rapamycin increases Kv1.1 expression in dendrites of hippocampal pyramidal neurons (Raab-Graham et al., 2006; Sosanya et al., 2013; Sosanya et al., 2015; Niere & Raab-Graham, 2017). In PV interneurons, as in other neurons, reduction in Kv1.1 lowers the threshold and latency for action potential firing (Goldberg et al., 2008; Li et al., 2011; Campanac et al., 2013; Giglio & Storm, 2014; Sosanya et al., 2015). Our results that the changes in repetitive firing were not associated with any change in threshold or latency of action potentials in PV INs with conditional hetero- or homozygous Rptor knock-out, suggest that Kv1 potassium channels may not be the target of mTORC1 regulation to modulate repetitive firing of PV cells. An alternative may be that mTORC1 regulates the expression of Kv3 channels (Jonas et al., 2004), however this remains to be demonstrated.

mTORC1 and LTPIE in PV INs

Previous work has shown that HFS applied to Schaffer collateral inputs induces a long-term increase in intrinsic excitability of CA1 fast-spiking PV INs in young rats which is prevented by rapamycin treatment, suggesting a role of mTORC1 signaling pathway (Campanac et al., 2013). However, mTOR signaling can occur via two distinct complexes, mTORC1 that contains Raptor, and mTORC2 that contains Rictor (Costa-Mattioli et al., 2009b). Hippocampal long-term synaptic plasticity and memory involve both mTORC1 (Stoica et al., 2011) and mTORC2 (Zhu et al., 2018) signaling. Although rapamycin is considered a more effective mTORC1 inhibitor (Kang et al., 2013), prolonged treatment (Sarbassov et al., 2006) or higher concentration (Foster & Toschi, 2009) of rapamycin also inhibits mTORC2. Thus, sensitivity to rapamycin treatment does not necessarily indicate mTORC1 implication. Our findings that HFS induced long-term increase of

PV INs intrinsic excitability in hippocampal slices from control mice, but failed to do so in mice with hetero- or homozygous conditional Rptor knock-out, clearly indicate that mTORC1 activity is required for LTPIE in PV INs, extending previous findings obtained with rapamycin treatment (Campanac et al., 2013).

Our results show that LTPIE is completely blocked in PV INs with heterozygous Rptor knock-out at 10-15 min and 25-30 min time points after HFS, but only at 10-15 min after induction in PV INs with homozygous Rptor knock-out, indicating a residual late component of LTPIE after complete Rptor knock-out. Our results share some similarities with previous findings that treatment of hippocampal slices with rapamycin suppressed LTPIE at 10-15 min after induction but did not block completely LTPIE at later times (25-30 min) (Campanac et al., 2013). Thus, our results indicate, first, that Rptor haploinsufficiency is sufficient to completely prevent LTPIE in PV INs, clearly showing a requirement for mTORC1 activity in LTPIE in PV INs. Second, they indicate that a residual component of LTPIE is present at later times in mice with full knock-out of Rptor. Further experiments will be necessary to identify the mechanisms possibly involved.

In CA1 fast-spiking PV INs, brief repetitive stimulation of Schaffer collaterals induces a rapamycin-sensitive LTPIE which is mediated by synaptic activation of mGluR5 and down-regulation of Kv1.1 channel activity (Campanac et al., 2013). Moreover, LTPIE involve a down-regulation of Kv1.1 channel activity since pharmacological blockers of Kv1.1 mimick LTPIE and occlude further induction of LTPIE (Campanac et al., 2013). Thus, our findings that LTPIE in PV INs is associated with a decrease in the latency and threshold of evoked action potentials, which consistent with previous findings (Campanac et al., 2013), and that LTPIE is impaired by conditional knock-out of Rptor in PV cells, provide a clear link between mTORC1 activation and regulation of Kv1.1 channel activity during LTPIE. These findings of mTORC1 requirement in LTPIE are consistent with previous evidence that mTORC1 activity regulates negatively Kv1.1 channel expression and activity in pyramidal cell dendrites (Raab-Graham et al., 2006; Sosanya et al., 2013; Sosanya et al., 2015). Our observations, thus, provide functional evidence of an mTORC1 regulation of Kv1.1 channel function during activity-dependent long-term plasticity of PV interneuron intrinsic excitability.

mTORC1 and hippocampal memory

Multiple lines of evidence indicate an important role of PV IN activity and synaptic plasticity in hippocampus-dependent memory function. Long-term structural plasticity of excitatory and inhibitory synapses of PV INs contributes to contextual fear learning and memory consolidation, as well as maze navigation learning (Donato et al., 2013). Pharmacogenetic inhibition of PV INs prevents contextual fear conditioning-induced changes in network oscillations and impairs fear memory consolidation (Ognjanovski et al., 2017). In addition, genetic deletion of γCaMKII in PV INs prevents LTP at their excitatory input synapses from Schaffer collaterals and impairs fear memory consolidation (He et al., 2021). Although there is no evidence of a role of mTORC1 in these synaptic plasticity mechanisms, our observations that contextual fear memory and context discrimination are intact in mice with conditional Rptor knock-out in PV cells, indicate that mTORC1 signaling is not involved in the roles of these plasticity mechanisms of PV INs in hippocampus-dependent memory tasks. These conclusions are in contrast with evidence in hippocampal principal cells and in somatostatin interneurons that mTORC1 signaling plays a critical role in long-term synaptic plasticity and in hippocampus-dependent learning and memory consolidation (Stoica et al., 2011; Artinian et al., 2019), pointing to cell type-specific mTORC1 mechanisms in long-term synaptic plasticity and memory consolidation.

Moreover, our findings that mice with conditional Rptor knock-out in PV cells show deficits in LTPIE and intact hippocampal-dependent contextual fear memory and context discrimination, indicate that mTORC1-dependent LTPIE in PV INs is dispensablemay not be necessary for these hippocampus-dependent memory tasks. This is in contrast with excitatory cells where plasticity of intrinsic excitability, also expressed as a change in action potential firing, plays an important role in memory allocation, consolidation, and updating (Zhang & Linden, 2003; Debanne et al., 2018; Chen et al., 2020). Given that LTPIE promotes PV INs firing in the gamma range and facilitates their recruitment by pyramidal cells (Campanac et al., 2013) which may favor synchronization of pyramidal cells activity and generation of network oscillations (Hu et al., 2014), our results raise the question of when is mTORC1-dependent LTPIE in PV INs critical for hippocampus-dependent learning and memory consolidation? Impairment of inhibition by hippocampal PV INs results in impaired spatial working memory and intact spatial learning and spatial reference memory (Murray et al., 2011). Thus, LTPIE and regulation of PV INs firing in

the generation of network oscillations (Hu et al., 2014) could be important for learning during spatial navigation (Hasselmo et al., 2002; Burgess, 2008; Buzsaki, 2015). Interestingly, increased mTORC1 activity in mice with conditional heterozygous knock-out of Tsc1 in Nkx2.1 expressing interneurons, which include somatostatin and parvalbumin interneurons, impaired hippocampus-dependent long-term spatial working memory but not spatial reference memory (Haji et al., 2020). Thus, mice with conditional Rptor knock-out in PV INs could be useful to determine if mTORC1-mediated LTPIE is implicated in long-term spatial working memory.

Interneuron type-specific mTORC1 function is important in pathological conditions. The eukaryotic translation initiation factor 4E-binding protein 2 (4E-BP2) is a translational repressor downstream of mTORC1. Genetic ablation of 4E-BP2 in inhibitory but not excitatory neurons causes an increase in the susceptibility to pentylenetetrazole-induced seizures (Sharma et al., 2021). Moreover, mice lacking 4E-BP2 in parvalbumin, but not in somatostatin or vasoactive intestinal peptide-expressing (VIP) inhibitory neurons exhibit a lowered threshold for seizure induction and reduced number of parvalbumin neurons (Sharma et al., 2021). Thus, increased mTORC1-dependent translation in parvalbumin neurons is implicated in the pathophysiology of epilepsy (Sharma et al., 2021). Such a role is consistent with PV IN dysfunction contributing to epileptiform discharges and abnormalities in oscillatory rhythms, network synchrony, and memory in human amyloid precursor protein (hAPP) mouse model of Alzheimer disease (Verret et al., 2012). In addition, deletion of 4E-BP2 in GABAergic inhibitory neurons results in impairments in social interaction and vocal communication (Wiebe et al., 2019). Thus, mTORC1 signaling via 4E-BP2 has an inhibitory cell-specific role in engendering autism related behaviors (Wiebe et al., 2019). These findings are consistent with a loss of hippocampal PV INs, impaired perisomatic inhibition, gamma and sharp wave ripples activity, as well as spatial discrimination, in the Cntnap2 mouse model of autism spectrum disorder (Paterno et al., 2021). Thus, an implication of mTORC1-mediated LTPIE in PV INs in interneuron-specific pathological conditions would be important to investigate.

In conclusion, we found that mTORC1 activity regulates CA1 PV IN repetitive firing and LTPIE but is dispensablemay not be necessary for consolidation of long-term contextual fear memory and context discrimination. Thus, mTORC1 plays cell-specific roles in synaptic plasticity

of hippocampal inhibitory interneurons that are differentially involved in hippocampus-dependent learning and memory.

Limitations

Some limitations should be considered when interpreting our results. First, although our interpretations discussed in the study are concordant with impaired mTORC1 activity at least in CA1 PV INs of mice with conditional homozygous knock-out of Rptor in PV cells, functional alterations of PV INs in other hippocampal and neocortical regions could also influence the behavioral tasks in our study. Although we tested a behavioral task known to engage the hippocampus (contextual fear memory), a region-specific deletion approach would be helpful to confirm the role of CA1 PV INs. Second, we used immunohistochemical assays for Raptor expression and phospho-specific S6 immunohistochemical assay for mTORC1 signaling and we could detect a reduction of Raptor protein expression level and mTORC1 activity in PV INs from mice with conditional homozygous Rptor knock-out but not in mice with heterozygous Rptor knock-out. However, we did find phenotypes in electrophysiological experiments in PV INS of both hetero- and homozygous Rptor knock-out mice, suggesting a reduction in Raptor expression level with Rptor haploinsufficiency. A more sensitive assay, such as quantitative single cell PCR would be necessary to confirm the effective knock-down of Rptor in mice with heterozygous deletion. Third, previous studies focusing on mTORC1 in the regulation of synaptic transmission, revealed that reducing mTORC1 activity with rapamycin or by knocking out Raptor, decreased the efficacy of excitatory transmission via pre- and postsynaptic mechanisms in hippocampal excitatory neurons (Wang et al., 2006; Weston et al., 2012; McCabe et al., 2020). Thus, if similar mechanisms occur in PV INs, excitatory synaptic inputs in PV INs could be reduced in mice with conditional hetero- or homozygous Rptor knock-out, which may reduce the postsynaptic efficacy of HFS to activate mGluR5 and induce LTPIE. Thus, characterization of synaptic transmission in conditional Rptor knock-out mice would be necessary to rule out such changes. However, in our experimental protocol, the strength of synaptic stimulation was adjusted to elicit similar EPSPs prior to induction of LTPIE and control for putative differences in presynaptic release in the different genotypes. Fourth, we found that conditional hetero- or homozygous Rptor knock-out mice showed altered repetitive firing and a block of LTP-IE, indicating a role of mTORC1.

However, we did not test in parallel the possible role of mTORC2. Similar experiments using conditional Rictor knock-out mice would be useful to assess this possibility. Fifth, our conclusion that mTORC1 function in PV interneurons may not be necessary for contextual fear memory and discrimination is based on a single type of behavioral experiments (contextual fear memory) that showed no difference between wild-type and transgenic mice. Thus, additional behavioral verifications with other hippocampus-dependent tasks would be necessary to confirm our conclusion. Finally, a last limitation to consider is that our whole cell recordings were obtained from cells in slices that came from a smaller number of transgenic mice. However, all whole cell recordings were obtained from a single cell per slice which are considered independent experiments. Nonetheless, additional experiments in a larger number of mice would clarify this issue.

List of abbreviations

aCSF: artificial cerebrospinal fluid

AP: Action potential

AHP: after hyperpolarization

CaMKII: Ca2+/calmodulin-dependent protein kinase II

CFC: Contextual fear memory

ERK: Extracellular signal-regulated kinase

FS-PV INs: Fast-spiking parvalbumin-expressing interneurons

HFS: High frequency stimulation

LTD: Long-term depression

LTDIE: Long-term depression of intrinsic excitability

LTP: Long-term potentiation

LTPIE: Long-term potentiation of intrinsic excitability

mGluR5: Type 5 metabotropic glutamate receptors

mTORC1: Mammalian target of rapamycin complex 1

PI3K: Phosphoinositide 3-kinase

PKA: Protein kinase A

PKC: Protein kinase C

PV INs: Parvalbumin-expressing interneurons

Raptor: Regulatory-Associated Protein of mTOR

Rin: Input resistance

RMP: Resting membrane potential

SOM INs: Somatostatin interneurons

TSC2: Tuberous Sclerosis Complex 2

γCaMKII: Gamma Ca2+/calmodulin-dependent protein kinase II

Ethics approval

All animal procedures and experiments were performed in accordance with the Université de Montréal animal care committee regulations.

Consent for publication

All authors have given their consent for publication.

Availability of data and materials

The datasets used and/or analyzed during the current study are available from the corresponding author on reasonable request.

Competing interests

The authors declare that they have no competing interests.

Funding

This work was supported by grants to J.C.L. from the Canadian Institutes of Health Research (CIHR MOP-125985 and PJT-153311) and a Research Centre grant (Centre Interdisciplinaire de Recherche sur le Cerveau et l'Apprentissage; CIRCA) from the Fonds de la Recherche du Québec – Santé (FRQS). J.C.L. is the recipient of the Canada Research Chair in Cellular and Molecular Neurophysiology (CRC 950-231066) and a member of the Research Group on Neural Signaling and Circuitry (GRSNC) at Université de Montréal.

Author Contributions

A.K. and J.-C.L. designed the project; A.K., E.H., I.L., performed experiments and analyzed data; A.K., E.H., I.L., and J.-C.L. wrote the paper. All authors read and approved the final manuscript.

Acknowledgments

Not applicable

Author information

The authors Abdessattar Khlaifia and Eve Honoré shared first authorship in the study

References

Aika, Y., Ren, J.Q., Kosaka, K. & Kosaka, T. (1994) Quantitative analysis of GABA-like-immunoreactive and parvalbumin-containing neurons in the CA1 region of the rat hippocampus using a stereological method, the disector. Exp Brain Res, 99, 267-276.

Angliker, N., Burri, M., Zaichuk, M., Fritschy, J.M. & Ruegg, M.A. (2015) mTORC1 and mTORC2 have largely distinct functions in Purkinje cells. Eur J Neurosci, 42, 2595-2612.

Artinian, J., Jordan, A., Khlaifia, A., Honore, E., La Fontaine, A., Racine, A.S., Laplante, I. & Lacaille, J.C. (2019) Regulation of Hippocampal Memory by mTORC1 in Somatostatin Interneurons. J Neurosci, 39, 8439-8456.

Biever, A., Valjent, E. & Puighermanal, E. (2015) Ribosomal Protein S6 Phosphorylation in the Nervous System: From Regulation to Function. Front Mol Neurosci, 8, 75.

Bonito-Oliva, A., Pallottino, S., Bertran-Gonzalez, J., Girault, J.A., Valjent, E. & Fisone, G. (2013) Haloperidol promotes mTORC1-dependent phosphorylation of ribosomal protein S6 via dopamine- and cAMP-regulated phosphoprotein of 32 kDa and inhibition of protein phosphatase-1. Neuropharmacology, 72, 197-203.

Burgess, N. (2008) Spatial cognition and the brain. Ann N Y Acad Sci, 1124, 77-97.

Buzsaki, G. (2015) Hippocampal sharp wave-ripple: A cognitive biomarker for episodic memory and planning. Hippocampus, 25, 1073-1188.

Campanac, E., Gasselin, C., Baude, A., Rama, S., Ankri, N. & Debanne, D. (2013) Enhanced intrinsic excitability in basket cells maintains excitatory-inhibitory balance in hippocampal circuits. Neuron, 77, 712-722.

Castillo, P.E., Chiu, C.Q. & Carroll, R.C. (2011) Long-term plasticity at inhibitory synapses. Curr Opin Neurobiol, 21, 328-338.

Chandra, N. & Barkai, E. (2018) A non-synaptic mechanism of complex learning: Modulation of intrinsic neuronal excitability. Neurobiol Learn Mem, 154, 30-36.

Chattopadhyaya, B. & Cristo, G.D. (2012) GABAergic circuit dysfunctions in neurodevelopmental disorders. Front Psychiatry, 3, 51.

Chen, L., Cummings, K.A., Mau, W., Zaki, Y., Dong, Z., Rabinowitz, S., Clem, R.L., Shuman, T. & Cai, D.J. (2020) The role of intrinsic excitability in the evolution of memory: Significance in memory allocation, consolidation, and updating. Neurobiol Learn Mem, 173, 107266.

Chittajallu, R., Auville, K., Mahadevan, V., Lai, M., Hunt, S., Calvigioni, D., Pelkey, K.A., Zaghloul, K.A. & McBain, C.J. (2020) Activity-dependent tuning of intrinsic excitability in mouse and human neurogliaform cells. Elife, 9.

Costa-Mattioli, M. & Monteggia, L.M. (2013) mTOR complexes in neurodevelopmental and neuropsychiatric disorders. Nat Neurosci, 16, 1537-1543.

Costa-Mattioli, M., Sonenberg, N. & Richter, J.D. (2009a) Translational regulatory mechanisms in synaptic plasticity and memory storage. Prog Mol Biol Transl Sci, 90, 293-311.

Costa-Mattioli, M., Sossin, W.S., Klann, E. & Sonenberg, N. (2009b) Translational control of long-lasting synaptic plasticity and memory. Neuron, 61, 10-26.

D'Adamo, M.C., Liantonio, A., Rolland, J.F., Pessia, M. & Imbrici, P. (2020) Kv1.1 Channelopathies: Pathophysiological Mechanisms and Therapeutic Approaches. Int J Mol Sci, 21.

Debanne, D., Inglebert, Y. & Russier, M. (2018) Plasticity of intrinsic neuronal excitability. Curr Opin Neurobiol, 54, 73-82.

Donato, F., Rompani, S.B. & Caroni, P. (2013) Parvalbumin-expressing basket-cell network plasticity induced by experience regulates adult learning. Nature, 504, 272-276.

Foster, D.A. & Toschi, A. (2009) Targeting mTOR with rapamycin: one dose does not fit all. Cell Cycle, 8, 1026-1029.

Freund, T.F. & Buzsáki, G. (1996) Interneurons of the hippocampus. Hippocampus, 6, 347-470.

Giglio, A.M. & Storm, J.F. (2014) Postnatal development of temporal integration, spike timing and spike threshold regulation by a dendrotoxin-sensitive K(+) current in rat CA1 hippocampal cells. Eur J Neurosci, 39, 12-23.

Gobert, D., Topolnik, L., Azzi, M., Huang, L., Badeaux, F., Desgroseillers, L., Sossin, W.S. & Lacaille, J.C. (2008) Forskolin induction of late-LTP and up-regulation of 5' TOP mRNAs translation via mTOR, ERK, and PI3K in hippocampal pyramidal cells. J Neurochem, 106, 1160-1174.

Goldberg, E.M., Clark, B.D., Zagha, E., Nahmani, M., Erisir, A. & Rudy, B. (2008) K+ channels at the axon initial segment dampen near-threshold excitability of neocortical fast-spiking GABAergic interneurons. Neuron, 58, 387-400.

Haji, N., Riebe, I., Aguilar-Valles, A., Artinian, J., Laplante, I. & Lacaille, J.C. (2020) Tsc1 haploinsufficiency in Nkx2.1 cells upregulates hippocampal interneuron mTORC1 activity, impairs pyramidal cell synaptic inhibition, and alters contextual fear discrimination and spatial working memory in mice. Mol Autism, 11, 29.

Hara, K., Maruki, Y., Long, X., Yoshino, K., Oshiro, N., Hidayat, S., Tokunaga, C., Avruch, J. & Yonezawa, K. (2002) Raptor, a binding partner of target of rapamycin (TOR), mediates TOR action. Cell, 110, 177-189.

Hasselmo, M.E., Bodelon, C. & Wyble, B.P. (2002) A proposed function for hippocampal theta rhythm: separate phases of encoding and retrieval enhance reversal of prior learning. Neural Comput, 14, 793-817.

He, X., Li, J., Zhou, G., Yang, J., McKenzie, S., Li, Y., Li, W., Yu, J., Wang, Y., Qu, J., Wu, Z., Hu, H., Duan, S. & Ma, H. (2021) Gating of hippocampal rhythms and memory by synaptic plasticity in inhibitory interneurons. Neuron, 109, 1013-1028 e1019.

Honore, E., Khlaifia, A., Bosson, A. & Lacaille, J.C. (2021) Hippocampal Somatostatin Interneurons, Long-Term Synaptic Plasticity and Memory. Front Neural Circuits, 15, 687558.

Hu, H., Gan, J. & Jonas, P. (2014) Interneurons. Fast-spiking, parvalbumin(+) GABAergic interneurons: from cellular design to microcircuit function. Science, 345, 1255263.

Incontro, S., Sammari, M., Azzaz, F., Inglebert, Y., Ankri, N., Russier, M., Fantini, J. & Debanne, D. (2021) Endocannabinoids tune intrinsic excitability in O-LM interneurons by direct modulation of post-synaptic Kv7 channels. J Neurosci.

Jaworski, J. & Sheng, M. (2006) The growing role of mTOR in neuronal development and plasticity. Mol Neurobiol, 34, 205-219.

Jonas, P., Bischofberger, J., Fricker, D. & Miles, R. (2004) Interneuron Diversity series: Fast in, fast out--temporal and spatial signal processing in hippocampal interneurons. Trends Neurosci, 27, 30-40.

Kang, S.A., Pacold, M.E., Cervantes, C.L., Lim, D., Lou, H.J., Ottina, K., Gray, N.S., Turk, B.E., Yaffe, M.B. & Sabatini, D.M. (2013) mTORC1 phosphorylation sites encode their sensitivity to starvation and rapamycin. Science, 341, 1236566.

Kullmann, D.M. & Lamsa, K.P. (2007) Long-term synaptic plasticity in hippocampal interneurons. Nat Rev Neurosci, 8, 687-699.

Laplante, M. & Sabatini, D.M. (2012) mTOR signaling in growth control and disease. Cell, 149, 274-293.

Li, K.X., Lu, Y.M., Xu, Z.H., Zhang, J., Zhu, J.M., Zhang, J.M., Cao, S.X., Chen, X.J., Chen, Z., Luo, J.H., Duan, S. & Li, X.M. (2011) Neuregulin 1 regulates excitability of fast-spiking neurons through Kv1.1 and acts in epilepsy. Nat Neurosci, 15, 267-273.

Marin, O. (2012) Interneuron dysfunction in psychiatric disorders. Nat Rev Neurosci, 13, 107-120.

Martina, M., Schultz, J.H., Ehmke, H., Monyer, H. & Jonas, P. (1998) Functional and molecular differences between voltage-gated K+ channels of fast-spiking interneurons and pyramidal neurons of rat hippocampus. J Neurosci, 18, 8111-8125.

McCabe, M.P., Cullen, E.R., Barrows, C.M., Shore, A.N., Tooke, K.I., Laprade, K.A., Stafford, J.M. & Weston, M.C. (2020) Genetic inactivation of mTORC1 or mTORC2 in neurons reveals distinct functions in glutamatergic synaptic transmission. Elife, 9.

Murray, A.J., Sauer, J.F., Riedel, G., McClure, C., Ansel, L., Cheyne, L., Bartos, M., Wisden, W. & Wulff, P. (2011) Parvalbumin-positive CA1 interneurons are required for spatial working but not for reference memory. Nat Neurosci, 14, 297-299.

Niere, F. & Raab-Graham, K.F. (2017) mTORC1 Is a Local, Postsynaptic Voltage Sensor Regulated by Positive and Negative Feedback Pathways. Front Cell Neurosci, 11, 152.

Ognjanovski, N., Schaeffer, S., Wu, J., Mofakham, S., Maruyama, D., Zochowski, M. & Aton, S.J. (2017) Parvalbumin-expressing interneurons coordinate hippocampal network dynamics required for memory consolidation. Nat Commun, 8, 15039.

Panja, D. & Bramham, C.R. (2014) BDNF mechanisms in late LTP formation: A synthesis and breakdown. Neuropharmacology, 76 Pt C, 664-676.

Paterno, R., Marafiga, J.R., Ramsay, H., Li, T., Salvati, K.A. & Baraban, S.C. (2021) Hippocampal gamma and sharp-wave ripple oscillations are altered in a Cntnap2 mouse model of autism spectrum disorder. Cell Rep, 37, 109970.

Pelkey, K.A., Chittajallu, R., Craig, M.T., Tricoire, L., Wester, J.C. & McBain, C.J. (2017) Hippocampal GABAergic Inhibitory Interneurons. Physiol Rev, 97, 1619-1747.

Pelletier, J.G. & Lacaille, J.C. (2008) Long-term synaptic plasticity in hippocampal feedback inhibitory networks. Prog Brain Res, 169, 241-250.

Petilla Interneuron Nomenclature, G., Ascoli, G.A., Alonso-Nanclares, L., Anderson, S.A., Barrionuevo, G., Benavides-Piccione, R., Burkhalter, A., Buzsaki, G., Cauli, B., Defelipe, J., Fairen, A., Feldmeyer, D., Fishell, G., Fregnac, Y., Freund, T.F., Gardner, D., Gardner, E.P., Goldberg, J.H., Helmstaedter, M., Hestrin, S., Karube, F., Kisvarday, Z.F., Lambolez, B., Lewis, D.A., Marin, O., Markram, H., Munoz, A., Packer, A., Petersen, C.C., Rockland, K.S., Rossier, J., Rudy, B., Somogyi, P., Staiger, J.F., Tamas, G., Thomson, A.M., Toledo-Rodriguez, M., Wang, Y., West, D.C. & Yuste, R. (2008) Petilla terminology: nomenclature of features of GABAergic interneurons of the cerebral cortex. Nat Rev Neurosci, 9, 557-568.

Pouille, F. & Scanziani, M. (2001) Enforcement of temporal fidelity in pyramidal cells by somatic feed-forward inhibition. Science, 293, 1159-1163.

Pouille, F. & Scanziani, M. (2004) Routing of spike series by dynamic circuits in the hippocampus. Nature, 429, 717-723.

Raab-Graham, K.F., Haddick, P.C., Jan, Y.N. & Jan, L.Y. (2006) Activity- and mTOR-dependent suppression of Kv1.1 channel mRNA translation in dendrites. Science, 314, 144-148.

Ran, I., Laplante, I., Bourgeois, C., Pepin, J., Lacaille, P., Costa-Mattioli, M., Pelletier, J., Sonenberg, N. & Lacaille, J.C. (2009) Persistent transcription- and translation-dependent long-term potentiation induced by mGluR1 in hippocampal interneurons. J Neurosci, 29, 5605-5615.

Roux, L. & Buzsaki, G. (2015) Tasks for inhibitory interneurons in intact brain circuits. Neuropharmacology, 88, 10-23.

Ruvinsky, I. & Meyuhas, O. (2006) Ribosomal protein S6 phosphorylation: from protein synthesis to cell size. Trends Biochem Sci, 31, 342-348.

Sarbassov, D.D., Ali, S.M., Sengupta, S., Sheen, J.H., Hsu, P.P., Bagley, A.F., Markhard, A.L. & Sabatini, D.M. (2006) Prolonged rapamycin treatment inhibits mTORC2 assembly and Akt/PKB. Mol Cell, 22, 159-168.

Sharma, V., Sood, R., Khlaifia, A., Eslamizade, M.J., Hung, T.Y., Lou, D., Asgarihafshejani, A., Lalzar, M., Kiniry, S.J., Stokes, M.P., Cohen, N., Nelson, A.J., Abell, K., Possemato, A.P., Gal-

Ben-Ari, S., Truong, V.T., Wang, P., Yiannakas, A., Saffarzadeh, F., Cuello, A.C., Nader, K., Kaufman, R.J., Costa-Mattioli, M., Baranov, P.V., Quintana, A., Sanz, E., Khoutorsky, A., Lacaille, J.C., Rosenblum, K. & Sonenberg, N. (2020) eIF2alpha controls memory consolidation via excitatory and somatostatin neurons. Nature, 586, 412-416.

Sharma, V., Sood, R., Lou, D., Hung, T.Y., Levesque, M., Han, Y., Levett, J.Y., Wang, P., Murthy, S., Tansley, S., Wang, S., Siddiqui, N., Tahmasebi, S., Rosenblum, K., Avoli, M., Lacaille, J.C., Sonenberg, N. & Khoutorsky, A. (2021) 4E-BP2-dependent translation in parvalbumin neurons controls epileptic seizure threshold. Proc Natl Acad Sci U S A, 118.

Somogyi, P. & Klausberger, T. (2005) Defined types of cortical interneurone structure space and spike timing in the hippocampus. J Physiol, 562, 9-26.

Sosanya, N.M., Brager, D.H., Wolfe, S., Niere, F. & Raab-Graham, K.F. (2015) Rapamycin reveals an mTOR-independent repression of Kv1.1 expression during epileptogenesis. Neurobiol Dis, 73, 96-105.

Sosanya, N.M., Huang, P.P., Cacheaux, L.P., Chen, C.J., Nguyen, K., Perrone-Bizzozero, N.I. & Raab-Graham, K.F. (2013) Degradation of high affinity HuD targets releases Kv1.1 mRNA from miR-129 repression by mTORC1. J Cell Biol, 202, 53-69.

Stoica, L., Zhu, P.J., Huang, W., Zhou, H., Kozma, S.C. & Costa-Mattioli, M. (2011) Selective pharmacogenetic inhibition of mammalian target of Rapamycin complex I (mTORC1) blocks long-term synaptic plasticity and memory storage. Proc Natl Acad Sci U S A, 108, 3791-3796.

Switon, K., Kotulska, K., Janusz-Kaminska, A., Zmorzynska, J. & Jaworski, J. (2017) Molecular neurobiology of mTOR. Neuroscience, 341, 112-153.

Tasic, B., Yao, Z., Graybuck, L.T., Smith, K.A., Nguyen, T.N., Bertagnolli, D., Goldy, J., Garren, E., Economo, M.N., Viswanathan, S., Penn, O., Bakken, T., Menon, V., Miller, J., Fong, O., Hirokawa, K.E., Lathia, K., Rimorin, C., Tieu, M., Larsen, R., Casper, T., Barkan, E., Kroll, M., Parry, S., Shapovalova, N.V., Hirschstein, D., Pendergraft, J., Sullivan, H.A., Kim, T.K., Szafer, A., Dee, N., Groblewski, P., Wickersham, I., Cetin, A., Harris, J.A., Levi, B.P., Sunkin, S.M., Madisen, L., Daigle, T.L., Looger, L., Bernard, A., Phillips, J., Lein, E., Hawrylycz, M., Svoboda, K., Jones, A.R., Koch, C. & Zeng, H. (2018) Shared and distinct transcriptomic cell types across neocortical areas. Nature, 563, 72-78.

Tremblay, R., Lee, S. & Rudy, B. (2016) GABAergic Interneurons in the Neocortex: From Cellular Properties to Circuits. Neuron, 91, 260-292.

Udakis, M., Pedrosa, V., Chamberlain, S.E.L., Clopath, C. & Mellor, J.R. (2020) Interneuron-specific plasticity at parvalbumin and somatostatin inhibitory synapses onto CA1 pyramidal neurons shapes hippocampal output. Nat Commun, 11, 4395.

Urbanska, M., Gozdz, A., Swiech, L.J. & Jaworski, J. (2012) Mammalian target of rapamycin complex 1 (mTORC1) and 2 (mTORC2) control the dendritic arbor morphology of hippocampal neurons. J Biol Chem, 287, 30240-30256.

Verret, L., Mann, E.O., Hang, G.B., Barth, A.M., Cobos, I., Ho, K., Devidze, N., Masliah, E., Kreitzer, A.C., Mody, I., Mucke, L. & Palop, J.J. (2012) Inhibitory interneuron deficit links altered network activity and cognitive dysfunction in Alzheimer model. Cell, 149, 708-721.

Wang, H., Kunkel, D.D., Schwartzkroin, P.A. & Tempel, B.L. (1994) Localization of Kv1.1 and Kv1.2, two K channel proteins, to synaptic terminals, somata, and dendrites in the mouse brain. J Neurosci, 14, 4588-4599.

Wang, Y., Barbaro, M.F. & Baraban, S.C. (2006) A role for the mTOR pathway in surface expression of AMPA receptors. Neurosci Lett, 401, 35-39.

Weston, M.C., Chen, H. & Swann, J.W. (2012) Multiple roles for mammalian target of rapamycin signaling in both glutamatergic and GABAergic synaptic transmission. J Neurosci, 32, 11441-11452.

Wiebe, S., Nagpal, A., Truong, V.T., Park, J., Skalecka, A., He, A.J., Gamache, K., Khoutorsky, A., Gantois, I. & Sonenberg, N. (2019) Inhibitory interneurons mediate autism-associated behaviors via 4E-BP2. Proc Natl Acad Sci U S A, 116, 18060-18067.

Younts, T.J., Monday, H.R., Dudok, B., Klein, M.E., Jordan, B.A., Katona, I. & Castillo, P.E. (2016) Presynaptic Protein Synthesis Is Required for Long-Term Plasticity of GABA Release. Neuron, 92, 479-492.

Yu, Y., Zeng, Z., Xie, D., Chen, R., Sha, Y., Huang, S., Cai, W., Chen, W., Li, W., Ke, R. & Sun, T. (2021) Interneuron origin and molecular diversity in the human fetal brain. Nat Neurosci, 24, 1745-1756.

Zhang, W. & Linden, D.J. (2003) The other side of the engram: experience-driven changes in neuronal intrinsic excitability. Nat Rev Neurosci, 4, 885-900.

Zhu, P.J., Chen, C.J., Mays, J., Stoica, L. & Costa-Mattioli, M. (2018) mTORC2, but not mTORC1, is required for hippocampal mGluR-LTD and associated behaviors. Nat Neurosci, 21, 799-802.

Chapitre VI

Discussion

Notre hypothèse de départ était que les différents interneurones qui peuplent l'hippocampe et les différentes formes de plasticité qu'ils expriment contrôlent différents aspects des fonctions mnésiques de l'hippocampe. Dans l'optique d'étudier cette question, nous avons examiné deux types d'interneurones principaux du CA1 dorsal, avec en premier lieu le rôle des SOM-INs et leur plasticité synaptique dans la régulation des réseaux de l'hippocampe et de différents types de mémoire. Ensuite nous avons étudié le rôle des PV-INs et la plasticité de leur excitabilité intrinsèque (PLT_{EI}) dans la mémoire contextuelle de peur.

6.1. Résultats principaux

6.1.1. Rôle des interneurones somatostatinergiques

Tout d'abord, nous avons conçu un protocole de stimulation optogénétique (le TBS_{opto}) capable d'induire une PLT aux synapses CP-SOM dans l'hippocampe dorsal *in vitro* (figure 1) (Chapitre II). Nous avons démontré que la stimulation des axones des cellules pyramidales (CP) de CA1 est suffisante pour induire la PLT des synapses excitatrices de SOM-INs, il n'y a donc pas de nécessité de coactivation des afférences extrahippocampiques. Ensuite, nous avons caractérisé cette PLT optogénétique (PLT_{opto}), et démontré que tout comme celle induite auparavant par une stimulation électrique, la PLT_{opto} est Hebbienne, dépend des mêmes fréquences de stimulation, de l'activation des mGluR1s et de la traduction d'ARNm via mTORC1, mais pas de la transcription (Asgarihafshejani A. *et al.*, 2022). Cette PLT n'est donc pas persistante (pouvant durer 24 h), mais transitoire (dure au moins 30 min à quelques heures). De plus, ce protocole d'induction n'induit pas de PLT dans les PV-INs.

Grâce au TBS_{opto} nous avons pu vérifier que la PLT CP-SOM était suffisante pour moduler l'activité du réseau de CA1 (Chapitre II). En effet, cette PLT n'affecte pas le niveau de transmission de base, ni des afférences de CA3, ni de celles provenant du cortex entorhinal. Cependant, elle augmente la PLT des synapses des CP CA3-CA1 et diminue celle entre le cortex entorhinal et les CP de CA1 (figure 1).

Au niveau de la synapse CP-SOM, il semble exister une interaction entre la plasticité induite par une stimulation optogénétique et celle induite par une autre forme de stimulation donnée ultérieurement (Chapitre II et III). Si on effectue deux inductions électriques consécutives, on observe un phénomène d'addition des PLT. La PLT électrique sature une PLT_{opto} subséquente. Une première PLT_{opto} sature également une PLT_{opto} consécutive. Enfin l'induction d'une PLT électrique suivant une PLT_{opto} produit une dépotentialisation des synapses (figure 4 Chapitre II). De façon analogue, la PLT_{opto} bloque la synthèse protéique normalement produite par l'induction chimique de la PLT des SOM-INs (Chapitre III).

Si on donne le TBS_{opto} avant un conditionnement à la peur, la mémoire de peur à long terme s'en trouve fortement diminuée, de même que l'activité spontanée et évoquée des synapses CP-SOM (figure 1) (Chapitre II). Étant donné que le conditionnement à la peur induit une PLT aux synapses CP-SOM (Artinian J. *et al.*, 2019). Ces résultats concordent avec le fait que la PLT_{opto} interfère avec les potentialisations induites ultérieurement par d'autres formes de stimulation des synapses CP-SOM.

D'autre part, si on donne le TBS_{opto} avant l'entraînement à une tâche de mémorisation de localisation d'objets sous le seuil d'apprentissage, on augmente la mémoire de localisation d'objets (figure 1) (Chapitre IV). Nous ne savons pas si ce type d'apprentissage induit une PLT aux synapses CP-SOM, mais étant donné qu'un défaut de PLT des SOM-INs dans les souris SOM-EYFP-Raptor KO altère la mémoire spatiale, nous pensons que c'est une possibilité (Artinian J. *et al.*, 2019). Cependant, comme l'entraînement était sous le seuil d'apprentissage, il n'a probablement pas provoqué de PLT mais une forme de plasticité à court terme. Dans nos travaux la PLT_{opto} pourrait avoir fait passer la plasticité induite par l'entraînement d'un état transitoire à un état persistant, ce qui a permis de conserver le souvenir de la localisation des objets seulement dans les souris qui ont reçu le TBS_{opto}.

L'ensemble de ces travaux sont illustrés conceptuellement dans la figure 1. Ceux-ci démontrent que la PLT des synapses CP-SOM du CA1 dorsal est nécessaire et suffisante pour contrôler la formation des mémoires aversives et contextuelles, de même que des mémoires peu saillantes épisodiques et spatiales. De plus, nous montrons qu'il est nécessaire que cette PLT soit induite lors de l'apprentissage pour la formation de la mémoire.

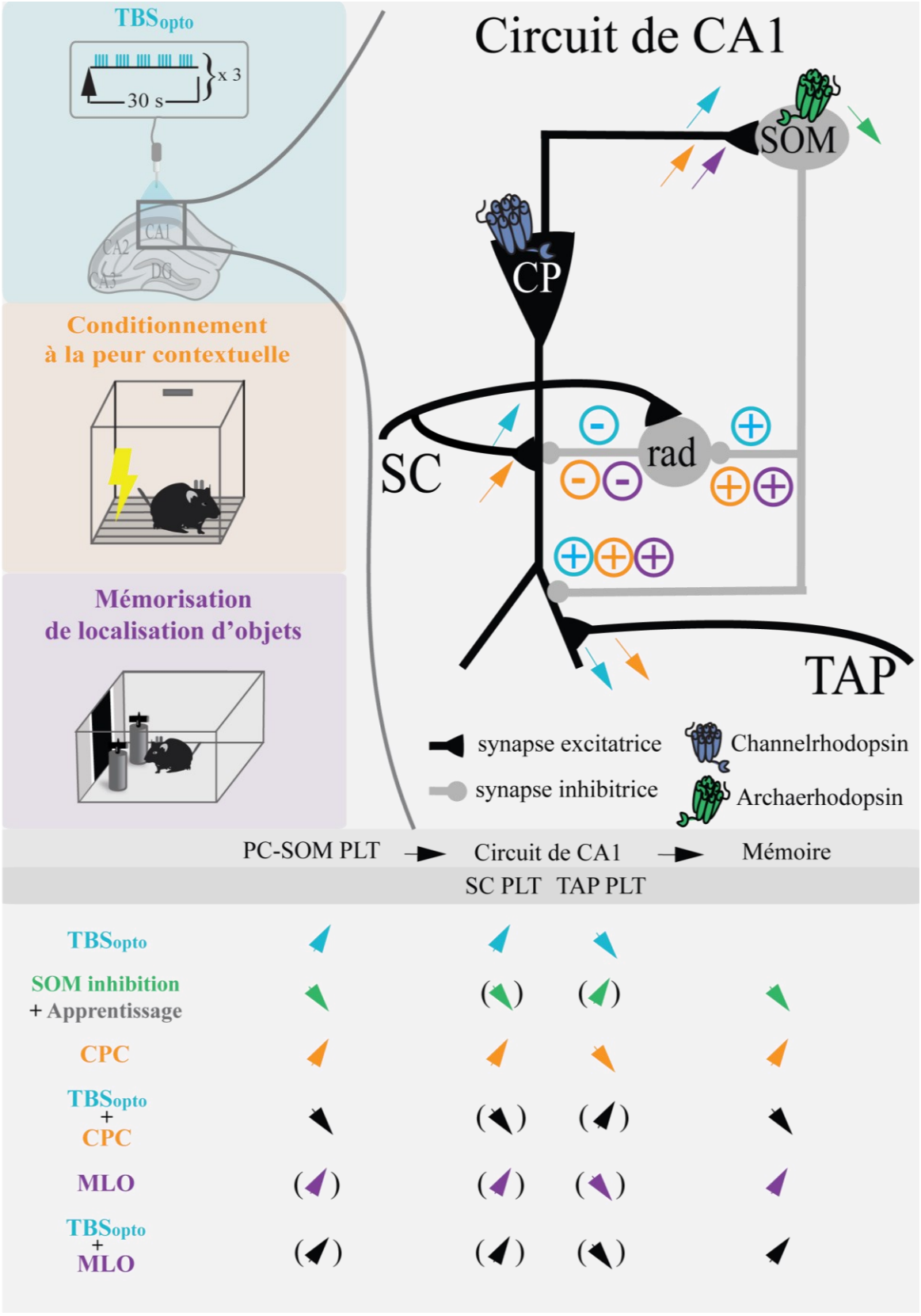
TBSopto
x 3
30 s
CA1
CA2
CA3
DG
Conditionnement
à la peur contextuelle
Mémorisation
de localisation d'objets
Circuit de CA1
SOM
CP
SC
rad
TAP
synapse excitatrice
synapse inhibitrice
Channelrhodopsin
Archaerhodopsin
PC-SOM PLT
Circuit de CA1
Mémoire
SC PLT
TAP PLT
TBSopto
SOM inhibition
+ Apprentissage
CPC
TBSopto
+
CPC
MLO
TBSopto
+
MLO

Figure 1 Rôles de la PLT des SOM-INs sur le circuit de CA1. L'induction d'une PLT aux synapses CP-SOM par le TBS_{opto} provoque une augmentation de l'inhibition des dendrites distales des CP et des interneurones de la couche radiatum (rad). Ceci a pour conséquence la diminution de la PLT de la voie temporoammonique (TAP) et l'augmentation de la PLT des collatérales de Schaffer (SC). L'inhibition des interneurones SOM pendant l'apprentissage bloque la PLT des SOM ceci a pour effet potentiel (flèches entre parenthèses) de diminuer la PLT des SC et augmenter celles de la TAP. Cela a pour conséquence une diminution de la mémoire. Le conditionnement à la peur (CPC) induit une PLT aux synapses CP-SOM, ceci a pour conséquence l'augmentation de la PLT des SC et la diminution de celle de la TAP, et la formation de la mémoire de peur. L'induction de la PLT aux synapses CP-SOM suivie d'un conditionnement à la peur induit une dépotentialisation des synapses CP-SOM. Ce qui a l'effet potentiel de diminuer la PLT des SC et augmenter celles de la TAP. Cela a pour conséquence une diminution de la mémoire. L'induction de la PLT aux synapses CP-SOM suivie d'une tâche de mémorisation de localisation d'objet (MLO) sous le seuil, induit probablement une PLT durable aux synapses CP-SOM. Ceci a pour conséquence potentielle l'augmentation de la PLT des SC et la diminution de celle de la TAP, et la consolidation de la mémoire de localisation d'objet. Donc la MLO aurait besoin de la PLT des synapses CP-SOM pour former la mémoire de localisation d'objet.

6.1.2. Rôle des interneurones parvalbuminergiques

Dans un second temps, nous avons montré que dans les PV-INs, au moins une copie du gène Rptor est nécessaire pour que l'activité du complexe mTORC1 mène à la phosphorylation de la sous-unité ribosomique S6. Cependant, deux copies fonctionnelles de ce gène sont nécessaires pour le fonctionnement normal des PV-INs. La délétion hétérozygote et homozygote de Rptor diminue la fréquence de décharge répétée des PV-INs mais pas les propriétés de base du potentiel d'action. La PLT de l'excitabilité intrinsèque (PLT_{EI}) des PV-INs est bloquée par ces mutations, ce qui indique que cette forme de plasticité nécessite l'activité de mTORC1. Cependant, étant donné que les souris ayant une délétion hétérozygote ou homozygote de Rptor (PV-Raptor KO) n'ont pas de déficit de la mémoire de peur contextuelle ni de la discrimination de contextes, ni l'activité de mTORC1 ni la PLT_{EI} ne sont nécessaires pour l'encodage de la mémoire contextuelle de peur ni la précision de cette mémoire (figure 2) (Chapitre V).

Ces résultats contrastent avec ceux obtenus dans les SOM-INs où la délétion de Rptor ne changent pas les propriétés de décharge de base mais bloque l'induction de la plasticité synaptique.

De plus, contrairement aux souris PV-Raptor KO, les souris SOM-Raptor KO présentent un déficit de la mémoire de peur contextuelle, et une augmentation de la discrimination de contextes (Artinian J. *et al.*, 2019).

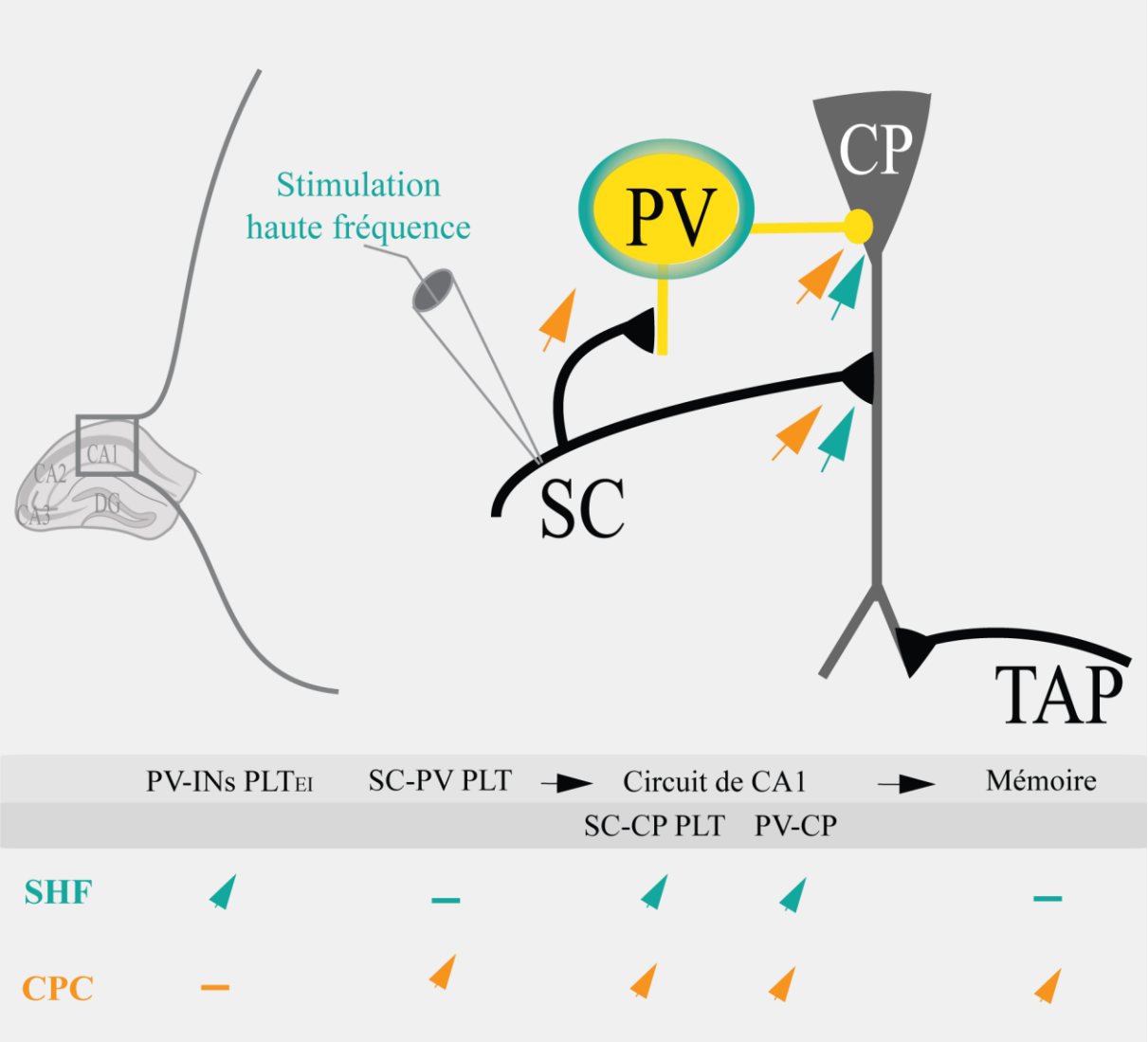

Figure 2 Rôles des différentes formes de PLT des PV-INs sur le circuit de CA1. La stimulation à haute fréquence (SHF) des collatérales de Schaffer (SC) provoque l'induction de la PLT des synapses SC-CP et de la PLT_{EI} des PV-INs. Ceci a pour conséquence une augmentation de la chance de recrutement des PV-INs et donc une augmentation de leur inhibition des CP. Cependant, cette plasticité n'influence pas la mémoire de peur. Le conditionnement à la peur contextuelle (CPC) induit une PLT aux synapses SC-PV. Cela augmente également l'inhibition des CP par les PV-INs et contribue à la formation de la mémoire de peur.

6.2. Implications des résultats dans la formation et la régulation des fonctions mnésiques.

6.2.1. Rôle des différents interneurones et de leur plasticité dans la régulation des circuits de CA1 dans les fonctions mnésiques.

Le rôle des différents interneurones dans la régulation des fonctions mnésiques de l'hippocampe dépend de nombreux paramètres dont l'influence demeure à être démontrée dans la majorité des cas.

Encodage de la mémoire de peur contextuelle.

Pour l'encodage de la mémoire contextuelle de peur, nos travaux et ceux d'autres équipes montrent que l'activité des SOM-INs et l'induction de la PLT des synapses CP-SOM sont importantes durant l'apprentissage (figure 1) (Lovett-Barron M. *et al.*, 2014; Asgarihafshejani A. *et al.*, 2022) alors que l'activité et la PLT des PV-INs sont importantes durant la consolidation (Lovett-Barron M. *et al.*, 2014; Ognjanovski N. *et al.*, 2017; He X. *et al.*, 2021). Néanmoins, il semblerait que tous les PV-INS n'encodent pas tous les types de mémoire.

Il existe des sous-types de cellules en panier parvalbuminergiques (CPn-PV) qui répondent différemment en fonction de la forme d'apprentissage (tableau 1). On différencie ces cellules par rapport au moment où elles sont apparues durant la neurogenèse des PV-INs (entre les jours embryonnaires (E) 9.5 et 15.5 chez la souris) (Donato F. *et al.*, 2015). Les CPn-PV nées tôt (avant E13.5) voient leur parvalbumine et leur glutamate décarboxylase 67 augmentées, ainsi que leurs entrées excitatrices augmentées spécifiquement à la suite d'un apprentissage en une fois, tel que le conditionnement à la peur contextuelle, ou à la fin d'un apprentissage progressif. En retour, elles inhibent plus particulièrement les cellules pyramidales profondes. Les CPn-PV qui sont nées tardivement (après E13.5) voient l'expression de la parvalbumine et glutamate décarboxylase 67

diminuées, ainsi que leurs entrées inhibitrices augmentées spécifiquement à la suite d'un enrichissement de l'environnement, ou au début d'un apprentissage spatial progressif comme la piscine de Morris. Ces cellules innervent plus particulièrement les cellules pyramidales superficielles. (Donato F. *et al.*, 2013; Donato F. *et al.*, 2015). Ainsi tous les PV-INs ne sont pas intégrés au réseau de la même façon en fonction de l'avancée de l'encodage d'un souvenir. Les CPn-PV nées tardivement promeuvent donc la plasticité du circuit en diminuant leur inhibition des cellules pyramidales superficielles durant l'apprentissage. Une fois que l'apprentissage est fini, les CPn-PV nées tôt promeuvent la stabilité du circuit hippocampique en augmentant leur contrôle des cellules pyramidales profondes (Donato F. *et al.*, 2015).

Un élément supplémentaire distingue les CPn-PV nées tôt et celles nées tard. Les premières ont une diminution de l'expression du *myocyte Enhancer Factor 2* (MEF2), un facteur de transcription dépendant de l'activité, à la suite d'un conditionnement à la peur, alors que les CPn-PV nées tard ont une diminution du MEF2 après un apprentissage spatial (Donato F. *et al.*, 2013). MEF2 peut être activé par une augmentation du calcium intracellulaire et l'activation de la voie de signalisation PI3K-AKT (Chen X. *et al.*, 2017). Ces signaux d'activité déclenchent également la voie de signalisation de mTORC1 (Costa-Mattioli M. *et al.*, 2009). Dans nos expériences, l'activité de mTORC1 et la PLT_{EI} des PV-INs qui en dépend n'étaient pas nécessaires pour la mémoire de peur contextuelle (Chapitre V). Il serait intéressant de voir si elles sont impliquées dans la spécialisation des CPn-PV nées tard et l'apprentissage progressif.

Tableau 1 : récapitulatif des changements entraînant la spécialisation des CPn-PV

	CPn-PV nées tôt	*CPn-PV nées tard*
Conditionnement à la peur ou fin d'apprentissage	↗ PV, GAD 67, ↗ Synapses excitatrices ↗ Inhibition des CP profondes ↘ MEF2	Pas de changement
Début d'apprentissage progressif	Pas de changement	↘ PV, GAD 67, ↗ Synapses inhibitrices ↘ Inhibition des CP superficielles ↗ MEF2

CPn-PV cellules en panier parvalbuminergiques, PV : parvalbumine, GAD 67 glutamate décarboxylase 67, MEF2 : *myocyte Enhancer Factor 2,* ↗ augmentation, ↘ diminution.

Les SOM-INs proviennent de deux origines embryonnaires, l'éminence ganglionnaire médiane et l'éminence ganglionnaire caudale. Celles qui émergent de l'éminence ganglionnaire médiane expriment le marqueur spécifique des neurones de cette aire, le facteur de transcription NK2 homeobox 1 (Nkx-2.1), alors que celles qui émergent de l'éminence ganglionnaire caudale expriment le récepteur à la sérotonine 5-HT-$_{3A}$. Les deux types d'interneurones participent aux oscillations de CA1 de façon différente et le recrutement des SOM-INs qui expriment 5-HT-$_{3A}$ dépend fortement de la présence de sérotonine (Chittajallu R. *et al.*, 2013). De plus, la neurogenèse de ces deux groupes de SOM-INs ne se fait pas en même temps, dans l'éminence ganglionnaire caudale elle a lieu de E 9.5 à E 15.5 alors que dans l'éminence ganglionnaire médiane elle a lieu de E 12.5 à E 16.5 (Miyoshi G. *et al.*, 2010). Il serait donc intéressant d'étudier si ces deux types de SOM-INs encodent des apprentissages différents comme les CPn-PV nées tôt ou nées tard.

Encodage de la mémoire spatiale.

Dans le chapitre II, nous montrons que la PLT des synapses CP-SOM est suffisante pour moduler la métaplasticité du réseau de CA1, résultant en une diminution de PLT de la voie temporoammonique (TAP) sur les dendrites distales des CP-CA1 et une augmentation de la PLT des collatérales de Schaffer (SC) sur les dendrites proximales des CP-CA1 (figure 1).

Lors de l'apprentissage spatial dans une piste linéaire, durant les premières sessions, l'activité des CP-CA1 est fortement influencée par les afférences de la TAP. Au fur et à mesure de l'apprentissage, les SC vont prendre le dessus sur la TAP dans l'influence de la décharge des CP-CA1, ce qui augmente le couplage des rythmes de CA3 et CA1 en fin d'apprentissage (Fernández-Ruiz A. *et al.*, 2017). En fait, ces changements de couplage n'ont pas lieu de la même façon dans toutes les CP de CA1. Lors des premières sessions d'exploration d'un apprentissage, l'activité des CP profondes est entrainée par les entrées du cortex entorhinal. En conséquence, ces CP ont un taux de décharge plus important lors des premiers essais, qui diminue au cours de l'apprentissage. Par opposition les CP superficielles sont plus particulièrement entrainées par les entrées de CA3 et ont une activité faible lors des premiers essais, qui augmente au fur et à mesure de l'apprentissage. Les CP superficielles ont une probabilité de transmission de décharge égale pour les PV-INs que pour les SOM-INs, alors que les CP profondes ont une probabilité de transmission accrue pour les SOM-INs (Fernández-Ruiz A. *et al.*, 2017). Ceci concorde avec nos résultats selon lesquels l'apprentissage provoque la PLT des synapses CP-SOM et le rôle de cette PLT dans la métaplasticité du réseau. Cela corrobore également le fait que les PV-INs nés tôt augmentent l'inhibition des CP profondes à la fin de l'apprentissage, alors que les PV-INs nés tard, qui inhibent les CP superficielles ont leurs propres entrées inhibitrices augmentées lors de l'apprentissage ce qui désinhibe progressivement les CP ciblées (Donato F. *et al.*, 2013).

Au cours d'une tâche d'alternance retardée dépendante de la mémoire spatiale et épisodique dans un labyrinthe en 8, les souris commencent leur exploration dans le bras central et doivent apprendre à choisir en alternance entre tourner à gauche ou à droite pour recevoir une récompense. Une fois que la tâche est apprise, la cohérence entre les rythmes gamma de CA3 et de CA1 est plus forte dans le bras central que dans les bras périphériques. À l'inverse, le couplage entre l'activité du cortex entorhinal et CA1 est plus fort dans les bras périphériques. Ces changements de couplages n'ont pas lieu dans les sessions où l'animal se trompe, ce sont donc des

phénomènes liés au fonctionnement de la mémoire (Fernández-Ruiz A. *et al.*, 2017). Dans le bras central, l'animal doit se référer à ses souvenirs pour prédire dans quel bras la récompense se trouvera, il utilise donc en priorité les informations venant de CA3 (Montgomery S. M. & Buzsáki G., 2007; Schomburg Erik W. *et al.*, 2014; Fernández-Ruiz A. *et al.*, 2017; Colgin L. L., 2020). Alors qu'une fois que ce choix est fait, il doit se diriger vers la récompense, et pour cela mettre en relation ses souvenirs venant de CA3 et les informations spatiales venant du cortex entorhinal (Knierim J. J. *et al.*, 2014; Schomburg Erik W. *et al.*, 2014; Fernández-Ruiz A. *et al.*, 2017; Colgin L. L., 2020). Ainsi, le routage de l'information diffère en fonction de l'état de l'apprentissage, et de la tâche effectuée (Schomburg Erik W. *et al.*, 2014; Fernández-Ruiz A. *et al.*, 2017; Colgin L. L., 2020). Par conséquent, le recrutement des interneurones par les différentes CP devrait différer aussi en fonction de la tâche effectuée, si elle nécessite que l'on se repose plus ou moins sur les connaissances acquises ou sur les informations disponibles dans l'environnement.

De tels changements dans les préférences de connexions entre les différentes CP et les PV-INs ou les SOM-INs sont observés selon la complexité de l'environnement dans lequel l'animal évolue. Lors de la navigation dans un environnement riche en indices, les CP profondes sont plus susceptibles de former des champs de lieu (Sharif F. *et al.*, 2021). L'activation majoritaire des CP profondes dans ce type d'environnement vient de leurs connexions préférentielles avec le cortex entorhinal (Sharif F. *et al.*, 2021) qui transmet les nombreuses informations spatiales disponibles dans cet environnement (Knierim J. J. *et al.*, 2014). Durant de ce type de tâche, les PV-INs sont majoritairement recrutées, mais une grande variété d'interneurones semble activée dans ce type de navigation (Sharif F. *et al.*, 2021). Les CP superficielles de leur côté sont plus susceptibles de former des champs de lieu dans un environnement pauvre en indices, où elles reçoivent des informations principalement de CA3 (Sharif F. *et al.*, 2021). Ce qui suggère que dans ce cas, la navigation se base sur la prédiction de la position avec l'association d'éléments contextuels (Montgomery S. M. & Buzsáki G., 2007). Pendant ce type de navigation, ce sont les SOM-INs, qui sont majoritairement recrutés (Sharif F. *et al.*, 2021).

Dans leur ensemble, ces travaux suggèrent que lors de l'apprentissage les CP profondes sont activés par leurs entrées du cortex entorhinal et recrutent plus particulièrement les SOM-INs ce qui sélectionne les entrées pertinentes du cortex entorhinal, diminue globalement ces entrées et

graduellement promeut la PLT des entrées de CA3 qui seront réactivées lors des rappels. De leur côté les CPn-PV nées tard inhibent les CP superficielles.

À la fin de l'apprentissage CPn-PV nées tard sont fortement inhibées, les CP superficielles ont leur activité augmentée par les entrées de CA3 et recrutent les SOM-INs, et les CPn-PV nées tôt, ce qui inhibe les CP profondes. Lors de la prise de décision, ou la navigation dans un environnement pauvre en indices, l'activité du réseau ressemble à celle à la fin de l'apprentissage avec l'entraînement par CA3 des CP superficielles, mais ici ces CP recrutent plus particulièrement les SOM-INs. Enfin dans un environnement familier où il est facile de se repérer, une grande variété d'interneurones sont recrutés, mais particulièrement les PV-INs.

En conséquence, il est critique de déterminer précisément les conditions dans lesquelles on étudie le rôle des interneurones de l'hippocampe. Cependant, il faut noter que dans la globalité, les SOM-INs est les PV-INs sont plutôt actifs pendant la locomotion et plutôt inactifs durant l'immobilité mise à part durant les SWR pour les PV-INs (Geiller T. *et al.*, 2020). De plus, tout comme les CP, un sous ensemble discret de PV-INs et SOM-INs a une préférence de lieu et peut démontrer une corrélation positive ou négative avec un endroit précis de l'environnement (Colgin L. L., 2020; Geiller T. *et al.*, 2020). Cela suggère que l'activité de ces interneurones est liée à celle des cellules de lieu de leur réseau. Comme dans CA1 la majorité des cellules qui composent l'engramme sont des cellules de lieu, cet ensemble d'interneurones montrant une préférence de lieu pourrait également être lié à l'engramme (Colgin L. L., 2020; Josselyn S. A. & Tonegawa S., 2020).

6.2.2. Rôle des interneurones dans la régulation de l'engramme

Activité des interneurones durant la formation de l'engramme

La sélection des neurones qui composent l'engramme se fait notamment par une augmentation de l'excitabilité intrinsèque des CP (Josselyn & Frankland, 2018). Le conditionnement au clignement de l'œil différé provoque une augmentation de l'excitabilité intrinsèque des CP de CA1 médié par une augmentation de l'excitabilité intrinsèque des SOM-INs aussi produite durant ce conditionnement (McKay B. M. *et al.*, 2013). Mais nous ne savons pas si des formes d'apprentissage induisent une augmentation de l'excitabilité intrinsèque des PV-INs.

L'augmentation de l'excitabilité intrinsèque d'un neurone accroit sa réponse indépendamment de modifications synaptiques. Or, pour que la mémoire soit fidèle, il faut que seule une fraction des CP fasse partie de l'engramme (Josselyn S. A. & Tonegawa S., 2020). Il y a donc nécessité d'un processus de sélection des cellules qui vont être plus particulièrement excitées afin de conserver la précision d'un souvenir.

Dans le gyrus denté, l'inhibition chémogénétique des SOM-INs durant le conditionnement à la peur contextuelle et sa consolidation, puisque la fenêtre d'activation avec cet outil est de plusieurs heures (Campbell E. J. & Marchant N. J., 2018), provoque une augmentation de la taille de l'engramme et du comportement d'immobilité durant les tests 24 h ou une semaine après le conditionnement. Augmenter l'activité des SOM-INs réduit la taille de l'engramme et le comportement d'immobilité durant le test une semaine après. Ce qui démontre que ces interneurones ont un rôle de sélection des CP faisant partie de l'engramme (Stefanelli T. *et al.*, 2016). Par opposition, l'activation chémogénétique des PV-INs durant ce conditionnement et sa consolidation, n'a pas d'effet sur la mémoire de peur ni la taille de l'engramme (Stefanelli T. *et al.*, 2016).

Dans CA1 c'est différent puisque l'inactivation optogénétique des SOM-INs durant le conditionnement réduit fortement la mémoire de peur dans le test 24 h après (Lovett-Barron M. *et al.*, 2014; Asgarihafshejani A. *et al.*, 2022) et l'inactivation chémogénétique des PV-INs durant la consolidation diminue la mémoire de peur, la réactivation cohérente des ensembles neuronaux et la stabilité du réseau (Ognjanovski N. *et al.*, 2017).

Dans CA1, l'activité des interneurones tout comme les CP est différente selon la position de l'animal dans l'environnement. Lors du passage dans un champ de lieu l'activité des SOM-INs augmente (Royer S. *et al.*, 2012; Fernández-Ruiz A. *et al.*, 2017). Cela accroit l'encodage spatial en synchronisant les entrées corticales et inhibant les informations hors cible dans le champ de lieu (Royer S. *et al.*, 2012; Grienberger C. *et al.*, 2017). De leur côté, les PV-INs qui hyperpolarisent le corps cellulaire et l'axone des CP (Glickfeld L. L. *et al.*, 2009), sont donc inhibés lors du passage dans le champ de lieu, ce qui désinhibe CP et augmente leur fréquence de décharge (Royer S. *et al.*, 2012; Fernández-Ruiz A. *et al.*, 2017). Cependant, ce n'est pas le cas pour tous les SOM-INs et PV-INs puisque dans certains de ces interneurones l'activité inverse est observée en relation à la

position de l'animal dans l'environnement (Geiller T. *et al.*, 2020). Ainsi, ces interneurones semblent avoir une activité adaptée aux CP qu'ils contactent.

Si on essaye d'induire des champs de lieu de façon artificielle, en même temps dans plusieurs CP proches, cette induction sera moins fructueuse que si l'on induit un champ de lieu dans une seule CP (Rolotti S. V. *et al.*, 2022). Ceci est dû au phénomène de compétition entre les CP pour faire partie de l'engramme. Lors de l'apprentissage ou de la stimulation d'un groupe de CP, plusieurs CP vont voir leur excitabilité augmenter. Parmi ces CP un petit groupe des cellules les plus excitables sera alloué à l'engramme. Plusieurs études supportent le fait que ce mécanisme de compétition est régulé par les interneurones (Rao-Ruiz P. *et al.*, 2019). En effet, inhiber l'activité des interneurones durant l'induction artificielle de champ de lieu dans plusieurs CP contiguës diminue fortement le phénomène de compétition (Rolotti S. V. *et al.*, 2022). Par conséquent, l'augmentation de l'activité des interneurones dans le champ de lieu pourrait refléter cette compétition. La population de CP activées entrainant l'augmentation de l'activité des interneurones, qui en retour inhibent l'activité de cette population de CP et seule la CP la plus excitée gagne l'allocation. Néanmoins il semble que ce ne soit pas le seul mécanisme par lequel l'inhibition puisse réguler l'allocation des CP. Au contraire, les interneurones qui contactent la CP dans laquelle le champ de lieu a été formé ont une légère baisse d'activité dans le champ de lieu ainsi créé. Cette reconfiguration de l'inhibition n'a pas lieu tout de suite après l'induction du champ de lieu, mais entre la session d'induction et la session d'exploration suivante, ce qui suggère un mécanisme de plasticité à long terme (Geiller T. *et al.*, 2022). Malheureusement, ces travaux ne permettent pas de savoir quels types d'interneurones ont leur activité diminuée ou augmentée en fonction du fait qu'ils innervent les cellules de lieu formée ou non. Mais cela concorde avec le fait que les PV-INs qui sont l'un des types majoritaires d'interneurone ont leur activité diminuée à l'entrée du champ de lieu (Royer S. *et al.*, 2012; Pelkey K. A. *et al.*, 2017).

Collectivement, ces études semblent montrer que l'activité des interneurones est différente selon qu'ils régulent les CP qui font partie d'un engramme, ou qu'ils contrôlent les autres CP qui doivent rester silencieuses à ce moment-là, afin que la mémoire soit précise. De plus ces changements ne se faisant pas de manière instantanée, mais après une période de consolidation, il semble que la plasticité des interneurones joue un rôle clef dans la formation et la régulation des engrammes.

Le contrôle sélectif de l'activité des CP par la plasticité des synapses inhibitrices.

Les SOM-INs et PV-INs contactent en moyenne 1500 et 2500 CP respectivement (Pelkey K. A. *et al.*, 2017). Puisque les interneurones sont moins nombreux que les CP, et qu'à chaque moment seulement une partie des CP encodent pour un lieu, les régulations de l'activité des CP par les interneurones doivent être très dynamique et spécifique à une cellule pour exercer un contrôle différent des cellules qui doivent être activées et celles qui doivent être silencieuses. Au cours de cette thèse, nous avons beaucoup présenté les régulations de l'entrée des interneurones, c'est-à-dire leur compartiment postsynaptique. Mais une autre façon d'effectuer un contrôle sélectif des différentes cibles neuronales est de réguler la sortie des interneurones, c'est-à-dire leur compartiment présynaptique. La stimulation optogénétique en bouffée thêta des SOM-INs provoque la potentialisation de leurs synapses inhibitrices (I-PLT) sur les CP, tandis que la même stimulation des PV-INs provoque une dépression de leurs synapses inhibitrices (I-DLT) sur les CP. Il est important de noter que ces mécanismes plastiques sont dépendant de la dépolarisation concomitante des CP. En fait, les synapses inhibitrices des PV-INs et SOM-INs sur les CP (PV-CP et SOM-CP) suivent une plasticité dépendante du temps de décharge (*spike-timing dependent*) (Udakis M. *et al.*, 2020). Ces règles de plasticité sont cohérentes avec la préférence de phase de ces interneurones et des CP dans le cycle thêta. Lors des oscillations thêta, les PV-INs ont une préférence de phase dans la pente descendante du thêta, 60 ms avant les SOM-INs et CP qui eux déchargent légèrement après le creux du thêta (Somogyi P. *et al.*, 2014). Dans cette configuration du circuit, les PV-INs sont stimulés 60 ms avant la stimulation des CP, cela induit une légère I-DLT des synapses PV-CP. Les SOM-INs sont stimulés en même temps que les CP, et cela produit une I-PLT des synapses SOM-CP. Dans les deux cas, si les CP sont stimulées 60 ms avant les interneurones, il n'y a pas de plasticité (Udakis M. *et al.*, 2020). Lors de la traversée d'un champ de lieu, l'activité de la cellule de lieu se décale progressivement plus tôt dans le cycle, on appelle cela la précession de phase. Typiquement, ce décalage de la décharge des CP est de 180 degrés, donc proche de la préférence de phase des PV-INs (Somogyi P. *et al.*, 2014; Drieu C. & Zugaro M., 2019). Dans cette configuration du circuit, les PV-INs sont stimulées en même temps que les CP, ce qui provoque une I-DLT des synapses PV-CP plus prononcée. Les CP sont stimulée 60 ms avant les SOM-INs ce qui ne provoque pas de plasticité. Enfin, si les CP sont stimulées 60 ms après les SOM-INs, cela provoque une I-DLT (Udakis M. *et al.*, 2020). Par conséquent, la stimulation

des interneurones aura un effet différent sur le contrôle de l'activité des CP selon le moment où elles déchargent durant le cycle thêta.

Rôle des interneurones dans la consolidation de l'engramme.

Une autre étape importante de la formation de l'engramme est sa consolidation. À travers leur régulation des SWR les PV-INs ont un rôle important dans cette étape de la formation de la mémoire (Ognjanovski N. *et al.*, 2017). En effet, les fibres de CA3 sont spécialisées dans un type d'information (par exemple visuelle, olfactive, somesthésique). Seules les afférences de CA3 comportant des informations pertinentes relatives à une expérience vécue en voie d'être consolidées sont réactivées durant les réactivations séquentielles alors que les afférences qui apportent des informations non pertinentes sont supprimées (Terada S. *et al.*, 2022). Ainsi la régulation de la consolidation par les PV-INs semble spécifique au fait que la cellule appartient ou non à l'engramme. Étant donné que la majorité des cellules ne font pas partie d'un engramme donné, il serait intéressant d'étudier si la PLT_{EI} des PV-INs joue un rôle dans la suppression des informations non pertinentes. Dans nos travaux, nous n'avons pas vu de modification de la discrimination dans les PV-Raptor KOs (qui ont un déficit de la PLT_{EI} des PV-INs) par rapport aux souris contrôles. Cependant nous avons utilisé un protocole de conditionnement à la peur contextuelle très fort, et la diminution du comportement d'immobilité dans le contexte neutre était subtile. Ceci montre que ce type de conditionnement induit une forte généralisation, donc probablement une moindre sélection des informations pertinentes. Il serait donc intéressant de voir si dans un apprentissage moins massif, tel que la mémorisation de localisation d'objets (Korotkova T. *et al.*, 2010), la PLT_{EI} des PV-INs joue un rôle dans la suppression des informations non pertinentes.

6.2.3. Implication des afférences neuromodulatrices

Notre observation de l'interaction du TBS_{opto} avec la PLT des synapses CP-SOM induite par le conditionnement à la peur contextuelle soulève la question intéressante de l'origine de cette interaction. Pour rappel, nous avons étudié ces mécanismes en tranche, et trouvé que deux inductions électriques consécutives produisent des PLT des synapses PC-SOM qui s'additionnent. Une première PLT électrique sature une PLT_{opto} subséquente. De même qu'une première PLT_{opto}

sature la PLT_{opto} suivante. Enfin, la PLT_{opto} est dépotentialisée par l'induction d'une PLT électrique. La différence entre les inductions optogénétique et électrique est ce qui est stimulé. Le TBS_{opto} n'active que les terminaisons des CP locales, il y a donc stimulation des récepteurs glutamatergiques des synapses CP-SOM. La stimulation électrique recrute toutes les fibres locales, y compris les afférences neuromodulatrices venant des structures sous-corticales, tout comme l'apprentissage. Ainsi, les différentes interactions entre les protocoles d'inductions de PLT des synapses CP-SOM pourraient émerger du fait qu'il y ait ou non recrutement d'afférences neuromodulatrices.

De nombreux travaux démontrent que les neuromodulateurs contribuent à la formation de la mémoire à travers leur rôle de modulateurs de la plasticité (Palacios-Filardo J. & Mellor J. R., 2019). Les SOM-INs de CA1 expriment de nombreux récepteurs à l'acétylcholine, dopamine, sérotonine, et adrénaline (Cox D. J. *et al.*, 2008; Tricoire L. *et al.*, 2011; Mikulovic S. *et al.*, 2015; Puighermanal E. *et al.*, 2017; Nicholson E. & Kullmann D. M., 2021).

L'acétylcholine

Le septum et la bande diagonale de Broca sont les sources majeures d'acétylcholine dans l'hippocampe (Haam J. & Yakel J. L., 2017). L'activation des récepteurs cholinergiques seuls induit une PLT des courants excitateurs des interneurones de l'oriens/alvéus. Cependant, elle produit une occlusion de la PLT électrique subséquente, de même qu'une première PLT électrique produit une occlusion de la PLT cholinergique (Nicholson E. & Kullmann D. M., 2021). Dans le néocortex, de tous les neuromodulateurs, l'acétylcholine est celui qui augmente le plus les courants excitateurs entre les CP et les SOM-INs, non pas lors d'une coactivation des afférences cholinergiques et glutamatergiques, mais lorsque les afférences glutamatergiques sont stimulées 200 ms après l'activation des afférences cholinergiques, ce qui suggère que le timing précis de l'entrée cholinergique est important pour son rôle dans la régulation des synapses PC-SOM (Urban-Ciecko J. *et al.*, 2018). Dans CA1, l'activation des fibres cholinergiques est nécessaire pour la formation de la mémoire de peur (Lovett-Barron M. *et al.*, 2014), elle-même dépendante de la PLT des SOM-INs (Asgarihafshejani A. *et al.*, 2022). Dans les souris APP/PS1 modèles de la maladie d'Alzheimer, le nombre d'entrées cholinergiques des SOM-INs est diminué tandis que le nombre de neurones cholinergiques est inchangé. Ces souris souffrent d'un déficit de la mémoire de peur

contextuelle, accompagné d'une perte de l'augmentation des épines des SOM-INs liée à l'apprentissage. Cette augmentation des épines des SOM-INs liée à l'apprentissage est dépendante des entrées cholinergiques (Schmid L. C. *et al.*, 2016). Ainsi l'acétylcholine a un effet potentialisateur des synapses des SOM-INs durant l'apprentissage, qui pourrait s'additionner à la PLT mGluR1 dépendante. Cependant il se pourrait que la PLT cholinergique bloque d'autres inductions subséquentes, la dynamique de libération de l'acétylcholine est donc un point clef de la régulation de la mémoire.

La dopamine

La transmission dopaminergique de l'hippocampe provient de deux sources. L'aire tegmentale ventrale innerve particulièrement la partie ventrale de l'hippocampe et dans une moindre mesure la partie dorsale dont la source principale de dopamine provient des neurones noradrénergiques du locus coeruleus (Kempadoo K. A. *et al.*, 2016). Le rôle de la dopamine dans la régulation de la plasticité des SOM-INs demeure inconnu, cependant dans les PV-INs de l'aire CA3 ventrale l'activation des récepteurs à la dopamine de type 1 plusieurs heures après l'induction d'une PLT ou l'apprentissage est nécessaire pour la consolidation de leur plasticité synaptique et la mémoire de peur. Des résultats similaires sont obtenus dans CA1, mais l'effet est plus grand dans la portion ventrale de CA3 (Karunakaran S. *et al.*, 2016). La libération de dopamine ne se faisant pas de façon synaptique, mais par transmission de volume (Descarries L. & Mechawar N., 2000; Liu C. *et al.*, 2021). On peut imaginer que les SOM-INs qui expriment aussi les D1 pourraient également avoir leur PLT consolidée par la dopamine. Cependant il faut tenir compte du fait que les PV-INs et SOM-INs expriment également les récepteurs à la dopamine de type 2 qui sont des récepteurs métabotropes inhibiteurs (Puighermanal E. *et al.*, 2017). Les récepteurs D2 sont 10 à 100 fois plus sensibles à la dopamine que les D1 et sont donc activés par une libération tonique de dopamine à faible concentration. Les D1 quant à eux sont activés lors de décharges en bouffées des neurones dopaminergiques (Martel J. C. & Gatti McArthur S., 2020). Une réduction de la consolidation peut donc également être médiée par la dopamine. Ce neuromodulateur peut réguler la plasticité des collatérales de Schaffer induite par l'apprentissage de façon bidirectionnelle via l'activation des récepteurs de la famille D1. L'activation de ces récepteurs durant l'apprentissage et le début de la consolidation (injection intracérébroventriculaire d'un agoniste) module la mémoire spatiale et de localisation d'objets, mais leur blocage par un antagoniste n'affecte pas ces

mémoires (Lemon N. & Manahan-Vaughan D., 2006). ll reste à montrer dans quelles conditions les D1 ou les D2 sont activés dans les interneurones de l'hippocampe.

La noradrénaline

Le rôle de la noradrénaline dans la régulation de la plasticité des SOM-INs n'est pas non plus connu. Or, le locus coeruleus envoie des afférences noradrénergiques à CA1 apportant des informations liées aux états émotionnels d'anxiété, de vigilance, et d'attention (Benarroch E. E., 2018). La stimulation des récepteurs noradrénergiques de l'hippocampe dorsal augmente la consolidation de la mémoire de peur et la mémoire de localisation d'objet (Bevilaqua L. *et al.*, 1997; Song Q. *et al.*, 2021). L'activation des afférences du locus coeruleus augmente l'encodage spatial par les cellules de lieu, mais seulement à proximité d'une zone de récompense (Kaufman A. M. *et al.*, 2020). Cependant, les fibres du locus coeruleus libèrent également de la dopamine, donc cet effet pourrait être lié à la libération de l'une, l'autre, ou la co-libération des deux catécholamines (Kempadoo K. A. *et al.*, 2016). Comme la dopamine, la noradrénaline module de façon bidirectionnelle la plasticité. La direction de la modulation dépend des récepteurs activés. Les récepteurs β adrénergiques potentialisent les synapses tandis que l'effet des récepteurs α 1 dépend de la dose de noradrénaline accumulée. Plus elle s'accumule, plus elle provoque de DLT (Dyer-Reaves K. *et al.*, 2019). Les SOM-INs expriment les récepteurs β 1 et 2 (récepteurs métabotropiques couplés aux Gs), mais aussi α1 (récepteurs métabotropiques couplés aux Gq) (Papay R. *et al.*, 2006; Cox D. J. *et al.*, 2008). Ces interneurones sont donc largement équipés pour être modulés par les entrées noradrénergiques.

Les neuromodulateurs sont libérés par transmission de volume (Marder E., 2012). Les astrocytes ont leur activité modulée par les neuromodulateurs, régulent la concentration de neurotransmetteur extracellulaire, et la transmission pré et post-synaptique des SOM-INs. Ce type cellulaire majoritaire dans le système nerveux central pourrait donc jouer un rôle important dans la régulation de la plasticité par les neuromodulateurs (Pacholko A. G. *et al.*, 2020; Honore E. *et al.*, 2021; Wahis J. & Holt M. G., 2021).

Interaction du TBS_{opto} avec la libération tonique de neuromodulateurs.

À la lumière de toutes ces informations, on peut alors se demander si les interactions opposées entre le TBS_{opto}, le conditionnement à la peur (diminution), et la tâche de mémorisation de localisation d'objets (augmentation) sont seulement dues au fait que l'un ait probablement induit une PLT subséquente et donc dépotentialisé les synapses CP-SOM alors que l'autre n'a probablement pas induit une potentialisation. L'activité tonique ou phasique des neurones dopaminergiques qui active les D2 et D1 respectivement encode des types de mémoire différents. Des souris dont l'activité phasique des interneurones dopaminergiques est supprimée ont une mémoire spatiale de travail et une mémoire de reconnaissance d'objets intacte alors que leur mémoire de peur indicée est diminuée de même que la mémoire spatiale dans la piscine de Morris, et la préférence de place conditionnée (Zweifel L. S. *et al.*, 2009). L'activité tonique ou phasique des neurones du locus coeruleus est aussi différente dans les tâches qui requièrent de l'attention ou dirigées par un but par rapport aux comportements exploratoires (Usher M. *et al.*, 1999). Une explication alternative de l'interaction différente entre le TBS_{opto}, le conditionnement à la peur, et la tâche de mémorisation de localisation d'objets, serait que les cocktails de neuromodulateurs, leur répartition dans le temps et l'espace pourraient être différents selon les types de mémoire à encoder et qu'ils aient interagi de façon différente avec la PLT optogénétique des SOM-INs.

6.3 Développements futurs

Bien que nos expériences démontrent un effet du TBS_{opto} sur les propriétés synaptiques des SOM-INs *in vivo*, une question demeure irrésolue : 'Le TBS_{opto} a-t-il effectivement induit une PLT aux synapses PC-SOM *in vivo* ?'. Étant donné que la PLT induite par le TBS_{opto} est transitoire *in vitro*, nous supposons qu'il en est de même *in vivo*. Donc pour prouver que ce protocole induit une PLT des synapses CP-SOM *in vivo*, il faut enregistrer l'activité synaptique des SOM-INs *in vivo*. Pour cela, on pourrait imager les signaux calciques transitoires dendritiques des SOM-INs qui traduisent l'activité synaptique de ces neurones (Oh J. *et al.*, 2019). Pour induire le TBS_{opto}, il faudrait utiliser la même channelrhodopsine que dans nos expériences, ou une autre ayant une cinétique d'activation au moins aussi rapide exprimée dans les CP. Les channelrhodopsines sont fusionnées à des protéines fluorescentes pour pouvoir facilement identifier leur lieu d'expression.

Il faudrait donc une combinaison telle que la longueur d'onde d'excitation de la channelrhodopsine ainsi que de sa protéine fluorescente et celle de l'indicateur calcique soient suffisamment distantes pour que la visualisation de l'indicateur calcique ne stimule pas la channelrhodopsine. Il faut également vérifier que l'émission de l'indicateur calcique ne stimule pas la channelrhodopsine. De tels outils existent et pourraient être utilisés dans nos souris SOM-Cre, la channelrhodopsine ChETA (spectre d'excitation 425 à 550 nm (Renault R. *et al.*, 2015)), fusionnée à la EYFP (spectre d'excitation 450 à 590 nm 1 photon ; pic à 970 nm 2 photons, olympus-lifescience fpcolorpalette (Spiess E. *et al.*, 2005)) exprimée dans les cellules pyramidales de CA1, et l'indicateur calcique rouge jRGECO1a, exprimé dans les SOM-INs, stimulé en fin de pic d'excitation (excitation 1150 nm 2 photons, émission 650 nm (Dana H. *et al.*, 2016)). Ainsi, puisque la plasticité des SOM-INs est liée à une augmentation en amplitude et en fréquence des évènements synaptiques spontanés (Artinian J. *et al.*, 2019; Asgarihafshejani A. *et al.*, 2022), une augmentation en amplitude et en fréquence des évènements calciques transitoires refléterait une potentialisation des synapses CP-SOM. Cependant la stimulation du jRGECO1a pourrait stimuler légèrement la EYFP ce qui augmenterait le bruit de fond et pourrait rendre la détection des évènements calciques transitoires difficiles (Spiess E. *et al.*, 2005; Dana H. *et al.*, 2016).

Suivant cette question, nous avons également soulevé le fait que nous ne savons pas si la plasticité induite par le TBS_{opto} a lieu aux synapses de toutes les SOM-INs. En effet, dans CA1 il existe de nombreux sous-types de SOM-INs. Notamment les cellules oriens-lacunosum moleculare, les cellules bistratifiées et les cellules de projection (Honore E. *et al.*, 2021). En utilisant la même méthode que dans le paragraphe précédent, couplée à l'enregistrement de potentiels de champs locaux dans l'hippocampe controlatéral, nous pourrions identifier les cellules bistratifiées par leur capacité à décharger lors des SWR (Geiller T. *et al.*, 2020) puis identifier des dendrites appartenant à ces cellules pour les imager avant et après le $TBS_{opto.}$ Étant donné l'importance des neuromodulateurs sur le recrutement et la plasticité des cellules oriens-lacunosum moleculare (Leao R. N. *et al.*, 2012; Chittajallu R. *et al.*, 2013), nous pourrions aussi vérifier s'il y a un effet différent du TBS_{opto} sur les cellules oriens-lacunosum moleculare exprimant le récepteur nicotinique CHRNA2 grâce aux souris Chrna2-cre (Leao R. N. *et al.*, 2012). Finalement, peu de choses sont connues sur les SOM-INs de projection. Cependant, ils semblent avoir un rôle dans la synchronisation des structures connectées à l'hippocampe et des deux hippocampes ensemble (Wang Y. *et al.*, 2014; Kang D. *et al.*, 2017; Sun Y. *et al.*, 2019). Il serait donc intéressant de voir

si ces interneurones, qui peuvent exprimer mGluR1 (Jinno S. *et al.*, 2007), sont potentialisés par le TBS_{opto}. Pour le savoir, il faudrait utiliser un vecteur viral infectant de façon rétrograde et dont l'expression dépend de la recombinase cre pour faire exprimer l'indicateur calcique jRGECO1 dans les SOM-INs en injectant ce virus dans les structures cibles de ces interneurones

Une autre question soulevée par nos travaux est : 'Comment le TBS_{opto} interagit-il avec la plasticité induite par l'apprentissage ?' Le conditionnement à la peur contextuelle provoque une PLT des synapses PC-SOM (Artinian J. *et al.*, 2019; Asgarihafshejani A. *et al.*, 2022) et une augmentation du nombre d'épines dendritiques des SOM-INs (Schmid L. C. *et al.*, 2016). Puisque la PLT est liée à l'augmentation du nombre d'épines (Malenka R. C. & Bear M. F., 2004), une façon de répondre à cette question serait d'imager les dendrites des SOM-INs *in vivo*, dans des souris exprimant une protéine fluorescente dans les SOM-INs dont le spectre d'excitation est loin de celui de la channelrhodopsine, avant, et après le conditionnement dans des souris ayant reçu le TBS_{opto} et d'autres qui ne l'ont pas reçu (Schmid L. C. *et al.*, 2016). Ceci peut être fait grâce à l'utilisation de la même channelrhodopsine ChETA mentionnée dans le paragraphe précédent, exprimée dans les CP, et l'expression de la protéine fluorescente mCherry (spectre d'excitation 450 à 625 nm excitée à son pic d'absorption 595 nm, émission entre 590 et 775 nm avec un pic à 620 nm, olympus-lifescience fpcolorpalette) dans les SOM-INs. Ainsi, nous pourrions savoir si le TBS_{opto} interfère avec la plasticité structurelle induite par le comportement (Malenka R. C. & Bear M. F., 2004; Schmid L. C. *et al.*, 2016) ou si elle diminue l'activité des synapses CP-SOM par un autre mécanisme.

Finalement, nous avons montré que la PLT_{EI} des PV-INs n'était pas nécessaire pour la formation de la mémoire contextuelle de peur et la précision de cette mémoire contrairement à la plasticité synaptique de ces interneurones. Pour autant, cela ne veut pas dire que la PLT_{EI} n'est pas nécessaire dans d'autres types de mémoire. L'augmentation de l'activité de mTORC1 dans les PV-INs par la délétion cellule spécifique du gène qui encode TSC2 n'a pas d'effet non plus sur la transmission de base des PV-INs ni sur leur inhibition des CP (Zhao J.-P. & Yoshii A., 2019). Cependant, les animaux présentant cette mutation ont un déficit de comportement et mémoire sociaux. Ceci n'est peut-être pas lié à une augmentation de la $PLT_{EI,}$ mais a des changements de connectivité des PV-INs durant le développement (Amegandjin C. A. *et al.*, 2021). De plus dans les CPn-PV né tard, l'augmentation de MEF2 et des synapses inhibitrices pourrait être lié à PLT_{EI}

(Donato F. *et al.*, 2013). Cette forme de plasticité des PV-INs pourrait donc jouer un rôle dans la consolidation de la mémoire qui s'acquiert de façon graduelle. En outre, la PLT_{EI} promeut la décharge des CPn-PV à la fréquence gamma lente (Campanac E. *et al.*, 2013). La cohérence entre le rythme gamma lent de CA3 et de CA1 augmente graduellement au cours de l'apprentissage spatiale, et est un marqueur de l'activité de rappel et de prise de décision (Colgin L. L., 2015; Fernández-Ruiz A. *et al.*, 2017). Étant donné le rôle des PV-INs dans la synchronisation des rythmes gamma de CA3 et CA1 (Zemankovics R. *et al.*, 2013), la PLT_{EI} pourrait réguler d'autres types de comportements que la mémoire contextuelle de peur tels que la reconnaissance sociale ou une tâche d'alternance retardée, qui est un apprentissage spatial graduel.

6.4 Conclusion

En conclusion les travaux de cette thèse démontrent que l'activité et la plasticité des interneurones de l'hippocampe contrôlent différents aspects de la formation de la mémoire. L'activité des SOM-INs et l'induction de la plasticité des synapses CP-SOM dépendante des récepteurs mGluR1 et de mTORC1 sont nécessaire durant l'apprentissage. Ils sont aussi suffisants pour réguler l'apprentissage de la mémoire de peur et la mémorisation de localisation d'objets, ainsi que les réseaux de CA1. L'activité des PV-INs et la plasticité synaptique des PV-INs sont nécessaires durant la consolidation de l'apprentissage mais pas la plasticité de l'excitabilité intrinsèque dépendante de mTORC1.

Cependant, ceci n'est peut-être pas le cas pour tous les SOM-INs et PV-INs. Il est possible que certains SOM-INs ne démontrent pas de PLT dépendante des mGluR1 et de mTORC1 aux synapses CP-SOM. Ou encore, il se pourrait que dans certains sous types la PLT des synapses CP-SOM soit dépendante de la présence de neuromodulateurs (par exemple dans les OLM exprimant 5-HT-3A ou le récepteur nicotinique α2). De même, la PLT_{EI} dépendante de l'activité de mTORC1 pourrait être importante dans les PV-INs nés tard, qui ne sont pas recrutés dans le type de mémoire que nous avons testé.

Pour mieux comprendre la subtilité des régulations du réseau par les interneurones et la complexité des fonctions qui en émergent, il faudra prendre en compte plus de détails sur ces interneurones. Quel est leur sous-type au sein de leur classe par exemple les PV-INs nés tôt, né

tard, ou les OLM-5-HT-3A ou OLMα2. À quel moment sont-ils activés ou inactivés au cours des tâches précises (1ere ou 5ème présentation d'un environnement, cet environnement est-il riche ou pauvre en indices, fort ou faible en saillance, aversif ou attractif, est-ce que la tâche nécessite le rappel d'informations ou une prédiction. etc.). Il faudra également prendre en compte les changements plastiques qui s'opèrent dans les différents interneurones (plasticité synaptique des afférences excitatrices ou inhibitrices, ou plasticité de l'excitabilité intrinsèque) et comment ces changements modifient les dynamiques du réseau. Finalement, la régulation des interneurones dans la formation d'un champ de lieu ou de la mémoire représente la majorité des données dont nous disposons. Le maintien de la majorité des CP silencieuses lorsqu'elles ne sont pas impliquées dans le processus mnésique est tout aussi important et l'étude de ces mécanismes pourrait être approfondie.

Ainsi, les travaux de cette thèse ont permis de mettre en évidence les rôles spécifiques de la plasticité des interneurones somatostatinergiques et parvalbuminergiques dans les mécanismes de mémoire dépendants de l'hippocampe.

Références

Amegandjin, C.A., Choudhury, M., Jadhav, V., Carriço, J.N., Quintal, A., Berryer, M., Snapyan, M., Chattopadhyaya, B., Saghatelyan, A. & Di Cristo, G. (2021) Sensitive period for rescuing parvalbumin interneurons connectivity and social behavior deficits caused by TSC1 loss. *Nature Communications*, **12**, 3653.

Artinian, J., Jordan, A., Khlaifia, A., Honore, E., La Fontaine, A., Racine, A.S., Laplante, I. & Lacaille, J.C. (2019) Regulation of Hippocampal Memory by mTORC1 in Somatostatin Interneurons. *J Neurosci*, **39**, 8439-8456.

Asgarihafshejani, A., Honoré, È., Michon, F.-X., Laplante, I. & Lacaille, J.-C. (2022) Long-term potentiation at pyramidal cell to somatostatin interneuron synapses controls hippocampal network plasticity and memory. *iScience*, **25**, 104259.

Banko, J.L., Hou, L., Poulin, F., Sonenberg, N. & Klann, E. (2006) Regulation of eukaryotic initiation factor 4E by converging signaling pathways during metabotropic glutamate receptor-dependent long-term depression. *J Neurosci*, **26**, 2167-2173.

Bartos, M., Alle, H. & Vida, I. (2011) Role of microcircuit structure and input integration in hippocampal interneuron recruitment and plasticity. *Neuropharmacology*, **60**, 730-739.

Benarroch, E.E. (2018) Locus coeruleus. *Cell and Tissue Research*, **373**, 221-232.

Bevilaqua, L., Ardenghi, P., Schörder, N., Bromberg, E., Schmitz, P.K., Schaeffer, E., Quevedo, J., Bianchin, M., Walz, R., Medina, J.H. & Izquierdo, I. (1997) Drugs acting upon the cyclic adenosine monophosphate/ protein kinase A signalling pathway modulate memory consolidation when given late after training into rat hippocampus but not amygdala. *Behavioural Pharmacology*, **8**.

Bezaire, M.J. & Soltesz, I. (2013) Quantitative assessment of CA1 local circuits: knowledge base for interneuron-pyramidal cell connectivity. *Hippocampus*, **23**, 751-785.

Bliss, T.V. & Lomo, T. (1973) Long-lasting potentiation of synaptic transmission in the dentate area of the anaesthetized rabbit following stimulation of the perforant path. *J Physiol*, **232**, 331-356.

Booker, S.A., Harada, H., Elgueta, C., Bank, J., Bartos, M., Kulik, A. & Vida, I. (2020) Presynaptic GABAB receptors functionally uncouple somatostatin interneurons from the active hippocampal network. *Elife*, **9**.

Booker, S.A., Loreth, D., Gee, A.L., Watanabe, M., Kind, P.C., Wyllie, D.J.A., Kulik, A. & Vida, I. (2018) Postsynaptic GABABRs Inhibit L-Type Calcium Channels and Abolish Long-Term Potentiation in Hippocampal Somatostatin Interneurons. *Cell Rep*, **22**, 36-43.

Booker, S.A. & Vida, I. (2018) Morphological diversity and connectivity of hippocampal interneurons. *Cell and Tissue Research*, **373**, 619-641.

Campanac, E., Gasselin, C., Baude, A., Rama, S., Ankri, N. & Debanne, D. (2013) Enhanced Intrinsic Excitability in Basket Cells Maintains Excitatory-Inhibitory Balance in Hippocampal Circuits. *Neuron*, **77**, 712-722.

Campbell, E.J. & Marchant, N.J. (2018) The use of chemogenetics in behavioural neuroscience: receptor variants, targeting approaches and caveats. *Br J Pharmacol*, **175**, 994-1003.

Cardin, J.A., Carlen, M., Meletis, K., Knoblich, U., Zhang, F., Deisseroth, K., Tsai, L.H. & Moore, C.I. (2010) Targeted optogenetic stimulation and recording of neurons in vivo using cell-type-specific expression of Channelrhodopsin-2. *Nature protocols*, **5**, 247-254.

Cenquizca, L.A. & Swanson, L.W. (2007) Spatial organization of direct hippocampal field CA1 axonal projections to the rest of the cerebral cortex. *Brain Res Rev*, **56**, 1-26.

Chen, X., Gao, B., Ponnusamy, M., Lin, Z. & Liu, J. (2017) MEF2 signaling and human diseases. *Oncotarget*, **8**.

Chittajallu, R., Craig, M.T., McFarland, A., Yuan, X., Gerfen, S., Tricoire, L., Erkkila, B., Barron, S.C., Lopez, C.M., Liang, B.J., Jeffries, B.W., Pelkey, K.A. & McBain, C.J. (2013) Dual origins of functionally distinct O-LM interneurons revealed by differential 5-HT3AR expression. *Nature Neuroscience*, **16**, 1598-1607.

Chiu, C.Q., Martenson, J.S., Yamazaki, M., Natsume, R., Sakimura, K., Tomita, S., Tavalin, S.J. & Higley, M.J. (2018) Input-Specific NMDAR-Dependent Potentiation of Dendritic GABAergic Inhibition. *Neuron*, **97**, 368-377 e363.

Choi, J.H., Sim, S.E., Kim, J.I., Choi, D.I., Oh, J., Ye, S., Lee, J., Kim, T., Ko, H.G., Lim, C.S. & Kaang, B.K. (2018) Interregional synaptic maps among engram cells underlie memory formation. *Science*, **360**, 430-435.

Colgin, L.L. (2015) Do slow and fast gamma rhythms correspond to distinct functional states in the hippocampal network? *Brain Research*, **1621**, 309-315.

Colgin, L.L. (2020) Five Decades of Hippocampal Place Cells and EEG Rhythms in Behaving Rats. *The Journal of Neuroscience*, **40**, 54-60.

Costa-Mattioli, M., Sossin, W.S., Klann, E. & Sonenberg, N. (2009) Translational control of long-lasting synaptic plasticity and memory. *Neuron*, **61**, 10-26.

Cox, D.J., Racca, C. & Lebeau, F.E.N. (2008) β-adrenergic receptors are differentially expressed in distinct interneuron subtypes in the rat hippocampus. *Journal of Comparative Neurology*, **509**, 551-565.

Croce, A., Pelletier, J.G., Tartas, M. & Lacaille, J.C. (2010) Afferent-specific properties of interneuron synapses underlie selective long-term regulation of feedback inhibitory circuits in CA1 hippocampus. *J Physiol*, **588**, 2091-2107.

Dana, H., Mohar, B., Sun, Y., Narayan, S., Gordus, A., Hasseman, J.P., Tsegaye, G., Holt, G.T., Hu, A., Walpita, D., Patel, R., Macklin, J.J., Bargmann, C.I., Ahrens, M.B., Schreiter, E.R., Jayaraman, V., Looger, L.L., Svoboda, K. & Kim, D.S. (2016) Sensitive red protein calcium indicators for imaging neural activity. *eLife*, **5**, e12727.

Descarries, L. & Mechawar, N. (2000) Ultrastructural evidence for diffuse transmission by monoamine and acetylcholine neurons of the central nervous system *Progress in Brain Research*. Elsevier, pp. 27-47.

Donato, F., Chowdhury, A., Lahr, M. & Caroni, P. (2015) Early- and Late-Born Parvalbumin Basket Cell Subpopulations Exhibiting Distinct Regulation and Roles in Learning. *Neuron*, **85**, 770-786.

Donato, F., Rompani, S.B. & Caroni, P. (2013) Parvalbumin-expressing basket-cell network plasticity induced by experience regulates adult learning. *Nature*, **504**, 272-276.

Drieu, C. & Zugaro, M. (2019) Hippocampal Sequences During Exploration: Mechanisms and Functions. *Frontiers in Cellular Neuroscience*, **13**.

Dyer-Reaves, K., Goodman, A.M., Nelson, A.R. & McMahon, L.L. (2019) Alpha1-Adrenergic Receptor Mediated Long-Term Depression at CA3-CA1 Synapses Can Be Induced via Accumulation of Endogenous Norepinephrine and Is Preserved Following Noradrenergic Denervation. *Frontiers in Synaptic Neuroscience*, **11**.

Fernández-Ruiz, A., Oliva, A., Nagy, G.A., Maurer, A.P., Berényi, A. & Buzsáki, G. (2017) Entorhinal-CA3 Dual-Input Control of Spike Timing in the Hippocampus by Theta-Gamma Coupling. *Neuron*, **93**, 1213-1226.e1215.

Freund, T.F. & Buzsáki, G. (1996) Interneurons of the hippocampus. *Hippocampus*, **6**, 347-470.

Fuhrmann, F., Justus, D., Sosulina, L., Kaneko, H., Beutel, T., Friedrichs, D., Schoch, S., Schwarz, M.K., Fuhrmann, M. & Remy, S. (2015) Locomotion, Theta Oscillations, and the Speed-Correlated Firing of Hippocampal Neurons Are Controlled by a Medial Septal Glutamatergic Circuit. *Neuron*, **86**, 1253-1264.

Geiller, T., Sadeh, S., Rolotti, S.V., Blockus, H., Vancura, B., Negrean, A., Murray, A.J., Rózsa, B., Polleux, F., Clopath, C. & Losonczy, A. (2022) Local circuit amplification of spatial selectivity in the hippocampus. *Nature*, **601**, 105-109.

Geiller, T., Vancura, B., Terada, S., Troullinou, E., Chavlis, S., Tsagkatakis, G., Tsakalides, P., Ócsai, K., Poirazi, P., Rózsa, B.J. & Losonczy, A. (2020) Large-Scale 3D Two-Photon

Imaging of Molecularly Identified CA1 Interneuron Dynamics in Behaving Mice. *Neuron*, **108**, 968-983.e969.

Glickfeld, L.L., Roberts, J.D., Somogyi, P. & Scanziani, M. (2009) Interneurons hyperpolarize pyramidal cells along their entire somatodendritic axis. *Nat Neurosci*, **12**, 21-23.

Grienberger, C., Milstein, A.D., Bittner, K.C., Romani, S. & Magee, J.C. (2017) Inhibitory suppression of heterogeneously tuned excitation enhances spatial coding in CA1 place cells. *Nat Neurosci*, **20**, 417-426.

Haam, J. & Yakel, J.L. (2017) Cholinergic modulation of the hippocampal region and memory function. *J Neurochem*, **142 Suppl 2**, 111-121.

He, X., Li, J., Zhou, G., Yang, J., McKenzie, S., Li, Y., Li, W., Yu, J., Wang, Y., Qu, J., Wu, Z., Hu, H., Duan, S. & Ma, H. (2021) Gating of hippocampal rhythms and memory by synaptic plasticity in inhibitory interneurons. *Neuron*, **109**, 1013-1028.e1019.

Hippenmeyer, S., Vrieseling, E., Sigrist, M., Portmann, T., Laengle, C., Ladle, D.R. & Arber, S. (2005) A developmental switch in the response of DRG neurons to ETS transcription factor signaling. *PLoS Biol*, **3**, e159.

Honore, E., Khlaifia, A., Bosson, A. & Lacaille, J.C. (2021) Hippocampal Somatostatin Interneurons, Long-Term Synaptic Plasticity and Memory. *Front Neural Circuits*, **15**, 687558.

Huang, Y.H., Sinha, S.R., Tanaka, K., Rothstein, J.D. & Bergles, D.E. (2004) Astrocyte glutamate transporters regulate metabotropic glutamate receptor-mediated excitation of hippocampal interneurons. *J Neurosci*, **24**, 4551-4559.

Huang, Y.Y. & Kandel, E.R. (2005) Theta frequency stimulation up-regulates the synaptic strength of the pathway from CA1 to subiculum region of hippocampus. *Proc Natl Acad Sci U S A*, **102**, 232-237.

Huber, K.M., Kayser, M.S. & Bear, M.F. (2000) Role for rapid dendritic protein synthesis in hippocampal mGluR-dependent long-term depression. *Science*, **288**, 1254-1257.

Jiang, X., Lupien-Meilleur, A., Tazerart, S., Lachance, M., Samarova, E., Araya, R., Lacaille, J.C. & Rossignol, E. (2018) Remodeled cortical inhibition prevents motor seizures in generalized epilepsy. *Ann Neurol*, **84**, 436-451.

Jinno, S., Klausberger, T., Marton, L.F., Dalezios, Y., Roberts, J.D., Fuentealba, P., Bushong, E.A., Henze, D., Buzsaki, G. & Somogyi, P. (2007) Neuronal diversity in GABAergic long-range projections from the hippocampus. *J Neurosci*, **27**, 8790-8804.

Josselyn & Frankland (2018) Memory allocation: Mechanisms and function. *Annual Review of Neuroscience*, **41**, 389-413.

Josselyn, S.A. & Tonegawa, S. (2020) Memory engrams: Recalling the past and imagining the future. *Science*, **367**.

Kang, D., Ding, M., Topchiy, I. & Kocsis, B. (2017) Reciprocal Interactions between Medial Septum and Hippocampus in Theta Generation: Granger Causality Decomposition of Mixed Spike-Field Recordings. *Frontiers in Neuroanatomy*, **11**.

Karunakaran, S., Chowdhury, A., Donato, F., Quairiaux, C., Michel, C.M. & Caroni, P. (2016) PV plasticity sustained through D1/5 dopamine signaling required for long-term memory consolidation. *Nature Neuroscience*, **19**, 454-464.

Katona, L., Lapray, D., Viney, T.J., Oulhaj, A., Borhegyi, Z., Micklem, B.R., Klausberger, T. & Somogyi, P. (2014) Sleep and movement differentiates actions of two types of somatostatin-expressing GABAergic interneuron in rat hippocampus. *Neuron*, **82**, 872-886.

Kaufman, A.M., Geiller, T. & Losonczy, A. (2020) A Role for the Locus Coeruleus in Hippocampal CA1 Place Cell Reorganization during Spatial Reward Learning. *Neuron*, **105**, 1018-1026.e1014.

Kempadoo, K.A., Mosharov, E.V., Choi, S.J., Sulzer, D. & Kandel, E.R. (2016) Dopamine release from the locus coeruleus to the dorsal hippocampus promotes spatial learning and memory. *Proceedings of the National Academy of Sciences*, **113**, 14835-14840.

Klausberger, T., Magill, P.J., Marton, L.F., Roberts, J.D., Cobden, P.M., Buzsaki, G. & Somogyi, P. (2003) Brain-state- and cell-type-specific firing of hippocampal interneurons in vivo. *Nature*, **421**, 844-848.

Klausberger, T. & Somogyi, P. (2008) Neuronal diversity and temporal dynamics: the unity of hippocampal circuit operations. *Science*, **321**, 53-57.

Knierim, J.J., Neunuebel, J.P. & Deshmukh, S.S. (2014) Functional correlates of the lateral and medial entorhinal cortex: objects, path integration and local-global reference frames. *Philosophical Transactions of the Royal Society B: Biological Sciences*, **369**, 20130369.

Korotkova, T., Fuchs, E.C., Ponomarenko, A., von Engelhardt, J. & Monyer, H. (2010) NMDA Receptor Ablation on Parvalbumin-Positive Interneurons Impairs Hippocampal Synchrony, Spatial Representations, and Working Memory. *Neuron*, **68**, 557-569.

Kullmann, D.M., Moreau, A.W., Bakiri, Y. & Nicholson, E. (2012) Plasticity of inhibition. *Neuron*, **75**, 951-962.

Lamsa, K.P., Heeroma, J.H., Somogyi, P., Rusakov, D.A. & Kullmann, D.M. (2007) Anti-Hebbian long-term potentiation in the hippocampal feedback inhibitory circuit. *Science*, **315**, 1262-1266.

Lapointe, V., Morin, F., Ratte, S., Croce, A., Conquet, F. & Lacaille, J.C. (2004) Synapse-specific mGluR1-dependent long-term potentiation in interneurones regulates mouse hippocampal inhibition. *J Physiol*, **555**, 125-135.

Leao, R.N., Mikulovic, S., Leao, K.E., Munguba, H., Gezelius, H., Enjin, A., Patra, K., Eriksson, A., Loew, L.M., Tort, A.B. & Kullander, K. (2012) OLM interneurons differentially modulate CA3 and entorhinal inputs to hippocampal CA1 neurons. *Nat Neurosci*, **15**, 1524-1530.

Lemon, N. & Manahan-Vaughan, D. (2006) Dopamine D₁/D₅ Receptors Gate the Acquisition of Novel Information through Hippocampal Long-Term Potentiation and Long-Term Depression. *The Journal of Neuroscience*, **26**, 7723-7729.

Liu, C., Goel, P. & Kaeser, P.S. (2021) Spatial and temporal scales of dopamine transmission. *Nature Reviews Neuroscience*, **22**, 345-358.

Lovett-Barron, M., Kaifosh, P., Kheirbek, M.A., Danielson, N., Zaremba, J.D., Reardon, T.R., Turi, G.F., Hen, R., Zemelman, B.V. & Losonczy, A. (2014) Dendritic inhibition in the hippocampus supports fear learning. *Science*, **343**, 857-863.

Lovett-Barron, M., Turi, G.F., Kaifosh, P., Lee, P.H., Bolze, F., Sun, X.H., Nicoud, J.F., Zemelman, B.V., Sternson, S.M. & Losonczy, A. (2012) Regulation of neuronal input transformations by tunable dendritic inhibition. *Nat Neurosci*, **15**, 423-430, S421-423.

Madisen, L., Zwingman, T.A., Sunkin, S.M., Oh, S.W., Zariwala, H.A., Gu, H., Ng, L.L., Palmiter, R.D., Hawrylycz, M.J., Jones, A.R., Lein, E.S. & Zeng, H. (2010) A robust and high-throughput Cre reporting and characterization system for the whole mouse brain. *Nat Neurosci*, **13**, 133-140.

Malenka, R.C. & Bear, M.F. (2004) LTP and LTD: an embarrassment of riches. *Neuron*, **44**, 5-21.

Marder, E. (2012) Neuromodulation of Neuronal Circuits: Back to the Future. *Neuron*, **76**, 1-11.

Martel, J.C. & Gatti McArthur, S. (2020) Dopamine Receptor Subtypes, Physiology and Pharmacology: New Ligands and Concepts in Schizophrenia. *Frontiers in Pharmacology*, **11**.

McBain, C.J. & Kauer, J.A. (2009) Presynaptic plasticity: targeted control of inhibitory networks. *Curr Opin Neurobiol*, **19**, 254-262.

McKay, B.M., Oh, M.M. & Disterhoft, J.F. (2013) Learning increases intrinsic excitability of hippocampal interneurons. *J Neurosci*, **33**, 5499-5506.

Mikulovic, S., Restrepo, C.E., Hilscher, M.M., Kullander, K. & Leao, R. (2015) Novel markers for OLM interneurons in the hippocampus. *Frontiers in Cellular Neuroscience*, **9**.

Miyoshi, G., Hjerling-Leffler, J., Karayannis, T., Sousa, V.H., Butt, S.J., Battiste, J., Johnson, J.E., Machold, R.P. & Fishell, G. (2010) Genetic fate mapping reveals that the caudal ganglionic eminence produces a large and diverse population of superficial cortical interneurons. *J Neurosci*, **30**, 1582-1594.

Montgomery, S.M. & Buzsáki, G. (2007) Gamma oscillations dynamically couple hippocampal CA3 and CA1 regions during memory task performance. *Proceedings of the National Academy of Sciences*, **104**, 14495-14500.

Muller, C. & Remy, S. (2014) Dendritic inhibition mediated by O-LM and bistratified interneurons in the hippocampus. *Front Synaptic Neurosci*, **6**, 23.

Nabavi, S., Fox, R., Proulx, C.D., Lin, J.Y., Tsien, R.Y. & Malinow, R. (2014) Engineering a memory with LTD and LTP. *Nature*, **511**, 348-352.

Nicholson, E. & Kullmann, D.M. (2021) Nicotinic receptor activation induces NMDA receptor independent long-term potentiation of glutamatergic signalling in hippocampal oriens interneurons. *J Physiol*, **599**, 667-676.

O'Mara, S.M., Commins, S. & Anderson, M. (2000) Synaptic plasticity in the hippocampal area CA1-subiculum projection: implications for theories of memory. *Hippocampus*, **10**, 447-456.

Ognjanovski, N., Schaeffer, S., Wu, J., Mofakham, S., Maruyama, D., Zochowski, M. & Aton, S.J. (2017) Parvalbumin-expressing interneurons coordinate hippocampal network dynamics required for memory consolidation. *Nature Communications*, **8**, 15039.

Oh, J., Lee, C. & Kaang, B.K. (2019) Imaging and analysis of genetically encoded calcium indicators linking neural circuits and behaviors. *Korean J Physiol Pharmacol*, **23**, 237-249.

Oleskevich, S., Descarries, L. & Lacaille, J.C. (1989) Quantified distribution of the noradrenaline innervation in the hippocampus of adult rat. *J Neurosci*, **9**, 3803-3815.

Pacholko, A.G., Wotton, C.A. & Bekar, L.K. (2020) Astrocytes—The Ultimate Effectors of Long-Range Neuromodulatory Networks? *Frontiers in Cellular Neuroscience*, **14**.

Palacios-Filardo, J. & Mellor, J.R. (2019) Neuromodulation of hippocampal long-term synaptic plasticity. *Current Opinion in Neurobiology*, **54**, 37-43.

Papay, R., Gaivin, R., Jha, A., Mccune, D.F., Mcgrath, J.C., Rodrigo, M.C., Simpson, P.C., Doze, V.A. & Perez, D.M. (2006) Localization of the mouse α1A-adrenergic receptor (AR) in the brain: α1AAR is expressed in neurons, GABAergic interneurons, and NG2 oligodendrocyte progenitors. *Journal of Comparative Neurology*, **497**, 209-222.

Pelkey, K.A., Chittajallu, R., Craig, M.T., Tricoire, L., Wester, J.C. & McBain, C.J. (2017) Hippocampal GABAergic Inhibitory Interneurons. *Physiol Rev*, **97**, 1619-1747.

Pelletier, J.G. & Lacaille, J.C. (2008) Long-term synaptic plasticity in hippocampal feedback inhibitory networks. *Prog Brain Res*, **169**, 241-250.

Perez, Y., Morin, F. & Lacaille, J.C. (2001) A hebbian form of long-term potentiation dependent on mGluR1a in hippocampal inhibitory interneurons. *Proc Natl Acad Sci U S A*, **98**, 9401-9406.

Pouille, F. & Scanziani, M. (2004) Routing of spike series by dynamic circuits in the hippocampus. *Nature*, **429**, 717-723.

Puighermanal, E., Cutando, L., Boubaker-Vitre, J., Honoré, E., Longueville, S., Hervé, D. & Valjent, E. (2017) Anatomical and molecular characterization of dopamine D1 receptor-expressing neurons of the mouse CA1 dorsal hippocampus. *Brain Structure and Function*, **222**, 1897-1911.

Ran, I., Laplante, I., Bourgeois, C., Pepin, J., Lacaille, P., Costa-Mattioli, M., Pelletier, J., Sonenberg, N. & Lacaille, J.C. (2009) Persistent transcription- and translation-dependent long-term potentiation induced by mGluR1 in hippocampal interneurons. *J Neurosci*, **29**, 5605-5615.

Rao-Ruiz, P., Yu, J., Kushner, S.A. & Josselyn, S.A. (2019) Neuronal competition: microcircuit mechanisms define the sparsity of the engram. *Current Opinion in Neurobiology*, **54**, 163-170.

Renault, R., Sukenik, N., Descroix, S., Malaquin, L., Viovy, J.-L., Peyrin, J.-M., Bottani, S., Monceau, P., Moses, E. & Vignes, M. (2015) Combining Microfluidics, Optogenetics and Calcium Imaging to Study Neuronal Communication In Vitro. *PLOS ONE*, **10**, e0120680.

Rolotti, S.V., Ahmed, M.S., Szoboszlay, M., Geiller, T., Negrean, A., Blockus, H., Gonzalez, K.C., Sparks, F.T., Solis Canales, A.S., Tuttman, A.L., Peterka, D.S., Zemelman, B.V., Polleux, F. & Losonczy, A. (2022) Local feedback inhibition tightly controls rapid formation of hippocampal place fields. *Neuron*, **110**, 783-794.e786.

Royer, S., Zemelman, B.V., Losonczy, A., Kim, J., Chance, F., Magee, J.C. & Buzsaki, G. (2012) Control of timing, rate and bursts of hippocampal place cells by dendritic and somatic inhibition. *Nat Neurosci*, **15**, 769-775.

Schmid, L.C., Mittag, M., Poll, S., Steffen, J., Wagner, J., Geis, H.R., Schwarz, I., Schmidt, B., Schwarz, M.K., Remy, S. & Fuhrmann, M. (2016) Dysfunction of Somatostatin-Positive Interneurons Associated with Memory Deficits in an Alzheimer's Disease Model. *Neuron*, **92**, 114-125.

Schomburg, Erik W., Fernández-Ruiz, A., Mizuseki, K., Berényi, A., Anastassiou, Costas A., Koch, C. & Buzsáki, G. (2014) Theta Phase Segregation of Input-Specific Gamma Patterns in Entorhinal-Hippocampal Networks. *Neuron*, **84**, 470-485.

Sengupta, S., Peterson, T.R., Laplante, M., Oh, S. & Sabatini, D.M. (2010) mTORC1 controls fasting-induced ketogenesis and its modulation by ageing. *Nature*, **468**, 1100-1104.

Sharif, F., Tayebi, B., Buzsáki, G., Royer, S. & Fernandez-Ruiz, A. (2021) Subcircuits of Deep and Superficial CA1 Place Cells Support Efficient Spatial Coding across Heterogeneous Environments. *Neuron*, **109**, 363-376.e366.

Sharma, V., Sood, R., Khlaifia, A., Eslamizade, M.J., Hung, T.Y., Lou, D., Asgarihafshejani, A., Lalzar, M., Kiniry, S.J., Stokes, M.P., Cohen, N., Nelson, A.J., Abell, K., Possemato, A.P., Gal-Ben-Ari, S., Truong, V.T., Wang, P., Yiannakas, A., Saffarzadeh, F., Cuello, A.C.,

Nader, K., Kaufman, R.J., Costa-Mattioli, M., Baranov, P.V., Quintana, A., Sanz, E., Khoutorsky, A., Lacaille, J.C., Rosenblum, K. & Sonenberg, N. (2020) eIF2alpha controls memory consolidation via excitatory and somatostatin neurons. *Nature*, **586**, 412-416.

Somogyi, P., Katona, L., Klausberger, T., Lasztóczi, B. & Viney, T.J. (2014) Temporal redistribution of inhibition over neuronal subcellular domains underlies state-dependent rhythmic change of excitability in the hippocampus. *Philosophical Transactions of the Royal Society B: Biological Sciences*, **369**, 20120518.

Song, Q., Bolsius, Y.G., Ronzoni, G., Henckens, M.J.A.G. & Roozendaal, B. (2021) Noradrenergic enhancement of object recognition and object location memory in mice. *Stress*, **24**, 181-188.

Spiess, E., Bestvater, F., Heckel-pompey, A., Toth, K., Hacker, M., Stobrawa, G., Feurer, T., Wotzlaw, C., Berchner-Pfannschmidt, U., PorwoL, T. & Acker, H. (2005) Two-photon excitation and emission spectra of the green fluorescent protein variants ECFP, EGFP and EYFP. *Journal of Microscopy*, **217**, 200-204.

Stefanelli, T., Bertollini, C., Lüscher, C., Muller, D. & Mendez, P. (2016) Hippocampal Somatostatin Interneurons Control the Size of Neuronal Memory Ensembles. *Neuron*, **89**, 1074-1085.

Sun, Y., Jin, S., Lin, X., Chen, L., Qiao, X., Jiang, L., Zhou, P., Johnston, K.G., Golshani, P., Nie, Q., Holmes, T.C., Nitz, D.A. & Xu, X. (2019) CA1-projecting subiculum neurons facilitate object–place learning. *Nature Neuroscience*, **22**, 1857-1870.

Sun, Y., Nguyen, A.Q., Nguyen, J.P., Le, L., Saur, D., Choi, J., Callaway, E.M. & Xu, X. (2014) Cell-type-specific circuit connectivity of hippocampal CA1 revealed through Cre-dependent rabies tracing. *Cell Rep*, **7**, 269-280.

Szonyi, A., Sos, K.E., Nyilas, R., Schlingloff, D., Domonkos, A., Takacs, V.T., Posfai, B., Hegedus, P., Priestley, J.B., Gundlach, A.L., Gulyas, A.I., Varga, V., Losonczy, A., Freund, T.F. & Nyiri, G. (2019) Brainstem nucleus incertus controls contextual memory formation. *Science*, **364**.

Taniguchi, H., He, M., Wu, P., Kim, S., Paik, R., Sugino, K., Kvitsiani, D., Fu, Y., Lu, J., Lin, Y., Miyoshi, G., Shima, Y., Fishell, G., Nelson, S.B. & Huang, Z.J. (2011) A resource of Cre driver lines for genetic targeting of GABAergic neurons in cerebral cortex. *Neuron*, **71**, 995-1013.

Taube, J.S. (1993) Electrophysiological properties of neurons in the rat subiculum in vitro. *Exp Brain Res*, **96**, 304-318.

Terada, S., Geiller, T., Liao, Z., O'Hare, J., Vancura, B. & Losonczy, A. (2022) Adaptive stimulus selection for consolidation in the hippocampus. *Nature*, **601**, 240-244.

Topolnik, L., Azzi, M., Morin, F., Kougioumoutzakis, A. & Lacaille, J.C. (2006) mGluR1/5 subtype-specific calcium signalling and induction of long-term potentiation in rat hippocampal oriens/alveus interneurones. *J Physiol*, **575**, 115-131.

Tricoire, L., Pelkey, K.A., Erkkila, B.E., Jeffries, B.W., Yuan, X. & McBain, C.J. (2011) A Blueprint for the Spatiotemporal Origins of Mouse Hippocampal Interneuron Diversity. *The Journal of Neuroscience*, **31**, 10948-10970.

Tyan, L., Chamberland, S., Magnin, E., Camire, O., Francavilla, R., David, L.S., Deisseroth, K. & Topolnik, L. (2014) Dendritic inhibition provided by interneuron-specific cells controls the firing rate and timing of the hippocampal feedback inhibitory circuitry. *J Neurosci*, **34**, 4534-4547.

Udakis, M., Pedrosa, V., Chamberlain, S.E.L., Clopath, C. & Mellor, J.R. (2020) Interneuron-specific plasticity at parvalbumin and somatostatin inhibitory synapses onto CA1 pyramidal neurons shapes hippocampal output. *Nat Commun*, **11**, 4395.

Urban-Ciecko, J., Jouhanneau, J.-S., Myal, S.E., Poulet, J.F.A. & Barth, A.L. (2018) Precisely Timed Nicotinic Activation Drives SST Inhibition in Neocortical Circuits. *Neuron*, **97**, 611-625.e615.

Usher, M., Cohen, J.D., Servan-Schreiber, D., Rajkowski, J. & Aston-Jones, G. (1999) The Role of Locus Coeruleus in the Regulation of Cognitive Performance. *Science*, **283**, 549-554.

van Hooft, J.A., Giuffrida, R., Blatow, M. & Monyer, H. (2000) Differential expression of group I metabotropic glutamate receptors in functionally distinct hippocampal interneurons. *J Neurosci*, **20**, 3544-3551.

Vasuta, C., Artinian, J., Laplante, I., Hebert-Seropian, S., Elayoubi, K. & Lacaille, J.C. (2015) Metaplastic Regulation of CA1 Schaffer Collateral Pathway Plasticity by Hebbian MGluR1a-Mediated Plasticity at Excitatory Synapses onto Somatostatin-Expressing Interneurons. *eNeuro*, **2**.

Wahis, J. & Holt, M.G. (2021) Astrocytes, Noradrenaline, α1-Adrenoreceptors, and Neuromodulation: Evidence and Unanswered Questions. *Frontiers in Cellular Neuroscience*, **15**.

Wang, Y., Toprani, S., Tang, Y., Vrabec, T. & Durand, D.M. (2014) Mechanism of highly synchronized bilateral hippocampal activity. *Exp Neurol*, **251**, 101-111.

Whitlock, J.R., Heynen, A.J., Shuler, M.G. & Bear, M.F. (2006) Learning induces long-term potentiation in the hippocampus. *Science*, **313**, 1093-1097.

Younts, T.J., Monday, H.R., Dudok, B., Klein, M.E., Jordan, B.A., Katona, I. & Castillo, P.E. (2016) Presynaptic Protein Synthesis Is Required for Long-Term Plasticity of GABA Release. *Neuron*, **92**, 479-492.

Yuan, S. & Burrell, B.D. (2013) Endocannabinoid-dependent long-term depression in a nociceptive synapse requires coordinated presynaptic and postsynaptic transcription and translation. *J Neurosci*, **33**, 4349-4358.

Zemankovics, R., Veres, J.M., Oren, I. & Hájos, N. (2013) Feedforward Inhibition Underlies the Propagation of Cholinergically Induced Gamma Oscillations from Hippocampal CA3 to CA1. *The Journal of Neuroscience*, **33**, 12337-12351.

Zhao, J.-P. & Yoshii, A. (2019) Hyperexcitability of the local cortical circuit in mouse models of tuberous sclerosis complex. *Molecular Brain*, **12**, 6.

Zweifel, L.S., Parker, J.G., Lobb, C.J., Rainwater, A., Wall, V.Z., Fadok, J.P., Darvas, M., Kim, M.J., Mizumori, S.J.Y., Paladini, C.A., Phillips, P.E.M. & Palmiter, R.D. (2009) Disruption of NMDAR-dependent burst firing by dopamine neurons provides selective assessment of phasic dopamine-dependent behavior. *Proceedings of the National Academy of Sciences*, **106**, 7281-7288.